

**Development of a Test Protocol for Industry to
Predict and Optimise Flow Behaviour of Blended
Powders utilising Particle to Bulk Scale Models**

Jose Carmelo Santana Perdomo

This thesis is submitted in partial fulfilment of the requirements for the
award of the degree of Doctor of Philosophy

This research was carried out at The Wolfson Centre for Bulk Solids
Handling Technology
University of Greenwich

September 2015

DECLARATION

I certify that this work has not been accepted in substance for any degree, and is not concurrently being submitted for any degree other than that of Doctor of Philosophy being studied at the University of Greenwich. I also declare that this work is the result of my own investigations except where otherwise identified by references and that I have not plagiarised the work of others.

Jose Carmelo Santana Perdomo

Candidate

Professor Michael S.A. Bradley

First Supervisor

Dr Robert Berry

Second Supervisor

ACKNOWLEDGEMENTS

I would like to thank all staff of The Wolfson Centre for Bulk Solids Handling Technology for their support in the last four years. Special acknowledgements to Mr. Jonathan Larkin, Mr. Trevor Mortley, Mrs. Caroline Chapman, Mr. Richard Farnish, Mr. Tony Kelly, Dr. Stefan Zigan, Dr. Tong Deng, Dr. Karol Ariza Zafra, Dr. Oscar Andres Angulo Pinzon and Dr. Tariq Hussain; their friendship made me feel very welcome at The Wolfson Centre.

I am indebted to my supervisors Professor Mike Bradley and Dr. Robert Berry for believing in me and being always willing to share their knowledge; they always guided and advised me through the research project and helped me to become a better researcher.

My sincere gratitude to everyone who made contributions to this research project with discussions, brilliant ideas and theoretical support during my stay at The Wolfson Centre.

I wish to dedicate the entire work to my parents, my brother and my wife; they have always been supportive and encouraging no matter what and my life would not be the same without their sincere love.

ABSTRACT

Reformulation of blended particulate materials has been always a problem for powder industry because formulators have difficulty in measuring, controlling and/or modifying the bulk flow properties of powders. A recently developed powder flow tester (PFT) by The Wolfson Centre for Bulk Solids Handling Technology, University of Greenwich is now available for industry to measure quickly and accurately the flow behaviour of single and blended particulate materials.

This new powder flow tester helps to characterise quantitatively the blends which show good flow behaviour in the industrial process lines and define the desirable standards for blends with poor flow behaviour. However, the current process of reformulation is basically a trial and error procedure based on the prior experience of the formulator with other blends reformulated. There is clearly a lack of practical understanding of the links between the particle and bulk scale of powders and how changes in the particle properties and/or blend compositions would affect the flow behaviour of blended powders.

The aim of this research work was to develop an “empirical understanding” of the links between the particle properties and bulk flow properties in order to predict the bulk flow properties of blended powders based on changes to the particle properties or blend components. This has been achieved evaluating analytical well-established models found in the literature linking particle and bulk scale for practical purposes in industry, developing new empirical models to predict the flow behaviour of single and blended powders based on the experimental work undertaken in this research and identifying methods or techniques that formulators in industry could use to predict the flow behaviour of their blended powders.

The solution provided is a test protocol which in combination with the standard characterisation tests commonly used in industry and the prediction tool called Virtual Powder Blending Laboratory (recently developed by The Wolfson Centre for Bulk Solids Handling Technology using the experimental and modelling work undertaken in this work) will help formulators and process engineers to formulate the composition of blended powders with the desirable flow behaviour in industrial process lines.

CONTENTS

Chapter 1	Background.....	1
1.1	Introduction.....	1
1.2	Common flow issues in industrial processes.....	2
1.3	Problems in the blended food powder industry.....	8
1.4	Current practice for new or modified blended powders.....	9
1.5	Aim of the research.....	10
1.6	Programme objectives.....	10
1.7	Contributions to Knowledge.....	10
1.8	Project preview.....	11
Chapter 2	Literature Review.....	13
2.1	Introduction.....	13
2.2	Particle property measurements.....	14
2.2.1	Particle size and distribution.....	14
2.2.2	Particle density.....	16
2.2.3	Particle shape.....	16
2.2.4	Other particle properties.....	18
2.3	Bulk flow properties.....	18
2.3.1	Practical measurements of bulk flow properties.....	21
2.3.2	Brookfield Powder Flow Tester.....	24
2.3.3	Comparison to other commonly used shear testers.....	25
2.4	Theoretical links between particle and bulk scale.....	26
2.4.1	Packing of monosized spheres.....	26
2.4.2	Effect of particle properties.....	30
2.4.3	Interparticle forces.....	33
2.4.4	Dry particulate materials.....	34

2.4.5	Wet particulate materials	38
2.4.6	Effect of free flow additives	43
2.5	Research studies linking particle and bulk scale	46
2.5.1	Effect of particle shape	46
2.5.2	Effect of particle size and distribution	47
2.5.3	Effect of liquid content.....	48
2.5.4	Rabinovich model	51
2.6	Review of Industrial Practice	51
2.7	Summary	53
Chapter 3	Characterisation of materials	55
3.1	Introduction.....	55
3.2	Sampling and tests conditions	55
3.2.1	Dry single and blended powders.....	56
3.2.2	Wet single and blended powders	58
3.2.3	Wet single and blended powders with free flow additives.....	59
3.3	Particle property measurements.....	59
3.3.1	Particle size and distribution	59
3.3.2	Particle density	63
3.3.3	Particle shape.....	64
3.4	Bulk property measurements	65
3.5	Liquid property measurements	67
3.6	Results	69
3.6.1	Particle characterisation	69
3.6.2	Bulk characterisation	77
3.6.3	Liquid characterisation	90
3.7	Summary	91
Chapter 4	The structure of the investigation	92

4.1	Introduction.....	92
4.2	Research methodology	92
4.3	Industrial case study method.....	95
4.4	Experimental investigations.....	99
4.4.1	Effect of deconstructed particle size distribution.....	102
4.4.2	Effect of particle shape, size and liquid content on powders.....	103
4.4.3	Effect of particle size on dry blends	104
4.4.4	Effect of particle shape and size on wet blends.....	105
4.4.5	Interaction between oil and free flow additives	106
4.4.6	Effect of free flow additives	106
4.5	Summary	107
Chapter 5	Models for prediction of the bulk flow properties	109
5.1	Introduction.....	109
5.2	Modelling strategy	109
5.3	Limitations of the modelling work	110
5.4	Particle contact mechanisms for a single material.....	111
5.4.1	Dry powders.....	112
5.4.2	Wet powders.....	115
5.4.3	Surface coating of particles.....	118
5.5	Blended powders.....	120
5.6	Summary	121
Chapter 6	Experimental results	122
6.1	Introduction.....	122
6.2	Industrial case study	122
6.2.1	Effect of particle size and oil level with different free flow additives	124
6.2.2	Effect of different fillers	127
6.2.3	Trial blends	131

6.3	Experimental investigations.....	133
6.3.1	Effect of deconstructed particle size distribution.....	133
6.3.2	Effect of particle shape, size and liquid content on powders.....	137
6.3.3	Effect of particle size on dry blends	140
6.3.4	Effect of particle shape and size on wet blends.....	144
6.3.5	Interaction between oil and free flow additives	148
6.3.6	Effect of free flow additives	151
6.4	Summary	156
Chapter 7	Empirical calibration of established analytical models.....	157
7.1	Introduction.....	157
7.2	Analytical models for single powders.....	157
7.2.1	Dry powders.....	157
7.2.2	Wet powders.....	166
7.2.3	Surface coating of particles.....	179
7.3	Model proposed for dry blends	179
7.4	Summary	193
Chapter 8	Development of new empirical models.....	196
8.1	Introduction.....	196
8.2	Single particulate materials	196
8.2.1	Dry powders.....	196
8.2.2	Effect of liquid content.....	208
8.2.3	Effect of free flow additives	220
8.3	Blended particulate materials.....	229
8.4	Summary	232
Chapter 9	Development of the test protocol for industry.....	234
9.1	Introduction.....	234
9.2	Virtual Powder Blending Laboratory.....	234

9.2.1	Benefits of the prediction tool.....	234
9.2.2	Current limitations of the prediction tool.....	235
9.2.3	Powder testing and sampling.....	235
9.2.4	Interpretation of the results.....	236
9.2.5	Prediction of the flow behaviour of powders.....	236
9.2.6	Development of a Data Base.....	239
9.2.7	Application of the prediction tool	241
9.3	Test protocol for Industry	241
9.3.1	Common solutions for issues with the formulation of blends.....	241
9.3.2	Recommendations for non-tested conditions.....	242
9.4	Summary	247
Chapter 10	Conclusions and suggestions for further work	248
10.1	Achievement of aim and objectives.....	248
10.2	Contributions to knowledge.....	249
10.3	Critical assessment of the research approach.....	250
10.4	Conclusions	251
10.5	Recommendations for further work	252
References.....		254
Appendix A: Modelling Work.....		261
Appendix B: Experimental Work.....		312
Appendix C: Industrial Case Study		337

FIGURES

<i>Figure 1: The basic flow patterns defined by Jenike et al. a) Mass flow and b) Core flow (The Wolfson Centre for Bulk Solids Handling Technology, University of Greenwich, England).....</i>	<i>3</i>
<i>Figure 2: The three principal types of obstruction to flow a) Mechanical arch, b) Cohesive arch & c) Cohesive rat-hole (The Wolfson Centre for Bulk Solids Handling Technology, University of Greenwich, England).....</i>	<i>4</i>
<i>Figure 3: Effect of rolling segregation during the process of filling a silo (The Wolfson Centre for Bulk Solids Handling Technology, University of Greenwich, England).....</i>	<i>6</i>
<i>Figure 4: Variation of the particle size fraction within discharge stream as a function time, through the complete discharge cycle from a core flow vessel (The Wolfson Centre for Bulk Solids Handling Technology, University of Greenwich, England) For full explanation refer to the text</i>	<i>6</i>
<i>Figure 5: Effect of radial segregation arising from tangential pneumatic filling of a silo (The Wolfson Centre for Bulk Solids Handling Technology, University of Greenwich, England).....</i>	<i>7</i>
<i>Figure 6: Effect of lateral segregation arising from perpendicular pneumatic filling of a silo (The Wolfson Centre for Bulk Solids Handling Technology, University of Greenwich, England).....</i>	<i>8</i>
<i>Figure 7: System variables considered in the powder model.....</i>	<i>13</i>
<i>Figure 8: Characterisation of particle shapes (Benn et al. 1993).....</i>	<i>17</i>
<i>Figure 9: Stages of uniaxial consolidation test (Schulze, 2008).....</i>	<i>19</i>
<i>Figure 10: Instantaneous flow function (FF) and lines of flowability (Schulze, 2008).</i>	<i>20</i>
<i>Figure 11: Linear model of shear strength of a bulk solid material (The Wolfson Centre for Bulk Solids Handling Technology, University of Greenwich, England)</i>	<i>22</i>
<i>Figure 12: Yield locus and Mohr stress circles defining the unconfined yield strength and the consolidation stress: analogy to the uniaxial compression test</i>	<i>23</i>
<i>Figure 13: Open packing structure for monosized spheres (German et al. 1989).....</i>	<i>28</i>
<i>Figure 14: Close packing structure for monosized spheres (German et al. 1989).....</i>	<i>28</i>
<i>Figure 15: Small sphere filling the voidage of large spheres (German et al. 1989)....</i>	<i>32</i>
<i>Figure 16: Schematic diagram illustrating the effect of the particle size on the packing structure of dry glass beads (Yu et al. 2003).....</i>	<i>35</i>

<i>Figure 17: Different states of saturation for an assembly of random packing of monosized spheres (Iveson et al. 2002)</i>	38
<i>Figure 18: Schematic of a pendular bridge between two monosized spheres (Iveson et al. 2002)</i>	39
<i>Figure 19: Discrete and continuous coating of guest particles (Pfeffer et al. 2001) ...</i>	45
<i>Figure 20: The influence of fine particle content on the flow behaviour of blends – Comparison of the Rathole Index values (Hann et al. 2007)</i>	48
<i>Figure 21: Measuring device for the particle size distribution and laser diffraction technique a) Instrument to measure the particle size distribution of powders named Mastersizer 2000 b) Principles of the laser diffraction technique which is used in the Mastersizer 2000</i>	60
<i>Figure 22: Different sieving devices and test sieves a) Automatic PC – controlled device for sieve analysis processes named Gradex 2000 b) Digital sieve shaker named Octagon D200 Digital c) Standard test sieves for European specifications (40 mm depth and stainless steel frame)</i>	61
<i>Figure 23: Ultrapyc 1200e Pycnometer and standard sample cells: a) Automatic Pycnometer b) Standard sample cells supplied in stainless steel (10, 50 and 135 cm³ nominal volume; 24, 40 and 49 mm internal diameter; 23, 39 and 75 mm internal depth)</i>	63
<i>Figure 24: Brookfield Powder Flow Tester (PFT) and components for sample preparation: a) the shear tester b) accessories to prepare samples using the standard volume cell (263 cc volume and 150 mm outer diameter)</i>	67
<i>Figure 25: Schematic representation of a particle size distribution measured by weight percentage</i>	70
<i>Figure 26: Schematic representation of a particle size distribution measured by volume percentage</i>	70
<i>Figure 27: Average Flow Function of six standard flow function tests for a snack flavour named Flame Grilled Steak</i>	79
<i>Figure 28: Average Bulk Density of six standard flow function tests for a snack flavour named Flame Grilled Steak</i>	79
<i>Figure 29: Flow function of six grades of lactose</i>	80
<i>Figure 30: Bulk density of six grades of lactose</i>	80
<i>Figure 31: Friction function of six grades of lactose</i>	81
<i>Figure 32: Compaction curves of six grades of lactose</i>	81

<i>Figure 33: Voidage of six grades of lactose</i>	82
<i>Figure 34: Arch span of six grades of lactose</i>	83
<i>Figure 35: Cohesion of six grades of lactose</i>	84
<i>Figure 36: Internal friction of six grades of lactose</i>	85
<i>Figure 37: Tensile strength of six grades of lactose</i>	86
<i>Figure 38: Flow function of different full blended flavours</i>	93
<i>Figure 39: Arch span of different full blended flavours</i>	94
<i>Figure 40: Ingredient break-down of the Flame Grilled Steak standard flavour</i>	96
<i>Figure 41: Ingredient break-down of the Flame Grilled Steak flavour after removing monosodium glutamate of the standard composition</i>	124
<i>Figure 42: Flow function of full bended powders made with 2.4%wt of TCP</i>	126
<i>Figure 43: Flow function of full bended powders made with 1.2%wt of silica</i>	127
<i>Figure 44: Ingredient break-down of the proposed trial blends of Flame Grilled Steak flavour without MSG</i>	128
<i>Figure 45: Arch span of full blended flavours made with coarse fillers</i>	129
<i>Figure 46: Arch span of full blended flavours made with fine fillers</i>	130
<i>Figure 47: Arch span of the trials blends of the reformulated full blended flavour</i>	132
<i>Figure 48: Flow function of particle size fractions of dextrose</i>	134
<i>Figure 49: Flow function of particle size fractions of maltodextrin</i>	134
<i>Figure 50: Flow function of particle size fractions of sodium chloride</i>	135
<i>Figure 51: Flow function of six grades of glass beads</i>	135
<i>Figure 52: Variation of the bulk strength as a function of the particle size for six grades of lactose</i>	136
<i>Figure 53: Variation of the bulk density as a function of the particle size for six grades of lactose</i>	136
<i>Figure 54: Bulk strength of grades of glass beads blended with de-ionised water</i> ...	138
<i>Figure 55: Bulk strength of grades of glass beads blended with Miglyol oil 818</i>	138
<i>Figure 56: Bulk strength glass beads, crushed glass and sodium chloride blended with Miglyol oil 818</i>	139
<i>Figure 57: Bulk strength of glass beads blended with olive oil, Miglyol oil 818 and Miglyol oil 829</i>	139
<i>Figure 58: Flow function of three grades of lactose</i>	141
<i>Figure 59: Flow function of trinary blends of lactose</i>	141
<i>Figure 60: Flow function of five powders</i>	142

<i>Figure 61: Flow function of blends with five ingredients.....</i>	<i>142</i>
<i>Figure 62: Bulk strength of binary blends made with glass beads.....</i>	<i>143</i>
<i>Figure 63: : Voidage of binary blends made with glass beads.....</i>	<i>144</i>
<i>Figure 64: Bulk strength of a binary blend (glass beads D50 = 33 μm and sodium chloride D50 = 212 μm) and its individual components mixed with Miglyol oil 818 ..</i>	<i>145</i>
<i>Figure 65: Bulk strength of a binary blend (glass beads D50 = 63 μm and sodium chloride D50 = 212 μm) and its individual components mixed with Miglyol oil 818 ..</i>	<i>146</i>
<i>Figure 66: Bulk strength of a binary blend with two grades of glass beads and its individual components mixed with Miglyol oil 818.....</i>	<i>146</i>
<i>Figure 67: Bulk strength of a binary blend (glass beads D50 = 212 μm and sodium chloride D50 = 212 μm) and its individual components mixed with Miglyol oil 818 ..</i>	<i>147</i>
<i>Figure 68: Bulk strength of binary blend (crushed glass D50 = 212 μm and sodium chloride D50 = 212 μm) and its individual components mixed with Miglyol oil 818 ..</i>	<i>147</i>
<i>Figure 69: Bulk strength of binary blend (glass beads D50 = 212 μm and crushed glass D50 = 212 μm) and its individual components mixed with Miglyol oil 818 ..</i>	<i>148</i>
<i>Figure 70: Saturation of silicon dioxide adding Miglyol oil 818.....</i>	<i>149</i>
<i>Figure 71: Saturation of tricalcium phosphate adding Miglyol oil 818.....</i>	<i>150</i>
<i>Figure 72: Saturation of magnesium carbonate adding Miglyol oil 818.....</i>	<i>150</i>
<i>Figure 73: Bulk strength of wet maltodextrin as a function of the %wt of the free flow additives for three different free flow additives.....</i>	<i>152</i>
<i>Figure 74: Bulk strength of wet lactose as a function of the %wt of flow agents for three different free flow additives.....</i>	<i>152</i>
<i>Figure 75: Bulk strength of dry lactose as a function of the %wt of flow agents for three different free flow additives.....</i>	<i>153</i>
<i>Figure 76: Bulk strength of dry maltodextrin as a function of the %wt of the free flow additives for three different free flow additives.....</i>	<i>153</i>
<i>Figure 77: Bulk strength of wet glass beads as a function of the %wt of the free flow additives for different levels of oil content.....</i>	<i>154</i>
<i>Figure 78: Bulk strength of wet glass beads as a function of the %wt of the free flow additives for different levels of oil content.....</i>	<i>154</i>
<i>Figure 79: Bulk strength of a full blended flavour as a function of the %wt of the free flow additives for two types of flow agents.....</i>	<i>155</i>
<i>Figure 80: Bulk strength of wet glass beads as a function of the %wt of the free flow additives for two types of flow agents.....</i>	<i>155</i>

<i>Figure 81: Comparison of measured and predicted values of voidage for six grades of lactose</i>	161
<i>Figure 82: Comparison of measured and predicted values of voidage for size fractions of sodium chloride</i>	161
<i>Figure 83: Comparison of measured and predicted values of voidage for size fractions of dextrose</i>	162
<i>Figure 84: Comparison of measured and predicted values of voidage for six grades of glass beads</i>	162
<i>Figure 85: Comparison of measured and predicted values of voidage for size fractions of maltodextrin</i>	163
<i>Figure 86: Comparison of measured and predicted values of bulk strength for six fractions of glass beads</i>	164
<i>Figure 87: Comparison of measured and predicted values of bulk strength for six fractions of lactose</i>	164
<i>Figure 88: Comparison of measured and predicted values of bulk strength for size fractions of dextrose</i>	165
<i>Figure 89: Comparison of measured and predicted values of bulk strength for size fractions of maltodextrin</i>	165
<i>Figure 90: Comparison of measured and predicted values of bulk strength for size fractions of sodium chloride</i>	166
<i>Figure 91: Experimental voidage of glass beads mixed with Miglyol oil 818 at 9 kPa of consolidation stress</i>	170
<i>Figure 92: Experimental voidage of glass beads mixed with de-ionised water at 9 kPa of consolidation stress</i>	171
<i>Figure 93: Range of Rumpf model application for wet powders</i>	173
<i>Figure 94: Range of Rumpf model application for size fractions of glass beads mixed with de-ionised water</i>	173
<i>Figure 95: Range of Rumpf model application for size fractions of glass beads mixed with Miglyol oil 818</i>	174
<i>Figure 96: Range of Rumpf model application for saturation of size fractions of glass beads mixed with Miglyol oil 818</i>	174
<i>Figure 97: Range of Rumpf model application for saturation of size fractions of glass beads mixed with de-ionised water</i>	175
<i>Figure 98: Factor of calibration for glass beads mixed with Miglyol oil 818</i>	177

<i>Figure 99: Factor of calibration for glass beads mixed with de-ionised water</i>	177
<i>Figure 100: Comparison of the predicted, measured and calibrated bulk strength of wet glass beads $D_{50} = 33 \mu\text{m}$</i>	178
<i>Figure 101: Comparison of the predicted, measured and calibrated bulk strength of wet glass beads $D_{50} = 33 \mu\text{m}$</i>	178
<i>Figure 102: Measured and predicted flow function for maltodextrin</i>	182
<i>Figure 103: Measured and predicted flow function for sodium chloride</i>	183
<i>Figure 104: Measured and predicted flow function for dextrose</i>	183
<i>Figure 105: Measured and predicted flow function for blended lactose 15:15:70</i>	185
<i>Figure 106: Measured and predicted flow function for blended lactose 25:25:50</i>	185
<i>Figure 107: Measured and predicted flow function for blended lactose 33:33:33</i>	186
<i>Figure 108: Measured and predicted flow function for blended lactose 70:15:15</i>	186
<i>Figure 109: Measured and predicted flow function for blended lactose dextrose 10:90</i>	188
<i>Figure 110: Measured and predicted flow function for blended lactose dextrose 20:80</i>	189
<i>Figure 111: Measured and predicted flow function for blended lactose dextrose 30:70</i>	189
<i>Figure 112: Measured and predicted flow function for blended lactose dextrose 50:50</i>	190
<i>Figure 113: Measured and predicted flow function for blended powder 10:10:10:35:35</i>	190
<i>Figure 114: Measured and predicted flow function for blended powder 20:20:20:20:20</i>	191
<i>Figure 115: Measured and predicted flow function for blended powder 35:35:10:10:10</i>	191
<i>Figure 116: Comparison of the predicted and measured values of inverse flow factor ratio for lactose at 0.6 kPa</i>	200
<i>Figure 117: Comparison of the predicted and measured values of inverse flow factor ratio for lactose at 1.2 kPa</i>	200
<i>Figure 118: Comparison of the predicted and measured values of inverse flow factor ratio for lactose at 2.4 kPa</i>	201
<i>Figure 119: Comparison of the predicted and measured values of inverse flow factor ratio for lactose at 4.8 kPa</i>	201

<i>Figure 120: Comparison of the predicted and measured values of inverse flow factor ratio for lactose at 9 kPa.....</i>	<i>202</i>
<i>Figure 121: Comparison of the predicted and measured values of inverse flow factor ratio for lactose at 10 kPa.....</i>	<i>202</i>
<i>Figure 122: Measured flow function values of six grades of lactose.....</i>	<i>203</i>
<i>Figure 123: Predicted flow function values of six grades of lactose.....</i>	<i>203</i>
<i>Figure 124: Predicted flow function values of a grade of lactose $D_{50} = 4 \mu\text{m}$.....</i>	<i>204</i>
<i>Figure 125: Predicted flow function values of a grade of lactose $D_{50} = 9 \mu\text{m}$.....</i>	<i>204</i>
<i>Figure 126: Predicted flow function values of a grade of lactose $D_{50} = 32 \mu\text{m}$.....</i>	<i>205</i>
<i>Figure 127: Predicted flow function values of a grade of lactose $D_{50} = 70 \mu\text{m}$.....</i>	<i>205</i>
<i>Figure 128: Predicted flow function values of a grade of lactose $D_{50} = 96 \mu\text{m}$.....</i>	<i>206</i>
<i>Figure 129: Predicted flow function values of a grade of lactose $D_{50} = 100 \mu\text{m}$.....</i>	<i>206</i>
<i>Figure 130: Values of the parameter C of the empirical model for dry single powders developed in the research.....</i>	<i>207</i>
<i>Figure 131: Values of the parameter C of the empirical model for dry single powders developed in the research.....</i>	<i>208</i>
<i>Figure 132: Value of the parameter A of the empirical model for wet powders in funicular and capillary states for de-ionised water and Miglyol oil 818.....</i>	<i>211</i>
<i>Figure 133: Comparison of the measured an predicted values of the bulk strength of glass beads $D_{50} = 212 \mu\text{m}$ mixed with Miglyol oil 818.....</i>	<i>212</i>
<i>Figure 134: Comparison of the measured an predicted values of the bulk strength of glass beads $D_{50} = 212 \mu\text{m}$ mixed with de-ionised water.....</i>	<i>212</i>
<i>Figure 135: Comparison of the measured an predicted values of the bulk strength of glass beads $D_{50} = 112 \mu\text{m}$ mixed with Miglyol oil 818.....</i>	<i>213</i>
<i>Figure 136: Comparison of the measured an predicted values of the bulk strength of glass beads $D_{50} = 112 \mu\text{m}$ mixed with de-ionised water.....</i>	<i>213</i>
<i>Figure 137: Comparison of the measured an predicted values of the bulk strength of glass beads $D_{50} = 63 \mu\text{m}$ mixed with Miglyol oil 818.....</i>	<i>214</i>
<i>Figure 138: Comparison of the measured an predicted values of the bulk strength of glass beads $D_{50} = 63 \mu\text{m}$ mixed with de-ionised water.....</i>	<i>214</i>
<i>Figure 139: Comparison of the measured an predicted values of the bulk strength of glass beads $D_{50} = 45 \mu\text{m}$ mixed with Miglyol oil 818.....</i>	<i>215</i>
<i>Figure 140: Comparison of the measured an predicted values of the bulk strength of glass beads $D_{50} = 33 \mu\text{m}$ mixed with Miglyol oil 818.....</i>	<i>215</i>

<i>Figure 141: Comparison of the measured and predicted values of the bulk strength of glass beads $D_{50} = 33 \mu\text{m}$ mixed with de-ionised water</i>	216
<i>Figure 142: Predicted and measured flow function of lactose $D_{50} = 96 \mu\text{m}$ with 2.5%wt of Miglyol oil 818</i>	219
<i>Figure 143: Predicted and measured flow function of maltodextrin $D_{50} = 70 \mu\text{m}$ with 2.5%wt of Miglyol oil 818</i>	219
<i>Figure 144: Schematic representation of the model developed in this research for the prediction of the effect of flow agents on wet powders</i>	222
<i>Figure 145: Measured and predicted effect of the free flow additives on lactose 2.5%wt with 1%wt silica</i>	224
<i>Figure 146: Measured and predicted effect of the free flow additives on lactose 2.5%wt with 2%wt silica</i>	224
<i>Figure 147: Measured and predicted effect of the free flow additives on lactose 2.5%wt with 3%wt silica</i>	225
<i>Figure 148: Measured and predicted effect of the free flow additives on lactose 2.5%wt with 4%wt silica</i>	225
<i>Figure 149: Measured and predicted effect of the free flow additives on lactose 2.5%wt with 5%wt silica</i>	226
<i>Figure 150: Measured and predicted effect of the free flow additives on maltodextrin 2.5%wt with 1%wt silica</i>	226
<i>Figure 151: Measured and predicted effect of the free flow additives on maltodextrin 2.5%wt with 2%wt silica</i>	227
<i>Figure 152: Measured and predicted effect of the free flow additives on maltodextrin 2.5%wt with 3%wt silica</i>	227
<i>Figure 153: Measured and predicted effect of the free flow additives on maltodextrin 2.5%wt with 4%wt silica</i>	228
<i>Figure 154: Measured and predicted effect of the free flow additives on maltodextrin 2.5%wt with 5%wt silica</i>	228
<i>Figure 155: Measured and predicted values of the flow function of a dry blended powder</i>	230
<i>Figure 156: Measured values of the flow function of a blended powder at different conditions</i>	231
<i>Figure 157: Predicted values of the flow function of a blended powder at different conditions</i>	231

<i>Figure 158: Predicted values of the flow function of a blended powder at different conditions</i>	<i>232</i>
<i>Figure 159: Interface of the Virtual Powder Blending Laboratory</i>	<i>237</i>
<i>Figure 160: Interface of the data base in the Virtual Powder Blending Laboratory ..</i>	<i>240</i>
<i>Figure 161: Interface of the data base in the Virtual Powder Blending Laboratory ..</i>	<i>240</i>
<i>Figure 162: Interface of the data base in the Virtual Powder Blending Laboratory ..</i>	<i>241</i>

TABLES

<i>Table 1: Established models for normalised coordination numbers.....</i>	29
<i>Table 2: Size ratios required for different coordination numbers</i>	33
<i>Table 3: Interparticles forces and the mechanisms associated to these forces.....</i>	33
<i>Table 4: Particulate materials characterised with laser diffraction and mechanical sieving techniques</i>	62
<i>Table 5: Test conditions of the laser diffraction and mechanical sieving techniques .</i>	62
<i>Table 6: Test conditions of the Ultrapyc 1200e Pycnometer technique.....</i>	64
<i>Table 7: Test conditions of the scanning electron microscope technique.....</i>	65
<i>Table 8: Test conditions of the Brookfield powder flow tester technique.....</i>	67
<i>Table 9: Test conditions of the LV DV3 Ultra rheometer.....</i>	69
<i>Table 10: Particle properties of 6 grades of lactose.....</i>	71
<i>Table 11: Particle properties of different whey powders</i>	71
<i>Table 12: Particle properties of different maltodextrin powders.....</i>	72
<i>Table 13: Particle properties of different fillers.....</i>	72
<i>Table 14: Particle properties of idealised powders.....</i>	73
<i>Table 15: Particle properties of 6 grades of glass beads.....</i>	73
<i>Table 16: Particle properties of different flow agents.....</i>	74
<i>Table 17: SEM images of particulate materials</i>	75
<i>Table 18: SEM images of free flow additives.....</i>	77
<i>Table 19: Bulk flow properties of six grades of lactose</i>	87
<i>Table 20: Bulk flow properties of different whey powders.....</i>	87
<i>Table 21: Bulk flow properties of different maltodextrin powders</i>	88
<i>Table 22: Bulk flow properties of different fillers.....</i>	88
<i>Table 23: Bulk flow properties of idealised particulate materials</i>	89
<i>Table 24: Bulk flow properties of six grades of glass beads.....</i>	89
<i>Table 25: Bulk flow properties of different flow agents.....</i>	90
<i>Table 26: Liquid characterisation of different liquids.....</i>	91
<i>Table 27: Range of experimental investigations undertaken in the research.....</i>	102
<i>Table 28: Range of tests undertaken to study the effect of particle size and levels of oil content with different free flow additives on the reformulated Flame Grilled Steak..</i>	125
<i>Table 29: Dust emissions of full blended powders made with 2.4%wt TCP.....</i>	126
<i>Table 30: Dust emissions of full blended powders made with 1.2%wt silica</i>	127

<i>Table 31: Dust emissions of full blended flavours made with coarse fillers</i>	129
<i>Table 32: Dust emissions of full blended flavours made with fine fillers</i>	130
<i>Table 33: Dust emissions of the trial blends of the reformulated full blended flavour</i>	132
<i>Table 34: Estimated values of Hamaker constant, separation distance (Seville et al. 2000 & Li et al. 2006) and factor of proportionality powders tested</i>	159
<i>Table 35: Average factor of proportionality of glass beads mixed with Miglyol oil 818 at pendular state</i>	168
<i>Table 36: Average factor of proportionality of glass beads mixed with de-ionised water at pendular state</i>	169
<i>Table 37: Average voidage of glass beads mixed with Miglyol oil 818 at 9 kPa of consolidation stress</i>	171
<i>Table 38: Average voidage of glass beads mixed with de-ionised water at 9 kPa of consolidation stress</i>	172
<i>Table 39: Dimensionless factor of calibration for glass beads mixed with Miglyol oil 818 at pendular state at different levels of consolidation stress</i>	176
<i>Table 40: Dimensionless factor of calibration for glass beads mixed with de-ionised water at pendular state at different levels of consolidation stress</i>	176
<i>Table 41: Deviation of the measured and predicted flow function for maltodextrin, sodium chloride and dextrose</i>	184
<i>Table 42: Deviation of the measured and predicted flow function for maltodextrin, sodium chloride and dextrose</i>	184
<i>Table 43: Deviation of the measured and predicted flow function for blended lactose</i>	187
<i>Table 44: Deviation of the measured and predicted flow function for blended lactose</i>	187
<i>Table 45: Deviation of the measured and predicted flow function for blended lactose dextrose</i>	192
<i>Table 46: Deviation of the measured and predicted flow function for blended lactose dextrose</i>	192
<i>Table 47: Deviation of the measured and predicted flow function for blended powder</i>	193
<i>Table 48: Deviation of the measured and predicted flow function for blended powder</i>	193

<i>Table 49: Values of the parameters KC and KD of the empirical model for wet powders developed in this research</i>	<i>209</i>
<i>Table 50: Value of the parameter A of the empirical model for wet powders in funicular and capillary states.....</i>	<i>210</i>
<i>Table 51: Values of the constant tau of the empirical model developed in this research</i>	<i>218</i>
<i>Table 52: Values of the oil capacity and efficacy factor for silicon dioxide and tricalcium phosphate</i>	<i>221</i>

NOMENCLATURE

A	Hamaker constant which is related to material properties
m	The slope of the failure locus called coefficient of internal friction
T	The apparent tensile strength
c	The cohesion of the powders
s	The separation distance between particles
R	The radius of the spherical particles
d	The diameter of the spherical particles; the diameter of the guest particles
ϵ	The void fraction; the dry based void fraction
r	The asperity radius assuming particles have a spherical profile
H	The bonding force at point of contact
k	The mean coordination number
v	The volume of the bridge for a single sphere around the contact area between two spheres
α	The surface tension of the liquid
2h	The gap distance between the spheres
a	The radius of the spheres
D	The diameter of the host particles
Gwt%	The weight % of guest particles for 100% surface coverage

ϵ_0	The initial void fraction under gravity forces
ϵ_{\max}	The maximum achievable void fraction
M_{cri}	The critical liquid content to give ϵ_{\max}
M	The liquid content in mass basis
ρ_p	The particle density
μ_v	The liquid viscosity
σ_T	The mean theoretical tensile strength
ρ_l	The liquid density
Pd(%wt)	The weight percentage of liquid in the powder
GB(%wt)	The equivalent weight percentage of liquid in glass beads
KC	A parameter of a model which value varies with the type of liquid being 52 for Miglyol oil and 29 for de-ionised water
KD	A parameter of a model which value varies with the type of liquid being 2 for Miglyol oil and 4.5 for de-ionised water
σ_{CW}	The predicted bulk strength at 9 kPa of consolidation stress
σ_{cp}	The predicted bulk strength at the consolidation stress selected σ_{1p}
σ_{cmax}	The bulk strength at 9 kPa of consolidation stress
σ_{1p}	The consolidated stress to predict the bulk strength
ρ_{GB}	The particle density of glass beads

Chapter 1 Background

1.1 Introduction

The drive for the current project came from the launch of the Brookfield Powder Flow Tester in 2010. This device was developed at The Wolfson Centre for Bulk Solids Handling Technology, University of Greenwich, through a DEFRA sponsored project in collaboration with the food industry. This Powder Flow Tester (PFT) allows industrial users to quickly and accurately measure the flow properties of their materials for a range of purposes from bench marking and quality control to assisting reformulation. Now in a position to measure the flow properties using PFT, the industrial sponsors' next question was "What can be done to modify the flow properties if the material is judged to be too free flowing or too cohesive".

This thesis describes a programme of work undertaken with industrial sponsors from the food industry to further understanding of how to control or modify the flow properties of blended powders. The drive for this from an industrial perspective is that processing efficiency is often compromised by undesirable flow behaviour of materials that are too free flowing resulting in uncontrolled flow of material through feeders or control valves causing flooding problems and spillage; or too cohesive or 'sticky' so that they do not flow from storage when required and build-up on conveyors rather than being transported. Such flow problems affect production in all industries which use powders and cause significant losses, reducing productivity and increasing the cost of the final product (Peschl et al. 2001).

Controlling the flow behaviour of the powders would allow industry to use their existing silos and hoppers more effectively, avoiding the high cost of replacing equipment that will not discharge cohesive powders. For a powder producer, it may be a competitive advantage to offer his customers a powder that flows with fewer problems than a competitor's product. In the pharmaceutical industries, it has in recent years become common to use formulations that are cohesive rather than free flowing, in order to reduce segregation of blend components in handling; but if the blends are too cohesive, problems of poor flow arise in manufacturing instead. Thus the background for this project is the industrial need for a technique that can be used to help formulators of blended materials to quickly and economically come up with a material that flows

acceptably. The following section gives an overview of how storage vessels work and the common operational problems.

1.2 Common flow issues in industrial processes

Silos, hoppers, vessels, chutes, feeders and pneumatic conveying systems are commonly used to store and transport tonnes of powders each year. Applications range from large scale manufacturing processes handling 1000s tonnes of product per hour, to small plant handling systems dosing minor ingredients at kilograms per hour. Industries have been handling bulk solids for many years and suffering the same common flow problems such as erratic flow, or no flow, due to arching or rat-holing of cohesive materials or dust and segregation issues for free-flowing materials.

Jenike established in the 1960's (Jenike et al. 1961 & 1964) a procedure for designing solids handling equipment (hoppers, silos, bins and bunkers) for reliable gravity flow based on measured flow properties of the powders. To develop this method, Jenike first considered the discharge patterns developed in the hopper when the material was flowing and secondly the forms of the flow obstruction when it ceased.

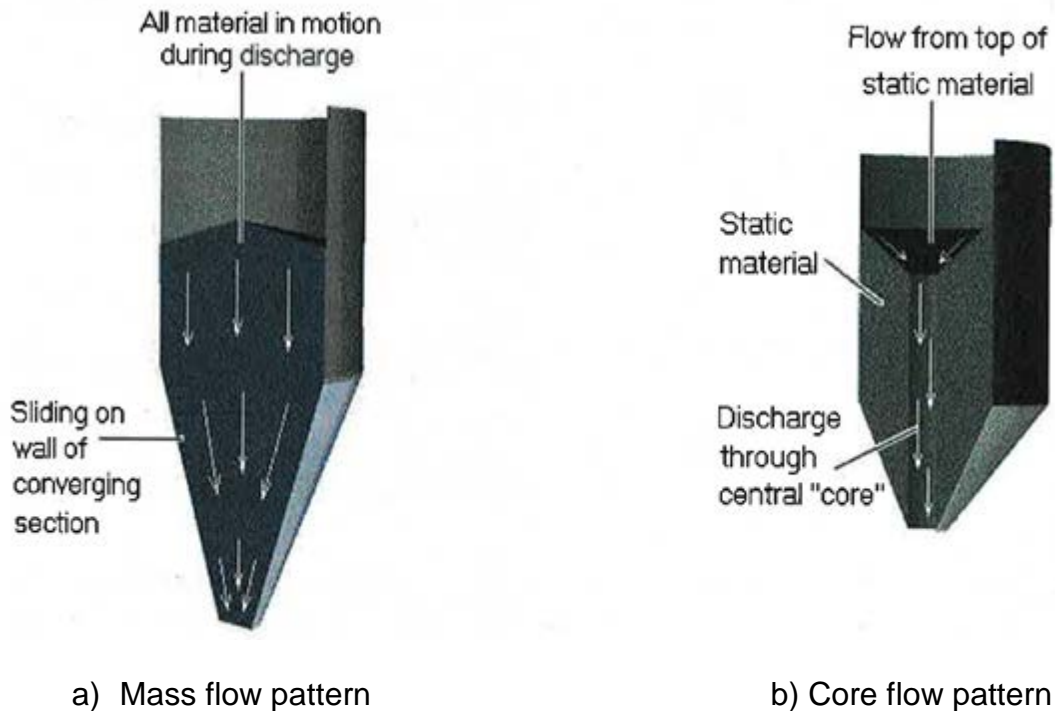


Figure 1: The basic flow patterns defined by Jenike et al. a) Mass flow and b) Core flow (The Wolfson Centre for Bulk Solids Handling Technology, University of Greenwich, England)

Two basic flow patterns were defined by Jenike: mass flow and core flow (or funnel flow) as shown in figure 1a & 1b respectively. In the case of mass flow, the entire bulk solid is in motion at every point of the bin whenever the material is discharged from the outlet. This regime gives a first-in first-out (FIFO) discharge but requires a converging section with walls that are sufficiently steep and smooth to allow material flow at the wall.

Core or funnel flow occurs when the material flows through the outlet in a channel formed within the bulk solid itself. The material around the wall is stationary and new material is fed into the flow channel from the top free surface which forms a drain down angle of repose. This gives a first-in last-out (FILO) discharge regime.

For the flow obstructions, the most trivial case is that of a mechanical obstruction. This occurs when the maximum particle size is large relative to the size of the hopper outlet. If several large particles flow through the hopper together, they can interlock and form a mechanical bridge across the outlet and prevent gravity discharge. To prevent this,

experience has shown that the minimum diameter of the outlet must be at least 8-10 times the length of the largest size normally handled.

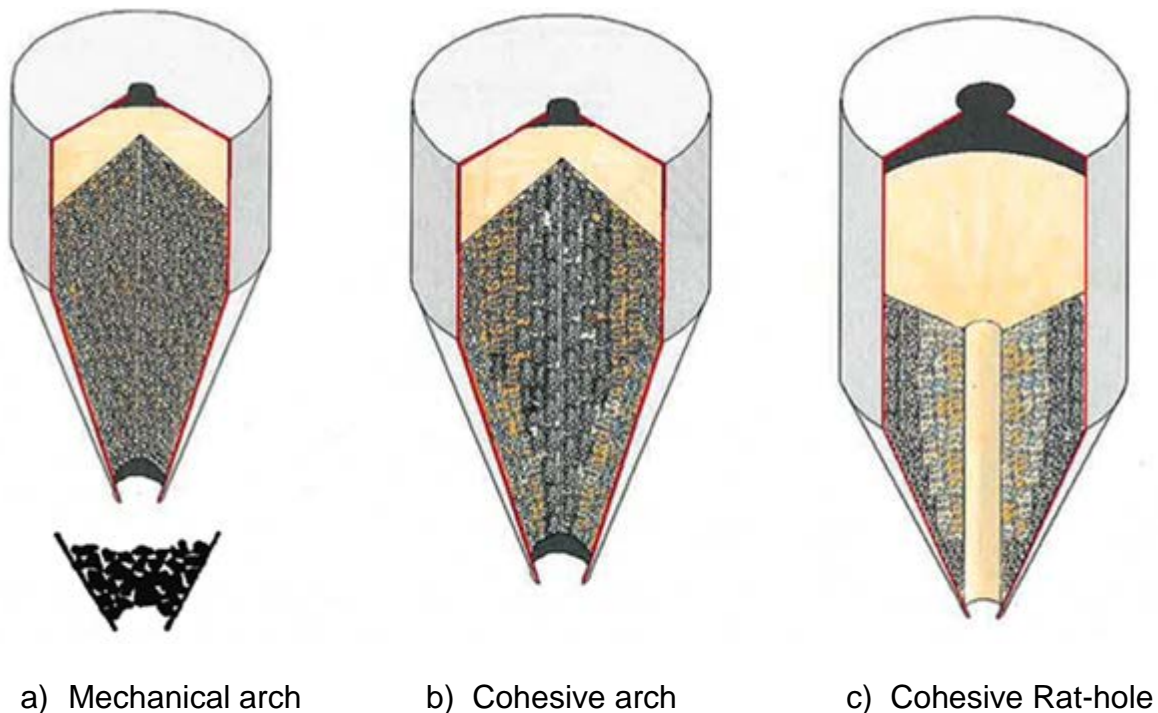


Figure 2: The three principal types of obstruction to flow a) Mechanical arch, b) Cohesive arch & c) Cohesive rat-hole (The Wolfson Centre for Bulk Solids Handling Technology, University of Greenwich, England)

The more complex problem that is to be considered here is that of cohesive strength occurring as the particle size reduces to below approximately 100 microns or in the presence of surface moisture. There are principally two different flow obstructions that can occur: cohesive arch and cohesive rat-hole as shown in figure 1b and 1c respectively. Cohesive arching is the flow limiting condition in a mass flow vessel and is formed due to the strength acquired by the powder because of its consolidation during storage. While arching can occur in a core flow bin, it is not the flow limitation condition. As the outlet is increased, the arch will increase in height until it breaks through to the top free surface forming a rat-hole. Rat-holing is characterised by a flow channel above the outlet discharge and leaves a stationary internal structure. This flow obstruction is the flow limiting condition in a core flow silo.

Segregation is defined as the demixing of a homogeneous mixture by differences in size, density or shape (Williams et al. 1976 & Bridgwater et al. 1985). Wide size distributions with a large difference in particle size have a high propensity for size

segregation. Powders which are too free flowing may segregate and generate dust causing problems such as flowing uncontrollably through the small clearances in dosing equipment.

There are two principal mechanisms of segregation: rolling (surface effect) and air induced. Rolling segregation occurs when material has a wide size distribution or a large difference in particle size between components. When the material is loaded into a vessel under gravity, the material forms a heap (angle of repose of the material). Larger particles have more momentum and larger radius (giving less resistance to rolling on the rough surface of the heap) so they roll further down the heap whereas the fines tend to remain where they land. This leads to a radial segregation pattern as shown in figure 3, where fines accumulate in the centre and the coarse around the wall. When the vessel discharges, if it operates in core-flow, the high concentration of fines in the centre of the vessel discharges first while the predominantly coarse material around the walls comes out last. This segregation pattern is illustrated in figure 4 which presents variation in the different size fractions through the complete discharge cycle of a core flow silo. Note that it has been stated that below 100 μ m particle size, the tendency of surface segregation is very low because material becomes cohesive (Williams et al. 1976 & Parsons et al. 1976).

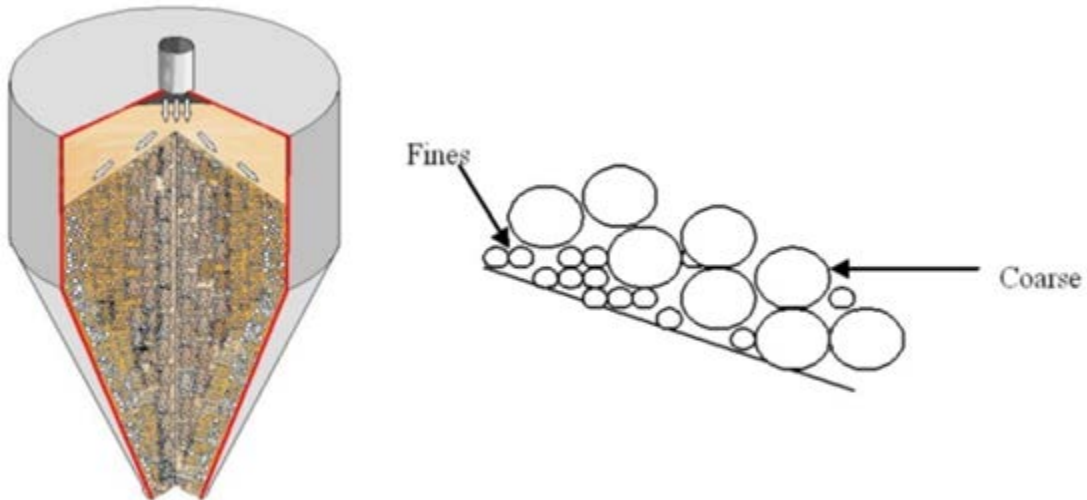


Figure 3: Effect of rolling segregation during the process of filling a silo (The Wolfson Centre for Bulk Solids Handling Technology, University of Greenwich, England)

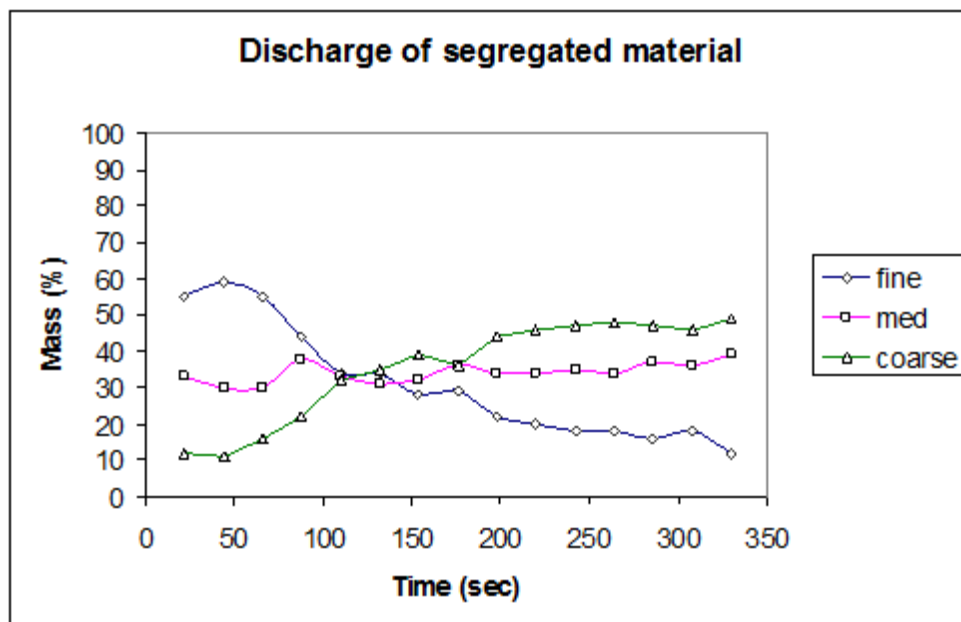


Figure 4: Variation of the particle size fraction within discharge stream as a function time, through the complete discharge cycle from a core flow vessel (The Wolfson Centre for Bulk Solids Handling Technology, University of Greenwich, England) For full explanation refer to the text

Air induced segregation occurs when material enters a confined space (silo chute) at high velocity; either through a pneumatic conveying system or following gravity free fall from a great height. Here the air displaced by the flow stream separates the fine

particles typically those below 50 microns which remain suspended as a dust cloud from the larger heavy particles that settle quickly. When these particles settle out, a layer on the top of accumulated particles is formed; over a number of filling cycles this generates stratified layers of fine particles. Figure 5 and 6 show the effect of radial segregation arising from tangential pneumatic filling and lateral segregation arising from perpendicular pneumatic filling respectively.

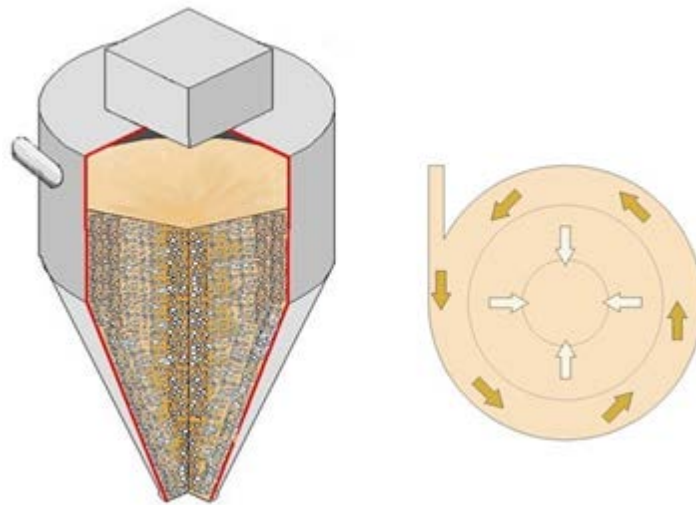


Figure 5: Effect of radial segregation arising from tangential pneumatic filling of a silo (The Wolfson Centre for Bulk Solids Handling Technology, University of Greenwich, England)

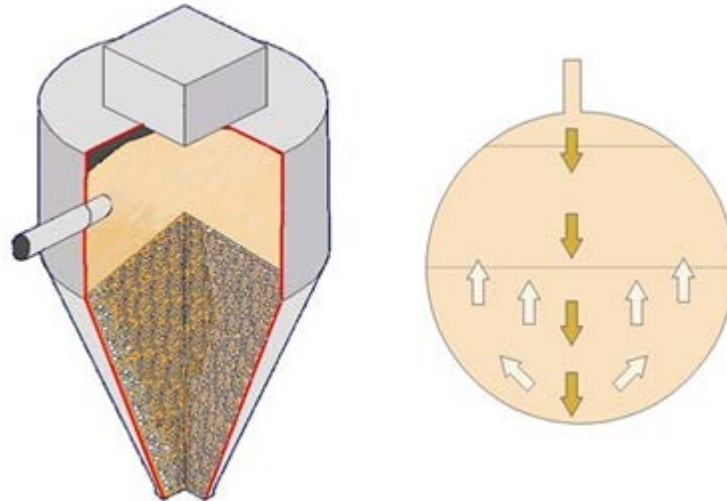


Figure 6: Effect of lateral segregation arising from perpendicular pneumatic filling of a silo (The Wolfson Centre for Bulk Solids Handling Technology, University of Greenwich, England)

1.3 Problems in the blended food powder industry

The above hopper flow issues and dust problems with materials are commonplace in the manufacturing and food industries, and cause significant stoppages and losses of production in many plants that handles powders.

Many food powders are “engineered”, i.e. made from mixtures of materials blended or co-processed to meet specified performance criteria, e.g. taste, texture, nutritional values etc., and their manufacturing processes can be controlled to adjust these parameters.

The flow properties can also be modified to suit the manufacturing process, but historically this has not been subject to much quantitative or qualitative study. There is a general lack of knowledge of how to select the best ingredients and additives to use to adjust the flow properties, or how much should be needed to obtain a given degree of flow property modification.

The flow behaviour of “engineered” powders affects the consistency of addition level and hence consistency of colour, texture and strength of aroma and flavour of the finished food product; poor flow causes irregular dosing, leading to variation between individual items or portions.

With powders applied by adhesion to snacks, the flow properties interact with their adhesion properties, e.g. when the powder is too free flowing:

- The blend components can segregate during handling leading variations in the taste, colour, etc.
- The flavour becomes dusty providing unpleasant working conditions, particularly if the material is spicy and loss of product.

When the powder is too cohesive, the flavour particles tend to stick together and cannot be dispersed evenly over the surface of the snack. Also, material tends to build-up on the feed chutes and in hoppers leading to flow problems such as cohesive arching and “rat-holing” causing a loss of product during industrial processes.

1.4 Current practice for new or modified blended powders

Addition of new ingredients to engineered food powders has been always a problem for powder industry. Historically, a bag test was undertaken where the material was shaken in a transparent bag and observed making a judgment based on whether it was dusty or sticky.

Nowadays, the blends are evaluated initially based on sensory factors such as the taste, aroma, colour and texture. Then the flow properties and the level of dust are measured using a powder flow tester and a dustiness test-rig respectively; after that, these are compared with existing flavours that are known to flow acceptably through the manufacturing process with an acceptable dust level. If they are similar then a one tonne batch is then manufactured for pilot scale industrial trials to assess flow reliability.

If the flow is considered unacceptable because it is significantly more cohesive or significantly more free-flowing than the desired flowability, then a series of reformulations are undertaken at a lab scale in order to try to bring the flow properties into the required window so that pilot scale manufacturing trials can be undertaken. At present this is very much a trial and error process based on the prior experience of the formulator, using oil to increase cohesion if the powder is too free flowing or too dusty and “free flow” additives to improve flow if it is too cohesive. If these modifications do not work then changes in the base ingredients are made and the process is repeated.

On top of this there is also pressure from legislation to reduce ingredients such as salt and monosodium glutamate which tend to be free flowing, to be replaced with materials which are poorer flowing.

1.5 Aim of the research

The aim of the project was to develop a practical understanding for the blended food powder industry of how to control powder flowability; an “empirical understanding” of the links between the particle properties (and single particle bond strength) and bulk flow properties which would help formulators and process engineers to predict the bulk flow properties of their single materials, or blended powders based on changes to the particle properties or blend components.

The project was directed heavily to the food industry by virtual of the industrial sponsors and DEFRA funding but the findings of the research have also been intended to be used in other industry sectors with similar flow problems with powders, such as pharmaceuticals, ceramics and powder metallurgy.

1.6 Programme objectives

The following objectives were proposed for this research programme:

- 1) To calibrate analytical well-established models found in the literature linking the primary particles properties (and single particle bond strength) to the secondary bulk flow properties. These high level models are calibrated empirically using a limited number of bulk flow property tests considering simplifications for practical use by the industrial partners.
- 2) To evaluate the applicability of these calibrated models to design powder handling equipment and assess the flow behaviour of single powder ingredients or “engineered” food powders in industrial processes.
- 3) To identify methods or techniques that process engineers could use to predict the bulk flow properties of their single materials, or blended powders based on changes to the particles properties or blend components.

1.7 Contributions to Knowledge

This project claims the following contributions to knowledge:

1. Understanding of the physics by which a variety of different additives to food powder blends act to modify their flow properties as a result of their interactions with commonly used ingredients.
2. Understanding the basics of how to select additional ingredients to give the best balance of controlled and desirable flow properties in industrial processes.

3. Development of new empirical particle to bulk scale models to predict the flow properties of single and blended particulate materials in dry and wet condition with and without free flow additives.
4. Development of a test protocol which in combination with the standard characterisation tests commonly used in the powder industry and the prediction tool called Virtual Powder Blending Laboratory (recently developed by The Wolfson Centre for Bulk Solids Handling Technology) will help formulators and process engineers to formulate the composition of blended powders with the desirable flow behaviour in industrial process lines.

1.8 Project preview

This thesis is structured as follows:

Chapter 2 presents a broad survey of the literature relating to particle properties (size, shape and texture), bulk solids properties (size and shape distribution, flow and packing properties) and analytical models linking particle scale to bulk scale considering packing structure, interparticle forces, liquid bridges and effect of free flow additives.

Chapter 3 presents the tests undertaken to characterise the powders at particle and bulk scale and the liquids used in this research.

Chapter 4 describes the methodology applied in the research and details of the experimental work in this investigation to develop an empirical understanding of the links between the particle and bulk flow properties of particulate materials.

Chapter 5 describes the calibration of the well-established analytical models found in the literature linking the particle properties to bulk scale behaviour.

Chapter 6 presents and discusses the results obtained from the experimental work undertaken at The Wolfson Centre and the industrial partners' plants and laboratories.

Chapter 7 presents the evaluation of the analytical models calibrated empirically and the discussion of the results obtained.

Chapter 8 presents the new empirical models developed in this research to predict the bulk flow properties of single and blended powders in wet and dry condition with or without free flow additives.

Chapter 9 presents the test protocol developed in this research work to predict and optimised the flow behaviour of blended powders.

Chapter 10 presents the conclusions of this research program and the further work proposed to advance the findings from this investigation.

Chapter 2 Literature Review

2.1 Introduction

Before commencing the review of the literature it is first useful to outline the key system variables considered in the model as listed below. These variables have been broken down into particle level, bulk level and agglomerate level as presented in figure 7. At agglomerate level, it is considered that agglomerates have sufficient strength that they will not break down during processing conditions and can thus be treated as a conglomerate of particles. These different system variables at different scales provide the structure of the literature discussed below.

PARTICLE SYSTEM BROKEN DOWN INTO DIFFERENT LEVELS

PARTICLE SCALE	BULK SCALE
<i>Particle size</i>	<i>Size distribution</i>
<i>Particle shape</i>	<i>Shape distribution</i>
<i>Particle texture</i> (Surface roughness)	<i>Packing structure</i> (Voidage, particle contacts)
<i>Particle structure</i> (Solid or porous)	<i>Blend constituents</i> (Particle and material properties)
<i>Material properties</i> (Surface energy, density)	<i>Moisture content</i> (Concentration, liquid-solid interaction)
AGGLOMERATE SCALE	<i>Flow agent content</i> (Concentration, liquid interaction)
<i>Particle structure</i> (Stable under process conditions)	<i>Material properties</i> (Characteristic for blend ingredients)

Figure 7: System variables considered in the powder model.

2.2 *Particle property measurements*

The characterisation of the particulates has significance in many industries due to its influence on the behaviour of bulk solids. Particle size, shape, texture and structure have a huge impact on the optimisation of the industrial processes.

2.2.1 Particle size and distribution

There are a wide range of systems to measure the size of the particulate such as physical, optical and electromagnetic techniques. The selection of the measurement system depends on the purpose of the size obtained and the accuracy needed. Generally, a compromise has to be made in order to achieve the best measurement of the particle size within the context of the purpose of the measurement.

It is not usual to measure the size of a single particle because it does not represent the particle size distribution of the powder. Particle size distribution is defined as an indication of the proportion of the sizes of the particles present in the sample measured.

A range of particle sizes is divided into separate intervals and the amount of particles which exist in each interval is expressed in percentage values in a frequency distribution. Cumulative distribution is also presented showing the percentage of a specific size or below. The data of the particle size is presented as a histogram or as a continuous distribution curve.

A common approach to define the distribution width is to cite three values on the axis, the D_{10} , D_{50} and D_{90} . The D_{50} is defined as the diameter where half of the amount of particles lies below this value. 90% of the distribution lies below the D_{90} and 10% lies below D_{10} . It is essential to mention these values because if only D_{50} is considered, fine and coarse particles of the sample could be omitted from consideration leading to many flow problems such as segregation or stoppages.

Particles normally are irregular shapes and they are almost never a sphere or a cube. Commonly, the indirect definition of *the equivalent spherical diameter* is used because irregular particles have different dimensions and, therefore, the size is expressed as the diameter of the equivalent circle or sphere which contains the irregular shape of the particle (McGlinchey et al. 2005).

It means that, unless the particle shape is a sphere, the sizes of irregular shaped particles measured by different techniques are not comparable because the principle

of measurement differs. Therefore, when the size of a particle is stated, the method and conditions used in the measurements must be specified (McGlinchey et al. 2005).

Direct methods of measurement can include sieving and microscopy. Static or electron microscopes produce an image of the particles and a certain amount of information is provided. This technique requires direct observation of the particles and the method is simple, however, the sample analysed is often not representative. It may be possible to identify the shape of the particle and powder blends could be analysed. The size range goes from 1 μm to 800 μm for optical microscopes and 1 nm to 15000 nm for electron ones (McGlinchey et al. 2005).

Sieving is also a simple method which separates fine from coarse material by means of a perforated sieve. The powder sample is shaken through a series of sieves in decreasing aperture size. All mesh sizes are covered by international standards. Fragile particles require wet sieving and the formation of agglomerates is a drawback for fine particles. The size distribution is reported as the mass of retained particles on the sieve size used. The size range goes from 20 μm to 425 μm (McGlinchey et al. 2005).

Laser diffraction is another common technique to determine the particle size distribution of powders. This method measures the angular variation in intensity of light dispersed when a laser beam goes through a sample of a powder. Light is scattered at small angles for large particles and at large angles for small particles relative to the laser beam. The particle size is described as a volume equivalent sphere diameter (Malvern website).

Optical properties of the particles and the dispersant are required. The size range goes from 0.01 to 3500 μm . The main sources of error are the incorrect refractive index and the instrument misalignments.

Sedimentation method by gravity or centrifugal force is not commonly used to measure the particle size except in very fine particles. It is based on the transport phenomena of particles utilising Stokes' Law to correlate the particle size to the settling velocity. In gravitational methods, the particle size is determined from the settling velocity and the undersize fraction by changes on concentration in a settling suspension. Samples are collected from a sedimenting suspension at predetermined times. A centrifuge is commonly used to reduce the sedimentation time (Sympatec website).

From sedimentation data, size distributions can be calculated assuming that the particles sink freely in the suspension and a volume concentration below 0.2% is recommended. Adequate dispersion of the particles prior to a sedimentation analysis is sometimes difficult, and hence, dispersing agents may be necessary (Sympatec website). The size range goes from 10 to 1000 μm for gravitational method and 0.05 to 25 μm for centrifugal one (McGlinchey et al. 2005).

2.2.2 Particle density

Particle density of a single particle is the mass of the particle divided by the volume occupied by the particle considering the pores on its surface. The average particle density of powders can be calculated measuring the mass of a representative sample material and dividing it by the volume occupied by the particles not including the voids between them.

2.2.3 Particle shape

The measurement of the particle shape of the particles is not very common in industries due to the complexity of its standardisation. Recently, a review and new methods of characterisation and classification of the particle shape has been published in 2008 by Blott et al. highlighting a number of techniques of which the favour approach (Benn et al. 1993) is to draw a cuboid around the particle to determine the longest L, intermediate I and the shortest S dimensions. The three extremes of the particle shape as shown in figure 8 below are equant (spherical) particles where $L = I = S$, the platy (flaky) particles where $L = I > S$ and the elongate (fibrous) particle where $L > I = S$. The distinction between rounded and angular particles is determined by the angularity of the particle by comparing the radius of the corners with the maximum diameter of the particle. Sphericity is determined by comparing the surface area of a particle with the surface area of a sphere of the same volume. These measurements are considered a level of detail out of the scope of the research.

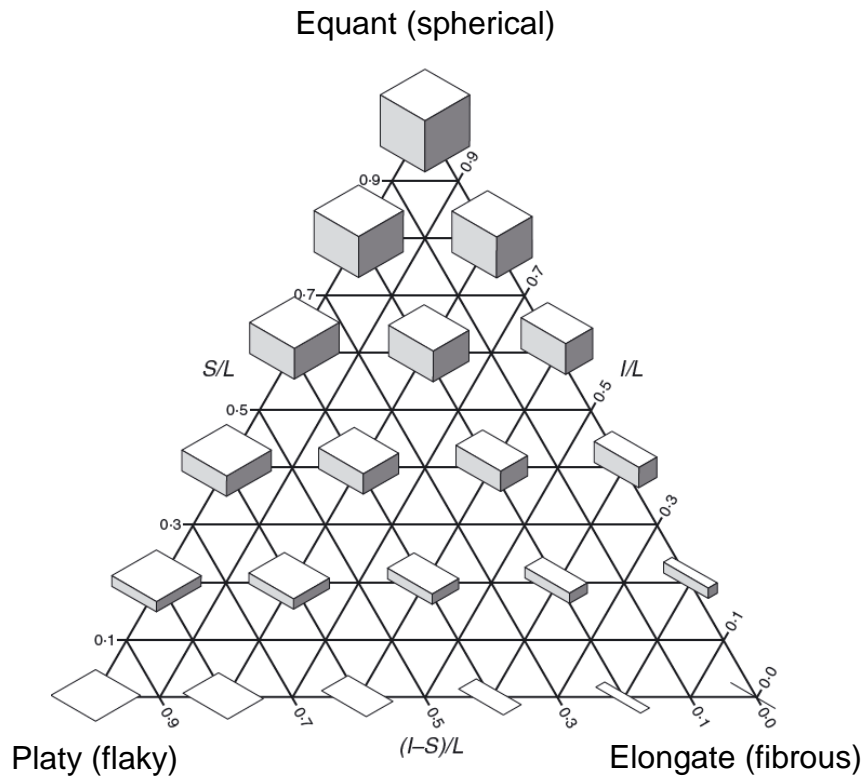


Figure 8: Characterisation of particle shapes (Benn et al. 1993)

Shape analysis compares the contour of irregular particles with well-known shapes like spheres or cubes for three-dimensional shape factors and circles or squares for two-dimensional shape factors. Then, the shape of the irregular particles is characterized based on simple methods like determination of the circularity and aspect ratio or sophisticated methods such as the use of Fourier analysis. To-date, no shape factor has been found applicable to all possible kind of shapes.

Researchers have been trying to find a better understanding of how to express the particle shape. Different classifications to define the shape of irregular particles have been proposed. To characterise this kind of particles, the average of length, breadth and thickness was commonly used; these values depend on the volume and the shape of the particles. For this reason, classifications based on roundness, angularity or sphericity were also proposed by many researchers.

In 1930's, Wadell et al. (1932, 1933 & 1935) published different articles highlighting the importance of considering the roundness and sphericity to classify the shape of irregular soil particles.

In 1937, Heywood et al. developed a three-dimensional shape factor assessing the irregular shapes of the particles. An expression of the volume shape factor was proposed regarding the length, the breadth and the thickness of the irregular particles. Two ratios were suggested: length to breadth (elongation shape factor) and breadth to thickness (flatness shape factor).

The three-dimensional shape factor appealed to many researchers in 1960's and was used to characterize powders. A drawback of the shape factor proposed was the fact that the more elongated the irregular particles are, the smaller breadth they have and, therefore, the elongation shape factor tends to infinity. Kaye, Clark and Liu (Kaye et al. 1992) tackled the issue and suggested that the shape factor would be the ratio of breadth or width to length (chunkiness shape factor), and then, the values of the new elongation shape factor proposed goes from zero to unit for very elongated particles.

2.2.4 Other particle properties

Particles properties such as surface area and pore size are important material characteristics in many processing applications, affecting the surface available to interact with surrounding fluids.

Sorption is a common method to measure the topography (surface area) and the internal structure (size and shape of pores) of an assembly of particles. Physical adsorption is a process in which a gas is brought into contact with a solid and part of it accumulates over the surface of the solid. It is a surface phenomenon between the adsorbate (molecules of liquid or gas) and the adsorbent (solid or liquid). Fine particles have large surface area and therefore act as good adsorbents.

2.3 *Bulk flow properties*

The internal friction of the powders is an important bulk flow property to be measured. Characteristic extreme values of the angle of internal friction for free flowing and very cohesive powders are 30° and 70° respectively, going through values in this range for easy-flowing and cohesive powders. The same tests used to measure the flow function flow property are the tests which measure the internal friction of the powders.

Bulk density was another important bulk flow property to be measured in this research work. Compression curves were used to study the changes of the bulk density in wet

blended powders at different levels of moisture content and dry multi component mixtures with different density ratios.

As mentioned in the introduction of the report, knowing the flow properties of a powder is necessary to design bulk solid handling equipment for reliable flow. The relationship between the consolidating stress and the strength generated by a solid is a characteristic property of bulk solids and its measurement is essential for hopper and silo designs.

The principle of this test is best illustrated by the uniaxial failure test or so-called “sand castle test” (see figure 9). Firstly, a quantity of the bulk solid is placed in a cylindrical mould with very low friction walls and cross sectional area A . Then the powder is consolidated under a load ($\sigma_1 A$) applied by a very low friction piston. After that, the consolidated cylinder of solid is removed from the mould and placed on a flat horizontal surface. An increasing compressive stress is applied to the consolidated sample; a stage will be reached where the powder collapses at certain load ($\sigma_c A$).

At the stress levels of interest for powder mechanics, during consolidation there is a reduction in the voidage due to the particle rearrangement. If the material has surface moisture at a level close to the point of saturation, then the reduction in voidage due to the consolidation may cause the material to exceed saturation and thus express excess moisture.

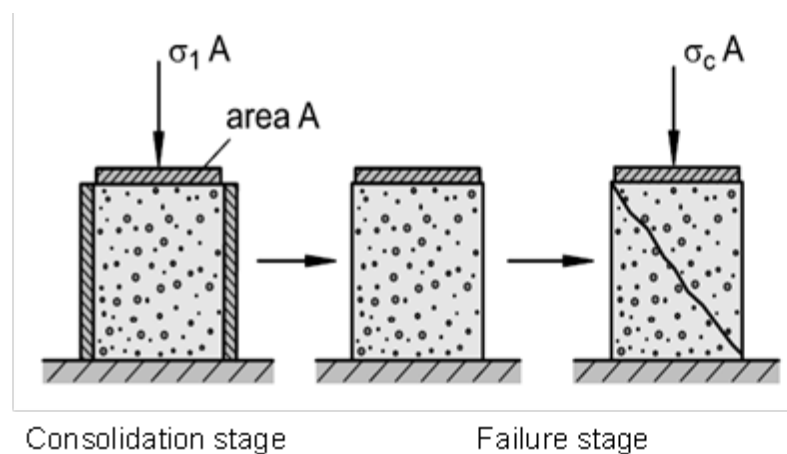


Figure 9: Stages of uniaxial consolidation test (Schulze, 2008)

This value of σ_c is called the compressive or unconfined failure strength corresponding to the consolidating stress σ_1 . If the compression test is repeated for several values of consolidating stress, for each value of σ_1 , a corresponding value of failure strength

σ_c will be obtained. If the compressive strength is plotted against the consolidating stress, the outcome is called the flow function of the material. Jenike et al. defined the flow factor ratio ff_c of consolidating stress to unconfined failure strength to characterise flowability numerically.

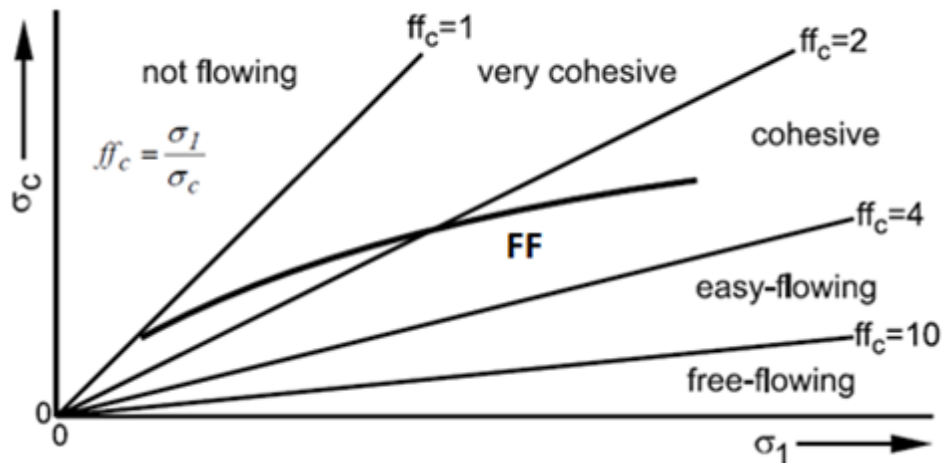


Figure 10: Instantaneous flow function (FF) and lines of flowability (Schulze, 2008)

For a given consolidating stress σ_1 , the strength gained varies from one powder to another. A free flowing material such as granular sugar has no strength and its flow function lies on the horizontal axis of the $\sigma_c - \sigma_1$ diagram as shown in figure 10. For more cohesive materials, the gradient of the lines of constant flowability increases.

While the “sand castle test” clearly illustrates the measurement principle, the direct (uniaxial) method of determining the flow properties explained above is not a very practical or reliable approach. For instance, the mould cannot be frictionless; it is very difficult to remove the consolidated cylinder of solid without causing a disturbance and also a uniform consolidation of the material is impossible to achieve with tall cylinders due to wall friction. Additionally, the test achieves poor repeatability due to variations in the precise position of the failure plane, and in the case of materials with moderate cohesiveness the self-weight of the powder above the failure plane contributes greatly to the failure, introducing a significant and rather variable error to the measurement.

For these reasons, it is more reliable to determine the flow function by indirect means using a shear tester. Another important bulk flow property to measure by shear testers are the bulk density (characterised as a compression curve) and the friction function,

which represents the internal friction between particles as a function of the consolidating stress.

2.3.1 Practical measurements of bulk flow properties

The application of any force to a powder tending to cause deformation by shear will result in an opposing resistive force. As the magnitude of the applied force increases, a point will be reached where the bulk solid begins to deform with the constituent particles sliding relative to each other. Shear strength of the material could be defined as the limiting value of the opposing resistive force when the powder is on the point of sliding.

The magnitude of the consolidating force on the powder has a major influence on the shear strength whereas other factors such as the nature of the particles themselves, particle size distribution, particle packing arrangement and moisture content have an effect as well.

The failure locus is the graphic representation of the relationship between the normal compressive stress (σ) and the resultant shear stress at failure (τ) for a powder subject to a specified consolidation. This failure locus is represented by a simple linear model $\tau = m\sigma + c = m\sigma + mT$ as shown in figure 11 where:

- m is the slope of the failure locus called coefficient of internal friction
- T is the apparent tensile strength, the value of σ for which the shear stress is zero
- c is the cohesion of the powder defined as the limiting value of τ for σ equal to zero

For a free flowing or non-cohesive material, cohesion is equal to zero and therefore the model is simplified as $\tau = m\sigma$. In this case, the failure locus passes through the origin.

Generally, the internal friction characteristics of the powders are indicated by the angle of internal friction (Φ), which is related to the coefficient of internal friction by the relationship $\Phi = \tan^{-1}m$. In powder mechanics, the consolidation stress levels to which the samples are exposed in processing equipment are typical 1 or 2 orders of magnitude lower than those of interest in soil mechanics. Samples used for strength tests are not an extracted in a consolidation condition; instead, a sample of loose

powder is consolidated in the shear over the stress range required and the strength is measured.

Cohesive powders show intrinsic shear strength under zero consolidation and the model is $\tau = m\sigma + mT$. However, the failure locus of these powders shows a significant curvature and the slope at any point defines the angle of internal friction Φ at that condition. This curvature can be represented with the Warren-Spring equation (Briscoe et al. 1987):

$$\left(\frac{\tau}{c}\right)^n = \frac{\sigma + T}{T} \quad \text{Equation 1}$$

This equation is applicable if the consolidation stress is smaller than the consolidation at the termination point of the yield locus. The loads index n varies between one and two (Briscoe et al. 1987).

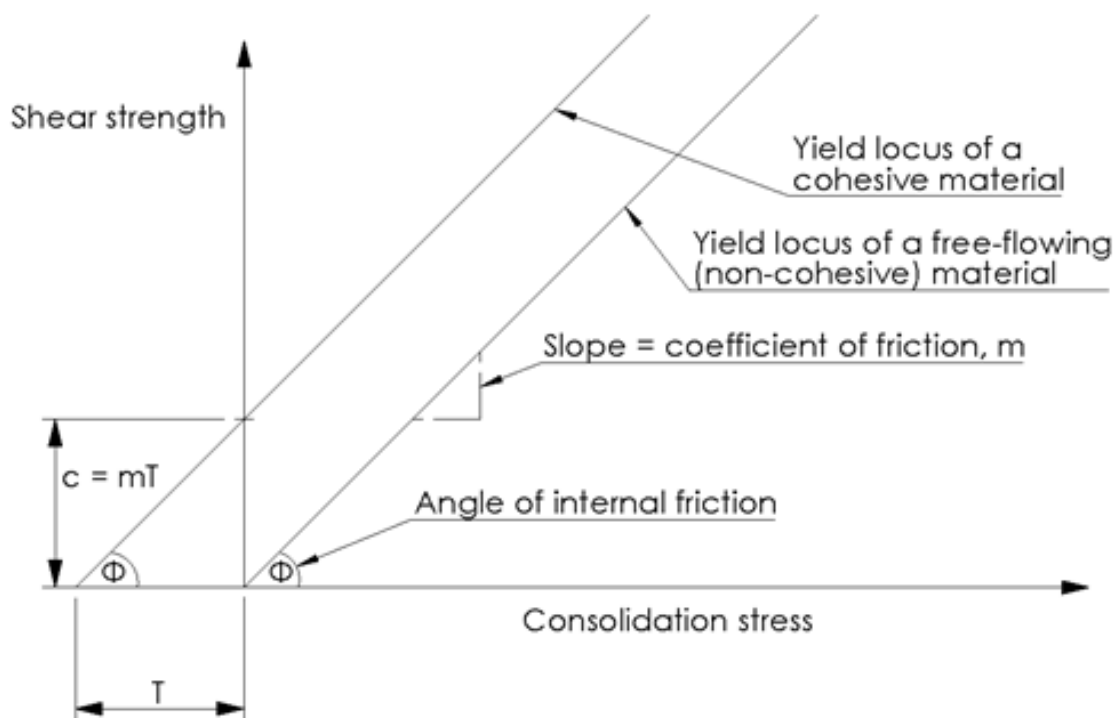


Figure 11: Linear model of shear strength of a bulk solid material (The Wolfson Centre for Bulk Solids Handling Technology, University of Greenwich, England)

Mohr semi-circles of stress define unconfined failure strength (σ_c) and major consolidating stress (σ_1) as shown in figure 12. The Mohr semi-circle of stress which defines σ_c passes through the origin of the $\tau - \sigma$ diagram and is tangential to the failure

locus. For the major consolidation stress (σ_1), the Mohr semi-circle is also tangential to the failure locus and passes through the point corresponding to the consolidated condition or preshear point.

The stress analysis for which the flow properties are used are generally 2 dimensional and behaviour is dominated by the magnitude of the difference in the major and minor principal consolidation stress.

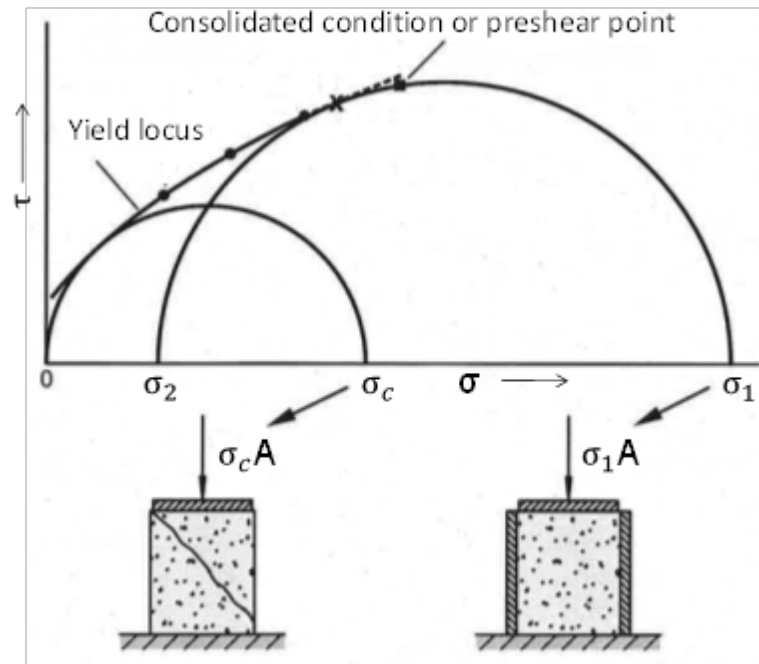


Figure 12: Yield locus and Mohr stress circles defining the unconfined yield strength and the consolidation stress: analogy to the uniaxial compression test

The apparent tensile strength is proportional to the unconfined failure strength and the coefficient of proportionality can be defined as follows:

$$\sigma_c = 2Kc = 2KmT \quad \text{Equation 2}$$

$$K = m + \sqrt{(1 + m^2)} \quad \text{Equation 3}$$

$$m = \tan \Phi \quad \text{Equation 4}$$

A straight line drawn through the origin and tangential to the consolidation Mohr semi-circle is called the effective failure locus. The angle between this failure locus and the horizontal axis of the diagram is named the effective angle of internal friction (δ). Further shearing of the material beyond the termination point of the yield locus is not

possible unless the normal stress applied is reduced which means allowing dilatation of the powder before being sheared.

The effective angle of internal friction represents the ratio of the major and minor principal stresses during steady state flow. This effective angle of friction is influenced by the magnitude of the internal friction, the cohesion as well as the consolidation stress level. Typically, the effective internal friction of a cohesive material increases significantly as the stress level reduces towards zero. This is because at very low stresses, minor principal stress of a cohesive powder tends to zero (at which point the effective angle of friction is 90°).

Different initial consolidating loads will give different failure loci which determine the corresponding values of σ_c and σ_1 . For such a family of failure loci these values of σ_c and σ_1 are used to plot the flow function of the powder. The other flow properties (effective friction function and bulk density curve) are usually as a function of σ_1 . Both the angle of effective internal friction and the bulk density vary with the consolidating stress. Therefore, it is important that the correct values are used in the design of bulk solid handling equipment.

Jenike et al. developed a translational shear tester for bulk solids and its procedure has been well-recognised and can be found in the ASTM standard D-6128. However, this tester requires a highly trained operator and is also extremely time consuming to use, i.e. undertaking the tests to characterise a single powder requires one whole day.

2.3.2 Brookfield Powder Flow Tester

Characterisation of a single powder using Brookfield Powder Flow Tester (PFT) takes approximately 45 minutes and requires operator attendance at the machine for around 5 minutes at start and end of test.

The test procedure of the PFT is as follows: initially, the sample is consolidated to the critical consolidation (preshear point N) and sheared which causes the material to flow under consolidation stress until the shear force reaches a steady value (S) achieving the steady-state or closely approached (NS).

Once steady-state flow is achieved, the sample is sheared under a reduced normal load N_1 giving the first maximum shear force S_1 for over-consolidated failure corresponding to the load applied N_1 . This procedure enables the points needed for

the failure locus. Three points are required to define the failure locus and the loads applied are one third ($N_1 = 0.33N$), two thirds ($N_2 = 0.66N$) of the critical consolidation N and the critical consolidation point.

The powder is tested at normal stresses mentioned (N , N_1 and N_2) and then an algorithm determines the best fit failure locus for these values. Based on this failure locus, the point of tangency in the Mohr semi-circles of stresses for σ_c is calculated. Powder is again consolidated and sheared under the normal load corresponding to the point of tangency (N_3) and the algorithm recalculates the best fit locus. Once the final failure locus is constructed, σ_c and σ_1 are calculated by the unconfined failure Mohr semi-circle and the consolidation Mohr semi-circle.

Five levels of consolidation stress are possible: 0.3, 0.6, 1.2, 2.4 and 4.8 kPa. The volume of powder required is 263cc for the standard cell and 43cc for the small cell. Flow function test requires 45 minutes and the resulting data gives the flow function ($\sigma_c - \sigma_1$ diagram), the friction function ($\tau - \sigma_1$ diagram) and the bulk density function ($\rho - \sigma_1$ diagram) of the powder tested. These functions are used to characterise the flow strength and the potential of arching and ratholing for the bulk solid. It is also possible to test the effect of time consolidation on powders by undertaking a time consolidated flow function test. It follows the same procedure as flow function test but the bulk solid is left under consolidation for a user defined time period for static storage.

The design of a mass flow hopper also requires information about the friction between the powder and a hopper wall. However, wall friction testing was considered outside the scope of this work as it would add another dimension to the experimental and modelling work. The omission of this is not so critical because industrial partners' plants were found to mostly operate in core flow.

2.3.3 Comparison to other commonly used shear testers

The magnitude of the flow property measurements generated by the Brookfield Powder Flow Tester has been compared with Jenike shear tester and Schulze Ring shear tester measurements in a recent published study (Berry et. al 2014). Round robin tests were undertaken with the Brookfield Powder Flow Tester using the standard BCR limestone powder (CRM-116) at three different laboratories in the USA and United Kingdom. The limestone powder was tested with seven different Brookfield Powder

Flow Testers undertaking seven repeat flow function tests using the standard and the small volume shear cells for each one.

Representation of the data obtained in the study showed a standard deviation of 95% confidence interval for the measured values of the flow functions, bulk density and effective internal friction functions. Comparison of the mean flow functions and effective internal friction functions were made with the results published in the literature for the tests undertaken with the same powder with the Jenike shear cell and Schulze cell. This comparison showed that Schulze cell measured 4° higher angles of internal friction compared to Jenike and PFT. Regarding the flow functions, the values of the unconfined failure strength obtained using these three shear testers are comparable with different standard deviations over the stress consolidation ranges; the PFT and the Schulze shear tester showed similar reproducibility with more scattered from the data published for the Jenike shear tester.

2.4 Theoretical links between particle and bulk scale

A broad survey of the literature is presented relating to analytical models linking particles properties to bulk properties considering:

- Packing structure
- Interparticle forces
- Liquid bridges
- Effect of free flow additives

2.4.1 Packing of monosized spheres

The packing of the particles is a key factor to determinate the behaviour of bulk solids under compaction forces, as it controls the average number of particle contacts and ultimately the bulk strength. German et al. (1989) stated that particle size and shape, agglomeration and friction between particles affect the packing structure. Powders are characterised by different particle size and shape distributions, agglomerates and surfaces areas.

Due to the complexity of the interaction of the variables, monosized spheres are commonly used to model and predict the packing behaviour. Characteristics such as density, porosity, permeability and strength are relevant in industrial processes to control the quality of the final products.

For the case of dry coarse particles (typically above 100 μm) gravity forces dominate over interparticle forces, the packing structures formed can be estimated based on a model for fitting monosized spheres in a confined space.

In general terms, packing structure can be classified as dense and ordered or non-dense and random packing. The volume occupied by the solids and voids are referred to as the solids fraction and the void fraction respectively. The coordination number describes the number of contacts points on each particle.

The maximum void fraction depends on the dimensions of the study considered. I.e. for a two-dimensional structure (equal size circles on a plane), the maximum solids fraction is 0.9069 and the highest coordination number is 6 and for three-dimensional structure (monosized spheres in a volume), 0.7405 and 12 respectively. For random packing of monosized particles, characteristic values of the solids fraction are 0.75 for one-dimension, 0.82 for two-dimension and 0.64 for three-dimension structures (German et al. 1989).

Ordered packing and loose or dense random packing are the characteristic structures for monosized spheres in three dimensions. Loose random packing represents the structure of particles in a container without vibration. Once the container is agitated, the particles are reorganised and the solids fraction increases reaching the dense random packing value.

The coordination number of the packing structures in three dimensions depends on the considerations made for each method to evaluate the contact between particles. As an example, for a random loose packing of monosized spheres, the coordination number reported by researchers varies from 6 to 9.5 (German et al. 1989).

Different packing models for ordered structures have been proposed to link the solids fraction and the associated coordination number (German et al. 1989). Mathematically, it is accepted that the maximum packing density for monosized spheres (close-packed structure) is characterised for a coordination number of 12 and a void fraction of 0.26. Open-packed structure is characterised for a coordination number of 6 and a void fraction of 0.48. Table 1 shows established models for normalised coordination numbers and open and close packing structures have been highlighted in the table and shown in figures 13 and 14 below.



Figure 13: Open packing structure for monosized spheres (German et al. 1989)

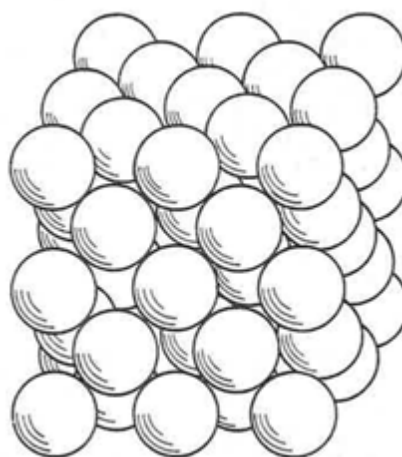


Figure 14: Close packing structure for monosized spheres (German et al. 1989)

<i>Packing of spheres</i>	<i>Coordination Number</i>	<i>Solids fraction</i>	<i>Void fraction</i>
Face-centred cubic	12	0.7405	0.2595
Face-centred cubic	11	0.7120	0.2880
Tetragonal – sphenoidal	10	0.7081	0.3019
Tetragonal – sphenoidal	9	0.6134	0.3866
Body-centred cubic	8	0.6802	0.3198
Orthorhombic	8	0.6046	0.3954
Orthorhombic	7	0.5612	0.4388
Cubic	6	0.5236	0.4764
Cubic	5	0.4031	0.5969
Diamond	4	0.3401	0.6599

Table 1: Established models for normalised coordination numbers

Several mathematical expressions have been proposed to link solids fraction and the coordination number for monosized spheres. Most of them make predictions for ordered packing structures. The simple units mentioned above have been used to find approximate correlations.

German et al. plotted the relation between very common mathematical expressions proposed by different researchers and the well-established packing data for monosized spheres. It was found that equations proposed by Ben Aim et al. and Gray et al. & Suzuki et al. fit reasonably the ordered packing data. However, these have a tendency to give a lower coordination number for random packings.

Ben Aim et al. developed the following expression where f is the solids fraction and N_c is the coordination number:

$$N_c = \pi / (1 - f) \quad \text{Equation 5}$$

Gray et al. & Suzuki et al. developed the following expression:

$$N_c = 2 \exp(2.4 f)$$

Equation 6

2.4.2 Effect of particle properties

Interparticle forces are raised by the irregularities on the surface of the particles. Both particle shape and surface texture have a significant effect on the packing density. In general terms, any particle differing from an ideal and smooth sphere or cubic decreases the values of the solids fraction. The further the particle is to being spherical or cubical, the lower the solid fraction.

However, the mixing of different particles shapes may increase the packing density if they are blended under vibration, particles might orient themselves and close packing structure could be possible, assuming that particles are sufficiently large for gravity forces to dominate over interparticle forces.

Another factor to take into account is the internal porosity of the particles involved in the packing density. Particles with open pores reduce the content of solid of the packing and, therefore, reduce the solid fraction. In case of very porous particles such as carbon black, it is very important to study its influence.

The effect of particle shape is strongly influenced by the packing structure, for close packed structure the shape affects the mobility of the particles. If we consider a uniaxial column of equant particles, when a stress is applied vertical a chain of contacts form in the powder and the ability of the particle contacts to rotate produces a lateral stress that is proportional to the axial stress. This is the stress ratio of the powder. If this conceptual experiment is conducted for the elongate materials they will naturally form a more open structure (higher void fraction) but the length and number of contacts along the length prevent the rotation of the particle so that the stress is supported axially and there is very low or zero lateral stress. The behaviour of the platy material is somewhere between the two extremes. While this analysis is valid for larger particles where gravity forces dominate over inter-particle forces, it is of little or no consequence for fine particles where an open packing structure is formed, which allows the particles the freedom rotate under applied stresses.

Particle size has a great influence on the solid fraction. Large dry particles with mean size over 100 μm are dominated by gravity forces and these forces do not affect the packing structure. Particles with the mean size below 100 μm decrease the packing

density due to increasing surface area, the lower mass of the particles and the influence of the weak forces like van der Waals forces and moisture. Therefore, the friction and bridging between particles is more relevant in the packing density, which is more restricted. The smaller the particles are, the lower the solid fraction will be.

Large spheres exhibit small difference between loose and random packing. German et al. stated that spherical particles with size greater than 100 μm do not show any significant change in void fraction under vibration. However, small and non-spherical particles show increases in the packing density under vibration. Generally, the smaller and more irregular the particles are, the greater the effect of the vibration in the packing density.

It is possible to increase the packing structure by adding smaller spheres to fill the voids between larger particles. The size ratio is a critical factor to obtain the most optimised structure with the highest possible solids fraction, along with the composition of the blend. An excess of any size fraction of the blend affects the packing density reducing its value. Geometry is used to calculate the diameter of the particles needed to fit in the voids. To get the most efficient packing, the smaller sphere should be touched by the three surrounding larger spheres as shown in figure 15. Therefore, the radius of the smaller particle can be calculated as follows:

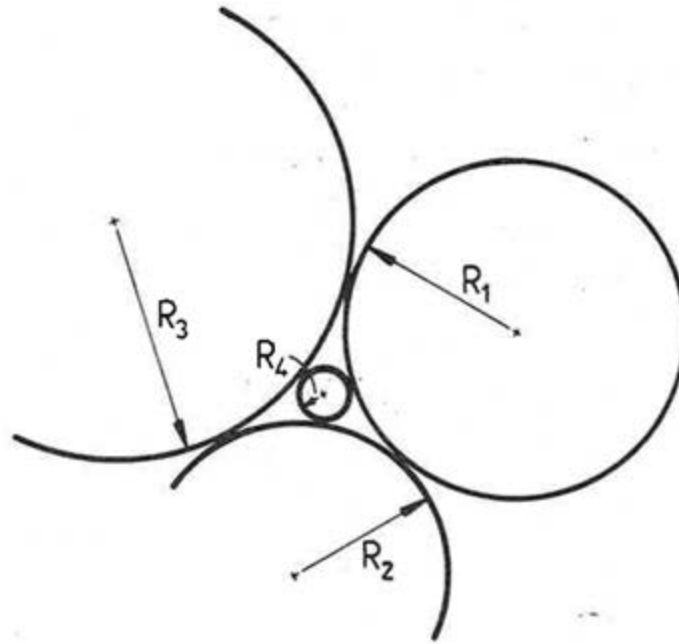


Figure 15: Small sphere filling the voidage of large spheres (German et al. 1989)

$$\frac{1}{R_4} = \frac{1}{R_1} + \frac{1}{R_2} + \frac{1}{R_3} + 2 \sqrt{\frac{1}{R_1 R_2} + \frac{1}{R_1 R_3} + \frac{1}{R_2 R_3}} \quad \text{Equation 7}$$

Where:

- R_4 is the radius of the smaller sphere
- R_1 , R_2 and R_3 are the radii of the larger spheres surrounding the smaller sphere

For the particular case of equal larger spheres, smaller particle has a radius of 1/6.464 or 0.1547 times the radius of the larger sphere. The process of filling can be repeated fitting spheres in the voids remaining after the first filling.

Hence, a general equation could express the solid fraction of the structure as a function of the sizes of the particles. A general size distribution of the particle sizes could also be used to predict and optimise the packing density (German et al. 1989).

Gilbert et al. (cited in German et al. 1989) provided a table giving the size ratios needed for different coordination numbers (see Table 2)

D_L/D_S	6.464	2.414	1.426	1.000	0.766	0.620	0.520	0.477
N_c	3	4	5	6	7	8	9	10

Table 2: Size ratios required for different coordination numbers

2.4.3 Interparticle forces

There are numerous interparticle force mechanisms that start to dominate the packing properties and cohesive strength of particulates as the particle size is reduced (Yu et al. 2003). Table 3 shows these forces and the mechanics associated to interparticles forces:

Forces	Mechanics
Van der Waals forces	Attraction forces between fine particles
Electrostatic forces	Attraction forces between fine particles
Magnetic forces	Attraction forces between solids
Chemical bonding	Chemical reactions between particles
Capillary forces	Forces due to the presence of liquid
Mechanical forces	Direct contact between particles
Gravity forces	Effect of gravity on particles

Table 3: Interparticles forces and the mechanisms associated to these forces

Gravity force drives the packing behaviour for coarse particles which depends on the particle size and shape (Yu et al. 2003). When particle size decreases, the magnitude of the gravity force decreases and other interparticle forces become higher than the gravity force. Mechanical forces are higher when the surface roughness increases; therefore smoother particles have lower tendency to interlock each other.

It has been stated that when a dry powder is in equilibrium with a dry atmosphere, the internal forces to take into consideration in terms of packing behaviour are electrostatic

forces, van der Waals forces, chemical bonding (or hydrogen bonding) and magnetic forces (Coelho et al. 1978).

The consensus of the literature is that both chemical and electrostatic forces are negligible relative to the van der Waals forces (Forsyth et al. 2001). The food grade materials under consideration for this project are non-magnetic so these forces can be also ignored. In the presence of surface liquid for non-magnetic particles, electrostatic forces are negligible (Iveson et al. 2002) and van der Waals forces are also negligible for particle systems with size greater than 10 μm (Rumpf et al. 1962).

Therefore, the bonding mechanisms considered in this project are van der Waals for dry materials and capillary forces for wet materials (presence of surface moisture).

2.4.4 Dry particulate materials

Van der Waals forces between atoms and molecules arise from the charge interactions of dipoles (Coelho et al. 1978 and Yu et al. 2003). It can be determined as follows for two spherical particles which contain molecules (Yu et al. 2003):

$$F_V = \frac{A}{6} \frac{64R^6(s + 2R)}{(s^2 + 4Rs)^2(s^2 + 4Rs + 4R^2)^2} \quad \text{Equation 8}$$

Where:

- A is the Hamaker constant which is related to material properties, with typical values about 10^{-19} J
- s is the separation distance between particles
- R is the radius of the spherical particles

The value of the Hamaker constant can be determined by different methods and techniques using atomic force microscopy (Argento et al. 1996, Lomboy et al. 2011 & Das et al. 2007). However, this measurement is considered a level of detail out of the scope of this research as disclosed in chapter 5, section 5.3 of the thesis.

These forces are more significant when “s” is small, and under the condition of $s \ll R$ [condition valid for industrial applications (Yu et al. 2003)], the equation is simplified as follows:

$$F_V = \frac{AR}{12s^2} \quad \text{Equation 9}$$

Yu et al. in 2003 plotted the force ratio between van der Waals force and gravity force on a spherical particle (glass beads) as a function of the particle size and different separation distances between 8.25×10^{-11} and 3.2×10^{-10} . It was found that van der Waals force is more significant than gravity for particles with size below $100 \mu\text{m}$. It also showed that these forces vanish rapidly with distance and, therefore, they are sensitive to surface roughness (Coelho et al. 1978).

The influence of the van der Waals force found by Yu is consistent with the experimental observations from Milewski et al., Mizuno et al. (both cited in Yu et al. 2003) and Yu et al. in 1997. It was observed that voidage was fairly constant for coarse monosized spheres under gravity force and increases for glass beads below $100 \mu\text{m}$ when particles size decreases because van der Waals force becomes dominant (Yu et al. 2003) as shown in figure 16 below.

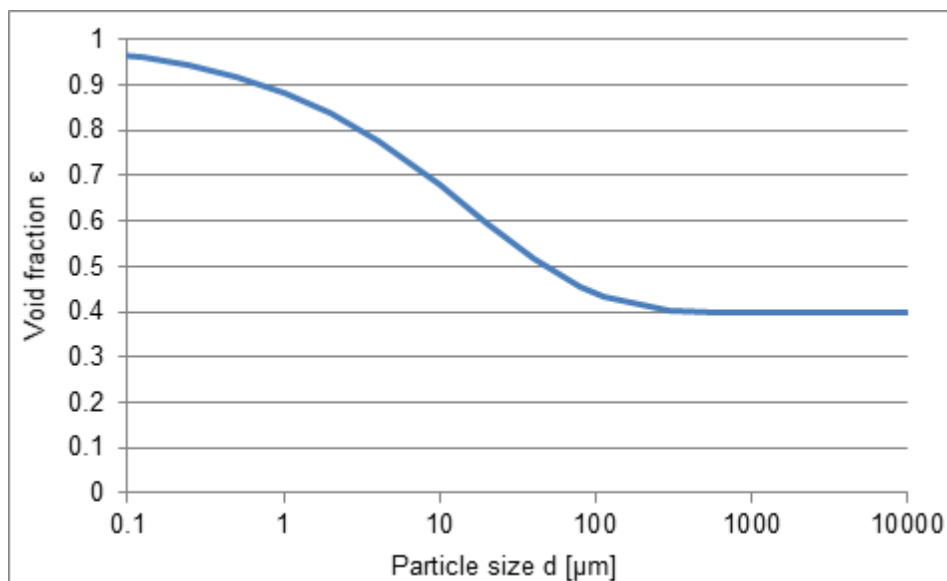


Figure 16: Schematic diagram illustrating the effect of the particle size on the packing structure of dry glass beads (Yu et al. 2003)

Furthermore, Yu et al. 2003 proposed empirical equations to predict the voidage of dry powders as a function of the particle size, particle density and material properties (Hamaker constant). These equations were developed by empirical curve fitting of the void fraction data as a function of the particle size taken from several resources with glass beads assumed in their calculations. These resources (Milewski et al., Mizuno

et al. and Yu et al. in 1997) measured the voidage at poured and tapped packing conditions which means that low consolidation stress was applied to the powder in their experimental work.

Initially, Yu et al. 2003 developed a general expression based on the empirical fitting of the measurements undertaken by Milewski et al., Mizuno et al. (both cited in Yu et al. 2003) and Yu et al. in 1997 for packing of fine sphere particles as follows:

$$\varepsilon = \varepsilon_0 + (1 - \varepsilon_0) \exp(-mR_F^{-n}) \quad \text{Equation 10}$$

Where:

- R_F is the ratio between the magnitudes of the interparticle force (van der Waals forces for dry materials) and the gravity force
- ε is the void fraction as a function of interparticles force
- ε_0 is the void fraction of the dry coarse spheres under gravity force
- m and n are fit constants of the experimental curve fitting of the measurements for packing of fine sphere particles

Meanwhile, Van der Waals forces were expressed as a function of surface roughness as follows:

$$F_V = AKR \quad \text{Equation 11}$$

Where K is the lumped parameter which depends on the surface roughness and the separation distance between particles. Experimental values of K for glass beads were fitted with the following equation:

$$K = b x d^c \quad \text{Equation 12}$$

Where:

- d is the diameter of the spherical particles
- b and c are fit constants (2.63×10^8 and -1.54 respectively) of the experimental lineal fitting of K values for glass beads

Substituting equations 11 and 12 into equation 10 gave an expression of the void fraction as a function of the particle properties (size and density) and material properties (Hamaker constant).

$$\varepsilon = \varepsilon_0 + (1 - \varepsilon_0) \exp\left(-m \left(\frac{3bA}{\pi\rho_p}\right)^{-n} d^{-n(c-2)}\right) \quad \text{Equation 13}$$

Where:

- A is the Hamaker constant
- ε is the void fraction as a function of particle properties
- d is the diameter of the spherical particles
- ρ_p is the particle density
- ε_0 is the void fraction of the dry coarse spheres under gravity force
- m and n are fit constants of the experimental curve fitting of the measurements for packing of fine sphere particles
- b and c are fit constants (2.63×10^8 and -1.54 respectively) of the experimental lineal fitting of K values

Yu et al. 2003 assumed a value of $\varepsilon_0 = 0.4$ for loose random packing and $\varepsilon_0 = 0.36$ for dense random packing and by fitting equation 13 to the plotted voidage data as a function of the particle size taken from the resources, obtained the values of m and n for these packings of spheres. Using these values, the void fraction can be expressed as follows:

- Loose random packing

$$\varepsilon = 0.4 + 0.6 \exp\left(-0.106 \left(\frac{\rho_p}{A}\right)^{0.156} d^{0.552}\right) \quad \text{Equation 14}$$

- Dense random packing

$$\varepsilon = 0.36 + 0.64 \exp\left(-0.178 \left(\frac{\rho_p}{A}\right)^{0.129} d^{0.457}\right) \quad \text{Equation 15}$$

Yu et al. in 2003 stated that van der Waals forces are composed by three components when the surface roughness is considered: attraction between particles, attraction between particles and asperities and attraction between asperities. Forsyth et al. in 2000 proposed an equation that considers the effect of asperities:

$$F_V = - \frac{2Ar^3}{3s^2(s+2r)^2} - \frac{2AR^3}{3(s+r)^2(s+r+2R)^2} \quad \text{Equation 16}$$

Where:

- r is the asperity radius assuming particles have a spherical profile

2.4.5 Wet particulate materials

The addition of liquid to bulk solids or even the presence of low moisture content in powders forms liquid bridges and cohesive forces between particles. This force is composed by two components: capillary and viscous. The strength of the liquid bond also depends on the interparticle friction (Iveson et al. 2001) which is activated by the capillary and surface tension forces in the liquid between particles.

The capillary component appears due to the surface tension of the liquid and the pressure deficiency in the liquid bridge, while the flow of the liquid in the bridge generates the viscous component (Yu et al. 2003).

Different regimes of liquid content for an assembly of random packing with monosized spheres have been well-established since 1958 when Newitt et al. described them for the first time (see figure 17).

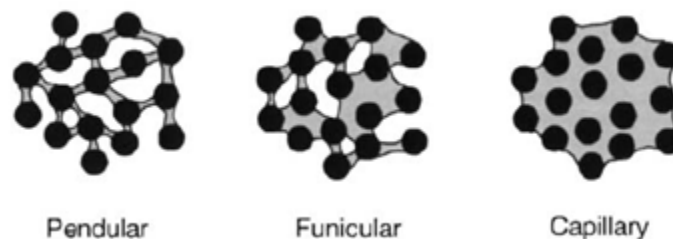


Figure 17: *Different states of saturation for an assembly of random packing of monosized spheres (Iveson et al. 2002)*

Initially liquid bridges are formed in the contact points holding the particles together (pendular state). Capillary state is characterised by the saturation of the particles (liquid fills all the voids). Funicular state is a transition between pendular and capillary states, liquid fills some of the voids whereas there is still some space left between particles. When the maximum amount of liquid that can be held by the particles is reached and more liquid is added, solid are held by liquid (droplet state). Another state called pseudo-droplet may be possible where unfilled voids are trapped inside the droplet (York et al.). It has been stated by several researchers (Sandell et al. 1993, Kristensen et al. 1995, Pierrat et al. 1997, Yang et al. 1999, Mitarai et al. 2006) that

the pendular state is characterised by a saturation lower than approximately 25%, the funicular state by a saturation approximately between 25% - 80% and the capillary state by a saturation greater than approximately 80%.

The bond strength of a particulate in the presence of surface moisture is characterised by two models: the static liquid bridge model for the pendular region and the dynamic viscosity based model for the funicular region. These are described below:

Static strength

As mentioned above, the strength of the static pendular bridge (see figure 18) depends on the surface tension at the contact line between liquid and particles and the pressure deficiency in the liquid bridge (Iveson et al. 2002 & Yu et al. 2003).

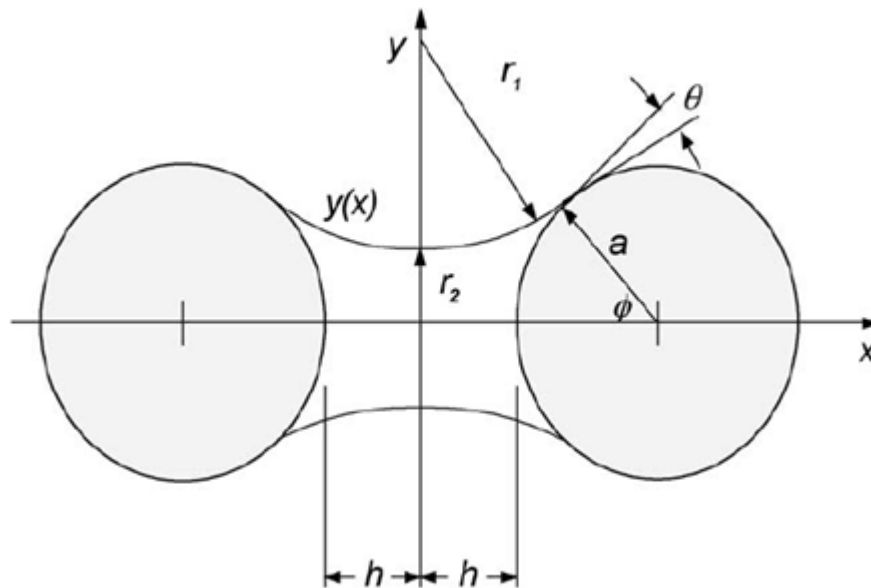


Figure 18: Schematic of a pendular bridge between two monosized spheres
(Iveson et al. 2002)

The capillary suction pressure difference across the curvature of the air-liquid interface is given by the Laplace-Young equation (Iveson et al. 2002):

$$\Delta P = \gamma_{LV} \left(\frac{1}{r_1} - \frac{1}{r_2} \right) \quad \text{Equation 17}$$

Where:

- γ_{LV} is the liquid surface tension

- r_1 and r_2 are the radii which defines the curvature of the surface bridge

This equation cannot be solved analytically and the common approach is to consider the liquid bridge profile as a toroid. However, this geometry figure has a variable surface curvature. Two theories have been developed about the evaluation of the surface tension and capillary pressure terms. By gorge method (Lian et al. 1993), these terms are evaluated at the middle point of the bridge; by boundary method (Lian et al. 1993), these are evaluated at the contact line with one of the spheres (Iveson et al. 2002). Therefore, two different equations are proposed for the estimation of the static bridge strength:

$$F_{gorge} = \pi \Delta P r_2^2 + 2\pi \gamma r_2 \quad \text{Equation 18}$$

$$F_{boundary} = \pi \Delta P a^2 (\sin \phi)^2 + 2\pi a \sin \phi \sin(\theta + \phi) \quad \text{Equation 19}$$

Another approach is the numerical full resolution of the equation and fit empirical expressions to the results. Willet et al. (cited in Iveson et al. 2002) solve the equation and proposed the following expression for $V/a^3 < 0.001$, where V is the volume of the bridge:

$$F_{static} = \frac{2\pi a \gamma_{LV} \cos \theta}{1.0 + 2.1 \left(\frac{ah^2}{V}\right)^{\frac{1}{2}} + 10.0 \left(\frac{ah^2}{V}\right)} \quad \text{Equation 20}$$

In the capillary state, the contribution of the surface tension component drops to zero whereas the suction pressure term is significant. Static strength drops to zero in droplet state (Iveson et al. 2002).

In 1962, Rumpf et al. developed a mathematical model to estimate the mean theoretical tensile static strength of the liquid bond for wet agglomerated granules or the interparticle force for binderless agglomerated granules. A basic equation was derived assuming spheres of the same size. The tensile strength is shown as a function of the particle size, the voidage and the bonding force at a point of contact. The following assumptions were considered:

- The sum of bonds formed in the stressed cross section of the agglomerate is significantly high. The bonds are uniformly distributed across the section and over the directions in space.
- The spheres are equally distributed in the agglomerate. Therefore, it was assumed that any cross section is homogenous and possesses the same void fraction and equal effective strength across its whole area.
- The effective bonding forces are distributed around a mean value which can replace them in calculations and it was assumed to be equal for different points of the cross section.

Based on these assumptions, the following equation was derived for a model:

$$\sigma_z = \frac{9(1-\varepsilon)}{8\pi d^2} kH \quad \text{Equation 21}$$

Where:

- H is the bonding force at point of contact (this force has a constant value due to the assumptions of the model and it is called “mean bonding force”)
- k is the mean coordination number (the average number of points of contact between one sphere and its neighbours)
- d is the diameter of the spherical particles
- ε is the void fraction within the total volume
- σ_z is the mean theoretical tensile strength

The approximate equation was previously published by Rumpf et al. (1958) but without the factor 9/8, which was introduced by taking an account of the statistical distribution of particles in the cross section.

The coordination number depends on the void fraction within the total volume. Using the results of Smith (Manegold et al. 1955), Rumpf et al. (1958) proposed a relation between coordination number and voidage for loose and jarred packing for monosized spheres:

$$k\varepsilon \approx 3.1 \approx \pi \quad \text{Equation 22}$$

Then equation 21 becomes a function of the particle size, the voidage and the bonding force at a point of contact:

$$\sigma_z = \frac{9(1-\varepsilon)H}{8\varepsilon d^2} \quad \text{Equation 23}$$

In this research, this equation of the model was adopted to calculate the bulk strength of dry single powders as a function of the particle size and the packing structure of the particulate materials.

Tanaka et al. gave an expression for the radius of the bridge for wet agglomerated granules:

$$r_2 = 0.82a \left(\frac{v}{a^3} \right)^{0.25} \quad \text{Equation 24}$$

Where:

- r_2 is the radius at the narrowest part of the bridge (the neck)
- v is the volume of the bridge for a single sphere around the contact area between two spheres

The model suggests that the bond fails only at the narrowest part of the bridges and all the liquid bridges are equal in geometry and strength. This means that the value obtained from the model can be considered as an average value (Christakis et al. 2006). In this research, the bonding force at point of contact was considered equal to the force produced in the neck of the bridge due to the surface tension of the liquid bonding the particles. With these assumptions, this equation can be developed into Rumpf's equation for wet particulate materials as follows:

$$\sigma_T = \alpha \cdot 2\pi r_2 \frac{9(1-\varepsilon)}{8\varepsilon} \left(\frac{1}{2a} \right)^2 \quad \text{Equation 25}$$

Where:

- σ_T is the mean theoretical tensile strength
- α is the surface tension of the liquid

Dynamic strength

The viscous force due to the flow of the liquid in a pendular bridge between two spheres surfaces can be approximated by the lubrication theory (Adams et al. 1987, cited in Iveson et al. 2002):

$$F_V = \frac{3\pi\mu_V a^2}{2h} \left(\frac{dh}{dt} \right) \quad \text{Equation 26}$$

Where:

- μ_V is the liquid viscosity
- $2h$ is the gap distance between the spheres
- a is the radius of the spheres
- dh/dt is the time derivate of h (i.e. half-gap velocity)

Adams et al. (cited in Yu et al. 2003) stated that the viscous component is significant when either the viscosity of the liquid is high or the relative velocity of the particles approaching each other is high. Mazzone et al. and Ennis et al. (cited in Iveson et al. 2002) verified the above equation and highlighted that the viscous component could exceed the capillary component by several orders of magnitude under certain conditions using viscous binders. It may explain the dramatic effect of small amounts of liquid on the flow properties of the powders.

However, other researchers found that the strength of pendular water bridges decreased as the rate of separation increased (Iveson et al. 2002). In general terms, the relative importance of the components dictates the effect of each term on the strength of the pendular bridge (Iveson et al. 2001). For example, in the case of water pendular bridges, capillary forces dominate over viscous forces (Iveson et al. 2002).

Goldman et al. proposed another equation based as well on the lubrication theory for small separation distances but it has not been well verified yet (Iveson et al. 2002). In the equation proposed, v_t is the relative velocity of the two spheres.

$$F_V = 6\pi a \mu_V v_t \left(\frac{8}{15} \ln \left(\frac{a}{2h} \right) + 0.9588 \right) \quad \text{Equation 27}$$

2.4.6 Effect of free flow additives

Free flow additives such as silicon dioxide, magnesium carbonate and tricalcium phosphate are common additives in the food industry. These flow agents improve the flowing and caking properties of the final food products like snack flavours. Generally they are used for either processing products or functional additives. As free flow and anti-caking agents, these additives aid the following functions:

- Prevent the packing of particles acting as a physical barrier when particles are moving
- Adsorb excess moisture from the atmosphere before it can be absorbed by the powder
- Sequester moisture from the surfaces of the particles
- Coat the surface of the particles reducing interparticle friction
- Adsorb moisture diffusing out of the bulk solid

Dry particle coating

A guest material which is an order of magnitude smaller in size, typically these are nanoparticles that have agglomerated to 1-10 μm .

The quantity required for complete surface coverage of the host can be estimated using the following equation based on difference in particle size and density (Yang et al. 2005):

$$Gwt\% = \frac{(Nd^3\rho_d)}{(D^3\rho_D) + (Nd^3\rho_d)} \times 100 \quad \text{Equation 28}$$

$$N = \frac{4(D + d)^2}{d^2} \quad \text{Equation 29}$$

Where:

- Gwt% is the weight % of guest particles for 100% surface coverage
- D is the diameter of the host particles
- d is the diameter of the guest particles
- ρ_D is the particle density of the host particles
- ρ_d is the particle density of the guest particles

Dry particle coating refers to techniques where a host material with large particle size is coated by a guest material characterised by very fine particles. This mechanical approach requires high-energy input to create collision and adhesion between core particles and the fine dry particles (Onwulata et al. 2005). Firstly, the agglomerates of the nanoparticles need to be break down and secondly, energy is required to spread them out across the surface of the larger particles.

Due to the fact that the size of the guest particles is very small (nanoparticles), van der Waals forces are strong enough to keep the fine particles attached to the host, and therefore, these fine particles cannot be easily removed (Onwulata et al. 2005). As such a discrete or continuous coating of guest particles (see figure 19) can be achieved depending on the operating conditions such as weight fraction of guest to host particles and process time (Pfeffer et al. 2001).

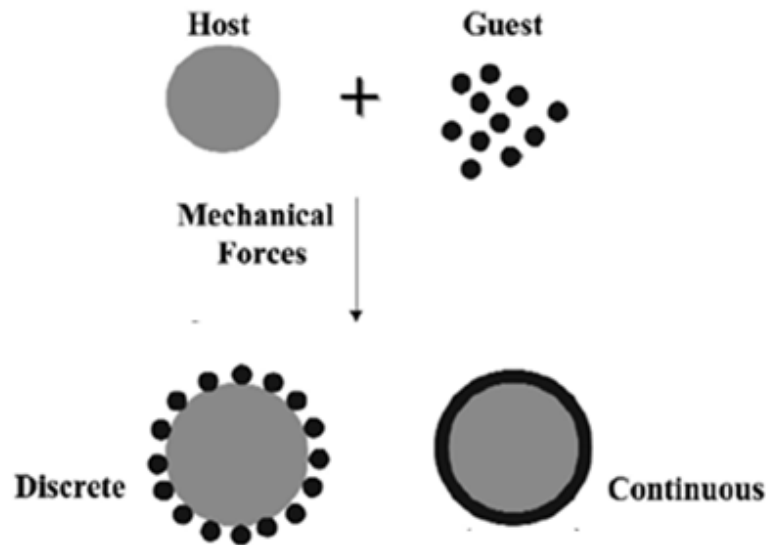


Figure 19: Discrete and continuous coating of guest particles (Pfeffer et al. 2001)

Mechanofusion

A mechanofusion machine is one of the devices used to achieve the strong force needed to coat the fine particles. The device consists of a rotating outer vessel, a stationary hammer inner piece and a stationary scraper. A measured amount of host and guest particles is placed into the rotating vessel. As the vessel rotates at speeds between 200 to 1600 rpm, the powder is forced to pass through the gap between the inner piece and the rotating drum. The scraper breaks-up any build-up of the powder on the walls of the vessel (Onwulata et al. 2005).

These particles are subjected to intense shearing and compressive forces. These forces generate sufficient heat energy to fuse the guest particles onto the surface of the host particles (mechanofusion). This process produces very strong bonds enhancing the dry particle coating (Onwulata et al. 2005).

During the process, the internal temperature may raise up to 60°C due to the high-energy required. This is an important factor to consider because many food ingredients are relatively soft and very sensitive to heat and can be deformed by the mechanical forces (Pfeffer et al. 2001). For these materials, soft dry coating systems are used ensuring minimum degradation of the particle size, shape and composition (Onwulata et al. 2005).

The High-Speed Elliptical-Rotor Type Mixer is a common example of a soft dry coating system. It consists of a slow rotating vessel (30 rpm) and a rotor rotating from 16 to 100 times faster. The rotor and the vessel rotate co-axially in opposite directions. The powder mixture inside the vessel is forced to pass through the clearance between the tip of the rotor and the vessel wall (Iwasaki et al. 2002).

2.5 *Research studies linking particle and bulk scale*

Many research studies have been undertaken trying to understand the effect of the particles properties on the bulk flow and packing properties. These studies are presented and discussed below.

2.5.1 Effect of particle shape

Researchers have found that particle shape, along with particle size, affects the flow behaviour of powders. Hann et al. 2007 investigated the effect of particle shape on the flow behaviour of limestone. A new attritor mill (Hann et al. 2006) was designed for the research to change the particle shape of the powder without modifying other properties.

Samples of limestone (milled and non-milled) were tested and compared utilising Johanson Hang-Up Indicizer (Roberts et al. 1995, Bell et al. 1994 & Johanson et al. 1992). Images of the samples showed that particles after the milling process were more rounded. The results showed that more rounded particles develop a greater failure strength than the more angular materials (0.64 kPa for milled particles and 0.36 kPa for non-milled particles) as they form denser packing structures (closer contacts), for identical consolidation conditions.

2.5.2 Effect of particle size and distribution

Many researchers have been trying to understand the effect of particle size and distribution on the bulk flow properties. In 1975, Kurz and Munz et al. determined the flow properties of different particle size distributions for limestone powders using a Jenike shear tester (Jenike et al. 1961 & 1967) and found that an increasing fraction of fines in the particle size distribution produced a significant effect on the strength of the powder, becoming more cohesive even with small variations of fines.

A few years later, in 1984, Molerus and Nywilt (Molerus et al. 1984) studied the effect of fine particles on the unconfined failure strength of binary mixtures of limestone. The samples were prepared by separating coarse and fine fractions from the particle size distribution. Fine size fraction of limestone was characterised by $D_{50} = 3.5 \mu\text{m}$ with a value of span ($D_{90} - D_{10}$) of $7 \mu\text{m}$; coarse size fraction of limestone was characterised by $D_{50} = 45 \mu\text{m}$ with a value of span of $40 \mu\text{m}$. The proportion of fines in the blends went from 0.5% to 35% at 5% blend increments. 100% fines and coarse samples were also tested. It was assumed that the particles were monosized spheres with a cubic packing arrangement and a packing structure with void fraction as 0.5. The researchers estimated that the fraction of fine particles which started dominating the flow behaviour of the blends, due to the embedding of the coarse particles by the fine ones, was 30%. The results showed that the angle of internal friction of the mixtures decreased as the proportion of fines increased and remained constant for any fraction higher than 25%. The flow properties were measured using a translational shear tester similar to the Jenike shear tester (Jenike et al. 1961 & 1967).

Recently, the study undertaken by Hann et al. 2007 utilised the Johanson Hang-Up Indicizer (Roberts et al. 1995, Bell et al. 1994 & Johanson et al. 1992) to investigate the effect of particle size and distribution on the flow properties of limestone. Changes in the flow properties were inferred from the measured rat-hole index for blends made with different proportions of coarse and fine. Rat-hole diameter (D_{rh}) gives the outlet size required for reliable discharge of core flow bins needed to prevent rat-holing (as described in section 1.2).

The research demonstrated that 100% coarse samples were effectively free flowing ($80 \text{ mm } D_{rh}$) as shown in figure 20 below. 100% fines samples had a $1500 \text{ mm } D_{rh}$ and this was consistent with flow properties of blend at 40-50% fines. The blend that

had the worst flowability was at 60% fines with a 2500 mm D_{rh} . The influence of fines particles was insignificant until 20% fine content and then rat-hole diameters increased steeply to reach a maximum value at 60% of fines; any further increase in fines decreased the values of the diameters.

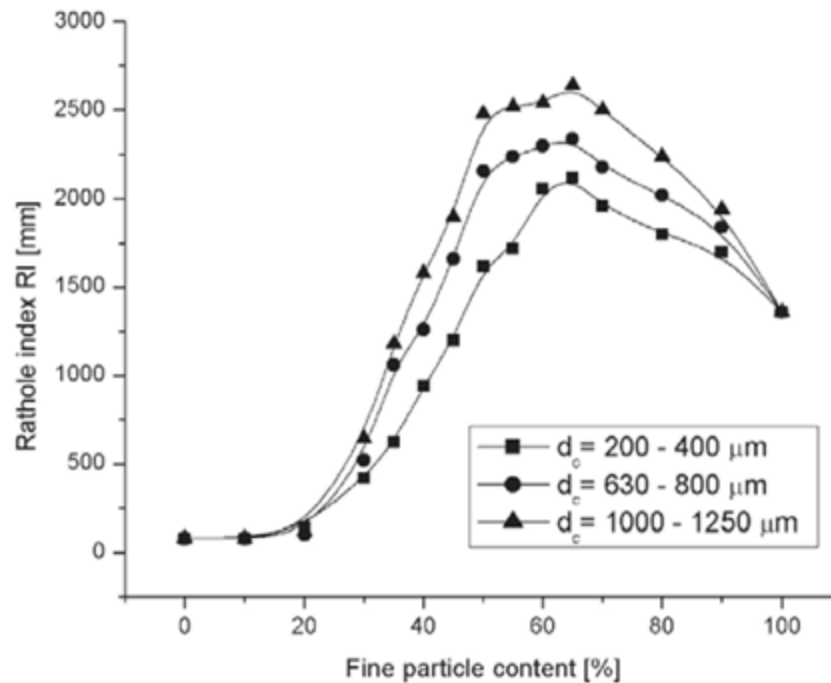


Figure 20: The influence of fine particle content on the flow behaviour of blends – Comparison of the Rathole Index values (Hann et al. 2007)

An increase in the width of the distribution was found to correlate to an increase in the critical rat-hole dimension. In summary, the study proved that fine particles have a significant influence on the flow properties of powders.

2.5.3 Effect of liquid content

Hann et al. 2007 studied the effect of moisture content (expressed by weight percentage) on the strength of limestone powder. Samples were wetted with different fractions of water at 0.5%wt and 1%wt moisture increments. The data obtained utilising Johanson Hang-Up Indicizer (Roberts et al. 1995, Bell et al. 1994 & Johanson et al. 1992) presented an increase in unconfined failure strength of limestone, even for small increases in liquid content. The research demonstrated that moisture content has an important influence on the flow properties of powders.

An experimental study of the packing of monosized coarse spheres and the effect of the addition of liquid was undertaken by Feng and Yu (Feng et al. 1998). Different liquids were used in order to understand the influence of liquid properties such as surface tension, viscosity and density. Glass beads with sizes over 200 μm were used to avoid the effect of van der Waals forces as it has been mentioned above. The research was conducted under loose random packing conditions because the use of external forces may overcome the effect of liquid additions. Three packing regimes were observed: wetting, filling and slurry as explained below.

Wetting

Initial addition of liquid wets the surface of the particles and increases the magnitude of the force; therefore, liquid bridges are formed between particles. These bridges hold the particles apart and generate a cohesive strength due to surface tension. This regime (wetting) is characterised by the increase of the void fraction with liquid content and the decrease of the bulk density until a critical value of liquid content is reached (M_{cri}). Three parameters are characteristic in this regime: the initial voidage (ϵ_0), the maximum achievable void fraction (ϵ_{max}) and the critical liquid content to give ϵ_{max} , (M_{cri}). At this stage, all particles are linked by liquid bridges.

Filling

After this critical point, further increase in liquid content reduces the void fraction on a dry basis as the liquid fills the voids. However, the cohesive strength of the bulk solid continues to increase due to the viscosity of the increasing thicknesses of the liquid bridges filling the voids. This regime (filling) is characterised by the increase of the bulk density and the decrease of the voidage on a wet basis (considering void fraction as the space left after the removal of the solid fraction and taking into account the liquid fraction and the voids). On a dry basis (removing solid and liquid fraction), voidage remains relatively constant as the liquid fills the void space.

Slurry

The maximum amount of liquid that can be held by the particles (M_{max}) is another critical value. As the point of saturation is approached, wet based void fraction decreases to zero, whereas, on a dry basis, shows a significant fall off due to the decrease of the magnitude of the capillary force. This regime (slurry) is characterised

by the decrease of the cohesive strength of the bulk solid, surface tension disappears at saturation levels and hence the bulk solid becomes freer-flowing slurry.

Empirical equations correlating the voidage and the bulk density with the liquid content in mass basis for wetting and filling regimes were proposed. It was assumed that the contact angle between liquid and solid was negligible. The viscosity of the liquids used in the study was not taken into account because this variable did not have an evident effect on the packing of materials. An equation for the maximum amount of liquid hold by the particles was also proposed for static packing regimes with limitations on its application.

$$\frac{\varepsilon - \varepsilon_0}{\varepsilon_{max} - \varepsilon_0} = \left(\frac{M}{M_{cri}}\right)^{0.423} \left[1 - 0.421 \ln \frac{M}{M_{cri}}\right] \quad \text{Equation 30}$$

$$\varepsilon_{max} = \varepsilon_0 + 0.048 \left(\frac{\sigma}{\rho_p g d^2}\right)^{0.266} \quad \text{Equation 31}$$

$$M_{cri} = 0.2545 \left(\frac{\rho_l}{\rho_p}\right)^{-1.057} \cdot \left(\frac{\sigma}{\rho_p g d^2}\right)^{0.4743} \quad \text{Equation 32}$$

$$M_{max} = 3.1934 \left(\frac{\rho_l}{\rho_p}\right)^{-0.7380} \cdot \left(\frac{\sigma}{\rho_p g d^2}\right)^{0.4008} \quad \text{Equation 33}$$

$$\rho_B = \rho_p (1 - \varepsilon) \left(1 + \frac{M}{100}\right) \quad \text{Equation 34}$$

Where:

- ε is the dry based void fraction
- ε_0 is the initial void fraction
- ε_{max} is the maximum achievable void fraction
- M_{cri} is the critical liquid content (mass basis) to give ε_{max}
- σ is the surface tension
- d is the particle size
- ρ_p is the particle density
- ρ_l is the liquid density
- M is the liquid content (mass basis)

The link between the packing regimes (wetting, filling and slurry) and the liquid content regimes (pendular, funicular and capillary) is not still very clear and more research needs to be done. In 1998, Yu et al. suggested that the maximum interparticle force corresponds to upper limit of the wetting regime could be regarded to the upper limit of the pendular regime. In this case, the equations proposed by Yu could estimate the transition from pendular to funicular regime under dynamic conditions. It was suggested that pendular and wetting regimes may be equivalent and the funicular regime could cover filling and slurry regimes.

2.5.4 Rabinovich model

In 2003, Rabinovich (Johanson et al. 2003) developed a first approximation model linking capillary forces between particles to unconfined failure strength of powders with moisture content. It was assumed capillary forces as the only bonding force acting among particles ignoring other inter-particle forces. Particles were considered spherical and the volume of the liquid bridge formed between particles was estimated constant under the shear process. The theory was based on the principle that the work needed to shear a powder is equal to the total effort required from the particles assembled to pass the adjacent particles during shearing. It was postulated that capillary forces generate unconfined failure strength proportional to $1/R$ where R is the particle diameter.

The hypothesis was tested measuring the strength of glass beads for various particle sizes adding oil at different proportions. The Schulze shear cell (ASTM standard D-6773) was utilised to undertake the tests for the study. The results showed that the strength of the wet powder decreased as particle size increased giving a fixed fraction of moisture content. It also showed that strength tended to reach a steady value as the proportion of oil increased for different consolidation stresses.

2.6 *Review of Industrial Practice*

The industrial process of the formulation of blended food powders has been reviewed to understand how the formulators and process engineers achieve the composition of their blends with the desirable flow behaviour in the industrial process lines. Changes in the composition of blended particulate materials have been always an issue for the powder industry because the new formulations must retain the sensory factors such as taste, aroma, colour and texture of the previous composition. Meanwhile, it is also

important the level of dust generated by the powder and the flow behaviour of the powder in the process lines. These factors must be considered when a blend is reformulated in the powder industry.

The reasons to reformulate an existing blend are generally the poor flow behaviour, the high level of dust generated and the need to change ingredients in the composition due to new legislations or new suppliers of powders. Initially, blends which show good flow behaviour and low level of dust under the extreme conditions of the process lines are characterised running tests in a powder flow tester and a dustiness tester to quantify the flowability and the level of dust respectively; particle size distribution is also measured using generally the laser diffraction method. The values obtained in the characterisation of these powders are used as a reference for future reformulations of powders.

The current process of reformulation is basically a trial and error procedure based on the prior experience of the formulator with other blends reformulated. The ingredients which characterised the sensory factors of the blend are not modified unless it is strictly necessary and only the components which affect the packing and bulk flow properties of the blends and the level of dust such as fillers, flow agents and liquids added could be modified in type and weight percentage content.

Liquids are used to increase the cohesion of powders sticking the particles to one another by the formation of liquid bridges and free flow agents are used to improve the flowability of the powder coating the surface of the particles and mitigating the effect of the liquid content. One of the challenges in the reformulation of blends is to understand the correlation of the level of liquid and free flow additive added in the flow behaviour of powders. Based on the experience along the years, formulators develop approximate equivalencies for the liquids and flow agents commonly used in their blended powders.

The filler powder is the bulk ingredient of the blend which helps the formulator to give weight to the blend using less expensive food powders. The challenge is to understand the effect of the particle and bulk properties of different fillers in the flow behaviour of the blended powders. At the moment, the selection of the type of filler is based on the experience of the formulator gained with previous blends with similar composition.

Once a possible composition of the reformulated blend is defined, the level of dust and the particle and bulk flow properties of the blend are measured to ensure that the new blend shows the desirable flow behaviour and level of dust. If different compositions are proposed, these new blends are characterised and compared with the flow behaviour of blends which show good behaviour under the extreme conditions of the process lines.

If the selected new blend compares favourably, factory trials will be run on a trial one tonne batch under a range of conditions to assess the reliability of the discharge behaviour. In the event that the reformulated blend is significantly worse than desirable standards, then the blend will be reformulated at a lab scale by making a series adjustments to either the free flow type or the balance of free flow and liquid, or changing the filler type so that pilot scale manufacturing trials can be undertaken again.

2.7 *Summary*

In this chapter, the measurement methods for particle and bulk flow properties of powders, the theoretical links between particle and bulk scale, published research studies linking particle and bulk flow properties of particulate materials and the common industrial practice for blended powders have been reviewed in details.

From the published work found in the literature, it can be appreciated the lack of practical understanding of the links between the particle and bulk flow properties for real single and blended powders. The analytical models and research studies found in the literature were developed under ideal conditions and in most cases using idealised particulate materials with no proven application to predict the bulk flow properties of real blended powders.

It is important to highlight the work developed by Rabinovich in the last decade looking at the development of the understanding of the links between particle and bulk flow properties. In 2003, Rabinovich (Johanson et al. 2003) developed a first approximation model linking capillary forces between particles to unconfined failure strength of powders with moisture content. It showed that this topic is a very broad research area and still a lot of work needs to be done by the future generations.

Standard characterisation testing techniques for powders at particle and bulk scale were reviewed in order to identify the suitable testing techniques for the purposes of the research. It was important to determine which measurement methods and particle

and bulk parameters are commonly used in the food industry to characterise powders. The information required for the task was gathered visiting industrial partner's plants and other food companies in the UK. This led to establish the testing techniques and the variables of the particle system that would be considered in this work as the purpose was to develop a test protocol for industry.

Existing well-established analytical models linking particle and bulk scale were reviewed in order to discern the potential useful models for this research. Several models have been developed for single powders considering packing structure, interparticle forces, liquid bridges and the effect of free flow agents. However, no well-established analytical model to predict the bulk flow properties of multicomponent blended powders was found in the literature.

Chapter 3 Characterisation of materials

3.1 *Introduction*

This chapter covers the standard characterisation tests undertaken and materials tested in order to build up the data base on which the research methodology and modelling strategy outlined in chapter 4 and 5 respectively is based on.

The key objective of this project is to develop the modelling strategy outlined in chapter 5 to predict the bulk flow properties of a blended powder based on the knowledge of the properties of the blend components. To meet this objective, it is required to characterise the particle properties, bulk flow properties and liquid properties of a large number of materials (approximately 40 particulate materials and 6 liquids) using standard techniques that are commonly used in process industries as the main objective is to develop a protocol for industry.

This chapter presents the test equipment and test procedures used in this research to: obtain samples for testing in section 3.2, characterise the particle properties in section 3.3, characterise the bulk flow properties in section 3.4 and characterise the liquid properties in section 3.5. For the common liquids and particulate materials used in food industry, details of the results from the characterisation tests undertaken are presented in section 3.6 and a summary of the chapter is presented in section 3.7

3.2 *Sampling and tests conditions*

Particle property, bulk flow property and liquid characterisation tests have been undertaken for a wide range of food grade powders provided by the industrial partners and other idealised standard materials selected for the research. A summary of properties of the food grade materials and additives and the properties of the idealised materials are presented in tables 10 - 25; table 26 shows the properties of the liquids used in this research.

The general characterisation tests of particle properties and bulk flow properties were undertaken under atmospheric conditions in the laboratories of The Wolfson Centre which are 15 to 20 °C and 45 to 50 %HR. These laboratories are equipped with a climate chamber which was used to prepare samples and test powders in specific test conditions when it was required. Prior to testing all particulate materials and liquids were stored in the laboratory in air tight containers.

In this research, it was necessary to measure the flow properties of prepared blends of multiple components or of materials prepared with controlled liquid contents and free flow additive levels and in this process sampling was an important part of the process. The main objectives of sampling are primarily ensuring that particle and bulk flow properties relate to the same sample and secondarily creating a data base of representative flow properties of the most common ingredients that industrial partners can use. Further details of the data base are disclosed in chapter 9 of the thesis. This data base is based on the sampling techniques explained in this section which are commonly used in the powder industry, therefore, a different sampling methods may lead to different results; in such a case, users of the test protocol developed in this work are advised to exercise caution when using data available in the data base running further repeated tests to ensure consistency of the results.

It is important to highlight the fact that the containers and sacks of powders received from industrial partners to be characterised at The Wolfson Centre may not be representative of the whole batch mixed in the industrial plants, however, tests undertaken at industrial partners' plant making the reformulated flavour of the case study (see chapter 4, section 3) for different batches from one kilogram to one tonne showed no significant variation of the bulk flow properties measured using PFT shear tester. Therefore, characterisation tests undertaken with the powders received were considered representative of the industrial batches.

3.2.1 Dry single and blended powders

Samples of dry single powders were prepared to be subjected to characterisation tests; particle and bulk flow properties were measured using different techniques explained in the following sections of the chapter. Each technique requires different amount of sample volume but the quality of the samples in terms of representation of the powder must be remained. As an example, the samples volumes obtained from mechanical sieving are similar to the volume required to test the powders in the shear tester, therefore, shear cell material can be sieved. For laser diffraction technique, small sample volume is required and riffle boxes are needed to subdivide mechanical sieved samples.

Particulate materials were sent by industrial partners and suppliers in 5 kg containers or 25 kg sacks. Most of the food and idealised powders tested were easy or free

flowing and for these the technique chosen to obtain samples was spin riffing; an automatic device designed by The Wolfson Centre produces up to one kilogram samples, the powder is discharged from a hopper by vibratory movement and a divider head collets samples rotating at constant velocity. The amplitude of the vibration and the speed of the rotation can be adjusted separately depending on the characteristics of the powder.

Then sub-samples were obtained subdividing these using riffle boxes until the amount required for each characterisation test was generated. When comparable size fractions from the full size distribution were needed, samples obtained from the spin riffing were mechanically sieved until sufficient material was generated in each fraction. Particle size distribution was measured and compared for various sub-samples of different one kilogram samples of powders to make sure that segregation did not happen during hopper discharge in the spin riffing device. The same procedure was used to compare different sacks or containers of the same powder.

Sampling cohesive powders demanded different techniques because these are poor flow and sticky particulate materials composed by very fine particles; there is no tendency of segregation but may not be homogenous in their composition due to their prior history. These particulate materials were received in 5 kg containers; firstly the powders were mixed in their containers using a hand mixer at low speed (540 rpm), two beaters were used to mix the powders thoroughly. After that, one kilogram samples were gathered onto a flat surface until the whole container was poured. For each one kilogram batch, the agglomerates were broken and the powder was divided in half and quarters; opposite quarters were combined to obtain two 500g samples. The whole process of dividing samples in half and quarters was repeated with the 500g samples, 250g samples and so on until the required amount was obtained. Particle size distribution was measured and compared for various samples of different batches such as one kilogram and 500g samples to ensure the homogeneity of the samples to be tested. This procedure was also used to compare different containers of the same powder.

Samples of dry blended powders were prepared to form homogeneous blends using a 700 ml bowl capacity food chopper (Morphy Richards 48561 Chopper 400W 700ml Bowl Red). The mixing procedure and the equipment used replicated the mixing process at laboratory scale in the industrial partners' plants. These blends were

subjected to bulk flow property tests using PFT shear tester, therefore, the sample volume required was the volume shear cell. A 500g sample was used as a reference weight giving sufficient material to fill the shear cell in all cases.

Samples of each component of the blends were prepared as explained above; multi-component blends were made adding the amount of ingredients required in each blend based on the weight percentage (%wt) of each component in the total weight of the blend sample (500g). Constituents of the blends were blended at low speed (500 rpm) for 5 minutes in the 700 ml bowl capacity food chopper making sure the blends are homogeneously mixed. The bowl was rotated during mixing process to avoid fine particles sticking to the wall and the corners.

Particle size distribution was measured and compared before and after these mixed conditions for single powder samples to make sure that degradation and particle breakage did not happen during the mixing process. This is an important aspect of the process because one of the key points of the experimental tests programme is to compare the effect of particle size and shape of powders at specific conditions (see chapter 4, section 4). An additional level of fines or significant changes in the shape of the particles may lead to wrong conclusions.

3.2.2 Wet single and blended powders

Samples of wet single and blended powders were prepared to be subjected to bulk flow property tests. A 700 ml bowl capacity food chopper was used to mix the dry powders with liquids such as de-ionised water and oil. Firstly, dry samples were prepared with no addition of liquid following the procedure explained in the previous section. After that, liquid was added to the dry single or blended samples for a wide range of content covering from 0.5%wt to 16%wt liquid content reaching the saturation of the powders. Different sizes of graduated pipettes were used to pour the liquid increasingly to the dry powders until reaching the weight percentage selected to be tested. This methodology was used to ensure that the final wet powders were homogeneously mixed and the liquid added was well distributed along the particles of the sample powders. An oil soluble called paprika oleoresin was used to evaluate the homogeneity of the wet blends. This oil is used as a colouring in the food industry so that the distribution of the oil in the blends can be evaluated visually.

3.2.3 Wet single and blended powders with free flow additives

Samples adding free flow additives to dry and wet single and blended powders were prepared to be subjected to bulk flow property tests. Using a 700 ml bowl capacity food chopper, the process explained above is repeated making dry blends before adding any liquid or free flow additive. Then wet blends were made repeating the process explained and finally the free flow additive was added in the percentage weight selected for each case. A 10ml and 20ml volume spoons were used to add the free flow additive increasingly until reaching the amount required to ensure the homogeneity of the final blend and its distribution along the particles of the sample powders. When liquid was not required, the additive was added to dry blends following the same procedure used for wet blends.

3.3 *Particle property measurements*

Particle size distribution and particle density have been measured and particle shape information has been obtained for all the single powders tested. Different techniques have been used to measure these properties to suit the characteristic particle properties of each powder as discussed in details in chapter 2.

3.3.1 Particle size and distribution

Due to the variations in the breadth of the particle size distribution (PSD) and levels of fines of the particulate materials to be measured, a range of different techniques had to be employed:

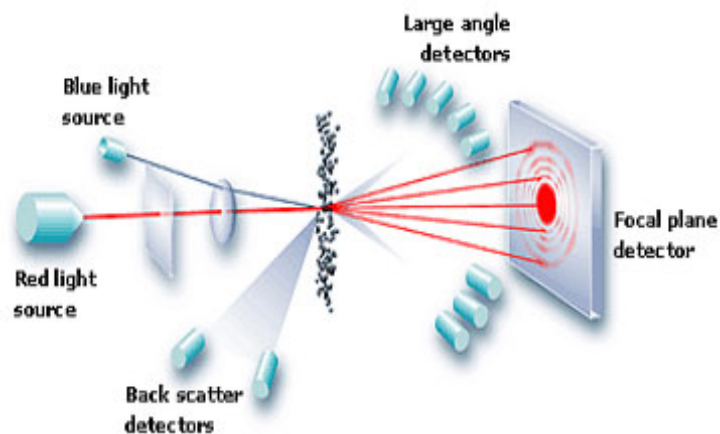
- Laser diffraction technique which can test a wide size range from 0.8 μm to 2 mm but does not actually measure the particle size (infers it from light scatter pattern as explained in chapter 2, section 2.2.1) and uses only a very small sample (1.5 ml) therefore is subject to sampling error.
- Mechanical sieving technique which measures a limiting intermediate particle dimension with a large sample volume (0.2 m^3) but only can test down to approximately 45 μm and may lead to particle degradation or agglomeration under certain conditions compromising accuracy.
- Air swept sieving technique which can accurately measure limiting intermediate particle dimension over the 10 to 200 μm range requiring a relatively small sample (20 g) but is extremely time consuming.

- Scanning electron microscopy (SEM) which can operate over a very wide size range from millimetres to 30 nm giving 2 dimensional images of a very limited number of particles (1-2g sample) from which particle size measurements can be obtained.

The laser diffraction and mechanical sieving techniques (disclosed in the literature review in section 2.2.1) which are shown in figures 21 and 22 are representative of the standard techniques used in the process industry and are used by all the project partners. Tables 4 and 5 present the test conditions for each technique including particulate materials tested, test sample volume, test time consuming and number of repetitions and range of sieve sizes tested when applicable.



a)



b)

Figure 21: Measuring device for the particle size distribution and laser diffraction technique a) Instrument to measure the particle size distribution of powders named Mastersizer 2000 b) Principles of the laser diffraction technique which is used in the Mastersizer 2000. Images obtained from the company website www.malvern.com



a)



b)



c)

Figure 22: Different sieving devices and test sieves a) Automatic PC – controlled device for sieve analysis processes named Gradex 2000 b) Digital sieve shaker named Octagon D200 Digital c) Standard test sieves for European specifications (40 mm depth and stainless steel frame). Images obtained from the company website www.rotex.com, www.glencreston.com and www.impact-test.com respectively

Powders tested	Laser diffraction	Mechanical sieving
Grades of lactose	●	
Whey powders	●	
Maltodextrin powders	●	
Dextrose	●	
Bread crumbs	●	
Rice flour	●	
Glass beads	●	●
Sodium chloride	●	●
Flow agents	●	

Table 4: *Particulate materials characterised with laser diffraction and mechanical sieving techniques*

Test conditions	Laser diffraction	Mechanical sieving
Sample volume	1.5 ml	0.2 m ³
Time consuming	5 minutes	20 minutes
Number of repetitions	3	3
Range of sieve sizes	Not applicable	56 – 425 µm

Table 5: *Test conditions of the laser diffraction and mechanical sieving techniques*

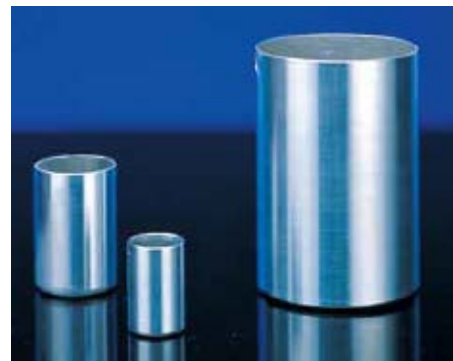
3.3.2 Particle density

Particle density is a measurement that is not commonly measured in the processing industry. However, the measurement of this particular property is crucial to determine the voidage of the particulate materials. For this reason, a material property data base was created with the food grades and idealised particulate materials tested. Literature values are available for a wide range of powders that can be used in the absence of a pycnometer. It must be highlighted that all the powders tested were non porous materials.

This property was measured using Ultracyc 1200e Pycnometer shown in figure 23 which operates with the Archimedes' principle of fluid displacement and gas expansion (Boyle's law); a nitrogen gas is used to penetrate into the voids of the sample materials and behaviour of an ideal gas is considered in the measurements. For blended powders, the particle density of the constituent ingredients of the blend must be measured individually. Table 6 presents the test conditions for this technique including volume of the cell used, test sample volume, test time consuming and number of repetitions.



a)



b)

Figure 23: Ultracyc 1200e Pycnometer and standard sample cells: a) Automatic Pycnometer b) Standard sample cells supplied in stainless steel (10, 50 and 135 cm³ nominal volume; 24, 40 and 49 mm internal diameter; 23, 39 and 75 mm internal depth). Images obtained from the company website www.quantachrome.com

Test conditions	Ultrapyc 1200e Pycnometer
Volume of the cell used	135 cm ³
Sample volume	90 cm ³
Time consuming	60 minutes
Average measured	40 runs per test
Number of repetitions	3
Gas used	Nitrogen

Table 6: Test conditions of the Ultrapyc 1200e Pycnometer technique

3.3.3 Particle shape

The particle shape of the powders was examined using scanning electron microscope SEM; limited tests were undertaken to obtain images at different range of magnifications depending on the particle size distributions of the sample materials. From these, the particle shape of powders was classified qualitatively using the terms explained in the literature such as equant, spherical, platy or elongate. These characterisation tests were undertaken by The School of Science at the University of Greenwich using SEM (JEOL JSM 5310 LV and Hitachi SU 8030 FE). This microscope does not required the sample to be coated in a film of gold leaf in order to retain particles during the measurement process, therefore, it gives a clear image of the particle shape and surface texture.

A quantitative study of the particle shape was not undertaken in this work because this would add an extra dimension to the experimental work and especially to the modelling work. In terms of experimental work, no shape factor has been found applicable to all possible kind of shapes (see chapter 2, section 2.2.3) and considering the wide range of materials to characterise, testing time taken might be increased by a factor of the number of shape factors considered. In terms of modelling work, the models found in

the literature review linking particle and bulk flow properties assumed spherical particles and the consideration of different particle shapes in the calibration of the models requires further studies to develop shape factors applicable to each model. This would also increase significantly the time required to finish this research work.

Table 7 presents the test conditions for this technique to obtain information of the particle shape including volume of the cell used, test sample volume, number of magnifications used, test time consuming and number of repetitions.

Test conditions	Scanning electron microscope SEM
Volume of the cell used	3.2 cm ³
Sample volume	3.2 cm ³
Time consuming	20 minutes per image taken
Number of repetitions	3
Range of magnifications used	20X to 2,000X

Table 7: Test conditions of the scanning electron microscope technique

3.4 Bulk property measurements

Bulk flow properties of the particulate materials such as flow function, friction function and bulk density have been measured using the Brookfield Viscometers Powder Flow Tester (PFT) shown in figure 24. While the modelling approach presented in chapter 5 could be used in conjunction with any shear tester, PFT was selected because this shear tester is used by all the project industrial sponsors for quality control and new products development as explained in chapter 1 of the thesis.

PFT shear tester can run a number of different tests but these were limited to only the standard flow function test. This generates a flow function, bulk density function and effective internal friction function which gives sufficient information to describe the flow

behaviour in a small core flow vessel that industrial partners use to process powders in the blended snack flavour industry.

The design of a mass flow hopper also requires information about the friction between the powder and the hopper wall. However, wall friction testing was considered outside the scope of this work as it would add another dimension to the experimental and modelling work. For instance, different wall materials may be considered for different applications therefore testing time taken might be increased by a factor of the number of the surfaces considered. The omission of wall friction is not so critical because project industrial sponsors' plants mostly operate in core flow.

The main focus of this research is to examine the links between the particle and the bulk flow properties and evaluate this link purely based on the internal strength of the powders. All tests were undertaken with the PFT using the standard volume cell (263 cc volume and 150 mm outer diameter) which limits the top particle size to 2 mm (adequate for the food grade and idealised powders tested) and has a maximum consolidation normal stress limit of 4.8 kPa. Table 8 presents the test conditions for the PFT including volume of the cell used, test sample volume, test time consuming and number of repetitions.

Measurements taken with the PFT for single and blended powders needed to be processed to convert the data from the derive consolidation stresses which vary due to the level of internal friction to a fixed consolidation stress for comparative purposes. A fitting equation was develop for this conversion (values required were interpolated between measurements) and a data base was created to evaluate the models developed at different levels of stress (2, 4 and 9 kPa) with the powders tested. More details of the interpolation of the measured values of the bulk flow properties of the particulate materials are presented in chapter 8.



Figure 24: Brookfield Powder Flow Tester (PFT) and components for sample preparation: a) the shear tester b) accessories to prepare samples using the standard volume cell (263 cc volume and 150 mm outer diameter). Images obtained from the company website www.brookfieldengineering.com

Test conditions	Brookfield Powder Flow Tester
Volume of cell used	263 cm ³
Sample volume	275 cm ³
Time consuming	60 minutes
Standard test run	Flow Function test
Number of repetitions	3

Table 8: Test conditions of the Brookfield powder flow tester technique

3.5 Liquid property measurements

Liquid properties such as density, viscosity and surface tension are measurements that are not commonly measured by industrial project partners. These are normally given by the suppliers in a limited range of tested conditions. The use of liquids in their snack flavours is reduced to one type of oil which is used for most of blended powders.

Miglyol oil 818 is used as a reference liquid in this research because its properties are similar to the ones of the oil mainly used by industrial partners. However, in terms of modelling, the use of various liquids to compare the effect of different viscosity and surface tension values is crucial to understand the flow behaviour of wet powders as explained in the literature review. Therefore, the effects of a wide range of liquids added at different proportions to single and blended powders were tested as presented in chapter 4, section 4.

The properties of these liquids were given by the suppliers at specific conditions (values of the density, viscosity and surface tension at 20°C) but in the absence of measured values, literature values are available for a wide range of liquids that can be used for properties such as surface tension.

To study the variation of the viscosity with temperature, these liquids were tested at 20°C and 25°C using LV DV3 Ultra rheometer. These characterisation tests were undertaken by Brookfield Viscometers Limited because The Wolfson Centre did not have the required equipment. A rheometer was used to measure the resistance of the Newtonian liquids to movement when a vane spindle was immersed in the liquid samples. Different rotational speeds (5-10 rpm and 10-50 rpm) were used due to the wide viscosity range of the liquids tested.

Table 9 presents the test conditions for the LV DV3 Ultra rheometer including, volume of the sample chamber used, rotational speeds, test sample volume, test time consuming and number of repetitions.

The density values of the liquids were measured under the atmospheric conditions of the laboratories of The Wolfson Centre (15°C to 20°C) and compared with the suppliers' values given at 20°C. Characterisation density tests were undertaken using a 20 ml graduated cylinder and a 3 decimal balance. The cylinder was weighed before and after pouring carefully the liquid to be measured. A pipette to reach 10 ml level accurately was used in the measurements. Density can be calculated knowing the mass and the volume of the liquids; the values obtained from these tests were in the range of the values given by the suppliers.

Test conditions	LV DV3 Ultra rheometer
Volume of the sample chamber	10 ml
Sample volume	7.1 ml
Time consuming	30 minutes
Rotational speeds	5-10 rpm and 10-50 rpm
Temperature tested	20°C and 25°C
Number of repetitions	3

Table 9: Test conditions of the LV DV3 Ultra rheometer

3.6 Results

As explained in the introduction, this section presents the results of the measured liquid, particle and bulk flow properties for a wide range of single powders and liquids characterised.

3.6.1 Particle characterisation

Particle properties of the more common food grade powders, free flow additives and idealised particulate materials are presented in this section. Table 10 - 18 shows the particle size and distribution and particle density of a wide range of food powders from very fine to coarse with different particle densities and the idealised particulate materials used in this work. The information of the particle shape was obtained for a limited number of powders because The Wolfson Centre does not have the required equipment and these characterisation tests undertaken by The School of Science at the University of Greenwich are very costly. Figures 25 and 26 show schematic representations of how the particle size distributions measured by weight and volume percentage are presented.

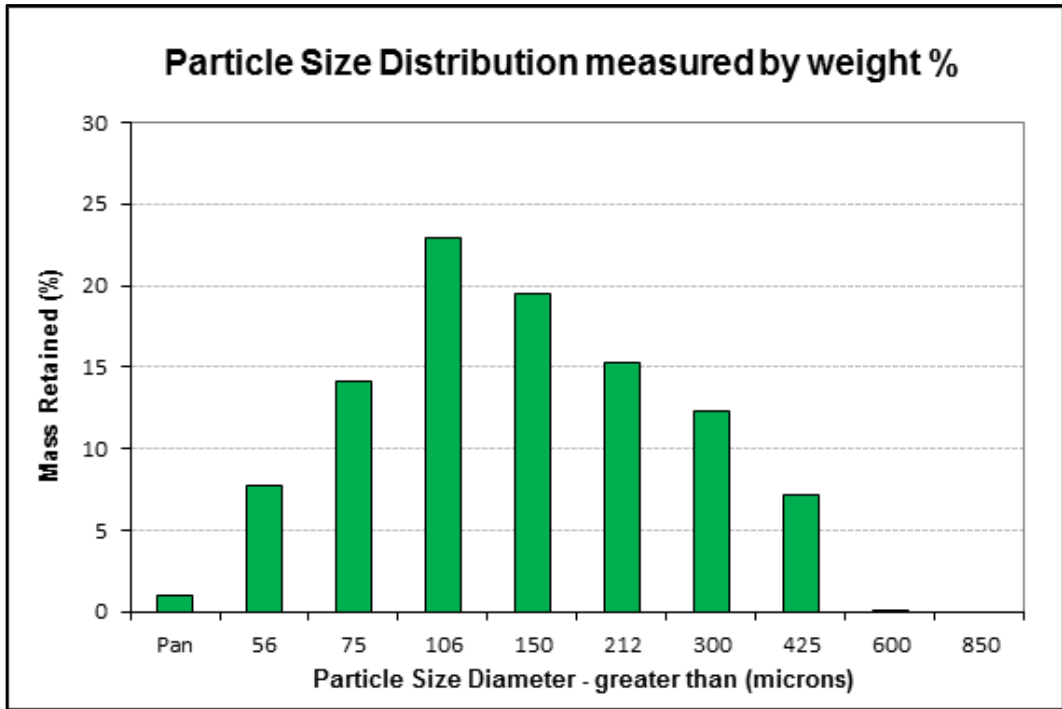


Figure 25: Schematic representation of a particle size distribution measured by weight percentage

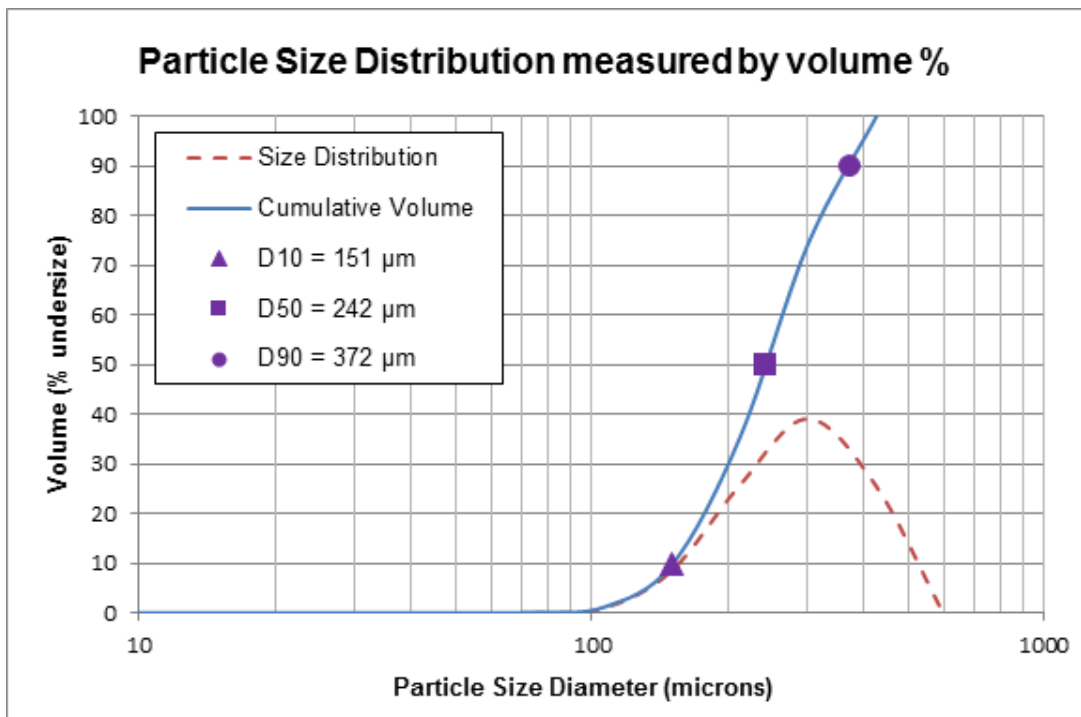


Figure 26: Schematic representation of a particle size distribution measured by volume percentage

Powder Name	D10 (µm)	D50 (µm)	D90 (µm)	Span (D90 – D10)	Particle density (kg/m³)
Lactohale 300	1	4	9	8	1584
Sorbolac 400	4	9	17	13	1567
Lactose 200	12	32	58	46	1560
Lactohale 200	32	70	112	80	1552
Inhalac 230	64	96	135	71	1547
Lactohale 100	75	100	148	73	1549

Table 10: Particle properties of 6 grades of lactose

Powder Name	D10 (µm)	D50 (µm)	D90 (µm)	Span (D90 – D10)	Particle density (kg/m³)
Whey PDR Lactose	12	67	172	160	1287
Whey PDR Protein	35	138	229	194	3277
Whey Dry Sweet	42	125	308	266	1439
Whey powder	74	130	324	250	1428

Table 11: Particle properties of different whey powders

Powder Name	D10 (µm)	D50 (µm)	D90 (µm)	Span (D90 – D10)	Particle density (kg/m³)
Maltodextrin Potato 8-14	10	35	73	63	1396
Maltodextrin Wheat 17-23	14	70	194	180	1417
Maltodextrin Maize 20-23	16	76	203	187	1512
Maltodextrin Potato17-20	23	65	233	210	1489

Table 12: Particle properties of different maltodextrin powders

Powder Name	D10 (µm)	D50 (µm)	D90 (µm)	Span (D90 – D10)	Particle density (kg/m³)
Rice Flour	16	82	185	169	1250
Bread crumbs	91	220	409	318	2450
Dextrose Wheat	51	185	574	523	1565
Dextrose	12	91	395	383	1563

Table 13: Particle properties of different fillers

Powder Name	D10 (µm)	D50 (µm)	D90 (µm)	Span (D90 – D10)	Particle density (kg/m³)
Crushed Glass	180	212	220	40	2600
Sodium Chloride	185	212	231	46	2160
Sodium Chloride Mesh 60	76	187	264	188	2160
Microfine Sodium Chloride	7	24	56	49	2160

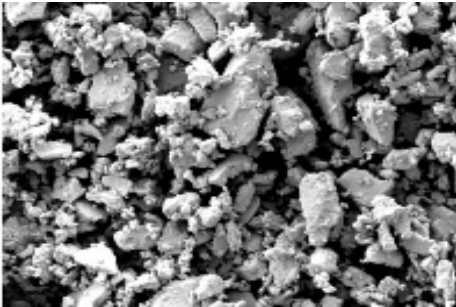
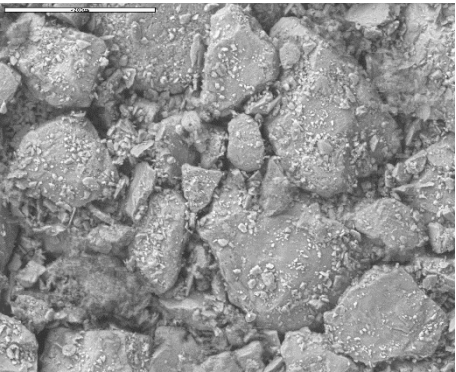
Table 14: Particle properties of idealised powders

Powder Name	D10 (µm)	D50 (µm)	D90 (µm)	Span (D90 – D10)	Particle density (kg/m³)
Glass Beads	10	33	50	40	2600
Glass Beads	20	45	60	40	2600
Glass Beads	40	63	80	40	2600
Glass Beads	90	112	130	40	2600
Glass Beads	190	212	230	40	2600
Glass Beads	320	338	360	40	2600

Table 15: Particle properties of 6 grades of glass beads

Flow Agent Name	D10 (µm)	D50 (µm)	D90 (µm)	Span (D90 – D10)	Particle density (kg/m³)
Silicon Dioxide	2	5	12	10	3215
Tricalcium Phosphate	1	3	7	6	3352
Magnesium Carbonate	1	5	17	16	2137

Table 16: Particle properties of different flow agents

Powder	SEM Image of the powder
Lactohale 300 (1µm scale) Angular shape	
Dextrose (200µm scale) Shard shape	

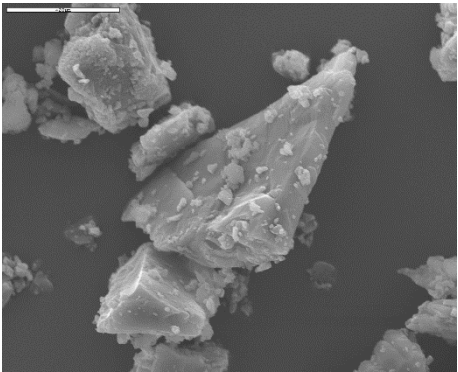

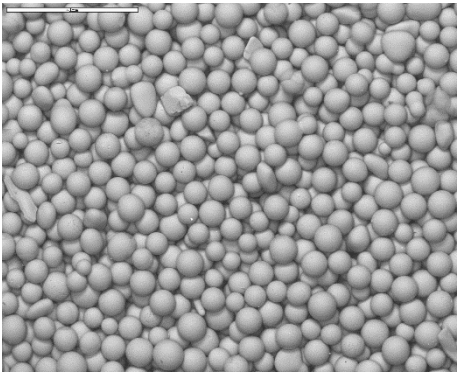

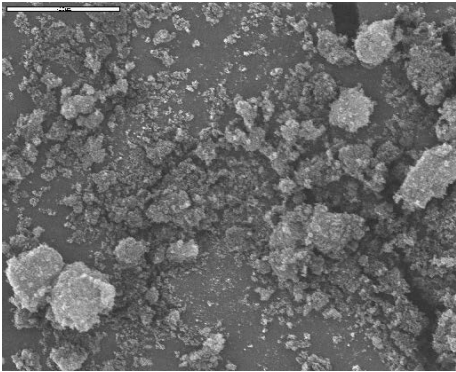
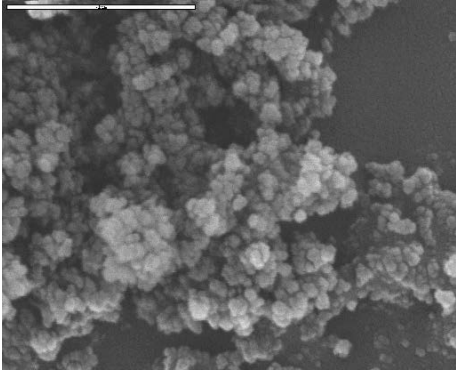
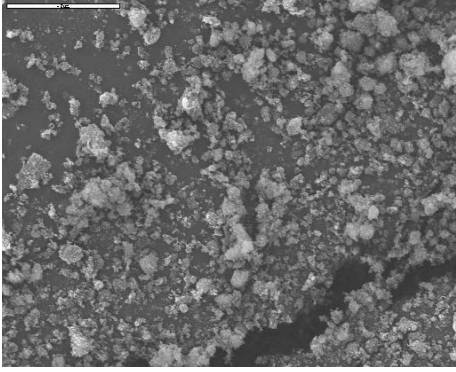
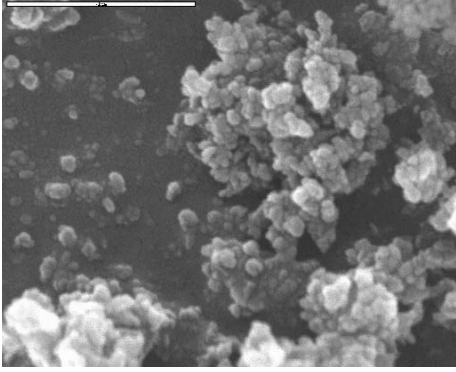
<p>Maltodextrin Wheat 17-23 (200μm scale) Shard shape</p>	
<p>Sodium Chloride (1mm scale) Cubic shape</p>	
<p>Glass Beads (1mm scale) Spherical shape</p>	
<p>Crushed Glass (1mm scale) Angular shape</p>	

Table 17: SEM images of particulate materials

Flow agent	SEM Image of the free flow additive
Silicon Dioxide (20 μm scale)	 Scanning electron micrograph (SEM) showing the morphology of Silicon Dioxide at a 20 micrometer scale. The image displays a dense, granular material with irregular, angular particles and some larger agglomerates. A white scale bar is visible in the top left corner of the image area.
Silicon Dioxide (1 μm scale) The image shows agglomerates of 1 to 10 μm	 Scanning electron micrograph (SEM) showing the morphology of Silicon Dioxide at a 1 micrometer scale. The image reveals a highly agglomerated structure, with individual particles appearing as small, rounded or angular units clustered together into larger, irregular agglomerates. A white scale bar is visible in the top left corner of the image area.
Tricalcium Phosphate (20 μm scale)	 Scanning electron micrograph (SEM) showing the morphology of Tricalcium Phosphate at a 20 micrometer scale. The image shows a granular material with irregular, angular particles and some larger agglomerates, similar in appearance to the Silicon Dioxide at the same scale. A white scale bar is visible in the top left corner of the image area.
Tricalcium Phosphate (1 μm scale) The image shows agglomerates of 1 to 10 μm	 Scanning electron micrograph (SEM) showing the morphology of Tricalcium Phosphate at a 1 micrometer scale. The image displays a highly agglomerated structure, with individual particles appearing as small, rounded or angular units clustered together into larger, irregular agglomerates, similar to the Silicon Dioxide at the same scale. A white scale bar is visible in the top left corner of the image area.

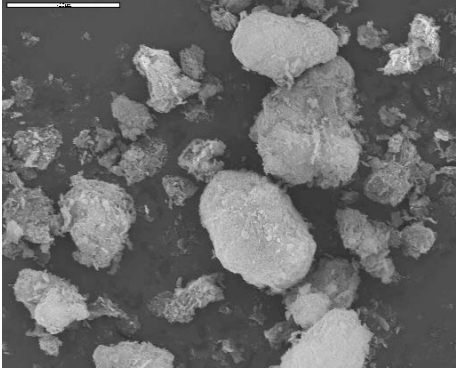
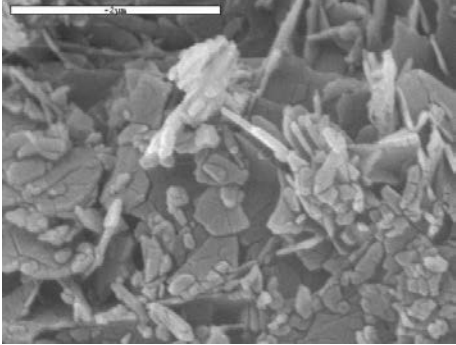
<p>Magnesium Carbonate (20μm scale)</p>	
<p>Magnesium Carbonate (1μm scale) The image shows agglomerates of 10 to 20μm</p>	

Table 18: SEM images of free flow additives

3.6.2 Bulk characterisation

The bulk flow properties (flow function, bulk density and effective internal friction) of the more common food grade powders, free flow additives and idealised particulate materials are shown in tables 19 - 25. Figures 29 - 37 show the wide range of bulk flow properties which can be measured or calculated to characterise particulate materials. These figures show the following flow properties for six grades of lactose:

- Flow function and arch span (normalised flow function)
- Bulk density, compaction curve and voidage
- Friction function, internal friction, cohesion and tensile strength

As explained in chapter 1, the two principal flow obstructions to flow are arch and rat-hole (see figure 2). For each single or blended powder, there is a minimum outlet dimension to avoid cohesive arch and cohesive rat-hole during the discharge which are called the critical rat-hole and the critical arching diameters. Arch span is defined as the critical arching diameter for plane and conical hoppers and represents the largest arch that a powder can support before collapsing under its self-weight. In this research, arch span has been calculated as shown in figure 34 assuming conical

hoppers (the value of the arch span for conical hoppers is twice as the one for plane hoppers). The representation of the consolidation stress vs arch span (see figure 34) is named normalised flow function and provides a comparison of the potential critical arching diameter of powders with different bulk flow properties. This is a version of the flow function graph (see figure 10) disclosed in the literature review and gives a better comparison for powders with very different flow behaviour.

During the preliminary studies undertaken to characterise the flow behaviour of blended powders with good and poor flow in the partner's industrial process lines explained in chapter 4, section 4.3 of the thesis, the bulk flow properties of different flavours were measured repeating the standard flow function test six times using the Brookfield Powder Flow Tester (PFT).

The objective was to study the repeatability of the results obtained from the PFT and the results for the snack flavour named Flame Grilled Steak are shown in figures 27 and 28. The error bars of these figures represent the standard deviation at 95% confidence interval which shows the good repeatability of the results.

Furthermore, results of seven repeat flow function tests for CRM-116 limestone powder presented in the comparison study of the PFT with other shear testers (Berry et. al 2014) confirm the good repeatability found in this research. For this reason, values of the bulk flow properties presented in this thesis represent the results of a single standard flow function test for each single and blended powder tested.

From the results presented in this section for six size fractions of lactose tested, it is important to highlight that the effect of agglomeration of fine particles is shown in figure 31; inspection of this figure shows that at low consolidation stresses, the fine particles of size fractions of lactose with D50 equal to 4 and 9 μm are agglomerating resulting in a lower friction than the coarser size fraction of lactose with D50 equal to 32 μm .

Another detail which needs to be highlighted is the scale in the horizontal axis in figures 32 and 33. The bulk density is measured during the standard flow function test (see figure 30) but it can also be measured by a specific test called bulk density test. This test only gives the values of the compaction curve of the powder at different levels of consolidation stress and the maximum compaction load applied to the powder is 5 kPa. Figure 32 and 33 show the compaction curve measured by the bulk density test and the voidage calculated based on this specific compaction curve.

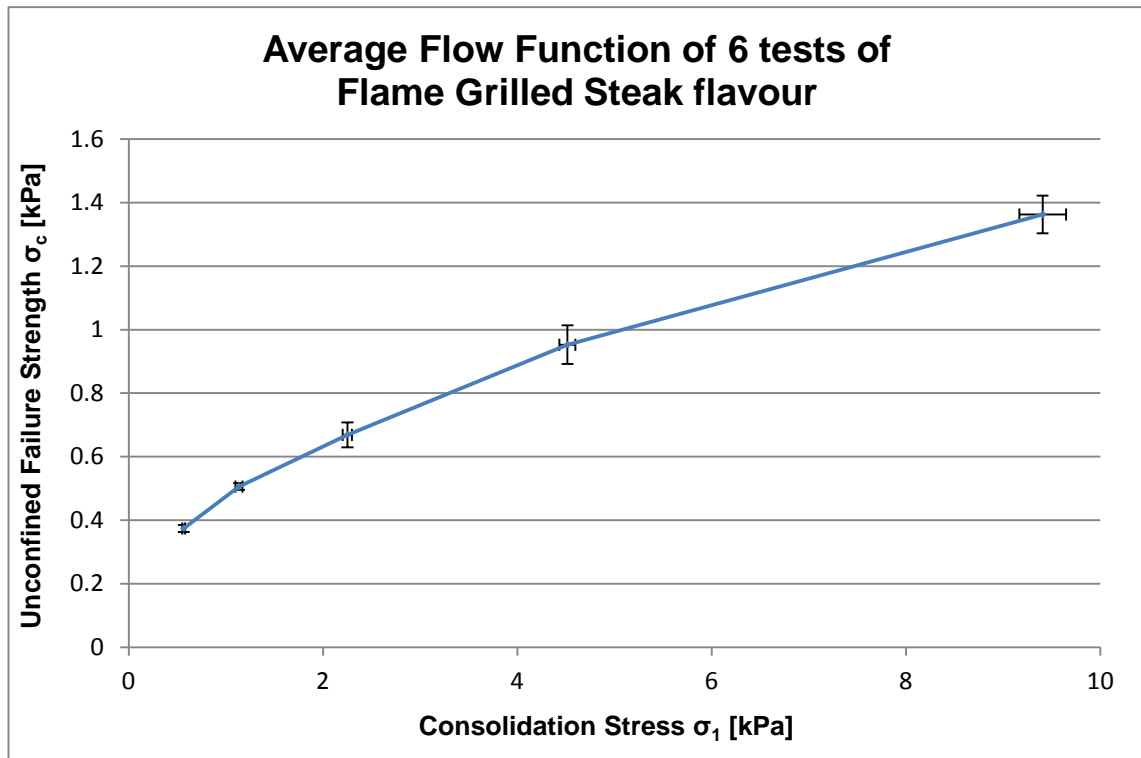


Figure 27: Average Flow Function of six standard flow function tests for a snack flavour named Flame Grilled Steak

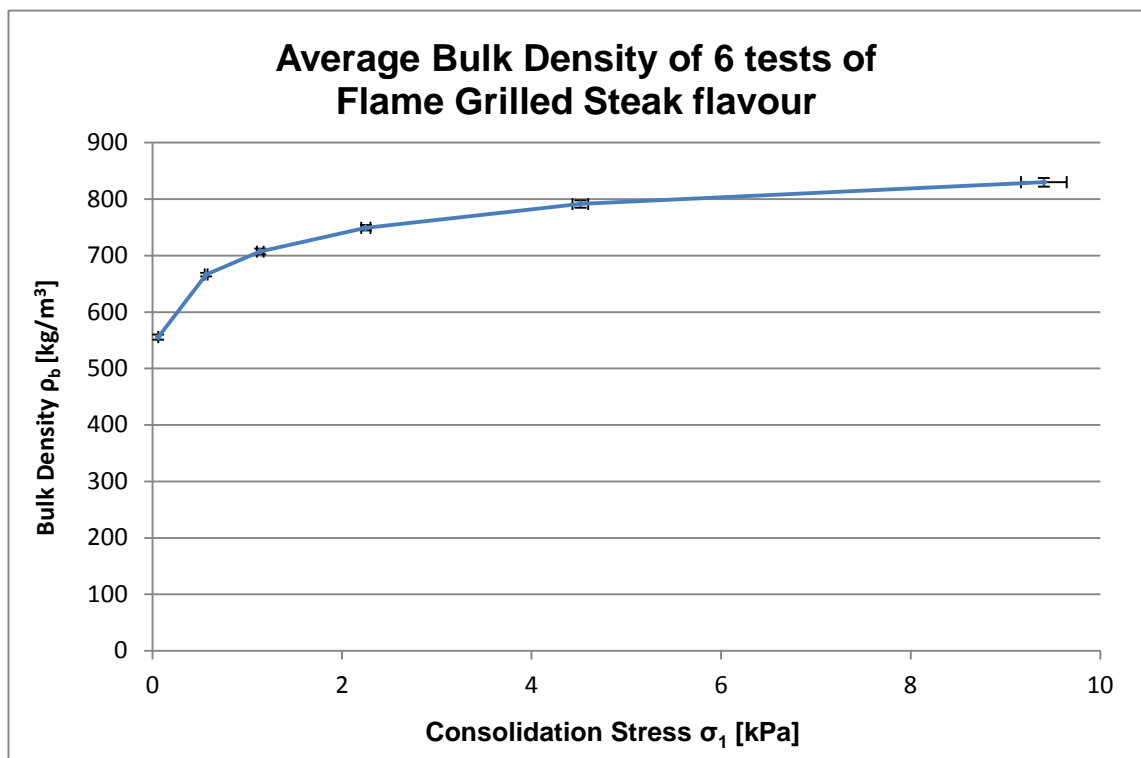


Figure 28: Average Bulk Density of six standard flow function tests for a snack flavour named Flame Grilled Steak

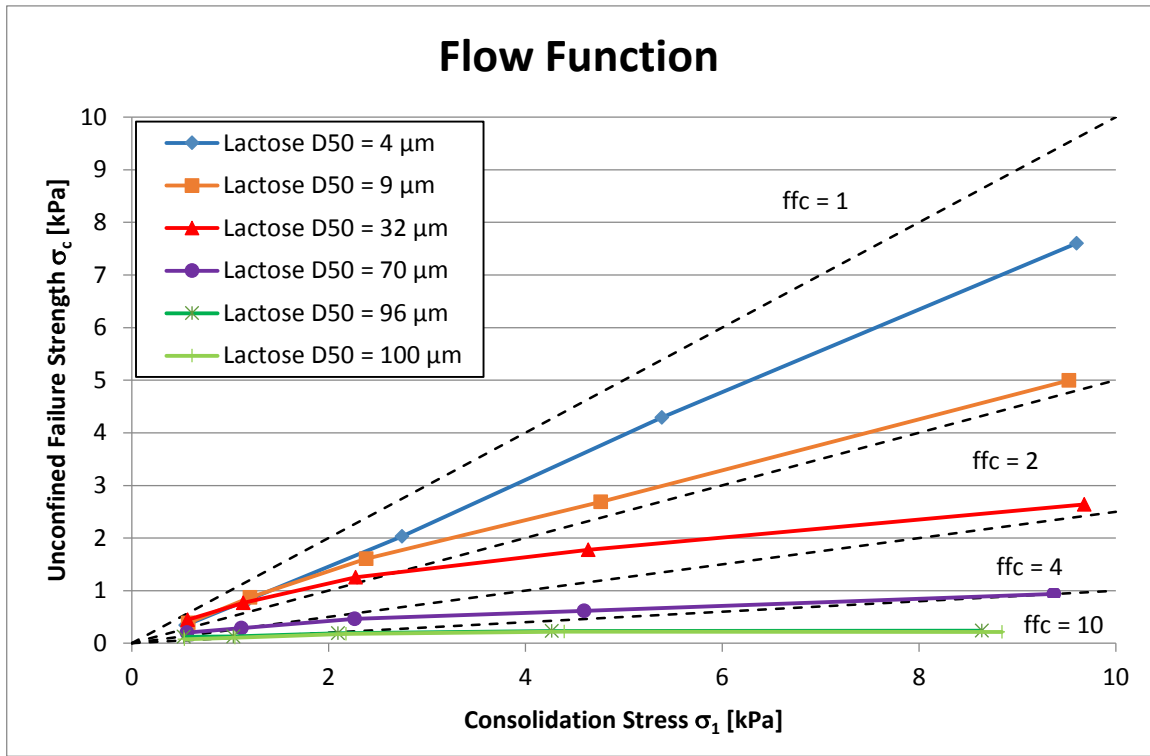


Figure 29: Flow function of six grades of lactose

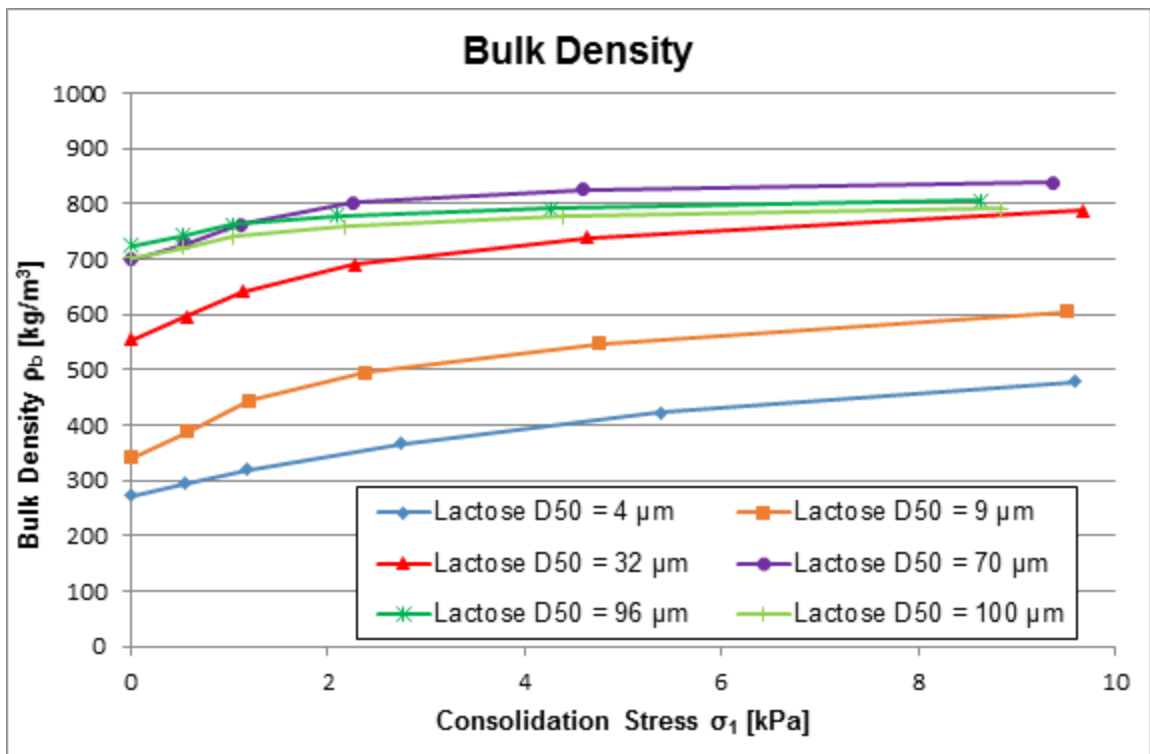


Figure 30: Bulk density of six grades of lactose

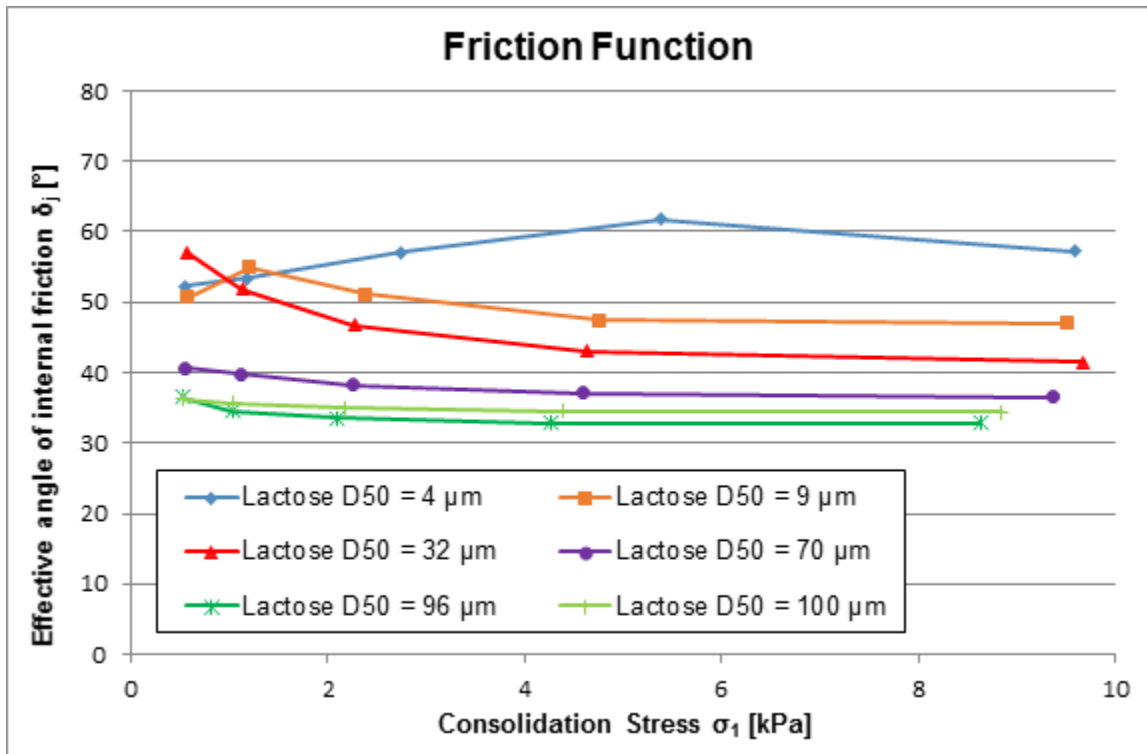


Figure 31: Friction function of six grades of lactose

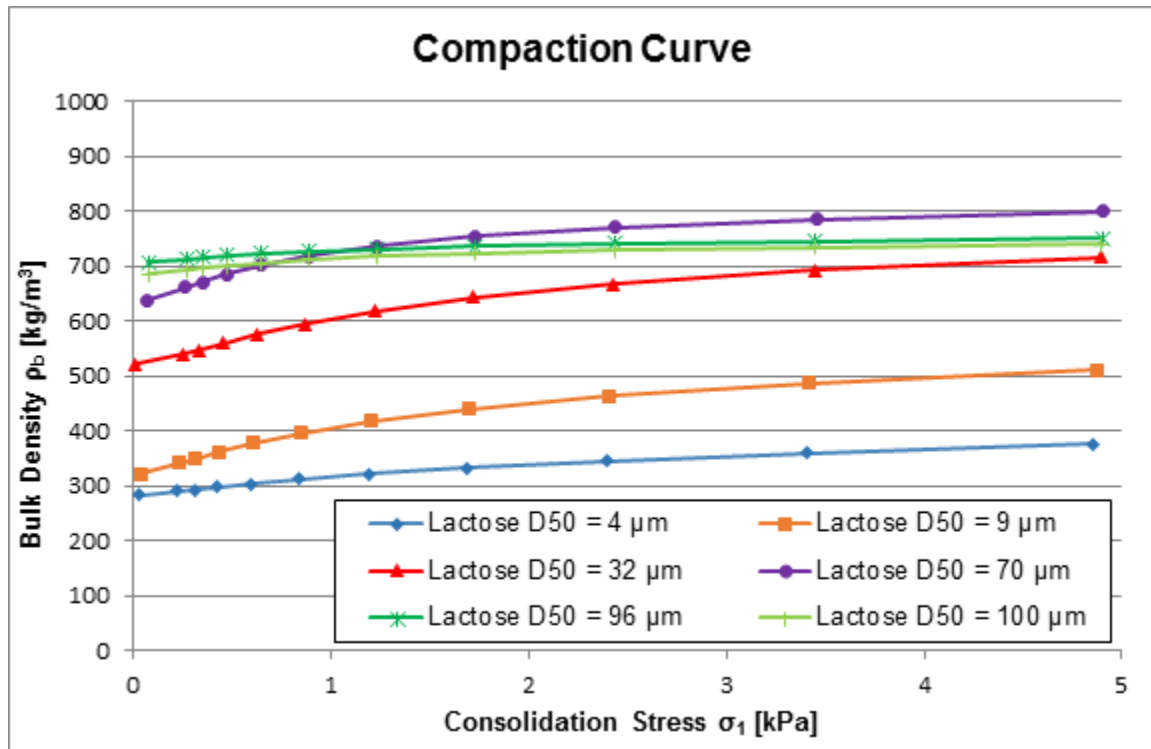


Figure 32: Compaction curves of six grades of lactose

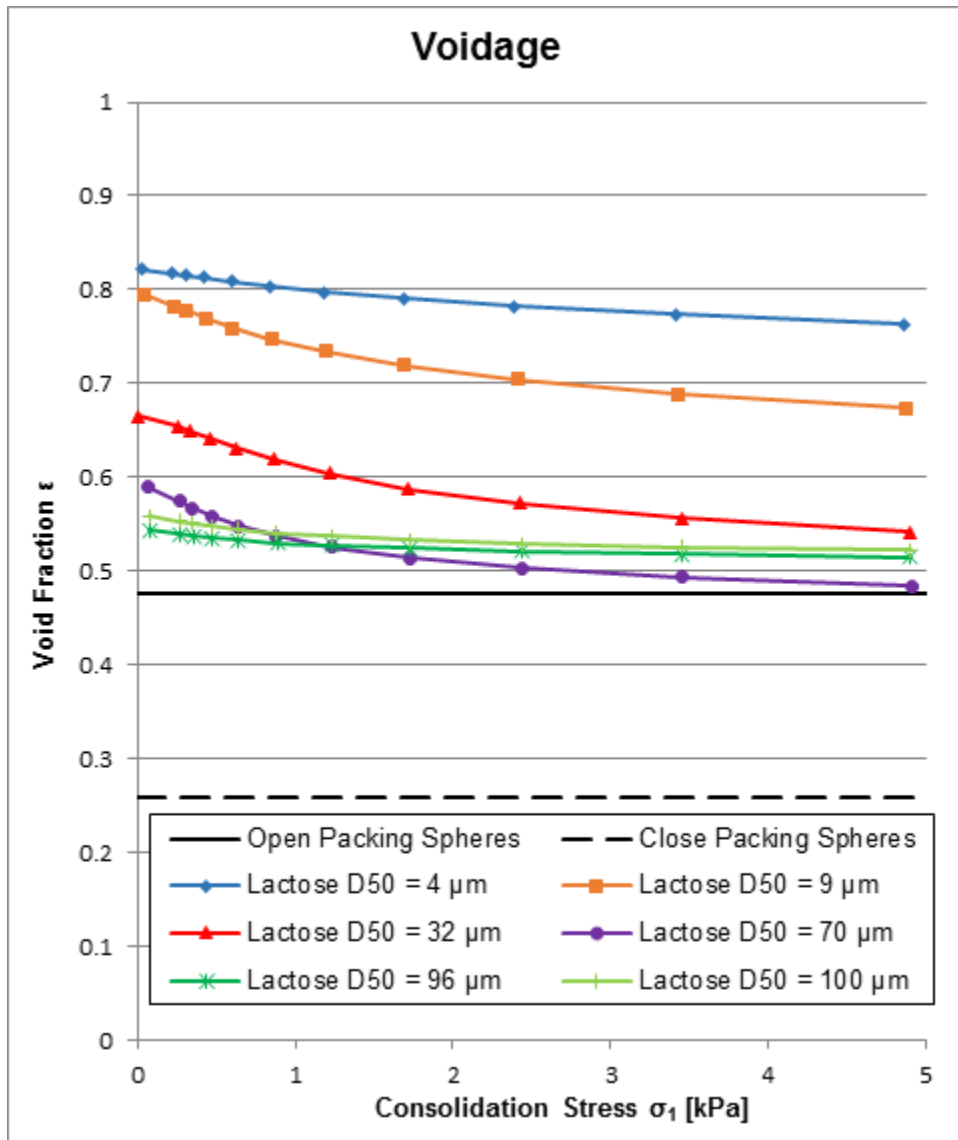


Figure 33: Voidage of six grades of lactose

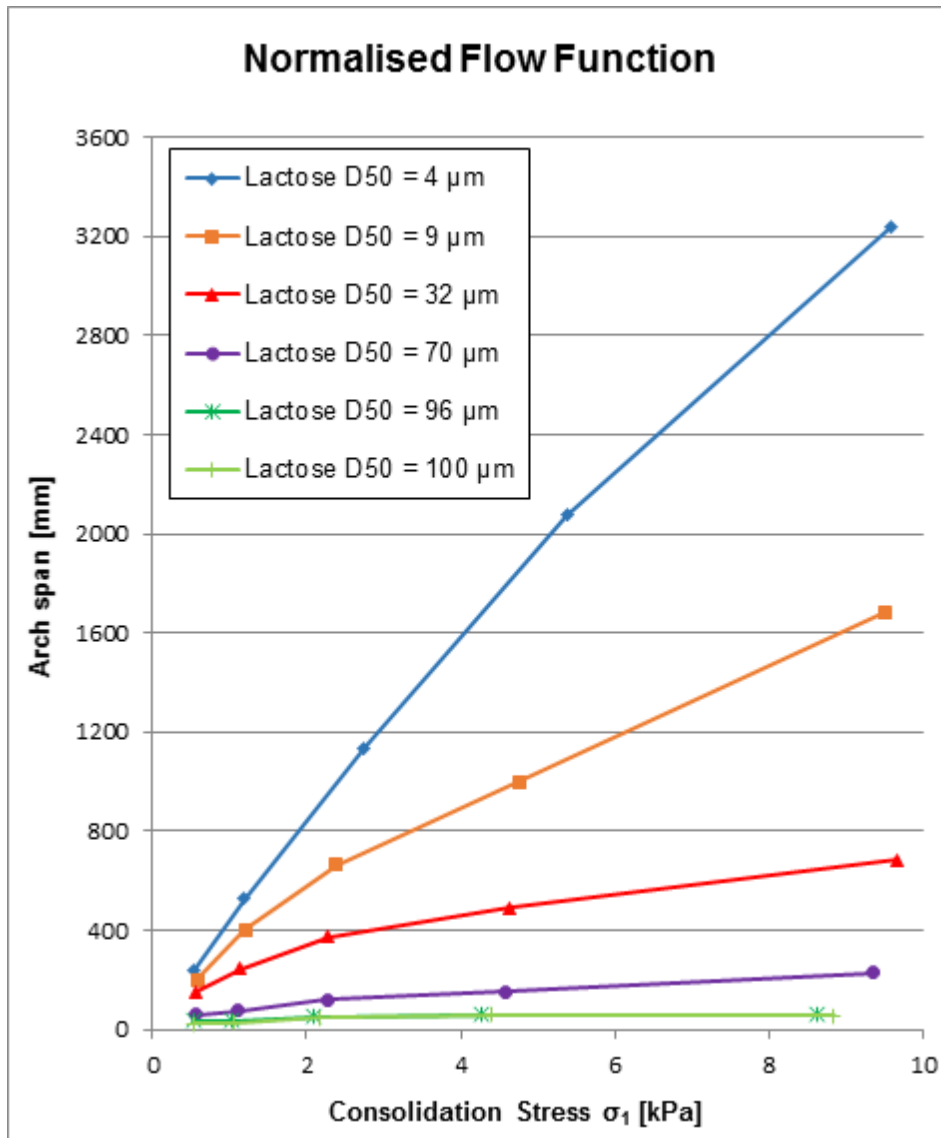


Figure 34: Arch span of six grades of lactose

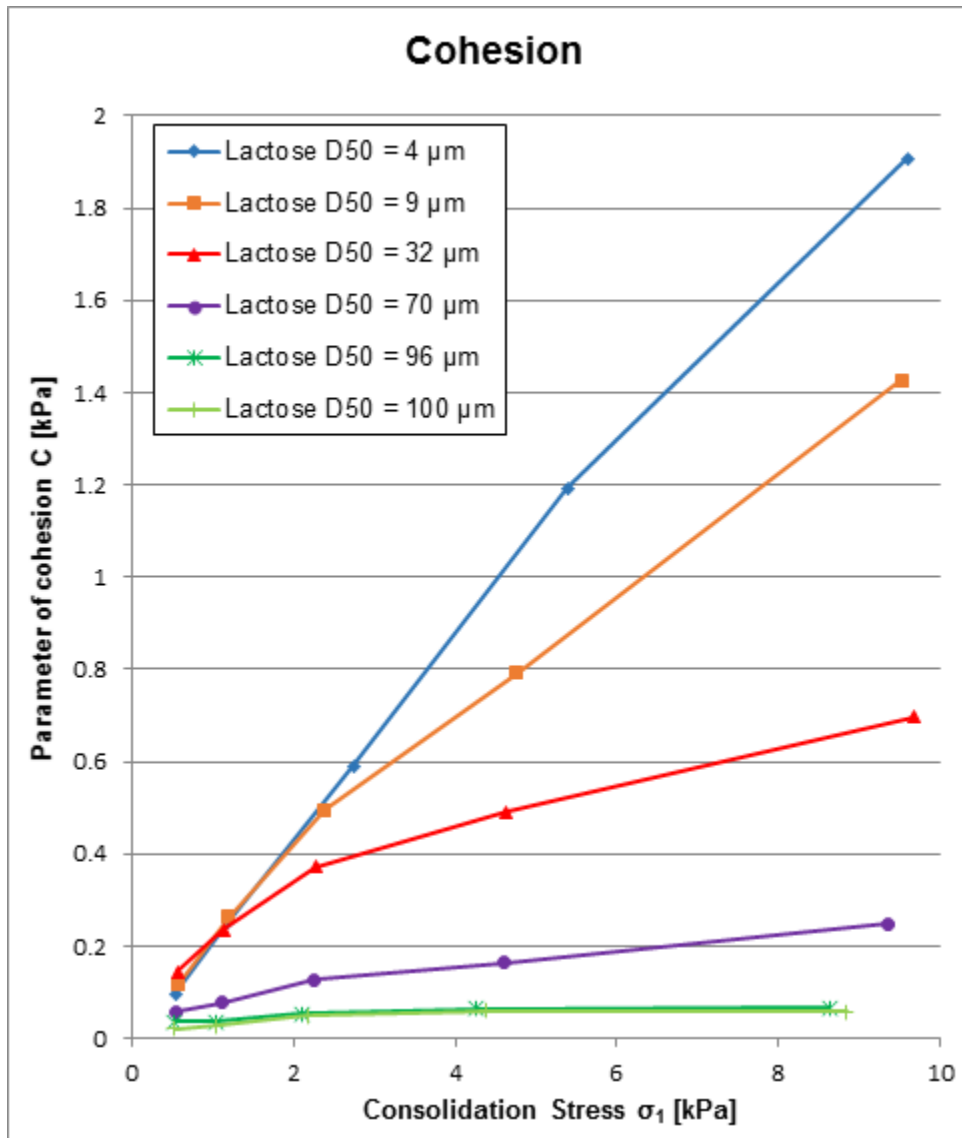


Figure 35: Cohesion of six grades of lactose

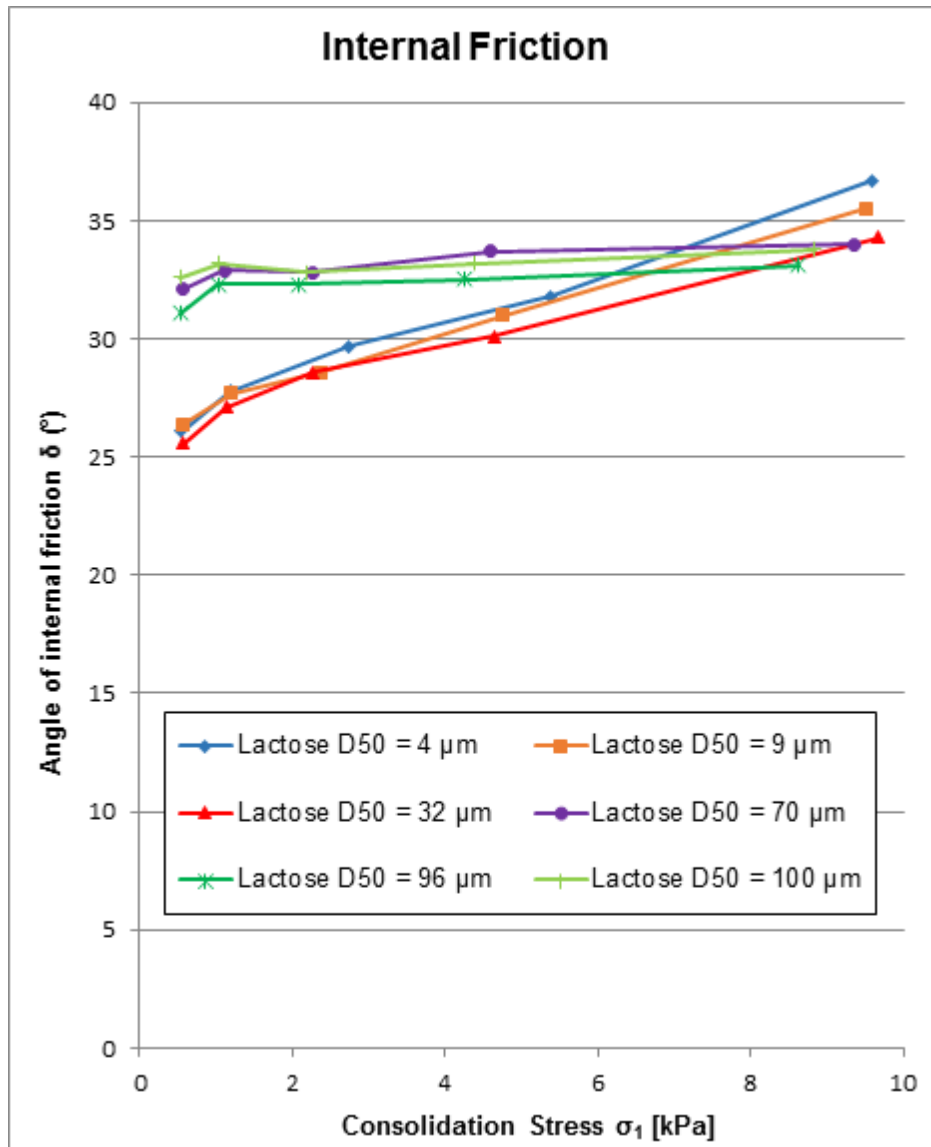


Figure 36: Internal friction of six grades of lactose

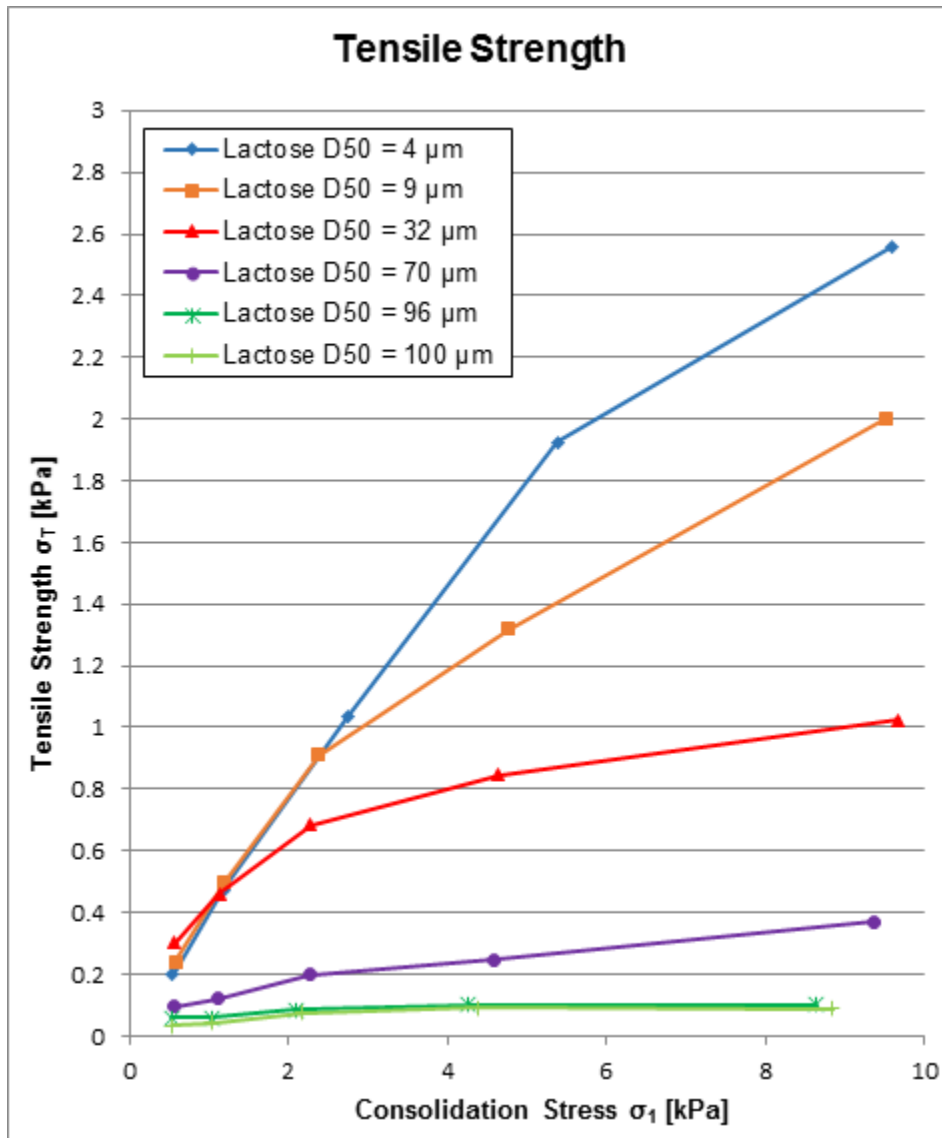


Figure 37: Tensile strength of six grades of lactose

	Bulk flow properties at 9 kPa of consolidation stress		
Name of the powder	Effective internal friction δ_j [°]	Bulk density ρ_b [kg/m ³]	Unconfined strength σ_c [kPa]
Lactohale 300	57.3	478	7.615
Sorbolac 400	47.2	605	4.958
Lactose 200	41.5	788	2.639
Lactohale 200	36.5	815	0.936
Inhalac 230	32.8	805	0.238
Lactohale 100	34.4	791	0.218

Table 19: Bulk flow properties of six grades of lactose

	Bulk flow properties at 9 kPa of consolidation stress		
Name of the powder	Effective internal friction δ_j [°]	Bulk density ρ_b [kg/m ³]	Unconfined strength σ_c [kPa]
Whey PDR Lactose	43.6	759.9	1.332
Whey PDR Protein	33.1	899.9	0.288
Whey Dry Sweet	39.3	759.1	1.119
Whey powder	42.3	667.2	0.871

Table 20: Bulk flow properties of different whey powders

Bulk flow properties at 9 kPa of consolidation stress			
Name of the powder	Effective internal friction δ_j [°]	Bulk density ρ_b [kg/m ³]	Unconfined strength σ_c [kPa]
Maltodextrin Potato 8-14	35.4	615.9	1.077
Maltodextrin Wheat 17-23	36.5	652.8	1.218
Maltodextrin Maize 20-23	35.4	650.8	0.997
Maltodextrin Potato17-20	36.9	650.5	1.443

Table 21: Bulk flow properties of different maltodextrin powders

Bulk flow properties at 9 kPa of consolidation stress			
Name of the powder	Effective internal friction δ_j [°]	Bulk density ρ_b [kg/m ³]	Unconfined strength σ_c [kPa]
Rice Flour	45.6	939.7	2.861
Bread crumbs	33.1	922.9	0.705
Dextrose Wheat	33.1	1049.1	0.304
Dextrose	36.6	1017.4	1.183

Table 22: Bulk flow properties of different fillers

Bulk flow properties at 9 kPa of consolidation stress			
Name of the powder	Effective internal friction δ_j [°]	Bulk density ρ_b [kg/m ³]	Unconfined strength σ_c [kPa]
Crushed Glass	34.5	1379.7	0.252
Sodium Chloride	31.8	1248.7	0.128
Sodium Chloride Mesh 60	32.5	1307.5	0.247
Microfine Sodium Chloride	56.5	817.8	7.738

Table 23: Bulk flow properties of idealised particulate materials

Bulk flow properties at 9 kPa of consolidation stress			
Name of the powder	Effective internal friction δ_j [°]	Bulk density ρ_b [kg/m ³]	Unconfined strength σ_c [kPa]
Glass Beads D50 = 33 μm	30.1	1486.6	0.618
Glass Beads D50 = 45 μm	24.6	1525.5	0.336
Glass Beads D50 = 63 μm	22.6	1642.6	0.205
Glass Beads D50 = 112 μm	23.5	1609.8	0.128
Glass Beads D50 = 212 μm	22.8	1656.9	0.125

Table 24: Bulk flow properties of six grades of glass beads

	Bulk flow properties at 9 kPa of consolidation stress		
Name of the powder	Effective internal friction δ_j [°]	Bulk density ρ_b [kg/m ³]	Unconfined strength σ_c [kPa]
Silicon Dioxide	38.5	234.5	2.756
Tricalcium Phosphate	46.4	510.2	5.128
Magnesium Carbonate	44.8	298.4	5.236

Table 25: Bulk flow properties of different flow agents

3.6.3 Liquid characterisation

Table 26 shows the properties of the liquids (density, viscosity and surface tension) used in this work. These oils show a decrease in viscosity values with increasing temperature; a 5 degree temperature rise resulted in a drop in the viscosity values by approximately 5 to 15 mPa.s, being larger for the more viscous oils. Only Miglyol oil 829 with a viscosity value of 270 mPa.s at 20°C shows a large drop in viscosity with increasing temperature, a 5 degree temperature rise resulted in a drop in the viscosity values by approximately 66 mPa.s.

Liquid	Viscosity (mPa.s)	Surface tension (mN/m)	Density (Kg/m³)
Water	1	73	1000
Miglyol 818	33	30	940
Miglyol 829	270	30	1000
Miglyol 840	10	30	910
Olive oil	80	33	900
Sunfloweroil	75	33	940

Table 26: *Liquid characterisation of different liquids*

3.7 Summary

As the main objective of the project is to develop a test protocol to predict and optimise the flow behaviour of blended powders utilising particle to bulk scale models, the knowledge of the properties of the blends and their constituents plays an important role in this research work.

This chapter presents a complete description of the standard characterisation techniques used at liquid level, particle and bulk scale for a wide range of particulate materials and liquids used in this work. Details of each technique are presented including materials tested, volume of the cell used, test sample volume, test time consuming and number of repetitions.

Sampling is a key factor to ensure that the particle and bulk scale relate to the same sample; different techniques to prepare representative samples depending on the characteristics of the powders are explained along with the methodology applied to avoid problems such as segregation or heterogeneity of the samples.

The results of the characterisation tests were used to create a data base on which the research methodology and modelling strategy described in chapter 4 and 5 respectively is based on.

Chapter 4 The structure of the investigation

4.1 Introduction

This chapter presents the research methodology applied in this work; the approach taken is explained in detail along with the experimental investigations undertaken to understand the links between the particle and the bulk flow properties. The challenge was to develop a practical understanding of how to control powder flowability with applications to the blended food powder industry and how to predict the effect on the bulk flow properties of changes to the:

- Particle size
- Blend constituent ingredients
- Flow additive level and type (liquid content and/or free flow content)

The academic challenge is in applying/developing existing particle to bulk scale models so that they can be used to assist industrial users to understand how to control powder flowability.

4.2 Research methodology

The research approach can be divided into two different investigations; one investigation was to undertake a series of specific tasks to meet the requirements of the project industrial partners. These tasks are expanded in section 4.3 of the chapter and were to:

- Measure the particle and flow properties of a wide range of relevant materials used by industrial partners in their blends in order to build up a database of flow properties that can be used for the test protocol as disclosed in details in chapter 9.
- Survey the flow property-related handling issues disclosed in chapter 1 and currently present in the plants of the food industry partners, and determine the “window” of flow properties which would result in most desirable flow behaviour based on the experience of industrial partners and the level of modifications needed to reach this window. A target to aim for in terms of flow behaviour was defined based on the window of flowability of known flavours in partners plant measuring the flow properties of powders that exhibit flow problems to quantify how cohesive they are; measuring the flow properties of materials that are too

free flowing or dusty and quantifying the flowability and cohesion of these; then testing materials that flow acceptably which will lie between the two limits. Flavours with poor and good flow behaviour under extreme conditions were tested and compared as shown in figures 38 and 39 below.

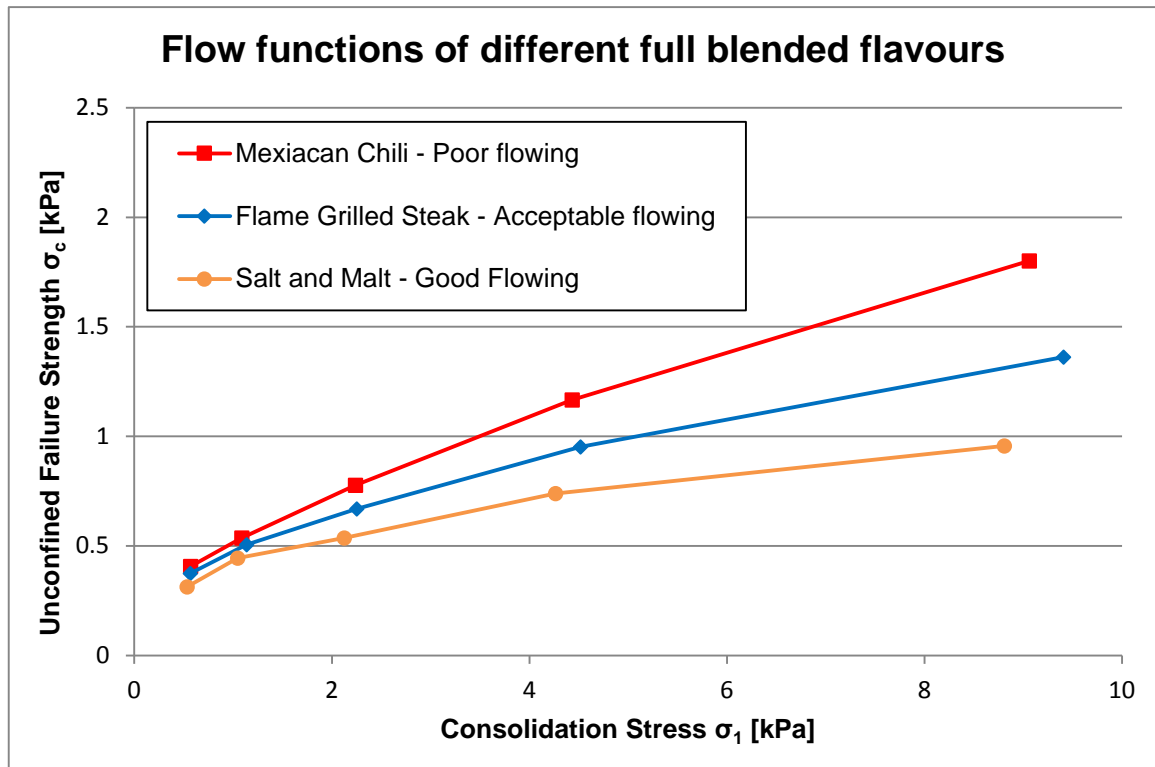


Figure 38: Flow function of different full blended flavours

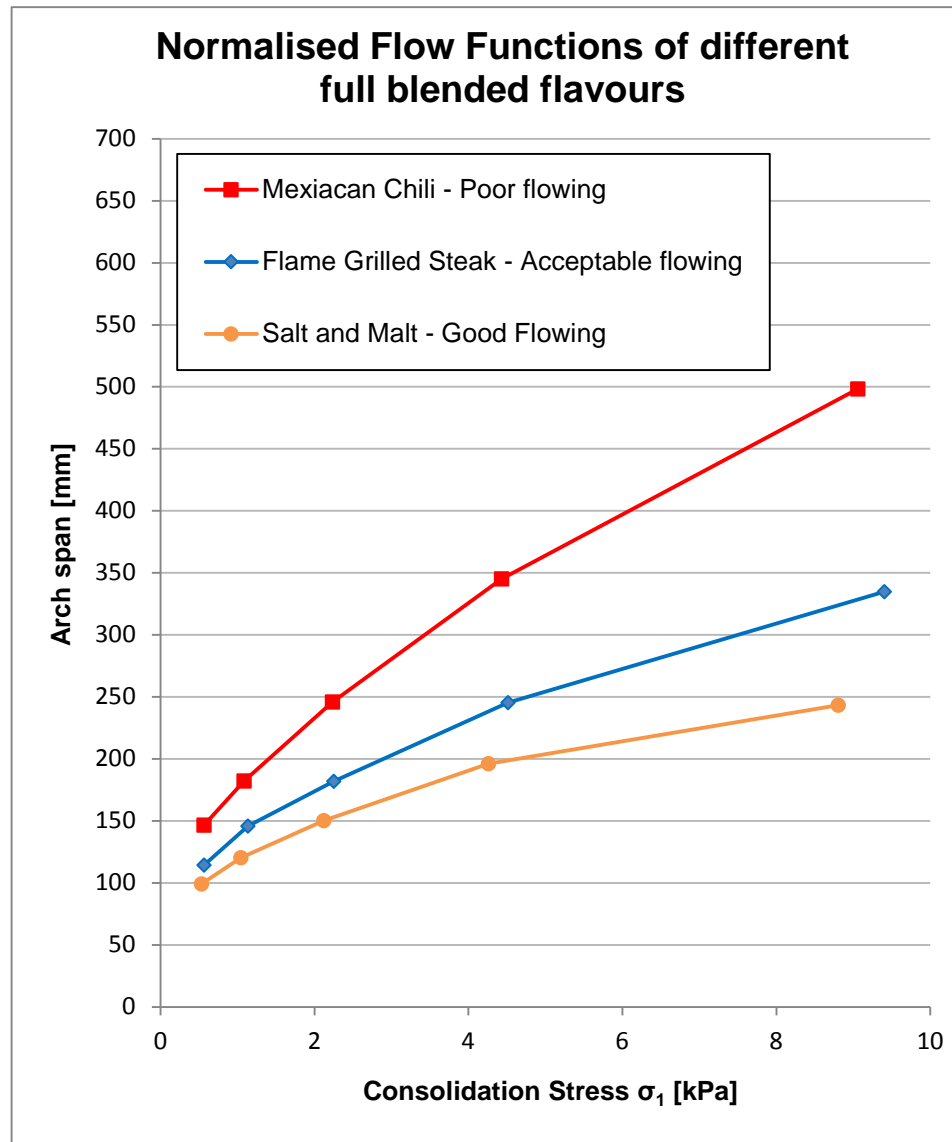


Figure 39: Arch span of different full blended flavours

- Identify the other key functional properties which need to be controlled to avoid flow powder handing issues in the industrial process lines of the partner's plants. These were the absence of dust, good adhesion to the snack and adequate flowability through feed hoppers and chutes as well as the critical taste, aroma, colour and texture.
- Investigate in detail the effect of oil used as a binder to prevent segregation of the blend components function and the effectiveness of the commonly used flow-property-modifying ingredients in the presence of a range of popularly-used main ingredients. These were limited to free flow additives namely magnesium carbonate, silicon dioxide and tricalcium phosphate which are the ones used

commonly by the project partners (This task may be considered as a fundamental investigation therefore it is expanded in section 4.4).

The other investigation was related to the academic challenge obtaining an understanding of the links between the particle and bulk scale. A series of fundamental investigations into the physics of the particle and bulk interactions for dry, wet and blended materials. These fundamental investigations are expanded in section 4.4 of the chapter and were to:

- Identify key mechanisms related to interparticle contacts, packing structure, moisture content, free flow additives and blending processes.
- Exploration of the above mechanisms using industrial partners' and idealised materials (simplified powder blends) to test the hypothesis presented and discussed in the literature review, before moving on to apply them to real blends, i.e. retrospectively applying the results of experiments to test whether the prediction correlated with the findings for the case study.

4.3 *Industrial case study method*

An industrial case study was undertaken with industrial partners, Intersnack, Givaudan and Brookfield Viscometers Ltd. as a preliminary test to understand the problems of the partners in their process lines. The aim of this investigation was to reformulate a Flame Grilled Steak snack flavour to remove monosodium glutamate (MSG) in order to conform the proposed regulation changes. The partners were expecting this to be a significant challenge because MSG is an easy flow material, whereas the replacement ingredient used to give a similar taste profile has much poorer flow properties. The industrial partners' requirements from this study were to:

- At least match and if possible improve the flow behaviour of the new formulated flavour compared to the standard flavour with MSG based on the flow function and bulk density curves.
- Reduce the level of dust to a limit of 0.019 wt% based on their experience in handling and processing snack flavours with a similar spice level. Dust in snack factory causes a loss of morale in the work force, this is particularly critical with spicy flavours where only a low level of dust can cause irritation to workers in the process lines.
- Ensure good adhesion of the reformulated flavour to the snack

- Evaluate the role of the filler material in the blended flavours on the above properties by running tests with a range of fillers of different particle sizes, which effect material cost.

Figure 40 shows the ingredient break-down of the Flame Grilled Steak standard flavour with MSG.

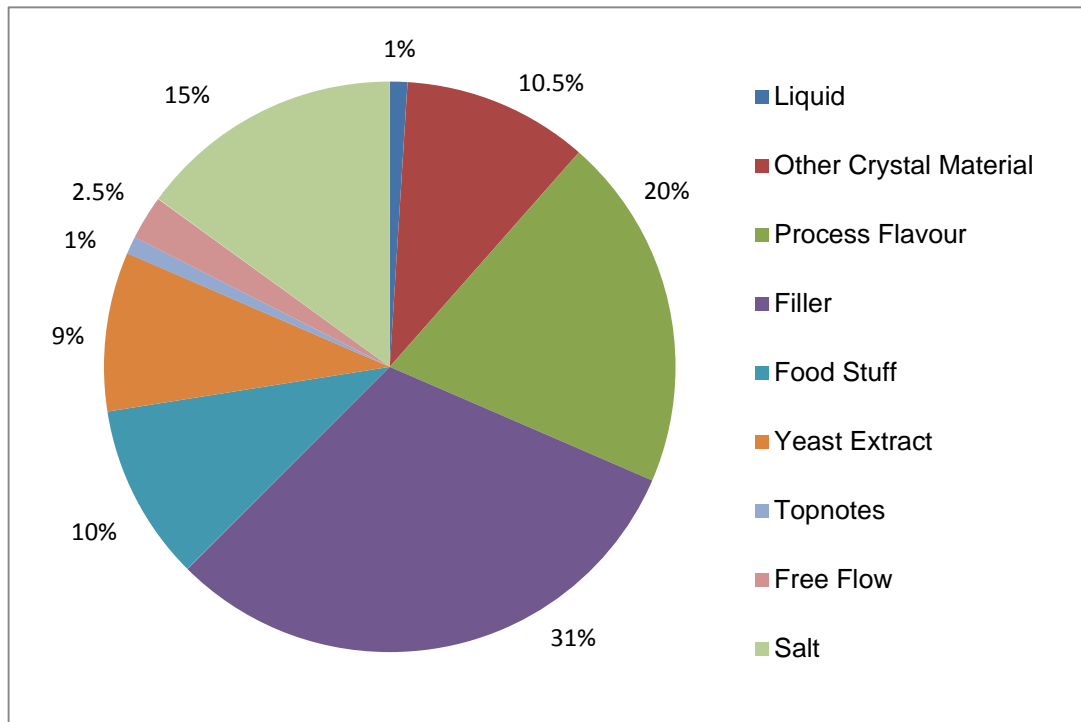


Figure 40: Ingredient break-down of the Flame Grilled Steak standard flavour

The investigation focused on the influence of free flow additive level and type, oil level and particle size variations of salt and fillers on the reformulated flavour. These ingredients contributed approximately 45wt% of the blended powder and it was anticipated that these variations would have a significant effect on the flow behaviour of the blended powder. The remaining 55wt% of the ingredients such as yeast extract, food stuff and process flavour control the flavour of the blend and were considered fixed in this case study in order not to significantly modify the taste, aroma, colour and texture.

A wide range of fillers from fine to coarse powders shown in the results of the case study presented in chapter 6 and commonly used by industrial partners and different grades of salt were characterised in this study. These powders were selected based on Givaudan experience providing a wide range of particle sizes and product costs.

From the range of the most common free flow additives used by project partners in their blends, silicon dioxide and tricalcium phosphate were selected for this case study due to their presence in most of their snack flavours; magnesium carbonate is rarely used and its applicability is limited to few flavours with specific partners' requirements. Miglyol 818 oil was selected for the case study because its liquid properties are similar to those of the common oil used by industrial partners. The levels of oil content added to the reformulated blends were in the working range normally used by Givaudan from 0.5 wt% to 2.5 wt%. A summary of the particle and bulk flow properties of these particulate materials and the liquid properties of the oil used are presented in chapter 3 of the thesis.

As explained in section 4.2, key functional properties of the blended powders such as dust emission and bulk flow properties need to be controlled to avoid flow powder handling issues in the industrial process lines so that bulk flow property and dust level measurements of different combinations of the flow-property-modifying ingredients, the oil level and the filler and salt grades in the reformulated flavour were undertaken at a range of different levels to evaluate their individual and combine effects.

Bulk flow properties were measured using Brookfield PFT shear tester and dust emission was measured using a dustiness tester. These characterisation tests were important to understand the role of each ingredient on the bulk flow properties and dust emissions of the final blended flavour. The range of conditions tested are disclosed in the results of the case study presented in chapter 6. Recommendations from Givaudan about the effect of these ingredients on the flow behaviour of the blended powders based on their experience in handling and processing their snack flavours were taken into consideration.

Givaudan had their own rule of thumb for assessing relative effectiveness of the different free flow additives but they did not understand the need to balance the level of free flow additive to the level of oil. If the flow properties were bad, they would carry on adding free flow additive to ensure flow properties improved. However, they would over dose leading to excess of free flow additive and high level of dust. Through testing it was demonstrated that there is an optimum level of free flow additive as presented in chapter 6, section 6.3.6, where strength is at a minimum value and beyond further addition has no effect and produces dust.

As detailed explained in the results of the case study presented in chapter 6, from these measurements, four different reformulated blends were selected to be trialled at the factory of Intersnack. The selection of the trial blended powders was based on the industrial partners' requirements as follows:

- Blend with similar flow properties to the current standard flavour but much lower dust level.
- Blend that is significantly freer flowing than the current standard flavour but with the same dust emission.
- Blend with slightly better flow properties than the current standard flavour with a lower dust level using a cheap filler.
- Blend with slightly better flow properties than the current standard flavour with a lower dust level using an expensive filler.

These reformulated blends were tested using the Rospen loss in weight feed hopper to demonstrate their effectiveness in an industrial environment under adverse environmental conditions (temperature 35°C and humidity 40%RH). These conditions are the same as the worst environmental conditions in the factory during summer. Different flavours with poor and good flow behaviour in the handling process at the factory were also tested and compared at the same environmental conditions as shown in figures 38 and 39 above.

The principle of the Rospen loss in weight feed hopper is to accurately control the dose weight output from the powder stored in the hopper using a feeder at its bottom. The powder is discharged as a function of the speed of the screw placed at the bottom of the hopper. The density of the powder stored determines the speed of the screw and the Rospen hopper unit varies this speed to obtain a controlled dose weight. An agitator placed over the feeder is an optional function of the unit to keep the powder moving during the discharge.

In the process lines of the industrial partners' plants, these Rospen hopper units are placed next to the snack and flavour mixing drums providing a controlled amount of flavour blended powder to the sliced fried potatoes rotating in the drum before being packed. The flavour particulate material and the snack are mixed in this step of the process line and it is critical to have a consistent dose weight over a complete discharge of the blended powder stored in the hopper in order to reduce the variability

of the dose in the discharge period. Fail to do so leads to slides potatoes with no much flavour or too much flavour which affects the quality of the final product of the industrial partners.

The discharge consistency decreased with time, the worst flowing materials had more erratic discharge rates from the loss in weight feeder hopper when run at a constant speed, demonstrating a link between the flow properties and the discharge behaviour, thus validating the focus on the flow function for characterising flowability.

Samples of these tested powders were taken every 30 minutes during their discharge from the Rospen loss in weight feeder hopper and subjected to measurements of their flow properties using PFT at the same environmental conditions. From these flow measurements, a target to aim for in terms of good flow behaviour was defined based on the windows of flowability of these known flavours in partners' plant.

The main results of the case study are presented in chapter 6, section 6.2 and full results plots of the tests undertaken are presented in appendix C. Most of the powders are relatively coarse and free flowing and it is the addition of the oil that provides the cohesion in the blended flavours. Tests undertaken under these adverse environmental conditions (temperature 35°C and humidity 40%RH) showed that the bulk strength of the blended powders increased with increasing exposure time. This fact leads to consider agglomeration of the powders so that an important issue for further work is to study the agglomeration tendencies of the flavour particulate materials in long term storage with the variation of temperature and humidity.

4.4 Experimental investigations

Fundamental investigations were made to discern the links between the particle properties and the bulk flow properties as identified in the literature review. After considering all the system variables that can be reasonably measured such as particle size or controlled like liquid properties, level of additives and so on, an investigation of the links between the particle and bulk scales has been undertaken.

Previously, an identification of the key bulk and particle properties was made for a wide range of industrial partners' and idealised materials such as particle size, particle density, bulk density, flowability, internal friction values and voidage. A summary of these properties for different food powders are presented in chapter 3 of the thesis. Liquid characterisation tests were also undertaken for the liquids used in this research

work and their properties (density, viscosity and surface tension) are presented chapter 3 of the thesis.

A range of investigations were carried out on different materials to understand the effect on bulk flowability and packing structure of:

- Deconstructed particle size distribution (PSD)
- Particle shape, size and liquid content (mass basis) on single powders
- Particle size on dry blends
- Particle shape and size on wet blends
- Interaction between oil and free flow additives
- Free flow additives

Test Program / Description	Test number	Single powder	Simplified blend	Blended flavour	Particle size	PSD	Particle shape	Free flow type	Free flow level	Liquid type	Liquid level
1. Influence of the particle size and distribution on four common filler materials (see section 4.4.1)	1.1	●			●						
	1.2	●				●					
2. Influence of the particle shape, surface liquid content, liquid type and particle size on four idealised materials (see section 4.4.2)	2.1	●					●				
	2.2	●					●				●
	2.3	●					●			●	●
	2.4	●			●						
	2.5	●			●						●
	2.6	●			●					●	●
3. Influence of the particle size of the constituent ingredients on dry blends of powders and idealised materials (see section 4.4.3)	3.1		●		●						
4. Influence of the particle shape and size of the components on	4.1		●				●				●

wet blended idealised materials (see section 4.4.4)	4.2		●		●						●
5. Interaction between three common free flow additives and oil at different liquid levels (see section 4.4.5)	5.1								●		●
	5.2							●	●		●
6. Influence of the level and type of free flow additive on three common filler powders, a blended flavour and idealised materials at different levels of oil (see section 4.4.6)	6.1	●						●	●		
	6.2	●						●	●		●
	6.3	●			●				●		●
	6.4	●						●	●		●
	6.5			●				●	●		●

Table 27: Range of experimental investigations undertaken in the research

4.4.1 Effect of deconstructed particle size distribution

The review of the literature indicated that particle size is the major contribution to cohesion and the bulk behaviour of the powders is dominated by the fines particles. These were evaluated by testing between particle size and material cohesion; a number of industrial materials were sieved into different size fractions so that bulk to particle factors could be evaluated. The outcome of this was that most of the industrial materials were easy or free flowing, with not enough material in the range of 0 to 100 μm to evaluate the relationship between particle size and bulk strength.

Therefore, it was the presence of a liquid binder that provides cohesion in the blended flavours, hence subsequent focus on wet materials in this study. To look at the effect of the particle size in more detail, tests were undertaken with lactose using different grades with narrow size distributions to generate the different particles sizes.

The effect of the breadth of the particle size distribution on the flow properties of four dry filler powders commonly used in the food manufacturing industry was investigated. These materials were tested at ambient conditions without adding any liquid or free flow additive.

Six different lactose grades to compare different particle size distributions – from wide to very narrow (see chapter 3) were selected. Size fractions of dextrose (wide size distribution), sodium chloride (fine grade) and maltodextrin wheat, both with narrower particle size distributions and presence of very fine particles below 45 μm , were removed by sieving analysis to be tested. These three powders have similar D50 approximately 100 μm as presented in chapter 3 of the thesis.

With the exception of the lactose grades, samples of powders were prepared to comparable size fractions; the test procedure was as follows:

- A large quantity of the full size powder was mechanically sieved using the technique described in chapter 3 until sufficient material was generated in each size fraction for a shear test.
- All the size fractions were then subjected to bulk flow property tests using PFT as described in chapter 3 and the flow properties were compared to those measured for the full size distribution. The results of this comparison are presented in chapter 6 of the thesis.

For the six different lactose grades with different particle D50 and spans, lactose samples were obtained from the full size powders for each grade and then subjected to measurements of their flow properties using PFT. These properties were compared and the results are presented in chapter 6 of the thesis.

4.4.2 Effect of particle shape, size and liquid content on powders

This section is focus on the effect of liquid as known from literature that the level and the properties of the liquids (viscosity and surface tension) have an important effect on the bulk strength as well as particle properties (particle size).

Tests were undertaken on idealised materials to control particle shape which is not considered in the models which are based on spheres and to ensure a non-porous particles so that all moisture was surface moisture.

To evaluate Rumpf model, different particles sizes and liquids were tested to pendular limit as this covers the relatively low level of liquid of interest to the industrial partners. Also the effect of the liquid to the point of saturation was investigated and there is a theory for this that can be evaluated as part of the further work. Limited tests were undertaken with real materials.

The second test programme investigates the influence of particle shape, surface liquid level, liquid type and particle size on three idealised materials. Wet powder samples were subjected to bulk flow property tests using PFT and the flow and packing properties were compared. Sampling for these wet powders is explained in details in chapter 3 of the thesis.

The test 2.1 compares the effect of particle shape on the bulk flow and packing properties for three idealised materials namely glass beads (spheres), crushed glass (shards) and sodium chloride (cubic) with similar particle densities, spans and D50 as presented in chapter 3 of the thesis.

The test 2.2 investigates the effect of increasing surface liquid content on the bulk strength and packing properties adding oil up to the point of the saturation for the same three idealised materials with different particle shapes named in the test 2.1. The test 2.3 studies the effect of the liquid properties repeating a limited range of the test 2.2 using distilled water. The comparison of the effect of particle shape, liquid content and liquid type is presented in chapter 6 of the thesis.

The test 2.4 studies the effect of particle size on the bulk flow and packing properties of glass beads at four reduced mean particle sizes. The test 2.5 investigates the effect of particle size and surface moisture on four grades of glass beads. The effect of the different liquid properties is studied in test 2.6 repeating a limited range of the test 2.5 adding distilled water and oils with dissimilar viscosities in the range of 33 to 300 mPa.s. The comparison of the effect of particle size, liquid content and liquid type is presented in chapter 6 of the thesis.

4.4.3 Effect of particle size on dry blends

As shown in the literature review, the presence of fine particles in blended powders has a critical effect on the packing and bulk flow properties of the final blends. The work developed by many researchers and presented in chapter 2 shown that a minimum amount of fines particles is required to affect the flow behaviour of the blends

becoming the powders more cohesive; below this level, the bulk flow properties of the blends are dominant by the coarsest particles.

The third test programme investigates the effect of the particle size of the constituent ingredients on dry multicomponent blends of common powders used by industrial partners and idealised materials was investigated. Food powders namely dextrose ex-wheat, dextrose, sodium chloride (different grades) and lactose (different grades) were mixed at different proportions and tested at ambient conditions without adding any liquid or free flow additive. Binary dry blends made with different grades of glass beads were also tested at the same conditions.

The dry blend samples prepared were subjected to bulk flow property tests using PFT and the flow and packing properties were compared. The results of this comparison are presented in chapter 6 of the thesis. Sampling preparation for these dry blends is explained in details in chapter 3 of the thesis.

4.4.4 Effect of particle shape and size on wet blends

The fourth test programme investigates the influence of the particle shape and size of the components on wet blended idealised materials. Wet blended powder samples were subjected to bulk flow property tests using PFT and the flow and packing properties were compared. Sampling preparation for these wet blended powders is explained in details in chapter 3 of the thesis.

The test 4.1 compares the effect of particle shape on the bulk flow and packing properties for blended wet idealised materials with constituent ingredients namely glass beads, crushed glass and sodium chloride with similar particle densities, spans and D50 as presented in chapter 3 of the thesis. The liquid used was Miglyol oil 818 and it was added up to the point of the saturation; this particular oil is used as a reference in the research because its properties are similar to the most common oil used by industrial partners in their snacks flavours.

The test 4.2 investigates the effect of the particle size of the ingredient components on wet blends repeating a limited range of the test 4.1 using glass beads at two reduced mean particle sizes. The comparison of the effect of particle shape and size of the blend components is presented in chapter 6 of the thesis.

4.4.5 Interaction between oil and free flow additives

In order to develop a better understanding of the interaction between liquids and free flow additives on the packing and bulk flow properties of particulate materials, the saturation level of the most commonly used free flow additives by industrial partners namely silicon dioxide, tricalcium phosphate and magnesium carbonate was investigated by adding Miglyol oil 818 at different liquid levels. Values of the level of saturation of the flow agents were considered an important parameter to understand their effectiveness and better predict their effect on wet powders.

Mixed powders samples were subjected to bulk flow property tests using PFT and the bulk flow and packing properties were compared. Sampling preparation for these blended powders is explained in details in chapter 3 of the thesis.

The fifth test programme compares the level of liquid content required to saturate these three flow-property-modifying ingredients adding the oil selected increasingly to a fixed amount of each free flow additive. The results of this comparison are presented in chapter 6 of the thesis.

4.4.6 Effect of free flow additives

SEM images of the free flow additives named silicon dioxide, tricalcium phosphate and magnesium carbonate presented in chapter 3 showed that these flow agents are characterised by an open structure of particles at a chain of nanoparticles. Silicon dioxide and tricalcium phosphate presented agglomerates of 1 to 10 μm and magnesium carbonate agglomerates of 10 to 20 μm as well as irregular particle shape.

Industrial partner's experience of working with these flow agents in the formulation of snack blended flavours showed that silicon dioxide seemed to be more effective than the others two free flow additives as less amount was required to reduce the effect of the oil content in the powders. Furthermore, tricalcium phosphate and magnesium carbonate seemed to produce similar effect on the wet blended particulate materials.

The sixth test programme investigates the influence of the level and type of free flow additive on three common filler powders, a blended flavour and idealised materials at different levels of oil. Blended powder samples were subjected to bulk flow property tests using PFT and the bulk flow and packing properties were compared. Sampling preparation for these blended powders is explained in details in chapter 3 of the thesis.

The test 6.1 compares the effect of the three most common free flow additives used by industrial partners on two grades of lactose. Free flow additive was added to these fillers at different levels without adding any liquid. The test 6.2 investigates the effect of these free flow additives on wet filler powders namely lactose and maltodextrin; Miglyol oil 818 was used to prepare wet filler powder samples at fixed level of 3 wt% before the addition of the free flow additives at different levels. The results of this comparisons are presented in chapter 6 of the thesis.

The test 6.3 investigates the effect of silicon dioxide on wet idealised materials at different grades to compare particle size distributions using glass beads; Miglyol oil 818 was added at 1 wt%, 2 wt% and 4 wt% covering the working range normally used by industrial partners in their snack flavours (up to 2.5 wt% normally but eventually can go as high as 4 wt%). The test 6.4 studies the effect of the type of free flow additive repeating a limited range of the test 6.3 using tricalcium phosphate; magnesium carbonate was not selected in these tests because its effect on dry and wet powders is similar to tricalcium phosphate as shown in the comparisons presented in chapter 6. The comparison of the effect of type and level of free flow additive on glass beads is also presented in chapter 6 of the thesis.

The test 6.5 compares the effect of silicon dioxide and tricalcium phosphate on a blended snack flavour; magnesium carbonate was no selected for the same reason mentioned in the previous paragraph. The flavour selected for the tests was Flame Grilled Steak snack flavour using the final re-formulation defined in the case study explained in this chapter. Oil was added at fixed amount of 1 wt% and free flow additives were added increasingly covering the working range normally used by industrial partners in their snack flavours (up to 5 wt% depending how free flowing they would like the flavour); the results of this comparison are presented in chapter 6 of the thesis.

4.5 *Summary*

The research methodology and the experimental investigations undertaken to develop a practical understanding of the links between the particle and the bulk flow properties of particulate materials have been presented in this chapter. The key points from the chapter are the following:

- The aim of the research was to understand how to control powder flowability with applications to the blended food powder industry and how to predict the effect on the bulk flow properties of changes to the blend compositions and the particle and bulk flow properties of the blend ingredients. Existing and well-established analytical particle to bulk scale models were calibrated empirically and new empirical models were developed in order to be used to assist industrial users to understand how to control powder flowability.
- The research approach was divided in two main investigations: one was to undertake a series of specific tasks to meet the requirements of the project industrial partners such as the development of a database of the bulk flow properties of a wide range of single powders and the characterisation of several blended powders which show good and poor flow behaviour in the industrial process lines. An industrial case study was undertaken to reformulate a Flame Grilled Steak snack flavour to remove monosodium glutamate (MSG) and, at the same time, improve the flow behaviour and reduce the dust emission of the new reformulated flavour compared to the standard with MSG. Results and conclusion of the case study are presented in chapter 6 of the thesis.
- The other investigation was to carry out a series of fundamental investigations into the physics of the particle and bulk interactions for blended powders in dry and wet condition in order to understand the links between the particle and bulk scale. These investigations studied the effect of the free flow additives, particle size and shape, interaction between oil and flow agents, liquid content and deconstructed particle size distribution on the bulk flow properties and packing structure of single and blended powders.

Next chapter presents the modelling strategy of the research and how the analytical models were calibrated to evaluate their applicability on real single and blended particulate materials.

Chapter 5 Models for prediction of the bulk flow properties

5.1 Introduction

Following the structure of the investigation, this chapter presents the modelling strategy of the research and how the analytical models found in the literature linking particle and bulk flow properties were calibrated to evaluate their applicability on predicting the packing and bulk flow properties of real single powders.

A new model for dry blended powders developed in this research due to the lack of established models for blends is also presented; this model predicts the average flow properties of multicomponent dry blends based on the particle and bulk flow properties of their constituent ingredients.

A review of the modelling strategy is presented in section 5.2; the limitations of the modelling work developed in this research are disclosed in section 5.3; the calibration process of the analytical models for single powders in dry and wet condition with free flow additives is explained in section 5.4; the new model developed for dry blended powders is presented in section 5.5 and a summary of the chapter is presented in section 5.6

5.2 Modelling strategy

The modelling strategy was to use analytical established models found in the literature to calculate the inter-particle forces based on particle size, voidage for different contact force mechanisms, e.g. van der Waals forces for dry blends and surface tension forces and viscous forces for wet blends.

These analytical models were calibrated empirically using a limited number of bulk flow property tests. The particle forces can then be determined by working back through the calibrated analytical model. Hence, the series of models can be used to predict the effect of changes in particle interaction properties or particle properties on the bulk flow behaviour.

There are a number of factors to consider and their effect needs to be calibrated independently. These include the variations in the:

- Granulometry (particle size and shape)
- Interaction methods (surface moisture, surface coating)

- Blended process (number of components, degree of mixedness)

This strategy combined a number of existing high level models with simplifications for practical use by the industrial partners. The analytical models calibrated in this research cover the following aspects:

- Dry contact (van der Waals forces) based on particles size
- Wet contact at low level of moisture (Rumpf liquid bridge strength) based on surface tension of liquid
- Effect of free flow additives which determine the critical addition level for surface coating based on particle sizes of the host and the additive

For individual materials these are calibrated against the measured strength. For a blended material the model uses an averaging function for the measured individual components based on the specific volume and surface area ratios of the blend components in the mixture.

5.3 *Limitations of the modelling work*

The analytical model developed in this research determines the optimised flow behaviour of blended food powders manufactured in the industrial partners' plants. This model can be used by non-powder specialist industrial users to assist in the optimisation of the flow properties of their blends predicting:

- The effect of changing particle interaction properties on the bulk flow behaviour of a single material
- The flow behaviour of a blended powder based on known particle and bulk properties of the constituent ingredients

The modelling approach was to combine and simplify a number of existing and well established analytical models to the point where they can be used in conjunction with industrial flow and particle property measurements. This led to take into account the following limitations in the modelling work:

- Consideration only of the particle properties that can be measured by industrial partners (see chapter 2)
- Calibration tests achievable by industrial partners using Brookfield PFT shear tester (see chapter 1)

In terms of simplifications of the models combined for practical use, the following assumptions were made:

- Assumed a random packing assembly of monosized spheres
- Reliance on tabulated values of material properties such as Hamaker constant that are difficult to measure by industrial users
- Assumed a grade of uncertainty inherent in the techniques used to measure the particle size (actual size can shift at significant margins which has implications for non-spherical particles)
- Assumed that particle shape is independent of the particle size based on limited SEM images of particles
- The effect of the surface roughness of the particles was not taken into account
- Assumed that models are being used at a high stress where material is in a compacted state. However, for a few examples, several models were calibrated at different stress levels to demonstrate the effect that this has on the bulk flow and packing properties of the powders

An important consideration in the modelling work was the fact that predicted unconfined failure strength (compressive strength) of blended and single powders was based on empirical calibration of models which predict the tensile strength of agglomerates. However, the compressive strength is proportional to the tensile strength as disclose in chapter 2 (see equations 2 - 4). Analytical models calibrated in this study presented the following simplifications:

- A single value of particle size characterises the powder
- Models valid for equal sized spheres
- Particle size distribution and different particle shapes are not considered in the models

5.4 Particle contact mechanisms for a single material

Models to cover the particle contact mechanisms required for a single material such as particle size, liquid content and surface coating were found in the extensive review of the literature.

5.4.1 Dry powders

In order to predict the bulk strength of dry powders, analytical models to calculate the interparticle forces, the tensile strength and the packing structure based on particle properties were calibrated empirically. As explained in chapter 2, the bonding mechanism considered for dry materials in this research project is van der Waals forces.

The tensile strength

Rumpf et al. proposed a model to predict the tensile static strength of agglomerates. A theory for granules under loads was developed based on the following assumptions explained in details in chapter 2:

- Particles forming the granule are equal sized spheres equally distributed in the agglomerate
- A cross section of a stressed agglomerate is formed by a large number of bonds uniformly distributed
- The effective bonding forces are distributed around a mean value which replaces them in calculations

This model relates the tensile strength of a single powder to the interparticles forces as a function of the packing structure and the particle size. As disclosed in chapter 2, the basic equation proposed by Rumpf can be written as a function of the particle size, the voidage and the bonding force at a contact point.

$$\sigma_z = \frac{9(1-\varepsilon)H}{8\varepsilon d^2} \quad \text{Equation 35}$$

Where:

- H is the mean bonding force at point of contact
- d is the diameter of the spherical particles
- ε is the void fraction within the total volume
- σ_z is the mean theoretical tensile strength

For dry powders (binderless agglomerate), van der Waals forces can be considered the principal bonding mechanism acting between particles (Salman et al. 2006). As illustrated in chapter 2, van der Waals forces for two spherical particles can be

expressed as a function of the particle size, material properties (Hamaker constant) and the contact distance assuming that $s \ll R$.

$$F_V = \frac{AR}{12s^2} \quad \text{Equation 36}$$

Where:

- A is the Hamaker constant
- s is the separation distance between particles
- R is the radius of the spherical particles

Coelho et al. disclosed that van der Waals forces are sensitive to surface roughness for particles with size below 100 μm . Different models have been proposed to predict these forces as a function of this particle property and an example of these models was developed by Yu et al. 2003 as explained in chapter 2. However, these models were not considered in the modelling work (see section 5.3 in this chapter).

Substituting equation 36 into equation 35 gives the Rumpf's equation as a function of the particle size, the voidage, material properties (Hamaker constant) and the contact distance.

$$\sigma_z = \frac{3}{64} \frac{(1 - \varepsilon)}{\varepsilon} \frac{A}{ds^2} \quad \text{Equation 37}$$

Where:

- σ_z is the mean theoretical tensile strength
- d is the diameter of the spherical particles
- ε is the void fraction within the total volume
- A is the Hamaker constant
- s is the separation distance between particles

The packing structure

Packing structure was predicted using the equations proposed by Yu et al. 2003. As explained in details in chapter 2, empirical equations were proposed to predict the void fraction of dry powders as a function of the particle size, particle density and material properties (Hamaker constant). These equations were obtained by empirical curve

fitting of the plotted void fraction data obtained from several resources (Milewski et al., Mizuno et al. and Yu et al. in 1997) using the following equation:

$$\varepsilon = \varepsilon_0 + (1 - \varepsilon_0) \exp\left(-m \left(\frac{3bA}{\pi\rho_p}\right)^{-n} d^{-n(c-2)}\right) \quad \text{Equation 38}$$

Where:

- A is the Hamaker constant
- ε is the void fraction as a function of particle properties
- d is the diameter of the spherical particles
- ρ_p is the particle density
- ε_0 is the void fraction of the dry coarse spheres under gravity force
- m and n are fit constants of the experimental curve fitting of the measurements for packing of fine sphere particles
- b and c are fit constants (2.63×10^8 and -1.54 respectively) of the experimental lineal fitting of K values

Yu et al. 2003 assumed a value of $\varepsilon_0 = 0.4$ for loose random packing and $\varepsilon_0 = 0.36$ for dense random packing and by fitting equation 38 to the measurements taken from the resources, obtained the values of m and n for these packings of spheres. Using these values, the void fraction can be expressed as follows:

- Loose random packing

$$\varepsilon = 0.4 + 0.6 \exp\left(-0.106 \left(\frac{\rho_p}{A}\right)^{0.156} d^{0.552}\right) \quad \text{Equation 39}$$

- Dense random packing

$$\varepsilon = 0.36 + 0.64 \exp\left(-0.178 \left(\frac{\rho_p}{A}\right)^{0.129} d^{0.457}\right) \quad \text{Equation 40}$$

Calibration process

This model predicts the bulk strength of single dry powders with particle size below approximately $100\mu\text{m}$. Yu et al. (2003) demonstrated that van der Waals forces become dominant when particle size is less than about $100\mu\text{m}$. As explained in chapter 2, for dry coarse particles above $100\mu\text{m}$, gravity forces dominate over

interparticles forces and the void fraction is fairly constant. Powders with coarse particles dominating the flow behaviour show very low bulk strength (free flowing materials) on dry conditions.

Particles smaller than 1 μm tend to agglomerate and the agglomerates formed dictate the flow behaviour of these mixtures of particles. It was considered that they have sufficient strength to be stable during processing conditions and therefore they can be treated as a conglomerate of particles.

One of the limitations in the prediction of the void fraction is that the equations proposed by Yu et al. for loose and dense random packing are based on the experimental fitting of measurements. The values of the fit constants (m, n, b and c) are valid for glass beads at the packing conditions tested but there is a lack of knowledge regarding the effect of others materials at different packing conditions.

The bulk strength and the packing properties were measured for different materials. These powders were tested using Brookfield PFT shear tester over a range of stresses as explained in chapter 2. Rumpf model to predict the tensile strength on dry granules (equation 37) was calibrated to the measured strength at the minimum particle size of each powder (a single calibration point) and this calibration factor was applied to the measurements calculated from the model.

5.4.2 Wet powders

The same approach considered for dry powders was developed for wet powders to predict the bulk strength of wet particulate materials. As explained in chapter 2, the bonding mechanism considered for wet materials (presence of surface moisture) in this research project is capillary forces.

The tensile strength

A model has been evaluated based on the basic equation proposed by Rumpf to estimate the mean tensile static strength of the liquid bonds as explained in chapter 2.

$$\sigma_T = \alpha \cdot 2\pi r_2 \frac{9(1-\varepsilon)}{8\varepsilon} \left(\frac{1}{2a}\right)^2 \quad \text{Equation 41}$$

$$r_2 = 0.82a \left(\frac{v}{a^3}\right)^{0.25} \quad \text{Equation 42}$$

Where:

- σ_T is the mean theoretical tensile strength
- α is the surface tension of the liquid
- r_2 is the radius at the narrowest part of the bridge (the neck)
- v is the volume of the bridge for a single sphere around the contact area between two spheres
- a is the radius of the spheres
- ε is the void fraction within the total volume

This model suggests that bonds only fail at the narrowest part of the liquid bridge and the radius of the neck represents an average value of the total bridges with the same strength.

The volume of the bridge was calculated using the definition of the moisture content as the ratio of the liquid mass to the mass of dry particles (Pierrat et al.) and the relation between the coordination number and void fraction for loose random packing (Tanaka et al.).

$$x_w = \frac{m_{liq}}{m_{sol}} = \frac{k \frac{v}{2} \rho_{liq}}{\frac{\pi d^3}{6} \rho_{sol}} = 6k \left(\frac{v}{2\pi d^3} \right) \frac{\rho_{liq}}{\rho_{sol}} \quad \text{Equation 43}$$

$$k\varepsilon \approx 3.1 \approx \pi \quad \text{Equation 44}$$

$$v = \frac{\varepsilon d^3 \rho_{sol} x_w}{3\rho_{liq}} \quad \text{Equation 45}$$

Where:

- m_{liq} is the mass of liquid
- m_{sol} the mass of dry particles
- k is the mean coordinator number
- ε is the void fraction
- d is the diameter of the spherical particles
- ρ_{liq} is the liquid density
- ρ_{sol} is the solid density

The packing structure

Packing structure was predicted using the equation proposed by Feng et al. As explained in details in chapter 2, an expression based on the empirical fitting of the measurements for loose random packing of coarse sphere particles was proposed as a function of particles properties (size and density), liquid properties (surface tension and density) and liquid content (mass basis).

$$\frac{\varepsilon - \varepsilon_0}{\varepsilon_{max} - \varepsilon_0} = \left(\frac{M}{M_{cri}}\right)^{0.423} \left[1 - 0.421 \ln \frac{M}{M_{cri}}\right] \quad \text{Equation 46}$$

$$\varepsilon_{max} = \varepsilon_0 + 0.048 \left(\frac{\alpha}{\rho_p g d^2}\right)^{0.266} \quad \text{Equation 47}$$

$$M_{cri} = 0.2545 \left(\frac{\rho_l}{\rho_p}\right)^{-1.057} \cdot \left(\frac{\alpha}{\rho_p g d^2}\right)^{0.4743} \quad \text{Equation 48}$$

$$\rho_B = \rho_p (1 - \varepsilon) \left(1 + \frac{M}{100}\right) \quad \text{Equation 49}$$

Where:

- ε is the dry based void fraction
- ε_0 is the initial void fraction (0.4 for loose random packing)
- ε_{max} is the maximum achievable void fraction
- M_{cri} is the critical liquid content (mass basis) to give ε_{max}
- α is the surface tension
- d is the particle size
- ρ_p is the particle density
- ρ_l is the liquid density
- M is the liquid content (mass basis)

It was assumed that contact angle was negligible and only surface tension was considered in the study.

Calibration process

This model predicts the flow behaviour of wet powders in the pendular state of liquid saturation assuming a random packing assembly of monosized spheres. The bulk

strength of wet glass beads has been calibrated for a wide range of grades of the powder adding de-ionised water and Miglyol oil 818. Then, the bulk strength of wet real powders in pendular state could be predicted with the results obtained from the calibration of the model with idealised particulate materials. Furthermore, to have a better understanding of the phenomena of the addition of liquid to powders, programmes of tests have been undertaken (see chapter 4) adding liquid up to saturation to idealised particulate materials.

Based on the experimental work undertaken and the findings from the literature review, Rumpf model has been calibrated to predict the bulk strength in the pendular state considering an upper saturation limit of 25% for the pendular and funicular transition states. Meanwhile, new empirical models have been developed based on the experimental work undertaken to predict the bulk strength of wet powders in the funicular and capillary states. These new models are presented and explained in details in chapter 8.

One of the limitations in the prediction of the void fraction is that the equations proposed by Feng et al. for loose random packing (see equation 46 - 49) are based on the experimental work undertaken with wet coarse sphere particles above 250 μ m avoiding the effect of particle size.

The packing properties and the bulk strength of idealised powders in wet condition have been measured using the Brookfield PFT shear tester. The adapted Rumpf model (equation 41) was calibrated by comparing the measured and predicted bulk properties and then calculating a factor of calibration for each grade of glass beads tested. The volume of the liquid bridge formed between particles was calculated considering the definition of the moisture content as the ratio of the liquid mass to the mass of dry particles (see equation 45).

5.4.3 Surface coating of particles

The effect of free flow additives on wet and dry powders has been studied in this research either calibrating an analytical model for dry particle coating to predict the total surface coverage of the host particles or undertaking a test programme to better understand and predict this effect on wet materials (see chapter 4).

Dry particle coating

For dry particle coating, the quantity requires for complete surface coverage of the host particles can be estimated using the following equation based on difference in particle size and density (Yang et al. 2005):

$$Gwt\% = \frac{(Nd^3\rho_d)}{(D^3\rho_D) + (Nd^3\rho_d)} \times 100 \quad \text{Equation 50}$$

$$N = \frac{4(D + d)^2}{d^2} \quad \text{Equation 51}$$

Where:

- Gwt% is the weight % of guest particles for total surface coverage
- D is the diameter of the host particles
- d is the diameter of the guest particles
- ρ_D is the particle density of the host particles
- ρ_d is the particle density of the guest particles

Yang et al. assumed that a monolayer of guest particles covers the total surface of the host particles and both particles are monosized spheres. It was also assumed that they have sufficient strength to be stable and do not deform during the coating process.

Wet particle coating

A test programme was undertaken to understand and predict the effect of free flow additives on the bulk flow and packing properties of wet powders as explained in chapter 4.

The optimum percentage of free flow additive was calculated with the measurements undertaken to define the shape of the bulk strength curves for different percentage of oil and free flow additives added. The saturation level of the three common free flow additives (magnesium carbonate, silicon dioxide and tricalcium phosphate) used by industrial partners was also studied; it was considered an important parameter to understand the effectiveness of these free flow additives and predict their effect on wet powders.

5.5 *Blended powders*

Well-established analytical models to predict the bulk flow and packing properties of multicomponent blended powders have not been found in the literature review. In this research work, a model for multicomponent dry blends has been proposed considering the limitations of the research. This averages the measured flow properties of the constituents of the blend using their proportion on specific volume or surface area.

A new model for dry blends has been developed to predict the average strength, internal friction and bulk density of dry blends without free flow additives based on specific volume and surface area ratios. The bulk and particle properties of each component of the blend required to predict the average blend values are:

- Flow function
- Bulk density function
- Internal friction function
- Particle density
- Particle size distribution (D_{10} , D_{50} and D_{90})

From these inputs along with the percentage basis by weight, the model calculates the following values of each component of the blend:

- Volume of an individual particle in each size fraction
- Surface area of a particle in each size fraction
- Number of particles in each size fraction
- Total surface area of all particles
- Specific volume of all particles assuming measured void fraction (i.e. bulk density and particle density)

An average strength, friction and bulk density are then determined by an average based on either the surface area or specific volume ratios of the blend components. It has been assumed monosized spheres and particle size distributions have not been considered in the model only taken into consideration the values of D_{50} . Evaluation and further details of the model have been presented in chapter 7.

5.6 Summary

The modelling strategy and how the well-established analytical models were calibrated to evaluate their applicability on predicting the packing and bulk flow properties of real single and blended powders have been presented in this chapter. The key points from the chapter are the following:

- Analytical established models found in the literature were calibrated empirically using a limited number of bulk flow property tests in order to use the models to predict the effect of changes in particle interaction properties or particle properties on the bulk flow behaviour of food blended powders. Simplifications for practical use of the models by the industrial partners of the research project were made considering only the particles properties that can be measured in the industry and calibration tests achievable by industrial partners.
- The model proposed by Rumpf et al. to predict the tensile strength of agglomerates relates the tensile strength of a single powder to the interparticle forces as a function of the packing structure and the particle size. As this model is valid for dry and wet powders, it was calibrated considering van der Waals forces for dry particulate materials and capillary forces for wet powders (presence of surface moisture).
- Packing structure of dry and wet powders was predicted using the empirical equations proposed by Yu et al. 2003 and Feng et al. respectively. These equations predict the voidage of the powders in dry and wet condition as a function of the particle size, particle density and material properties (Hamaker constant). The effect of the free flow additives on wet and dry powders has been also studied undertaking a test programme (see chapter 4) to better understand and predict this effect on powders.
- A new model for dry blends developed in this research has been presented; this new model predicts the flow properties of multicomponent dry blends based on the particle and bulk flow properties of their constituent ingredients.

Next chapter presents the results of the case study and the experimental investigations disclosed in chapter 4 to study the relationship between the flow properties of the blended powders and the changes made on their constituents at particle scale.

Chapter 6 Experimental results

6.1 Introduction

This chapter presents the results of the investigations on the effect of particle and liquid properties on the bulk flow and packing properties of blended powders. A series of test programs (see chapter 4) were undertaken under a variety of conditions to study the effects of changing surface liquid content and type, free flow additive content and type, particle shape, particle size and distribution on bulk flow properties and packing structure of particulate materials.

An industrial case study was carried out previously as preliminary study to quantitatively determine the most desirable bulk flow properties of the snack blended flavours in the industrial partners' plants as well as to identify the key functional properties of the blends to be considered for the successful use in the industrial process plants.

The main results of the case study are detailed in section 6.2 with full results plots presented in appendix C. Summary of the results of each test programme are detailed in section 6.3 with full results plots presented in appendix B. A summary of the chapter is given in section 6.4

6.2 Industrial case study

The case study aimed to reformulate a snack blended flavour named Flame Grilled Steak to meet specific flow and functional requirements from industrial partners disclosed in chapter 4. This reformulation was used as a preliminary study of the common undesirable flow behaviour of food powders explained in chapter 1, with the following main objectives:

- Identification of the flow and functional properties such as flow behaviour and dust emission which make a snack blended flavour adequate to flow through the industrial partners' plant equipment and maintain the environmental conditions in the plant suitable for the workers.
- Quantitatively determination of the most desirable flow properties based on industrial partners' known flavours which show both poor flow and good flow behaviour under extreme conditions during summer in the plants.

This section presents the main results and conclusions of the case study; detailed description is presented in chapter 4 with full results plots presented in appendix C. As explained in chapter 4, the investigation was focused on the influence of the free flow additive level and type, oil level and particle size variation of fillers and salt on the bulk flow properties of the snack blended flavour reformulated, evaluating their individual and combine effects.

The reformulation of the flavour was based on the new ingredient break-down shown in figure 41 removing monosodium glutamate from standard formulation (see chapter 4) and increasing significantly the amount of yeast extract in the blended powder based on Givaudan experience. Results are presented in different sections below highlighting the effect of the particle size and oil, free flow additives and different fillers. The last section presents the finished blends that were trialled at the factory of Intersnack as explained in chapter 4.

The dust emission presented in tables 29 – 33 was measured using the rotating drum style dustiness tester (Hjemsted et. al 1996, Breum et. al 1999, Liden et. al 2006 & Frew et. al 2013) developed at The Wolfson Centre for Bulk Solids Handling Technology based on the Standard BS EN 15051-2:2013 (Workplace exposure. Measurement of the dustiness of bulk materials. Rotating drum method). This dustiness tester consisted in a rotating closed drum connected to a filter in one of its ends; this drum was rotated at 40 rpm for a test period of 180 seconds generating dust from a 50g sample particulate material placed inside the drum. Dust was collected in the filter due to the vacuum produced at a controlled flow rate of 50 l/min. The dust emission in mass percentage was calculated as the ratio of the dust collected on the filter paper to the mass of the sample tested (50g).

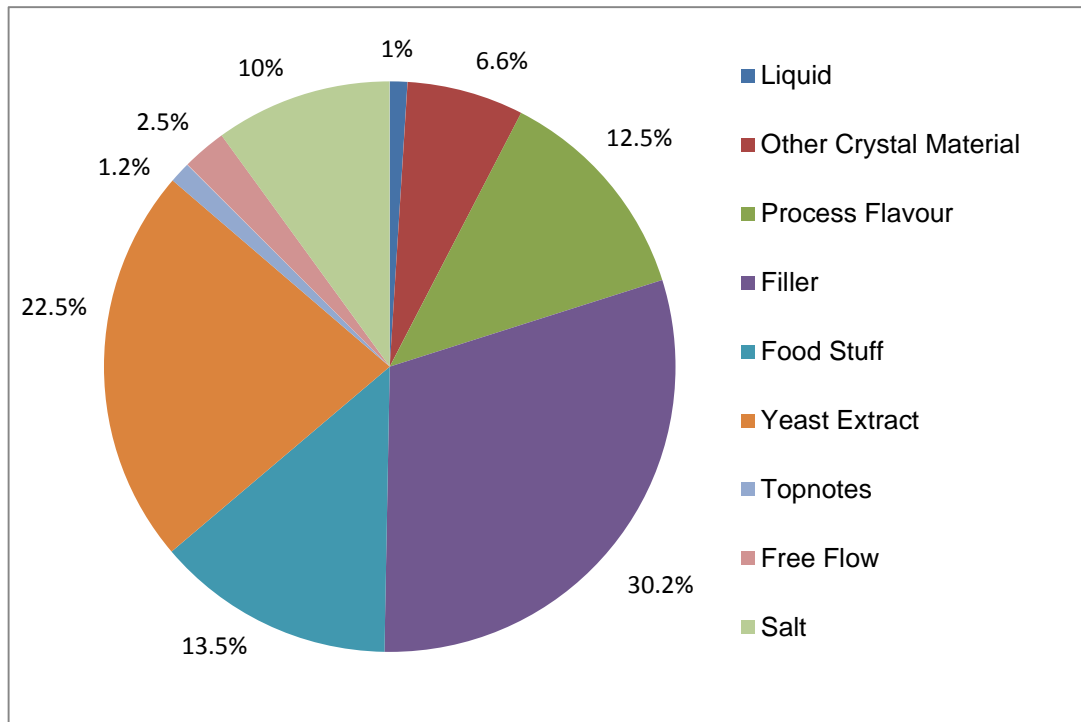


Figure 41: *Ingredient break-down of the Flame Grilled Steak flavour after removing monosodium glutamate of the standard composition*

6.2.1 Effect of particle size and oil level with different free flow additives

The effect of particle size (the extremes of the finest and coarsest grades of fillers and salts) and levels of oil with various free flow additives (see table 28) was investigated. Full blended flavours were prepared with the combinations of the maximum and minimum particle size available for the filler and salt added; in both cases, MCT oil was added at 1%wt & 2%wt and tricalcium phosphate (TCP) and silicon dioxide (SiO₂) were added at 2.4%wt and 1.2%wt respectively.

Reference	Filler	Grade of salt	OIL (%wt)	TCP (%wt)	SiO ₂ (%wt)
Blend 1	Lactose	Fine	1	2.4	-
Blend 2	Lactose	Fine	1	-	1.2
Blend 3	Lactose	Fine	2	2.4	-
Blend 4	Lactose	Fine	2	-	1.2
Blend 5	Bread Crumbs	Coarse	1	2.4	-
Blend 6	Bread Crumbs	Coarse	1	-	1.2
Blend 7	Bread Crumbs	Coarse	2	2.4	-
Blend 8	Bread Crumbs	Coarse	2	-	1.2

Table 28: Range of tests undertaken to study the effect of particle size and levels of oil content with different free flow additives on the reformulated Flame Grilled Steak

Inspection of figures 42 and 43 and tables 29 and 30 shows that blend 1 and blend 3 made with fine salt and fine filler using TCP as a free flow additive are close to the standard sample in terms of flowability and the effect of the oil content is clear in the levels of dust, with lower dust emission at higher oil content as vice versa as shown in figure 42 and table 29. Blend 7 made with coarse filler and coarse salt with 2%wt oil content flows slightly better than the standard sample with a lower dust emission whereas blend 5 made with coarse filler and coarse salt with 1%wt oil content shows better flow behaviour than standard sample but higher level of dust as shown in in figure 42 and table 29.

Figure 43 and table 30 show the results of the same tests adding silicon dioxide instead of tricalcium phosphate at 50% TCP level. These tests (blends 2, 4, 6 & 8) show a similar pattern of behaviour albeit slightly freer flowing to previous set of tests but dust emission is significantly higher.

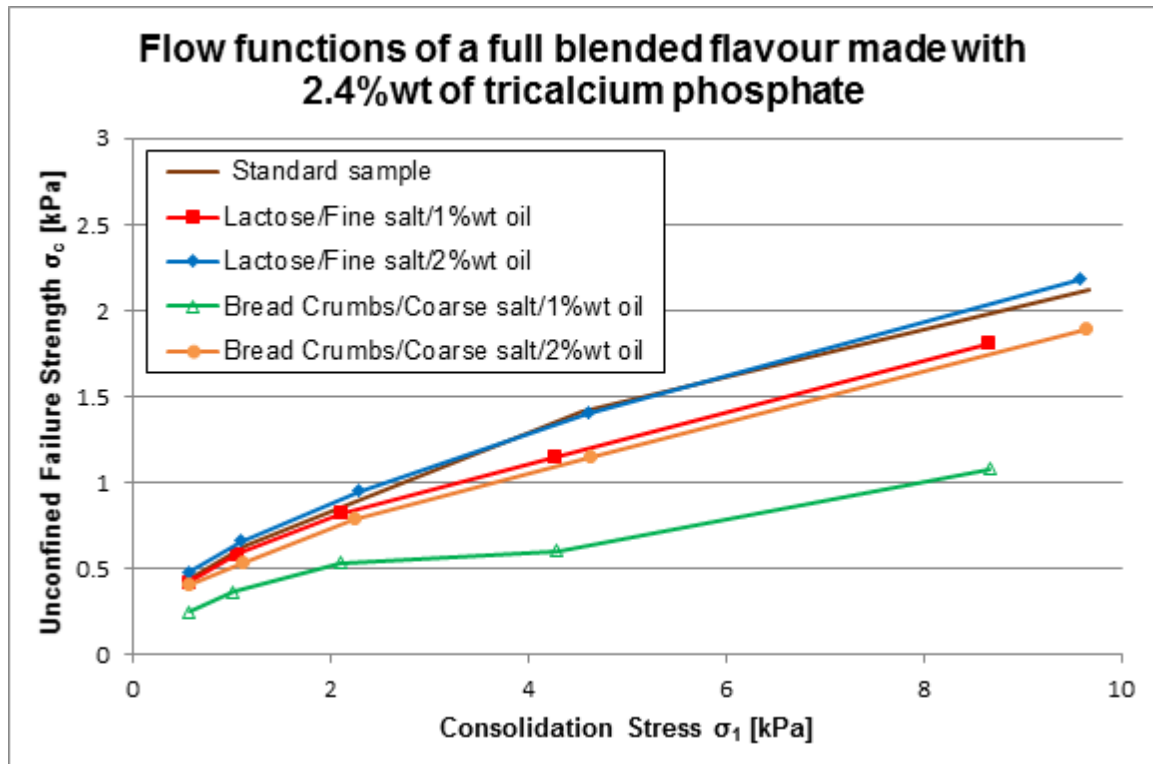


Figure 42: Flow function of full bended powders made with 2.4%wt of TCP

Ingredients of the blended flavour	Level of dust (wt%) with 2.4%wt TCP
Standard Flavour	0.0355
Lactose/Fine salt/1%wt oil	0.0275
Lactose/Fine salt/2%wt oil	0.0104
Bread Crumbs/Coarse salt/1%wt oil	0.0419
Bread Crumbs/Coarse salt/2%wt oil	0.0061

Table 29: Dust emissions of full blended powders made with 2.4%wt TCP

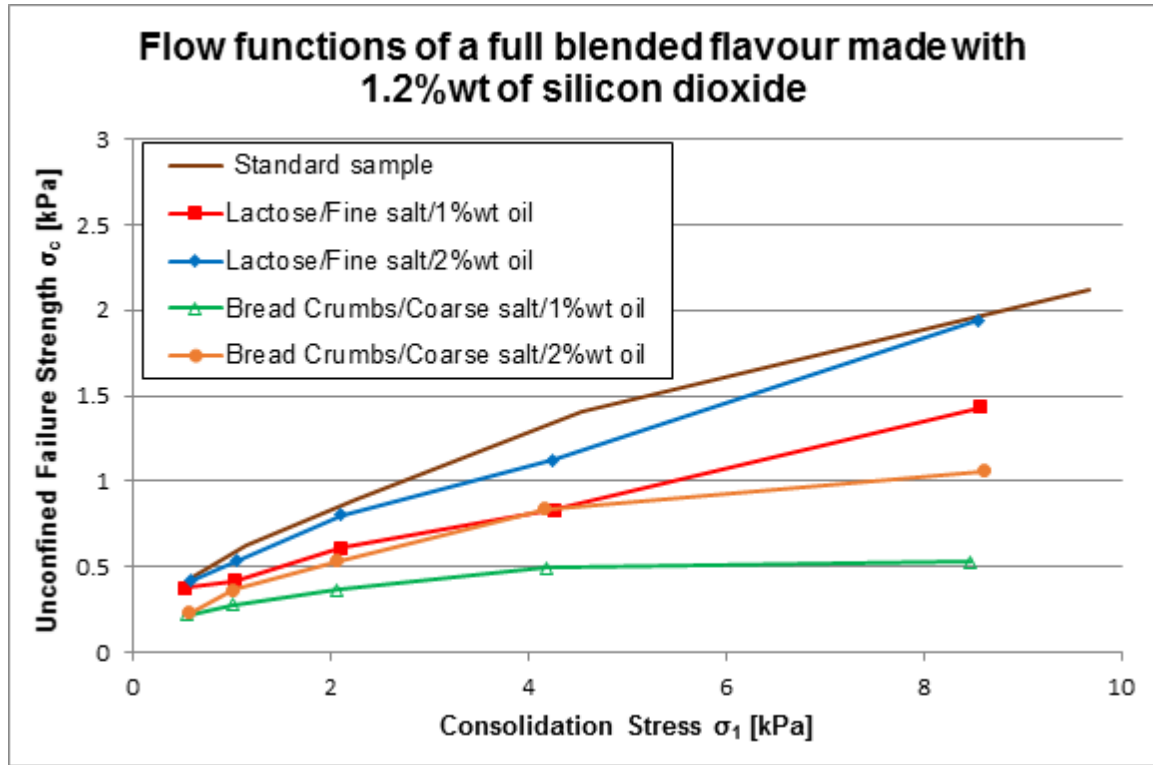


Figure 43: Flow function of full blended powders made with 1.2%wt of silica

Ingredients of the blended flavour	Level of dust (wt%) with 1.2%wt SiO ₂
Standard Flavour	0.0355
Lactose/Fine salt/1%wt oil	0.0610
Lactose/Fine salt/2%wt oil	0.0524
Bread Crumbs/Coarse salt/1%wt oil	0.0711
Bread Crumbs/Coarse salt/2%wt oil	0.0671

Table 30: Dust emissions of full blended powders made with 1.2%wt silica

6.2.2 Effect of different fillers

Based on the results from previous section, the percentage of oil and free flow additive in the trial blends was established as well as the type of free flow additive. Tricalcium phosphate was chosen instead of silicon dioxide due to the significant difference in dust emission for this particular flavour. Based on Givaudan experience, it was decided to use 5% of fine salt and 5% of coarse salt. Figure 44 shows the ingredient

break-down of the proposed trial blends of Flame Grilled Steak flavour without MSG. Test were undertaken to evaluate the effect of different coarse and fine fillers on the reformulated flavour; these were tested adding 1%wt MCT oil as 2%wt was considered an extreme oil content for the flavour blended powder.

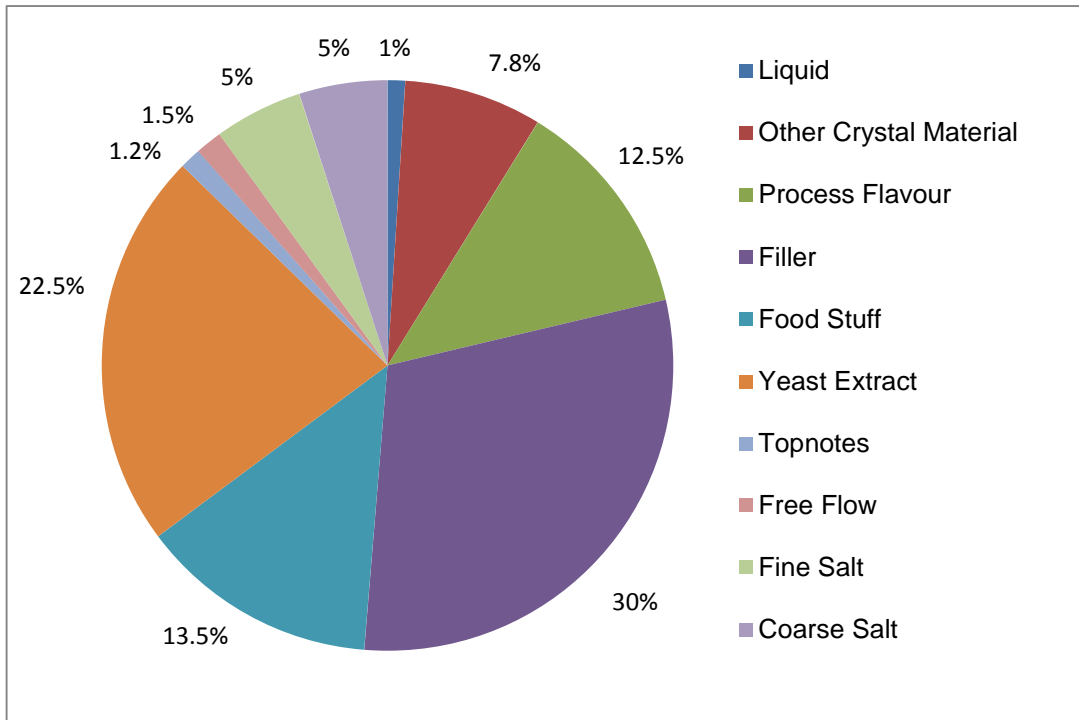


Figure 44: *Ingredient break-down of the proposed trial blends of Flame Grilled Steak flavour without MSG*

Inspection of figures 45 and 46 and tables 31 and 32 show that for the coarse fillers at the selected oil content (1%wt) and free flow level (1.5%wt), the filler type has no significant effect on the flow behaviour or dust emission of the flavour. For the finer fillers, there are significant variations in the bulk strength and dust emission as shown in figure 46 and table 32. The finest filler (lactose mesh 200) has the worst flow and the coarsest filler (lactose GG11519) the best flow behaviour; the bulk strength is range in the order of size. Regarding dust emissions, the freest flowing was the dustiest whereas the other three fine fillers show different flow behaviour but consistent low dust emission as shown in figure 46 and table 32.

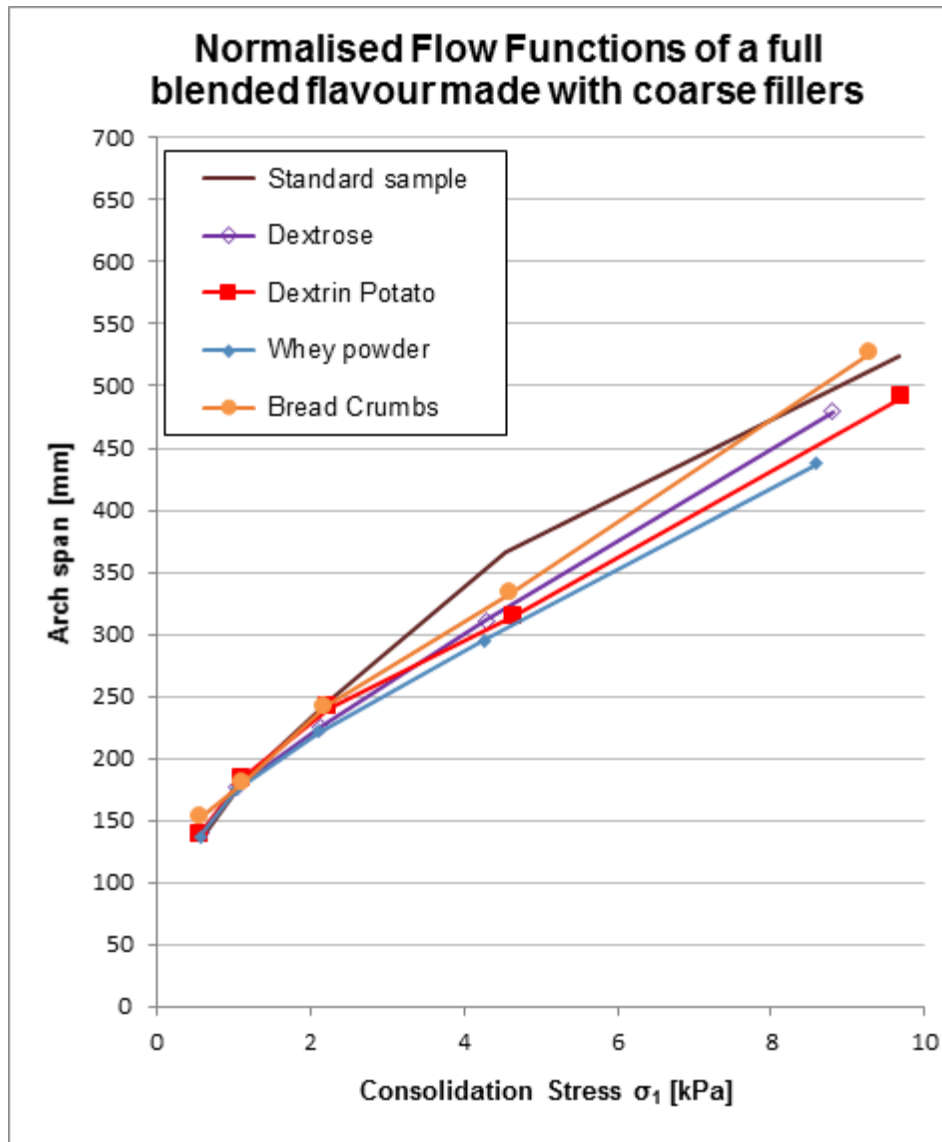


Figure 45: Arch span of full blended flavours made with coarse fillers

Main filler of the blended flavour	Level of dust in wt%
Standard Flavour	0.0355
Dextrose	0.0104
Maltodextrin Potato	0.0079
Whey powder	0.0079
Bread Crumbs	0.0039

Table 31: Dust emissions of full blended flavours made with coarse fillers

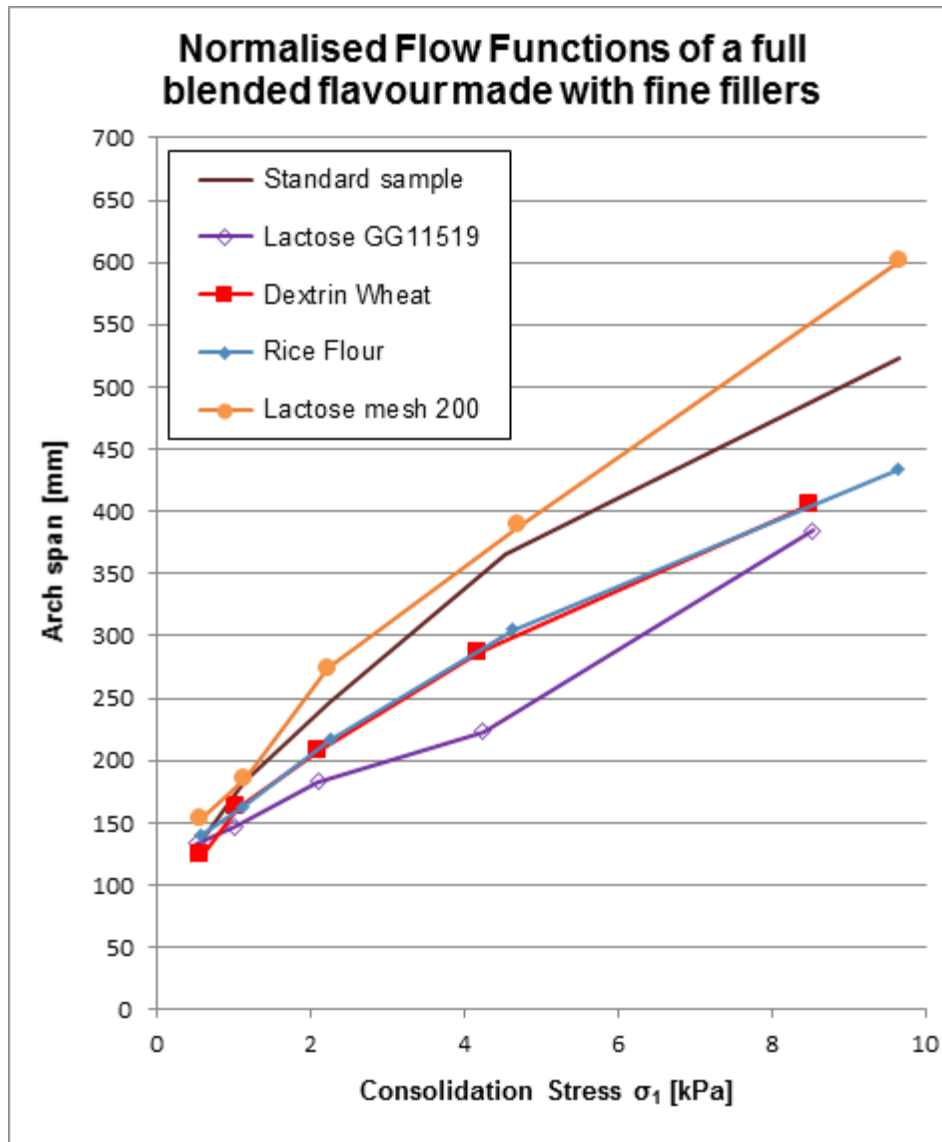


Figure 46: Arch span of full blended flavours made with fine fillers

Main filler of the blended flavour	Level of dust in wt%
Standard Flavour	0.0355
Lactose GG11519	0.0279
Maltodextrin Wheat	0.0125
Rice Flour	0.0104
Lactose mesh 200	0.0125

Table 32: Dust emissions of full blended flavours made with fine fillers

6.2.3 Trial blends

From the results presented in previous section, four different reformulated blends were selected (see figure 47 and table 33) to be trialled at the factory of Intersnack. The selection of the trial blended powders was based on the industrial partners' requirements (see chapter 4) as follows:

- Blend made with bread crumbs which shows similar flow properties to the current standard flavour but much lower dust level
- Blend made with lactose which is significantly freer flowing than the current standard flavour but with the same dust emission
- Blend made with whey powder which shows slightly better flow properties than the current standard flavour with a lower dust level using a cheap filler
- Blend made with maltodextrin potato which shows slightly better flow properties than the current standard flavour with a lower dust level using an expensive filler

Results of the tests using the Rospen loss in weight feed hopper to demonstrate the effectiveness of the blended powders in an industrial environment under adverse environmental conditions (temperature 35°C and humidity 40%RH) are presented in appendix C. These results showed that the trial blends presented a more consistent dose weight during the discharge than the standard sample whereas bridges were formed inside the hopper due to the exposition of the powders to these adverse conditions, even when the agitator was active. The issue was resolved choosing the trial blend made with whey powder for product costs considerations and adding 2%wt of tricalcium phosphate instead of 1.5%wt, this results in a final reformulated blended powder with similar behaviour to standard sample under the extreme conditions of the tests without bridges and showing a consistent dose weight during discharge and lower dust emission.

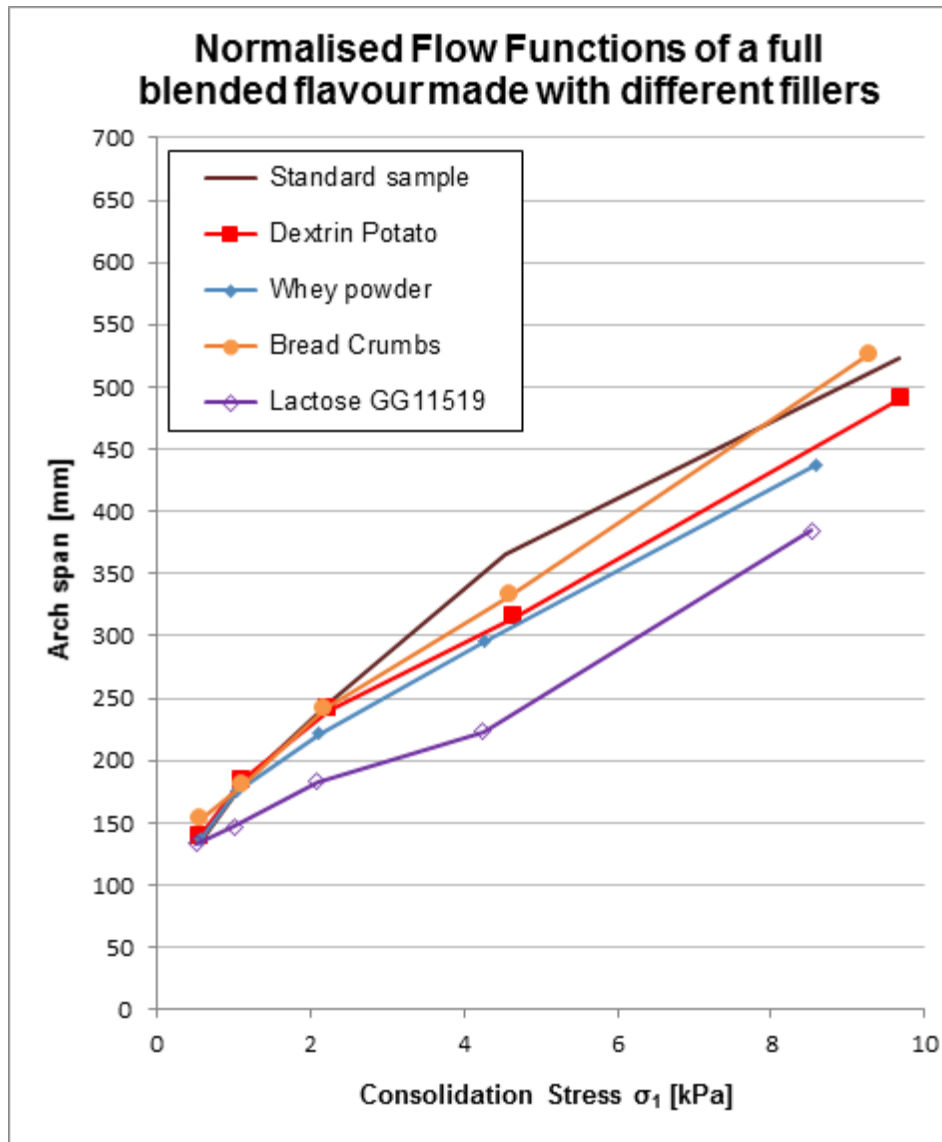


Figure 47: Arch span of the trials blends of the reformulated full blended flavour

Main filler of the blended flavour	Level of dust in wt%
Standard Flavour	0.0355
Maltodextrin Potato	0.0079
Whey powder	0.0079
Bread Crumbs	0.0039
Lactose GG11519	0.0279

Table 33: Dust emissions of the trial blends of the reformulated full blended flavour

6.3 *Experimental investigations*

This section describes the purpose of the test programmes undertaken in the experimental investigations along with the test parameters of each one (particles properties studied, type of powders tested, condition of the powders and additives added) and the main results. Complete description of the programs is presented in chapter 4 and a full set of results plots is presented in appendix B.

The bulk flow properties of a wide range of single and blended powders were measured studying the effect of particle size, surface moisture, level of free flow agent and the number of components and degree of mixedness for blends.

6.3.1 Effect of deconstructed particle size distribution

The aim of these test programmes is to study the influence of the particle size and distribution on four common filler materials named lactose, dextrose, sodium chloride and maltodextrin.

Test Parameters:

- Particle properties: size and breadths of the particle size distribution
- Type of powders: single food fillers
- Condition of the powders: dry
- Additives added: none

With the exception of lactose and maltodextrin, the dry powders tested showed size fractions in the free and easy flowing region as shown in figures 48 - 53. Only those two powders and glass beads presented size fractions with fine particle size below 50 μm , however, all the size fractions of glass beads showed no strength in dry condition as shown in figure 51. Figures 52 and 53 show how the unconfined failure strength and the bulk density vary as a function of the particle size of the size fractions of lactose; as expected, bulk strength decreases and bulk density increases (size fractions with fine particles show more open packing structure) as particle size increases.

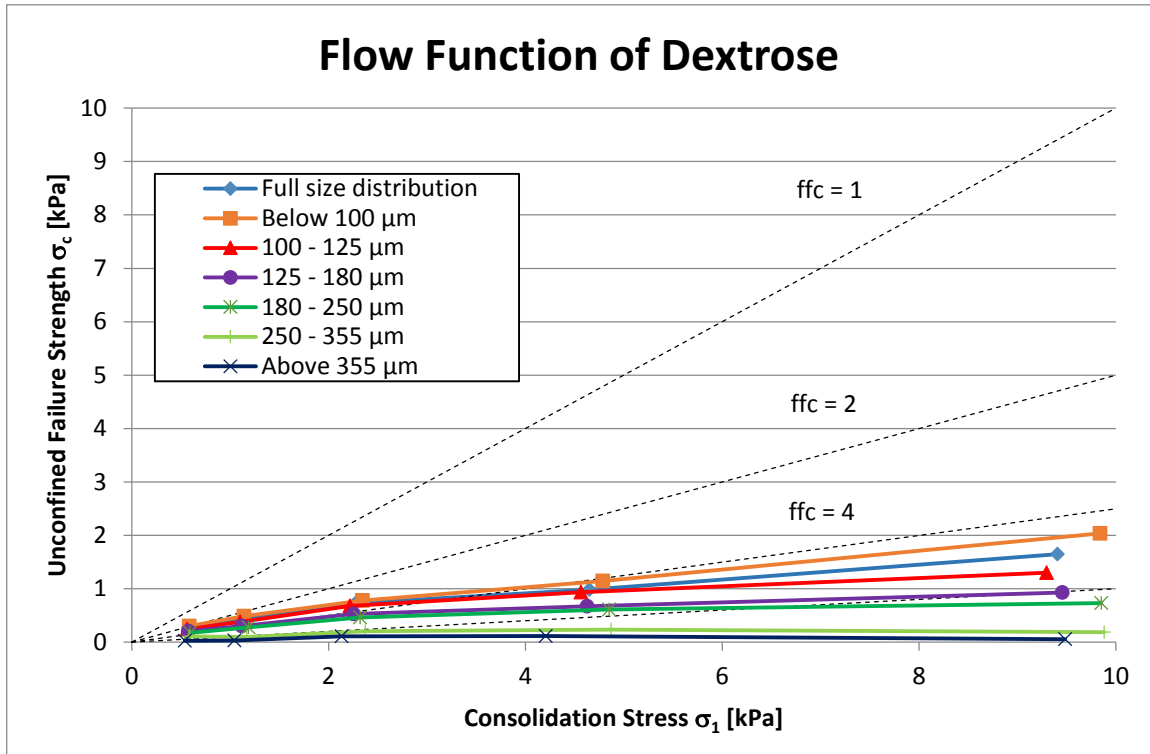


Figure 48: Flow function of particle size fractions of dextrose

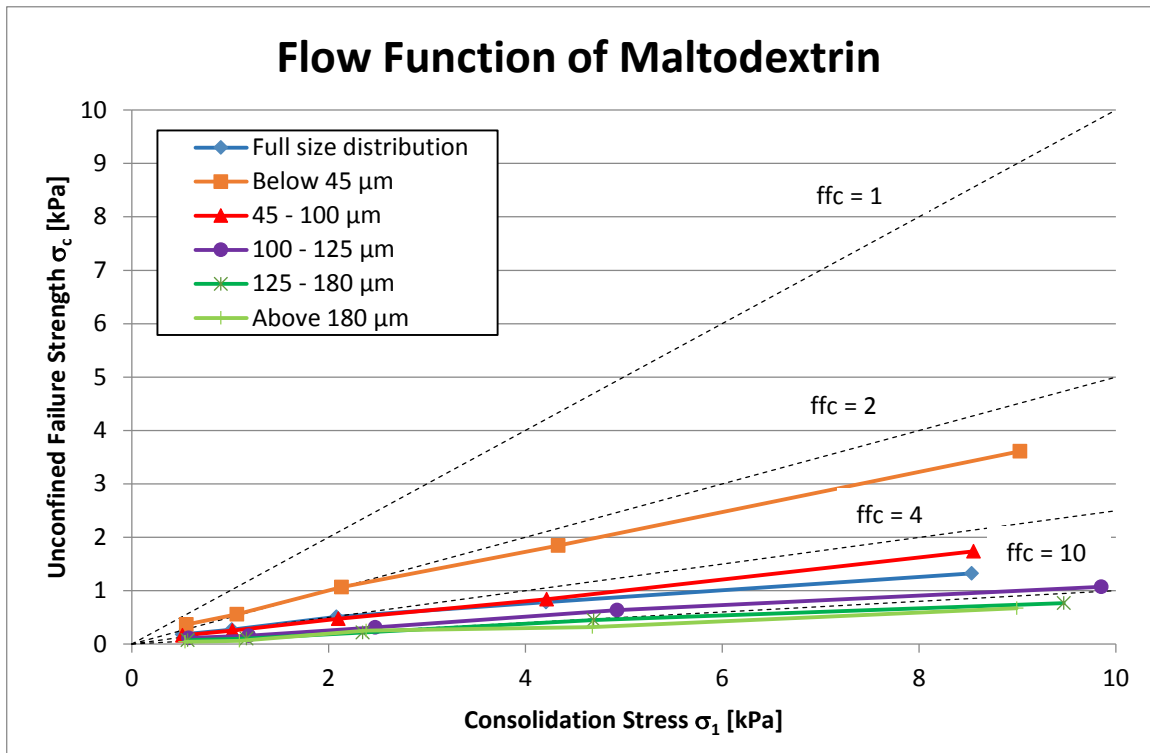


Figure 49: Flow function of particle size fractions of maltodextrin

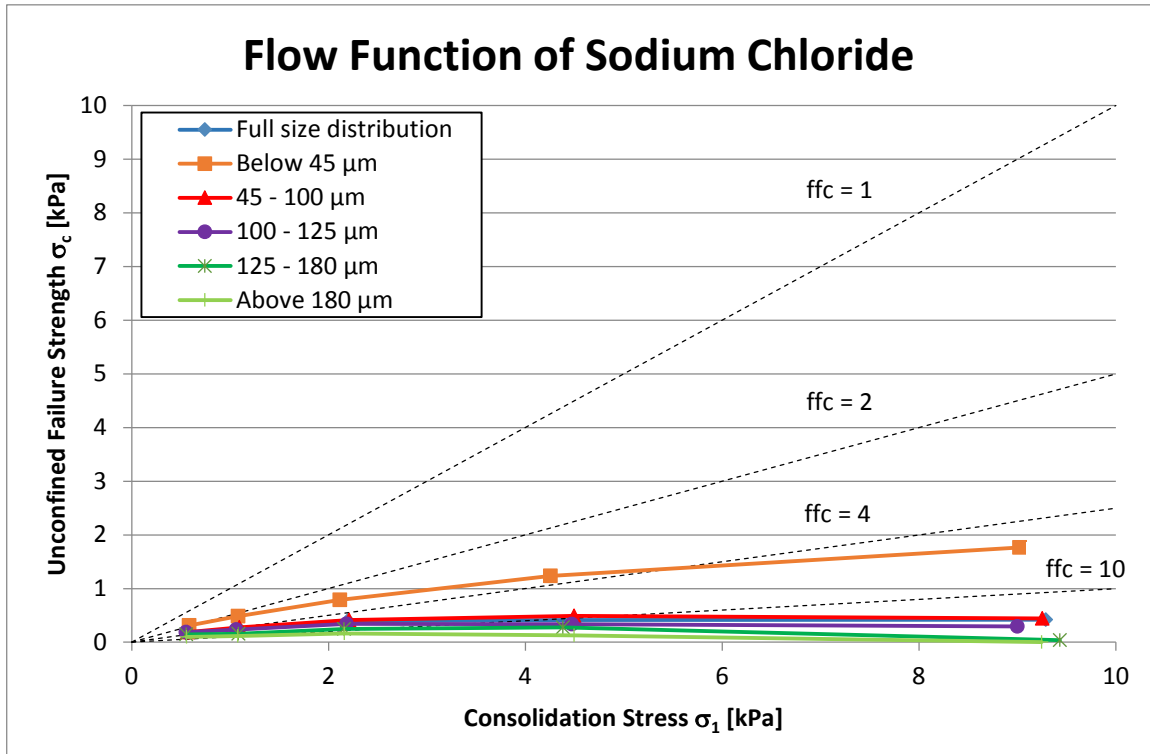


Figure 50: Flow function of particle size fractions of sodium chloride

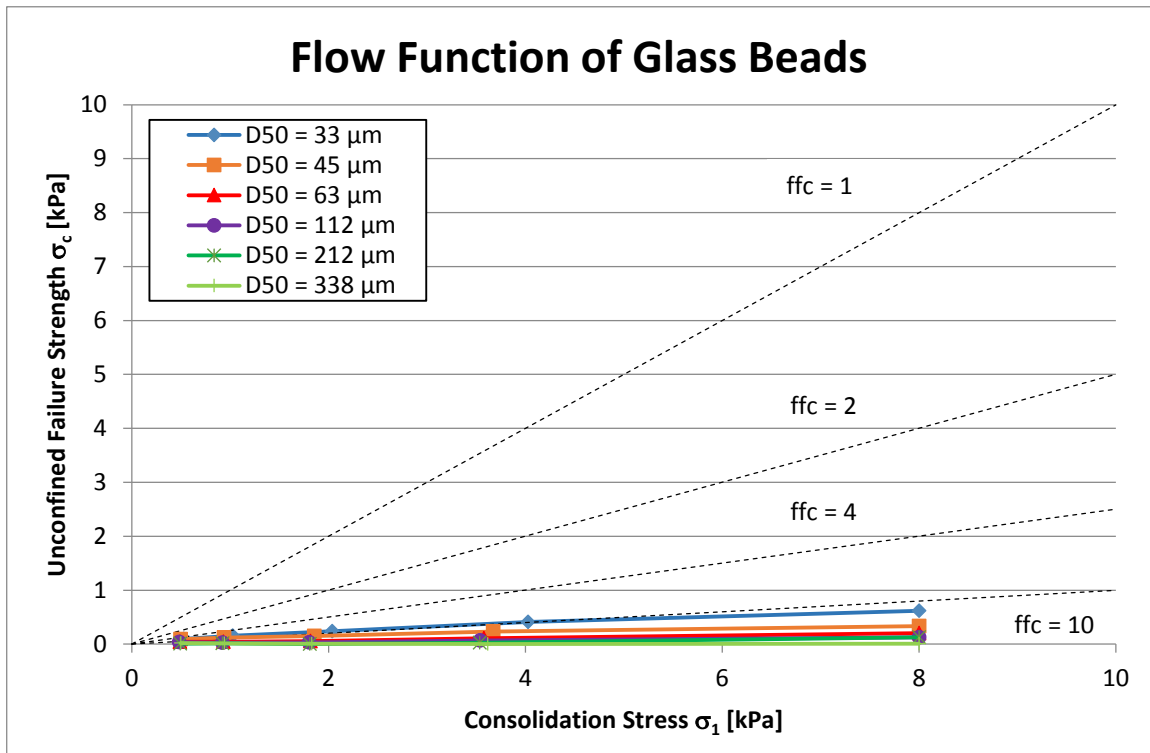


Figure 51: Flow function of six grades of glass beads

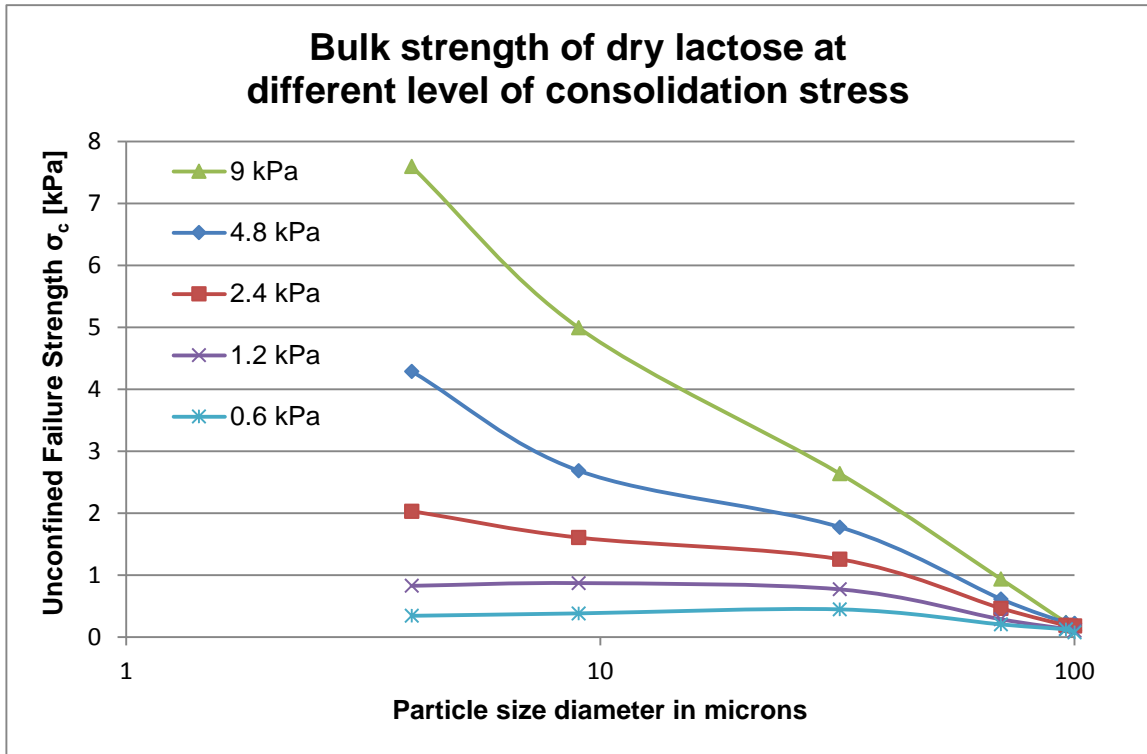


Figure 52: Variation of the bulk strength as a function of the particle size for six grades of lactose

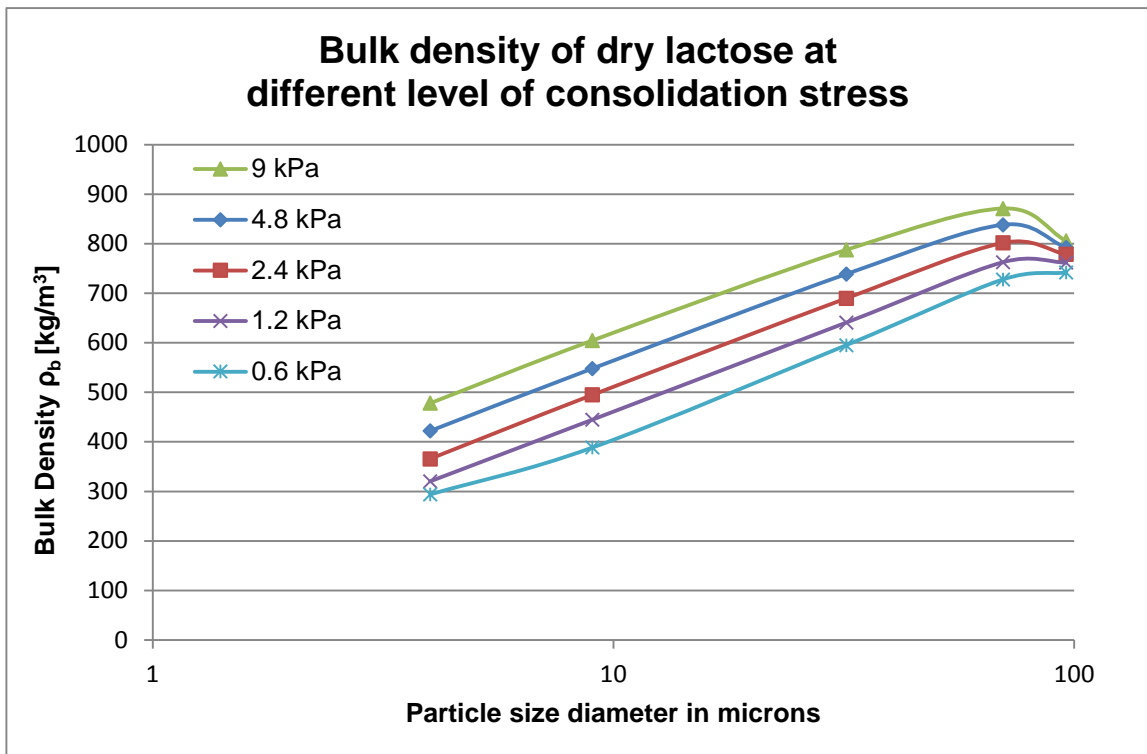


Figure 53: Variation of the bulk density as a function of the particle size for six grades of lactose

6.3.2 Effect of particle shape, size and liquid content on powders

The aim of these test programmes is to study the influence of the particle shape, surface liquid content, liquid type and particle size on three idealised materials named glass beads, crushed glass and sodium chloride.

Test Parameters:

- Particle properties: size and shape
- Type of powders: single idealised particulate materials
- Condition of the powders: dry and wet
- Additives added: liquids

Figure 54 - 57 show the results of the tests undertaken to study the influence of particle shape, size and liquid content (mass basis) on idealised particulate materials. These results showed that with the same particle size, the more irregular the particles are, the greater the bulk strength of the wet powder as shown in figure 56. Irregular particle shape enlarges the effect of the oil content as crushed glass showed the greatest bulk strength followed by sodium chloride and glass beads in decreasing order.

Regarding the effect of the liquid properties, figure 57 shows that the more viscous oils (Miglyol 829) may present bad distribution of the oil and the liquid bridges are not formed properly.

Figures 54 and 55 show the influence of the type of liquid on the bulk strength of different size fractions of glass beads tested. As expected, the finer the particles, the greater the effect of the liquid content. The results highlighted the effect of the surface tension at low liquid content (pendular state) showing a great increase of the bulk strength with a minimum amount of oil added to the powders. This effect is more remarkable in size fractions with particle size lower than 100 μm . In the funicular state of saturation, an approximately linear behaviour was found with values of the bulk strength showing a small variation.

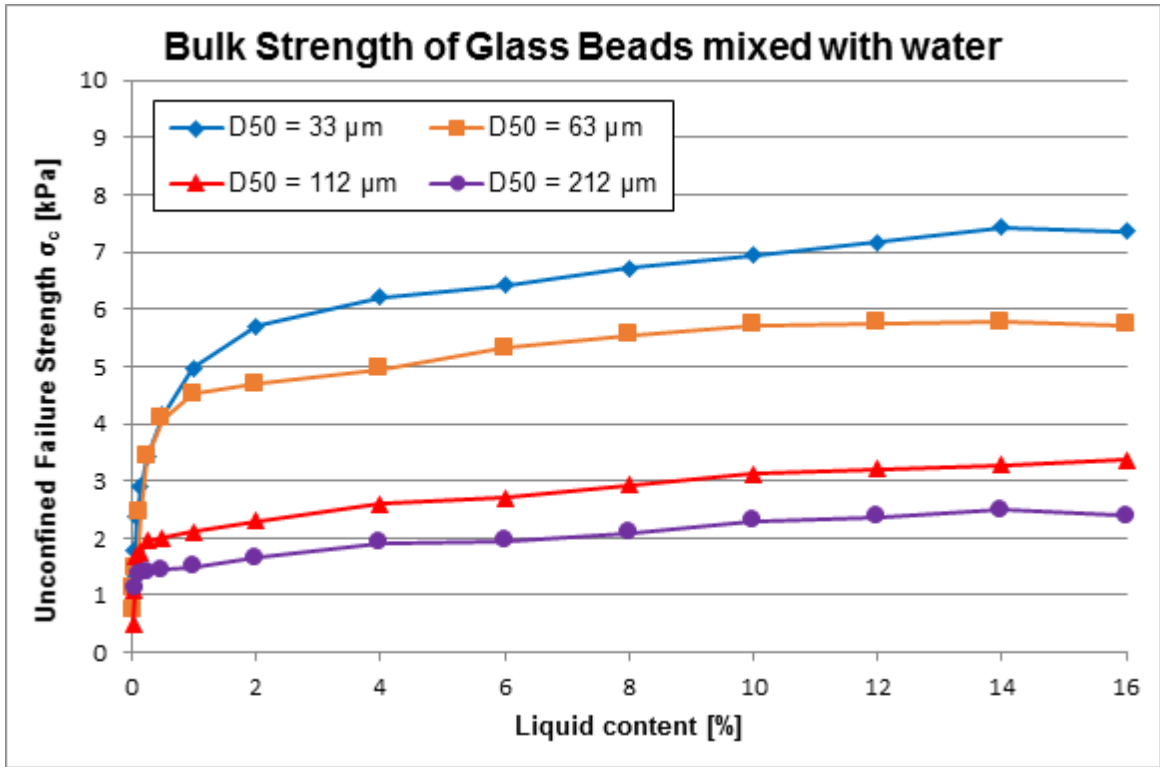


Figure 54: Bulk strength of grades of glass beads blended with de-ionised water

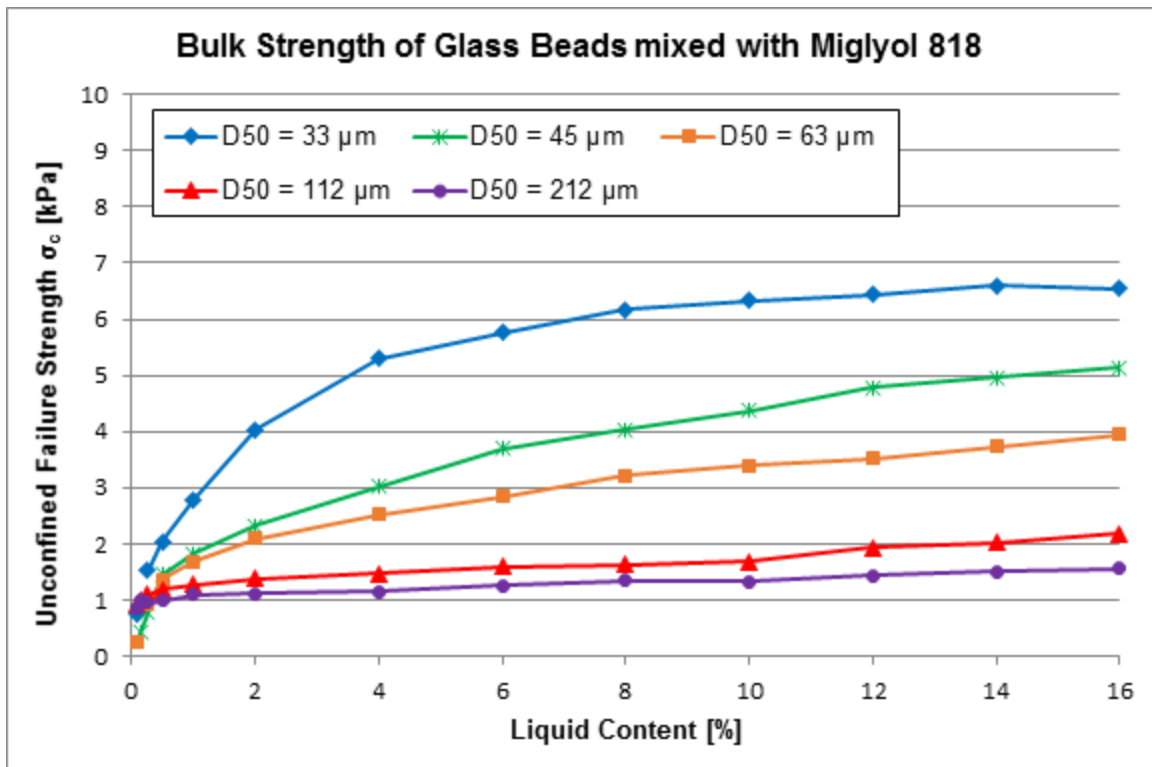


Figure 55: Bulk strength of grades of glass beads blended with Miglyol oil 818

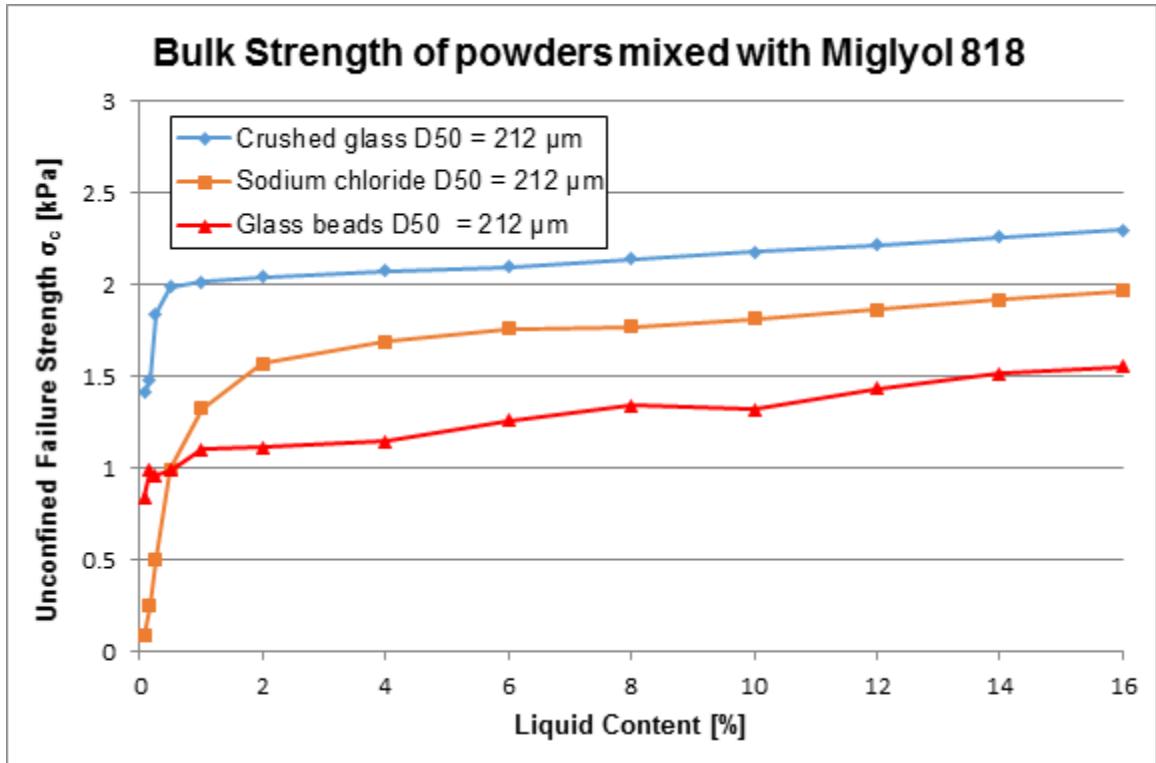


Figure 56: Bulk strength glass beads, crushed glass and sodium chloride blended with Miglyol oil 818

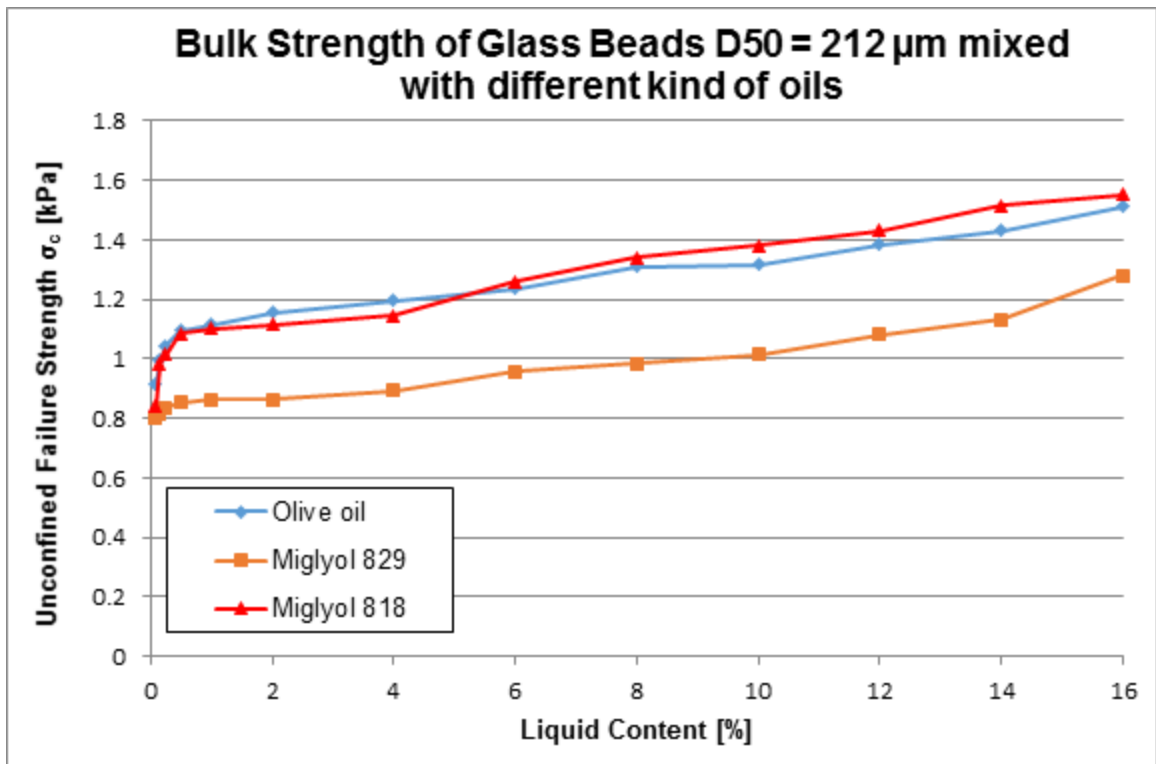


Figure 57: Bulk strength of glass beads blended with olive oil, Miglyol oil 818 and Miglyol oil 829

6.3.3 Effect of particle size on dry blends

The aim of this test programme is to study the influence of the particle size of the constituent ingredients on dry blends of powders and idealised materials named dextrose, dextrose-wheat, lactose, sodium chloride and glass beads.

Test Parameters:

- Particle properties: size
- Type of powders: multicomponent simplified blends of food powders and idealised materials
- Condition of the powders: dry
- Additives added: none

Figure 58 - 63 show the results of the tests undertaken to study the influence of the particle size on dry blended powders. These results showed how the presence of fine particles in blends makes the powders more cohesive. These also showed that a minimum amount of 30%wt of fine powders is required to become the final blend cohesive. However, this conclusion is based on limited amount of tests undertaken and further work is required with a wide range of blended powders with different contents of fine particles.

Figure 62 and 63 show the effect of packing on the bulk flow properties of binary blends of glass beads. Mixing size fractions of fine glass beads ($D_{50} = 33 \mu\text{m}$) with coarser size fractions ($D_{50} = 112 \mu\text{m}$ and $D_{50} = 338 \mu\text{m}$), voidage reaches a lowest value at the range of 30 – 40%wt of the finest particles showing the greatest bulk strength as the closest packing structure was obtained. Further addition of fine particles increases the voidage and decreases the unconfined bulk strength of the blended powders. Once the closest packing structure is achieved (maximum bulk strength and minimum voidage), the addition of more fine particles to the blend only increases the voidage and decreases the bulk strength reached.

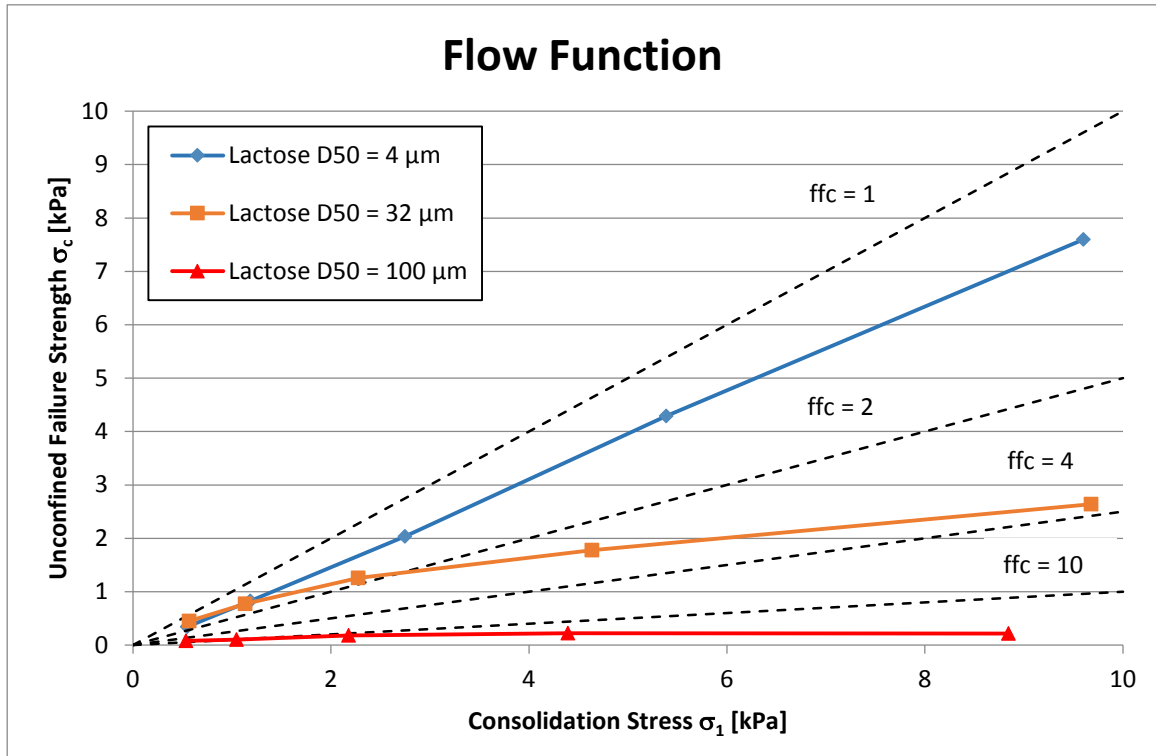


Figure 58: Flow function of three grades of lactose

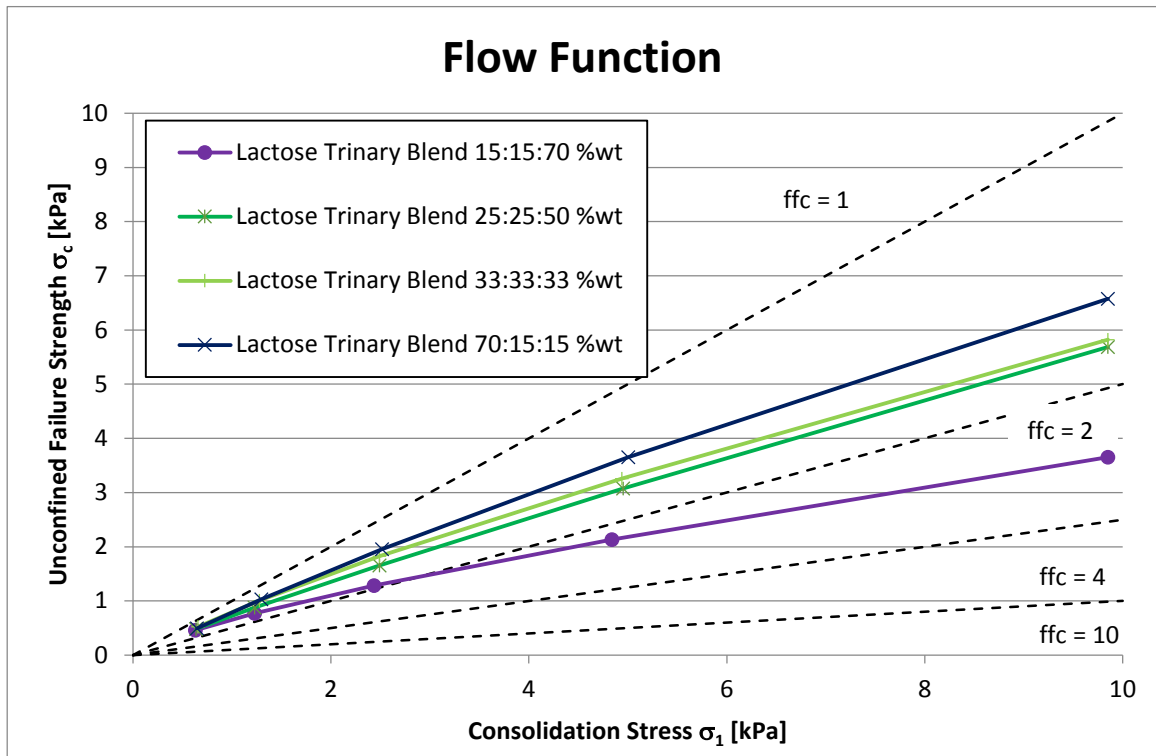


Figure 59: Flow function of trinary blends of lactose

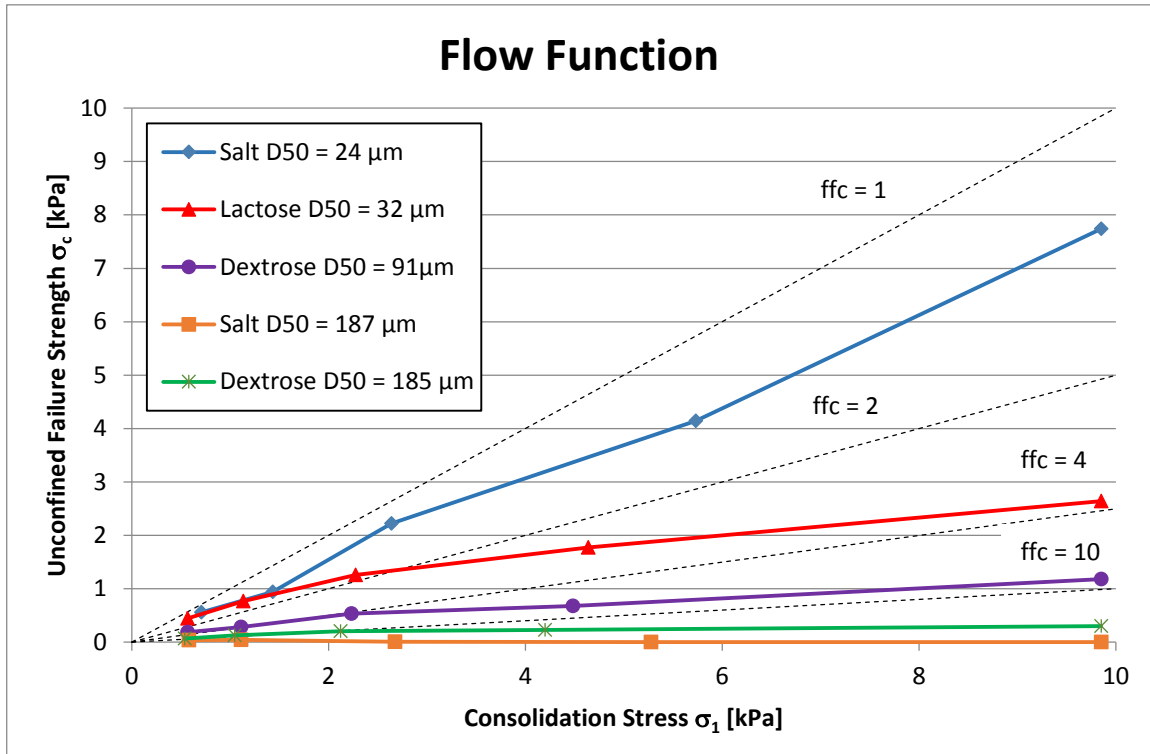


Figure 60: Flow function of five powders

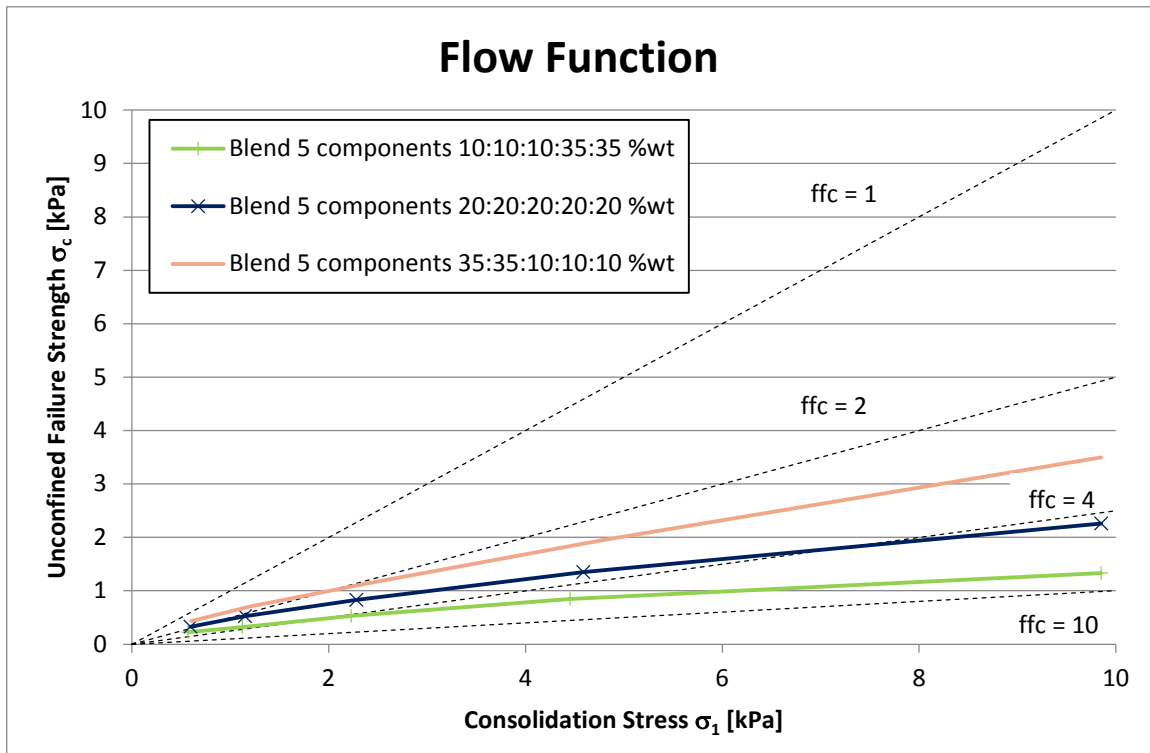


Figure 61: Flow function of blends with five ingredients

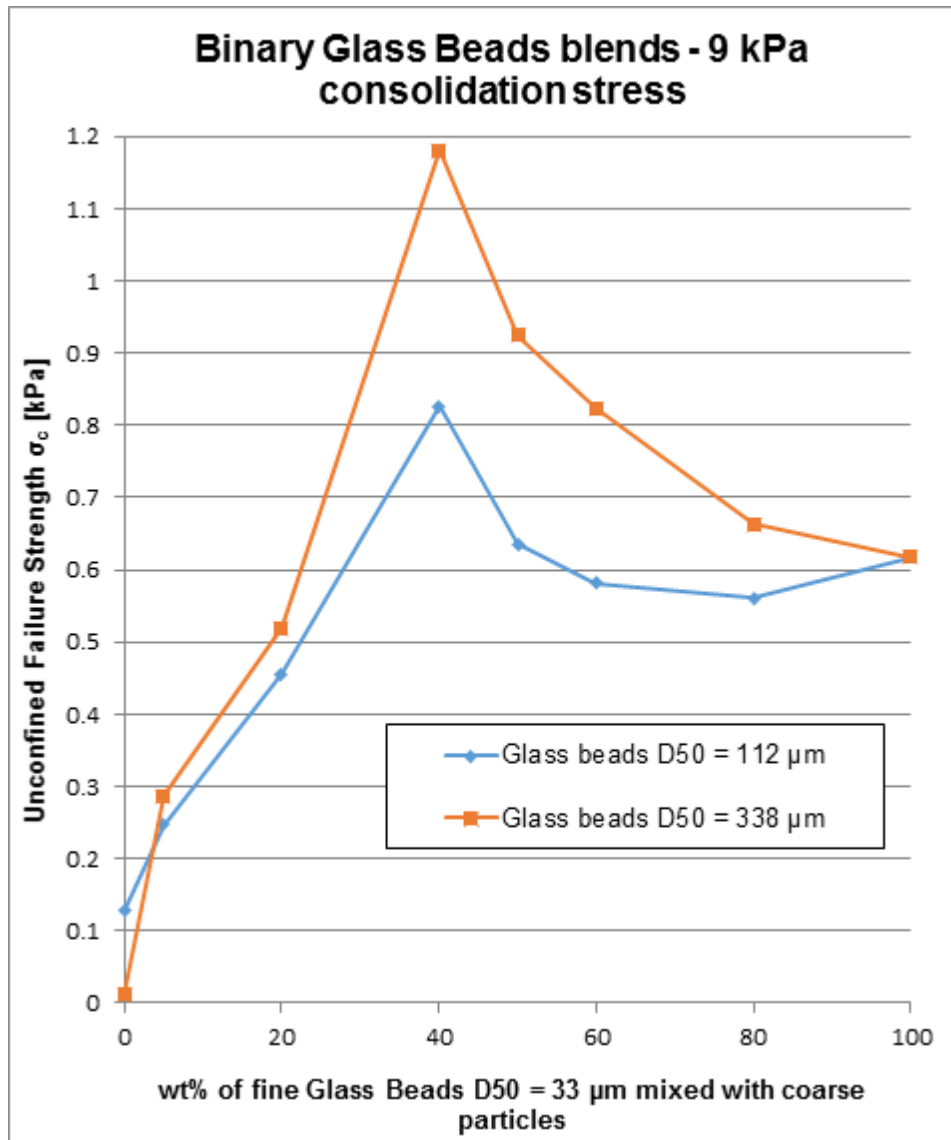


Figure 62: Bulk strength of binary blends made with glass beads

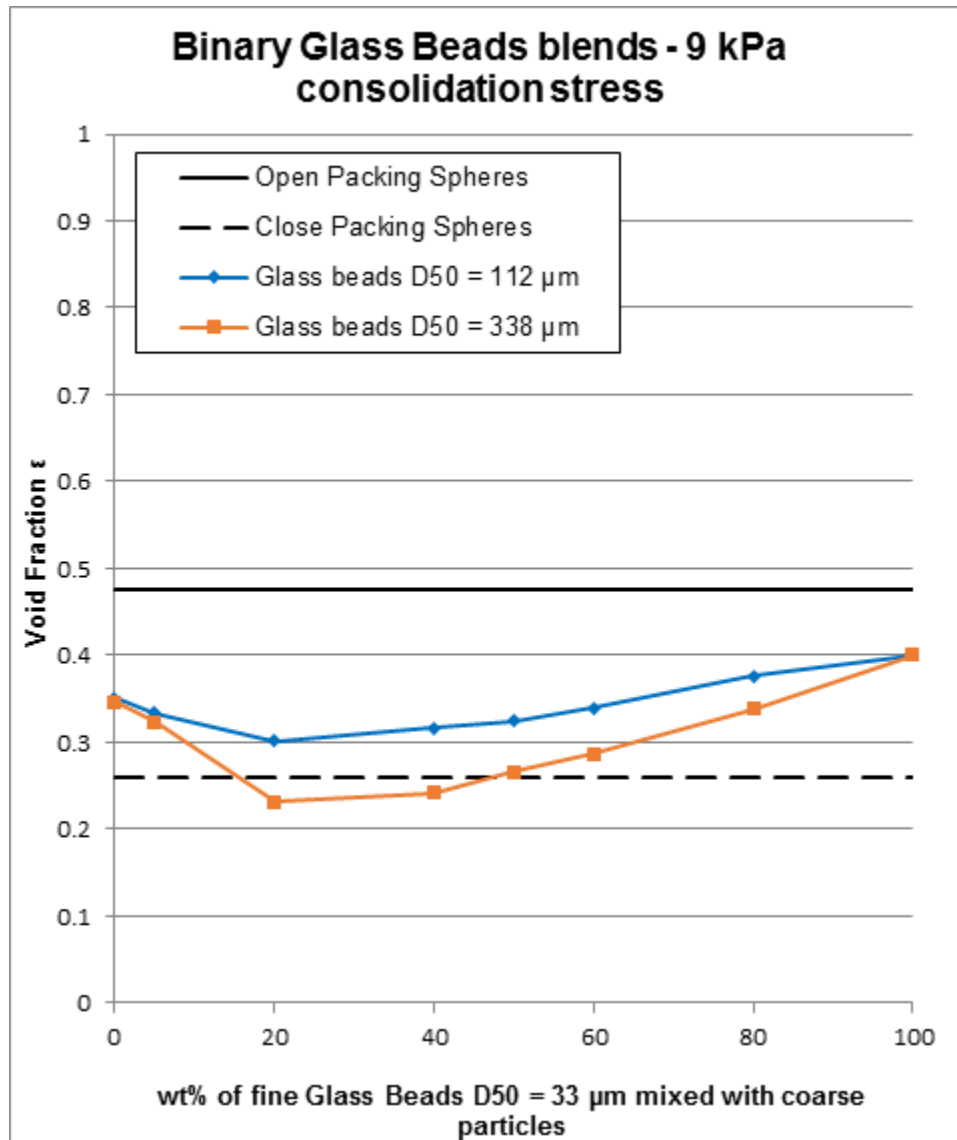


Figure 63: : Voidage of binary blends made with glass beads

6.3.4 Effect of particle shape and size on wet blends

The aim of these test programmes is to study the influence of particle shape and size of the components on wet blended idealised materials named glass beads, crushed glass and sodium chloride.

Test Parameters:

- Particle properties: size and shape
- Type of powders: multicomponent simplified blends of idealised materials
- Condition of the powders: wet
- Additives added: liquid

Figures 64 – 69 show the results of the tests undertaken to study the influence of particle shape and size on the bulk flow properties of blended idealised particulate materials. These results showed the effect of packing on the bulk flow properties of wet binary blends of idealised materials. As shown in figures 64 - 66, the finest the particles mixed with the coarse particles, the greatest the liquid content required to reach the maximum bulk strength of the binary blended powder. Once the closest packing structure is achieved (maximum bulk strength), the addition of more liquid content to the blend only decreases the bulk strength reached. Figures 62 and 63 presented and explained in the previous section of the chapter show the same effect on the packing and bulk flow properties of dry blends made with different grades of glass beads.

Regarding the particle shape, not much difference was found in the measured bulk strength of wet binary blends mixed in a 50:50 proportion using different idealised powders as shown in figures 67 - 69.

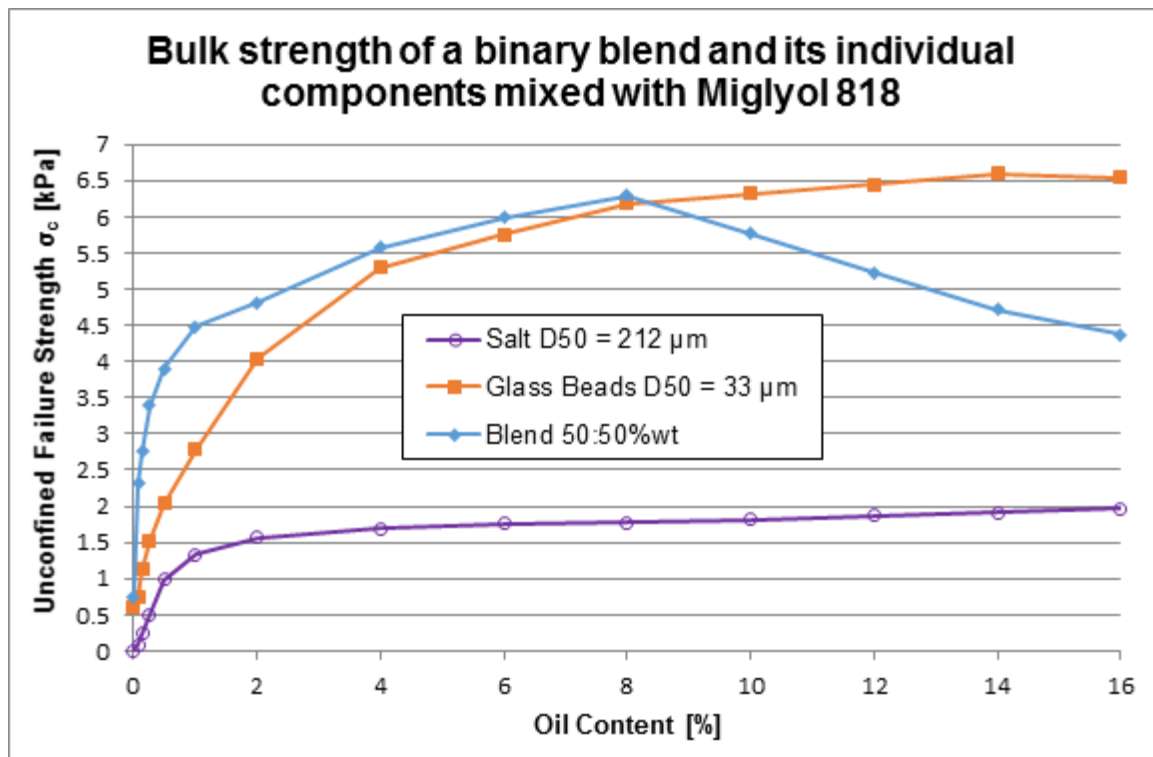


Figure 64: Bulk strength of a binary blend (glass beads $D_{50} = 33 \mu\text{m}$ and sodium chloride $D_{50} = 212 \mu\text{m}$) and its individual components mixed with Miglyol oil 818

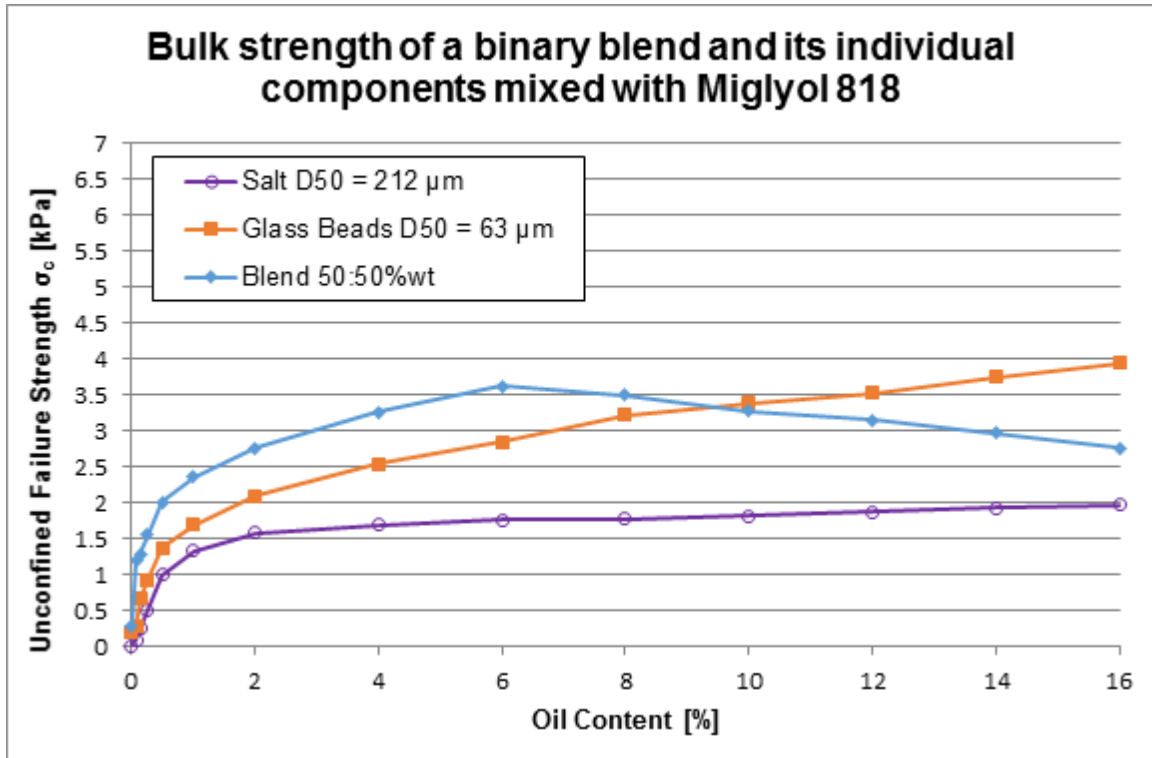


Figure 65: Bulk strength of a binary blend (glass beads D50 = 63 μm and sodium chloride D50 = 212 μm) and its individual components mixed with Miglyol oil 818

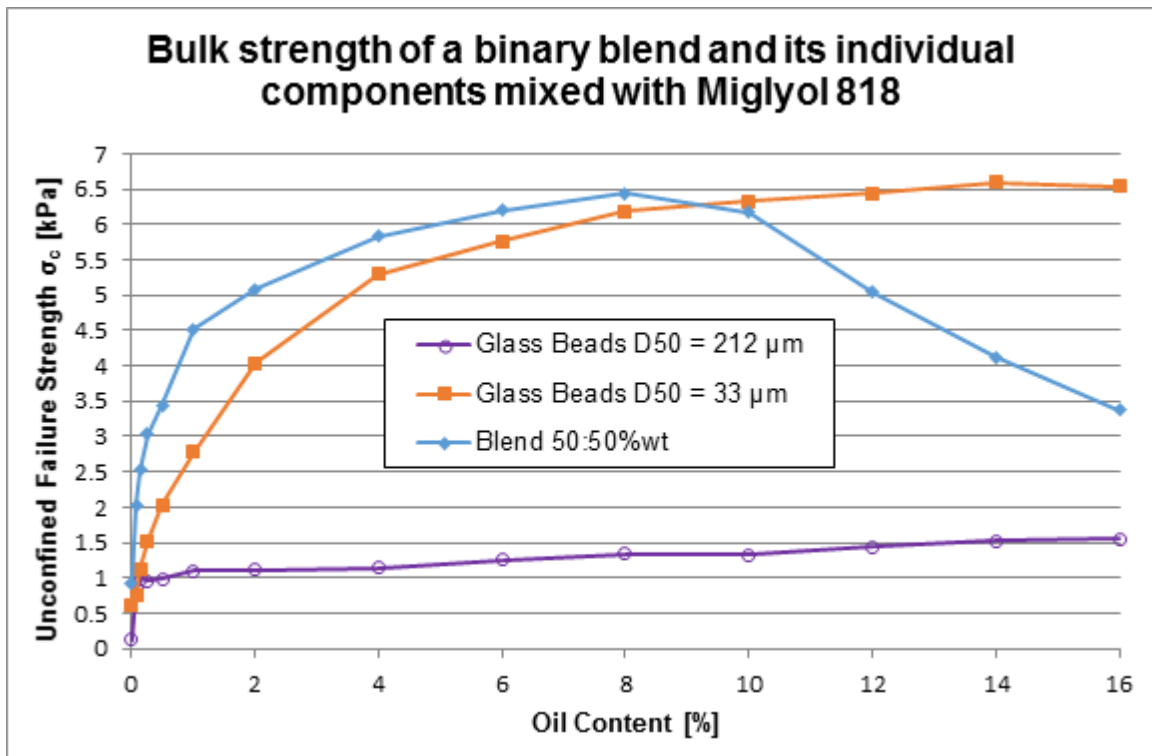


Figure 66: Bulk strength of a binary blend with two grades of glass beads and its individual components mixed with Miglyol oil 818

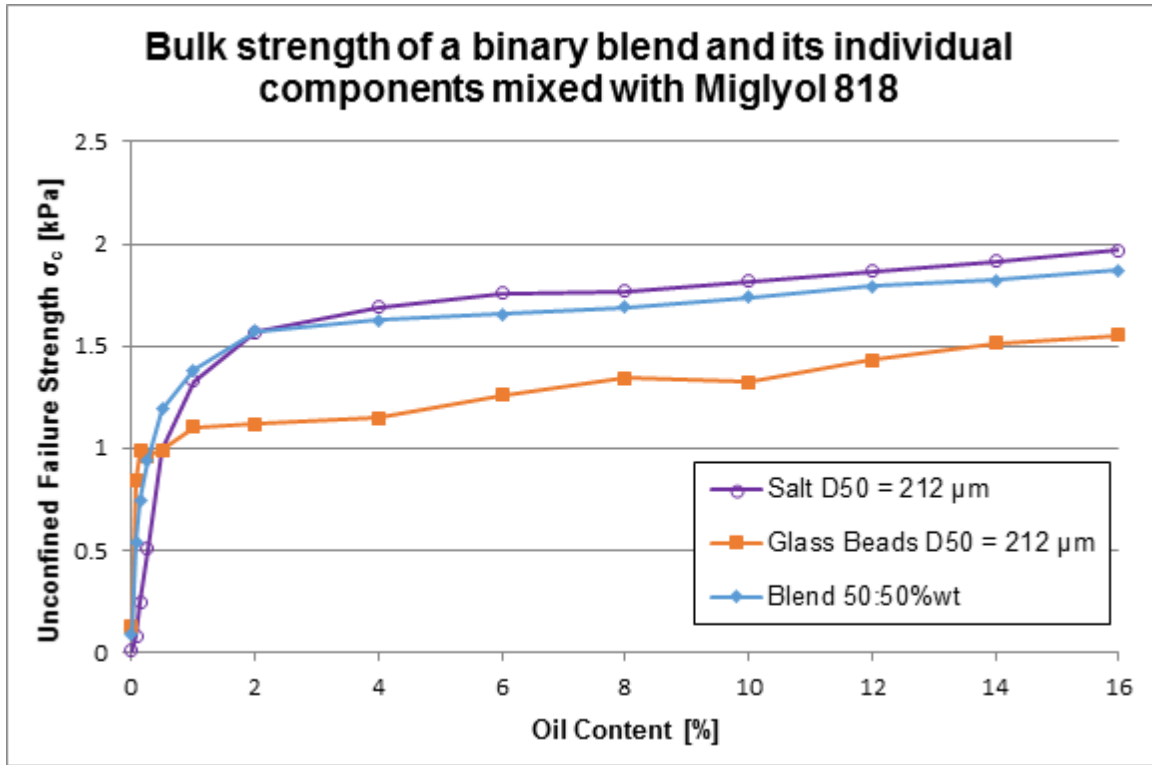


Figure 67: Bulk strength of a binary blend (glass beads D50 = 212 μm and sodium chloride D50 = 212 μm) and its individual components mixed with Miglyol oil 818

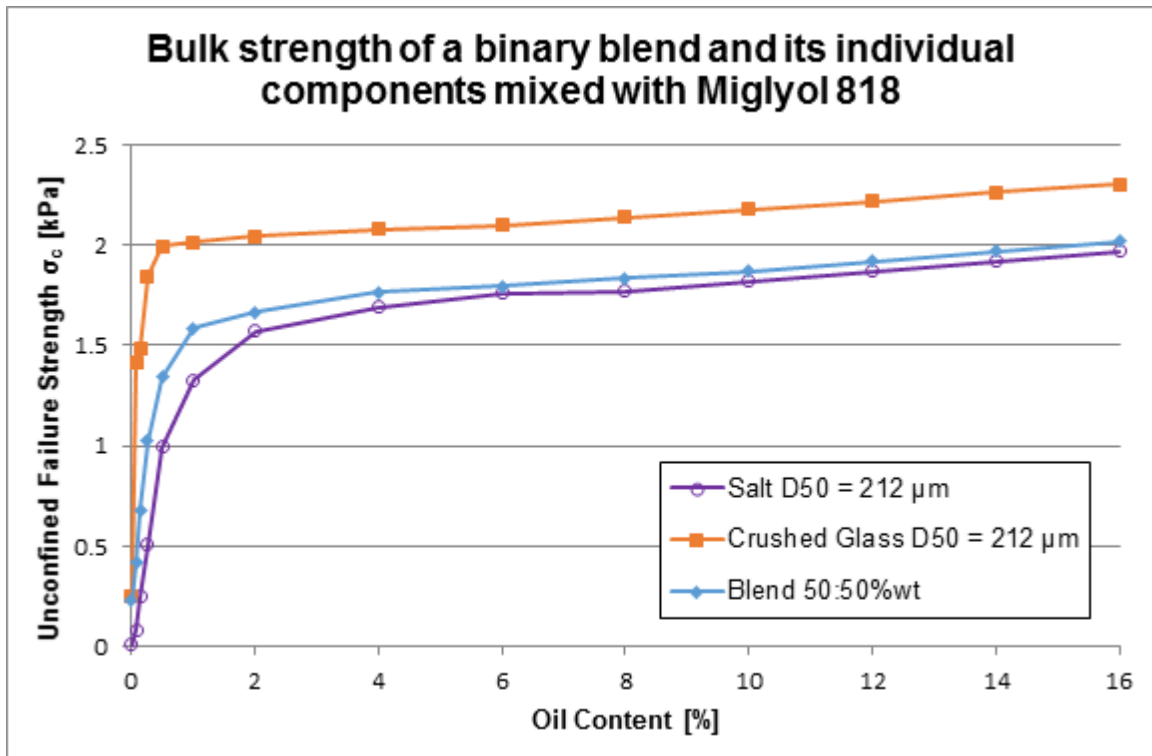


Figure 68: Bulk strength of binary blend (crushed glass D50 = 212 μm and sodium chloride D50 = 212 μm) and its individual components mixed with Miglyol oil 818

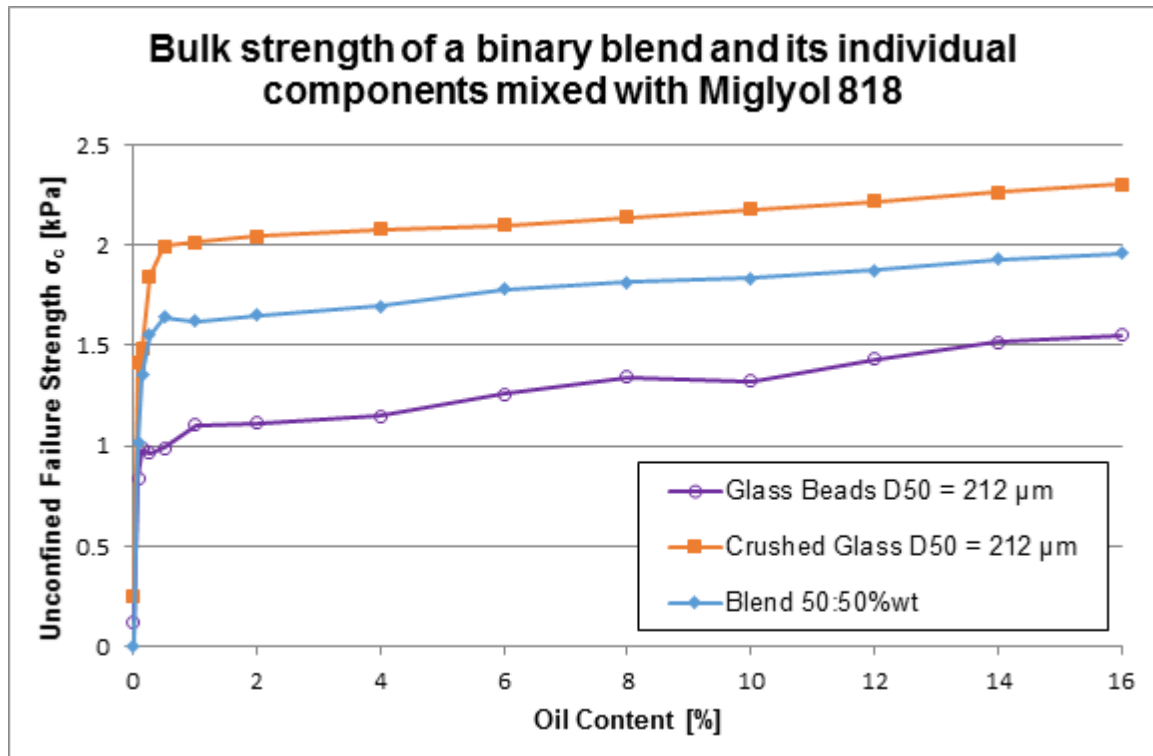


Figure 69: Bulk strength of binary blend (glass beads $D50 = 212 \mu\text{m}$ and crushed glass $D50 = 212 \mu\text{m}$) and its individual components mixed with Miglyol oil 818

6.3.5 Interaction between oil and free flow additives

The aim of these test programmes is to study the interaction between three common free flow additives named silicon dioxide, tricalcium phosphate and magnesium carbonate and oil at different liquid levels.

Test Parameters:

- Particle properties: none
- Type of powders: single flow property modifying ingredients
- Condition of the powders: wet
- Additives added: liquid and free flow additives

Figures 70 - 72 show the value of the saturation of dioxide, tricalcium phosphate and magnesium carbonate due to the addition of Miglyol oil 818. Silicon dioxide saturated when 200%wt of oil content was added whereas the other two flow agents saturated with lower values of oil content; 50%wt for tricalcium phosphate and 150%wt for magnesium carbonate.

From these saturation values, the amount of flow agent required to reduce the bulk strength due to the addition of the oil in powders and obtain the optimum and lowest strength could be predicted. However, these predictions do not match the experimental data presented in the next section of the chapter. It seems like the presence of a powder in addition to the free flow additive and the oil is need to study the effect of the flow agents.

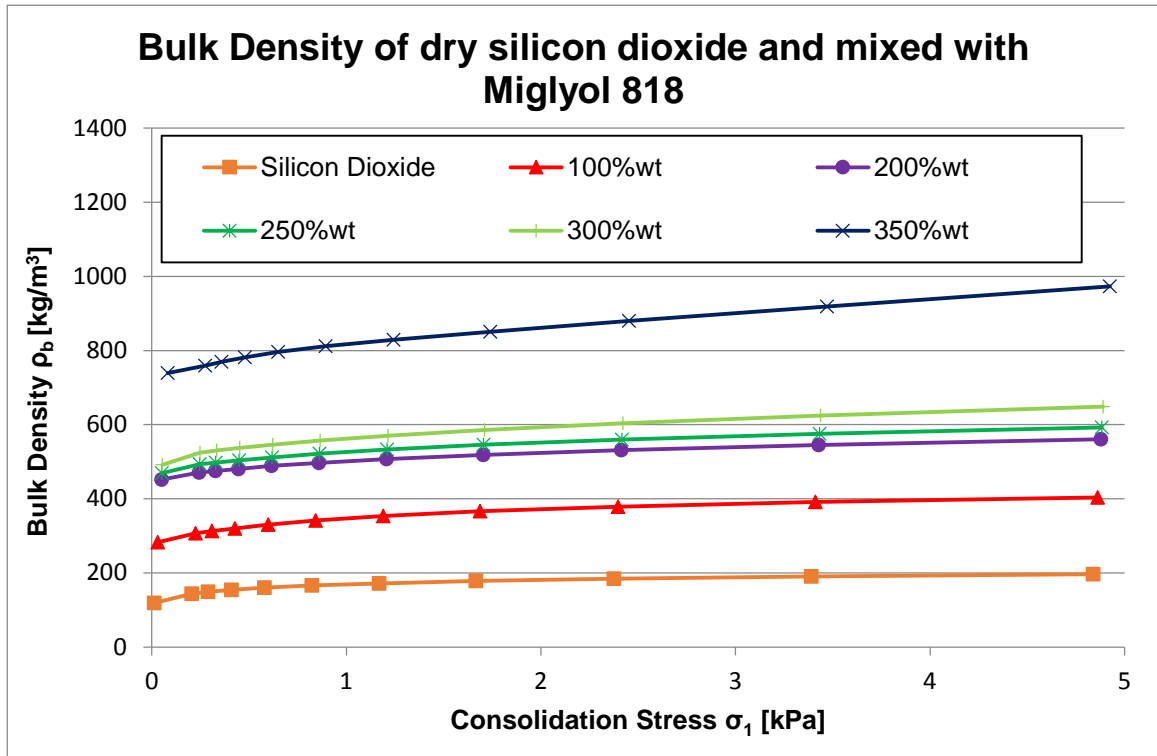


Figure 70: Saturation of silicon dioxide adding Miglyol oil 818

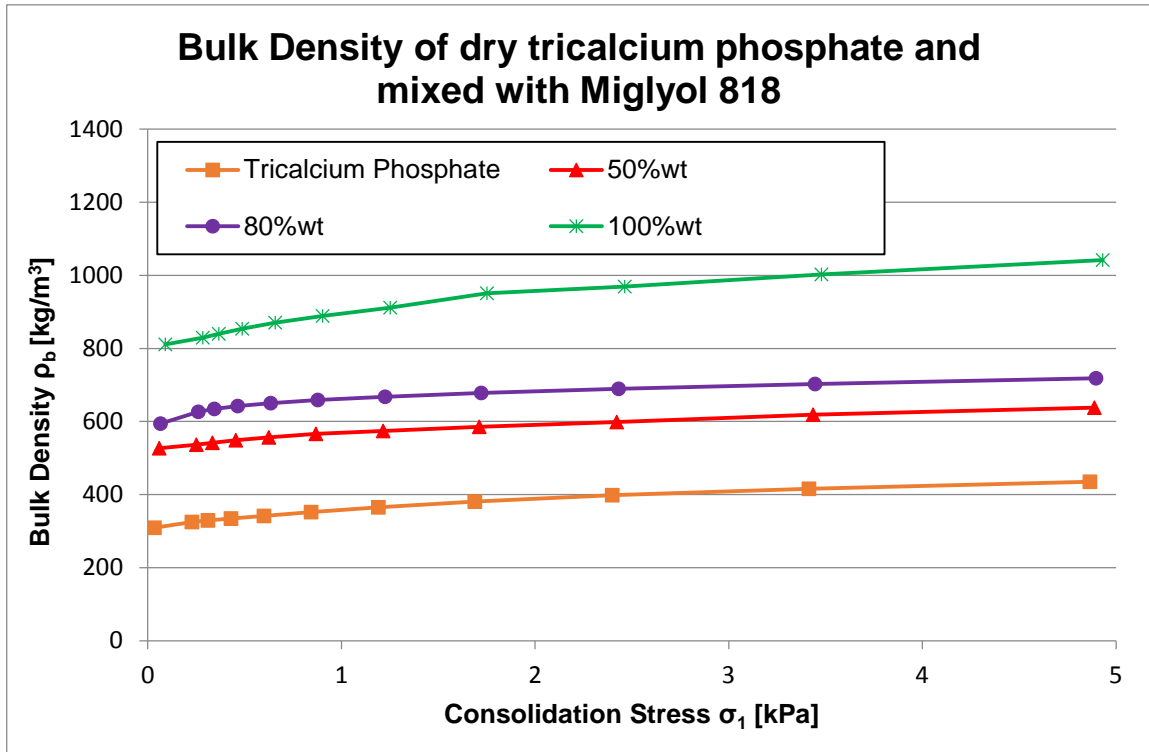


Figure 71: Saturation of tricalcium phosphate adding Miglyol oil 818

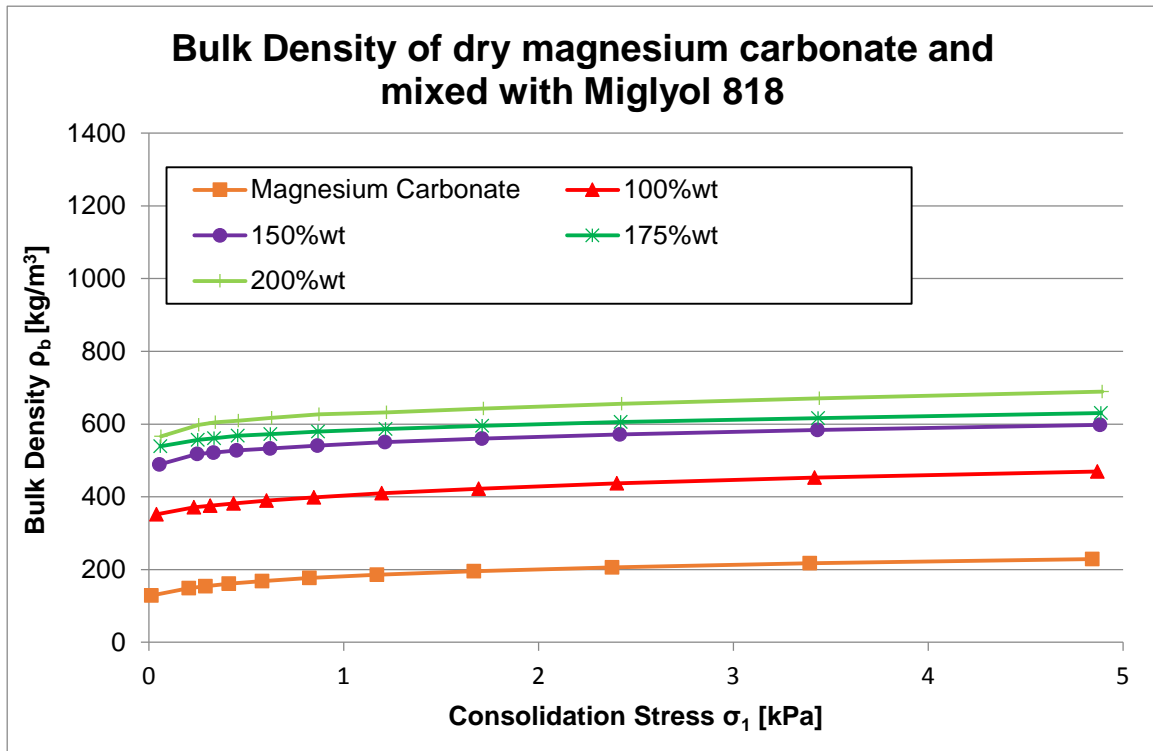


Figure 72: Saturation of magnesium carbonate adding Miglyol oil 818

6.3.6 Effect of free flow additives

The aim of these test programmes is to study the influence of the level and type of free flow additive on common filler powders (lactose and maltodextrin), idealised particulate materials (glass beads) and a blended snack flavour at different levels of oil.

Test Parameters:

- Particle properties: none
- Type of powders: blended snack flavour and single fillers & idealised materials
- Condition of the powders: dry and wet
- Additives added: liquid and free flow additives

Figures 73 - 80 show the result of the tests undertaken to define the shape of the bulk strength curves due to the addition of free flow agents to wet powders. These showed that the bulk strength is at maximum when only liquid is added to the powder; this is coming down at a low level of free flow additive added until the optimum strength is achieved and the additive covers the total surface of the host particle, further addition of additive increases the level of dust and the bulk strength significantly. This behaviour was consistent across different type of flow agents added to a full blended powder and different particles sizes of single real and idealised powders tested.

The results of the measured bulk flow properties of dry blends made with single powders and free flow additives (figures 75 and 76) showed that free flow additives are not effective on dry powders.

Approximately linear behaviour was found between the maximum bulk strength (no flow agent added) and the optimum strength as well as from this point to the value of the bulk strength at the maximum weight percentage of free flow additive added in the experimental work undertaken in the research.

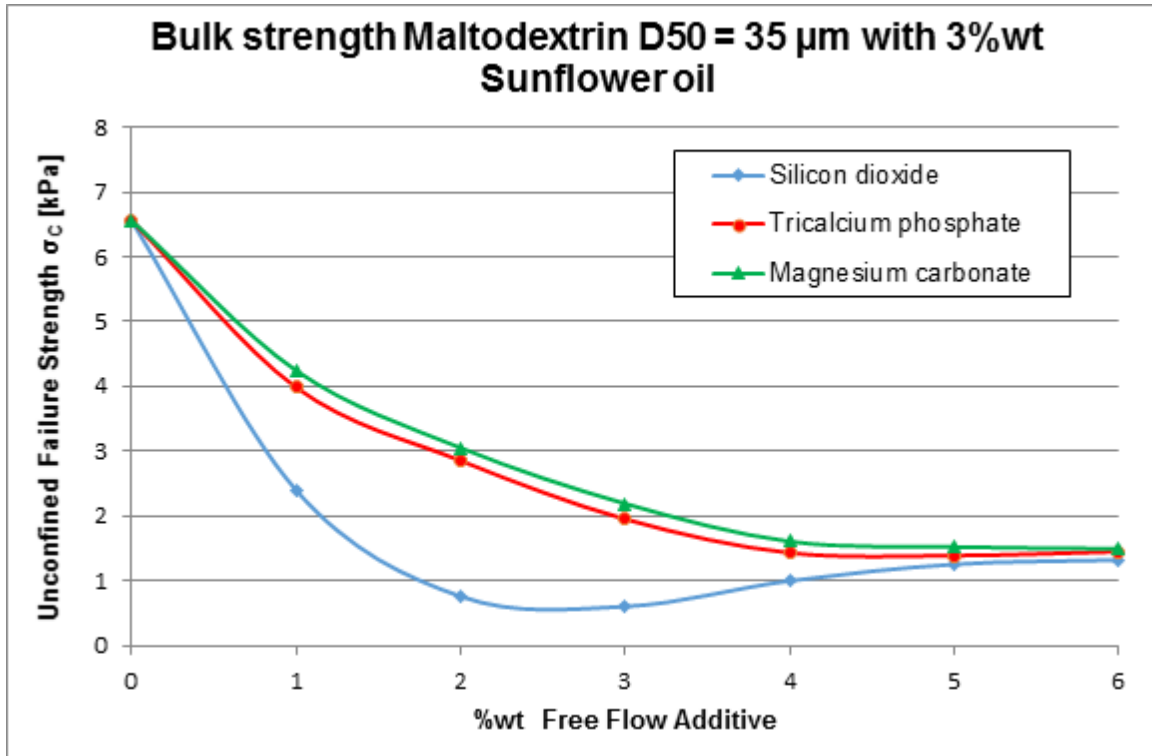


Figure 73: Bulk strength of wet maltodextrin as a function of the %wt of the free flow additives for three different free flow additives

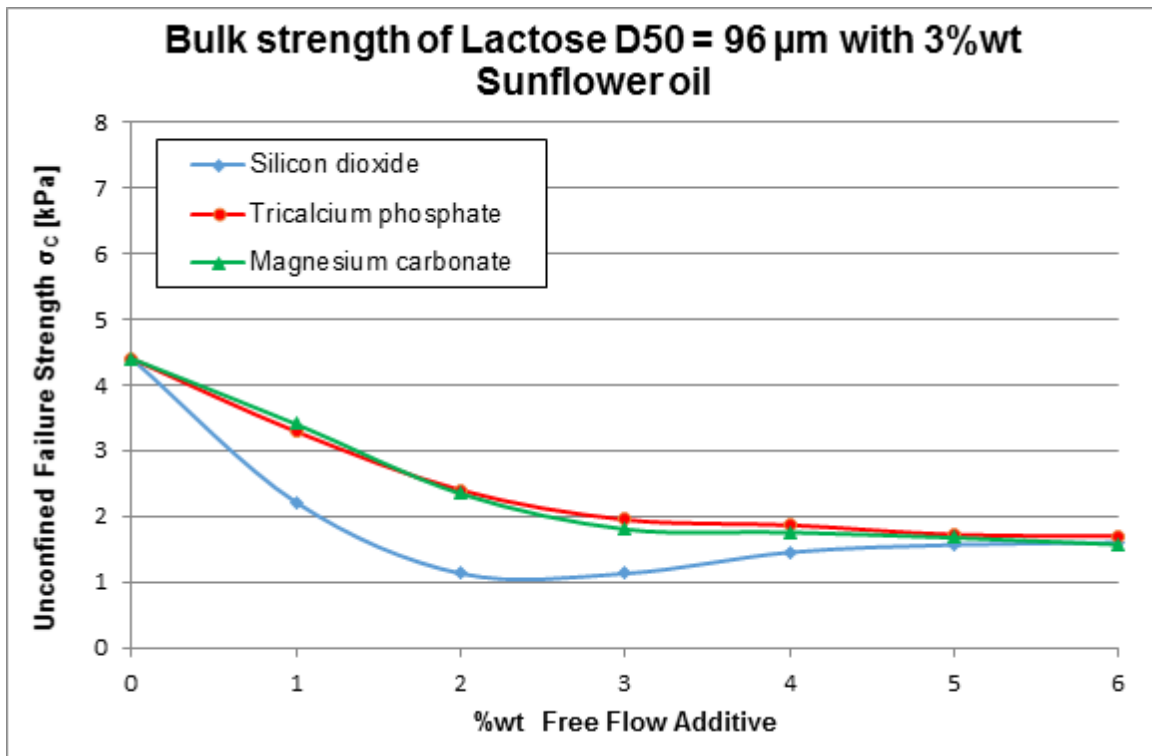


Figure 74: Bulk strength of wet lactose as a function of the %wt of flow agents for three different free flow additives

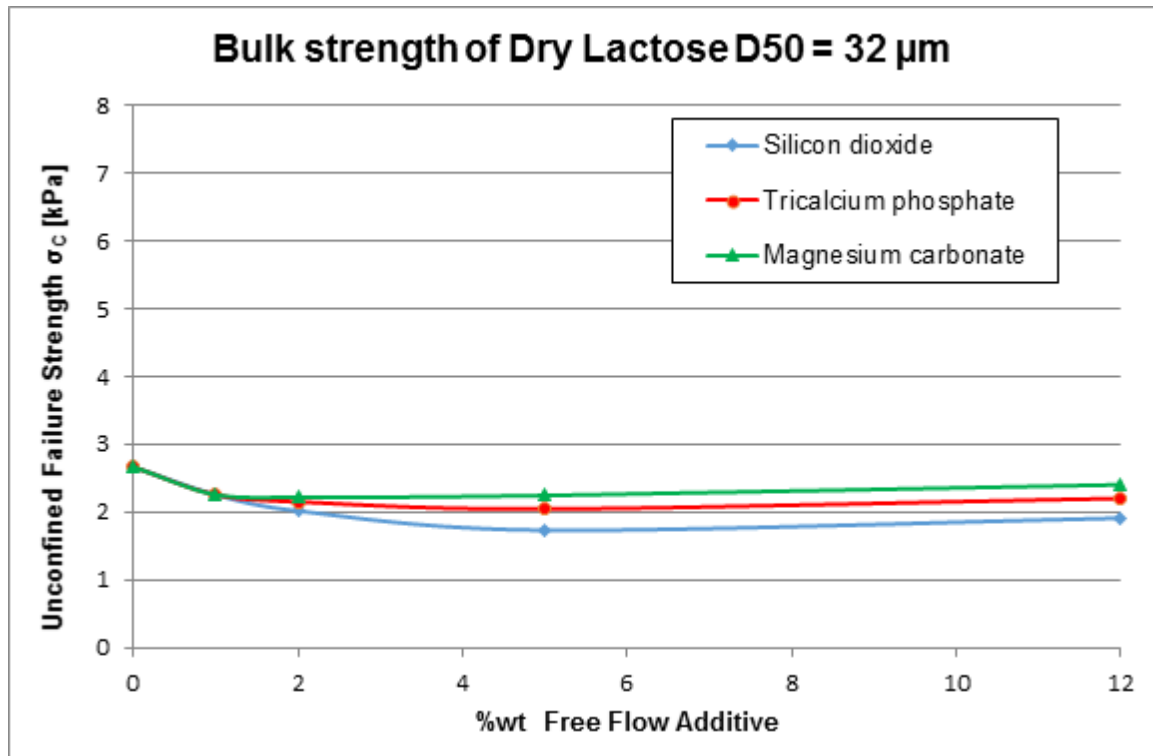


Figure 75: Bulk strength of dry lactose as a function of the %wt of flow agents for three different free flow additives

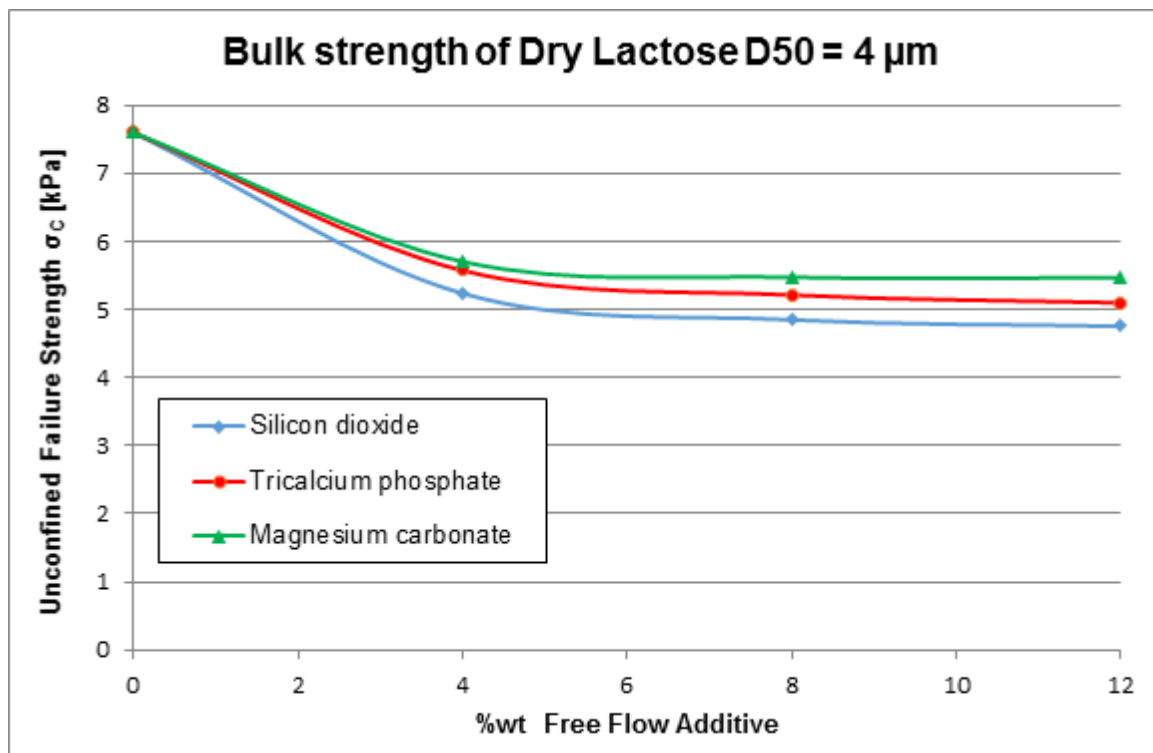


Figure 76: Bulk strength of dry maltodextrin as a function of the %wt of the free flow additives for three different free flow additives

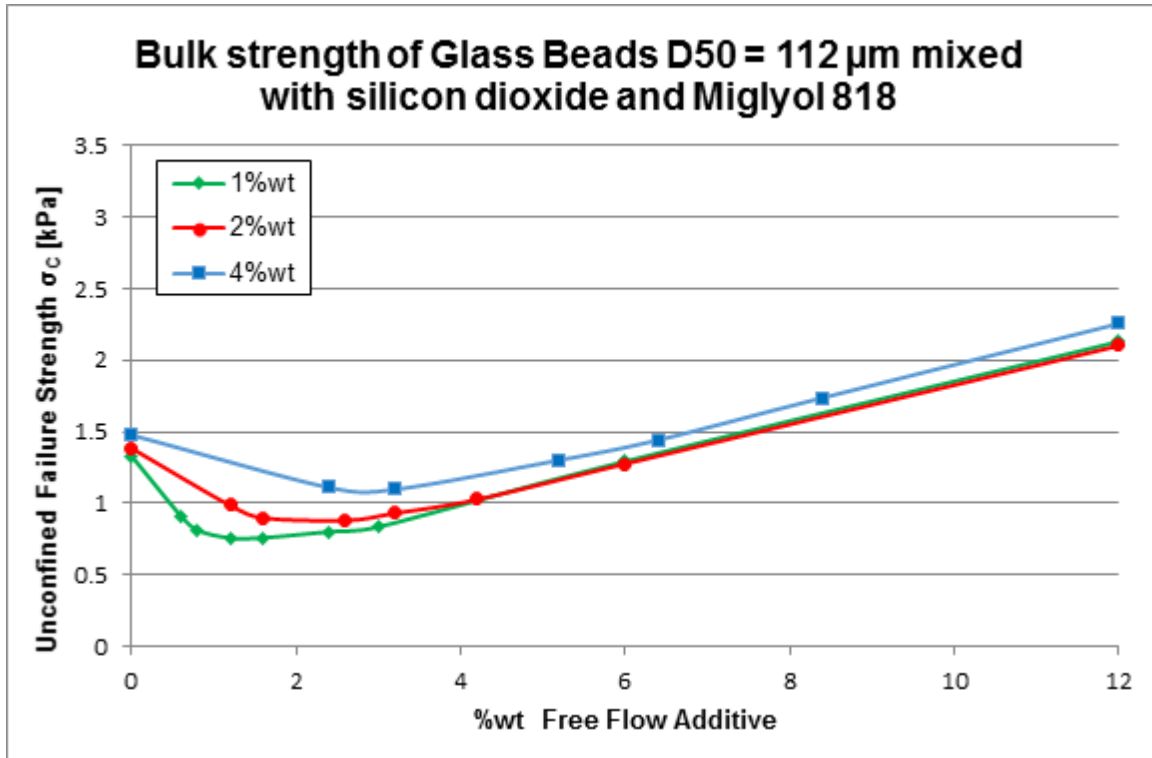


Figure 77: Bulk strength of wet glass beads as a function of the %wt of the free flow additives for different levels of oil content

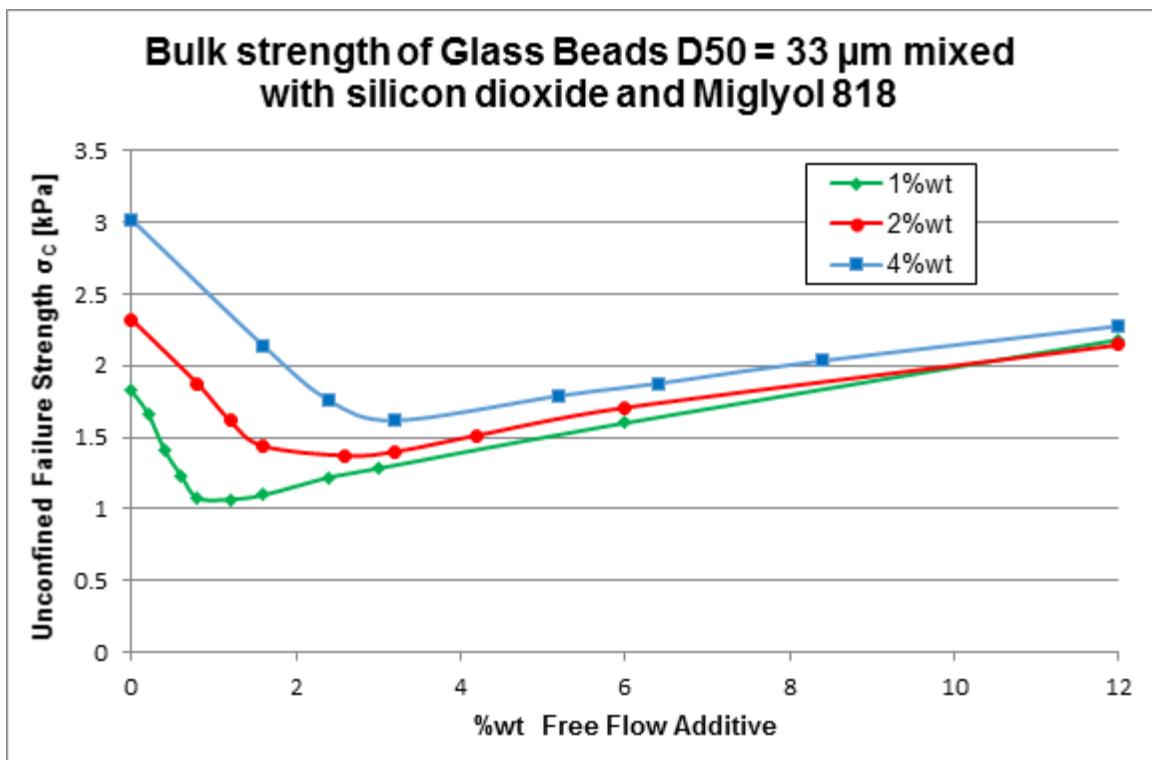


Figure 78: Bulk strength of wet glass beads as a function of the %wt of the free flow additives for different levels of oil content

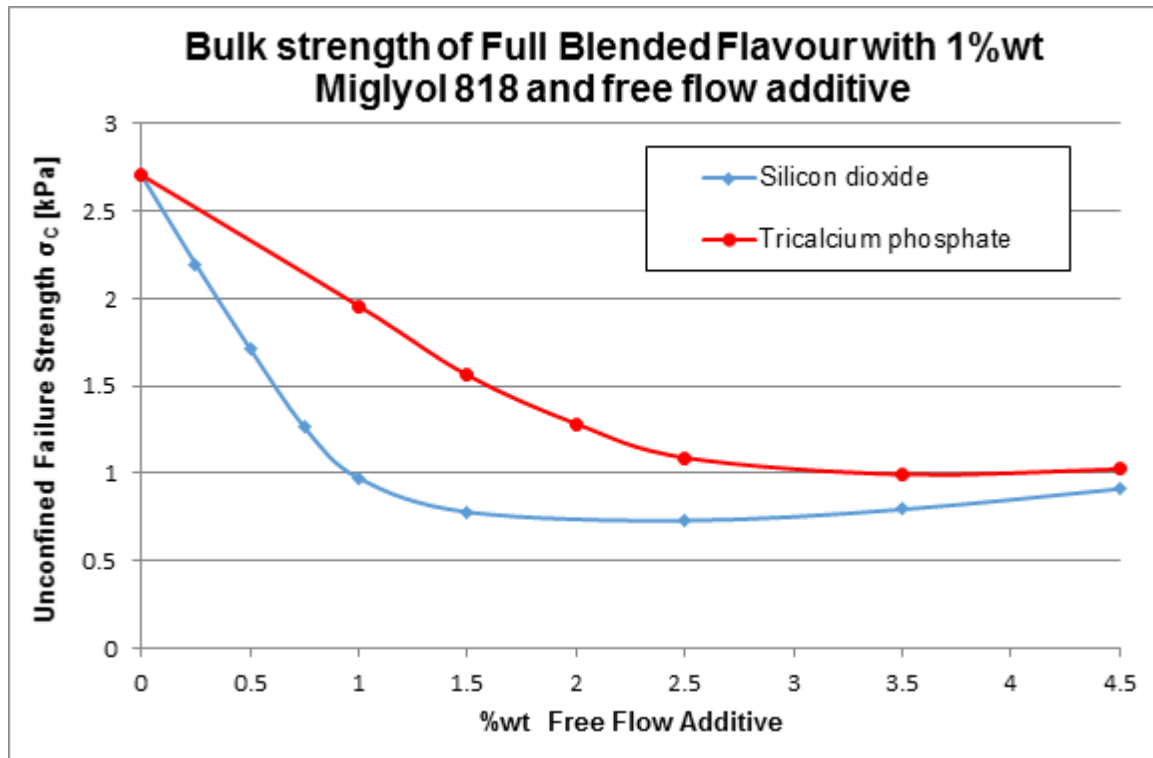


Figure 79: Bulk strength of a full blended flavour as a function of the %wt of the free flow additives for two types of flow agents

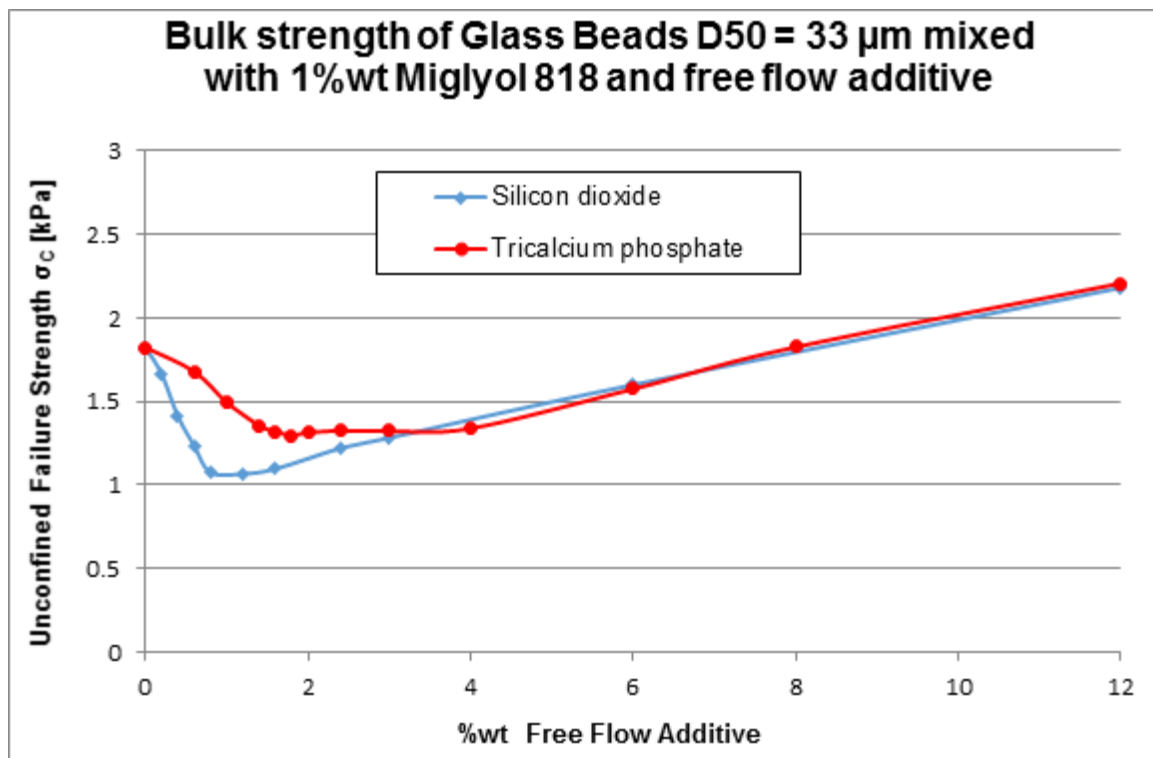


Figure 80: Bulk strength of wet glass beads as a function of the %wt of the free flow additives for two types of flow agents

6.4 Summary

The experimental results of the case study and the series of test programs undertaken under a variety of conditions to study the effects of changing particle properties, liquid properties and blend compositions on bulk flow properties of blended powders have been presented in this chapter. The key points from the chapter are the following:

- An industrial case study was undertaken as a preliminary study of the research to reformulate a Flame Grilled Steak snack flavour to remove monosodium glutamate (MSG) as a main objective. This reformulation was used as a preliminary study of the common undesirable flow behaviour of food powders present in the industrial partners' plants. Results of the case study presented in this chapter and also in appendix C showed that trial blends selected to be trialled at the partners' factory presented a more consistent dose weight during the discharge from the Rospen loss in weight feed hopper than the standard snack flavour with MSG. An increase in the amount of the free flow additive initially added to the reformulate blend resolved the problem of the bridges formed inside the hopper due to the exposition of the powders to adverse environmental conditions (temperature 35° and humidity 40%HR).
- The bulk flow properties of a wide range of single and blended powders were measured studying the effect of particle size, surface moisture, level of free flow additive and the number of components and degree of mixedness for blends. Results presented in this chapter and also in appendix C showed that most of the powders tested in this research are free flowing or easy flowing in dry condition therefore the cohesiveness of the blends is mainly due to the addition of oil. This cohesion is reduced by the addition of free flow additives but too much flow agent may increase the dust emission and the bulk strength of the blended powder. It is crucial to predict the right balance between the oil and flow agent to obtain the desired flow behaviour in the final snack blended flavour.

The experimental data presented in this chapter and the appendices B and C has been used in the calibration of the analytical particle to bulk scale models found in the literature and in the development of the new empirical models to better predict the bulk flow properties of single and blended particulate materials.

Chapter 7 Empirical calibration of established analytical models

7.1 Introduction

This chapter presents the results of the calibration of the analytical models found in the literature review linking particle and bulk flow properties. These models were calibrated comparing the experimental results presented in chapter 6 with the predictions to evaluate their applicability on predicting the packing and bulk flow properties of real single and blended powders. The new model for dry blended powders presented in chapter 5 was also evaluated comparing the measured and predicted results obtained using the specific volume and surface area ratios.

Results of the empirical calibration of the analytical models for single powders in dry and wet condition with free flow additives are discussed and presented in section 7.2; results of the evaluation of the new model developed for dry blended powders are discussed and presented in section 7.3 and a summary of the chapter is given in section 7.4

7.2 Analytical models for single powders

The model proposed by Rumpf et al. to predict the tensile strength of agglomerates has been empirically calibrated for dry and wet single powders and idealised materials looking at the effect of the particle size, surface liquid content and type, level of consolidation stress applied to the powder and the packing properties of the powders. The empirical fitting equations proposed by Yu et al. 2003 and Feng et al. to predict the void fraction of dry and wet powders respectively were also evaluated.

7.2.1 Dry powders

In this research, the model proposed by Rumpf which is also valid for binderless granules was adopted to calculate the bulk strength of dry single powders based on interparticle forces as a function of the particle size and the packing structure of the powders. As explained in chapter 2, the bonding mechanisms considered in this project are van der Waals for dry materials and capillary forces for wet materials (presence of surface moisture). As illustrated in chapter 2, van der Waals forces for two spherical particles can be expressed as a function of the particle size, material properties (Hamaker constant) and the contact distance. Then Rumpf's equation can be expressed as follows:

$$F_V = \frac{AR}{12s^2} \quad \text{Equation 52}$$

$$\sigma_T = \frac{3}{64} \frac{(1 - \varepsilon)}{\varepsilon} \frac{A}{ds^2} \quad \text{Equation 53}$$

This model estimates the theoretical tensile strength of the dry powders; in order to predict the bulk strength, it was necessary to develop the general correlation between the unconfined failure strength and the tensile strength of the dry powders as presented in chapter 2 of the thesis (see equations 2 - 4). Then, the Rumpf's equation can be expressed as follows:

$$\sigma_c = (2Km) \cdot \frac{3}{64} \frac{(1 - \varepsilon)}{\varepsilon} \frac{A}{ds^2} \quad \text{Equation 54}$$

A single calibration point at the lower particle size of the materials tested was applied to calibrate the shape of the curve which predicts the bulk strength of the dry powders as a function of the particle size.

This model implies the prior calculation of the void fraction and the factor of proportionality between the tensile strength and the unconfined failure strength which can be calculated separately. Voidage was calculated using the empirical equations proposed by Yu et al. 2003 and the factor of proportionality was estimated using the values of the angle of the internal friction from the measurements taken with the powder flow tester. An average value was calculated for the values of the factor of proportionality (2km) of the size fractions of each powder at 9 kPa of consolidation stress to predict the unconfined failure strength using Rumpf model. Values of the separation distance (s) and Hamaker constant (A) have been assumed based on the experimental work undertaken by others researchers (Seville et al. 2000 & Li et al. 2006) found in the literature review as shown in table 34 below.

Powder Name	Hamaker constant (J)	Separation distance (nm)	Factor of proportionality (2km)
Lactose	7.2×10^{-20}	2.5	2.8
Dextrose	7.2×10^{-20}	2.5	2.3
Maltodextrin	7.2×10^{-20}	2.5	2.3
Sodium Chloride	6.5×10^{-20}	2.5	2.3
Glass Beads	6.5×10^{-20}	2.5	1.6

Table 34: Estimated values of Hamaker constant, separation distance (Seville et al. 2000 & Li et al. 2006) and factor of proportionality powders tested

Prediction of the packing structure

The empirical equations proposed by Yu et al. 2003 to predict the void fraction of dry powders as a function of the particle size, particle density and material properties (Hamaker constant) was evaluated comparing the measured and predicted values for dense random packing condition. As explained in chapter 2, these equations were obtained by empirical curve fitting of the void fraction data obtained from several resources which measured this packing property at poured and tapped packing conditions, therefore, the use of these equations is limited to a low consolidation stress applied to the powders (tapped packing).

- Loose random packing

$$\varepsilon = 0.4 + 0.6 \exp\left(-0.106 \left(\frac{\rho_p}{A}\right)^{0.156} d^{0.552}\right) \quad \text{Equation 55}$$

- Dense random packing

$$\varepsilon = 0.36 + 0.64 \exp\left(-0.178 \left(\frac{\rho_p}{A}\right)^{0.129} d^{0.457}\right) \quad \text{Equation 56}$$

A comparison of the predicted and measured values of the void fraction at 2, 4 and 9 kPa of consolidation stresses is presented in figures 81 - 85. Results showed that for dextrose and sodium chloride, measured values fit reasonably well with the predicted

values at different levels of consolidation stresses whereas for lactose the predicted values were only close at 2 kPa of consolidation stress (see figure 81).

Glass beads and maltodextrin showed no agreement between the predicted and measured values for different reasons. For maltodextrin, the measured values are fairly constant and independent of the consolidation stress as shown in figure 85 with an average value of 0.59 for size fractions with particles above 45 μm and 0.64 for particles below 45 μm . These values are higher than the predicted value of the void fraction from the model (0.36) for particle size greater than 100 μm .

As these equations do not consider the effect of high consolidation stress on the packing properties of the powders, for particulate materials such as lactose and glass beads with most of the size fractions below 100 μm (see figures 81 and 84), measured values of the void fractions at 4 and 9 kPa of consolidation stresses are lower than predicted values so the model over-predicts the void fraction at these stresses. In the case of glass beads, values are over-predicted even at 2 kPa of consolidation stress.

Sodium chloride and dextrose present most of the size fractions above 100 μm (see figures 82 and 83) so the change in the voidage at high stress is less remarkable because there is no much difference between the values of the void fraction measured for the coarse size fractions of these powders.

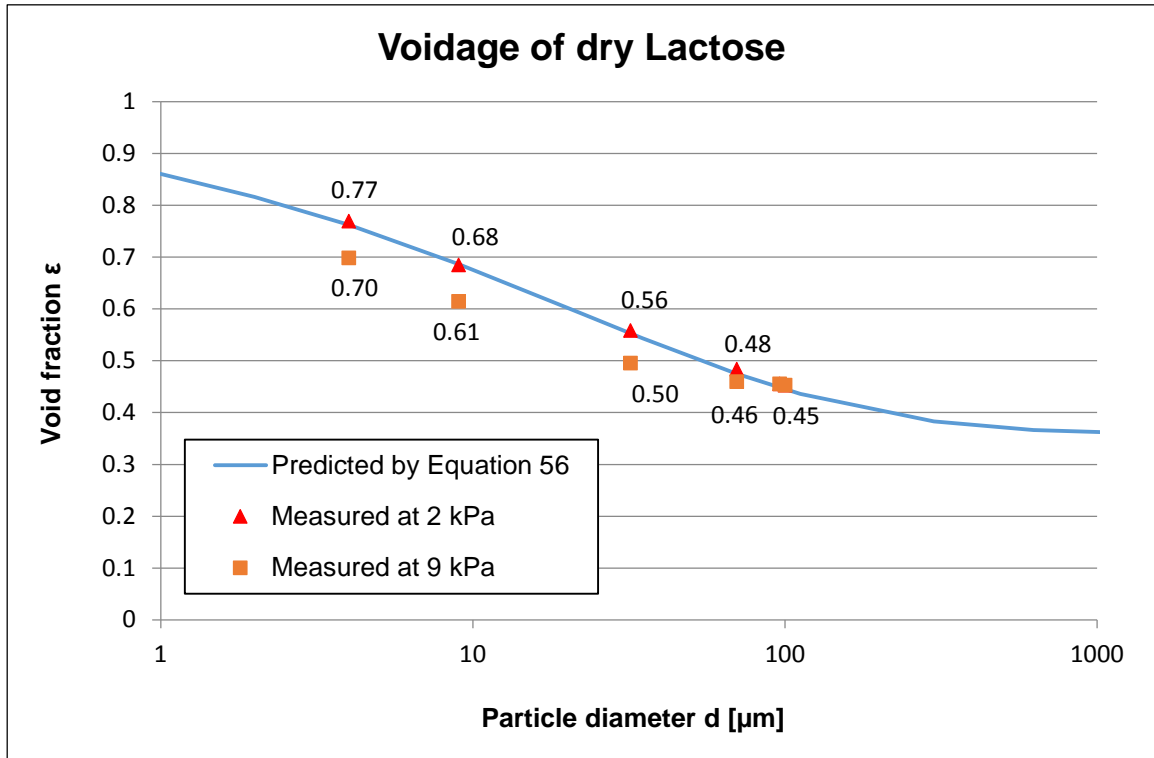


Figure 81: Comparison of measured and predicted values of voidage for six grades of lactose

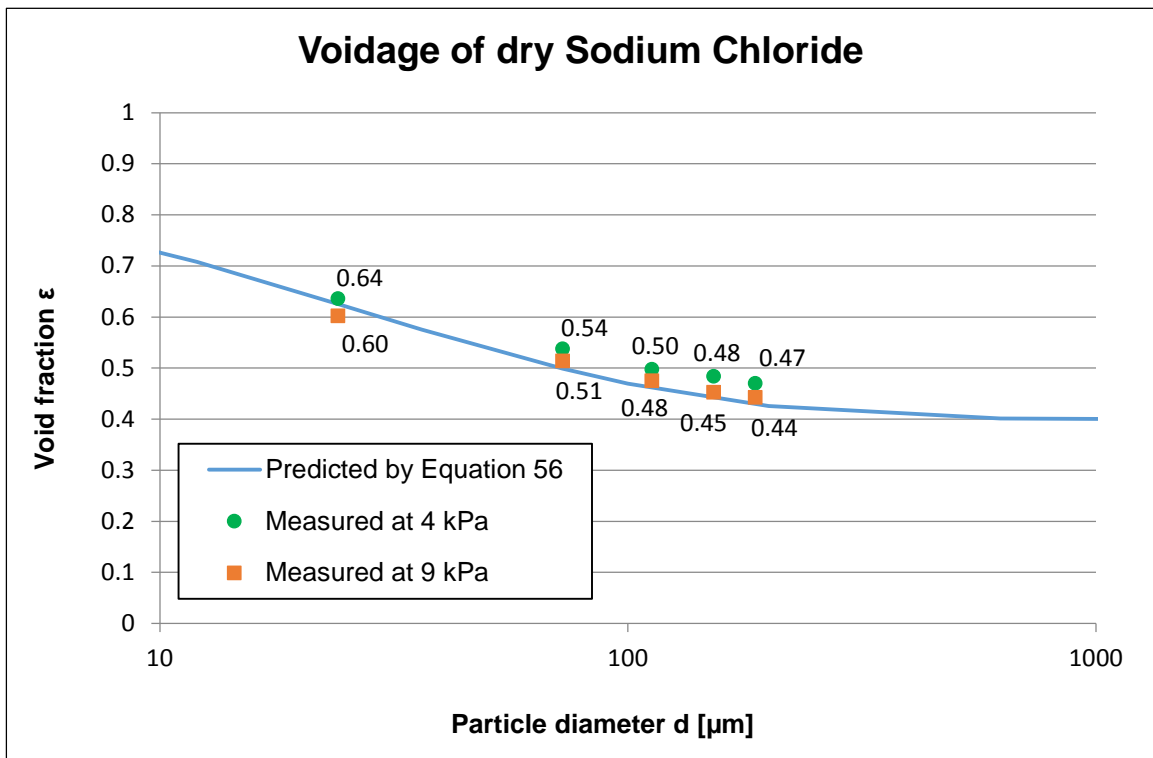


Figure 82: Comparison of measured and predicted values of voidage for size fractions of sodium chloride

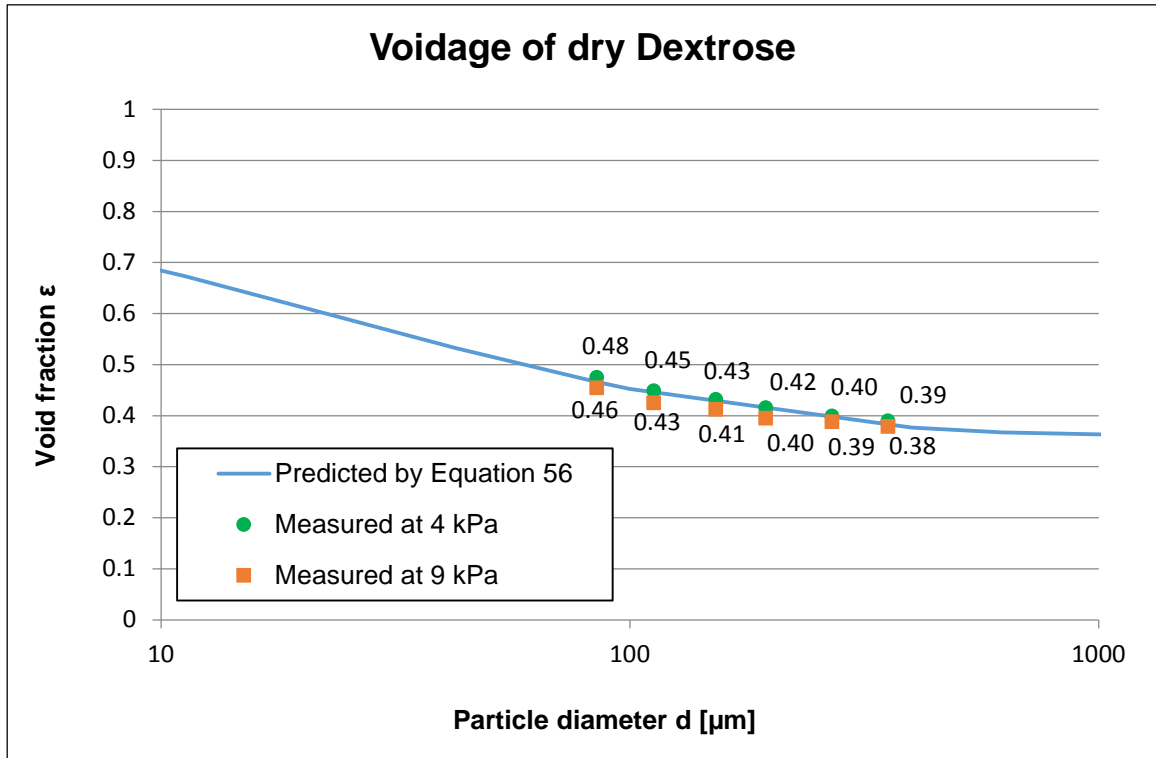


Figure 83: Comparison of measured and predicted values of voidage for size fractions of dextrose

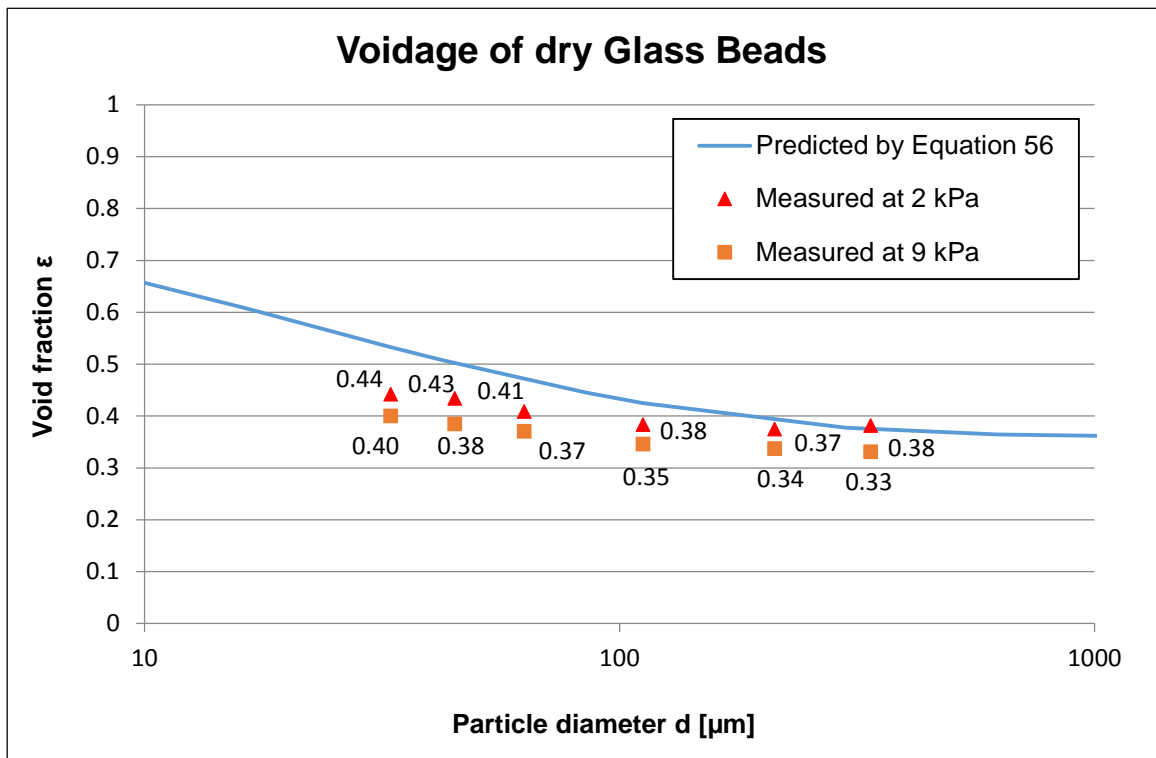


Figure 84: Comparison of measured and predicted values of voidage for six grades of glass beads

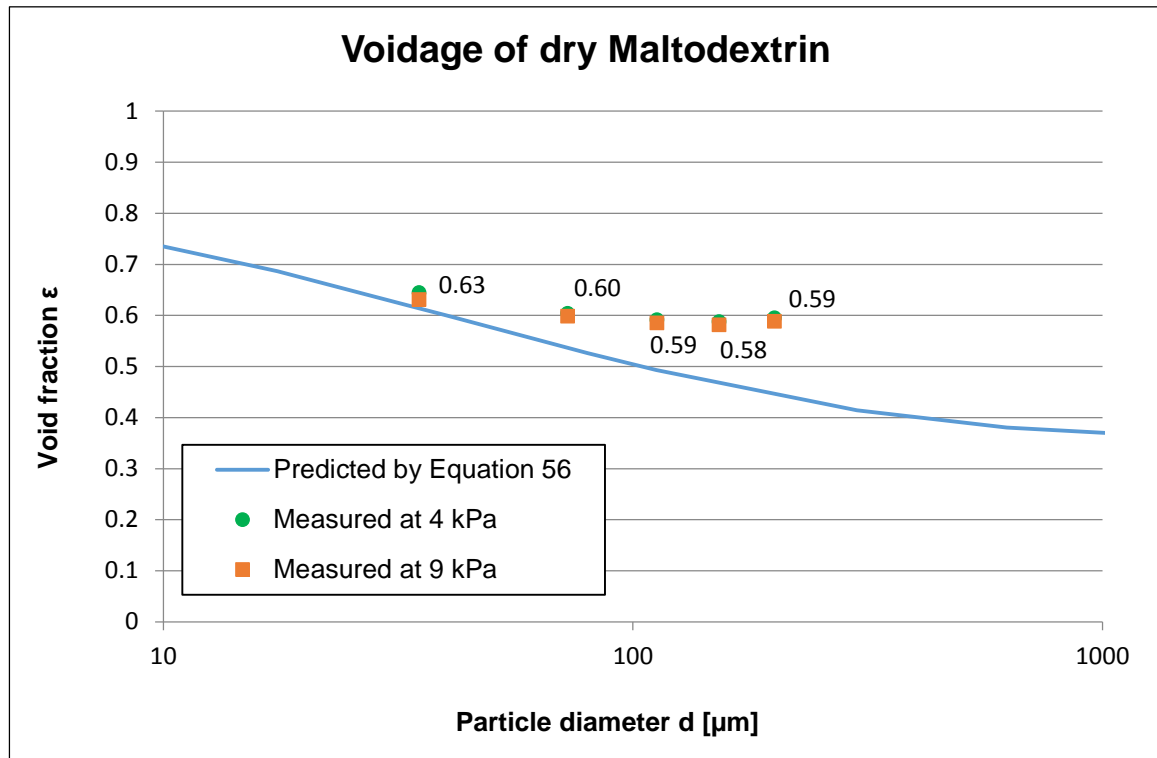


Figure 85: Comparison of measured and predicted values of voidage for size fractions of maltodextrin

Prediction of the bulk strength

This model predicts the bulk strength of dry single powders with particle size below approximately 100 μm where interparticles forces dominate over gravity forces as demonstrated by Yu et al. 2003. The behaviour of dry coarse particles with particle size above approximately 100 μm are dominated by gravity as explained in chapter 2 of the thesis.

A comparison of the predicted and measured values of the bulk strength at 9 kPa of consolidation stress is presented in figures 86 - 90. Results showed that the model does not fit the trend of the experimental data and with the exception of lactose, predicted and measured values only agreed at the lowest particle size of the powders as the model has been calibrated to the measured strength at the minimum particle size of each powder. Also the model does not consider the state of consolidation of the material by capping the strength at a value equal to the consolidation stress.

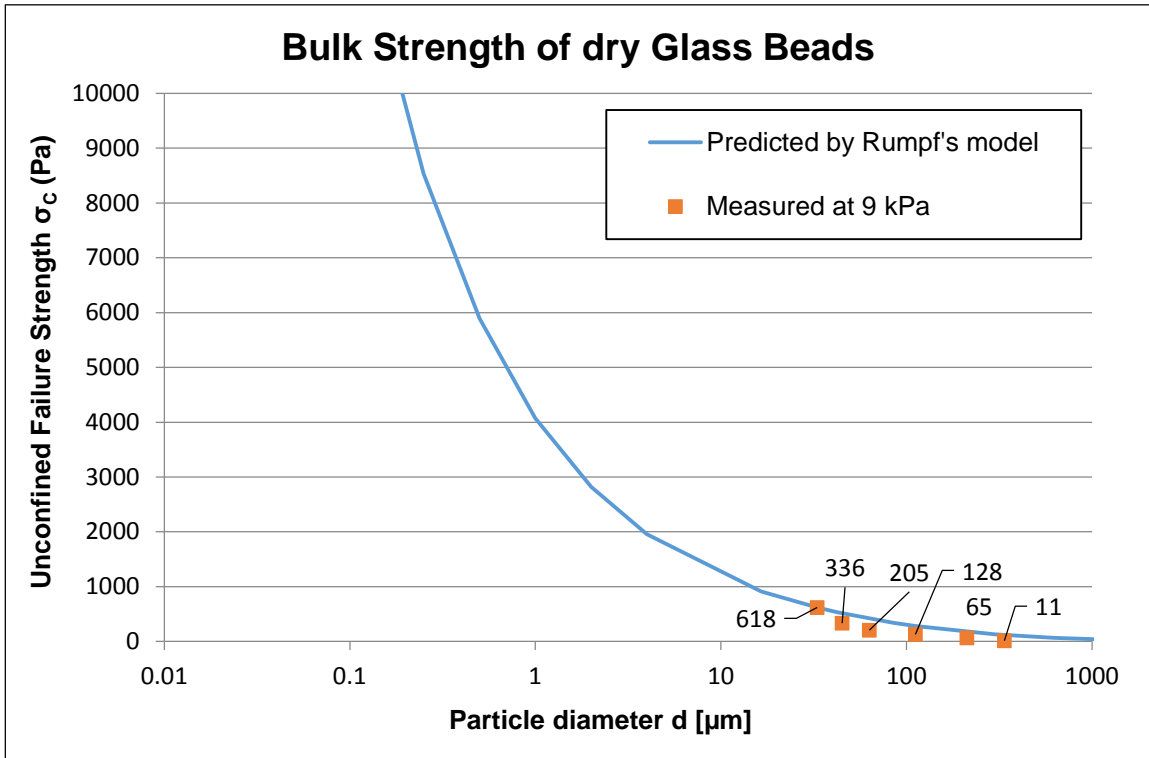


Figure 86: Comparison of measured and predicted values of bulk strength for six fractions of glass beads

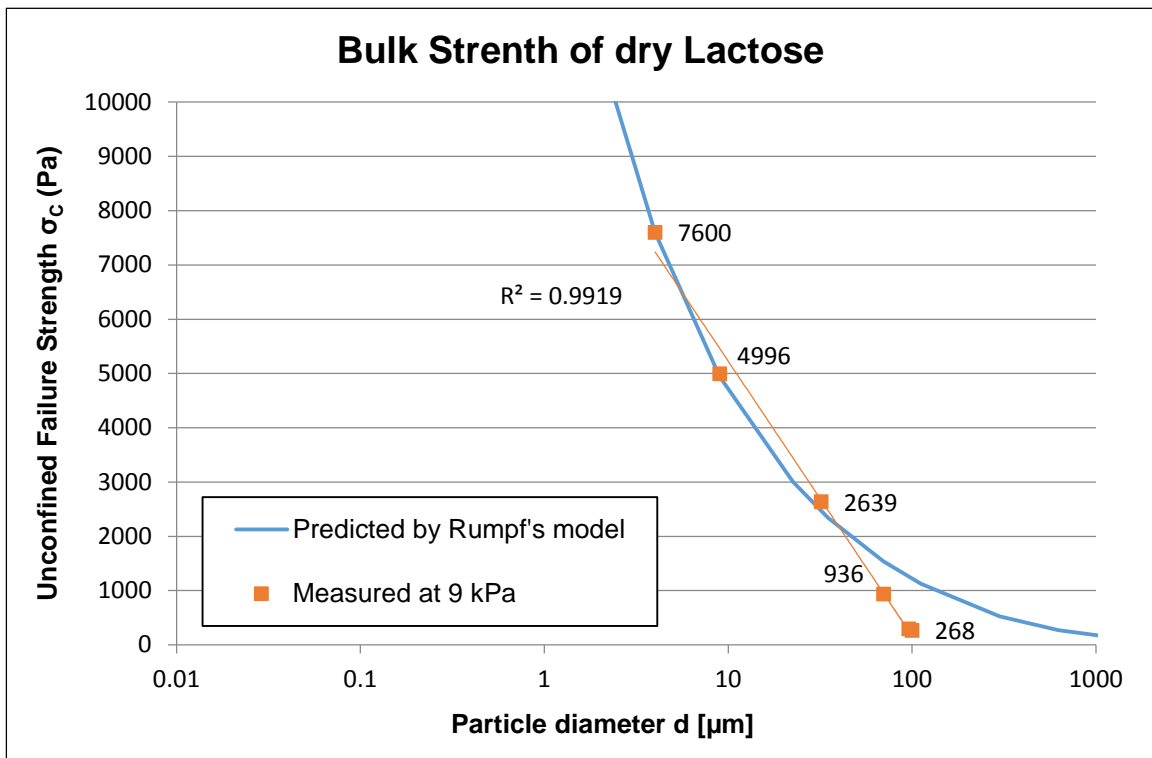


Figure 87: Comparison of measured and predicted values of bulk strength for six fractions of lactose

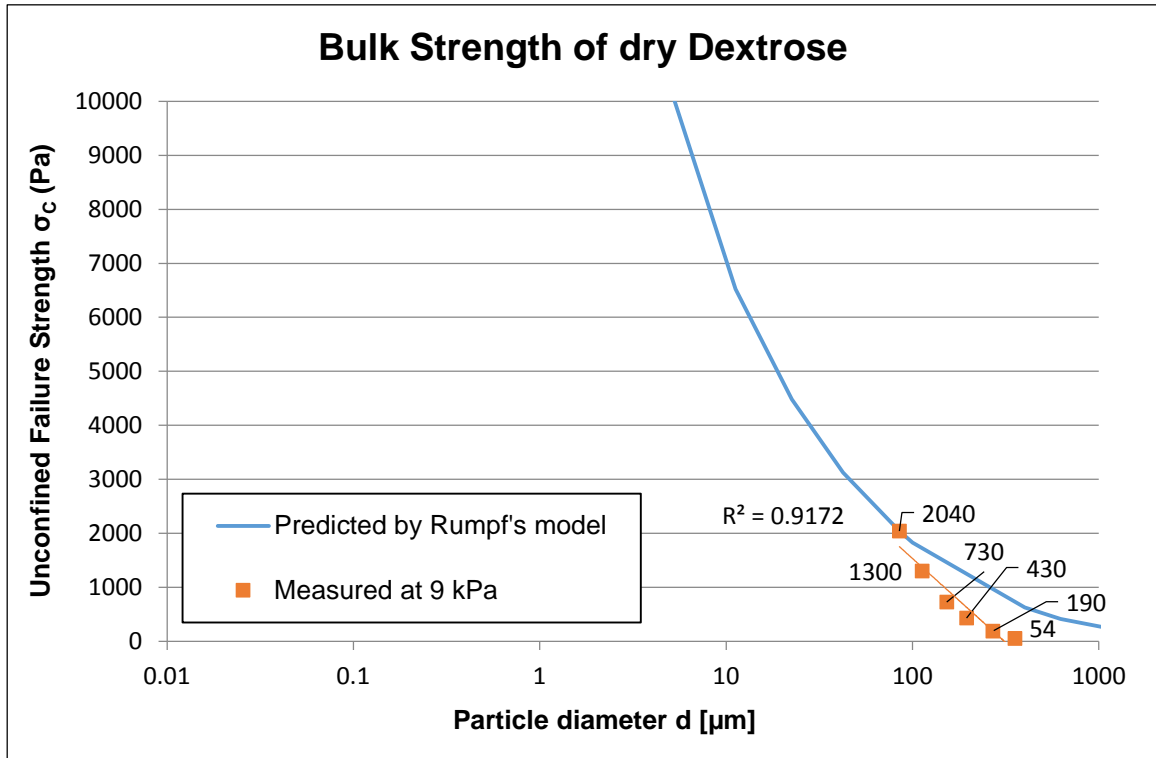


Figure 88: Comparison of measured and predicted values of bulk strength for size fractions of dextrose

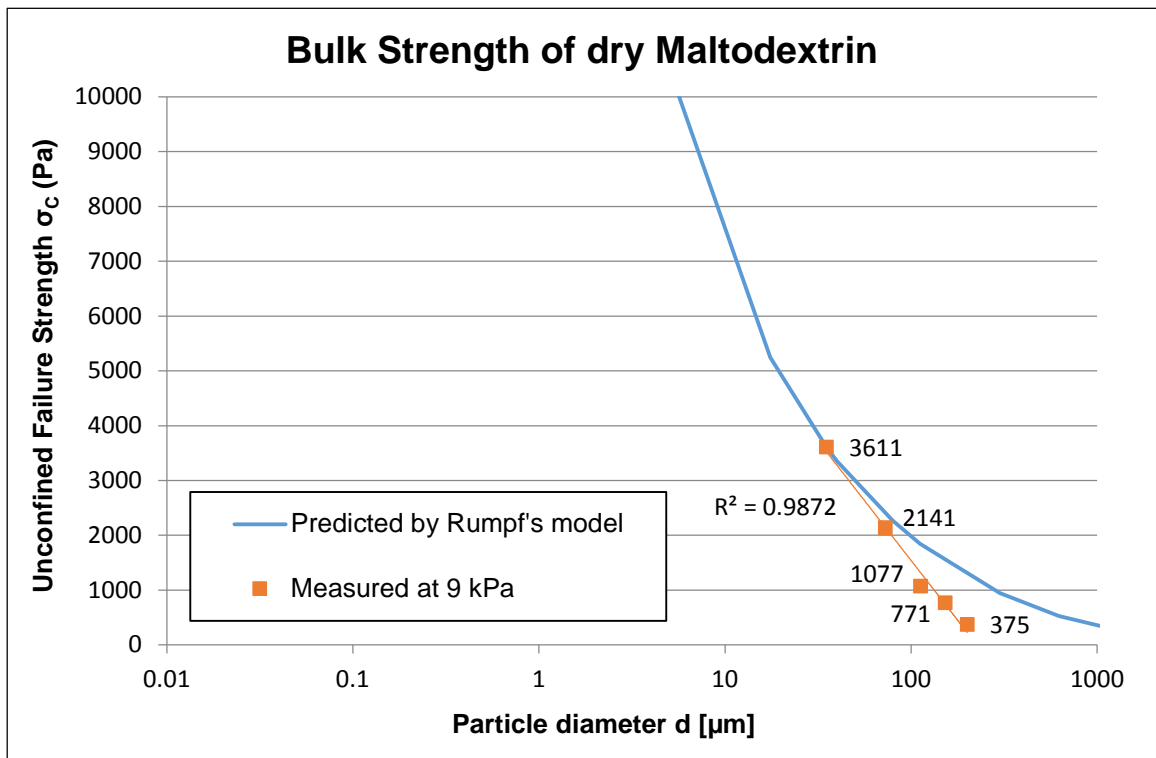


Figure 89: Comparison of measured and predicted values of bulk strength for size fractions of maltodextrin

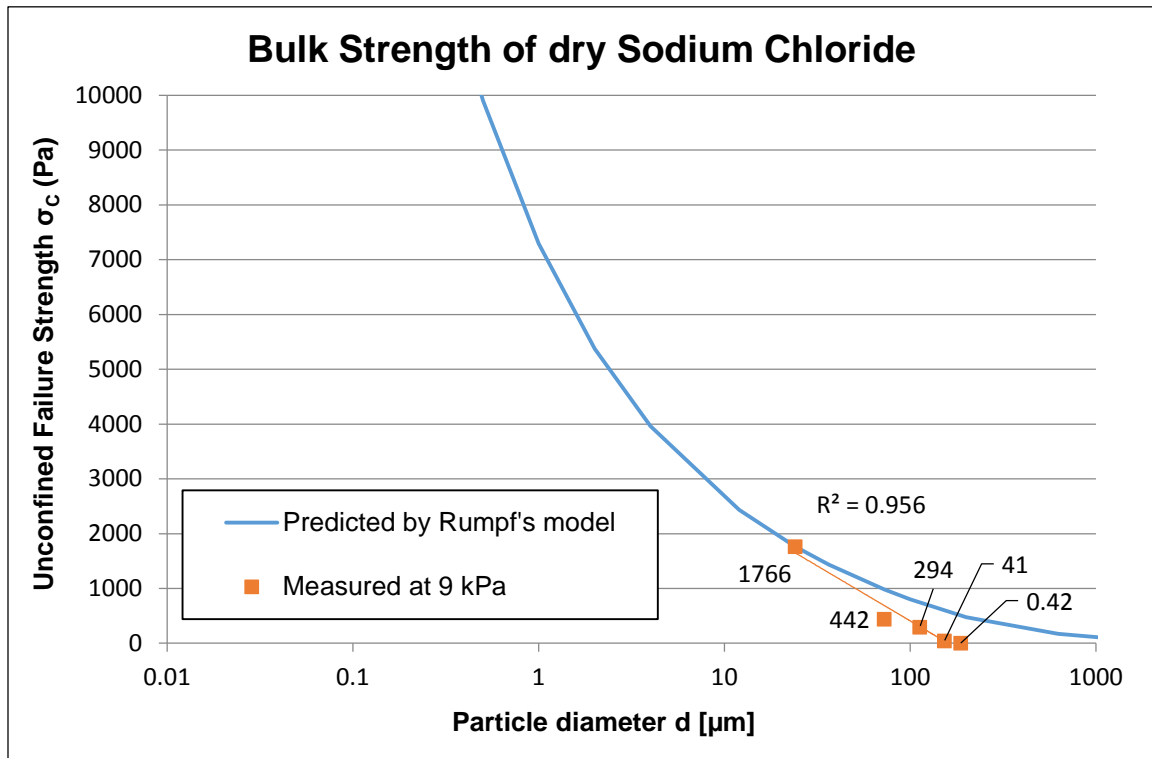


Figure 90: Comparison of measured and predicted values of bulk strength for size fractions of sodium chloride

A clear issue with this model is the fact that it predicts a trend for the decrease in strength which is an inverse power law whereas the measured data is closer to a linear decrease. As a result the calibrated model significantly over predicts the strengths as the particle size increases into the free flowing range. Furthermore, it is not possible to predict the increase in strength as size reduces because there is no cap on the maximum strength.

Based on these results, it would be better to use an empirical approach where the strength is measured at fine particle size (less than 50 μm) and assume a linear trend from zero at 100 microns through the measured point to a maximum strength which is equal to the consolidation stress. This empirical model has been developed in this research and it is presented and explained in details in chapter 8.

7.2.2 Wet powders

In this work, the well-established model developed by Rumpf for pendular state of liquid saturation of packed monosized spheres was adopted to calculate the bulk strength of wet single powders. As explained in chapter 5, this model has been calibrated for a wide range of grades of glass beads with narrow particle size distributions. The results

obtained in this calibration with idealised powders could be applied to real powders with non-spherical particles and wide particle size distributions as shown in chapter 8, section 8.2.3 below. When the pendular limit is exceeded, the empirical models developed in this research and presented in chapter 8 can be applied to predict the bulk strength of wet real particulate materials in funicular and capillary states.

The bonding force between particles due to the addition of liquid to the powder was assumed to be proportional to the product of the surface tension of the liquid added and the perimeter of the neck of the liquid bridge formed between particles in pendular state as explained in chapter 2 of the thesis. It was also assumed the expression for the radius of the liquid bridge for pendular state given by Tanaka et al. As presented in the literature review and chapter 5, the Rumpf's equation can be expressed as follows:

$$\sigma_T = \alpha \cdot 2\pi r_2 \frac{9(1-\varepsilon)}{8\varepsilon} \left(\frac{1}{2a}\right)^2 \quad \text{Equation 57}$$

$$r_2 = 0.82a \left(\frac{v}{a^3}\right)^{0.25} \quad \text{Equation 58}$$

This model estimates the theoretical tensile strength (pendular state) of a bulk solid due to the presence of liquid bonds between the surfaces of the particles of a consolidated bulk solid. Therefore, it was necessary to develop the general correlation between the unconfined failure strength of the wet powders tested with the PFT shear tester as presented in chapter 2 and the tensile strength that the model predicts. The Rumpf equation can be expressed as follows:

$$\sigma_c = (2Km) \cdot \alpha \cdot 2\pi r_2 \frac{9(1-\varepsilon)}{8\varepsilon} \left(\frac{1}{2a}\right)^2 \quad \text{Equation 59}$$

A dimensionless factor of calibration "C" (a single value) has been developed by comparing the measured and predicted bulk strength. A correlation for a range of different particle size and liquid properties has been found in this research. Then, the Rumpf's equation can be expressed as follows:

$$\sigma_c = C \cdot (2Km) \cdot \alpha \cdot 2\pi r_2 \frac{9(1-\varepsilon)}{8\varepsilon} \left(\frac{1}{2a}\right)^2 \quad \text{Equation 60}$$

This model (equation 60) implies the calculation of the void fraction (ϵ), the volume of the liquid bridges formed at pendular state (see equation 45 in chapter 5) and the radius of the narrowest part of the liquid bridges of the wet powders (equation 58); these elements are interdependent. Void fraction was calculated using the empirical equations proposed by Feng et al. and the volume of the liquid bridges formed at pendular state was determined using the calculated voidage, the percentage moisture content of the powder and the liquid and solid density (see equation 45 in chapter 5).

The factor of proportionality ($2k_m$) between the tensile strength and the unconfined failure strength was calculated separately. This factor was estimated using the values of the angle of the internal friction from the bulk flow properties measurements of the powders. An average value was calculated for the values of the factor of proportionality in the pendular state of each powder at 2, 4 and 9 kPa of consolidation stresses; these values are shown in table 35 and 36 below.

Average factor of proportionality ($2k_m$) of Glass Beads mixed with Miglyol 818 at pendular state and different levels of consolidation stress			
Mean size	2 kPa	4 kPa	9 kPa
D50 = 33 μm	1.5	1.5	1.5
D50 = 45 μm	1.4	1.4	1.4
D50 = 63 μm	1.2	1.2	1.2
D50 = 112 μm	1.3	1.3	1.3
D50 = 212 μm	1.4	1.4	1.4

Table 35: Average factor of proportionality of glass beads mixed with Miglyol oil 818 at pendular state

Average factor of proportionality (2km) of Glass Beads mixed with de-ionised water at pendular state and different levels of consolidation stress			
Mean size	2 kPa	4 kPa	9 kPa
D50 = 33 µm	1.3	1.3	1.3
D50 = 63 µm	0.9	0.9	0.9
D50 = 112 µm	1	1	1
D50 = 212 µm	1.1	1.1	1.1

Table 36: Average factor of proportionality of glass beads mixed with de-ionised water at pendular state

Prediction of the packing structure

The empirical equations proposed by Feng et al. to predict the void fraction of wet powders was evaluated comparing the measured and predicted values. These equations give higher values of void fraction compared to measured values at 2, 4 and 9 kPa of consolidation stresses.

$$\frac{\varepsilon - \varepsilon_0}{\varepsilon_{max} - \varepsilon_0} = \left(\frac{M}{M_{cri}}\right)^{0.423} \left[1 - 0.421 \ln \frac{M}{M_{cri}}\right] \quad \text{Equation 61}$$

$$\varepsilon_{max} = \varepsilon_0 + 0.048 \left(\frac{\alpha}{\rho_p g d^2}\right)^{0.266} \quad \text{Equation 62}$$

$$M_{cri} = 0.2545 \left(\frac{\rho_l}{\rho_p}\right)^{-1.057} \cdot \left(\frac{\alpha}{\rho_p g d^2}\right)^{0.4743} \quad \text{Equation 63}$$

These equations developed by Feng et al. were based on glass beads with a minimum size of 250 µm to avoid the effect of interparticle forces on the void fraction for particle size lower than approximately 100 µm. Furthermore, Feng et al. carried out the experimental work only for loose or poured packing conditions of wet glass beads. For these reasons, these equations over predict the packing structure of the wet powders

tested at different levels of consolidation stresses; these do not consider the fact that the void fraction decreases as the consolidation stress applied increases for particles of glass beads tested with a maximum size of 250 μm .

Due to the lack of models or empirical equations in the literature to predict the packing properties (void fraction) of wet powders considering different particle size below 250 μm and level of consolidation stress applied, it was decided to plot the measured values of void fraction for each powder tested in the range of the application of the model in pendular state (see figures 91 and 92 and tables 37 and 38) and characterise the powders with the average void fraction value for each case.

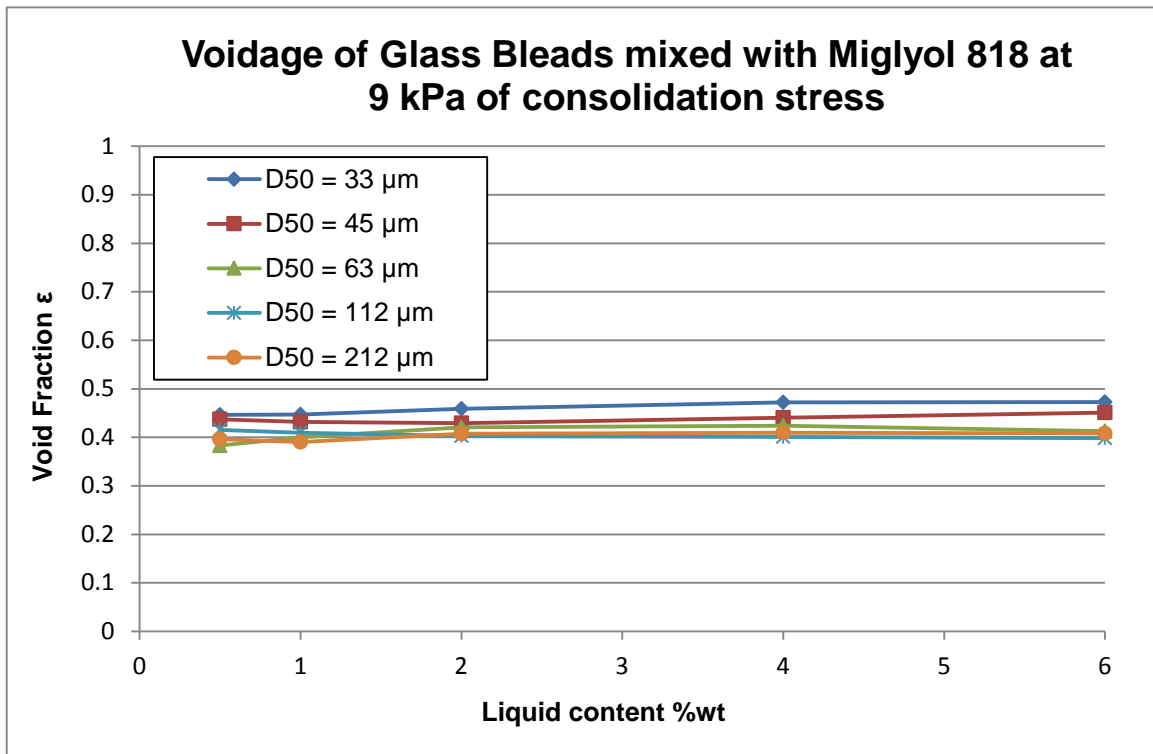


Figure 91: Experimental voidage of glass beads mixed with Miglyol oil 818 at 9 kPa of consolidation stress

Average void fraction of Glass Beads mixed with Miglyol 818 at pendular state and different levels of consolidation stress			
Mean size	2 kPa	4 kPa	9 kPa
D50 = 33 μm	0.52	0.48	0.46
D50 = 45 μm	0.50	0.46	0.43
D50 = 63 μm	0.48	0.44	0.41
D50 = 112 μm	0.46	0.43	0.40
D50 = 212 μm	0.45	0.42	0.40

Table 37: Average voidage of glass beads mixed with Miglyol oil 818 at 9 kPa of consolidation stress

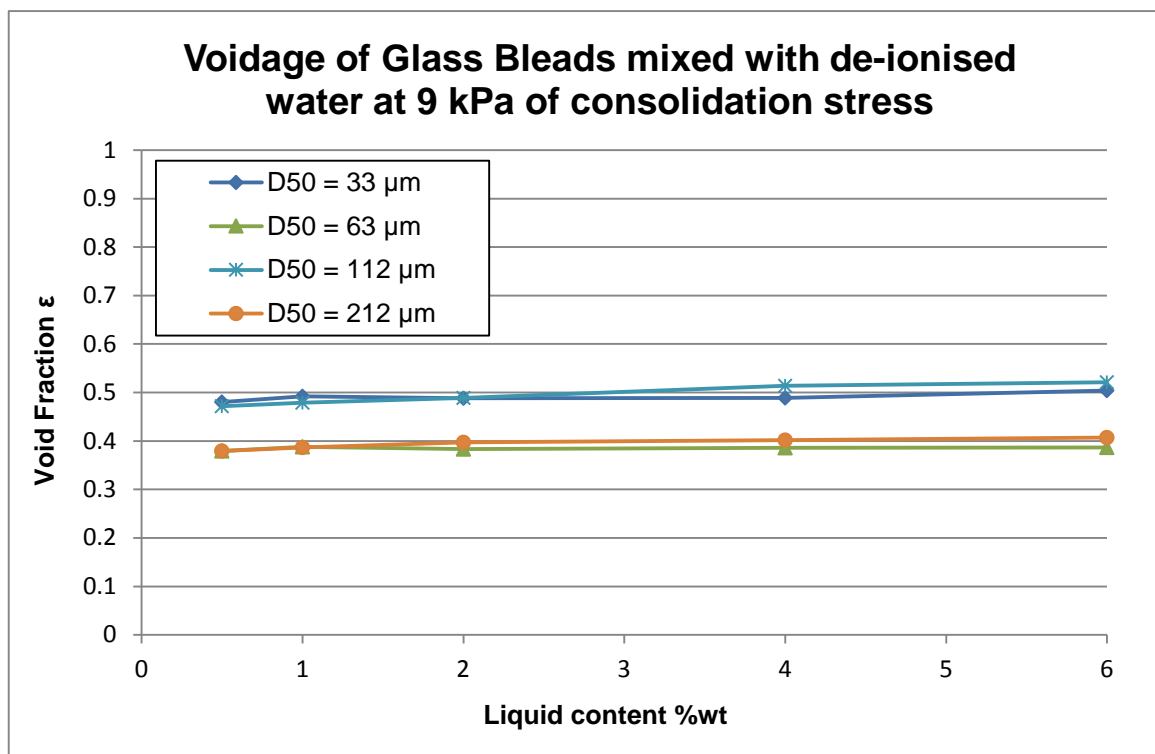


Figure 92: Experimental voidage of glass beads mixed with de-ionised water at 9 kPa of consolidation stress

Average void fraction of Glass Beads mixed with de-ionised water at pendular state and different levels of consolidation stress			
Mean size	2 kPa	4 kPa	9 kPa
D50 = 33 μm	0.59	0.55	0.49
D50 = 63 μm	0.57	0.53	0.47
D50 = 112 μm	0.49	0.43	0.39
D50 = 212 μm	0.47	0.42	0.38

Table 38: Average voidage of glass beads mixed with de-ionised water at 9 kPa of consolidation stress

Prediction of the bulk strength

As explained in the literature review, the upper limit of the transition from the pendular to funicular state has been defined as approximately 25% of saturation based on the work developed by others researchers and the experimental investigations undertaken in this research. Figures 93 - 97 presented below show the correlation between the upper limit of the pendular state and its corresponding value in percentage weight of liquid content. For this reason, the model (equation 60) has been calibrated up 6 %wt liquid content; this range covers the pendular state for all the idealised materials tested in this research as shown in figures 96 and 97. These figures show how the slope of the saturation lines changes at 6 %wt liquid content defining the limit between the pendular and funicular state. Empirical fitting modelling based on the experimental results showed in chapter 6 was developed for the funicular state as presented in chapter 8.

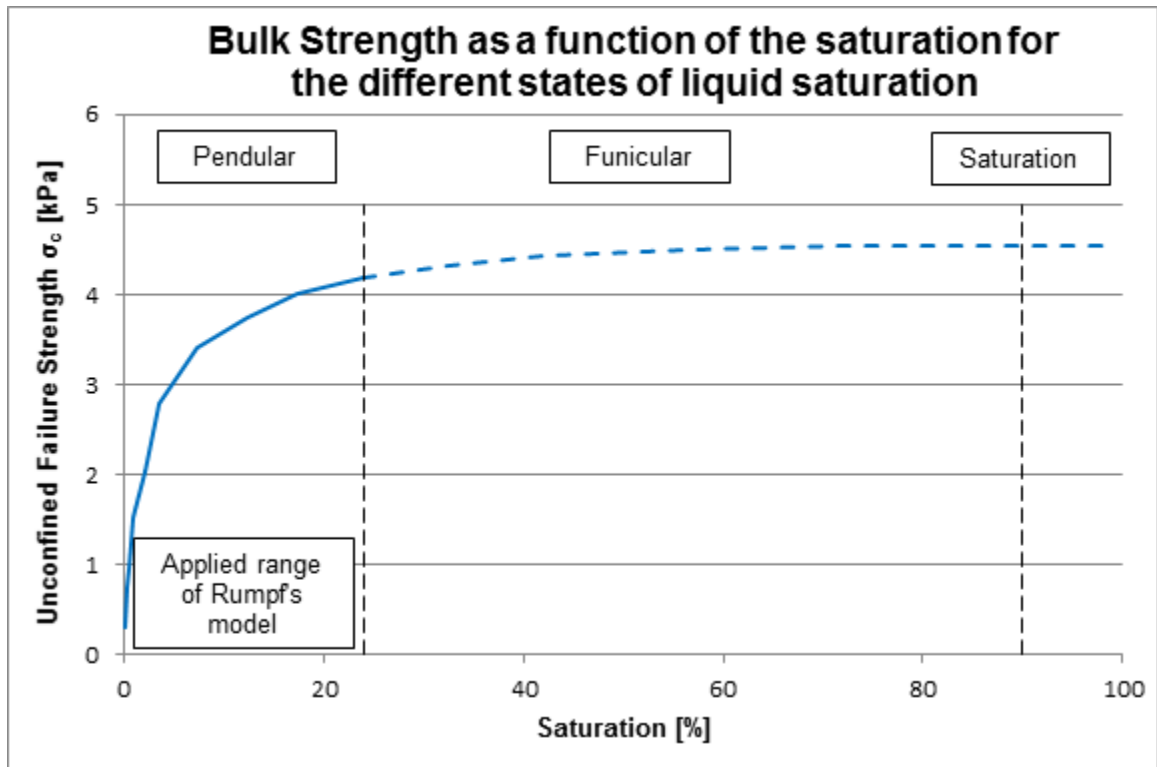


Figure 93: Range of Rumpf model application for wet powders

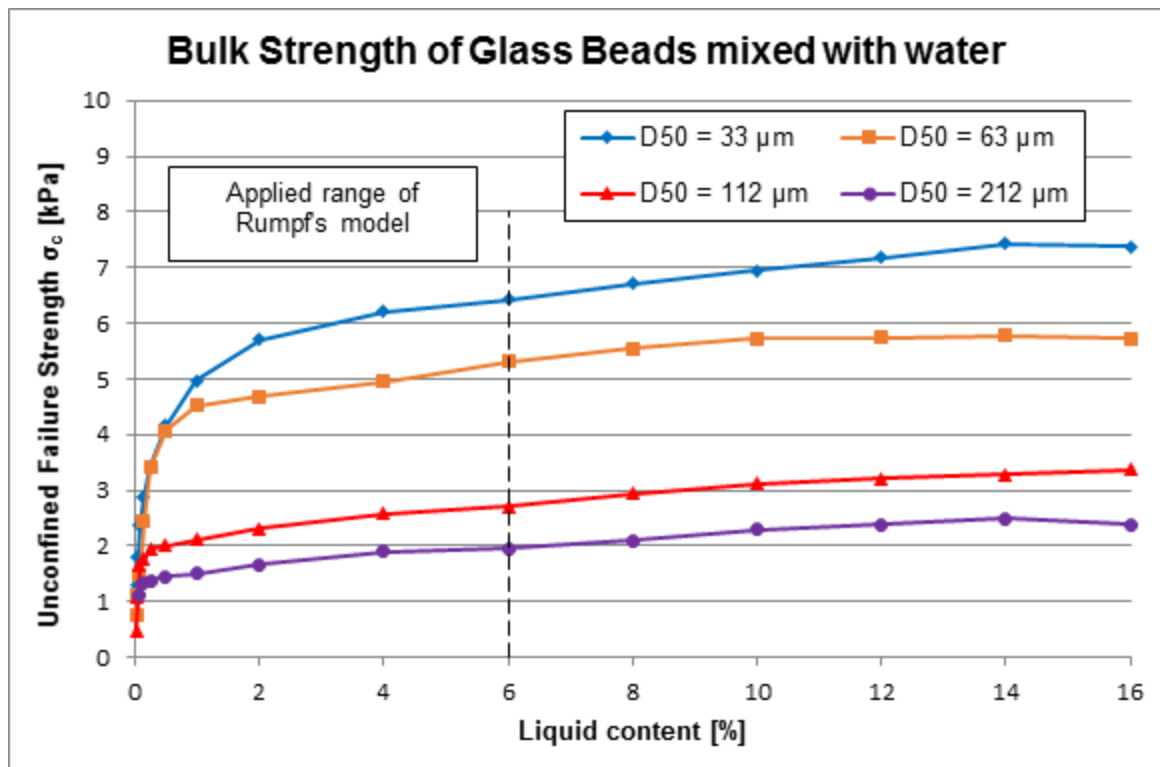


Figure 94: Range of Rumpf model application for size fractions of glass beads mixed with de-ionised water

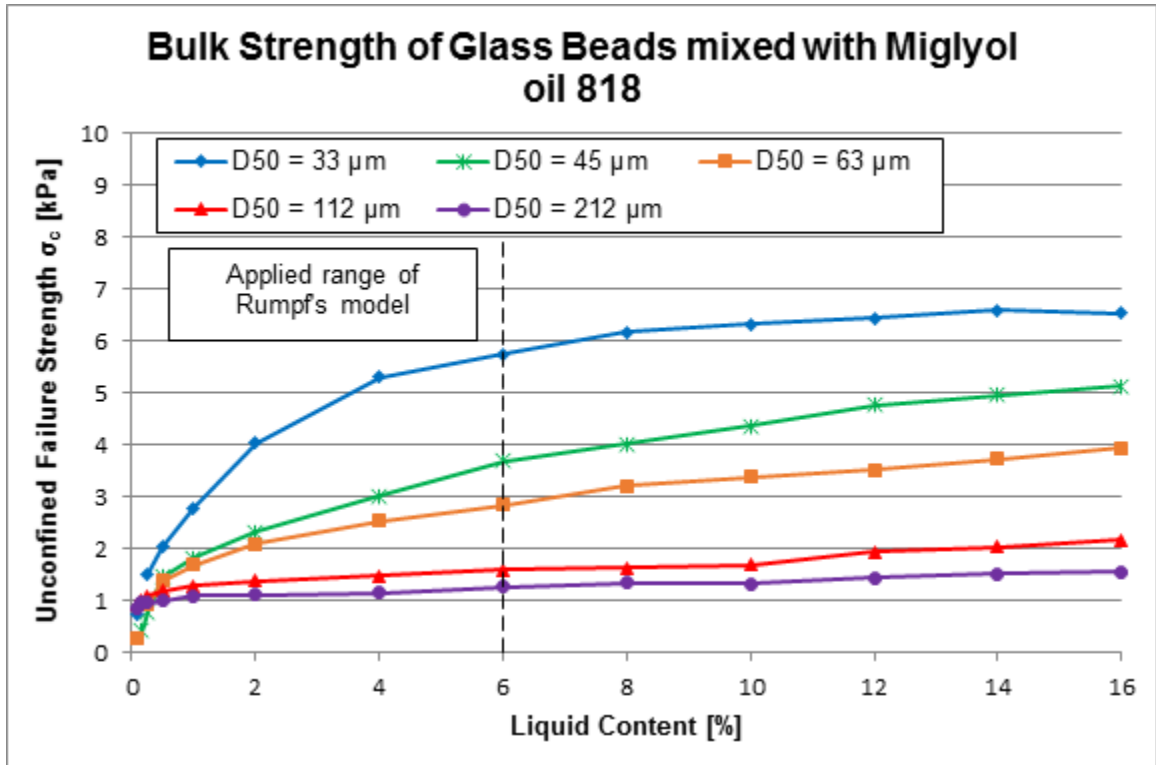


Figure 95: Range of Rumpf model application for size fractions of glass beads mixed with Miglyol oil 818

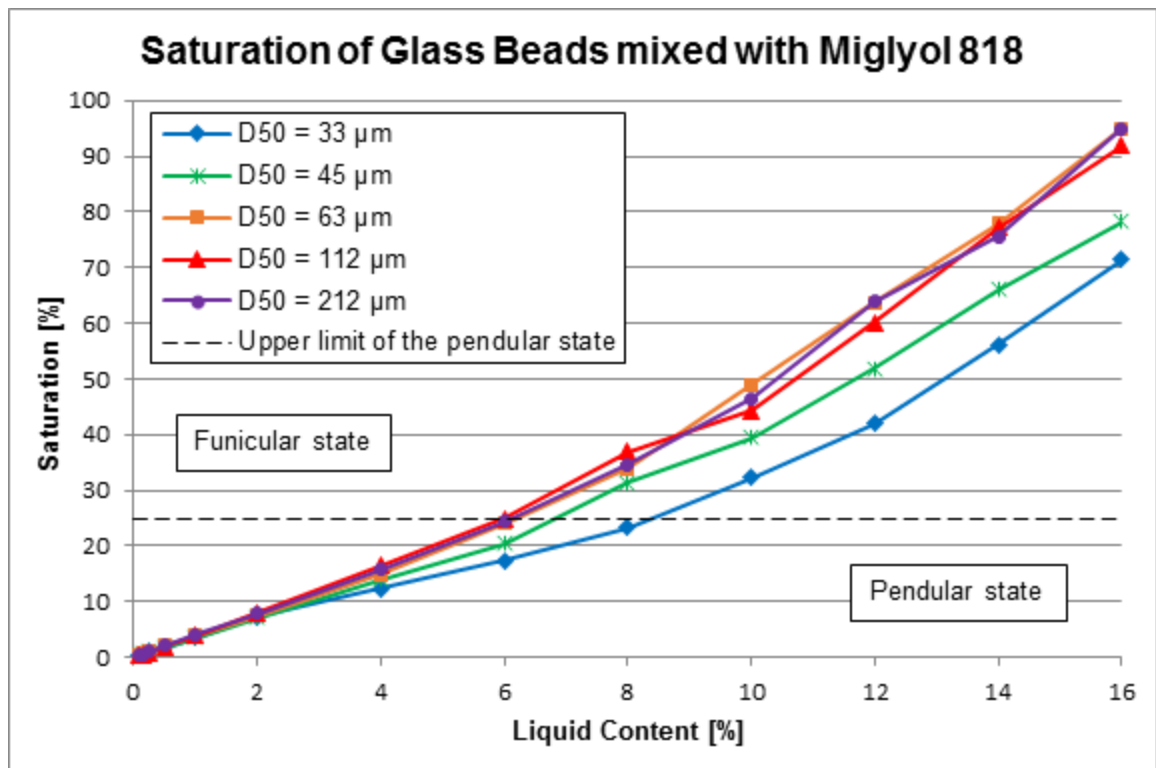


Figure 96: Range of Rumpf model application for saturation of size fractions of glass beads mixed with Miglyol oil 818

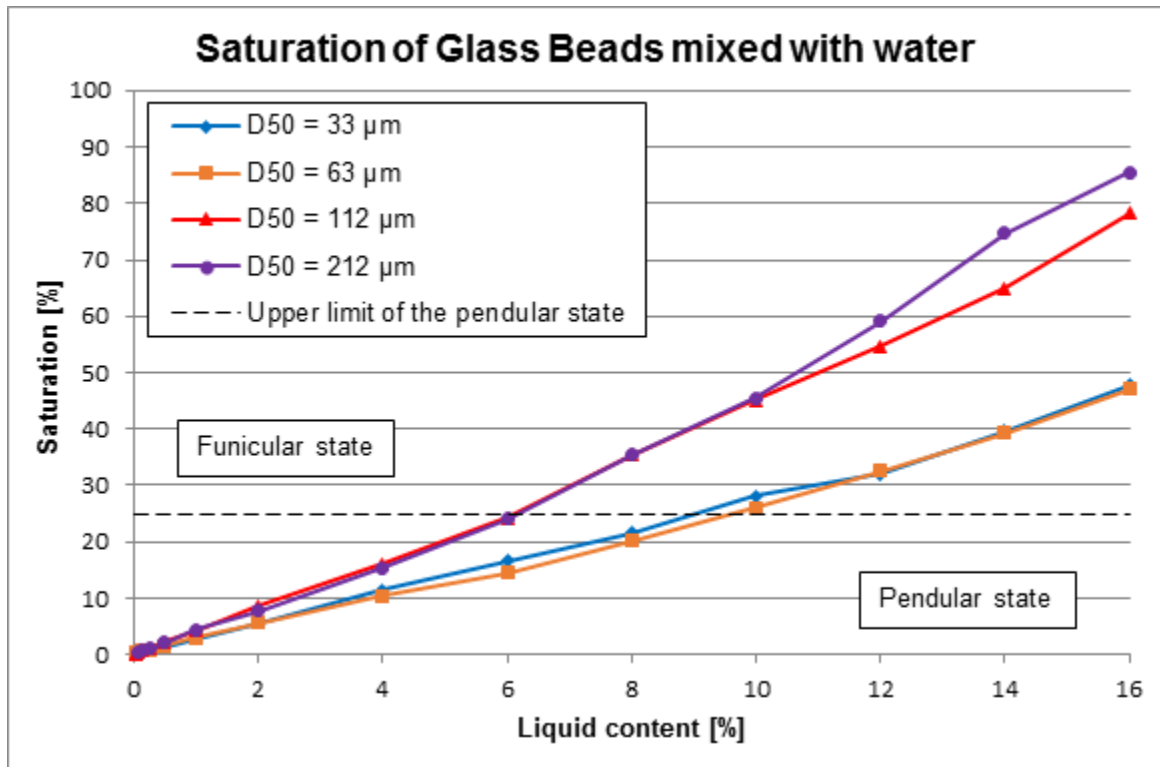


Figure 97: Range of Rumpf model application for saturation of size fractions of glass beads mixed with de-ionised water

The model (equation 60) has been applied at different levels of consolidation stresses for each powder tested. The following tables show the values of the factor of calibration “C” for different powders at 2, 4 and 9 kPa of consolidation stress. This has been developed by dividing the measured bulk strength by the predicted values obtained from the model in the range of application considered in this research. Then an average value of these differences for each wet powder tested has been used to calibrate the predicted results obtaining the single value which characterise the calibration of each powder. Table 39 and 40 and figures 98 and 99 show the values of the factor of calibration calculated in this research and how the factor of calibration varies with the consolidation pressure.

Dimensionless factor of calibration “C” for Glass Beads mixed with Miglyol 818 at pendular state and different levels of consolidation stress			
Mean size	2 kPa	4 kPa	9 kPa
D50 = 33 μm	-	-	-
D50 = 45 μm	0.24	0.31	0.37
D50 = 63 μm	0.32	0.38	0.42
D50 = 112 μm	0.44	0.48	0.52
D50 = 212 μm	0.60	0.66	0.72

Table 39: Dimensionless factor of calibration for glass beads mixed with Miglyol oil 818 at pendular state at different levels of consolidation stress

Dimensionless factor of calibration “C” for Glass Beads mixed with de-ionised water at pendular state and different levels of consolidation stress			
Mean size	2 kPa	4 kPa	9 kPa
D50 = 33 μm	0.21	0.29	0.34
D50 = 63 μm	0.32	0.38	0.44
D50 = 112 μm	0.44	0.48	0.54
D50 = 212 μm	0.58	0.64	0.71

Table 40: Dimensionless factor of calibration for glass beads mixed with de-ionised water at pendular state at different levels of consolidation stress

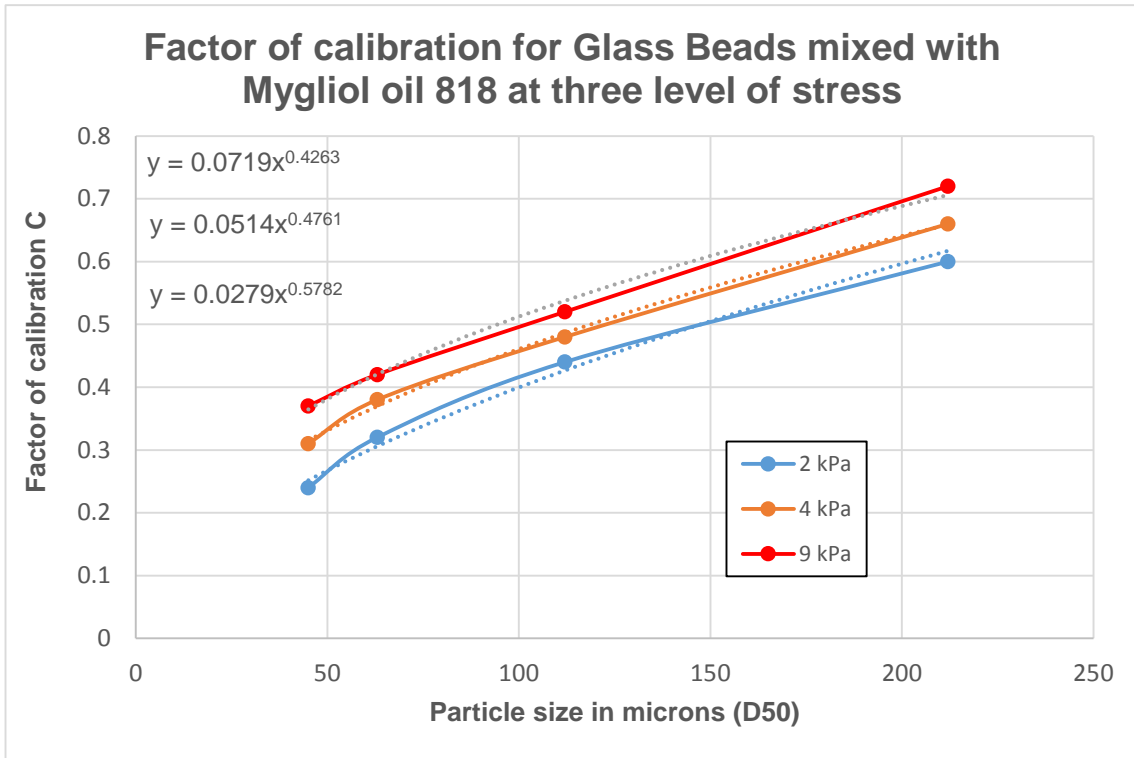


Figure 98: Factor of calibration for glass beads mixed with Miglyol oil 818

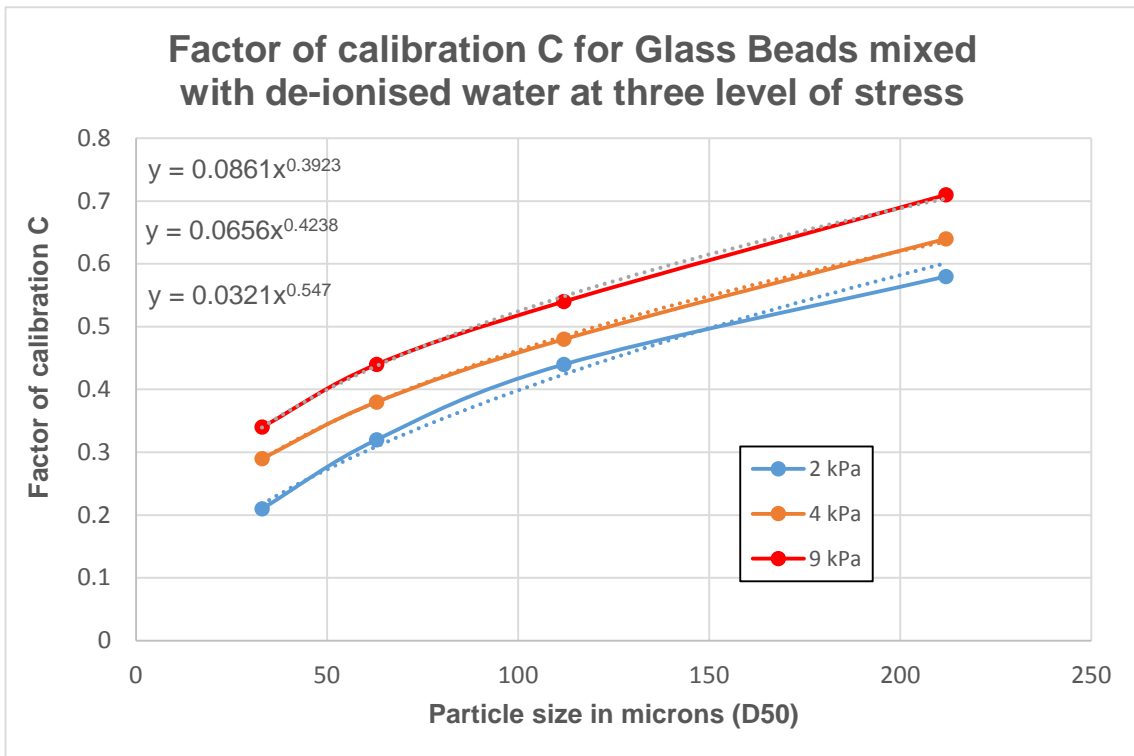


Figure 99: Factor of calibration for glass beads mixed with de-ionised water

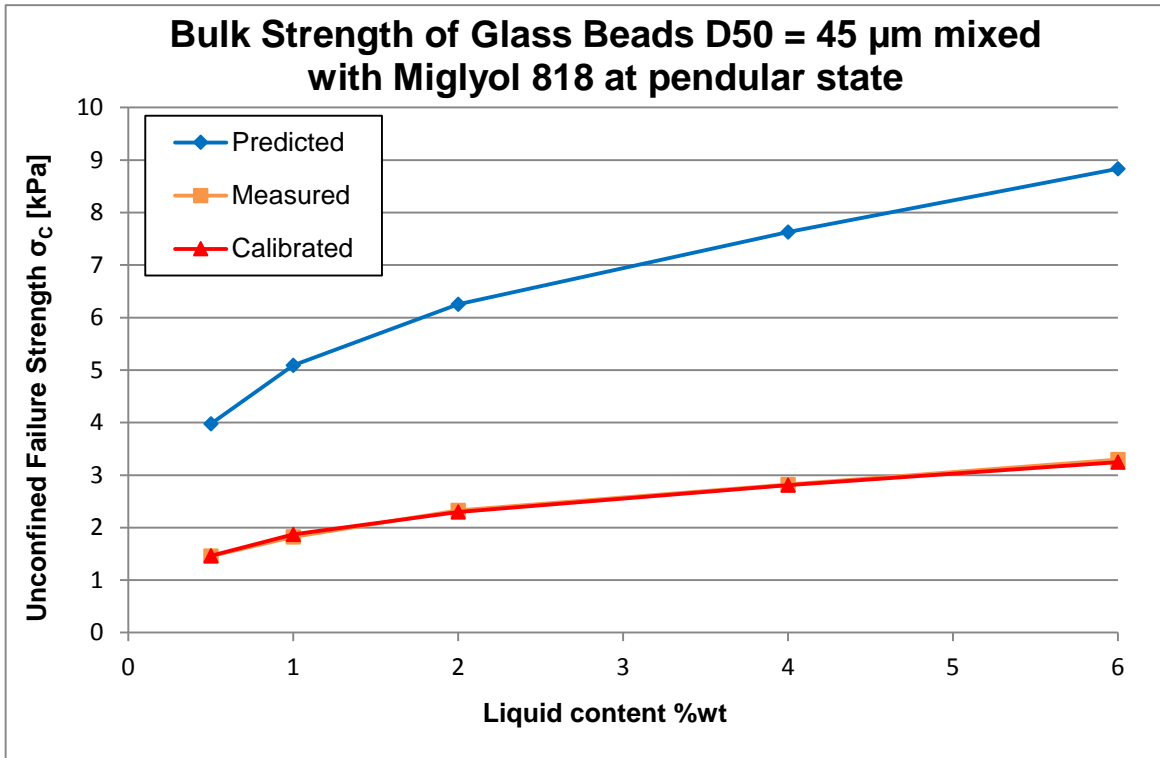


Figure 100: Comparison of the predicted, measured and calibrated bulk strength of wet glass beads D50 = 33 μm

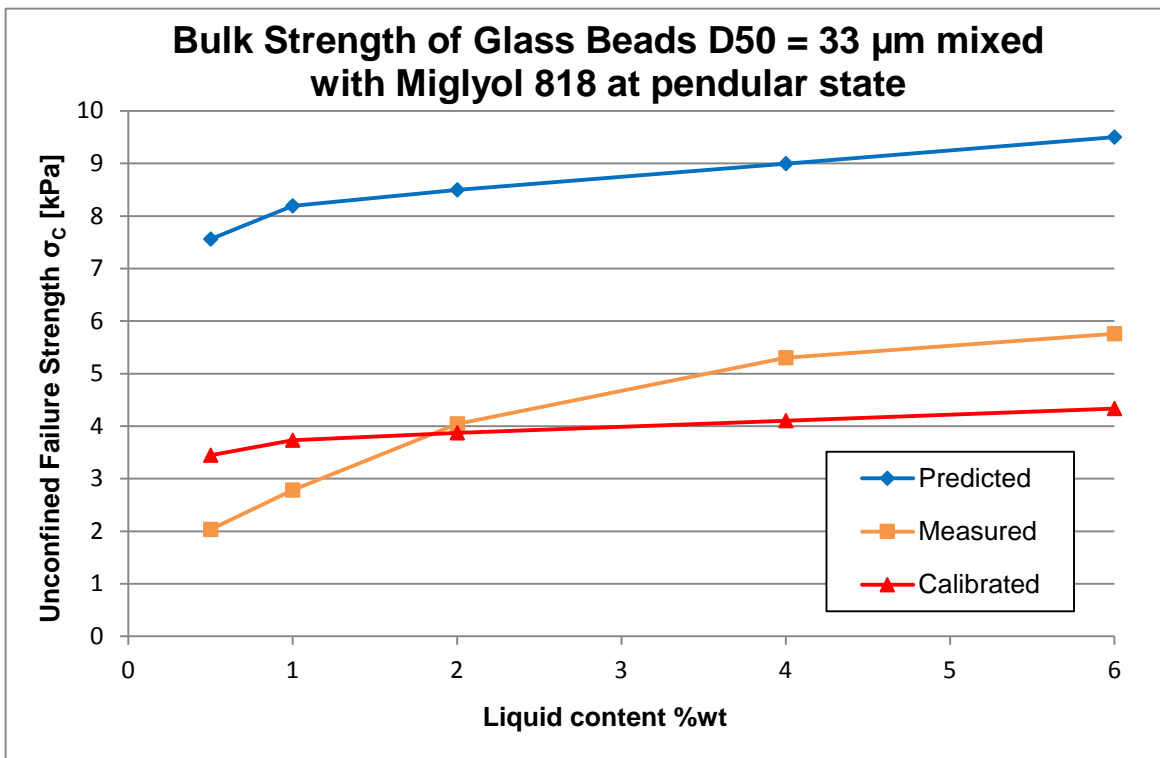


Figure 101: Comparison of the predicted, measured and calibrated bulk strength of wet glass beads D50 = 33 μm

Examples of the comparison between the measured and predicted bulk strength for different grades of glass beads are shown in figures 100 and 101. Results of the calibration of the model show that the bulk strength of wet glass beads with particle size above 40 μm can be calibrated with a single constant value. However, the shape of the curve for measured values of glass beads with particle size below 40 μm makes difficult to calibrate the model with a single constant value (see figure 101). For this case, it is necessary to develop an empirical fitting model of the measured values as an alternative approach to calibrated Rumpf model; this empirical model has been developed in this research and it is presented and explained in details in chapter 8.

Regarding to the predictions obtained from the model, these showed a similar trend to the measured values of the grades of glass beads tested whereas the model over-predicts the experimental data. This result is confirmed by the work developed by others researchers such as Pierrat et al. 1997 who predicted the tensile strength of glass beads using Rumpf model and compared the predictions with the experimental data. In this research, a correlation for a range of different particle sizes and liquid properties has been found as shown in figures 98 and 99 above.

7.2.3 Surface coating of particles

The results of the measured bulk flow properties of dry blends made with single powders and free flow additives (figures 75 and 76 in chapter 6, section 6.3.6) showed that free flow additives are not effective on dry powders and therefore the validation of the model for surface coating of dry particles became irrelevant in this research study.

It was considered more critical the development of an empirical model to predict the effect of free flow additives on wet powders based on the experimental work undertaken with blends made with glass beads, Miglyol oil 818 and different common free flow agents. The model developed to predict the bulk strength of wet blended powders with free flow additive is explained and presented in chapter 8, section 8.2.3 of the thesis.

7.3 *Model proposed for dry blends*

In chapter 5 a model has been introduced to predict the average values of the bulk strength, bulk density and internal friction for dry blends without free flow additives based on specific volume and surface area ratios of the blend components. This model

was evaluated measuring the packing and bulk flow properties of several multicomponent dry blends presented in chapter 6 and appendix B.

The model introduced in section 5.5 of the thesis has been applied at different consolidation stresses (0.6, 1.2, 2.4, 4.8 & 9 kPa) to predict the packing and bulk flow properties of different dry blended powders prepared and tested using Brookfield PFT shear tester. The predictions obtained based on the surface area and the specific volume ratios of the blend components have been plotted against the measured values to determine the accuracy of the proposed model. It has been assumed monosized spheres as explained in section 5.5 of the thesis.

Predictions based on the mass ratio of the blend components were initially made but the results obtained showed significant differences between the measured and predicted values in all cases. For this reason, this approach was not further considered in the model proposed for dry blends.

The equation of the model for the prediction of the bulk strength based on the average calculated with the specific volume ratio at the selected consolidation stress is as follows:

$$\sigma_{CAVG} (at \sigma_{1P}) = \sum_{i=1}^n \left(\sigma_{Ci} * \frac{X_i / \rho_{Bi}}{\sum_{i=1}^n (X_i / \rho_{Bi})} \right) \quad \text{Equation 64}$$

Where

- σ_{CAVG} is the predicted bulk strength at the consolidation stress selected σ_{1p}
- σ_{1p} is the consolidation stress selected to predict the bulk strength
- n is the number of the ingredients in the blended powder
- X_i is the weight ratio of each component of the blend
- σ_{Ci} is the measured bulk strength of each component of the blend at the consolidation stress selected σ_{1p}
- ρ_{Bi} is the measured bulk density of each component of the blend at the consolidation stress selected σ_{1p}

The average value of the mean particle size, the particle density, the internal friction and the bulk density based on the specific volume ratio are calculated substituting σ_{Ci} in the equation for the value of the variable to be predicted at the consolidation stress selected.

The equation of the model for the prediction of the bulk strength based on the average calculated with the surface area ratio at the selected consolidation stress is as follows:

$$\sigma_{CAVG} (at \sigma_{1P}) = \sum_{i=1}^n (\sigma_{Ci} * \frac{N_i * S_{Ai}}{\sum_{i=1}^n (N_i * S_{Ai})}) \quad \text{Equation 65}$$

$$N_i = \frac{X_i}{V_i * \rho_{Pi}} \quad \text{Equation 66}$$

Where

- N_i is the number of particles of each component of the blend
- S_{Ai} is the surface area of the particles of each component of the blend
- V_i is the volume of the particles of each component of the blend
- ρ_{Pi} is the particle density of each component of the blend

The average value of the internal friction based on the surface area ratio is calculated substituting σ_{Ci} in the equation for the value of the variable at the consolidation stress selected.

Percentage deviation of the predicted values from the measured values was calculated at different levels of consolidation stress. The values of the deviation (%) for each blended powder are shown in tables 41 - 48. It is important to highlight the fact that for free and easy flowing blends, the values of the high percentage deviation are not crucial if the predicted values are in the same range of flowability. However, values of the percentage deviation are critical for blended powders in the range of cohesive or very cohesive powders.

Overall, results suggested that the specific volume ratios on the blend components give a better agreement with the measured bulk flow properties than using surface area ratios. A good agreement was found for cohesive blended powders with greater deviations for free and easy flowing blended powders but still in the flow range of the measured blends. Different kind of dry blends were tested and compared as follows:

- 1) Blends made with size fractions of the same powder

The packing and bulk flow properties of three powders named dextrose, sodium chloride and maltodextrin were predicted applying the model with the data of the size fractions of each powder obtained from the study of the effect of deconstructed particle

size distribution presented in chapter 4. The flow function, bulk density curve and friction function of the full size distribution of these powders were tested and compared with the predicted functions of the dry blends considering in the calculations the equivalent weight ratios of each size fractions in the original particle size distribution of the powders. The main results are presented in this section in figures 102 - 104 and table 41 and 42 with full results plots presented in appendix A.

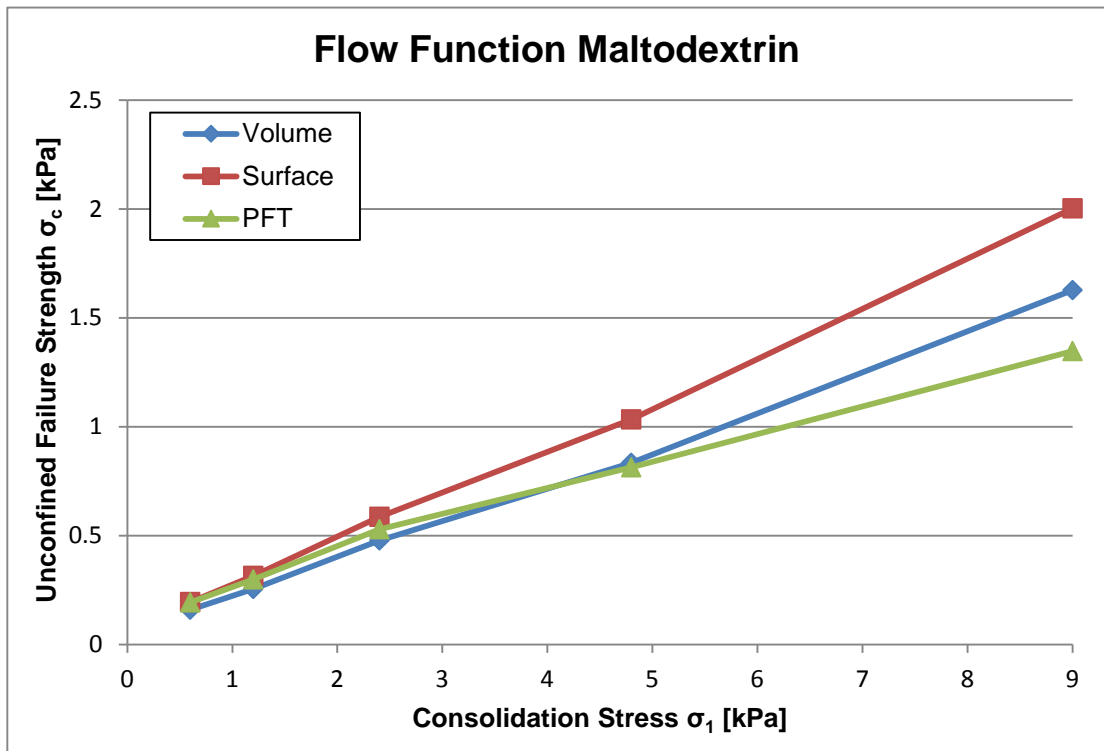


Figure 102: Measured and predicted flow function for maltodextrin

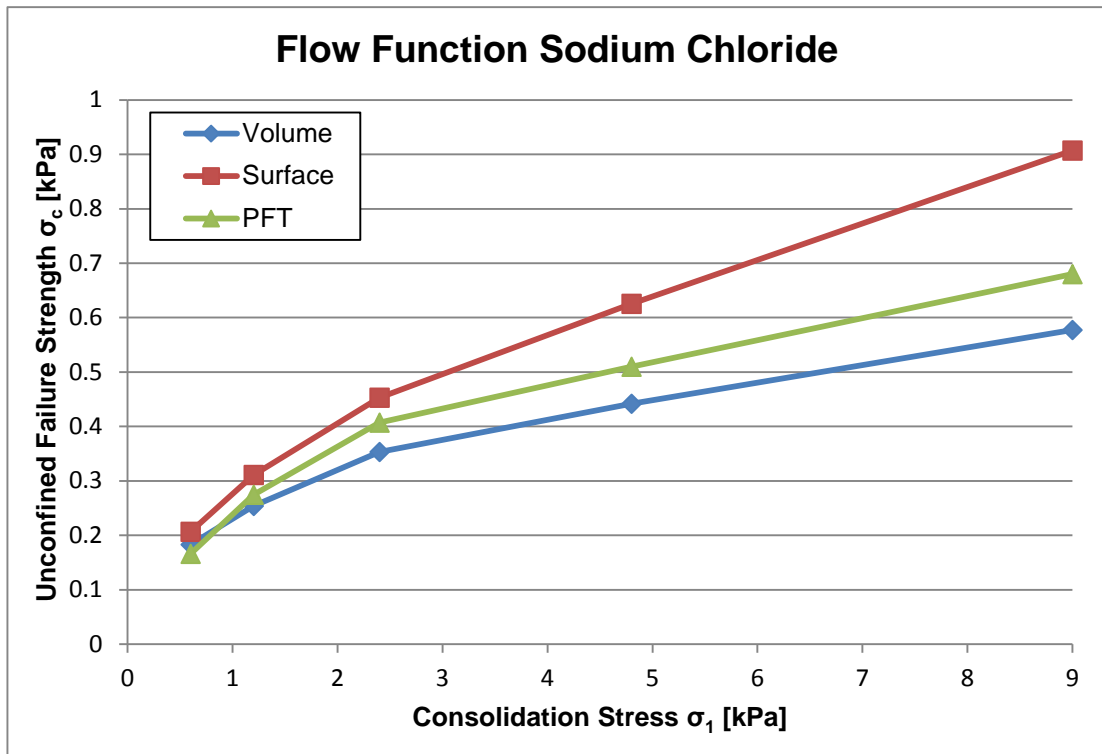


Figure 103: Measured and predicted flow function for sodium chloride

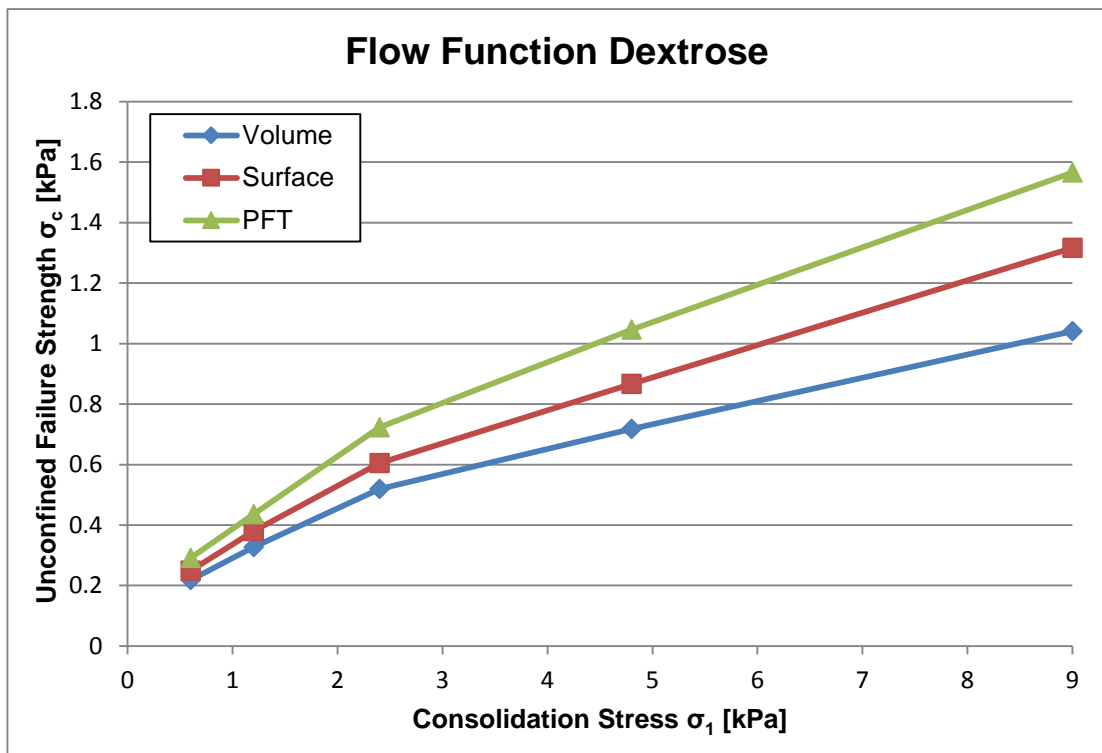


Figure 104: Measured and predicted flow function for dextrose

Deviation % from measured values based on specific volume ratio predictions	Values of consolidation stresses (kPa)				
	0.6	1.2	2.4	4.8	9
Maltodextrin	17.96	14.71	9.71	-2.57	-20.82
Sodium Chloride	-9.96	7.61	13.23	13.32	15.11
Dextrose	24.92	24.91	28.15	31.36	33.52

Table 41: Deviation of the measured and predicted flow function for maltodextrin, sodium chloride and dextrose

Deviation % from measured values based on surface area ratio predictions	Values of consolidation stresses (kPa)				
	0.6	1.2	2.4	4.8	9
Maltodextrin	-0.42	-5.50	-11.04	-27.10	-48.77
Sodium Chloride	-24.30	-13.20	-11.15	-22.69	-33.43
Dextrose	14.39	12.69	16.39	17.19	15.88

Table 42: Deviation of the measured and predicted flow function for maltodextrin, sodium chloride and dextrose

2) Blends made with different grades of the same powder

Three different grades of lactose with narrow particle size distributions and D50 values of 4, 32 and 100 μm were blended at different weight ratios to evaluate the model. Packing and bulk flow properties of these blends were measured and compared with the predicted values obtained from the application of the model. These three lactose grades were blended at the weight ratios of 15:15:70, 25:25:50, 33:33:33 & 70:15:15 to study the effect of the particle size in the predicted values. The main results are presented in this section in figures 105 - 108 and table 43 and 44 with full results plots presented in appendix A.

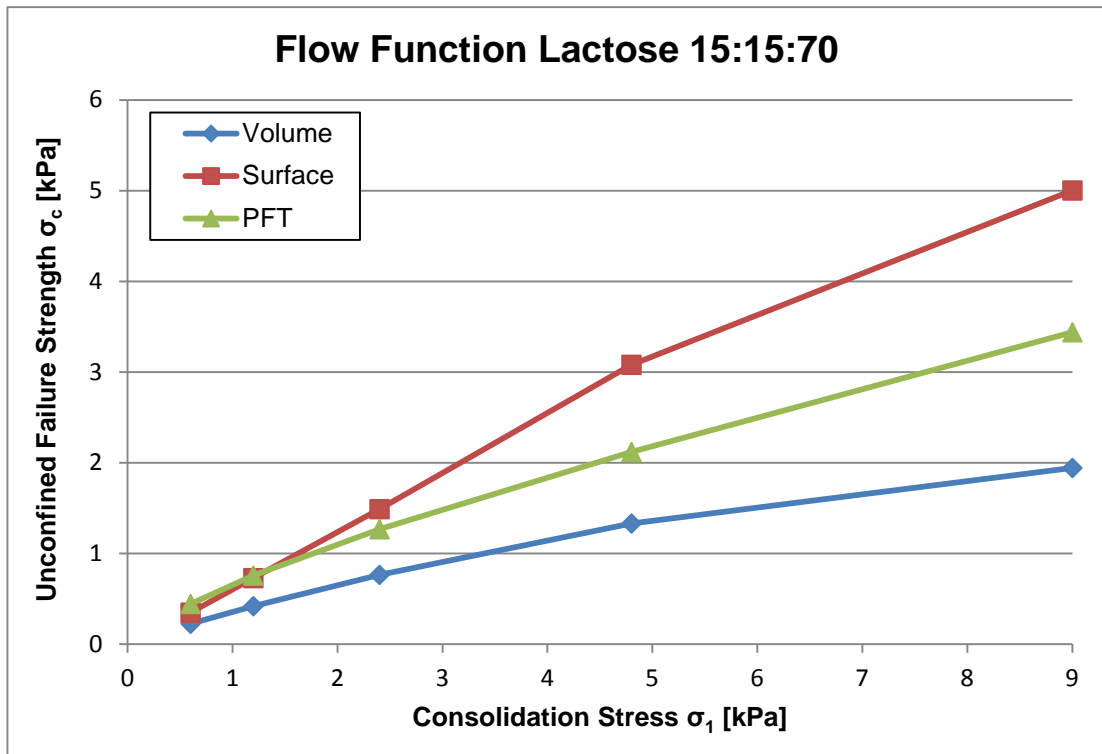


Figure 105: Measured and predicted flow function for blended lactose 15:15:70

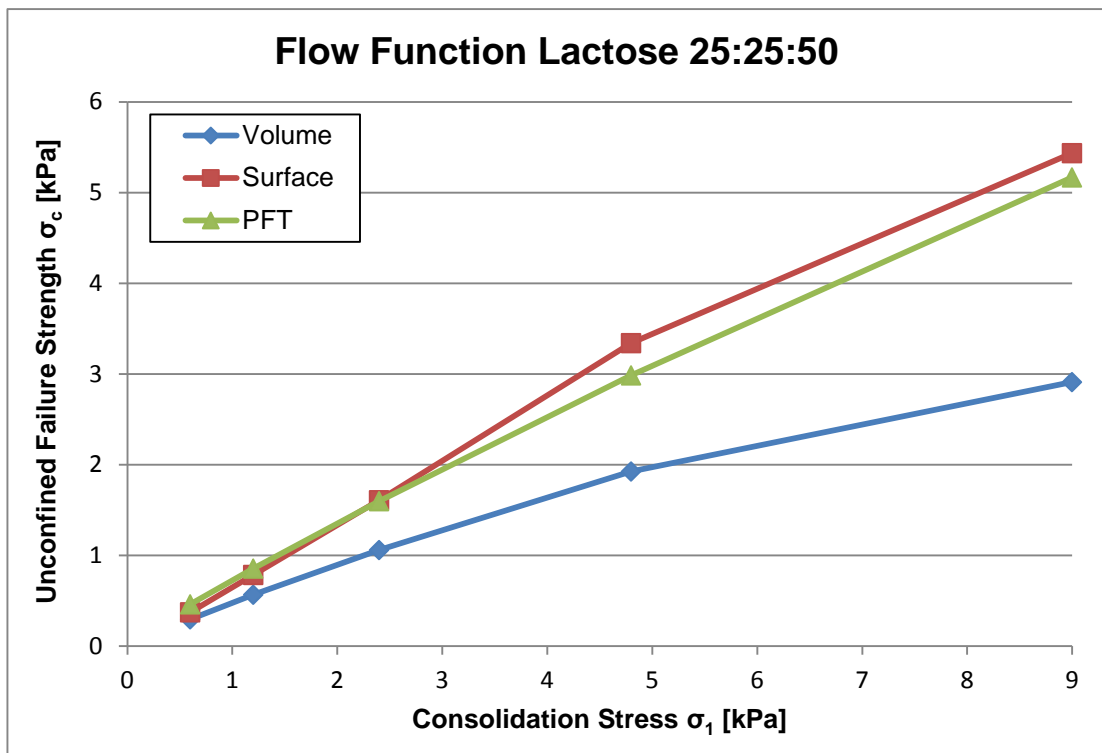


Figure 106: Measured and predicted flow function for blended lactose 25:25:50

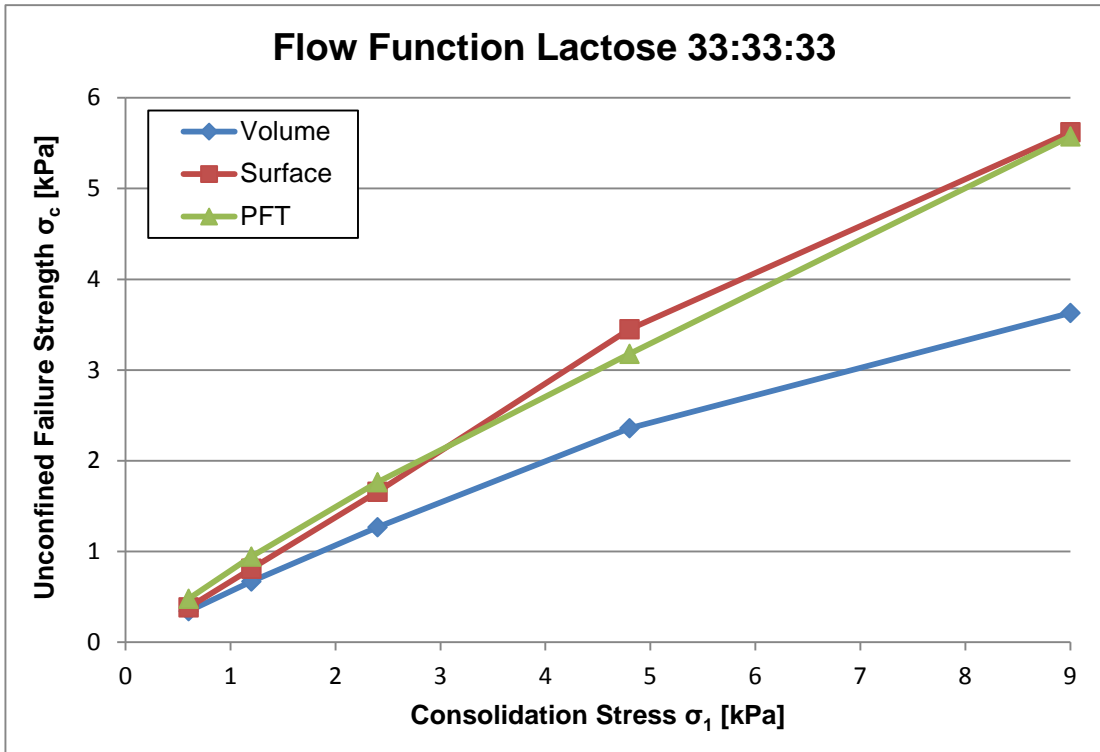


Figure 107: Measured and predicted flow function for blended lactose 33:33:33

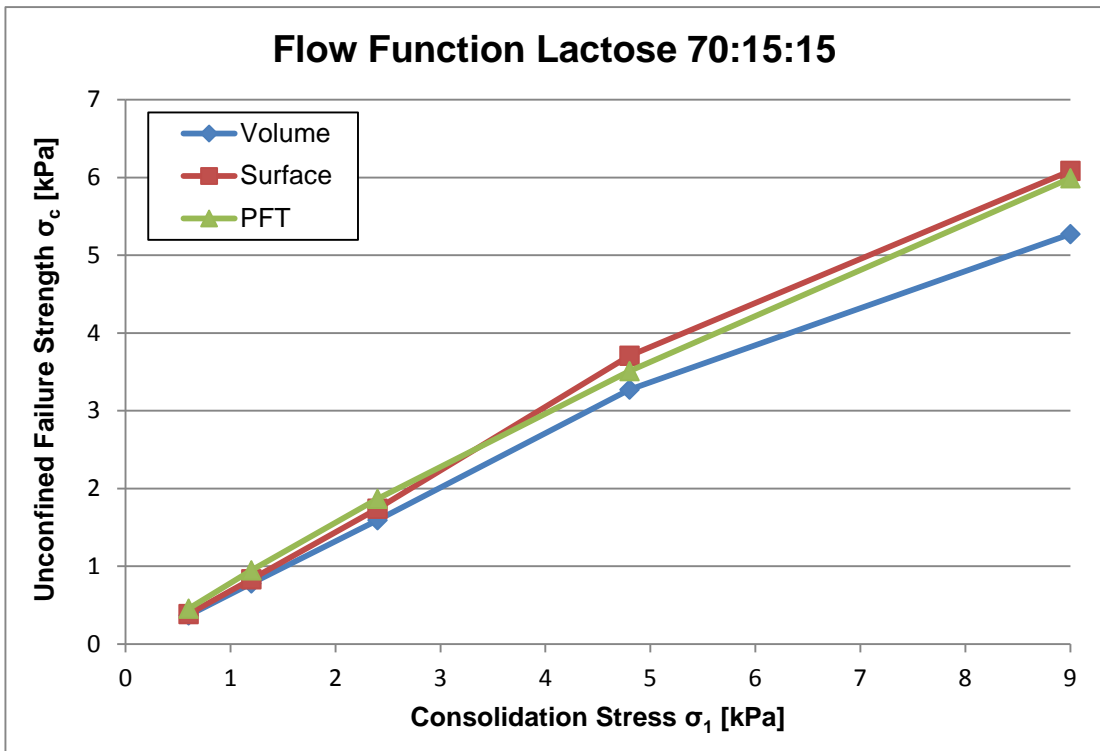


Figure 108: Measured and predicted flow function for blended lactose 70:15:15

Deviation % from measured values based on specific volume ratio predictions	Values of consolidation stresses (kPa)				
	0.6	1.2	2.4	4.8	9
Lactose 15:15:70	49.25	44.68	39.60	37.24	43.48
Lactose 25:25:50	35.96	33.88	33.59	35.48	43.65
Lactose 33:33:33	29.01	29.34	28.13	25.76	34.89
Lactose 70:15:15	18.51	17.83	14.79	6.80	12

Table 43: Deviation of the measured and predicted flow function for blended lactose

Deviation % from measured values based on surface area ratio predictions	Values of consolidation stresses (kPa)				
	0.6	1.2	2.4	4.8	9
Lactose 15:15:70	21.54	3.30	-17.68	-45.35	-45.43
Lactose 25:25:50	18.86	8.14	-0.68	-11.80	-5.17
Lactose 33:33:33	20.11	14.21	6	-8.54	-0.79
Lactose 70:15:15	15.25	12.32	6.82	-5.61	-1.63

Table 44: Deviation of the measured and predicted flow function for blended lactose

3) Blends made with different powders at various ratios of blend

Three powders named lactose, dextrose and sodium chloride were blended at different weight ratios to make 2 and 5 component blends. The binary blend was made with lactose (D50 = 32 μm) and dextrose (D50 = 185 μm) at the weight ratios of 10:90, 20:80, 30:70 and 50:50; the 5 component blend was made with fine sodium chloride (D50 = 24 μm), lactose (D50 = 32 μm), fine dextrose (D50 = 91 μm), coarse sodium chloride (D50 = 120 μm) and coarse dextrose (D50 = 185 μm) at the weight ratios of 10:10:10:35:35, 20:20:20:20:20 and 35:35:10:10:10 to analyse the influence of particle

size in the predictions made with the model. The main results are presented in this section in figures 109 - 115 and tables 45 - 48 with full results plots presented in appendix A.

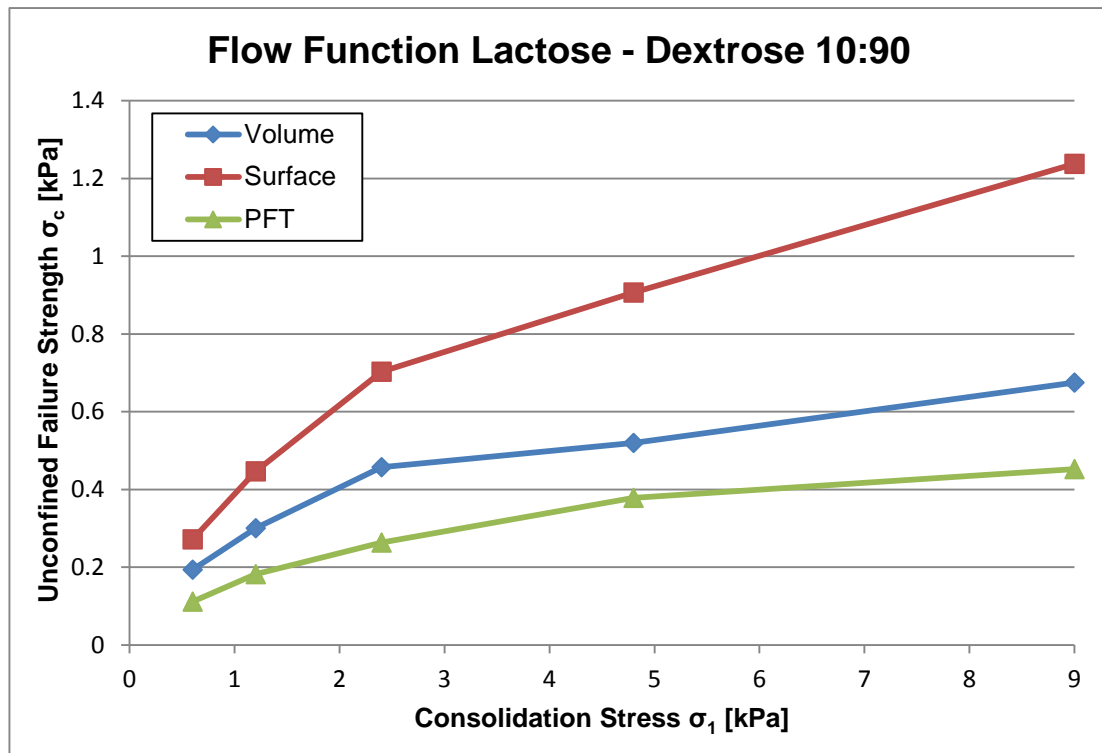


Figure 109: Measured and predicted flow function for blended lactose dextrose 10:90

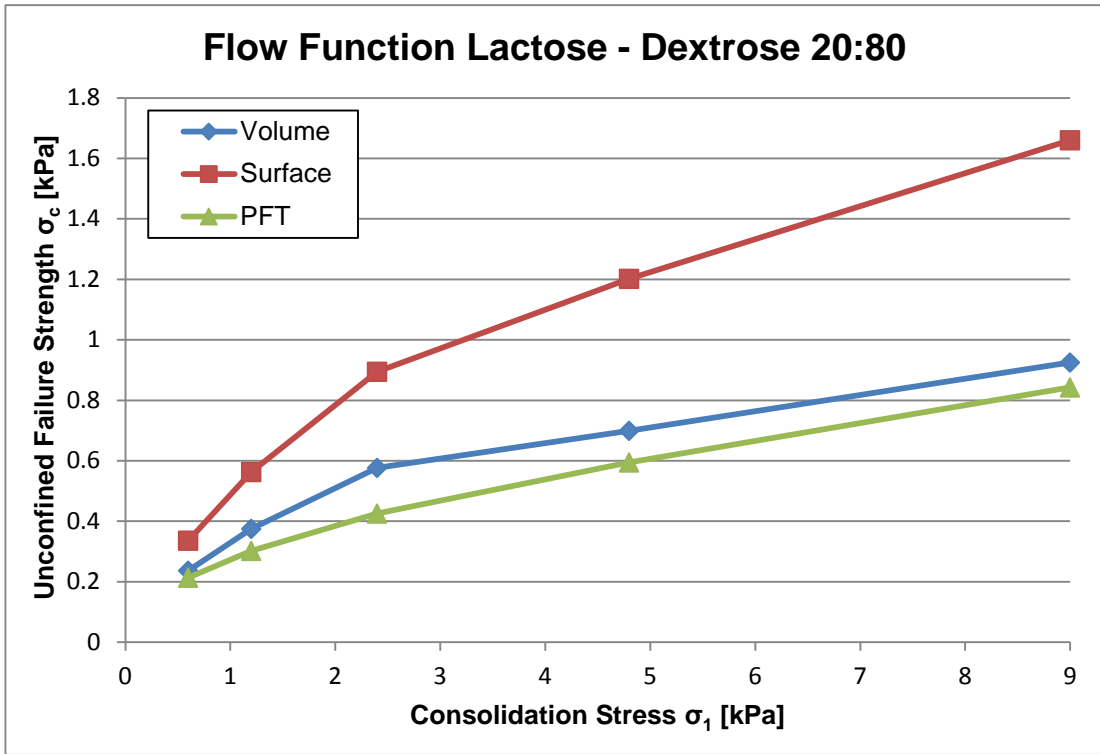


Figure 110: Measured and predicted flow function for blended lactose dextrose 20:80

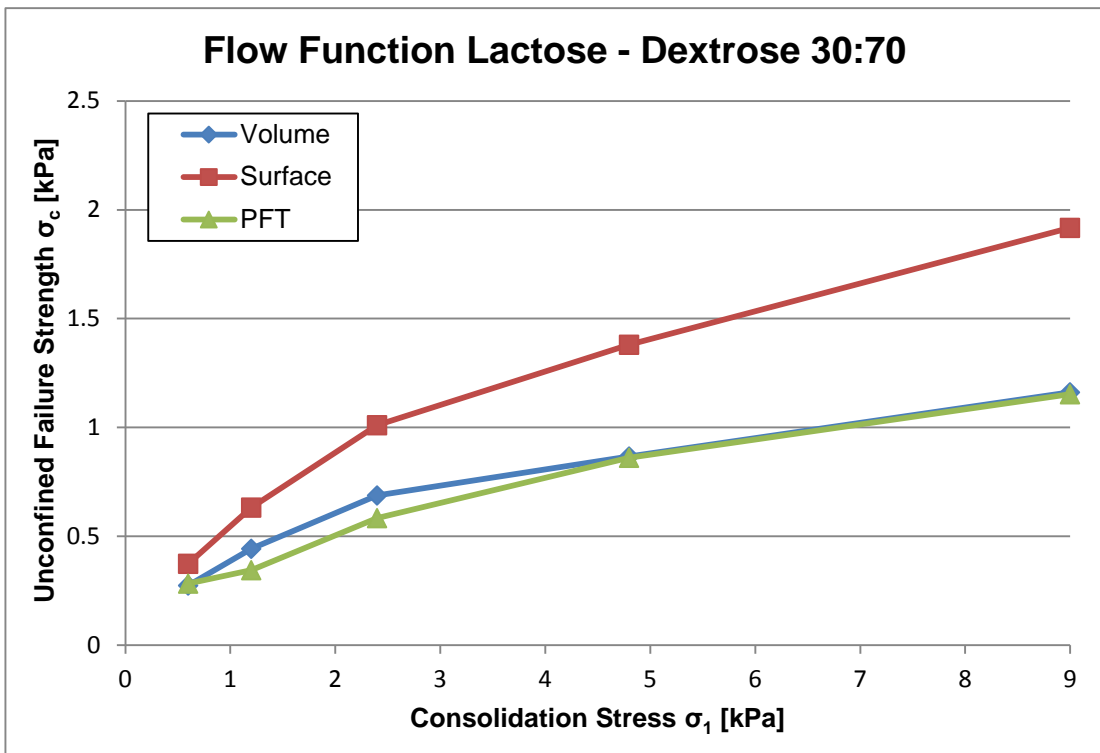


Figure 111: Measured and predicted flow function for blended lactose dextrose 30:70

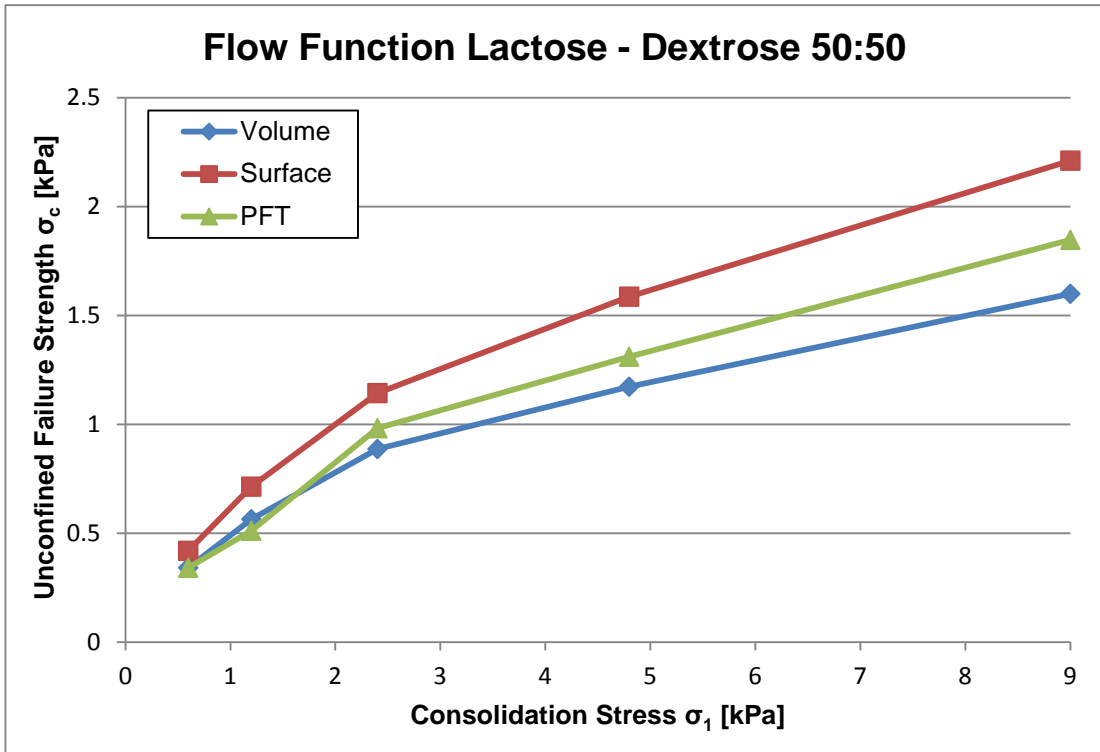


Figure 112: Measured and predicted flow function for blended lactose dextrose 50:50

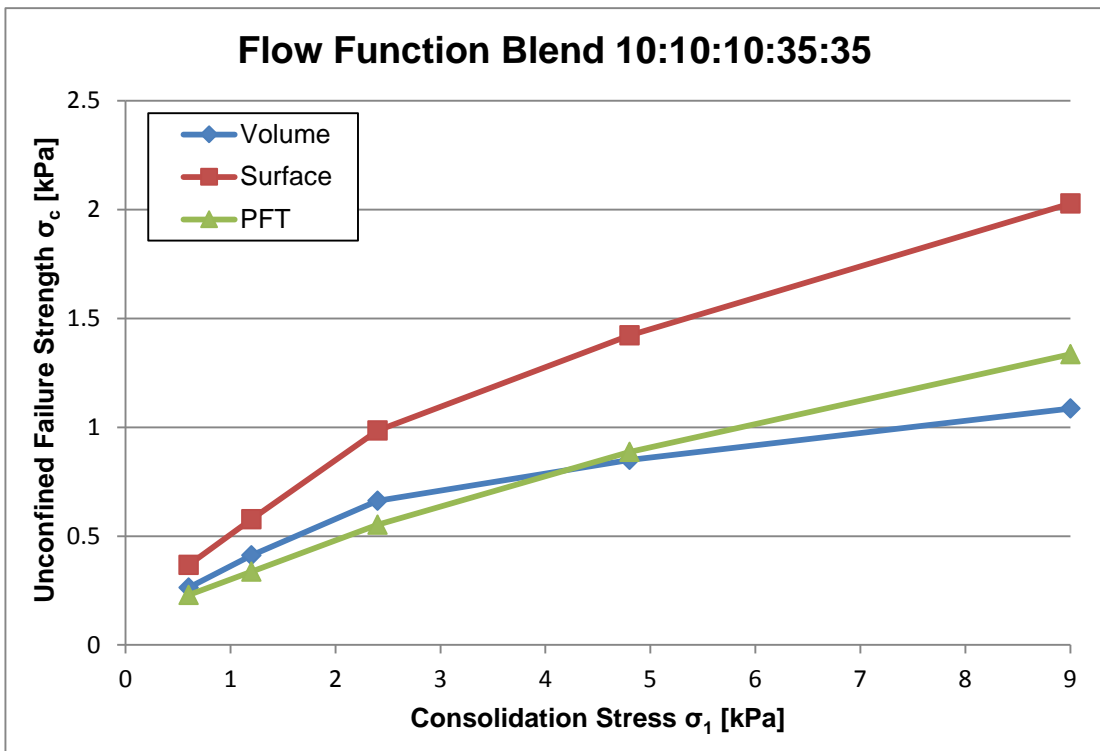


Figure 113: Measured and predicted flow function for blended powder 10:10:10:35:35

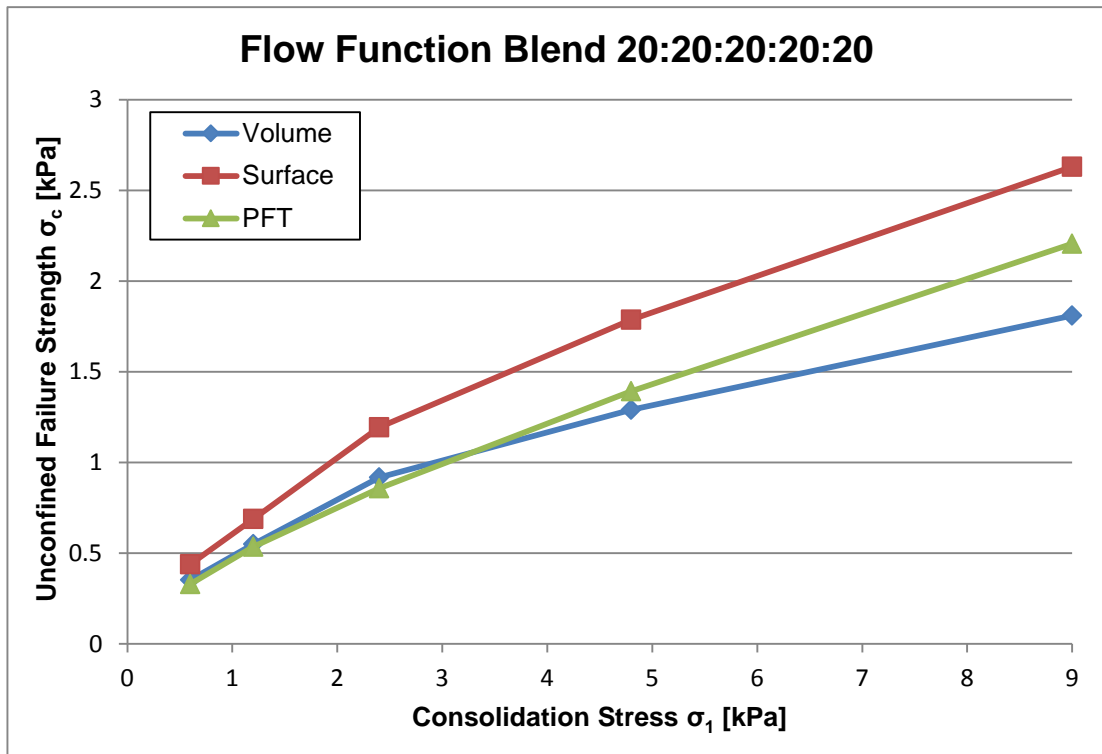


Figure 114: Measured and predicted flow function for blended powder 20:20:20:20:20

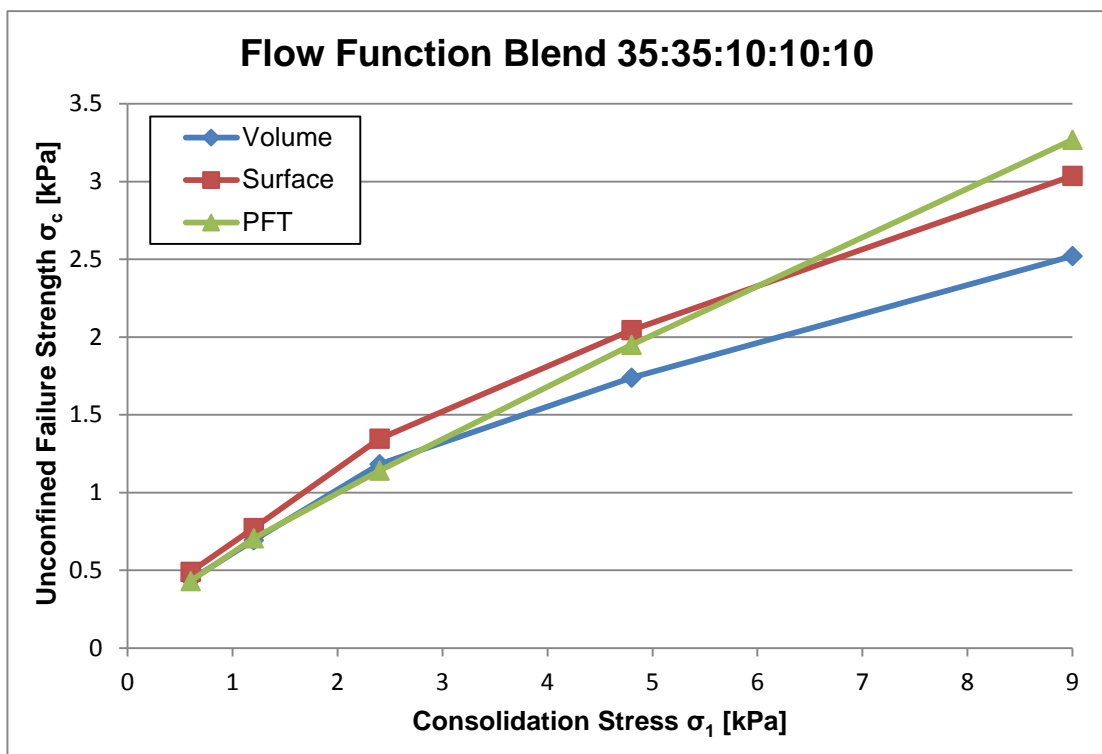


Figure 115: Measured and predicted flow function for blended powder 35:35:10:10:10

Deviation % from measured values based on specific volume ratio predictions	Values of consolidation stresses (kPa)				
	0.6	1.2	2.4	4.8	9
Lactose – Dextrose 10:90	-73.94	-64.82	-73.42	-37.35	-49.21
Lactose – Dextrose 20:80	-10.77	-24.13	-35.30	-17.44	-9.74
Lactose – Dextrose 30:70	3.19	-28.68	-17.71	-0.68	-0.73
Lactose – Dextrose 50:50	-0.15	-10.40	9.69	10.52	13.39

Table 45: Deviation of the measured and predicted flow function for blended lactose dextrose

Deviation % from measured values based on surface area ratio predictions	Values of consolidation stresses (kPa)				
	0.6	1.2	2.4	4.8	9
Lactose – Dextrose 10:90	-144.12	-144.89	-166.62	-139.57	-173.7
Lactose – Dextrose 20:80	-57.51	-86.14	-109.79	-101.95	-96.97
Lactose – Dextrose 30:70	-32.09	-83.60	-72.94	-60.37	-66.13
Lactose – Dextrose 50:50	-23.05	-39.59	-16.49	-21.02	-19.74

Table 46: Deviation of the measured and predicted flow function for blended lactose dextrose

Deviation % from measured values based on specific volume ratio predictions	Values of consolidation stresses (kPa)				
	0.6	1.2	2.4	4.8	9
Blend 10:10:10:35:35	-14.98	-22.28	-20	4.17	18.69
Blend 20:20:20:20:20	-6.68	-2.62	-6.89	7.26	17.95
Blend 35:35:10:10:10	-1.89	1.72	-3.63	10.83	22.85

Table 47: Deviation of the measured and predicted flow function for blended powder

Deviation % from measured values based on surface area ratio predictions	Values of consolidation stresses (kPa)				
	0.6	1.2	2.4	4.8	9
Blend 10:10:10:35:35	-60.06	-71.66	-78.37	-60.47	-51.84
Blend 20:20:20:20:20	-32.99	-28.57	-39.04	-28.37	-19.20
Blend 35:35:10:10:10	-13.75	-9.40	-18	-4.82	7.08

Table 48: Deviation of the measured and predicted flow function for blended powder

7.4 Summary

Analytical models found in the literature review linking particle and bulk flow properties and the new model for dry blended powders presented in chapter 5 were calibrated to evaluate their applicability on predicting the packing and bulk flow properties of real single and blended powders. The key points from the chapter are the following:

- The calibration of the empirical fitting equations proposed by Yu et al. 2003 to predict the voidage of dry powders showed that the equations over predict the voidage of dry powders at 2, 4 and 9 kPa of consolidation stress (see figures 81 and 84) for particulate materials with most of the size fractions below 100 μm . It is due to the fact that these equations do not consider the effect of stress consolidation on the packing properties of the powders. For powders with most

of the size fractions above 100 μm , the change in voidage due to the consolidation stress is not remarkable so the equations can make a good prediction (see figures 82 and 83). It is important to highlight that the measured values of voidage for size fractions of maltodextrin (see figure 85) shows a consistent trend in the data which needs to be studied in more details.

- The model proposed by Rumpf et al. to predict the tensile strength of agglomerates for dry powders predicts a trend for the decrease in strength which is an inverse power law. However, the measured data shows a linear decrease (see figures 86 - 90) so the model over predicts the strength as the particle size increases into the free flowing range. It would be better to develop a new empirical model based on the measured strength at fine particle size (less than 50 μm) and then assume a linear trend from zero at 100 μm through the measured point to a maximum strength which is equal to the consolidation stress. This model has been developed in this research and is presented in the next chapter.
- The calibration of the empirical equations proposed by Feng et al. to predict the voidage of wet powders showed that these equations over predict the voidage of wet particulate materials at 2, 4 and 9 kPa of consolidation stresses. It is due to the fact that these equations were developed using glass beads with a minimum size of 250 μm to avoid the effect of interparticles forces on the voidage for particle size lower than 100 μm . Furthermore, experiments to develop these equations were undertaken only for loose and poured packing conditions of wet glass beads. In this research, wet powders were characterised with the average measured value of the voidage as shown in figures 91 and 92 and tables 37 and 38.
- The calibration of the well-established model developed by Rumpf et al. for pendular state of liquid saturation of packed monosized spheres showed that the bulk strength of wet glass beads with particle size above 40 μm can be predicted by the model using a constant value of the factor of calibration "C" developed in this research (see figure 100); the value of the factor of calibration varies with the consolidation stress applied to the powder and the mean particle size of the size fraction of glass beads as shown in tables 39 and 40. For glass

beads with particle size below 40 μm , an empirical fitting model was developed and presented in the next chapter as the factor of calibration developed failed to predict the bulk strength with a constant value as shown in figure 101.

- The model proposed to predict the average values of the bulk strength, bulk density and internal friction for dry blends without free flow additives based on the specific volume and surface area ratios of the blend components was evaluated measuring the packing and bulk flow properties of multicomponent dry blends. Results of the evaluation suggested that the specific volume ratios on the blend components give a better agreement with the measured bulk flow properties rather than using surface area ratios. A good agreement was found for cohesive dry blended powders with greater deviations for free flowing dry blends but still in the flow range of the measured blends (free and easy flowing).

After analysing the results obtained from the calibration, new empirical models based on the experimental work of the research were developed to better predict the bulk flow properties of single and blended particulate materials; these models are explained and presented in the next chapter.

Chapter 8 Development of new empirical models

8.1 Introduction

An empirical approach has been developed in this research study to predict the bulk strength of dry single and blended powders and the effect of liquid content and the addition of free flow additives on their flow functions. Different empirical models have been developed to predict the flow functions of dry powders, wet powders and blended wet powders with free flow additives. This chapter presents these models and compares the predicted and measured values for several single and blended particulate materials.

Results of the evaluation of the new empirical models developed to predict the flow functions of single powders in dry and wet condition with free flow additives are discussed and presented in section 8.2; results of the application of these empirical models to blended powders are discussed and presented in section 8.3 and a summary of the chapter is given in section 8.4

8.2 Single particulate materials

This section presents the application of the empirical models developed to single powders. Each model is presented and validated with measured values of powders tested with PFT shear tester.

8.2.1 Dry powders

As explained in the conclusions of the calibration of Rumpf model to predict the bulk strength of dry powders, Rumpf model failed to give good predictions of the unconfined failure strength for dry particulate materials and for this reason an empirical approach was developed. This approach considered that the strength is measured at fine particle size (less than 50 μm) and then a linear trend is assumed from zero at 100 microns through the measured point to a maximum strength which is equal to the consolidation stress. This required a new logarithmic model to study the particle size scaling effect on dry powders.

The model proposed predicts the unconfined failure strength of powders with narrow particle size distributions and the bulk strength of size fractions of wide particle size distribution of powders. Once one size fraction or grade of a powder has been tested

using a shear tester, the values of the flow function obtained are used to predict the bulk strength of other grades or size fractions of the same powder. The equation of the model is as follows:

$$\sigma_c = \sigma_1(C - A \cdot \log D) \quad \text{Equation 67}$$

Where

- σ_c is the predicted bulk strength at the consolidation stress selected
- σ_1 is the consolidation stress selected for the prediction
- A is a parameter of the equation with constant value of 0.53; this parameter controls the gradient of the predicted function
- C is a parameter of the equation which varies for different powders; its value is defined for each powder by testing one size fraction or grade of the powder using a shear tester. Then, the value of the parameter is calculated using the equation of the model (equation 67) introducing the particle size tested and the value of the bulk strength at the selected consolidation stress. For a different consolidation stress, the value of the parameter needs to be recalculated using the bulk strength obtained at this level of consolidation stress.
- D is the D50 value in microns of the particle size distribution of the powder which bulk strength is going to be predicted

To predict the flow functions of size fractions or grades of a powder, initially one fraction or grade of the powder needs to be tested to obtain the values of the unconfined failure strength at different consolidation stresses required to apply the model; then the value of the parameter C can be calculated using the particles and bulk flow properties of the tested fraction or grade of the powder. This value of C is only valid at the point of the flow function selected as the values in the flow function curves vary from point to point. Once the value of C is calculated, the flow function of any other fraction or grade of the same powder can be predicted at the same level of consolidation stress considered.

The flow function of the size fractions of four powders named glass beads, dextrose, sodium chloride and maltodextrin were predicted and compared with the measured values obtained from the study of the effect of deconstructed particle size distribution presented in chapter 4. Also the flow properties of the six grades of lactose used in the same study have been predicted and compared with measured values to validate the accuracy of the model proposed.

The validation of the model included the predictions at 0.6, 1.2, 2.4, 4.8, 9 and 10 kPa based on each fraction of the powders or grade in case of lactose. Therefore, the model has been validated looking at the influence of the particle size tested to make the predictions at different levels of consolidation stress.

The equation of the model can be also expressed as a function of the flow factor value (FFc) which is defined as the ratio of the consolidation stress σ_1 to unconfined failure strength σ_c for every single point of the flow functions. Using this flow factor value which characterise the flowability numerically, the equation of the model is expressed as follows:

$$Z = \frac{1}{FFc} = \frac{\sigma_c}{\sigma_1} = C - A \cdot \log D \quad \text{Equation 68}$$

Where Z is a new parameter of the model and its value is the ratio of the unconfined failure strength to the consolidation stress for each point of the flow function (the inverse of the flow factor ratio). The value of this parameter must be in the range between 0 and 1 based on the maximum and minimum values of the flow factor ratio. Results of the model validation have been presented in two different type of graphs:

- 1) Plotting particle size against the values of Z for each powder at 0.6, 1.2, 2.4, 4.8, 9 and 10 kPa to study the effect of the consolidation stress selected on the accuracy of the predictions made by the model. The results for the six grades of lactose are presented in this section in figures 116 - 121 with full results plots presented in appendix A. These figures show how measured and predicted values fit for 4.8, 9 and 10 kPa whereas for lower consolidation stresses, a dispersion is presented in the measured values. This may be due to the fact that at low consolidation stresses, the fine particles of the size fractions of lactose are agglomerating resulting in a lower friction (see figure 31 in chapter 3) and more disagreement between the predicted and measured values than the coarser particles. The results presented in the appendix A for the rest of the powders tested showed a good agreement even at low consolidation stress.
- 2) Plotting the measured and predicted flow functions for each size fraction or grade of the powders to study the influence of the particle size selected as a reference to make the predictions on the accuracy of the model; these graphs

compare the predictions based on each size fraction or grade of the powder with the measured values of the flow functions. The results for the six grades of lactose are presented in this section in figures 122 - 129 with full results plots presented in appendix A. These figures show how the size fraction of lactose selected to make the predictions of the bulk strength has no relevant effect on the agreement between the predicted and measured values. For coarse particles of lactose (figures 127 - 129), it may seem to be a disagreement of the measured values with the model. However, looking at the scale of the vertical axis, it has been reduced in order to clarify the effect of the selection of the size fraction, but in a normal scale such as figures 122 - 125, these flow functions lies in the horizontal axis showing low unconfined failure strength in the free flowing range of flowability.

In this research, it has been shown that this logarithmic model could predict accurately the bulk strength of dry powders with narrow particle size distributions and narrow size fractions of particulate materials with wide particle size distributions. The next questions to answer are:

- What if the flow function of a full and wide particle size distribution (PSD) is used to make predictions with the model, would it be possible to predict the bulk strength of size fractions of a powder just measuring the full PSD?
- What size is required to be tested to predict the bulk strength of full and wide particle size distributions?
- Once a wide particle size distribution has been measured, would it be possible to predict other full PSD of the same powder?
- Is the constant value of the parameter A of the model valid for other particulate materials?

To answer these questions, it requires further work applying the model to a wide range of powders and making predictions based on the flow function of the particulate materials.

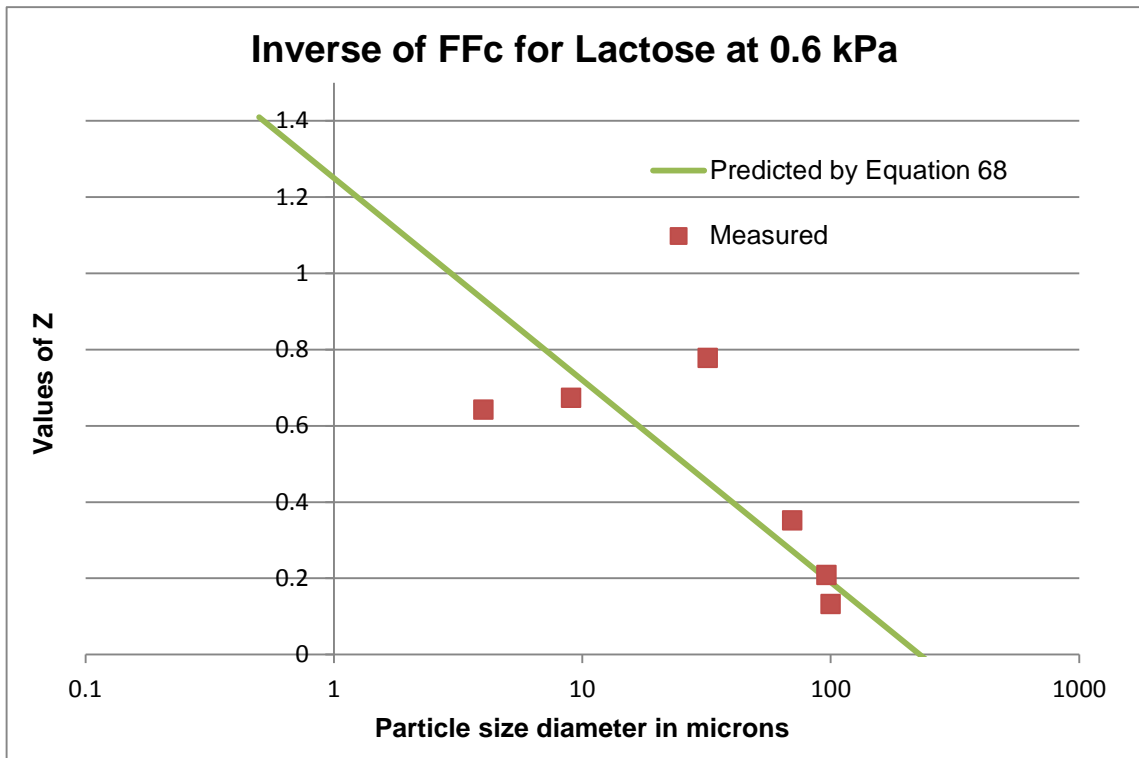


Figure 116: Comparison of the predicted and measured values of inverse flow factor ratio for lactose at 0.6 kPa

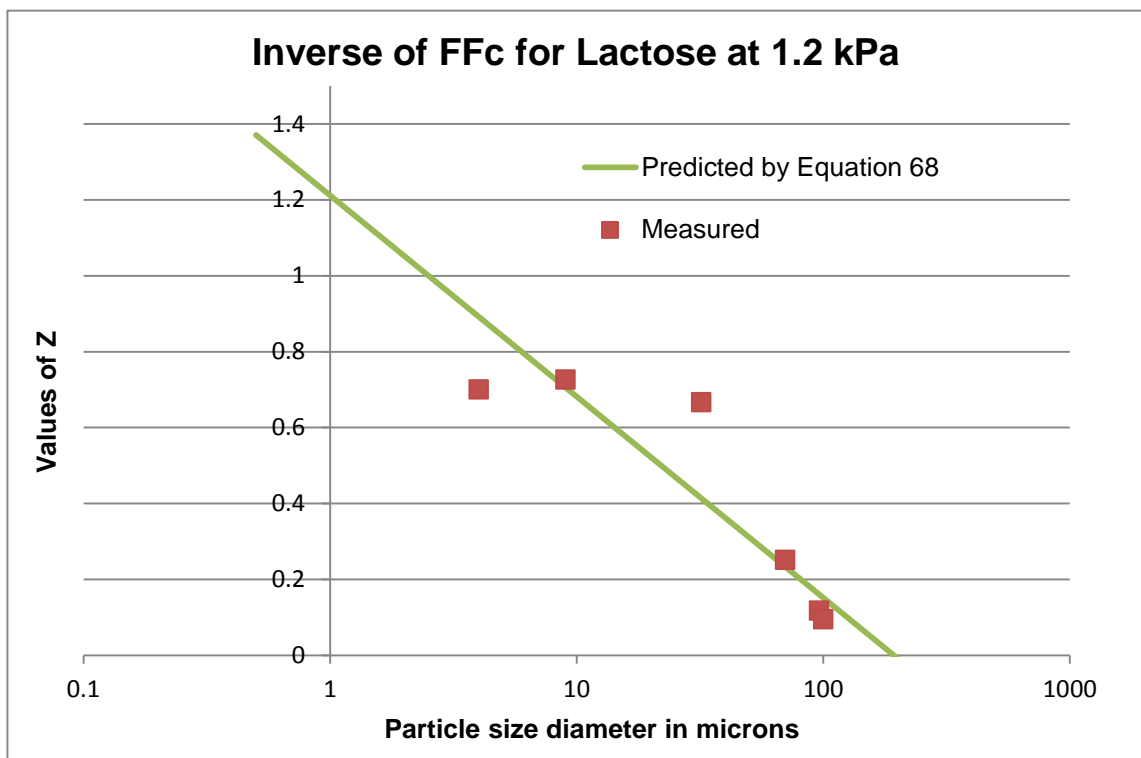


Figure 117: Comparison of the predicted and measured values of inverse flow factor ratio for lactose at 1.2 kPa

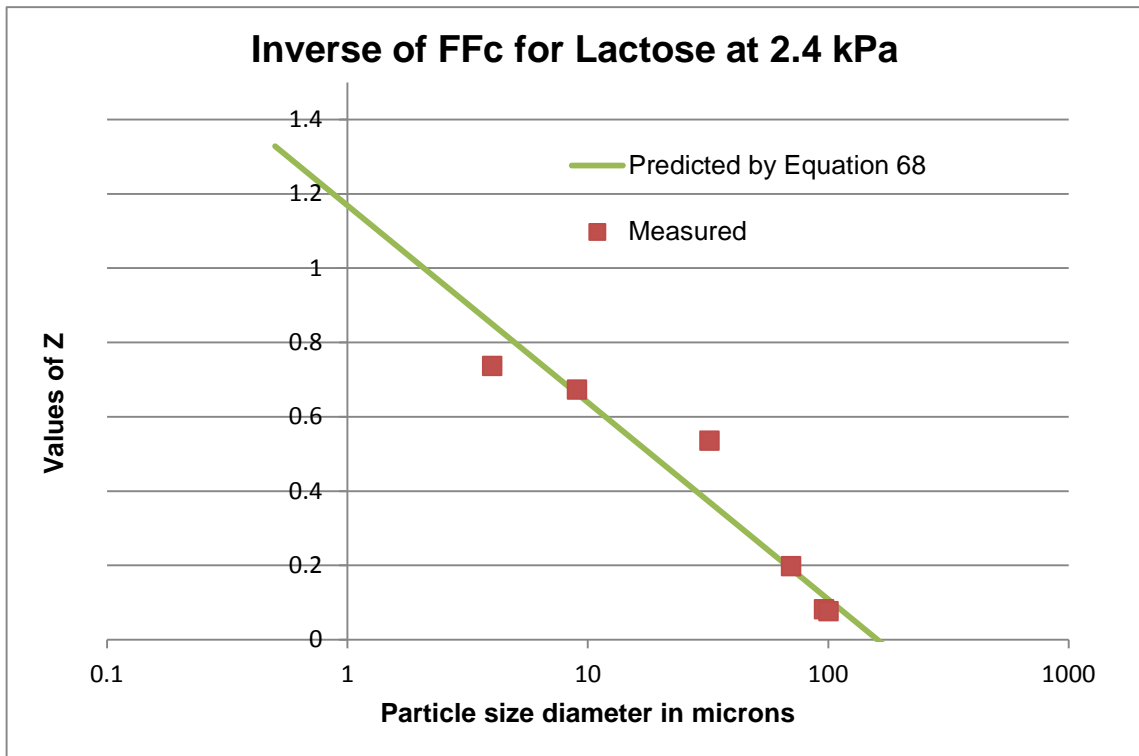


Figure 118: Comparison of the predicted and measured values of inverse flow factor ratio for lactose at 2.4 kPa

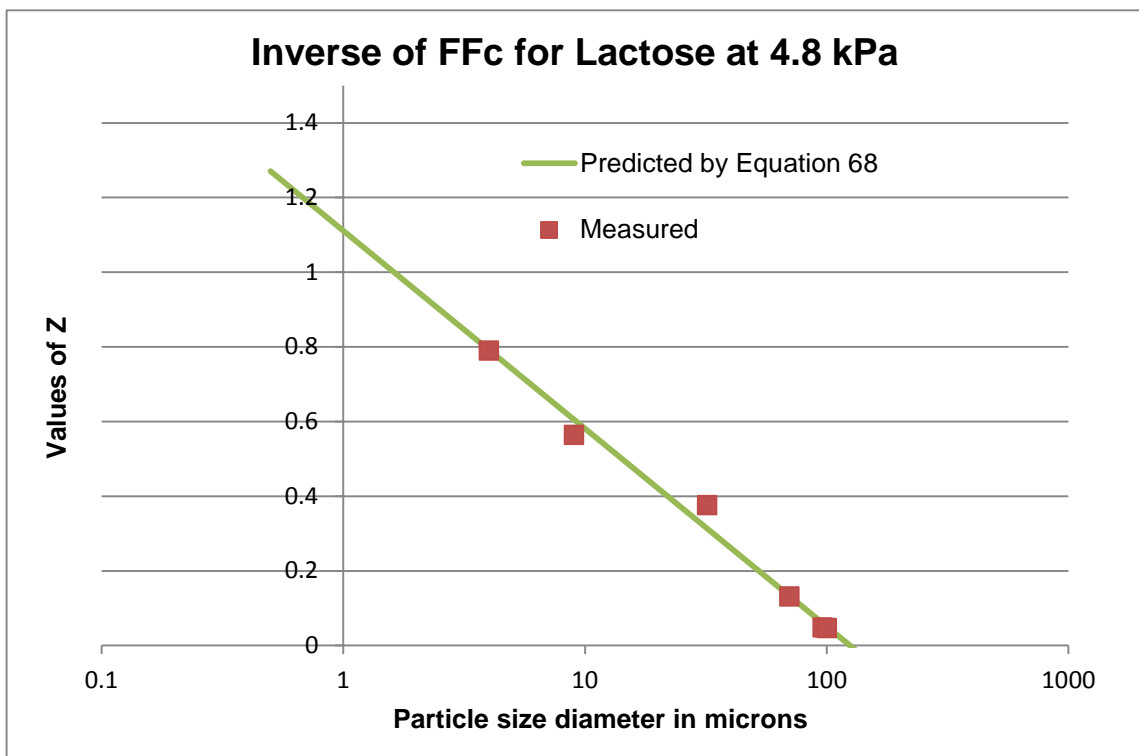


Figure 119: Comparison of the predicted and measured values of inverse flow factor ratio for lactose at 4.8 kPa

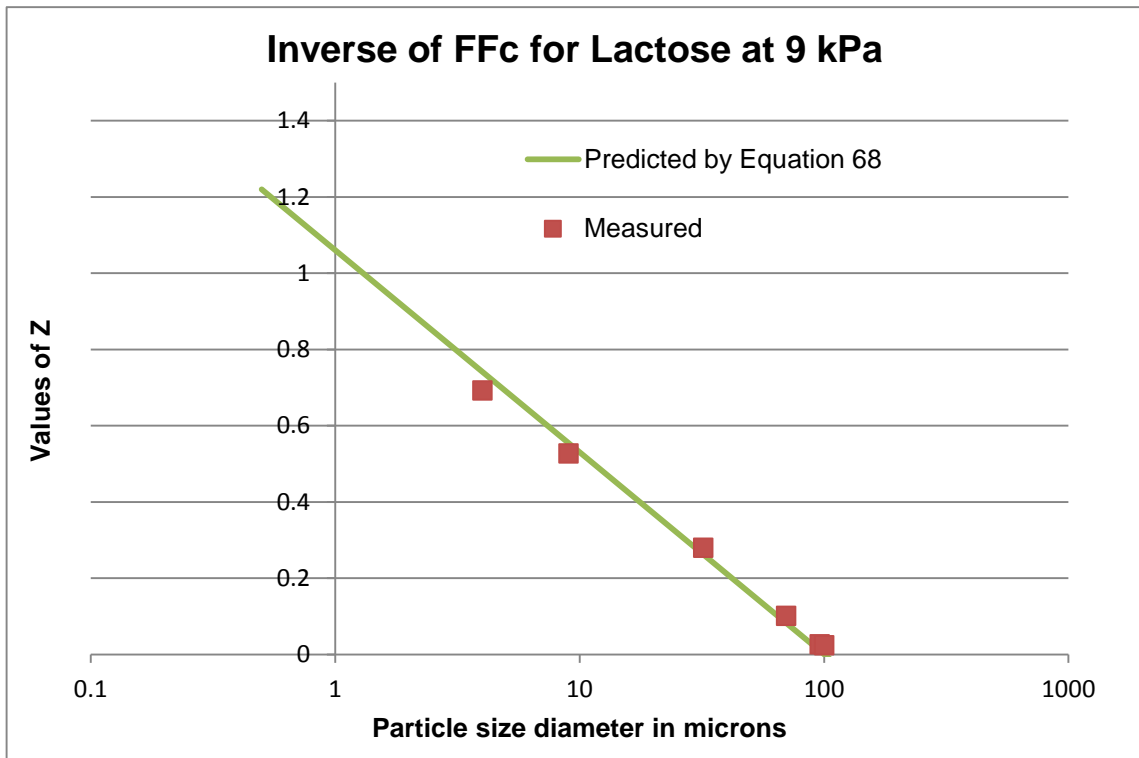


Figure 120: Comparison of the predicted and measured values of inverse flow factor ratio for lactose at 9 kPa

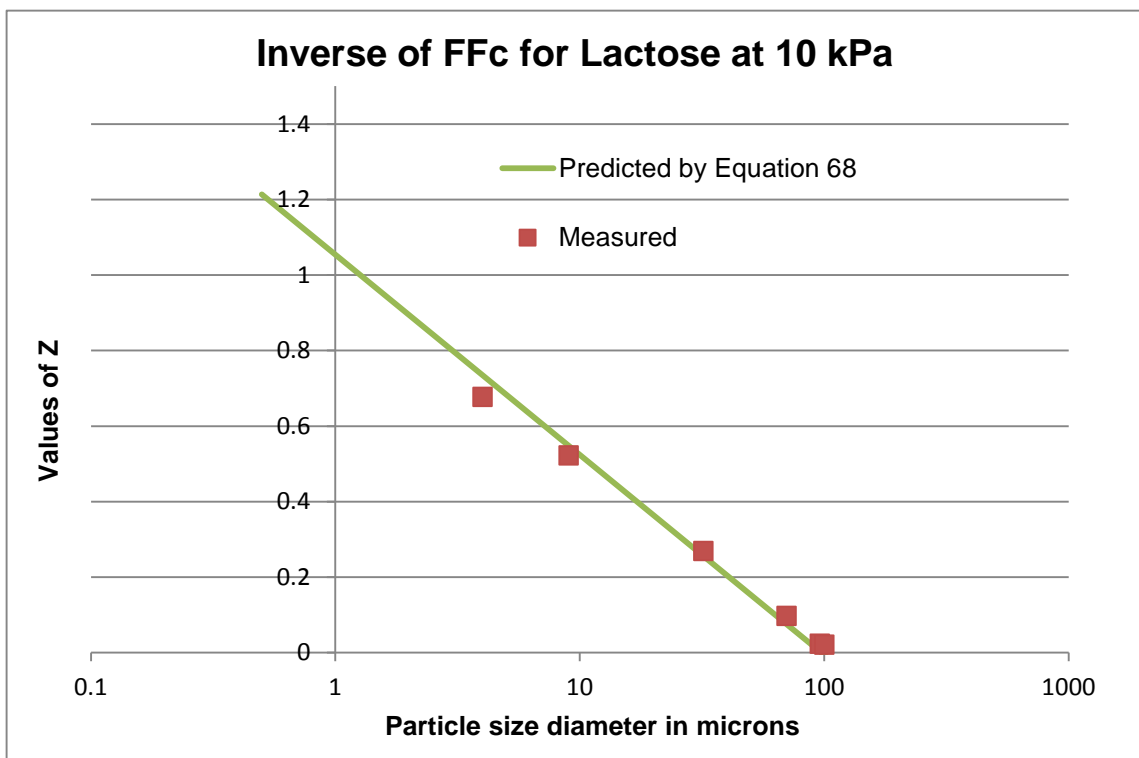


Figure 121: Comparison of the predicted and measured values of inverse flow factor ratio for lactose at 10 kPa

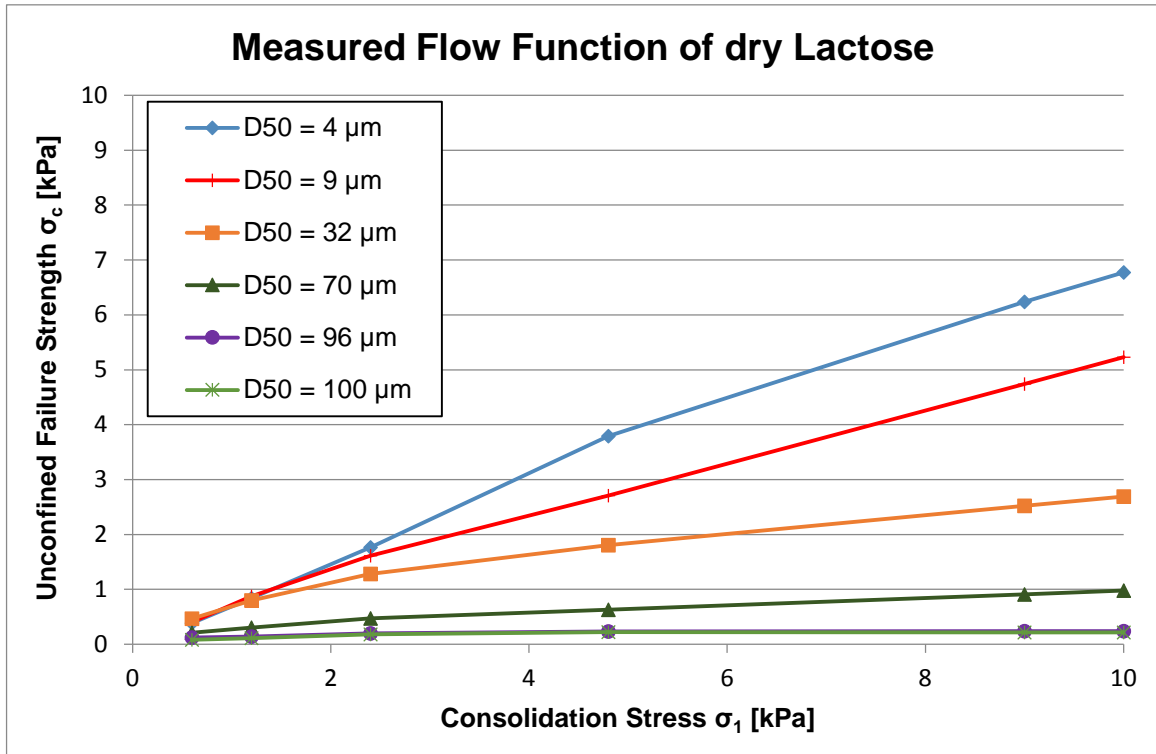


Figure 122: Measured flow function values of six grades of lactose

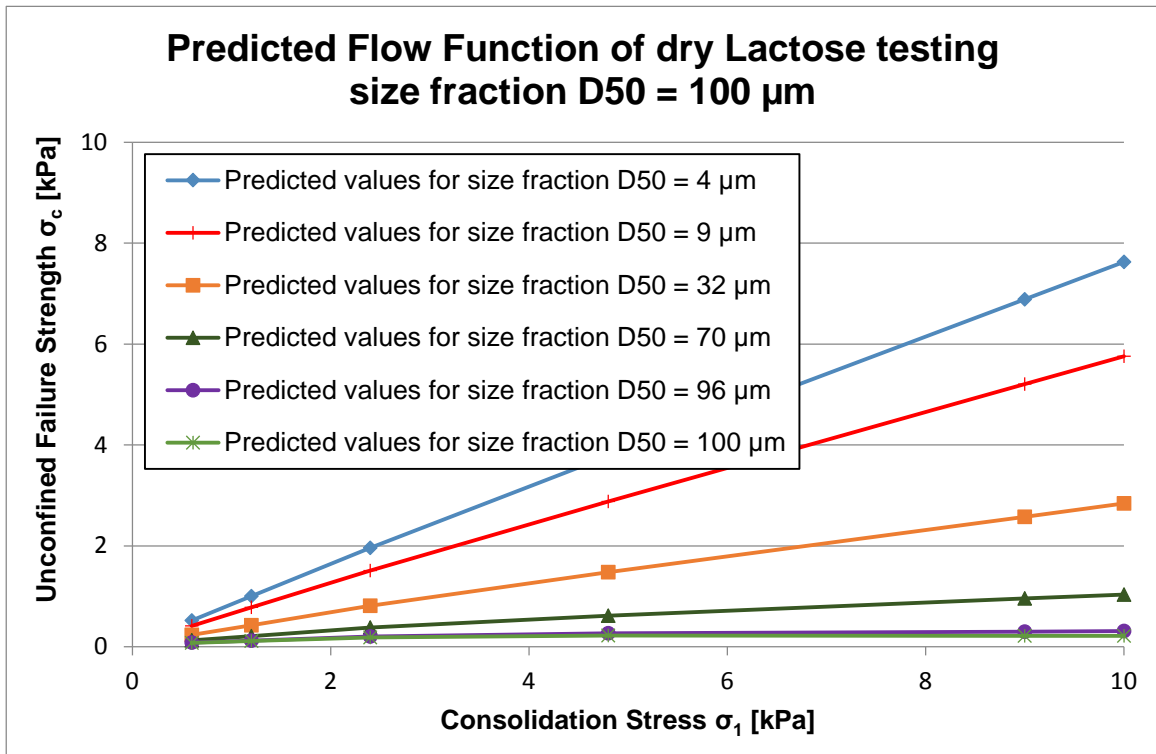


Figure 123: Predicted flow function values of six grades of lactose

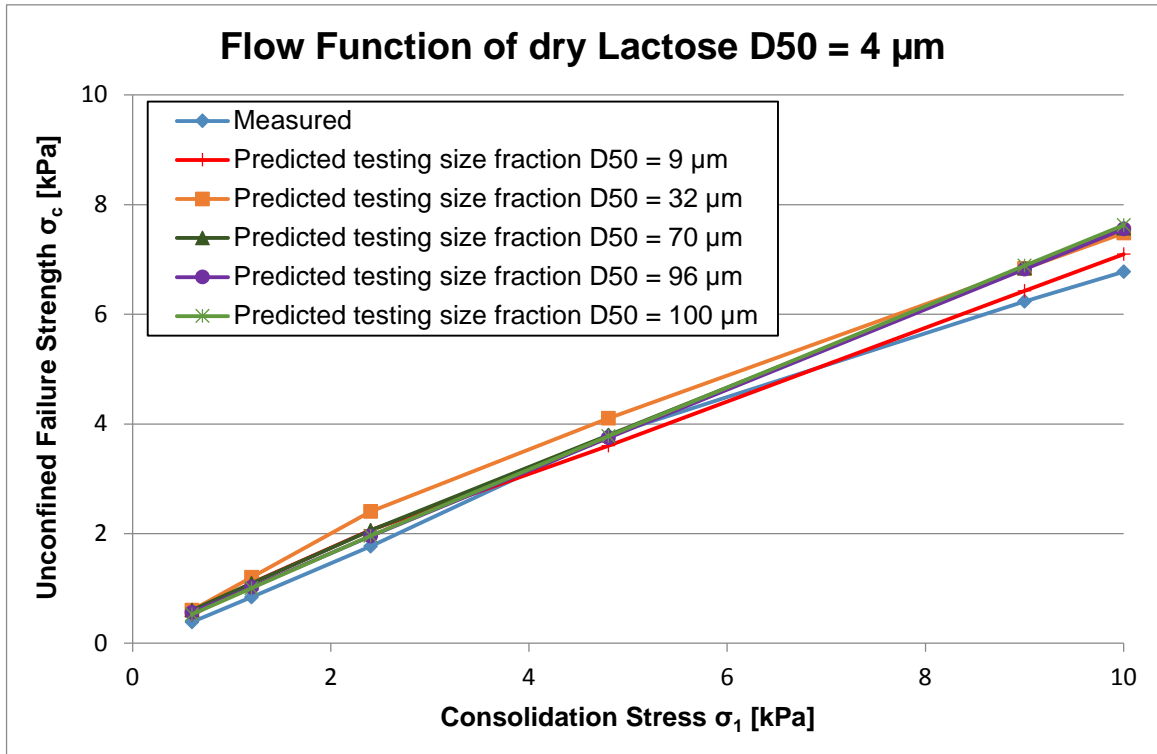


Figure 124: Predicted flow function values of a grade of lactose D50 = 4 μm

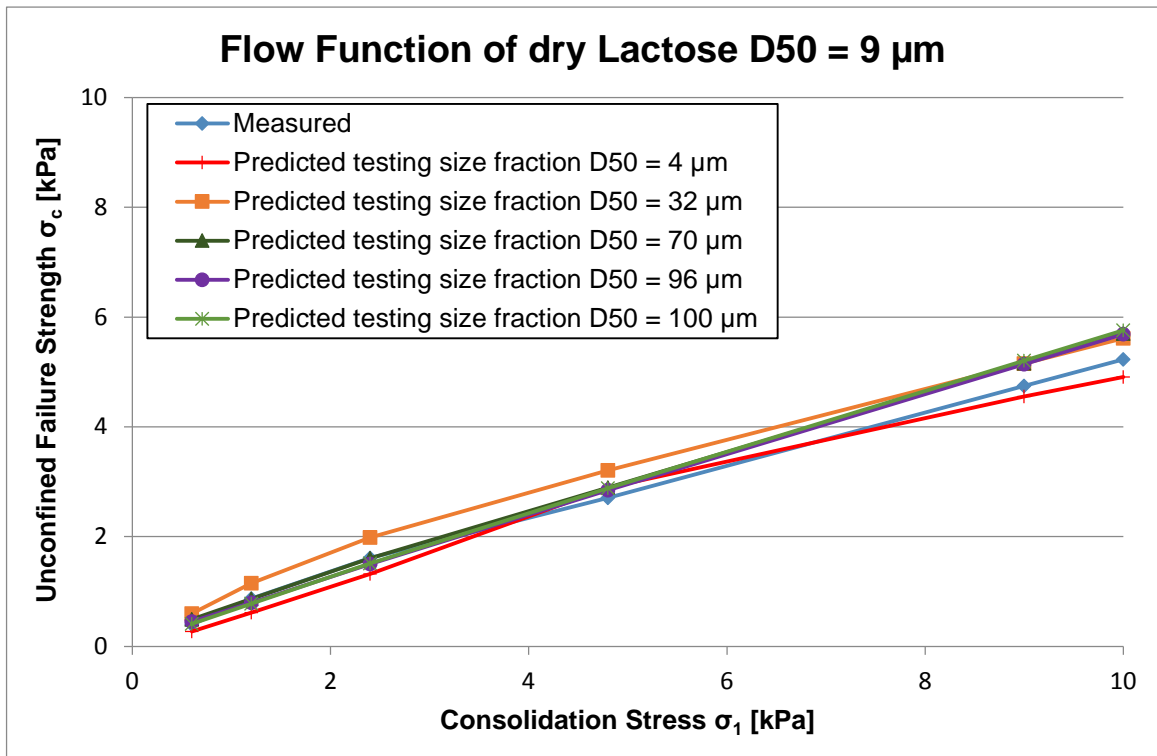


Figure 125: Predicted flow function values of a grade of lactose D50 = 9 μm

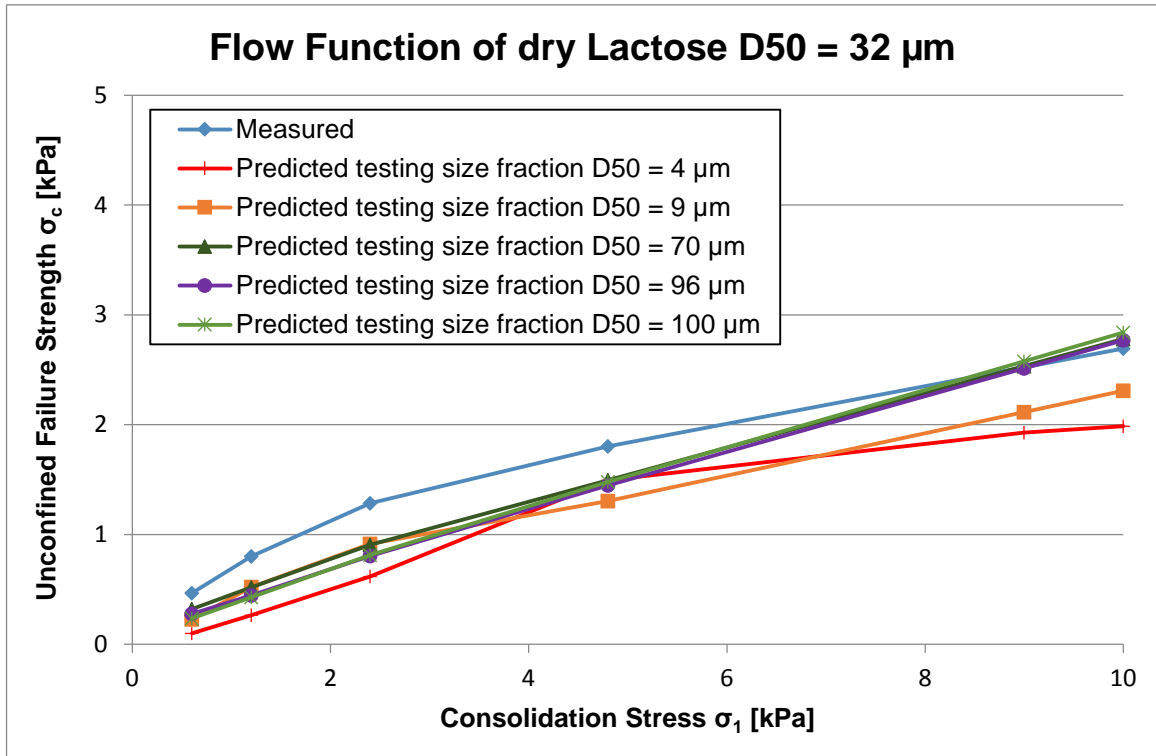


Figure 126: Predicted flow function values of a grade of lactose D50 = 32 μm

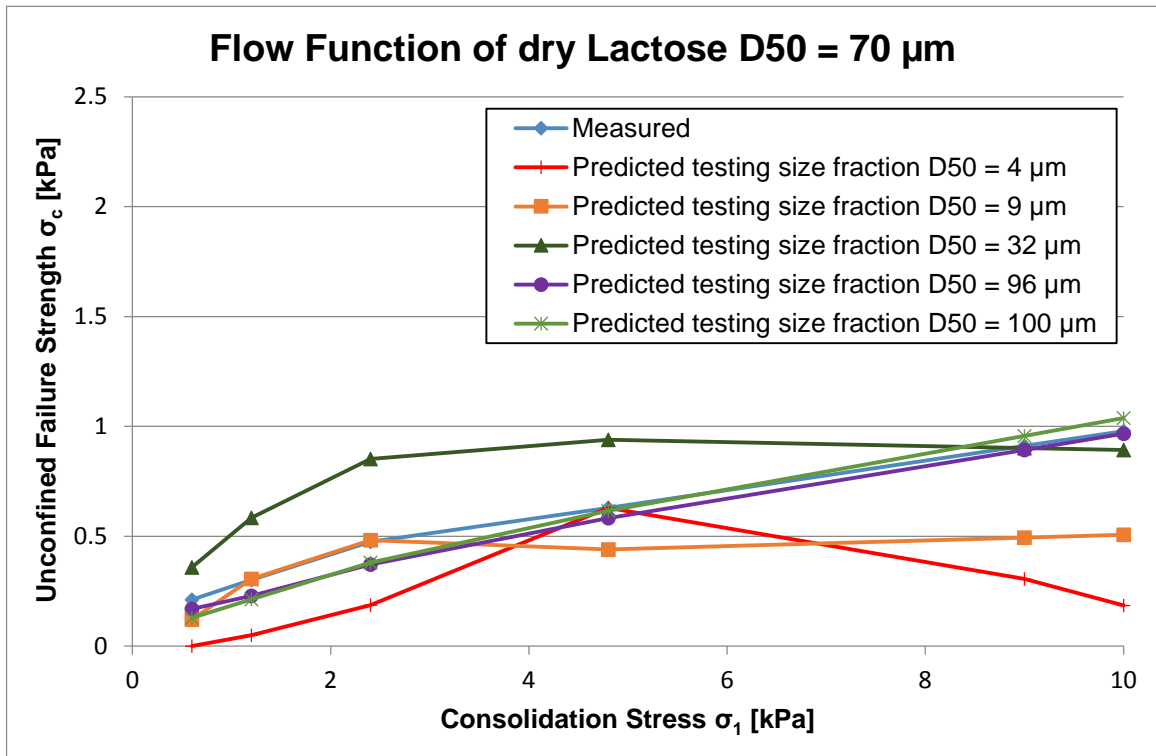


Figure 127: Predicted flow function values of a grade of lactose D50 = 70 μm

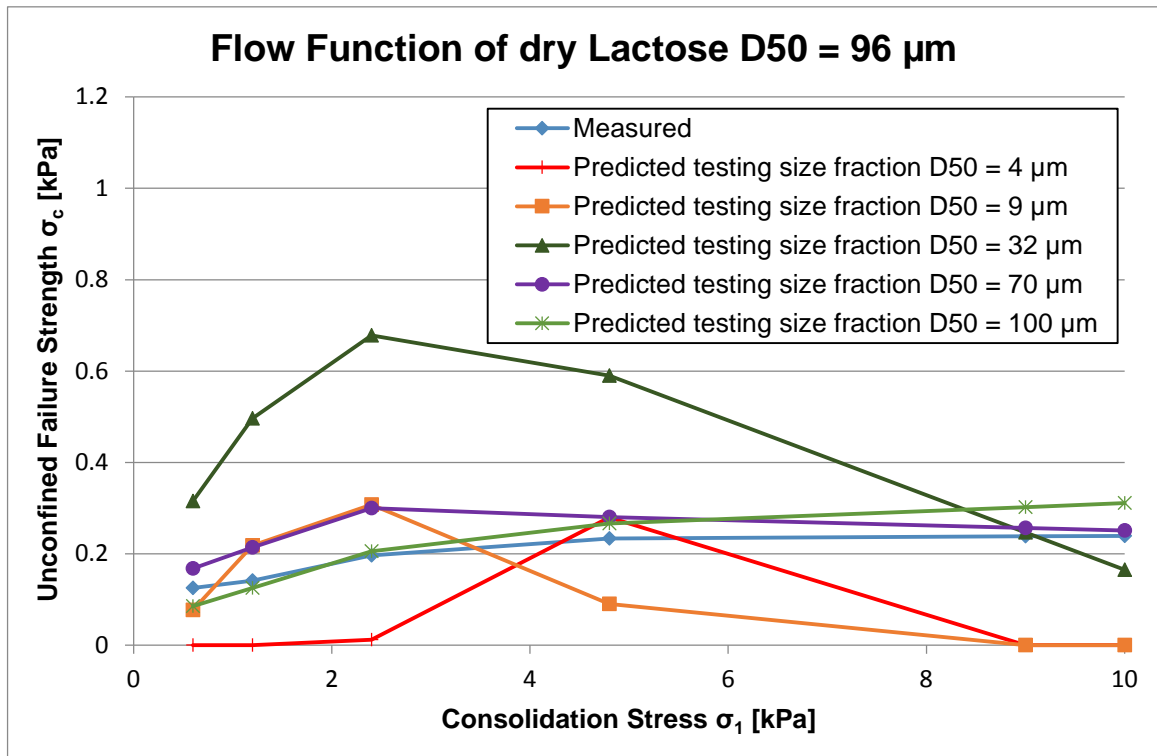


Figure 128: Predicted flow function values of a grade of lactose D50 = 96 μm

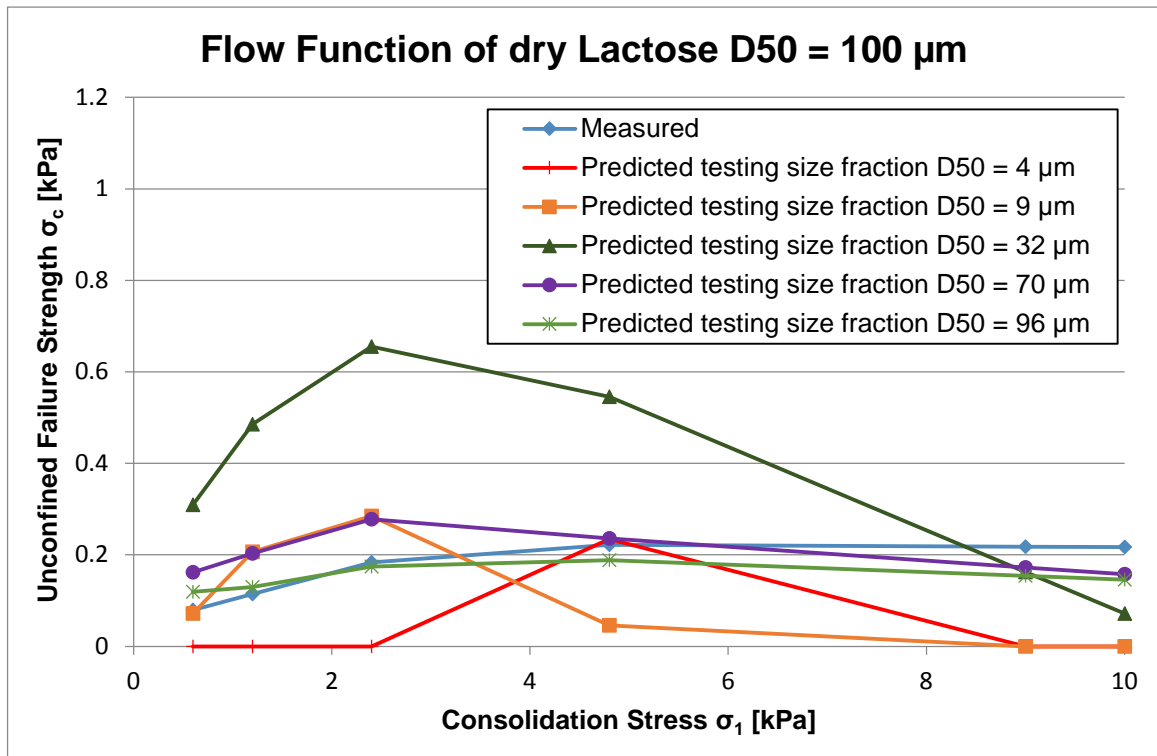


Figure 129: Predicted flow function values of a grade of lactose D50 = 100 μm

In order to keep developing the model, the value of Z was made equal to zero in the equation 69; then the value of the parameter C can be calculated as a function of the interception particle size in the x-axis (D_0) which is characteristic for each powder at

the consolidations stresses selected. Plotting the values of D_o and C against the values of consolidation stresses respectively gives the curves which represent the value of D_o and C at any value of consolidation stress for each powder. These curves (figures 130 and 131) give important correlations which are characteristic for each powder tested making the application of the model at different level of stresses more applicable to powder industry because less amount of tests would be required to predict the bulk strength of the dry particulate materials.

$$Z = C - A \cdot \log D = 0 \quad \text{Equation 69}$$

$$C = A \cdot \log D_o \quad \text{Equation 70}$$

$$D_o = 10^{C/A} \quad \text{Equation 71}$$

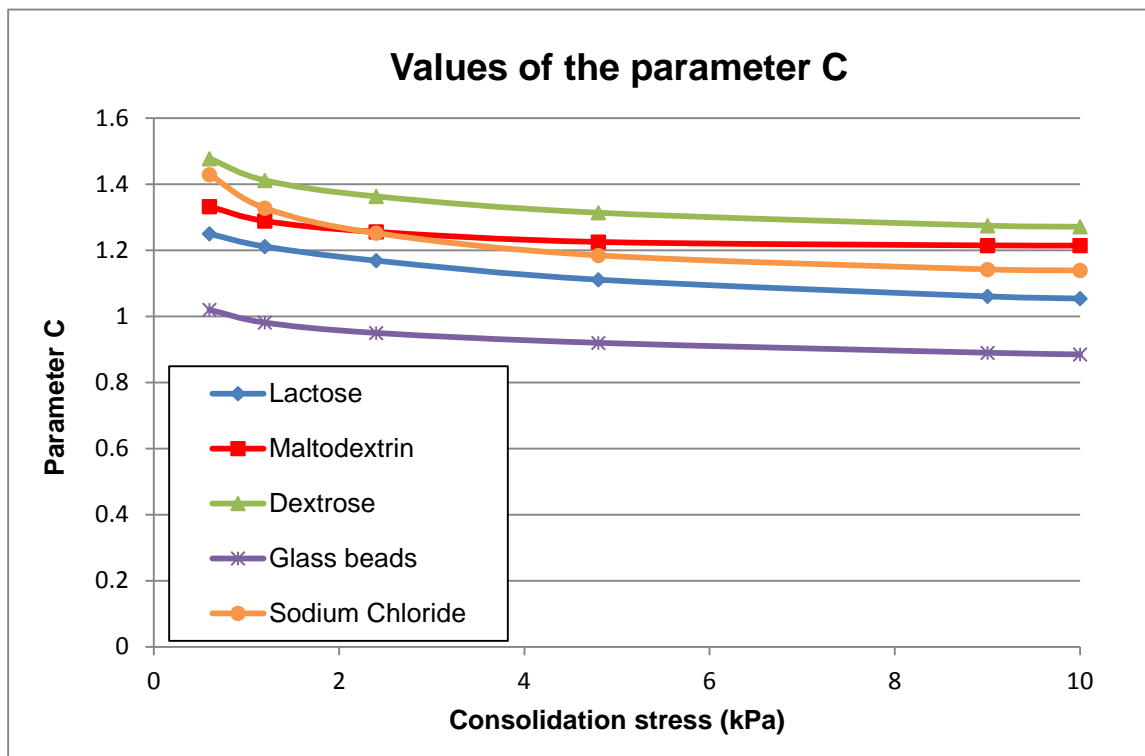


Figure 130: Values of the parameter C of the empirical model for dry single powders developed in the research

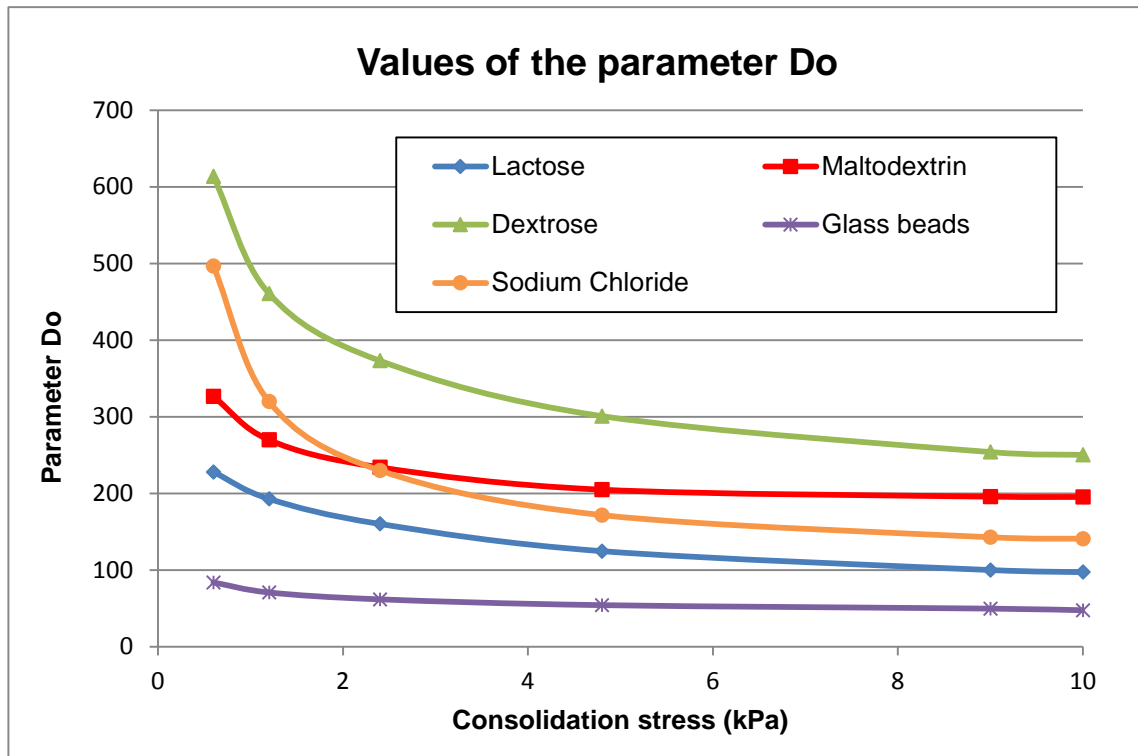


Figure 131: Values of the parameter C of the empirical model for dry single powders developed in the research

8.2.2 Effect of liquid content

As explained in the conclusions of the calibration of Rumpf model to predict the bulk strength of different grades of wet glass beads, calibrated Rumpf model failed to give good predictions of the unconfined failure strength for wet glass beads with particle size below $40\ \mu\text{m}$ and for this reason, it was necessary to develop an empirical fitting model of the measured values as an alternative approach to calibrated Rumpf model. Furthermore, empirical models were also developed to predict the bulk strength of wet particulate materials in the funicular and capillary states. These models were developed with the results obtained from the tests undertaken with idealised powders but these could be applied to real powders with non-spherical particles and wide particle size distributions as shown in chapter 8, section 8.2.3 below.

An empirical model was developed to predict the bulk strength of wet powders at 9 kPa of consolidation stress as a function of the medium particle size and the weight liquid content of the powder with the following equation:

$$\sigma_{CW} = \frac{Kc}{D^{0.667}} * Pd(\%wt)^{\frac{Kd}{D^{0.667}}} \quad \text{Equation 72}$$

Where

- σ_{CW} is the predicted bulk strength at 9 kPa of consolidation stress
- KC is a parameter of the model which value varies with the type of liquid being 52 for Miglyol oil and 29 for de-ionised water
- KD is a parameter of the model which value varies with the type of liquid being 2 for Miglyol oil and 4.5 for de-ionised water
- D is the medium particle size (D50) of the powder in microns
- Pd(%wt) is the weight percentage of liquid in the powder

The values of the parameters KC and KD shown in table 49 are valid for the two liquids added to glass beads tested in this research and therefore other liquids with different density, viscosity and surface tension values require further investigation; parameter KC is a straight multiplier and parameter KD affects the shape of the prediction curve.

Values of the parameter	Miglyol Oil 818 added	De-ionised water added
KC	52	29
KD	2	4.5

Table 49: Values of the parameters KC and KD of the empirical model for wet powders developed in this research

This model can be applied for the pendular, funicular and capillary stated as shown in figures 133 – 141 below. Predictions made with this model have been compared with the predictions made with the calibrated Rumpf model and the measured values presented in the chapter 6. The bulk strength data has been plotted against different weight liquid percentages up to the saturation of the powder tested as shown in figures 133 – 141 below.

Meanwhile, another empirical model was developed for the funicular and capillary regimes of liquid content to complete the predictions made with the calibrated Rumpf model which is limited to the pendular state. The equation of the model is as follows:

$$\sigma_c = A * e^{0.017 * Pd(\%wt)} \quad \text{Equation 73}$$

Where:

- σ_c is the predicted bulk strength at 9 kPa of consolidation stress
- A is a parameter of the empirical model which is function of the medium particle size and the type of liquid added to the powder
- Pd(%wt) is the weight percentage of liquid in the powder

Table 50 and figure 132 show the values of the parameter A of the model as a function of the particle size of glass beads tested in this study. These values have been calculated using a least square best fit curve to minimise the error in the predictions. A correlation between the values of the parameter A of the model and the particle size of the size fractions of glass beads was found as shown in figure 132.

Values of the parameter A	Miglyol Oil 818 added	De-ionised water added
D50 = 33 μm	4.8	6.2
D50 = 63 μm	2.8	4.2
D50 = 112 μm	1.7	2.7
D50 = 212 μm	1.2	1.9

Table 50: Value of the parameter A of the empirical model for wet powders in funicular and capillary states

Results of the comparison between the measured values and the predicted values obtained from the empirical fitting models and the calibrated Rumpf model are shown in figures 133 - 141. For glass beads with particle size below 40 μm (figures 140 and 141), empirical fitting model shows a good agreement with the experimental data. The predictions made with the calibrated Rumpf model and the empirical model developed for funicular and capillary states fit reasonably well with the measured values for size fractions with particle size above 40 μm . However, predictions of the empirical model

developed for pendular, funicular and capillary states show no agreement with experimental data for size fractions of glass beads blended with de-ionised water.

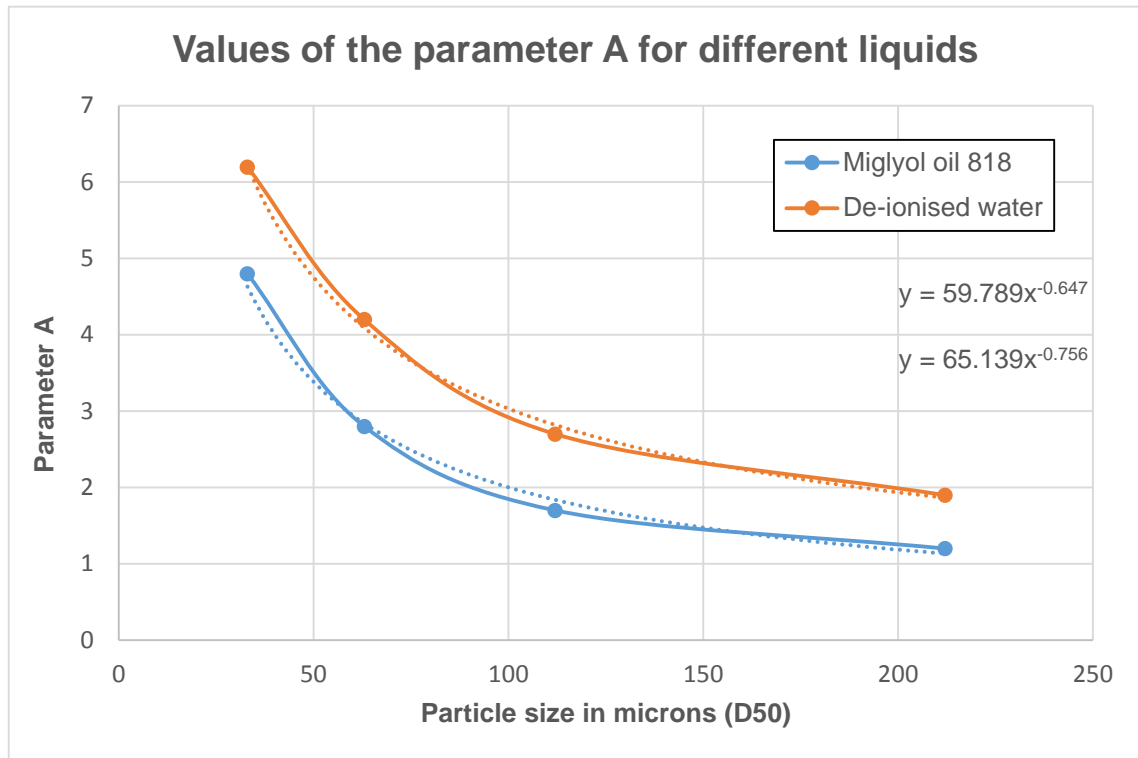


Figure 132: Value of the parameter A of the empirical model for wet powders in funicular and capillary states for de-ionised water and Miglyol oil 818

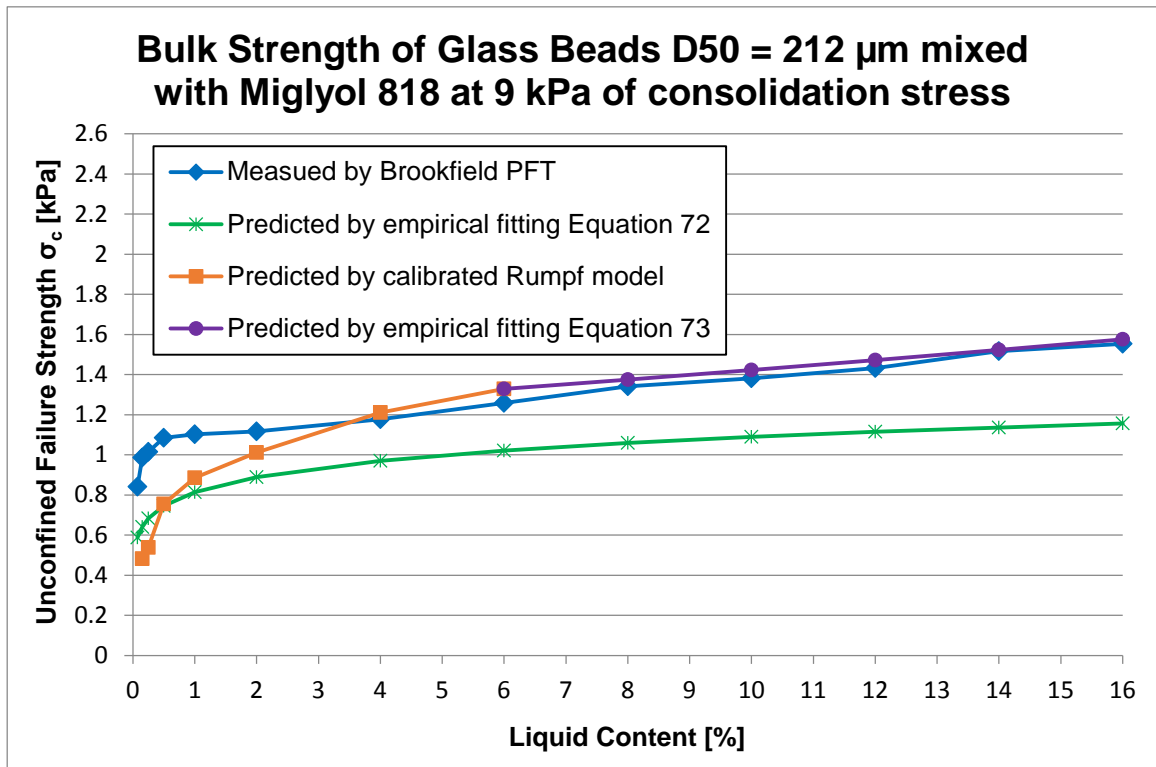


Figure 133: Comparison of the measured and predicted values of the bulk strength of glass beads D50 = 212 μm mixed with Miglyol oil 818

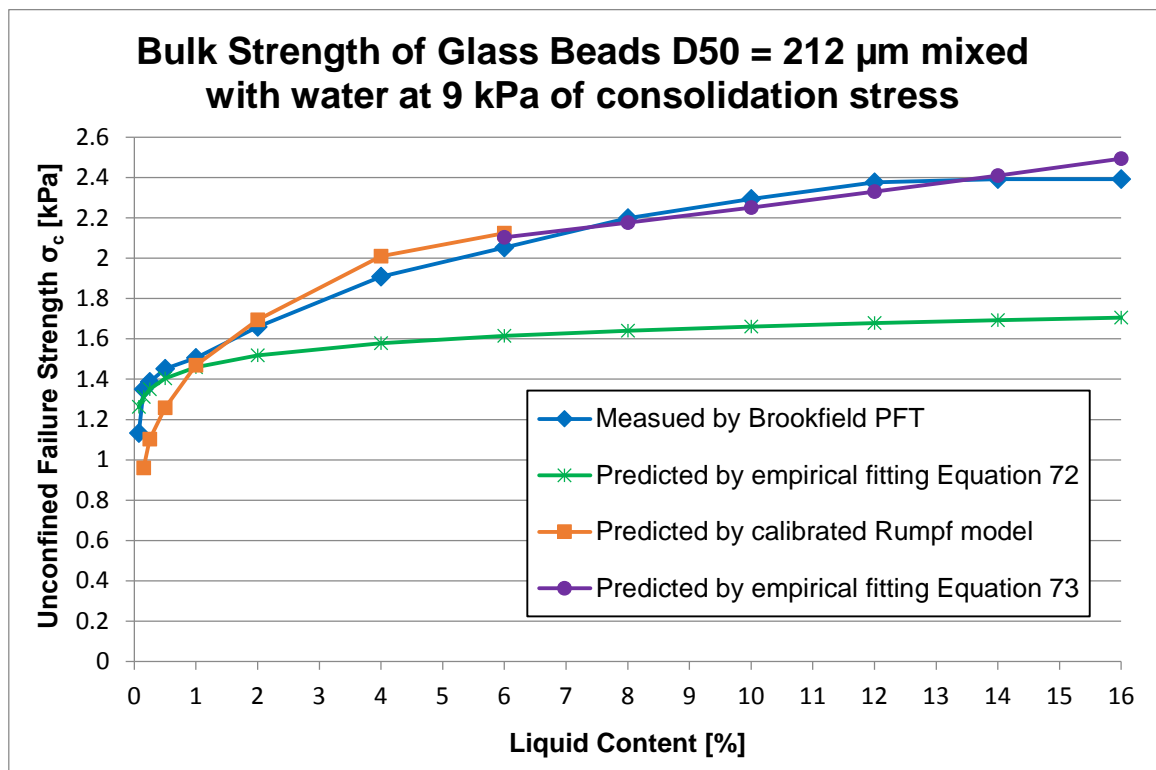


Figure 134: Comparison of the measured and predicted values of the bulk strength of glass beads D50 = 212 μm mixed with de-ionised water

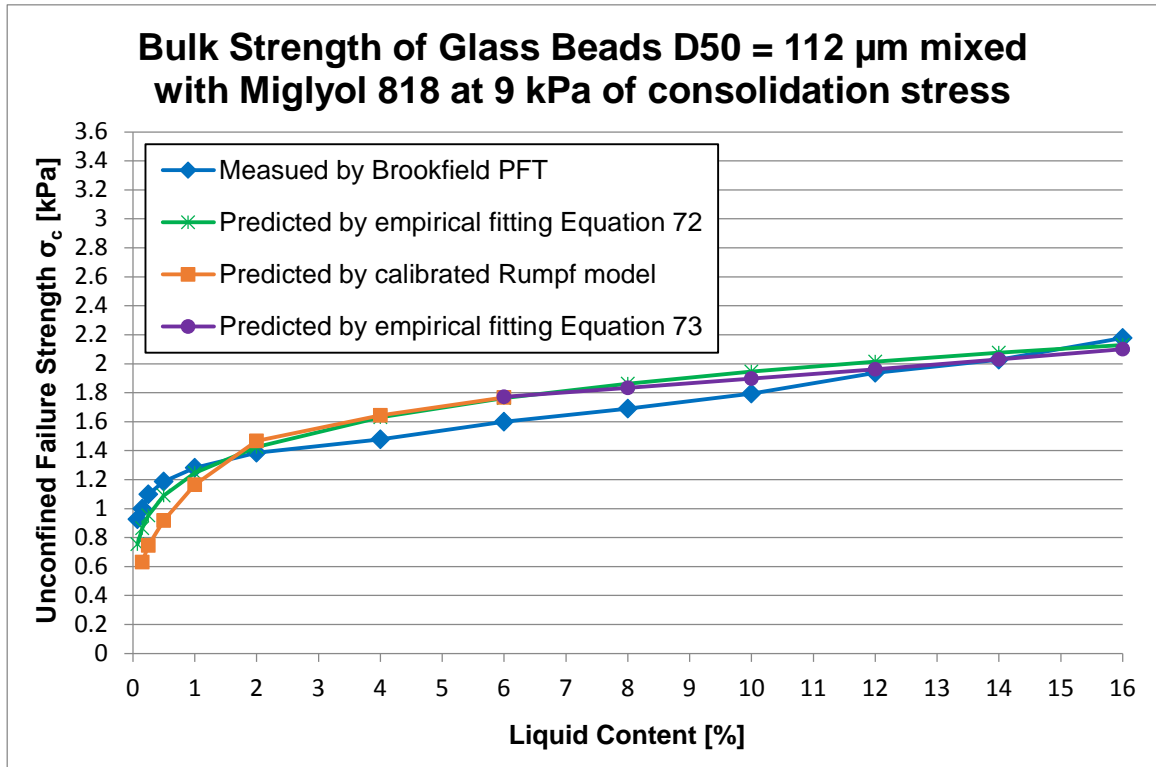


Figure 135: Comparison of the measured and predicted values of the bulk strength of glass beads D50 = 112 μm mixed with Miglyol oil 818

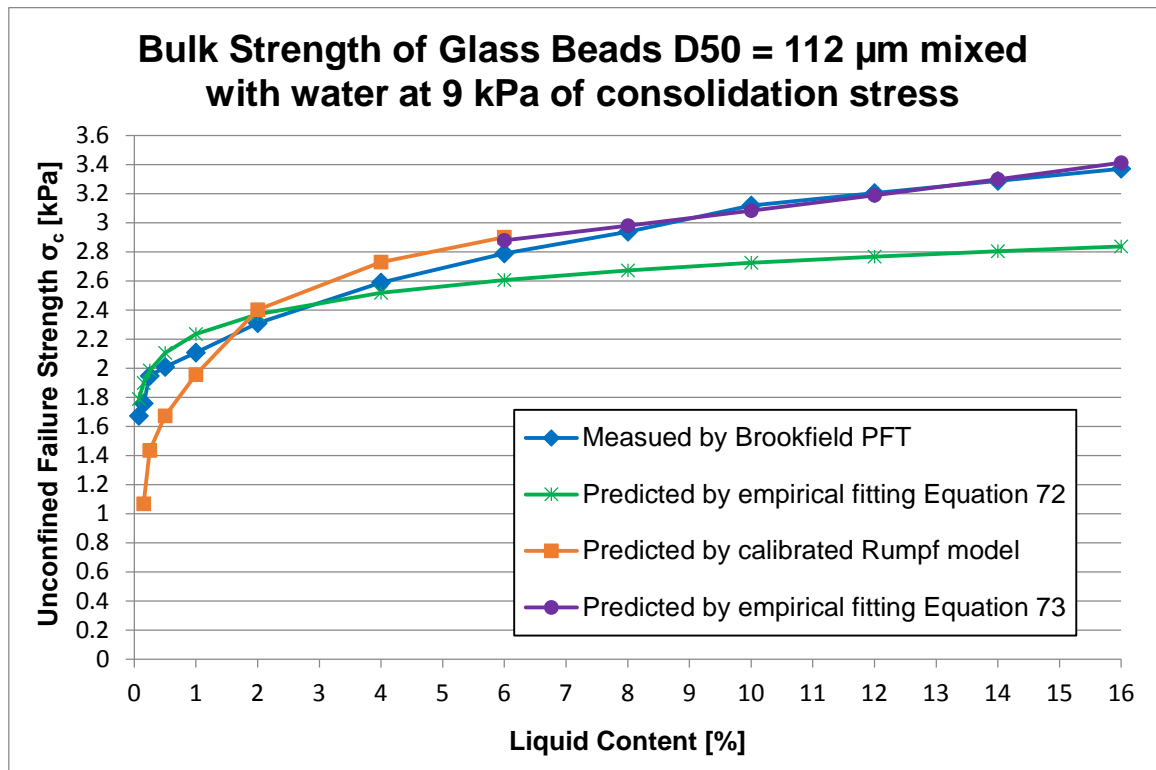


Figure 136: Comparison of the measured and predicted values of the bulk strength of glass beads D50 = 112 μm mixed with de-ionised water

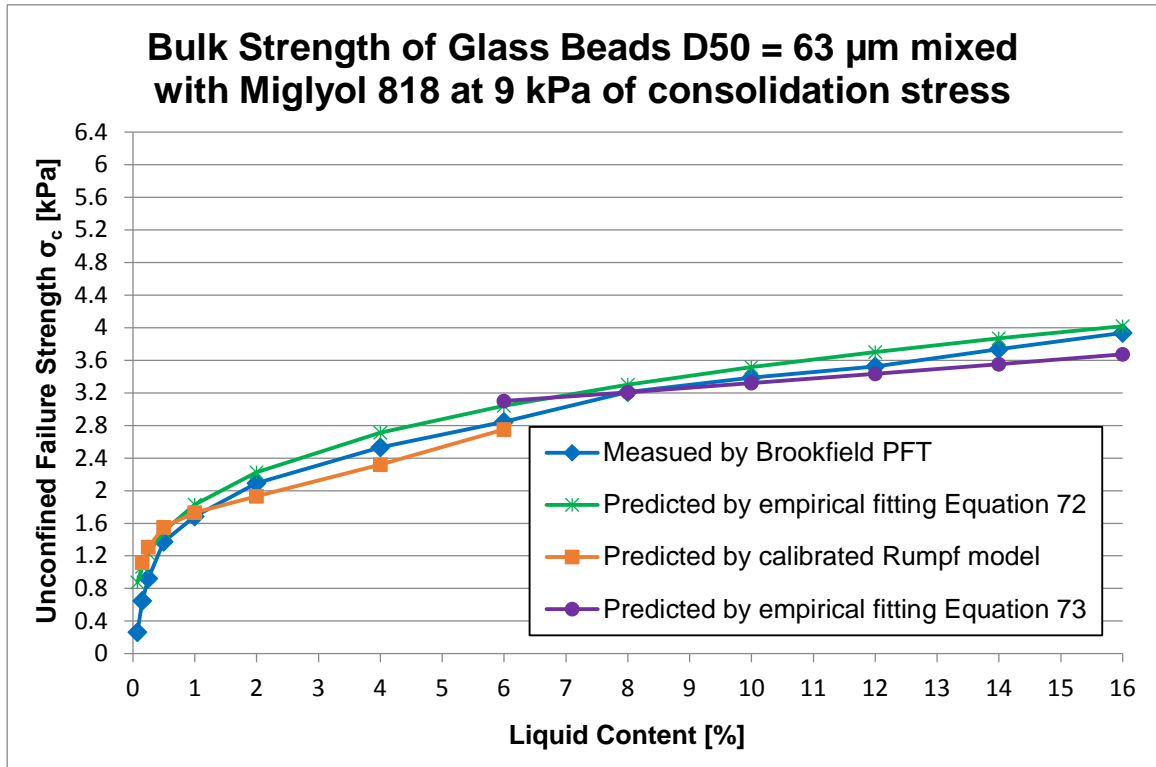


Figure 137: Comparison of the measured and predicted values of the bulk strength of glass beads D50 = 63 μ m mixed with Miglyol oil 818

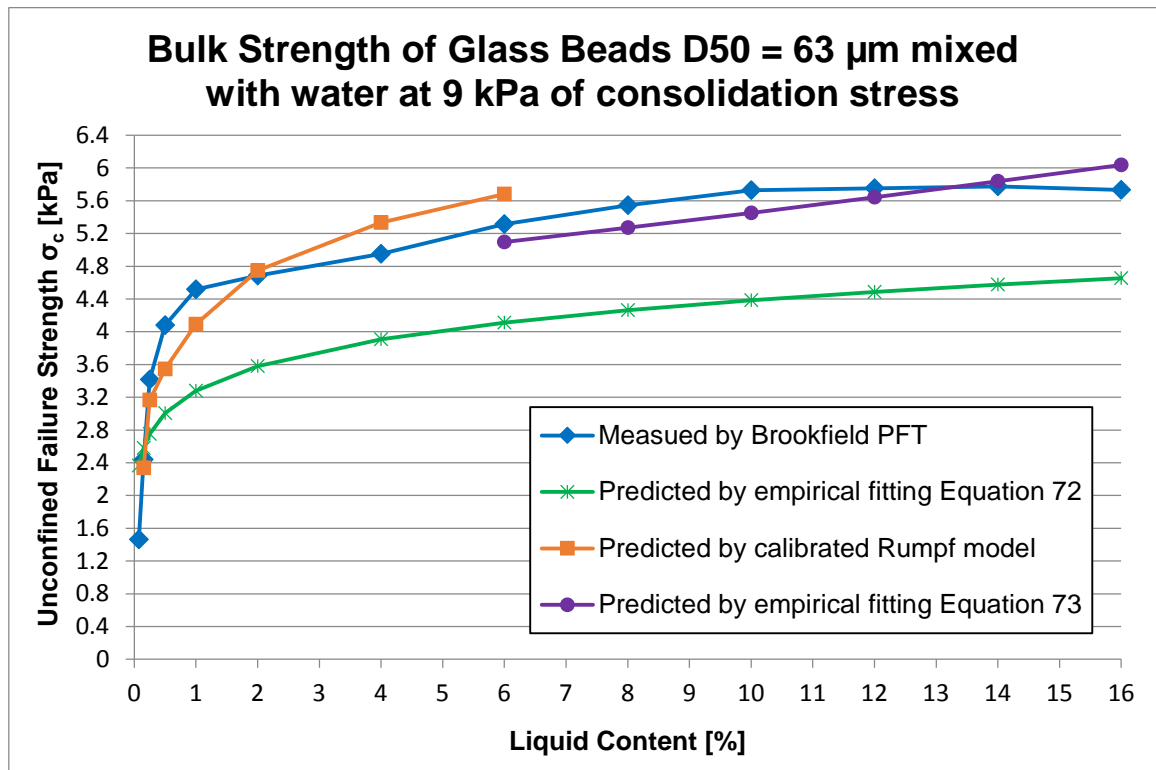


Figure 138: Comparison of the measured and predicted values of the bulk strength of glass beads D50 = 63 μ m mixed with de-ionised water

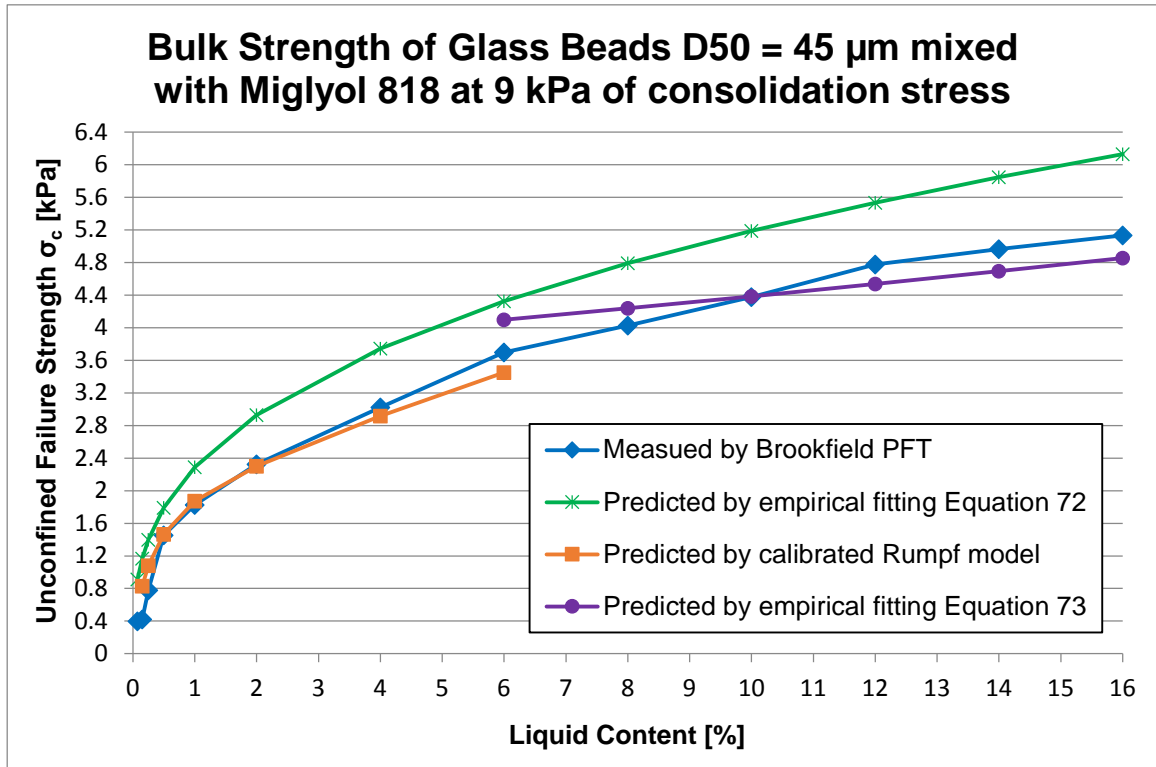


Figure 139: Comparison of the measured and predicted values of the bulk strength of glass beads D50 = 45 μm mixed with Miglyol oil 818

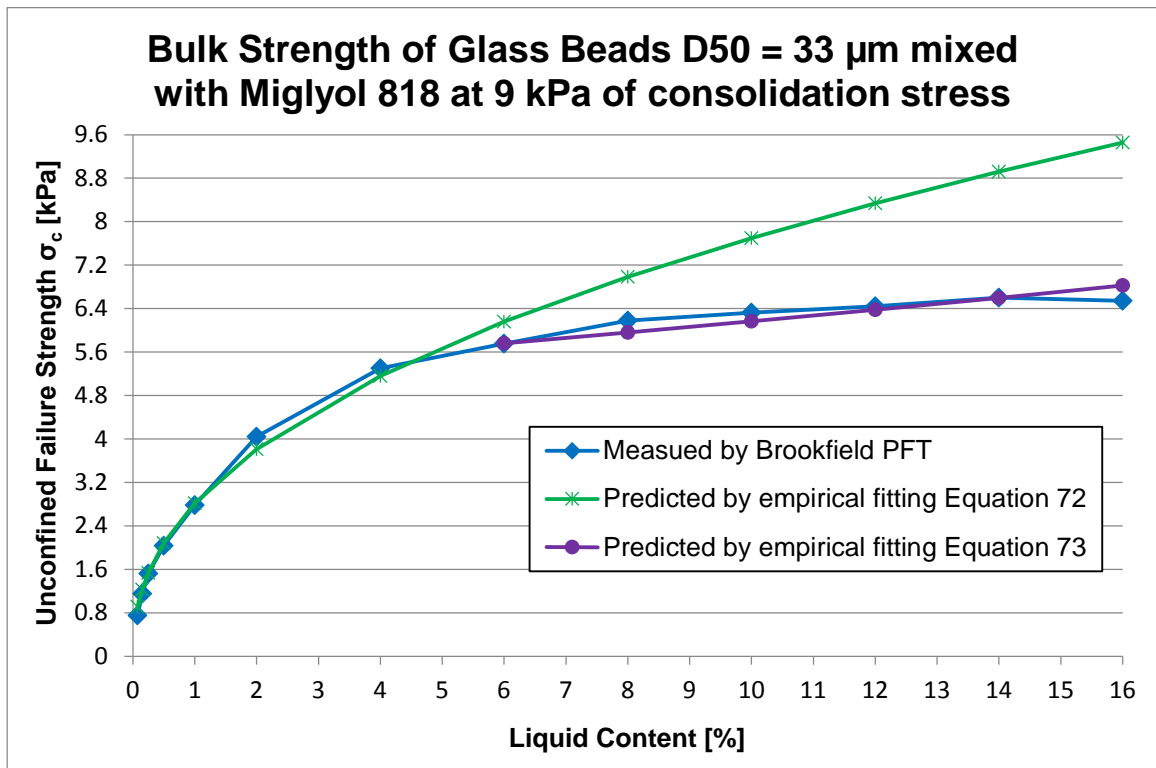


Figure 140: Comparison of the measured and predicted values of the bulk strength of glass beads D50 = 33 μm mixed with Miglyol oil 818

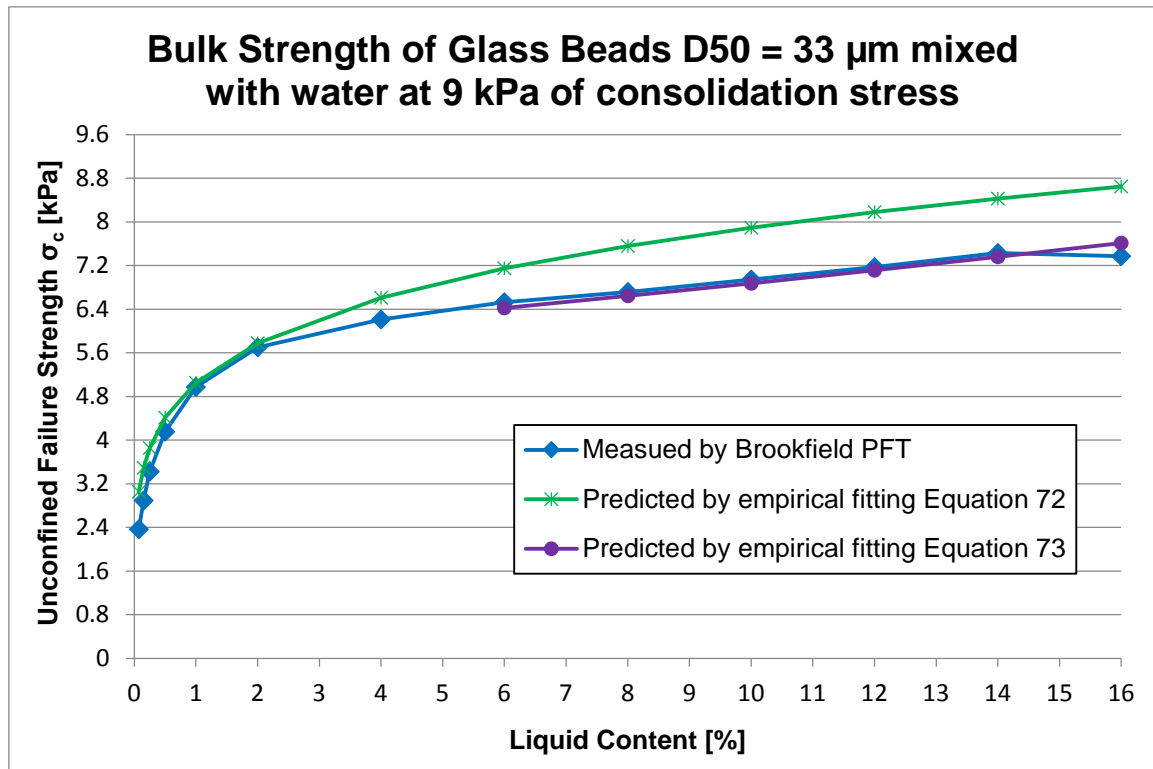


Figure 141: Comparison of the measured and predicted values of the bulk strength of glass beads D50 = 33 μm mixed with de-ionised water

In order to apply these models to real particulate materials, the effect of different particle density was considered by correcting the prediction of the strength for the change in volume. For the same volumetric proportion of liquid (the same level of saturation), if the particles are lighter, their mass will be lower in direct proportion. The same condition will occur in terms of saturation, showing higher percentage of liquid if the particles are lighter because with the same weight percentage, the same volume of liquid is a bigger proportion of the lighter particles.

Considering the particle density of glass beads as a reference, if the particle density of a powder is half the reference particle density of glass beads (2600 Kg/m³), then 2%wt Miglyol oil 818 in this powder is equal to 1%wt Miglyol oil 818 for glass beads in terms of saturation. To calculate the equivalent bulk strength for glass beads, the weight liquid percentage of a powder is multiplied by a factor as a function of the particle density of the powder. This factor is defined as the particle density of the powder divided to the particle density of glass beads. Then the reduced liquid content calculated is used to predict the bulk strength using the empirical models developed with the data obtained from glass beads tested.

$$GB(\%wt) = Pd(\%wt) * \frac{\rho_{Pd}}{\rho_{GB}} \quad \text{Equation 74}$$

Where:

- GB (%wt) is the equivalent weight percentage of liquid in glass beads
- Pd (%wt) is the weight percentage of liquid in the powder
- ρ_{Pd} is the particle density of the powder
- ρ_{GB} is the particle density of glass beads

As an example, if the density of a powder is 2160 Kg/m³ and the liquid content of the powder is 1%wt, then the equivalent liquid content for the model is equal to 0.83%wt as shown in the following calculation:

$$(2160 / 2600) \times 1\%wt = 0.83\%wt \quad \text{Equation 75}$$

The models developed are based on calculations at 9 kPa of consolidation stress; the gain in strength for lower consolidation stresses can be predicted by proportion of the values predicted at 9 kPa. As shown in the results obtained for glass beads mixed with Miglyol oil and de-ionised water, flow functions of the wet powders top up at high consolidation stress such as 9-10 kPa and therefore an exponential approach can be used to predict the flow functions of wet powders. An exponential model has been developed which predicts the shape of the flow function curves of wet powders based on the values calculated at 9 kPa of consolidation stress with the following equation:

$$\sigma_{cp}(at \sigma_{1p}) = 1.044 * \sigma_{cmax} * \left(1 - e^{-\sigma_{1p}/\tau}\right) \quad \text{Equation 76}$$

Where:

- σ_{cp} is the predicted bulk strength at the consolidation stress selected σ_{1p}
- σ_{cmax} is the bulk strength at 9 kPa of consolidation stress
- σ_{1p} is the consolidation stress selected to predict the bulk strength
- τ is a constant value which is a function of the particle size of the powder and type of liquid added to the powder

Table 51 shows the values of the constant τ as a function of the particle size of glass beads tested in this study. These values have been calculated using a least square best fit curve to minimise the error in the predictions.

Values of the constant τ	Miglyol Oil 818 added	De-ionised water added
D50 = 33 μm	5.4	5.4
D50 = 63 μm	4.6	4.6
D50 = 112 μm	2.85	2.85
D50 = 212 μm	2.85	2.85

Table 51: Values of the constant tau of the empirical model developed in this research

Figures 142 and 143 show the results obtained from the application of these empirical models to real particulate materials. The unconfined failure strength of two powders named lactose and maltodextrin with narrow and wide particle size distributions respectively was predicted. In both cases, these models under-predicted the bulk strength with a maximum deviation of 0.4 at 9 kPa consolidation stress in the easy flowing range of flowability. Particle and bulk flow properties of these two powders in dry condition are presented in chapter 3.

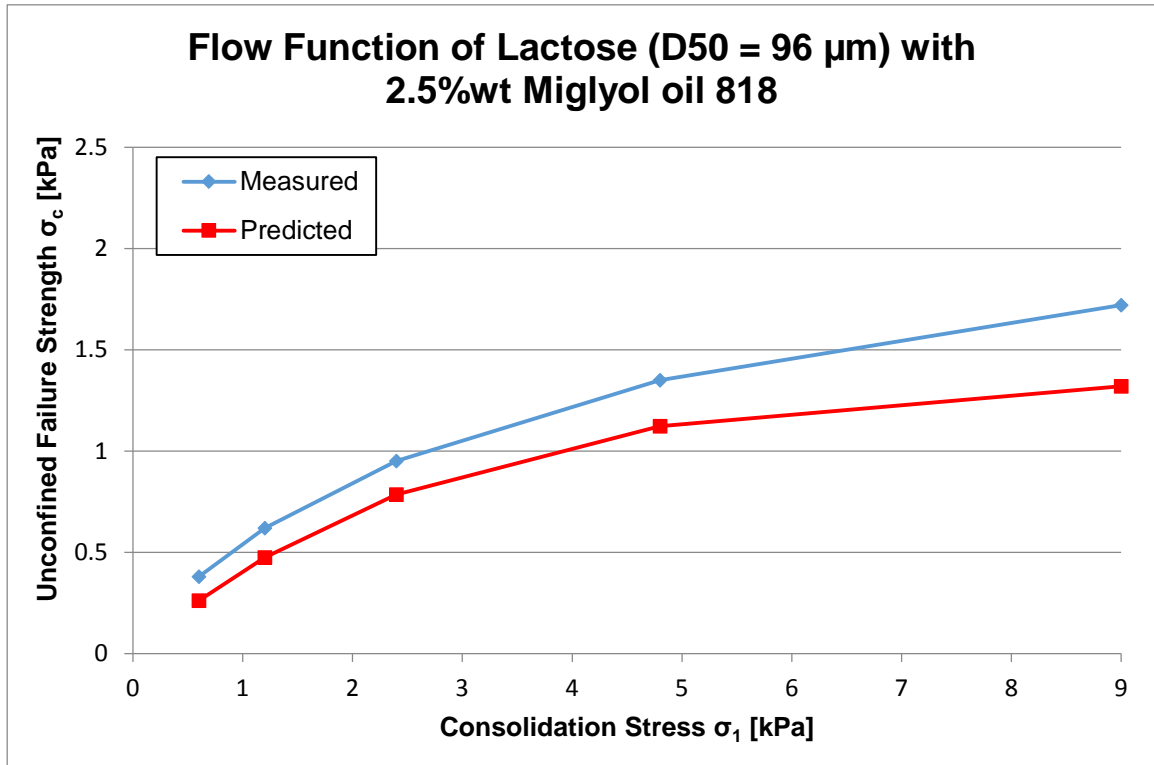


Figure 142: Predicted and measured flow function of lactose D50 = 96 μm with 2.5%wt of Miglyol oil 818

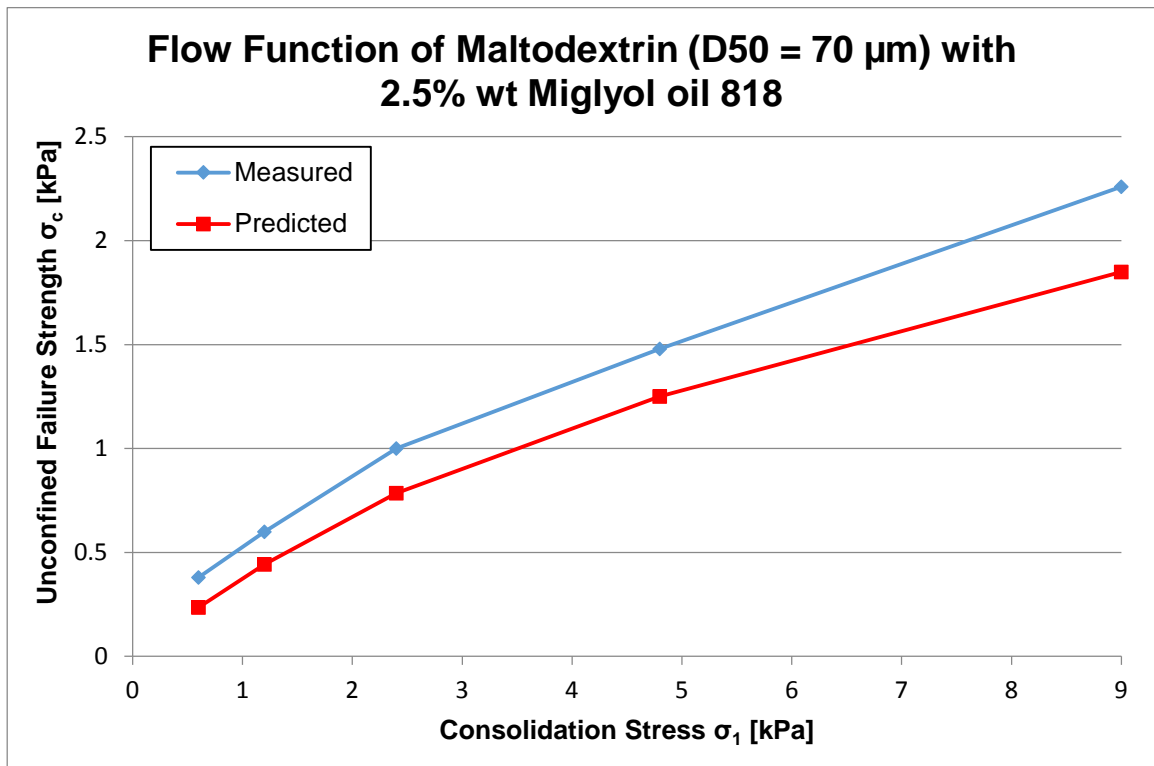


Figure 143: Predicted and measured flow function of maltodextrin D50 = 70 μm with 2.5%wt of Miglyol oil 818

The predicted results obtained for lactose and maltodextrin showed that further work applying these empirical models to a wide range of real powders is required to better understand the accuracy of the predictions. As new empirical models, further development would be necessary to get a good agreement between measured and predicted values for powders with a variety of particle sizes and shapes.

8.2.3 Effect of free flow additives

As disclosed in chapter 7, an empirical model was developed to predict the effect of flow agents on the bulk strength of wet blended powders. The development of the model was based on the experimental work undertaken with blends made with glass beads, Miglyol oil 818 and different common free flow agents such as silicon dioxide and tricalcium phosphate. The experimental data obtained is presented in chapter 6. The optimum percentage of free flow additive was calculated with the measurements undertaken to define the shape of the bulk strength curves for different percentage of oil and free flow additives added as shown in figures 73 -80 above.

The indication from the experimental data is that the effect of the free flow agent is effectively to mop up the oil and therefore reduce its contribution to the strength of the powder. For this reason, the model should work on mitigating only the effect of the liquid content on the bulk strength of the particulate material.

The principle of the model is to determine the optimum ratio of free flow agent to oil – the level of free flow additive which gives the minimum bulk strength. The reduction in strength is a ratio taken from experimental data; this gives the point which is the lowest strength and the optimum level of free flow additive tested. The following terms were defined for this model:

- Oil capacity (OC) is defined as the oil capacity of the free flow additive (mass ratio liquid content to the level of free flow additive at lowest strength).
- Efficacy factor (EF) is defined as the greatest reduction in liquid content contribution to the strength due to the presence of the free flow additive (ratio lowest strength with free flow additive to the bulk strength of the wet powder without free flow additive).

Table 52 shows the values of these terms for silicon dioxide and tricalcium phosphate which have been calculated as the average value of the ratios for the glass beads

tested at different weight percentages of liquid content as shown in chapter 6, figures 73- 80 above.

Values of the ratios for glass beads	Silicon Dioxide	Tricalcium phosphate
Oil capacity (OC)	1.06	0.55
Efficacy factor (EF)	0.65	0.7

Table 52: Values of the oil capacity and efficacy factor for silicon dioxide and tricalcium phosphate

The model developed is linear from the strength of the wet powder without free flow additive to the optimum level of flow agent and also from this point to the bulk strength of 100%wt free flow agent. As 12%wt of free flow additive was the maximum amount added to glass beads in this research study, a linear model from the optimum level of flow agent to the value of the bulk strength at the maximum weight percentage of free flow additive added to glass beads was also considered as an alternative approach. However, it is clear that this value of the bulk strength is only valid for glass beads and differs for other particulate materials as a function of the lowest bulk strength.

The ratios of the oil capacity and the efficacy factor of the flow agent added to the wet powder are used to predict the changes in bulk strength due to the effect of the level of the free flow additive. An excel spreadsheet was developed to make the predictions and the following steps must be followed to replicate the calculations developed in this research:

- 1) Define the values of the oil capacity (OC) and the efficacy factor (EF) ratios for the flow agent added to the wet powder
- 2) Define the weight percentage of liquid content of the wet particulate material Pd(%wt)
- 3) Measure the unconfined failure strength of the wet powder without free flow additive at 9 kPa of consolidation stress (σ_{Pd} at 9 kPa)
- 4) Measure the unconfined failure strength of 100% free flow additive at 9 kPa of consolidation stress ($\sigma_{100\% FFA}$ at 9 kPa)

- 5) Calculate the amount of the flow agent required to obtain the lowest bulk strength of the wet powder with free flow additive at 9 kPa of consolidation stress

$$\%wt \text{ flow agent at lowest strength} = \frac{Pd (\%wt)}{OC} \quad \text{Equation 77}$$

- 6) Calculate the lowest bulk strength of the wet powder with free flow additive at 9 kPa of consolidation stress (σ_{lowest} at 9 kPa)

$$\sigma_{lowest} \text{ at } 9 \text{ kPa} = EF * \sigma_{Pd} \text{ at } 9 \text{ kPa} \quad \text{Equation 78}$$

- 7) Calculate a first degree linear equation as shown in figure 144 between the following points:
- From the strength of the wet powder without free flow additive to the optimum level of flow agent
 - From the optimum level of flow agent to the bulk strength of 100%wt free flow agent

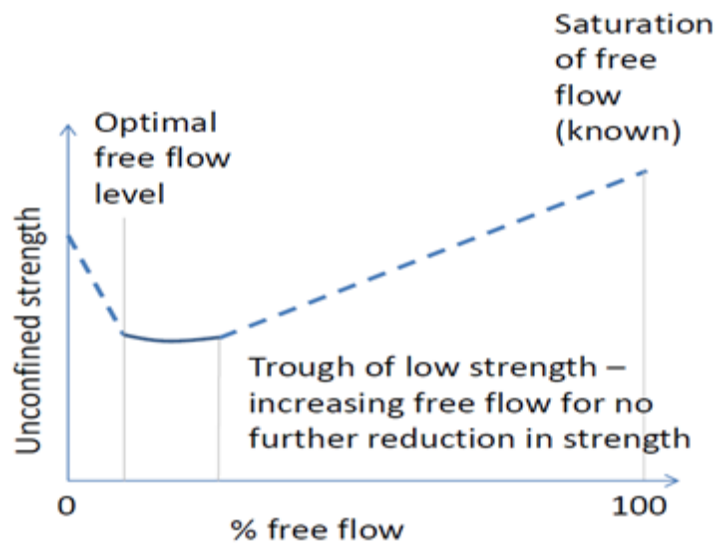


Figure 144: Schematic representation of the model developed in this research for the prediction of the effect of flow agents on wet powders

- Calculate the reduced oil contribution to the bulk strength of the wet powder due to the addition of the flow agent at the percentage of free flow additive selected using the linear equations from previous point
- Calculate the ratio bulk strength of the powder at the percentage of flow agent selected to the bulk strength of the wet powder without free flow additive. As

values are calculated at 9 kPa of consolidation stress, this ratio is used to proportionate down at lower stresses.

Figures 145 - 154 show the results obtained from the application of this empirical approach to real particulate materials to predict the effect of flow agents on wet powders. The unconfined failure strength of two powders named lactose (D50 = 96 μm) and maltodextrin (D50 = 70 μm) with narrow and wide particle size distributions respectively was measured after adding 2.5%wt of Miglyol oil 818. Then the effect of silicon dioxide and tricalcium phosphate up to 5%wt on the bulk strength of the wet powders was predicted and compared with the measured values obtained for the PFT shear tester. Comparison of the results obtained from the addition of silicon dioxide are presented in this section with full results plots presented in appendix A.

Analysing the experimental data, it was found that the impact of the weight percentage of the liquid content on the bulk strength reduction for the range tested in this research (1 – 4 %wt oil content) is insignificant as the values of the efficacy factor showed a small variation with a maximum difference of 0.1 from the average value for the case of coarse particles of glass beads.

Regarding the type of free flow additives, values of the OC and EF ratios presented in table 52 show that the weight percentage of free flow level required to obtain the lowest bulk strength for tricalcium phosphate is twice as much as the level needed for silicon dioxide as different free flow additives exhibit different optimum ratios. In terms of the optimum bulk strength, there is no much difference between these two flow agents and, therefore, the only difference is the amount of free flow additive required.

Predicted results for the powders tested showed that the upper limit of 12%wt or 100%wt of free flow additive considered in the calculation of the lineal equation gives similar agreement with the experimental data. It is important to highlight that in figures 145 - 154, the prediction made for 12%wt and 100%wt is the same if the values of the weight percentage of the free flow level added to the wet powders are lower than the weight percentage at the lowest strength.

The limitation of this work was that glass beads particles tested do not soak up the oil added therefore it is a factor to consider for the application of the model to real particulate materials. It is clear that further work is required to develop the empirical approach using more liquids and free flow additives for a wide range of powders.

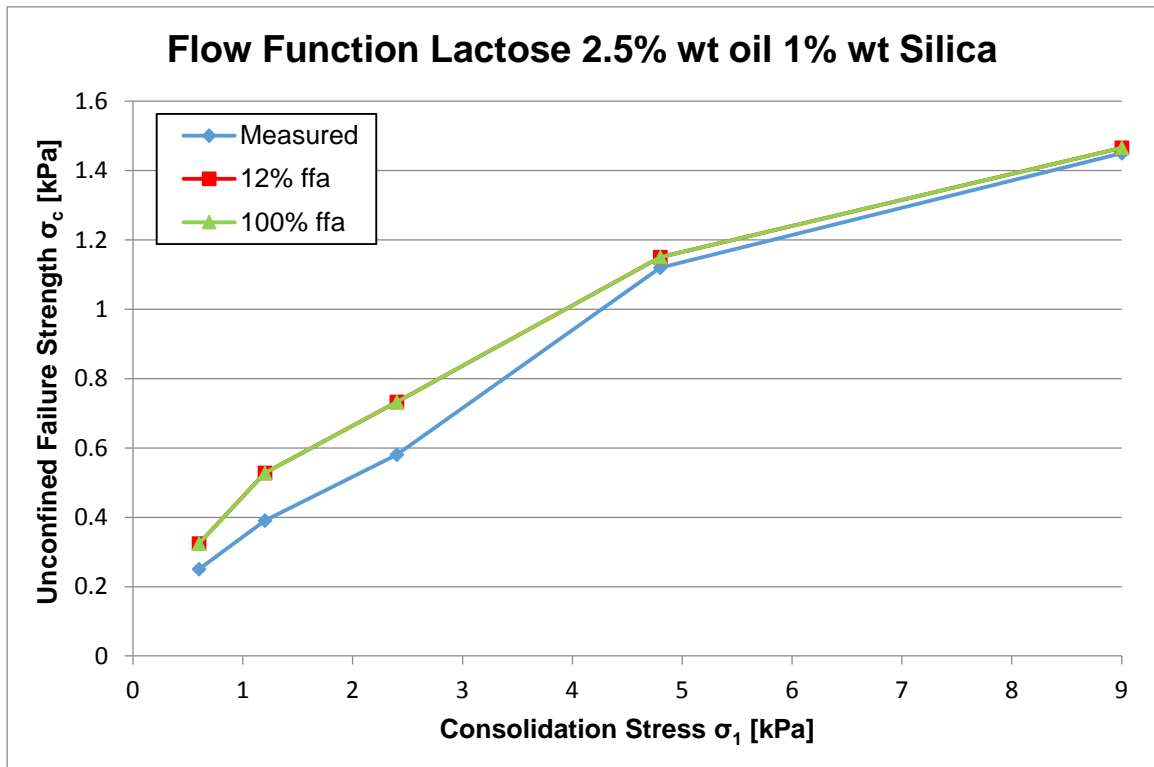


Figure 145: Measured and predicted effect of the free flow additives on lactose 2.5%wt with 1%wt silica

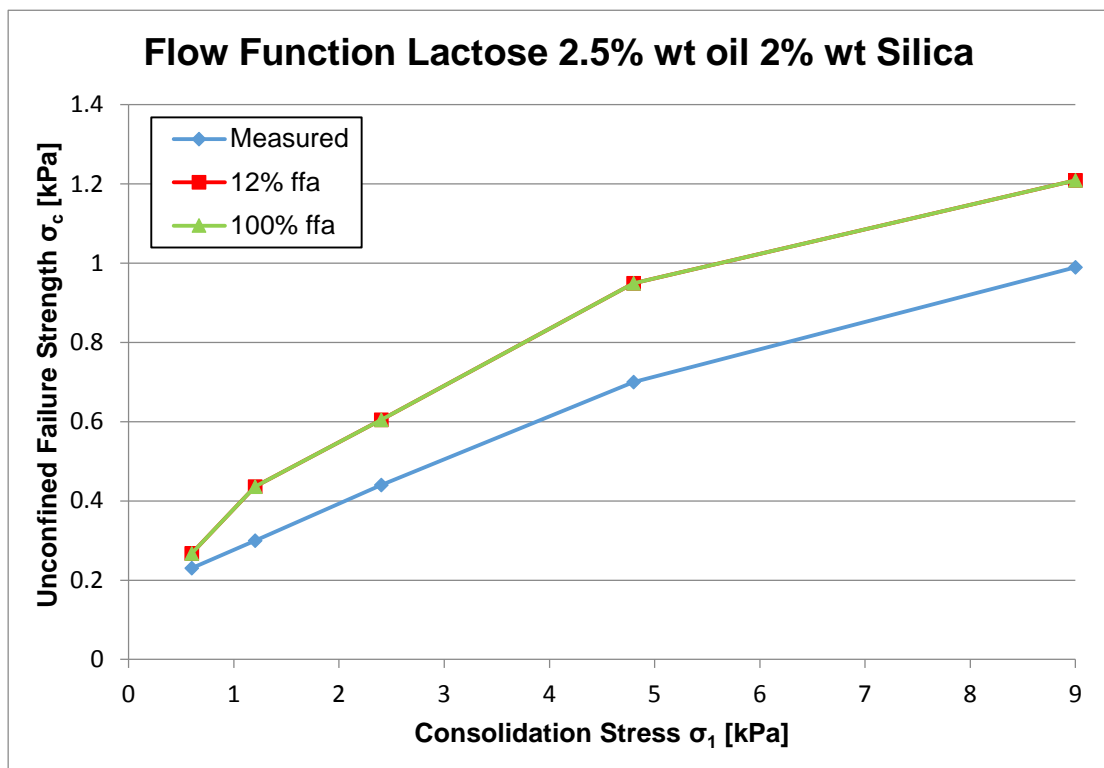


Figure 146: Measured and predicted effect of the free flow additives on lactose 2.5%wt with 2%wt silica

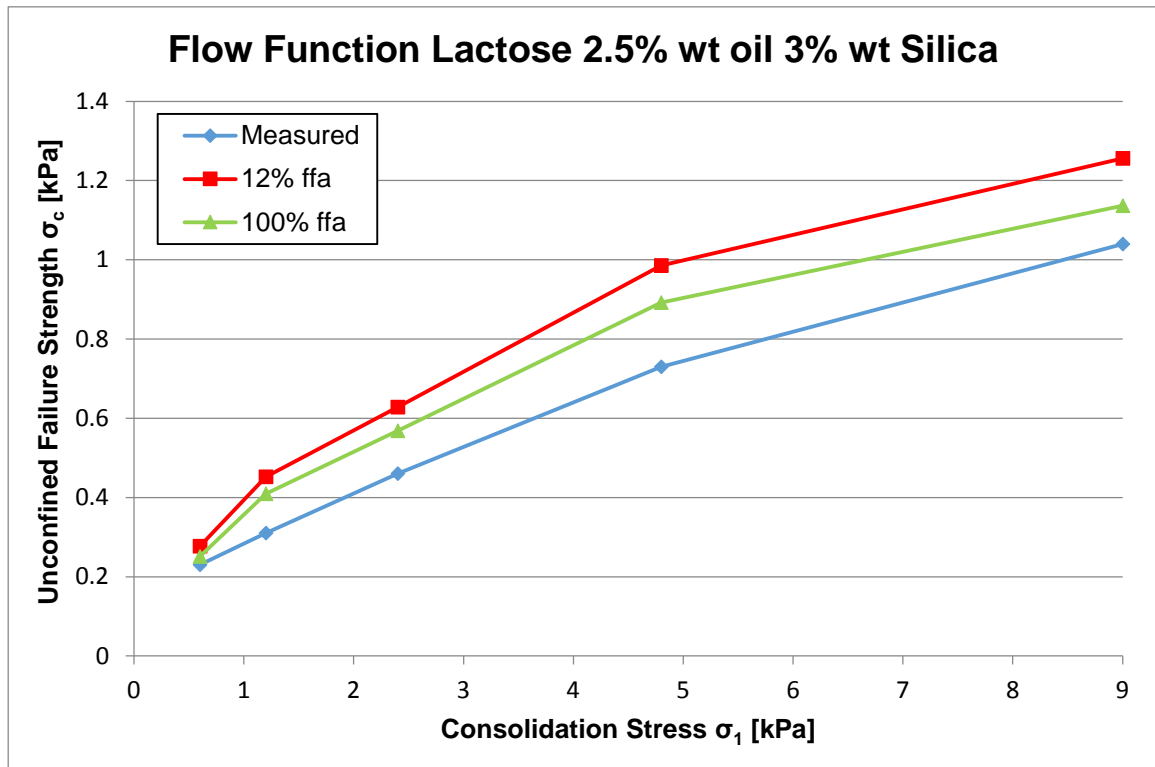


Figure 147: Measured and predicted effect of the free flow additives on lactose 2.5%wt with 3%wt silica

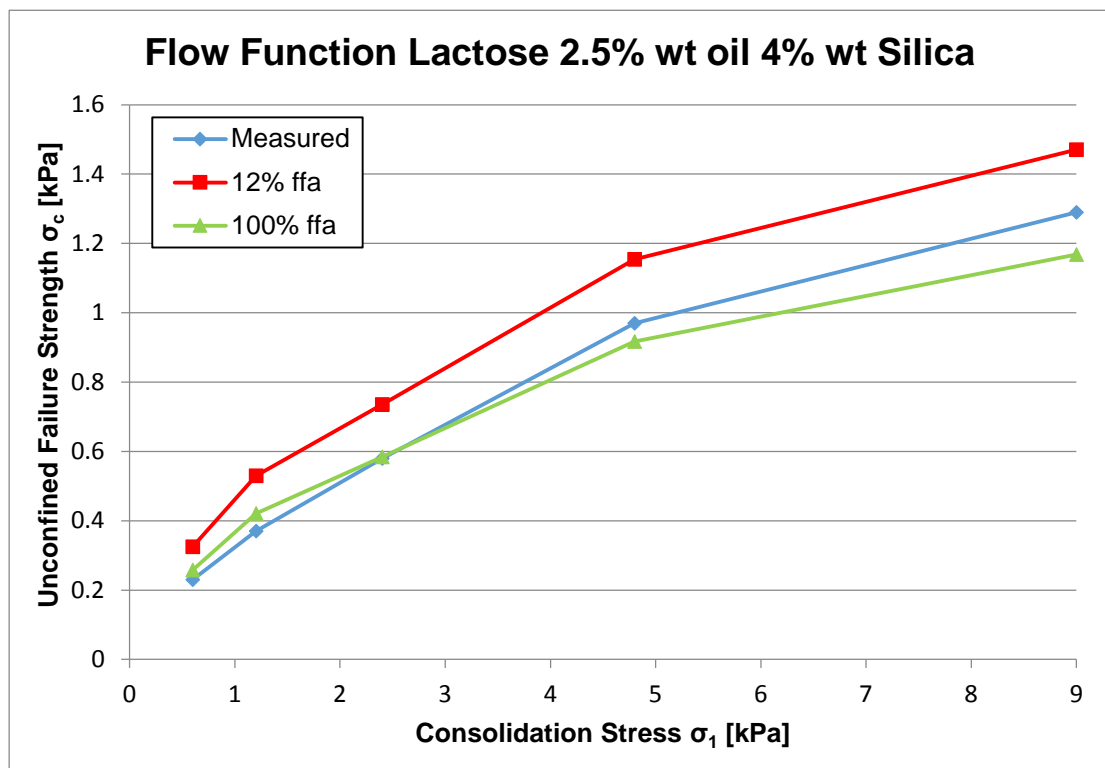


Figure 148: Measured and predicted effect of the free flow additives on lactose 2.5%wt with 4%wt silica

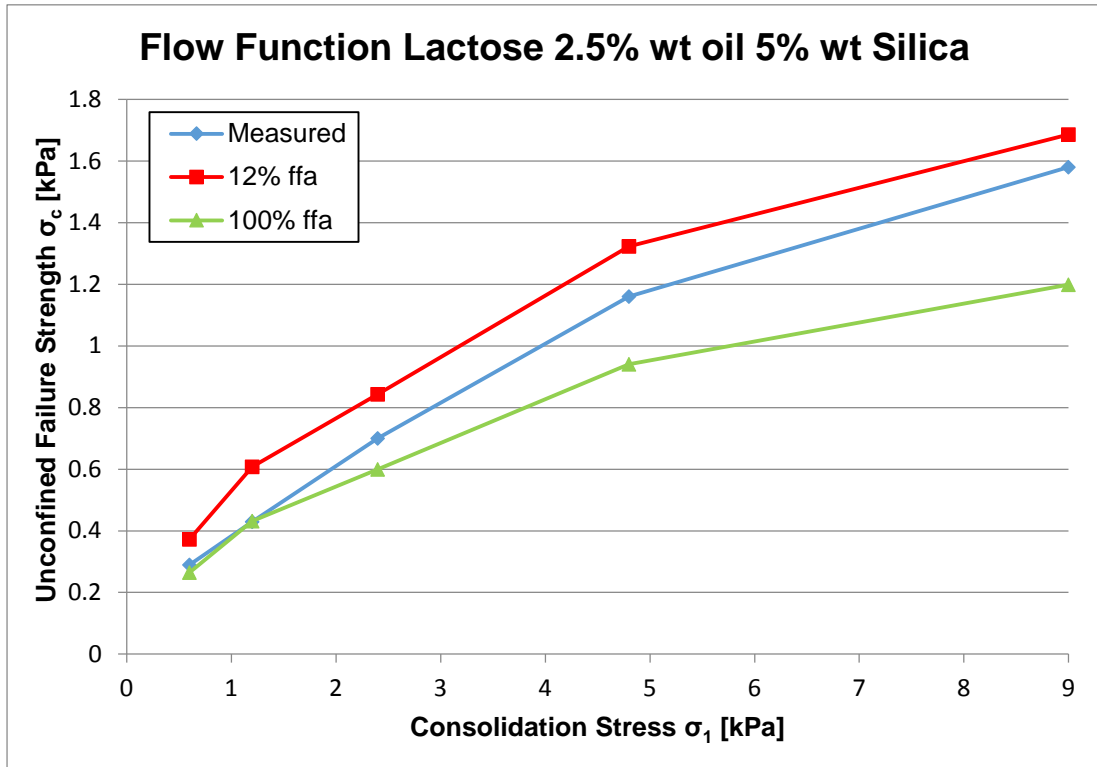


Figure 149: Measured and predicted effect of the free flow additives on lactose 2.5%wt with 5%wt silica

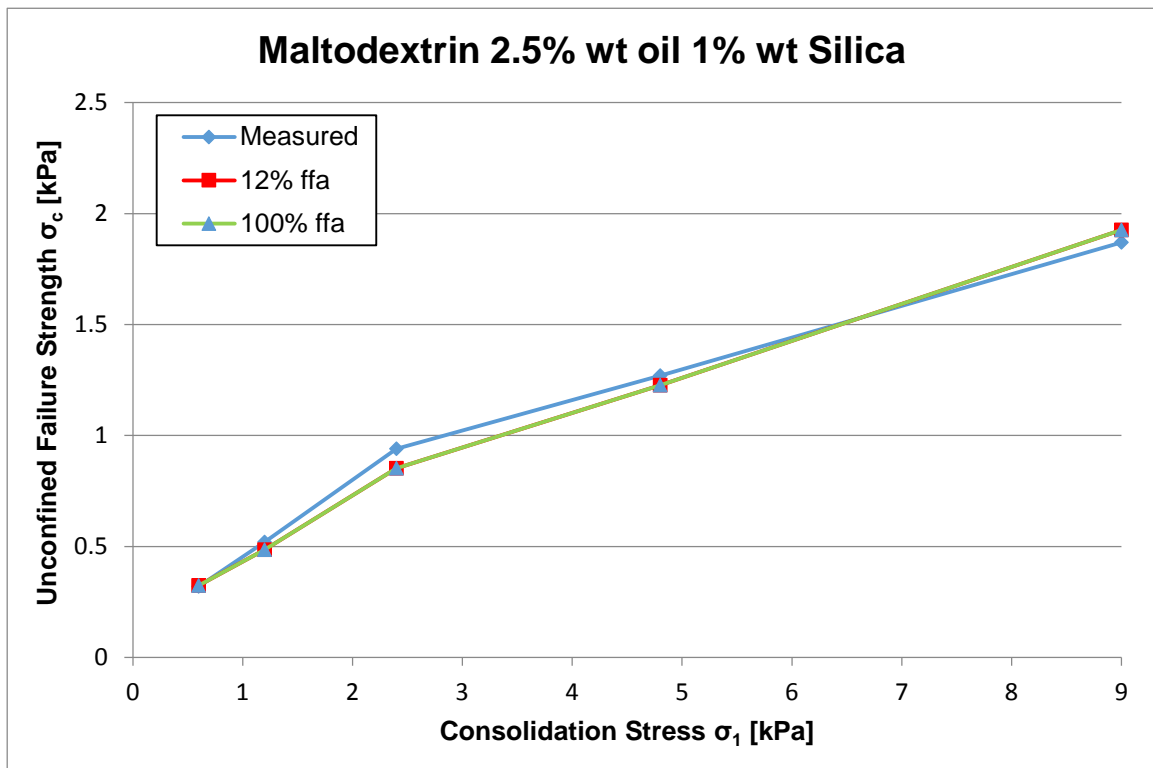


Figure 150: Measured and predicted effect of the free flow additives on maltodextrin 2.5%wt with 1%wt silica

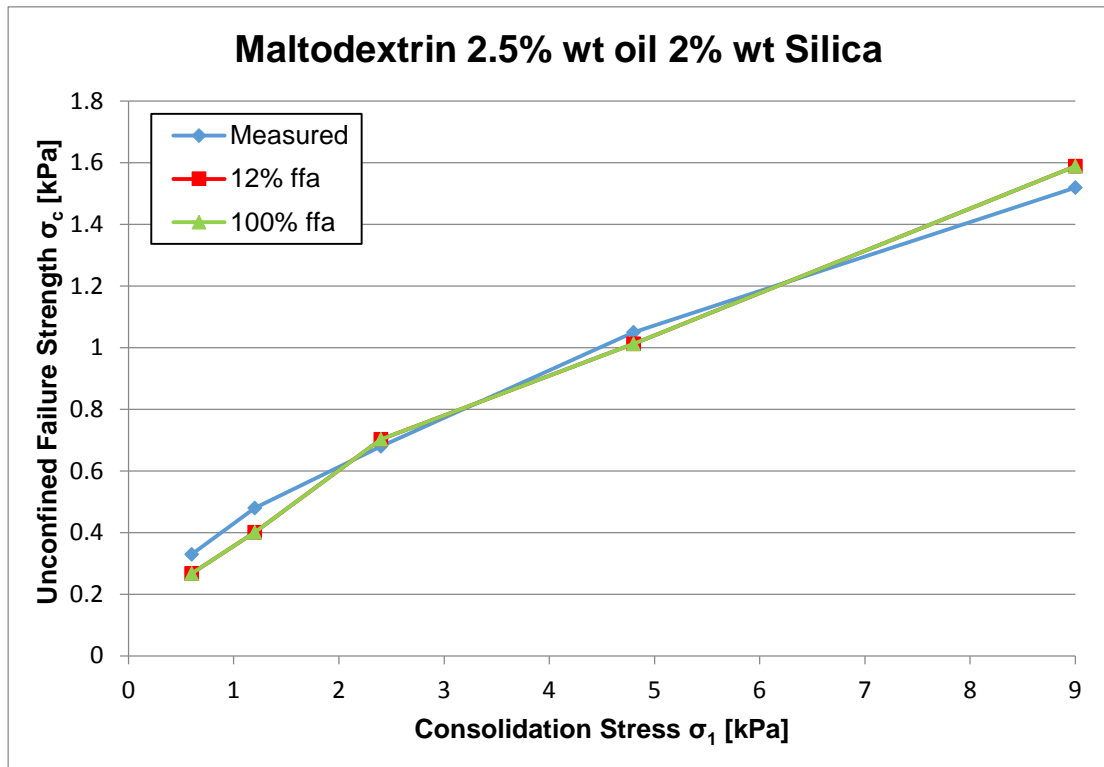


Figure 151: Measured and predicted effect of the free flow additives on maltodextrin 2.5%wt with 2%wt silica

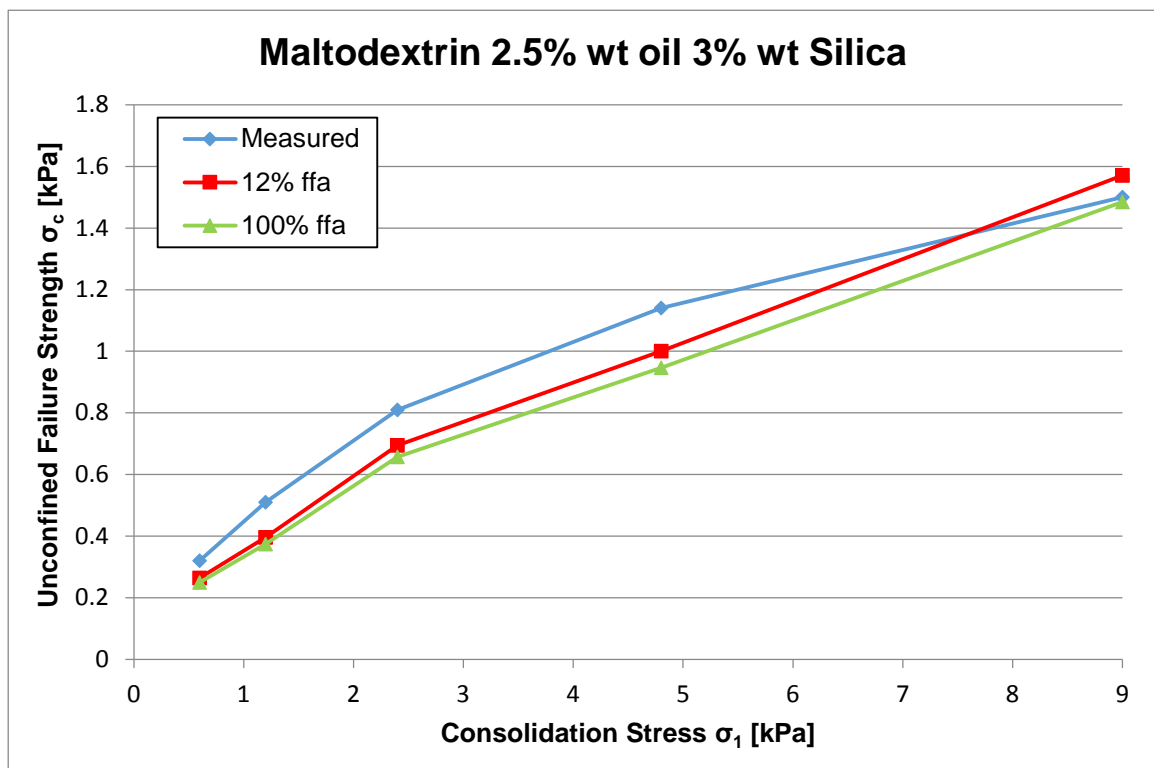


Figure 152: Measured and predicted effect of the free flow additives on maltodextrin 2.5%wt with 3%wt silica

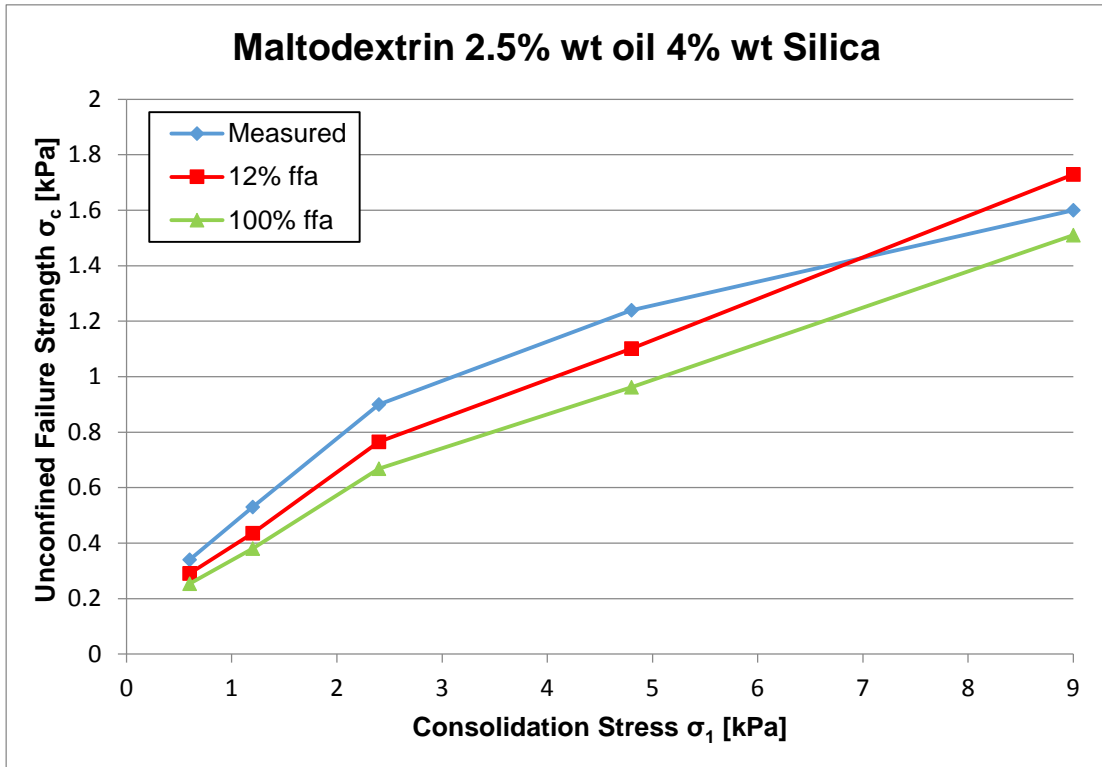


Figure 153: Measured and predicted effect of the free flow additives on maltodextrin 2.5%wt with 4%wt silica

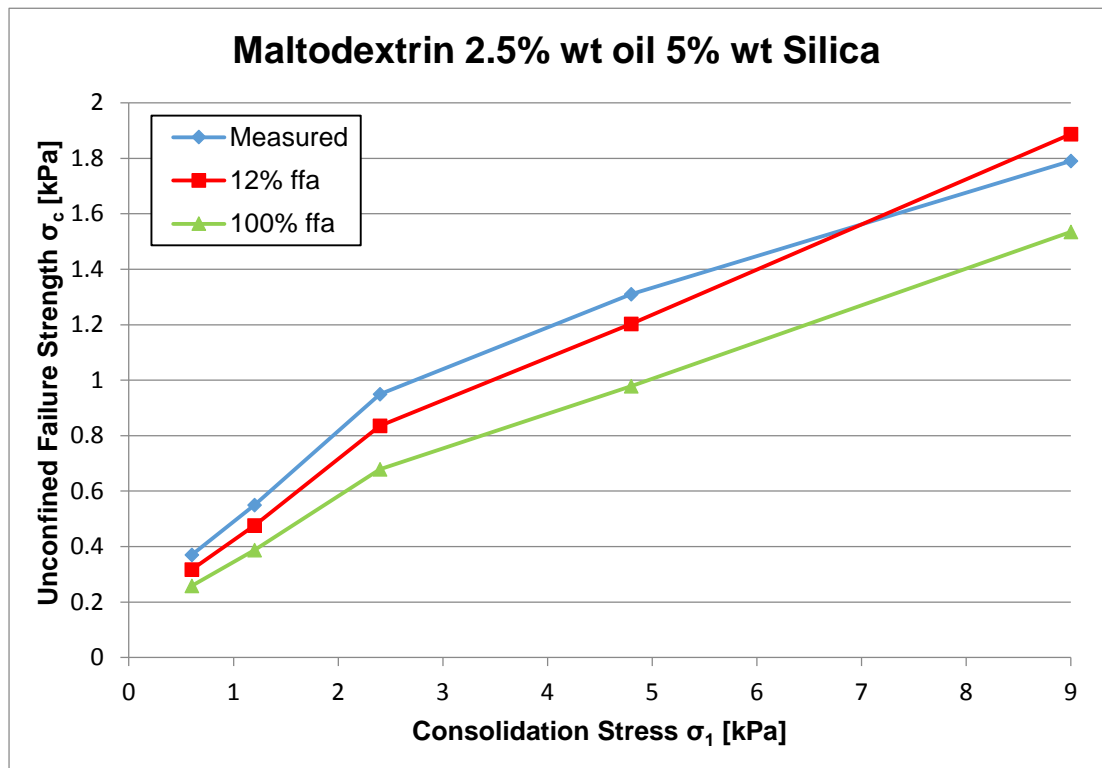


Figure 154: Measured and predicted effect of the free flow additives on maltodextrin 2.5%wt with 5%wt silica

8.3 *Blended particulate materials*

As disclosed in chapters 5 & 7, a new model to predict the bulk flow properties for dry blends without free flow additives has been developed and evaluated in this research work. This section presents the application of the new empirical models presented in this chapter to dry blended powders in order to predict the effect of liquid content and free flow additives. These models have been validated with measured values of a simplified food blended powder made with 5 ingredients. This blend was made with lactose (D50 = 90 μm), yeast (D50 = 60 μm), sodium chloride (D50 = 120 μm), dextrose (D50 = 185 μm) and whey powder (D50 = 130 μm) at the weight ratio of 50:11:15:11:13. Firstly, flow function of the dry blend was predicted applying the model for dry blends at 0.6, 1.2, 2.4, 4.8 & 9 kPa of consolidation stresses as a function of the surface area and specific volume ratios of the ingredients as shown in figure 155. The bulk strength is under-predicted and similar predictions were obtained using surface area and specific volume ratios.

Then 3%wt of Miglyol oil 818 was added to the blend and the bulk strength of the wet blend at 9 kPa of consolidation stress was predicted with the empirical models developed for wet powders. The models developed to predict the bulk strength at lower consolidation stresses and the effect of different particle density to glass beads were applied to calculate the flow function of the wet blended powder at 0.6, 1.2, 2.4, 4.8 & 9 kPa of consolidation stresses. At each level of stress, the calculated values of the bulk strength due to the addition of oil were added to the predicted values of the flow function for the dry blend giving the predicted flow function for the wet blended powder shown in figures 157 and 158 below.

The next step was the addition of 1%wt and 2%wt of silicon dioxide to the wet blend to predict the effect of the free flow agent in the bulk strength of the wet powder. Using the values of the efficacy factor and oil capacity for silicon dioxide given in table 52, the reduced oil strength proportion due to the content of free flow agent was calculated and used to scale across the consolidation stress range of 0.6 to 9 kPa. The predicted values of the flow function for the wet blend were multiplied by this proportion factor to obtain the predicted flow functions of the wet blend mixed with different weight percentages of silicon dioxide shown in figures 157 and 158 below.

It was found that the value of the efficacy factor obtained from the results of the tests undertaken with glass beads needs to be reconsidered for real blended powders. The predicted results for the effect of silicon dioxide over-predicts the experimental data as shown in figures 156 and 157. The predictions were recalculated with lower values of the efficacy factor and a value of 0.5 gave a better agreement with the measured values as shown in figures 156 and 158. A lower value of the efficacy factor means that the blended powder mitigates more oil than glass beads showing lower bulk strength at the optimum weight percentage of flow agent.

It is clear that further work on the predictions of the bulk flow properties of blended powders is required and new models need to be developed to better predict the effect of the liquid content and free flow additives on blends. The models developed in this research to make predictions for blended powders could be considered a starting point and further development is required to improve the accuracy of the predictions.

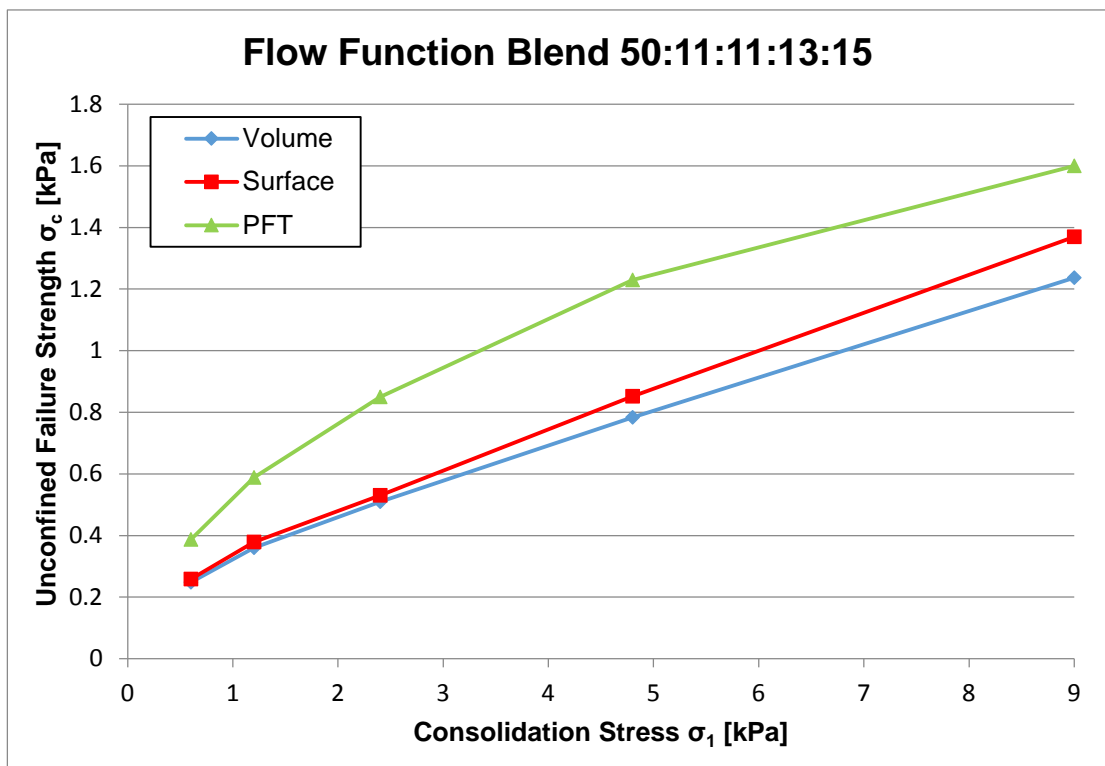


Figure 155: Measured and predicted values of the flow function of a dry blended powder

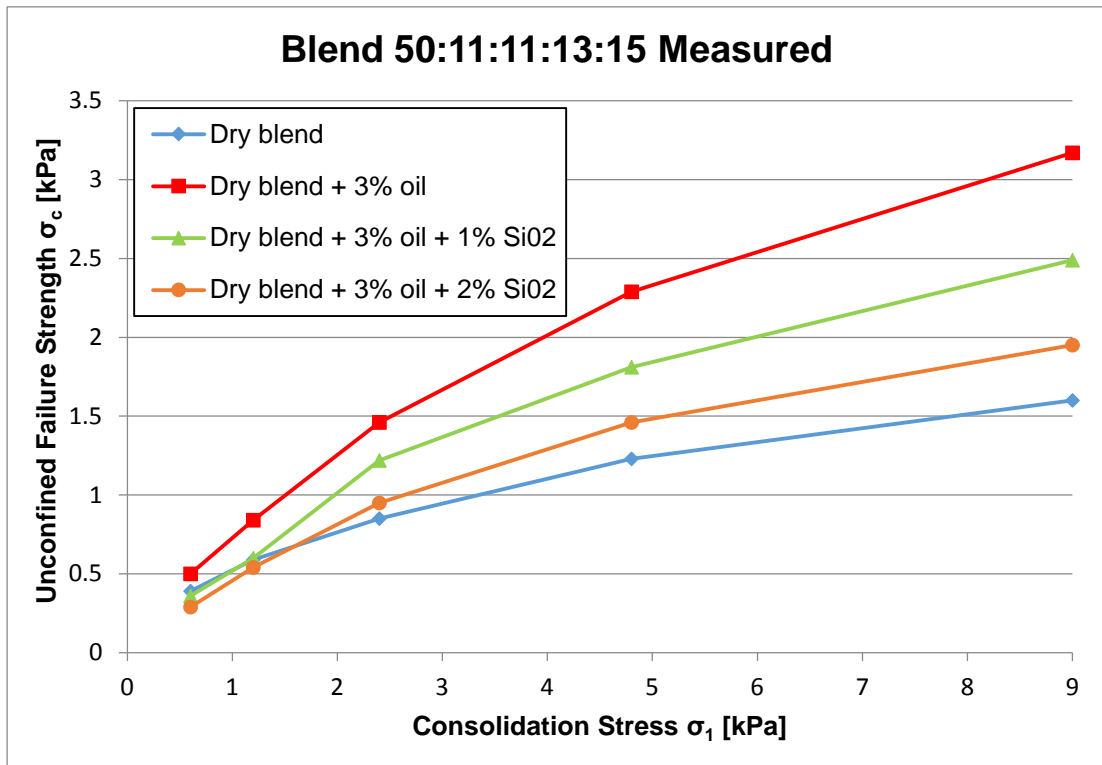


Figure 156: Measured values of the flow function of a blended powder at different conditions

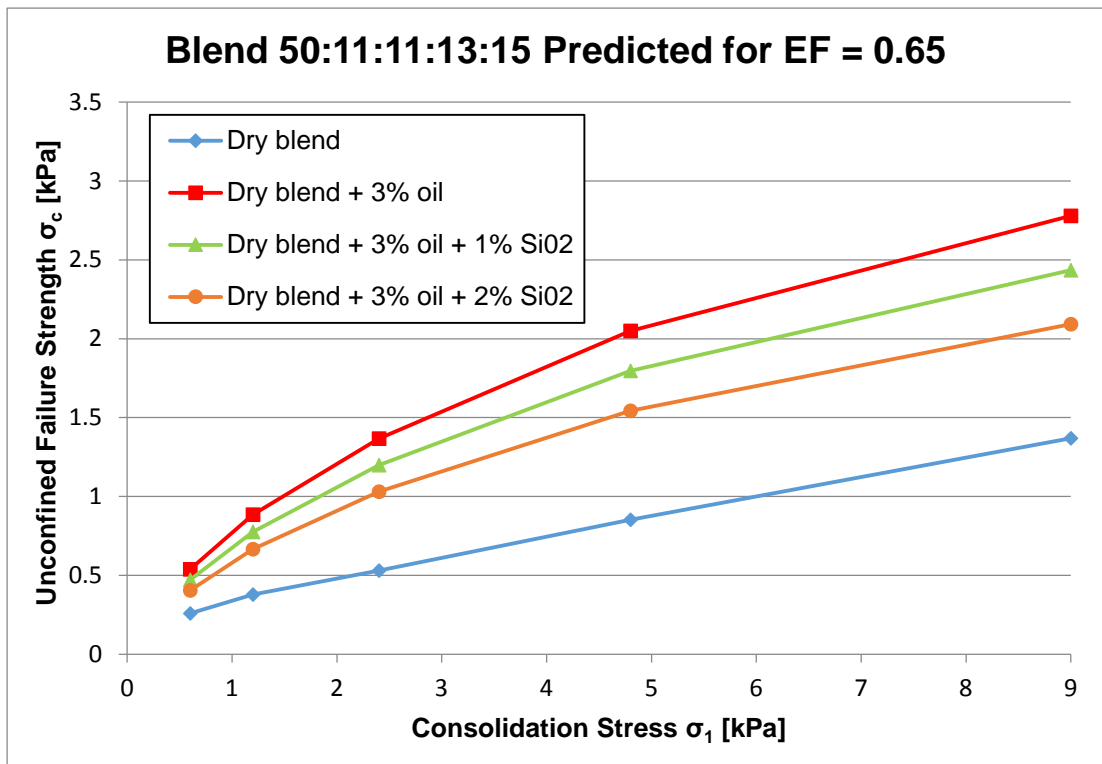


Figure 157: Predicted values of the flow function of a blended powder at different conditions

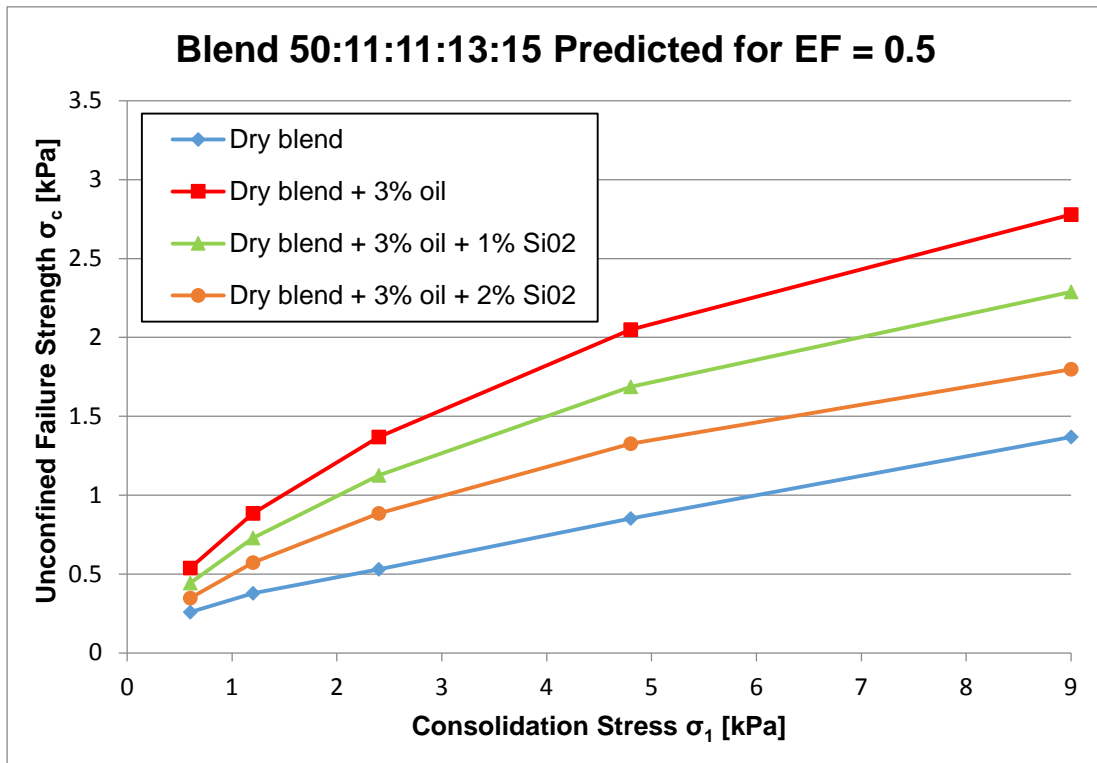


Figure 158: Predicted values of the flow function of a blended powder at different conditions

8.4 Summary

This chapter presents the evaluation of the new empirical models developed in this research to predict the bulk strength of dry single and blended powders and the effect of liquid content and the addition of free flow additives on their flow functions. The key points from the chapter are the following:

- A new empirical logarithmic model has been developed to predict the bulk strength of dry powders with narrow particle size distributions or the unconfined failure strength of size fractions of wide particle size distributions of powders. The flow function of the size fractions of five powders were predicted and compared with the measured values showing an agreement between both functions. Also predictions of the inverse of the flow factor ratio were made at different levels of consolidation stress and the results showed that the predicted values fit for most of the size fractions tested as the model failed in the predictions for lactose at low consolidation stresses. This may be due to the fact that at low consolidation stresses, the fine particles of the size fractions of lactose are agglomerating resulting in a lower friction (see figure 31, chapter 3)

leading to a greater disagreement compared to the coarse particles of the size fractions of lactose. Further work is required applying the model to a wide range of powders and making predictions based on the measured flow functions.

- Different empirical models were developed to predict the bulk strength of wet powders in the funicular and capillary states and also as an alternative approach to calibrated Rumpf model for the wet glass beads with particle size below 40 μm as explained in the conclusions of the previous chapter. These new models showed a good agreement with the experimental data both for glass beads with particle size below 40 μm in the pendular state and for any particle size of glass beads in the funicular and capillary states. The experimental work undertaken with idealised materials was used to develop these models but an example of their application to real powders with non-spherical particles is also presented in the chapter (see figures 142 and 143). Results showed that the models under predict the bulk strength of the powders named lactose and maltodextrin which means that further work is required to consider the effect of the particle shape and particle size distribution in the application of the models to real powders.
- A new empirical model has been developed to predict the effect of the free flow additives on the bulk strength of wet blended powders based on the experimental work undertaken in the research with glass beads. This empirical approach was evaluated predicting the effect of silicon dioxide and tricalcium phosphate up to 5%wt on the bulk strength of two powders named lactose and maltodextrin in wet condition after adding 2.5%wt of Miglyol oil 818. Results showed that further work is required as the predictions do not fit the measured values. One of the limitations of the models is the fact that glass beads do not soak up the oil added so the application of the model to real powders is limited.

This modelling work has been developed to arrive at a system (prediction tool) that gives a prediction of the flow function of single and blended powders in dry and wet conditions with or without free flow additive. This prediction tool is presented in the next chapter along with the test protocol for industry which gives recommendations about how to proceed in order to develop a blended powder.

Chapter 9 Development of the test protocol for industry

9.1 Introduction

This research work has been part of a wider Defra sponsored project to develop a prediction tool called Virtual Powder Blending Laboratory which has been recently developed by The Wolfson Centre for Bulk Solids Handling Technology. A data base of blended powders and their individual components with the measured particle and bulk flow properties has been developed in the form of a spreadsheet as part of this prediction tool.

The outcome of the research presented in this thesis is a test protocol for industry to predict and optimise the flow behaviour of blended powders. The test protocol is the recommendations about how a formulator faced with a problem should proceed using the standard characterisation tests presented in chapter 3 and the prediction tool together to get from his start point to his finished formulation of the desirable blended powder.

This research work is directed to the food industry by virtual of the industrial sponsors and Defra funding, however, the test protocol has the potential for applications in other industry sectors with similar flow problems with powders such as pharmaceuticals, ceramics and powder metallurgy.

9.2 Virtual Powder Blending Laboratory

This section describes the prediction tool called Virtual Powder Blending Laboratory which helps to investigate the effect of changing particle properties of single particulate materials or blend components on the bulk flow and packing properties of blended powders.

9.2.1 Benefits of the prediction tool

The benefits of using the prediction tool for formulators and process engineers are:

- Predict the bulk flow properties of single materials.
- Predict the bulk flow properties of blended powders based on changes to the particles properties or blend components.
- Compare the effectiveness of different free flow additives (anti-caking agents).

- Predict the effect of changing the amount of liquid and/or free flow additive in the blended powder instantaneously.
- Select the best combination of blend components to ensure the desirable flow behaviour of the final blended product.
- Evaluate the changes of the flow properties during industrial processes.
- Ensure the quality of the final blended products.

9.2.2 Current limitations of the prediction tool

The current limitations of the prediction tool are:

- Assume a random packing assembly of monosized sphere particles.
- Reliance on tabulated values of materials properties which are difficult to measure by industrial users such as Hamaker constant.
- Assume that particle shape is independent of the particle size based on limited SEM images of the particles.
- Assume a grade of uncertainty inherent in the techniques used to measure the particle size (actual size can shift at significant margins which has implications for non-spherical particles).
- Assume smooth and non-porous sphere particles (the effect of surface roughness and porosity of the particles need to be considered in further work).
- Assume unimodal normal particle size distribution of the powders.
- Effect of the variation of temperature and humidity on the flow behaviour of blended powders was considered outside the scope of this work as explained in chapter 2 of the thesis.
- Wall friction testing was considered outside the scope of this work as explained in chapter 2; therefore, this is only valid for core flow hopper design.

9.2.3 Powder testing and sampling

Standard characterisation tests commonly used in industry at particle and bulk scale were undertaken for a wide range of food powders and idealised particulate materials in order to make a data base on which the evaluation of the analytical models is based on. These tests were carried out under atmospheric conditions in the laboratories of The Wolfson Centre under controlled environment of 15 to 20°C and 35 to 50%HR; materials tested were stored in the laboratories in air tight containers.

The data base is based on the sampling techniques presented in chapter 3 and different sampling methods may lead to different results of the particle and bulk flow properties. Users of the prediction tool are advised to exercise caution when using the data base available if sampling methods are different and run further repeated tests to ensure consistency of the properties measured.

9.2.4 Interpretation of the results

To use the prediction tool and understand its predictions of the flow behaviour for single and blended powders, it is necessary to have some basic knowledge of the characterisation of the powders at particle and bulk scale and also how their flow behaviour is determined and numerically characterised. This knowledge has been presented in the literature review of the thesis, explaining the particle and bulk flow properties along with their practical measurements and the current industrial practice to develop the blended powders to meet the desirable flow behaviour of the final blended products.

9.2.5 Prediction of the flow behaviour of powders

A roadmap of the Virtual Powder Blending Laboratory is presented in this section including a general description of the user interface (see figure 159) and instructions for the user to input data in the prediction tool.

User interface of the prediction tool

The user interface of the prediction tool can be described as follows:

- The design and the combination of the colours make the interface attractive and pleasant to use calling attention to interface users
- It shows clearly how the application works which makes easy the learning process for the user
- At the same time, it is concise showing only the minimum explanations required to understand the features of the interface and the information presented
- It is familiar to use for the formulators and process engineers because with a simple look, you know what you can expect
- The user has the total control of the actions of the interface and the response of the selected options is direct and clear which makes the user feel in control of the actions happening

- The loading of the input data of a new ingredient is quick and the interface works fast
- It gives a feedback of the flowability of the process selected and defines the acceptable window of the flow functions
- It also shows the influence of the liquid content and the level of the free flow additive on the bulk strength of the blended powder

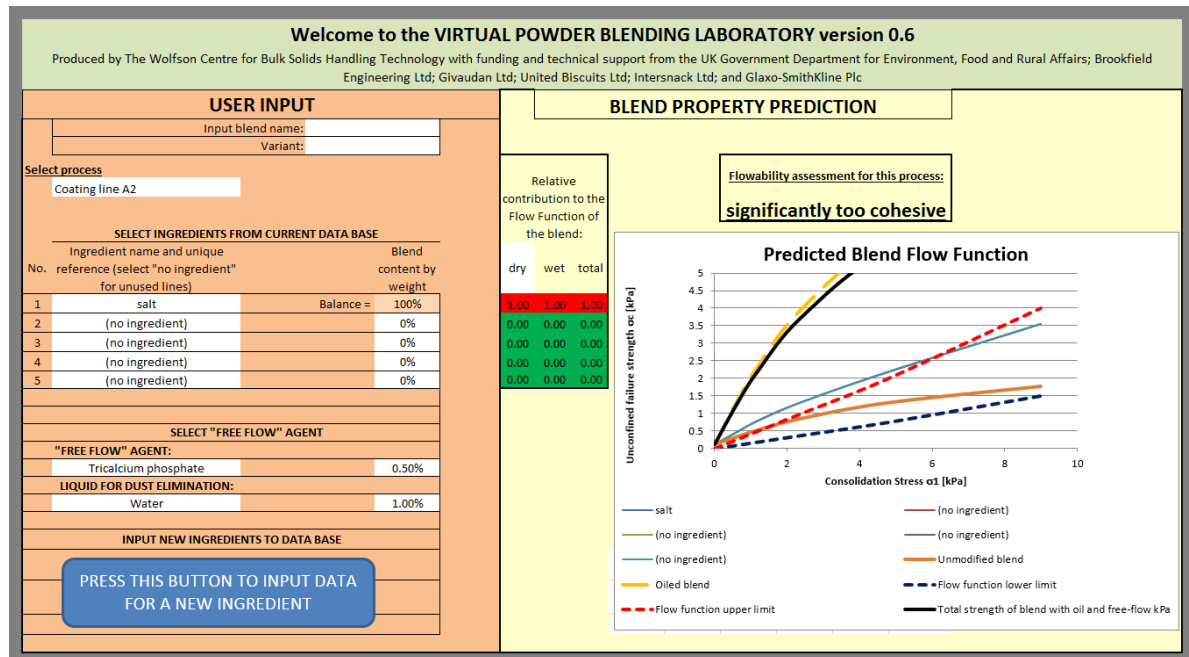


Figure 159: Interface of the Virtual Powder Blending Laboratory

Instructions for the user to input data in the prediction tool

The following steps should be followed by the users of the prediction tool for the first time to define the composition of the blend:

- Step 1: Name the input blend and its variant if applicable
- Step 2: Select the process from the list available (each process has a characteristic acceptable window of the predicted flow function so it is important to choose the right option)
- Step 3: Select the ingredients of the blend from the current database and the weight percentage content of each one in the blend in the numbered lines 1 to 5 (if any ingredient of the blend is not in the database, follow the instructions given in step 5)
- Step 4: Select "no ingredient" for unused numbered lines 1 to 5

- Step 5: The input data of a new ingredient (name of the powder; particle density; particle size values d_{10} , d_{50} and d_{90} ; data from the standard flow function test of the powder run in the PFT shear tester) can be added clicking on the button placed on the left bottom corner of the interface. Once the button is clicked, a window appears allowing the user to introduce the data for the new powder and when the input data is completed, clicking the button called “Insert Data” will return the user to the interface with the new powder available in the selection list of ingredients.
- Step 6: Select the liquid from the list available and its weight percentage content in the blend
- Step 7: Select the free flow agent from the list available and its weight percentage content in the blend

Understanding of the blend property prediction of the prediction tool

This initial guidance helps to understand the results predicted by the tool; once the composition of the blend has been defined in the user input section, the next step is to understand the prediction given by the Virtual Powder Blending Laboratory. Three panels are presented in the prediction view layout:

- Flowability assessment of the process
- Relative contribution to the Flow Function of the blend
- Predicted Blend Flow Function

The panel called “Flowability assessment of the process” placed on the top centre gives an assessment of the flowability for the process and blend composition selected by the user. It defines the flow behaviour of the blended powder in the following range based on the acceptable window of the flow function:

- Significantly too cohesive (Flow function significantly outside of the acceptable window in the cohesive zone of the $\sigma_c - \sigma_1$ diagram)
- Slightly too cohesive (Flow function slightly outside of the acceptable window in the cohesive zone of the $\sigma_c - \sigma_1$ diagram)
- Acceptable (Flow function inside the acceptable window of the process selected)
- Slightly too dusty (Flow function slightly outside of the acceptable window in the flowing zone of the $\sigma_c - \sigma_1$ diagram)

- Significantly too dusty (Flow function significantly outside of the acceptable window in the flowing zone of the $\sigma_c - \sigma_1$ diagram)

The panel called “Relative contribution to the Flow Function of the blend” placed on the top left corner gives the relative contribution of the dry blend and wet blend to the total bulk strength of the blend with liquid and free flow agent for each component selected. The contribution of each ingredient is presented by a sensitivity rating with the following colours at different grades:

- Severe contribution (red colour)
- Moderate contribution (orange colour)
- Slight or insignificant contribution (green colour)

The panel called “Predicted Blend Flow Function” presents a graph with the following data:

- Flow function of each ingredient of the blend in dry condition
- Flow function of the dry blended powder
- Flow function of the wet blended powder (effect of the addition of liquid to the dry blend)
- Flow function of the final blend with liquid and free flow additive (effect of the addition of free flow additive to the wet blend)
- Flow function lower and upper limit of the process selected by the user

9.2.6 Development of a Data Base

The data base of the Virtual Powder Blending Laboratory has been developed with the experimental work undertaken in this research. Currently, the data base of single powders includes particle and bulk properties values to characterise the powders. The particles properties considered are particle density and particle size distribution defined by the values of D10, D50 and D90. The flow properties considered are bulk density, unconfined failure strength, angle of internal friction and effective angle of internal friction measured using Brookfield Powder Flow Tester.

The data base can be updated adding data corresponding to new single powders and the flow properties are automatically recalculated at the specific consolidation stresses required using the fitting equation (lineal interpolation between measured values of the bulk flow properties) developed in this research as shown in figures 160 - 162.



Figure 160: Interface of the data base in the Virtual Powder Blending Laboratory

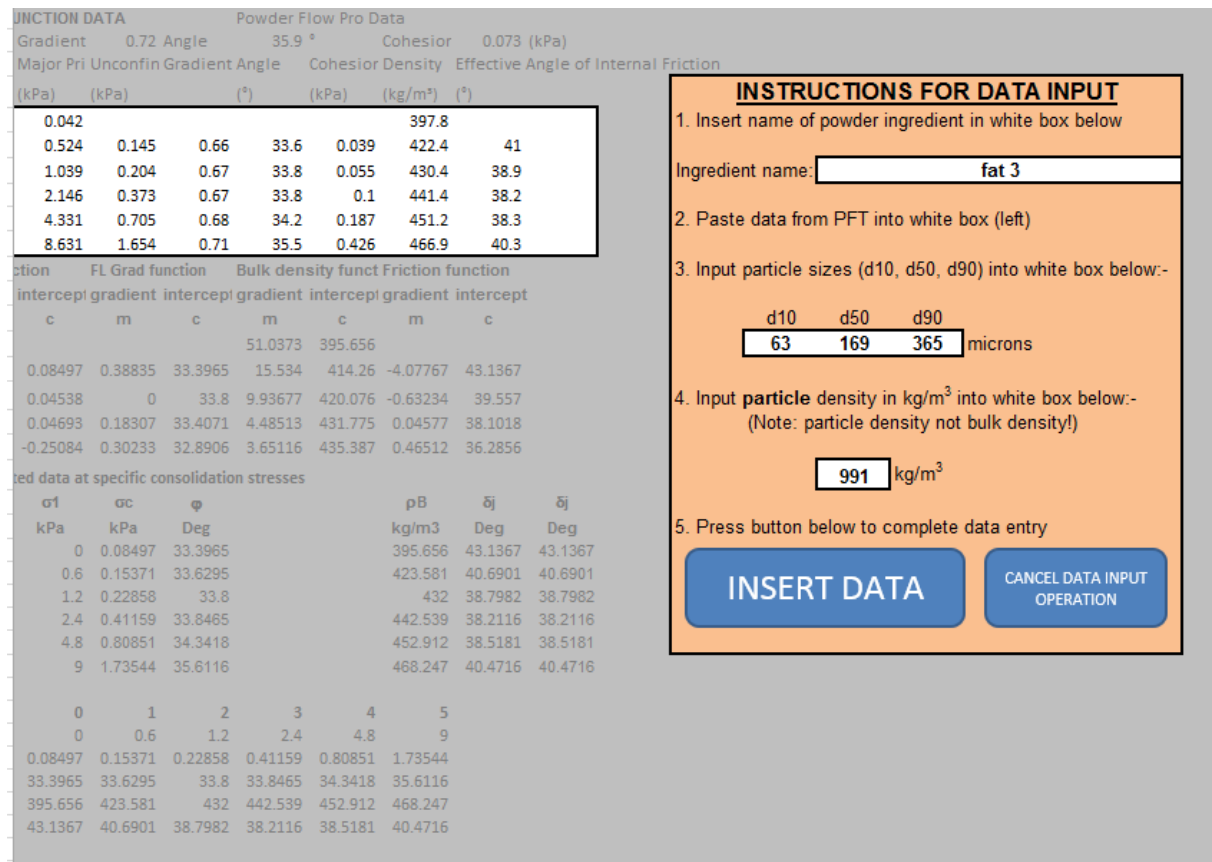


Figure 161: Interface of the data base in the Virtual Powder Blending Laboratory

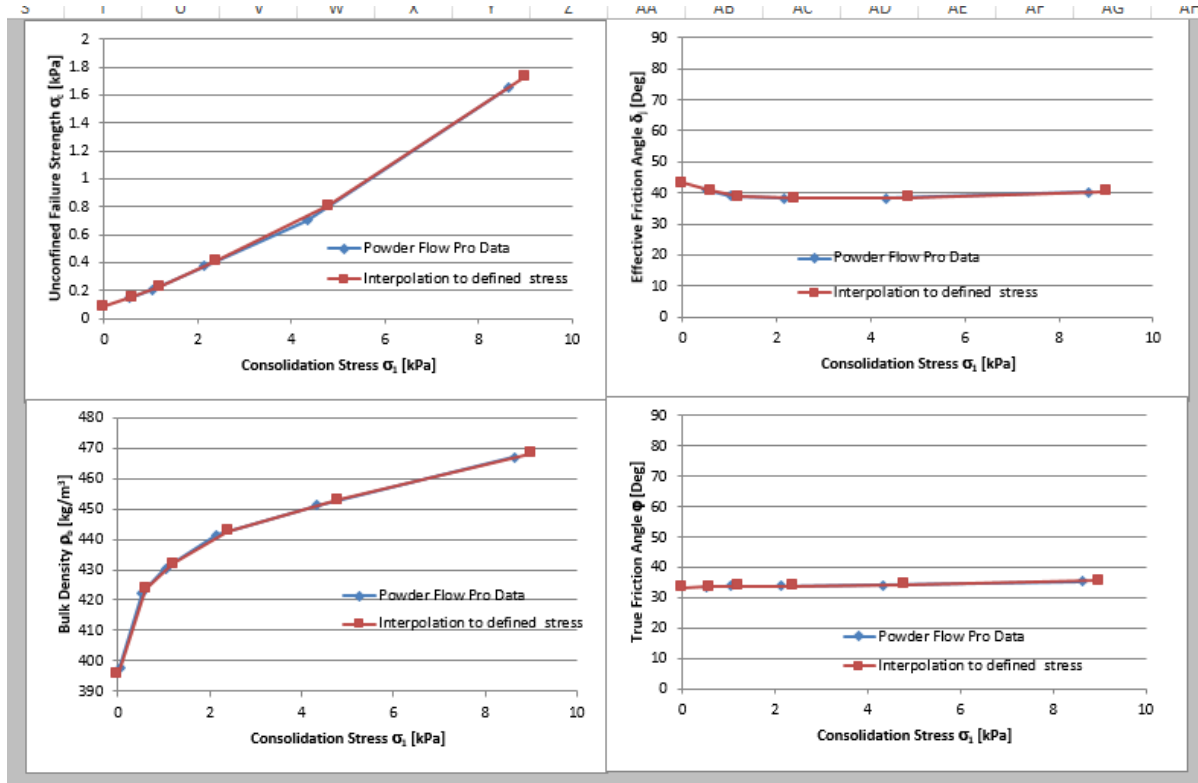


Figure 162: Interface of the data base in the Virtual Powder Blending Laboratory

9.2.7 Application of the prediction tool

This prediction tool has been intended to be a starting point for the prediction and optimisation of the flow behaviour of blended powders, however, the test protocol developed includes recommendations to generalise the use of the prediction tool in other powder conditions non-tested in this research work. Furthermore, recommendations for further work to improve the prediction tool have been made in the last chapter of the thesis, based on the experimental work undertaken and the results and conclusions obtained in this work.

9.3 Test protocol for Industry

The test protocol gives common solutions for issues with the formulation of blended powders and recommendations for users of the prediction tool in specific conditions non-tested in this work.

9.3.1 Common solutions for issues with the formulation of blends

Different common solutions for issues with formulation of blended powders have been presented to help formulators and process engineers to understand how to define the

blend composition with the desirable flow behaviour. Several ways to improve the flow behaviour of blended powders have been explained which could be combined or used independently in the formulated blends.

Blends too cohesive

When a composition of a blended powder is significantly too cohesive, one possible solution is to identify the ingredients which have severe contribution to make the flow behaviour too cohesive. These ingredients could be replaced by other powders which give the same functionality in the blend but have better flowability improving the flow behaviour of the blend. Another possibility is to consider different grades of the same powder in the flowability range of free flowing to cohesive and then a minor change is required to obtain the desirable flow behaviour.

Obviously, a clear solution is to increase the amount of free flow agent in the blend without making the blend significantly too dusty but in some cases, the level of dust generated by the blends in the process line is limited to a certain value and this solution is not a possibility to consider.

Blends too dusty

When a composition of a blended powder is significantly too dusty, one possible solution is to increase the weight percentage of the liquid content in the blend without making the blend significantly too cohesive. If a blend slightly too cohesive is acceptable for the process line, this gives a solution to the problem.

Another possibility is to consider a different free flow additive in the blend using a less dustier flow agent. In this case, the weight percentage content of the new flow agent might need to be increased to obtain the same reduction in the bulk strength due to the addition of liquid content. It makes the new free flow additive less effective but the problem of the level of dust generated will be solved. The use of a different grade of the powders which generate dust in the blend is also a possible solution without changing the type and content of the free flow additive.

9.3.2 Recommendations for non-tested conditions

This final section of the chapter presents the recommendations made for the use of the prediction tool under the following specific conditions of the powders:

- Effect of temperature and humidity
- Moisture adsorption of porous materials
- Effect of bimodal and trimodal particle size distributions
- Use of different liquids and flow agents tested in the research
- Bulk density for packing a variety of particle size

These conditions have been addressed in this protocol and the procedure required to follow when a formulator faces the challenge of predicting the flow behaviour of a blended powder under these conditions has been explained.

Effect of temperature and humidity

The current version of the prediction tool does not consider the effect of the variation of temperature and humidity on the flow behaviour of blended powders. In this research, characterisation tests were undertaken under atmospheric and controlled conditions of 15 to 20°C and 35 to 50%HR. The use of the prediction tool for blends exposed to higher temperature and humidity requires further experimental work running flow function tests in the PFT shear tester under the same environmental conditions of the blend which flow behaviour is going to be predicted.

At high temperature and humidity, it is essential to analyse the composition of the blended powder and identify which powders tend to cake at the specific environmental conditions of the blend. These powders need to be characterised individually running standard flow function tests at different temperatures to determine the conditions which make the powders cake and form agglomerates. The weight percentage content of these powders will determine if they are influential in the flow behaviour of the blend.

Anti-caking agents such as free flow additives need to be added to the blend to avoid flow problems such as erratic flow or no flow. Standard flow function tests should be run at the worst environmental condition of the blend adding an increasing amount of anti-caking agent to find the best composition of the blend.

Moisture absorption of porous particulate materials

The current version of the prediction tool does not consider the effect of porous powders on the components of the blends. The use of the prediction tool for blends made with porous ingredients requires further experimental work running flow function tests in the PFT shear tester. The weight percentage of these powders in the blend

determines their influence on the liquid content added to the blended powder. Generally, ingredients of the blends are added at different assemblies and the liquid is normally added at the beginning to make the blend from the first assemble sticky. The flow agent is normally added in the last assemble so the effect of porous materials in the blend will be noticed if their weight percentage content is high enough to make them influential.

Porous particulate materials are absorbent and contain cavities or interstices which retain part of the liquid added to the powder. These powders need to be characterised individually running standard flow function tests at different levels of liquid content to determine the weight percentage of the liquid which can be absorbed by the powder. This value gives a reference of how much liquid could be retained by the porous powder in the blend.

Once the porous powder is characterised with the liquid of the blend, the next step is to calculate how much liquid is retained by the powder based on its weight percentage in the blend. This requires standard flow function tests at different levels of liquid content to determine when the porous material stops retaining liquid added to the blend; this will be a characteristic value of the porous material in the blend.

The influence of the porous powders in the blends depends on the weight percentage of the particulate material and the particle and bulk flow properties of the components of the blends and therefore a data base should be created with the value of the liquid retained for blends with the same porous material and similar composition of powders.

Effect of bimodal and trimodal particle size distributions

The current version of the prediction tool does not consider the effect of bimodal, trimodal or multimodal particle size distributions of powders on the components of the blends. In the database, particle size distributions are considered unimodal and are characterised by the values of D10, D50 and D90. Powders with multimodal particle size distributions should be sieved in size fractions characterised by unimodal particle size distributions, then each size fraction will be considered a grade of the virgin multimodal powder in the database. Standard flow function tests should be run to characterise these size fractions and their particle size distributions should be characterised by the values of D10, D50 and D90.

Use of different flow agents tested in this research

The current version of the prediction tool offers a limited selection of free flow agents (silicon dioxide and tricalcium phosphate) to be considered in the composition of a blended powder. The use of the prediction tool for blends made with different free flow additives requires further experimental work running flow function tests in the PFT shear tester. Once one blend has been tested with the free flow agent to obtain the optimum free flow level, the prediction tool will determine the flow behaviour for other blends with the same flow agent and similar composition of powders.

Each free flow additive is characterised by its oil capacity (OC) and its efficacy factor (EF) which determine the level of the flow agent required to achieve the lowest strength of a wet powder blended with the free flow additive. Firstly, a standard flow function test of the flow agent is required to determine the bulk strength of 100%wt free flow additive. Secondly, to study the effect of the flow agent on mitigating the effect of the liquid content on the bulk strength of the powder, standard flow function tests of a crystallised particulate material mixed with free flow agent and liquid are required to find the optimum level of free flow additive which gives the lowest strength. It is recommended the use of a range of narrow particle size distributions of glass beads such as 4-45 microns and 75-150 microns to study the effect of the flow agent at different liquid contents such as 1, 2 and 4%wt.

Once different combinations of the flow agent and the liquid have been tested with idealised materials, the next step is to compare the predicted and measured values of a real blended powder applying the oil capacity and efficacy factor average values obtained. It is expected to find that real blends show lower efficacy factor than single idealised materials, however, the initial values of the oil capacity and efficacy factor from the tests undertaken with glass beads can be used as a reference for the predictions of the flow behaviour of any new blend. Particle and bulk flow properties of the components of the blends will determine the value of the efficacy factor and therefore a data base should be created with the value of the parameter for blends with similar composition of powders.

Use of different liquids tested in this research

The current version of the prediction tool offers a limited selection of liquids (Miglyol oil 818 and de-ionised water) to be considered in the composition of a blended powder. The addition of a different liquid such Miglyol oil 829 which is more viscous than Miglyol

oil 818 (300 and 30 mPa.s respectively) or Miglyol oil 840 (10 mPa.s) would not make a difference in the pendular regime of liquid content which upper saturation limit was defined in this research as 25%. In this regime only the capillary forces due to the surface tension and the pressure deficiency in the liquid bridge affect the bulk strength of the powders due to the addition of the liquid. In terms of weight percentage of liquid content, the upper limit of the pendular regime was defined as 6wt%. If the addition of the liquid is greater than this weight percentage limit, then the viscosity of the oil presents a high influence on the bulk strength of the powders.

The prediction of the effect of the addition of liquid on the bulk strength of particulate materials in the funicular and capillary regimes of liquid content was outside of the scope of this research. Further work is required to better understand and make predictions in these regimes with certain accuracy. Nevertheless, the addition of liquid greater than 6-8wt% tends to make the powders too cohesive and therefore the level of flow agent required to improve the flowability increases making the powder too dusty. It is highly recommended not to add a high level of liquid content as a solution for reformulation of blended powders unless it is strictly necessary. Instead, the formulator should think about different type and grade of fillers or different kind of flow agents in the blend.

Bulk density for packing a variety of particle size

One of the recommendations for further work regarding the model developed in this research for dry blended powders is to incorporate the possibility of fine particles packing into the voids between the coarse particles. This would help to predict the bulk density of dry blends more accurately in the Virtual Powder Blending Laboratory.

The best approach for formulators and process engineers to predict the bulk density of different compositions of reformulated blends is to run standard bulk density tests of the dry compositions using the powder flow tester. It is recommended to test several compositions and/or different grades of the same filler of the dry blend to find the combination of fillers which gives the desirable packing condition. This experimental work will help formulators to gain experience on the effect of the particle size on the packing conditions of powders. After the repetition of this process for several reformulations of blends, the user of the protocol and the prediction tool would be able to predict the suitable combination of ingredients based on the experience.

9.4 *Summary*

This chapter presents the outcome of the research which is a test protocol for industry to predict and optimise the flow behaviour of blended powders. However, this research project has been part of a wider Defra sponsored project to develop a prediction tool named Virtual Powder Blending Laboratory recently developed by The Wolfson Centre for Bulk Solids Handling Technology.

The test protocol contains the recommendations regarding how a formulator could face a powder flow problem using the standard characterisation tests disclosed in chapter 3 and the prediction tool Virtual Powder Blending Laboratory to achieve the desirable flow behaviour of a blended powder. This protocol gives common solutions for issues with the formulation of blended powders and recommendations for users of the prediction tool in specific conditions non-tested in this research project such as the effect of temperature and humidity or the effect of bimodal and trimodal particle size distributions.

The research project is directed to the food industry by virtual of the industrial sponsors and Defra funding but the test protocol has the potential for applications in other industry sectors with similar flow problems with particulate materials such as pharmaceuticals, ceramics and metallurgy.

A roadmap of the Virtual Powder Blending Laboratory has been presented including its benefits and current limitations, a description of the user interface (see figure 159), instructions for the user to input data and a guidance to help to understand the results predicted. A database of the particle and bulk flow properties of a wide range of particulate materials was developed in the form of a spreadsheet as part of the prediction tool. This database is based on the data obtained from the characterisation of materials undertaken in this research project using the sampling techniques disclosed in chapter 3 of the thesis and can be updated by the user adding the data corresponding to new single powders as shown in figures 160 – 162.

Chapter 10 Conclusions and suggestions for further work

10.1 Achievement of aim and objectives

The aim of the project was to develop an “empirical understanding” of the links between the particle properties and bulk flow properties of powders in order to predict the bulk flow properties of single particulate materials, or blended powders based on changes to the particle properties or blend components. To achieve this, the following objectives were proposed:

- 1) Calibration of analytical well-established models found in the literature linking the particle properties to the bulk flow properties of powders using a limited number of bulk flow property tests considering simplifications for practical use of the models.
- 2) Evaluation of the applicability of these calibrated models to design powder handling equipment and assess the flow behaviour of single particulate materials or blended powders in industrial processes.
- 3) Identification of methods or techniques that process engineers and formulators could use to predict the bulk flow properties of their single materials, or blended powders based on changes to the particles properties or blend components.

These aim and objectives were fully achieved by the programme of work devised in this research as follows:

- An extensive literature review was undertaken to review the suitable testing techniques for the purposes of the research at particle and bulk scale and find analytical models linking the particle properties to the bulk flow properties of powders.
- Visits to food industrial partners' plants to understand the flow property related handling issues present in the food industry and test a wide range of blended food powders with poor and good flow behaviour under different conditions.
- An industrial case study was undertaken as a preliminary experimental work of the research to reformulate a snack flavour to remove monosodium glutamate from the standard blended powder.
- Characterisation at particle and bulk scale of the food single powders, free flow agents and liquids commonly used in the blended flavours of the industrial partners to develop a database of these ingredients.

- A series of experimental test programmes were undertaken to evaluate the models found in the literature and develop a better understanding of the links between the particle and bulk scale studying the effects on bulk flow and packing properties of changing:
 - Particle size and distribution
 - Particle shape
 - Surface liquid content and type
 - Free flow agent content and type
- Development of new empirical particle to bulk scale models based on the experimental work undertaken and the practical understanding acquired of the links between the particle properties and bulk flow properties of powders.
- Development of a test protocol for industry to help formulators and process engineers to predict the effect of changes in particle properties and/or blend composition on the bulk flow behaviour of blended powders.

10.2 *Contributions to knowledge*

This project claims the following contributions to knowledge:

1. Understanding of the physics by which a variety of different additives to food powder blends act to modify their flow properties as a result of their interactions with commonly used ingredients.
2. Understanding the basics of how to select additional ingredients to give the best balance of controlled and desirable flow properties in industrial processes.
3. Development of new empirical particle to bulk scale models to predict the flow properties of single and blended particulate materials in dry and wet condition with and without free flow additives.
4. Development of a test protocol which in combination with the standard characterisation tests commonly used in the powder industry and the prediction tool called Virtual Powder Blending Laboratory (recently developed by The Wolfson Centre for Bulk Solids Handling Technology) will help formulators and process engineers to formulate the composition of blended powders with the desirable flow behaviour in industrial process lines.

10.3 Critical assessment of the research approach

It has been shown in this research that it is possible to predict the flow behaviour of blended powders based on the knowledge of the particle and bulk flow properties of their ingredients. The effect of changes in particle properties and/or blend composition on the bulk flow behaviour of blended powders can be predicted using the test protocol developed in this research.

The modelling approach followed was to calibrate empirically analytical models found in the literature using a limited number of bulk flow property tests and develop new empirical models based on the results obtained from the validation of the analytical models.

In order to make these predictions, it was initially required to develop the understanding of the links between the particle properties and bulk flow properties of powders using idealised and crystallised particulate materials such as glass beads, sodium chloride or crushed glass. These materials were used to test the hypotheses developed in the preliminary studies of the research before moving on to apply them to real single and blended powders.

There were a great number of factors to consider in the hypotheses and their effect needed to be studied independently. Due to the complexity of the particle system, it was necessary to take into account that the recommendations and procedures proposed in the test protocol should be based on particles and bulk flow properties measurable by industry and standard characterisation testing techniques commonly used in process industries.

This matter could be considered a limitation of the research, however, the particle and bulk flow properties used in this work cover the required parameters needed to characterise the powders. Some properties such as particle density are not common to be measured by industry, and for this reason, a material property database was created with the powders characterised in this work. This database covers most of the particulate materials used by industrial partners but it must be updated with the data of new ingredients present in the blended powders.

Another possible limitation of this work is the fact that simplifications were made in the development of the modelling work in order to develop an empirical and practical understanding of the link between particle and bulk scale. The scope of the work was

defined to make sure that the aim and objectives of the project were realistic and achievable. Obviously, further work is required to understand clearly the effect of the factors not considered in this work on the flow behaviour of blended powders. However, the test protocol gives recommendations for specific conditions non-tested in this research and how to use the Virtual Powder Blending Laboratory in these cases. The project was directed heavily to the food industry by virtual of the industrial sponsors and DEFRA funding but the findings of the research have also been intended to be used in other industry sectors with similar flow problems with powders, such as pharmaceuticals, ceramics and powder metallurgy.

10.4 Conclusions

The validation of the analytical models found in the literature showed that the existing well-established models are qualitatively encouraging but they need to be modified to be able to produce practical predictions for industry. These models present simplifications in terms of particle properties which reflects the complexity of considering variables such as particle size distributions or different particle shapes in the development of models to predict the bulk properties of powders.

Several models were found for single particulate materials but for blended powders, no well-established analytical model were found to predict the flow properties of blends. In this research, a new model has been developed for dry blended powders to predict the average bulk strength, internal friction and bulk density. The results obtained from this new model showed good agreement in the predictions but still the model requires further work in several aspects like consideration of the full size distribution in the input data of the powders and the possibility of fine particles packing into the voids between the coarse particles which will improve the predictions of the bulk density.

Also new empirical models were developed in this research based on the practical understanding acquired along the work undertaken in this project. These models predict the bulk strength for single dry powders and the effect of liquid content and free flow agent level on the bulk strength of single and blended powders.

10.5 *Recommendations for further work*

A test protocol for industry has been developed successfully to predict and optimise the flow behaviour of blended powders. This protocol is used in combination with the prediction tool Virtual Powder Blending Laboratory recently developed by The Wolfson Centre for Bulk Solids Handling Technology and the standard characterisation tests for particle and bulk flow properties commonly used in industrial processes. As the prediction tool is based on the work developed in this research, the following recommendations for further work based on the experimental work undertaken and the results and conclusions obtained could be used to improve the prediction tool.

- 1) A limited selection of free flow agents (silicon dioxide and tricalcium phosphate) and liquids (Miglyol oil 818 and de-ionised water) have been tested in the development of the empirical models and therefore, more experimental work needs to be done with different type of free flow additives and liquids.
- 2) The development of the empirical model for predicting the effect of the level of free flow additive on the bulk strength of wet powders was based on limited amount of tests undertaken with coarse and fine glass beads. The application of the model to real blended powders showed that real particulate materials presented lower efficacy factor than idealised materials. The values of efficacy factor obtained from glass beads can be used as a reference but further work needs to be done to investigate the mechanism of the mitigation of liquid content on the bulk strength of real blended powders.
- 3) In this research, the particle shape of powders was classified qualitatively based on limited tests using SEM; a quantitative study is required to understand the effect of the particle shape in the prediction of the flow behaviour of blended powders. The examination of this factor in the models developed would add an extra dimension to this work considering the wide range of particulate materials characterised.
- 4) The design of a mass flow hopper requires information about the friction between the powder and the hopper wall. However, wall friction testing was considered outside the scope of this work because it would add another dimension to the experimental and modelling work. For industrial plants operating in core flow as partners' ones, the findings of the research are applicable but further work is required for plants operating in mass flow.

- 5) The test protocol gives recommendations of how to use the Virtual Powder Blending Laboratory with powders under non-tested conditions in this research such as the effect of temperature and humidity, moisture adsorption of porous materials or bimodal and multimodal particle size distributions. These recommendations are only a guidance to help formulators and process engineers to deal with these untested conditions but further work is needed to have a better understanding of the effect of these conditions in the flow behaviour of blended powders.
- 6) Several variables of the particle system such as surface roughness or surface energy were not considered due to the practical approach of the research. These are difficult to be measured using standard characterisation testing techniques commonly used in industry. The omission of these variables is not critical considering the purpose of this research and further work is required to study their effect on the flow behaviour of blended powders.

References

- Adams M. J. & Perchard V. The cohesive forces between particles with interstitial liquid, International Chemical Engineering Symposium Series, No. 91, **1985**, 147 - 160
- Adams M. J. & Edmondson B. Forces between particles in continuous and discrete liquid media, in: B. J. Briscoe, M. J. Adams (Eds.), Tribology in Particulate Technology, A. Hilger, Bristol, England, **1987**, 154 – 172
- Alonso M. & Alguacil F. J. Stochastic Modelling of Particle Coating, American Institute of Chemical Engineers Journal (AIChE), 47(6), **2001**, 1303 – 1308
- Argento C. & French R. H. Parametric tip model and force – distance relation for Hamaker constant determination from atomic force microscopy, Journal of Applied Physics, 80, **1996**, 6081pp
- Arnold, P.C. Some observations on the importance of particle size in bulk solids handling, Powder Handling and Processing, 13 (1), **2001**, 35 – 40
- ASTM Standard D6128: Standard test method for shear testing of bulk solids using the Jenike shear cell. ASTM International, www.astm.org
- ASTM Standard D6773: Standard Shear Test Method for Bulk Solids Using the Schulze Ring Shear Tester. ASTM International, www.astm.org
- Bell, T. A., Ennis, B. J. & Grygo, R.J. Practical Evaluation of the Johanson Hang-up Indicizer, Bulk Solids Handling, 14 (1), **1994**, 117 – 125
- Ben Aim R. & Le Goff P. The Coordination Number of Disordered Stacks of Spheres – Application to Binary Mixtures of Spheres, Powder Technology, 2(1), **1968**, 1 – 12
- Benn, D.I. & Ballantyne, C. K. The description and representation of the particle shape, Earth Surface Processes and Landforms, 18(7), **1993**, 665 – 672
- Bernal J. D. Mason J. & Knight K. R. Radial Distribution of the Random Close Packing of Equal Spheres, Nature, 194, **1962**, 957 – 958
- Berry R.J. & Bradley, M.S.A. Development of the Brookfield Powder Flow Tester, Bulk Solids Europe 2010 Conference and IMechE Symposium in New Frontiers in Bulk Materials Handling, Glasgow, Sept. 9-10, **2010**

- Berry R.J. Bradley M.S.A. & McGregor R.G. Brookfield powder flow tester – Results of round tests with CRM-116 limestone powder, Proceedings of the Institution of Mechanical Engineers, Part E: Journal of Process Mechanical Engineering, **2014**, 1 – 16
- Blott, S.J. & Pye, K. Particle shape: A review and new methods of characterisation and classification, *Sedimentology* 55, **2008**, 31 – 63
- Breum N.O. The rotating drum dustiness tester: Variability in dustiness in relation to sample mass, testing time and surface adhesion, *The Annals of Occupational Hygiene*, 43(8), **1999**, 557 - 566
- Bridgwater J. Foo W. S. & Stephens D. J. Particle Mixing and Segregation in Failure Zones: Theory and Experiment, *Powder Technology*, 41(2), **1985**, 147 – 158
- Briscoe, B.J. & Adams, M.J. Tribology in Particulate Technology, IOP Publishing, Bristol, chapter 1.3, **1987**, p. 43
- Carr J. F. & Walker D. M. An annular shear cell for granular materials, *Powder Technology*, 1(6), **1968**, 369 – 373
- Coelho M. C. & Harnby N. Moisture Bonding in Powders, *Powder Technology*, 20(2), **1978**, 201 - 205
- Christakis N. Wang J. Patel M. K. Bradley M. S. A. Leaper M. C. & Cross M. Aggregation and caking processes of granular materials: continuum model and numerical simulation with application to sugar, *Advanced Powder Technology*, 17(5), **2006**, 543 – 565
- Das S. Sreeram P. A. & Raychaudhuri A. K. A method to quantitatively evaluate the Hamaker constant using the jump – into – contact effect in atomic force microscopy, *Nanotechnology*, 18(3), **2007**, 6pp
- Davis R. A simple feature-space representation of particle shape, *Powder Technology*, 12(2), **1975**, 111 - 124
- Ennis B. J. Li J. Tardos G. L. Pfeffer R. The influence of viscosity on the strength of an axially strained pendular liquid bridge, *Chemical Engineering Science*, 45(10), **1990**, 3071 - 3088

- Feng C. L. & Yu A. B. Effect of liquid addition on the packing of monosized coarse spheres, *Powder Technology*, 99(1), **1998**, 22 – 28
- Forsyth A.J. & Rhodes M. J., A simple model incorporating the effects of deformation and asperities into the van der Waals force for macroscopic spherical solid particles, *Journal of Colloid and Interface Science*, 223(1), **2000**, 133 – 138
- Forsyth A. J. Hutton S. R. Osborne C. F. & Rhodes M. J. Effects of Interparticle Force on the Packing of Spherical Granular Material, *Physical Review Letters*, 87(24), **2001**, 244301
- Frew I. Wypych P.W. & Mar L. Different modes of dust testing for bulk solids, ICBMH 2013 - 11th International Congress on Bulk Materials Storage, Handling and Transportation, Australia: The University of Newcastle, **2013**, pp 1 – 8
- German R. M. Particle Packing Characteristics, Metal Powder Industries Federation, Princeton, New Jersey, **1989**
- Gilbert E. N. Randomly Packed and Solidly Packed Spheres, *Canadian Journal of Mathematics*, volume 16, **1964**, 286 – 298
- Glor M. Electrostatic Hazards in Powder Handling, Research Studies Press Limited, Letchworth, Hertfordshire, England, John Wiley & Sons Inc. **1988**
- Goldman A. J. Cox R. G. & Brenner H. Slow viscous motion of a sphere parallel to a plane wall – Motion through a quiescent fluid, *Chemical Engineering Science*, 22(4), **1967**, 637 - 651
- Graton L. C. & Fraser H.J. Systematic Packing of Spheres with particular relation to Porosity and Permeability, *Journal of Geology*, 43(8), Part I, **1935**, 785 – 909
- Gray W. A. The Packing of Solids Particles, Chapman and Hall, London, UK, **1968**
- Hann D. and Strazisar J. Laboratory device for preparing round particles, 11th European Symposium on comminution, Book of Abstracts, Budapest, Hungary, October 9 – 12, **2006**
- Hann D. and Strazisar J. Influence of Particle Size Distribution, Moisture Content and Particle Shape on the Flow Properties of Bulk Solids, *Instrumentation Science and Technology*, 35 (5), **2007**, 571 – 584

- Herdan G. Small Particle Statistics. An account of Statistical Methods for the investigation of Finely Divided Materials, Second revised edition, London; Butterworths, **1960**, First edition, Amsterdam; Elsevier Publishing Co. With a guide to the experimental design of particle size determinations by M. L. Smith, **1953**
- Heywood H. Numerical definitions of particle size and shape, Chemical Technology and Biotechnology, 56(7), **1937**, 149 – 154
- Heywood H. Particle shape coefficients, Journal of the Imperial College Chemical Society, 8, **1954**, 15 – 33
- Hjemsted K. & Schneider T. Documentation of a dustiness drum test, The Annals of Occupational Hygiene, 40(6), **1996**, 627- 643
- Iveson S. M. Litster J.D. Hapgood K. & Ennis B. J. Nucleation, growth and breakage phenomena in agitated wet granulation processes: a review, Powder Technology, 117(1-2), **2001**, 3-39
- Iveson S. M. Beathe J. A. & Page N. W. The dynamic strength of partially saturated powder compacts: the effect of liquid properties, Powder Technology, 127(2), **2002**, 149 – 161
- Iwasaki T. Satoh M. & Ito T. Determination of optimum operating conditions based on energy required for particle coating in a dry process, Powder Technology, 123 (2-3), **2002**, 105 – 113
- Jenike A. W. Gravity Flow of Bulk Solids, Bulletin 108, Utah Engineering Station, **1961**
- Jenike A. W. Flow and Storage of Solids, Bulletin 123, Utah Engineering Station, **1964**
- Johanson J. R. The Johanson Indicizer system vs the Jenike shear tester, Bulk Solids Handling, 12(2), **1992**, 237 - 240
- Johanson K, Rabinovich Y, Moudgil B, Breece K & Taylor H, Relationship between particle scale capillary forces and bulk unconfined yield strength, Powder Technology, 138 (1), **2003**, 13 – 17
- Kaye B. H. Clark G. G. & Ying Liu Characterization the structure of abrasive fine particles, Particle and Particle Systems Characterization, 9(1), **1992**, 1 – 8
- Kristensen, H. G. Advances in Pharmaceutical Sciences (Volume 7): Particle Agglomeration, Academic Press, **1995**

- Kurz, H. P. & Munz, G. The influence of particle size distribution on the flow properties of limestone powders, *Powder Technology*, 11(1), **1975**, 37 - 40
- Liden, G. Dustiness Testing of Materials Handled at workplaces, *The Annals of Occupational Hygiene*, 50(5), **2006**, 437 - 439
- Lian, G. Thornton C. & Adams M. J. A theoretical study of the liquid bridge forces between two rigid spherical bodies, *Journal of Colloid and Interface Science*, 161 (1), **1993**, 138 – 147
- Lombay G. Sundararajan S. Wang K. & Subramaniam S. A test method for determining adhesion forces and Hamaker constants of cementitious materials using atomic force microscopy, *Cement and Concrete Research*, 41(11), **2011**, 1157 – 1166
- Manegold, E. Kapillarsysteme, Verlag Strassenbau, Chem. U. Technik Heidelberg, **1955**, p. 294
- Manson G. Radial Distribution Functions from Small Packings of Spheres, *Nature*, 217, **1968**, 733 - 735
- Mazzone D. N. Tardos G. I. & Pfeffer R. The behaviour of liquid bridges between two relatively moving particles, *Powder Technology*, 51(1), **1987**, 71 – 83
- McGlinchey D. *Characterisation of Bulk Solids*, Oxford Wiley Blackwell, **2005**
- McGlinchey D. *Bulk solids handling: equipment selection and operation*, Oxford Wiley Blackwell, **2008**
- Meiners K.E. *Process Handbook, Complex Metal Powder Shapes by Injection Molding*, Battelle Columbus Division, Columbus, OH, **1985**
- Milewski J. V. in H. S. Katz (Eds.) *Handbook of Fillers and Reinforcements for Plastics*, Van Nostrand – Reinhold, New York, **1987**, p. 14
- Mitarai, N. & Nori, F. *Wet Granular Materials, Advances in Physics*, Taylor & Francis, Volume 55, Issue 1-2, **2006**, p. 1 - 45
- Mizuno M. Fukaya A. Jimbo G. *KONA Powder Part 9*, **1991**, p. 19
- Molerus, O. & Nywlt, M. The influence of the fine particle content of the flow behaviour of bulk materials, *Powder Technology*, 37(1), **1984**, 145 – 154
- M. van der Kraan, *Techniques for the Measurement of the Flow Properties of Cohesive Powders*, PhD Dissertation Delft University, **1996**

- Newitt D. M. & Conway-Jones J. M. A contribution to the theory and practice of granulation, Transactions of the Institution of Chemical Engineers, 36, **1958**, 422 – 441
- Oger L. Troadec J. P. Bideau D. Dodds J. A. & Powell M. J. Properties of Disordered Sphere Packings I. Geometric Structure: Statistical Model, Numerical Simulations and Experimental Results, Powder Technology, 46(2-3), **1986**, 121 – 131
- Onwulata C. Encapsulated and Powdered Foods, Food Science and Technology, Boca Raton, London, Taylor & Francis, **2005**
- Parsons D. S. Particle Segregation in Fine Powders by Tapping as Simulation of Jostling During Transportation, Powder Technology, 13(2), **1976**, 269 – 277
- Peschl, I. Arching and rat-holing in silos, Powder Handling & Processing, 13 (4), **2001**, 357-363
- Pierrat, P. & Caram, H. S. Tensile Strength of Wet Granular Materials, Powder Technology, 91(2), **1997**, 83 – 93
- Pfeffer R. Dave R. N. Wei D. & Ramlakhan M. Synthesis of engineered particulates with tailored properties using dry particle coating, Powder Technology, 117(1-2), **2001**, 40 – 67
- Roberts, A. W. 100 years of Janssen, National Conference Publication, Institution of Engineers, Australia NCP, number 4/V1, **1995**, pp. 1 – 20
- Rumpf, H. Grundlagen und Methoden des Granulierens, Chemie Ingenieur Technik, 30(3), **1958**, 144 – 158
- Rumpf, H. The strength of granules and agglomerates, International Symposium on Agglomeration, Philadelphia, Pa., American Institute of Mining, Metallurgical and Petroleum Engineers, INC, W. A. Knepper, ed., Interscience, **1962**, pp. 379 - 418
- Salman, A.D., Hounslow, M.J. & Seville, J. P. K. Handbook of Powder Technology, Vol. 11 Granulation, Chapter 21, Breakage in Granulation, **2006**, pp 998
- Sandell, E. Industrial Aspects of Pharmaceuticals, Swedish Pharmaceutical Press, **1993**
- Schulze, D. Powder and Bulk Solids: Behaviour, Characterisation, Storage and Flow, Springer, **2008**
- Scott G. D. Packing of Equal Spheres, Nature, 188, **1960**, 908 – 909

- Scott G.D. & Kilgour D. M. The Density of Random Close Packing of Spheres, *Journal of Physics D: Applied Physics*, 2(6), **1969**, 863 – 866
- Seville J.P.K. Willet C.D. & Knight P.C. Interparticle forces in fluidisation: a review, *Powder Technology*, 113(3), **2000**, 261-268
- Suzuki M. Makino K. Yamada M. & Inoya K. A study on the coordination number in a System of Randomly Packed, Uniform-Sized Spherical Particles, *International Chemical Engineering*, 21, **1981**, 482 – 488
- Tanaka T. Evaluating the caking strength of powders, *Industrial and Engineering Chemistry Product Research and Development*, 17(3), **1978**, 241 – 246
- Wadell H. Volume, shape and roundness of rock particles, *Journal of Geology*, 40(5), **1932**, 443 - 451
- Wadell H. Sphericity and roundness of rock particles, *Journal of Geology*, 41(3), **1933**, 310 - 331
- Wadell H. Volume, shape and roundness of quartz particles, *Journal of Geology*, 43(3), **1935**, 250 - 280
- Williams J.C. The Segregation of Particulate Materials: A Review, *Powder Technology*, 15(2), **1976**, 245 – 251
- Yang, Wen-Ching, *Fluidization Solids Handling and Processing: Industrial Applications*, Noyes Publications, **1999**
- Yang, J. Sliva A. Banerjee A. Dave R. N. & Pfeffer R. Dry particle coating for improving the flowability of cohesive powders, *Powder Technology*, 158(1-3), **2005**, 21-33
- York P. & Rowe R. C. Monitoring granulation size enlargement processes using mixer torque rheometry, *First International Particle Technology Forum*, Denver, USA, **1994**
- Yu A. B. Standish N. & Lu L. Coal agglomeration and its effects on bulk density, *Powder Technology*, 82(2), **1995**, 177 – 189
- Yu A. B. Bridgwater J. Burbidge A. On the modelling of the packing of fine particles, *Powder Technology*, 92 (3), **1997**, 185 – 194
- Yu A. B. Feng C. L. Zou R. P. & Yang R. Y. On the relationship between porosity and interparticle forces, *Powder Technology*, 130(1-3), **2003**, 70 – 76

Appendix A: Modelling Work

A1 Introduction

The evaluation of the analytical models found in the literature and the empirical models developed in the research generated a large amount of data and it was not possible to show all the data in chapters 7 and 8; this appendix contains the data not presented in these chapters.

A2 Analytical models for single dry powders

This section shows more results of the measured and predicted packing structure and bulk strength as described in the chapter 7.

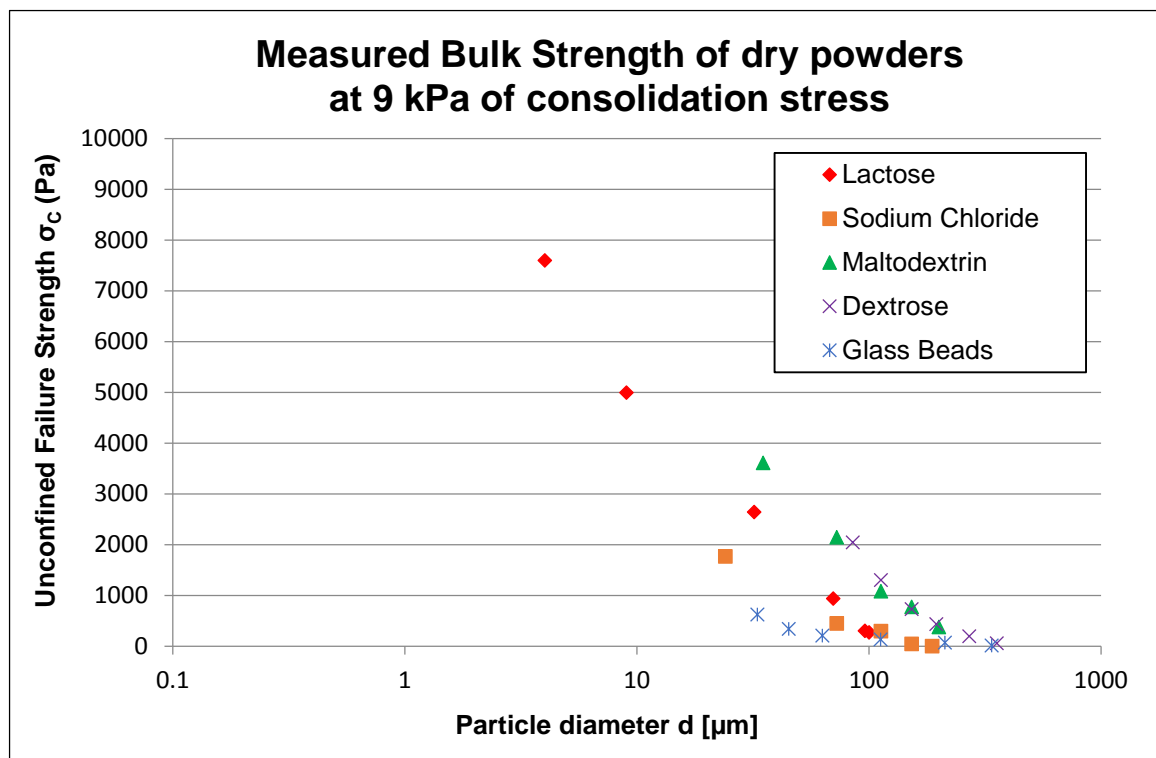


Figure A1

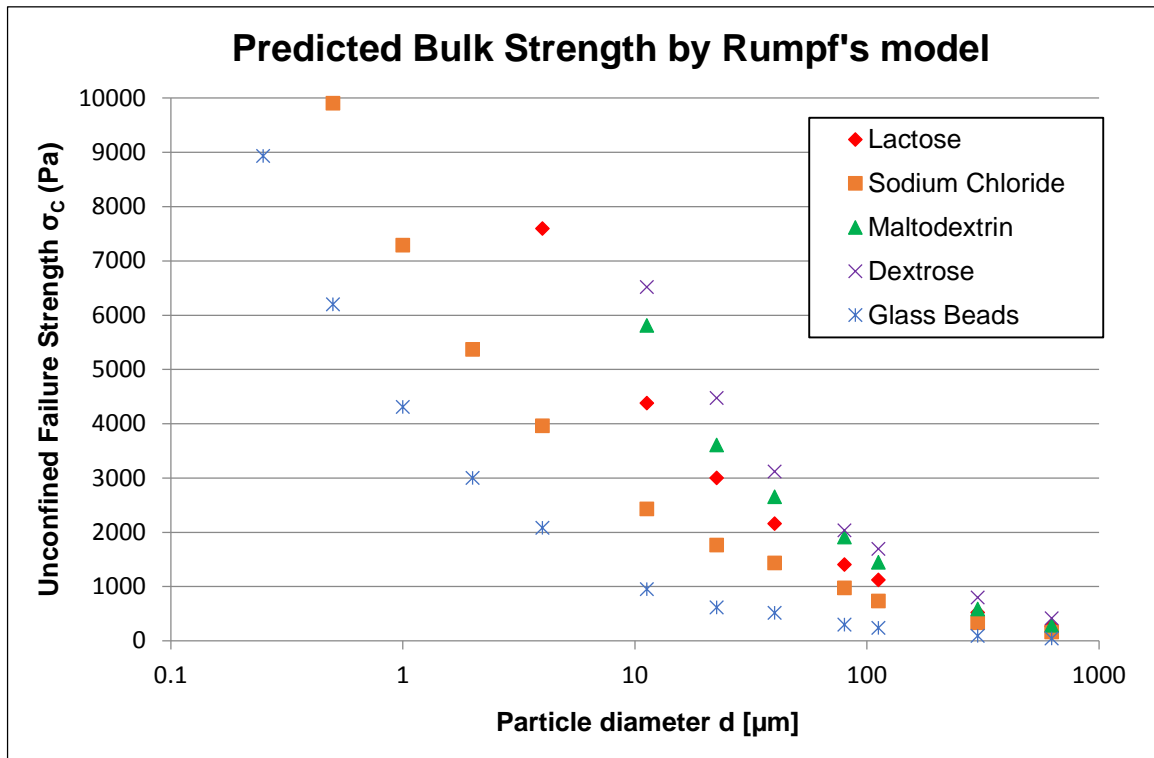


Figure A2

A3 Model proposed for dry blends

This section presents the measured and predicted bulk density and effective internal friction for the blends shown in chapter 7:

- Blends made with size fractions of the same powder
- Blends made with different grades of the same powder
- Blends made with different powders at various ratios of blend

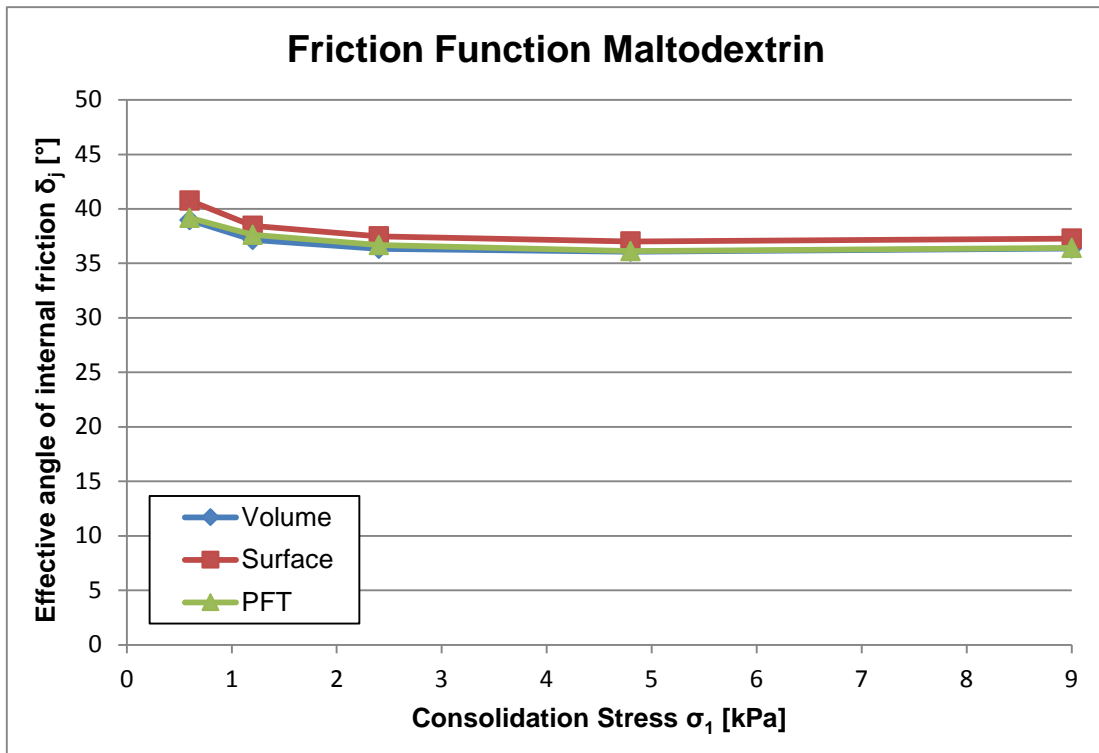


Figure A3

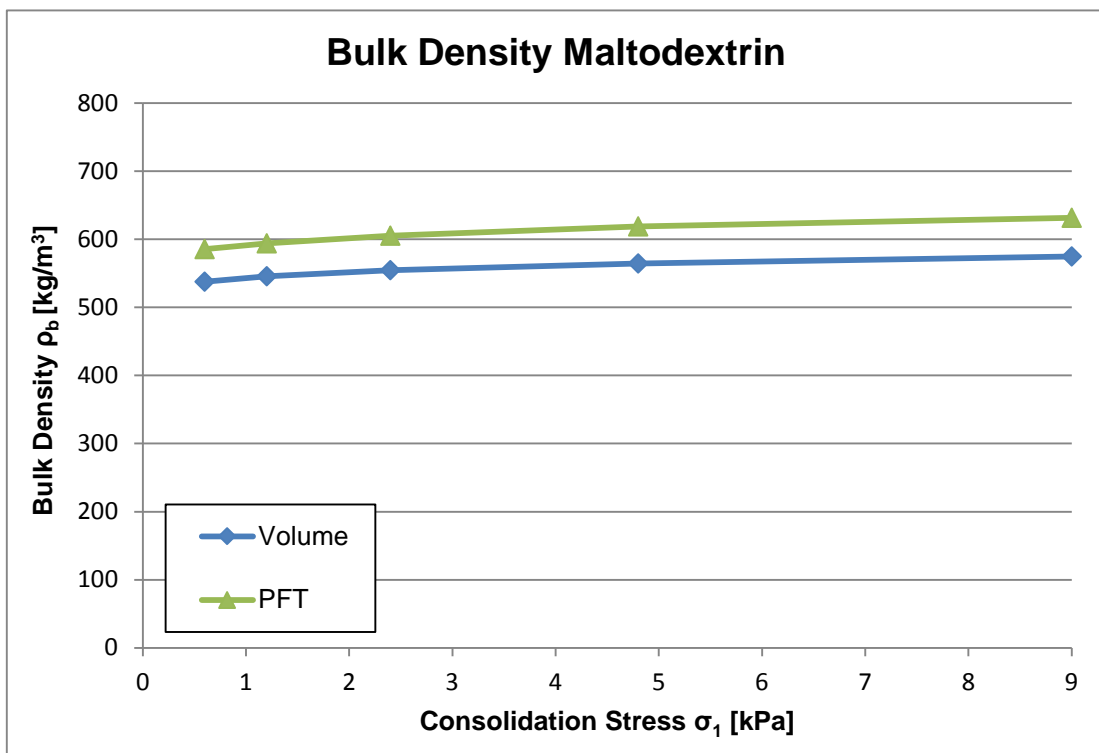


Figure A4

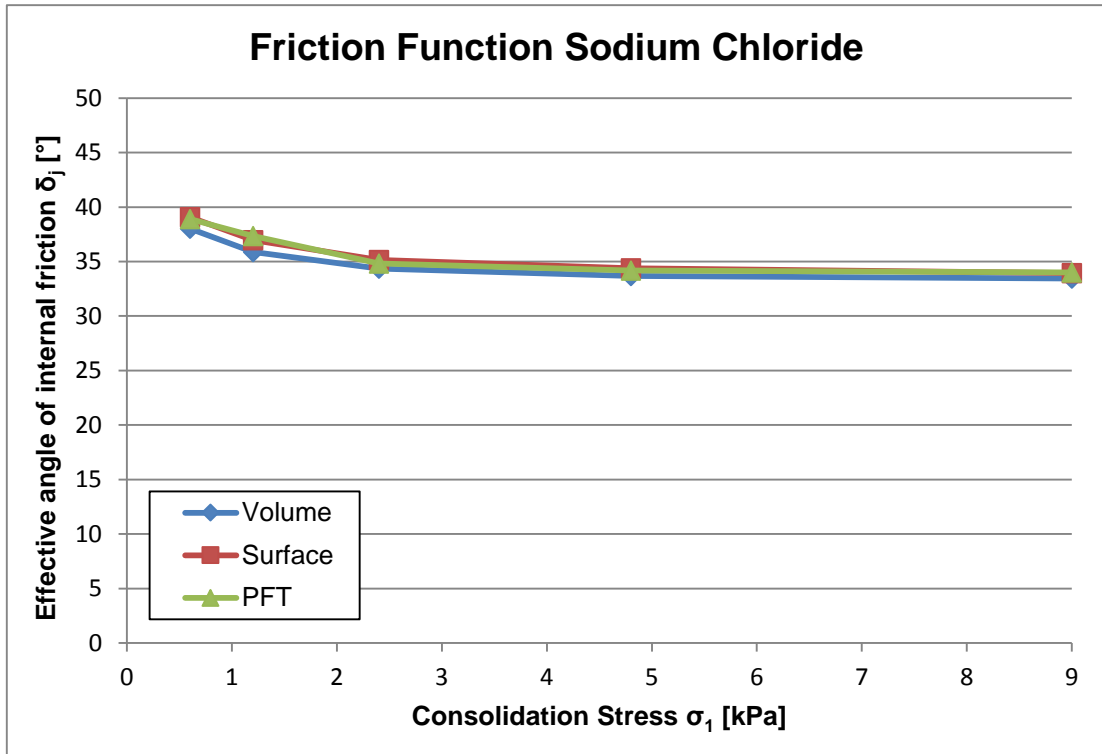


Figure A5

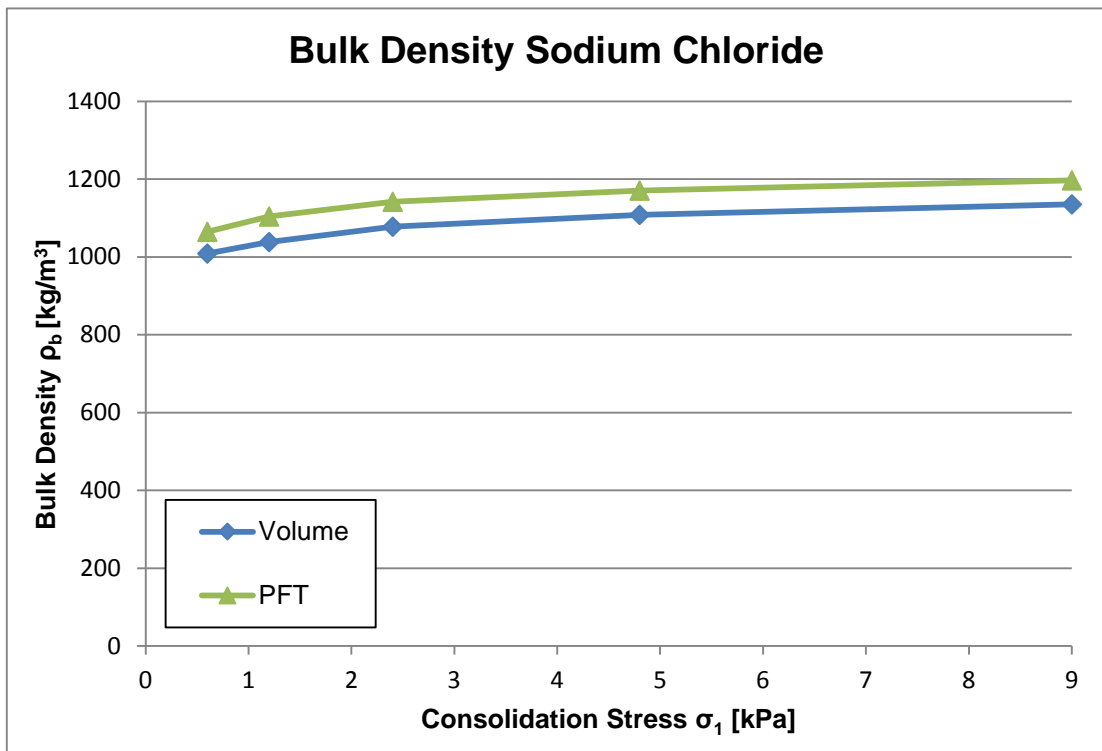


Figure A6

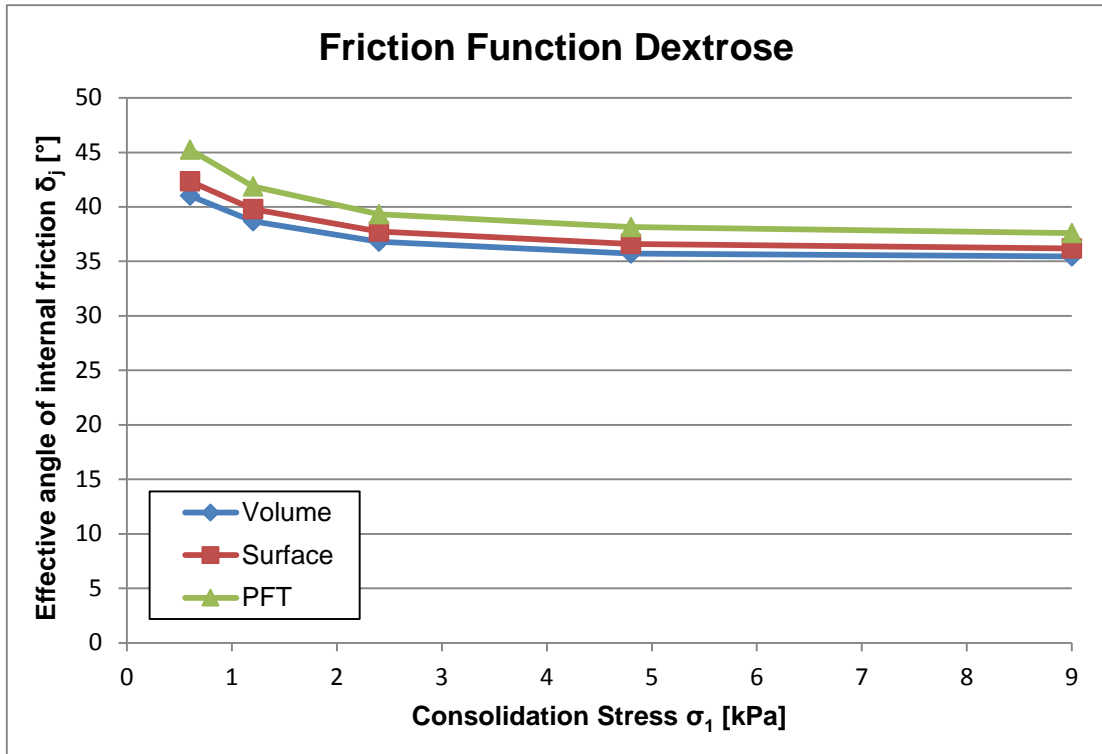


Figure A7

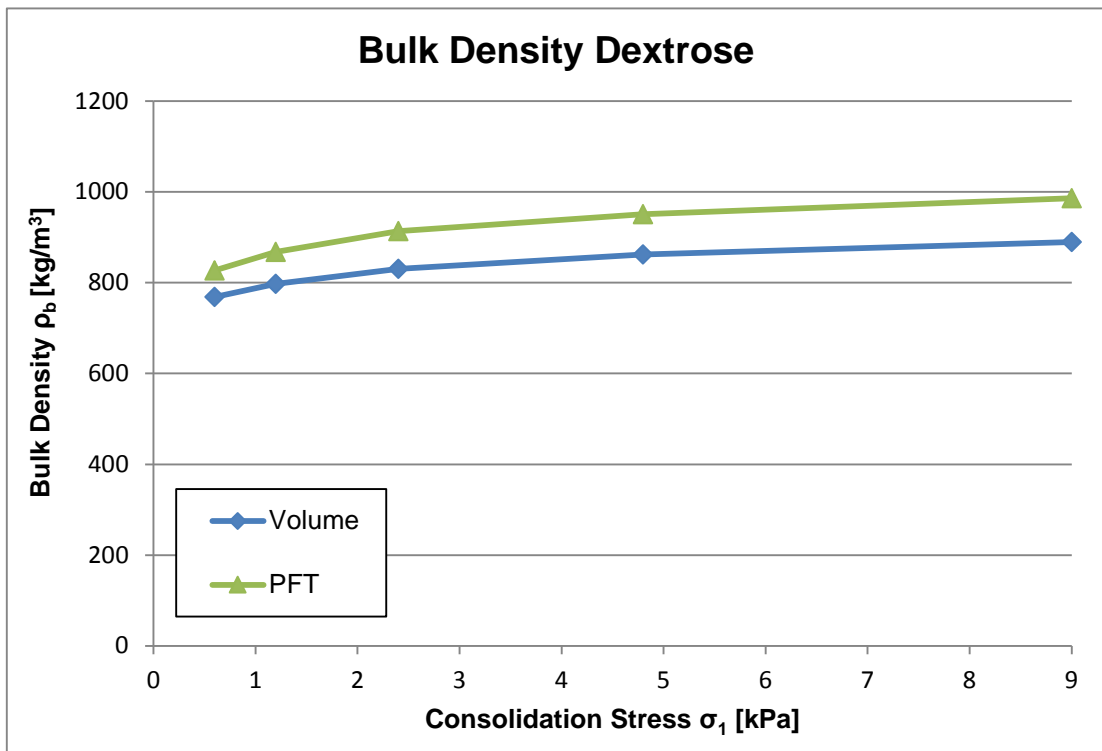


Figure A8

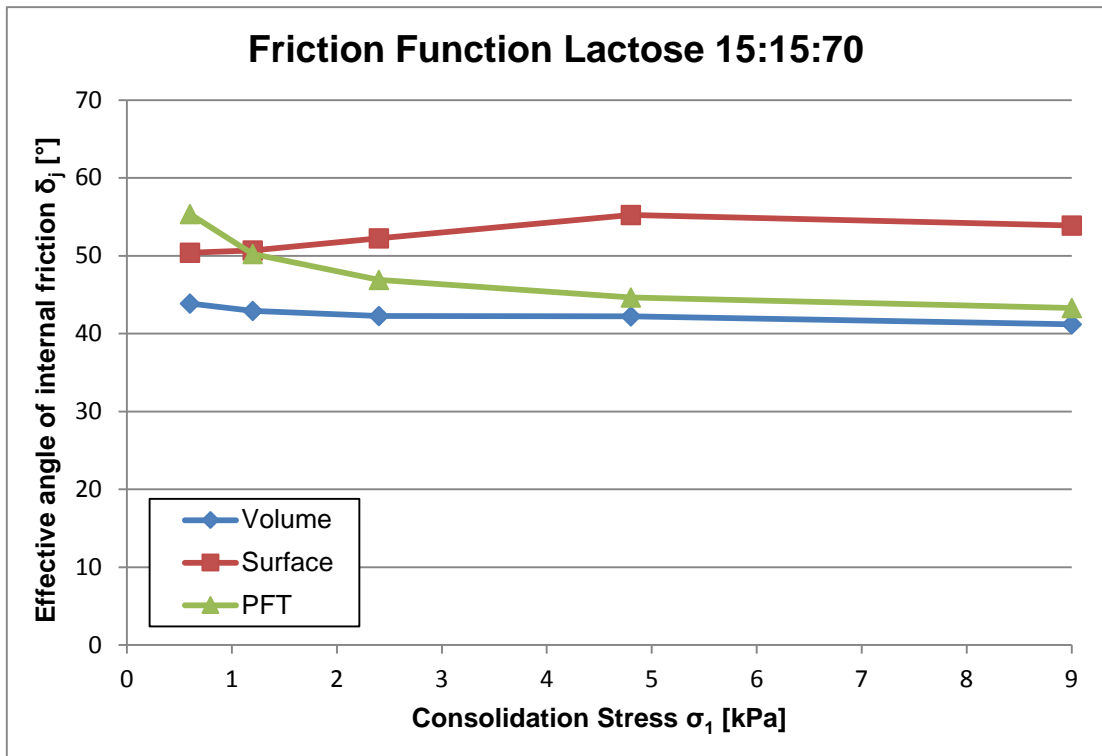


Figure A9

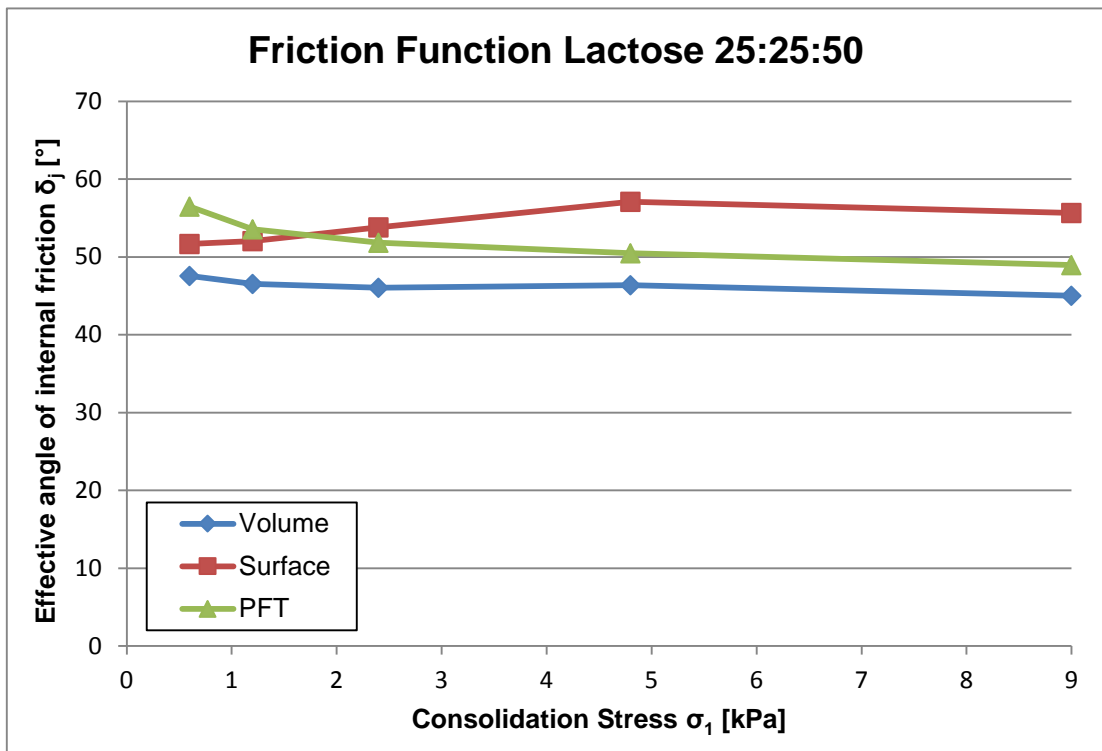


Figure A10

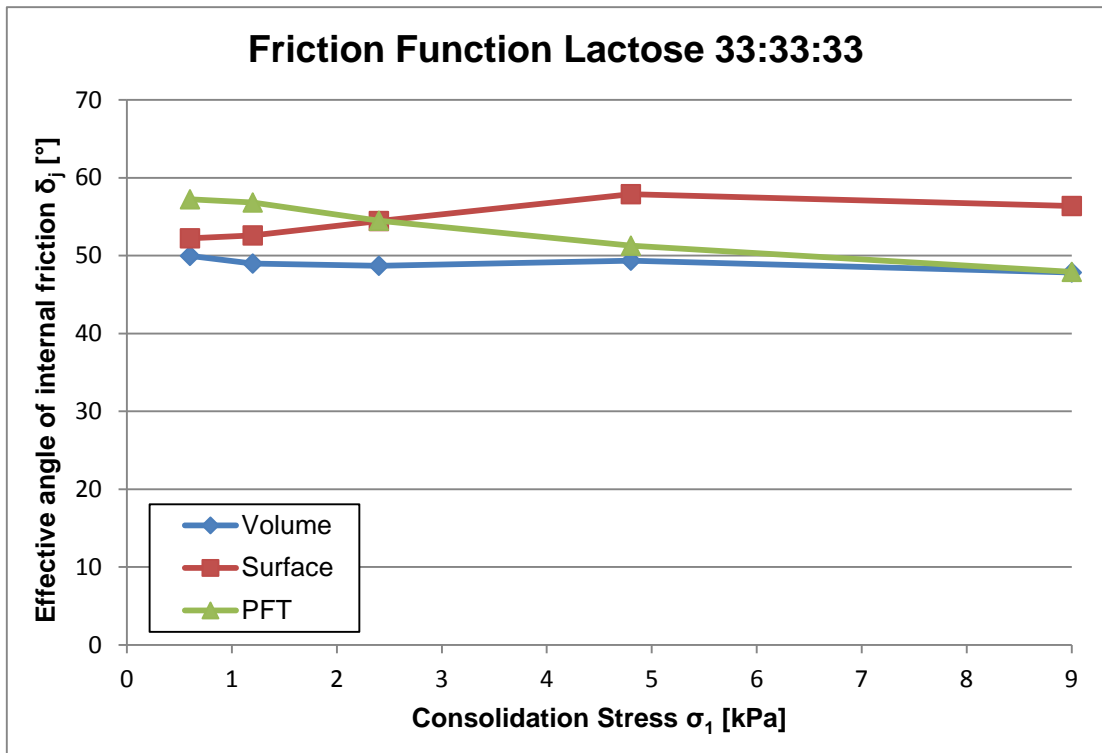


Figure A11

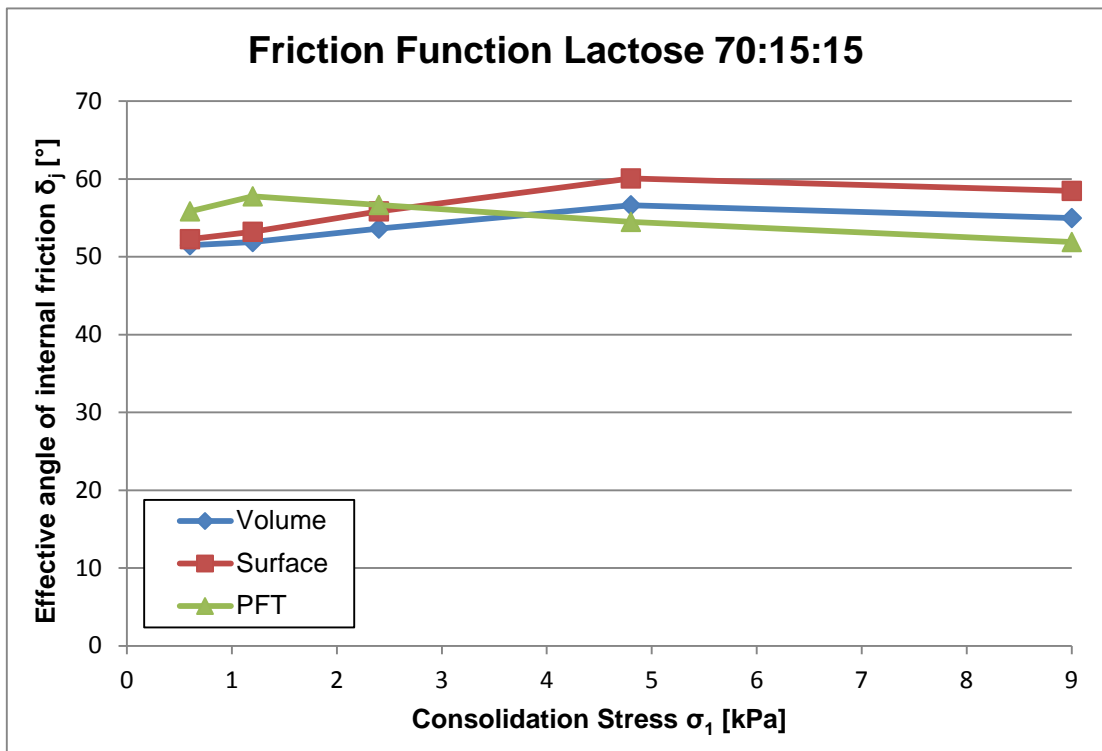


Figure A12

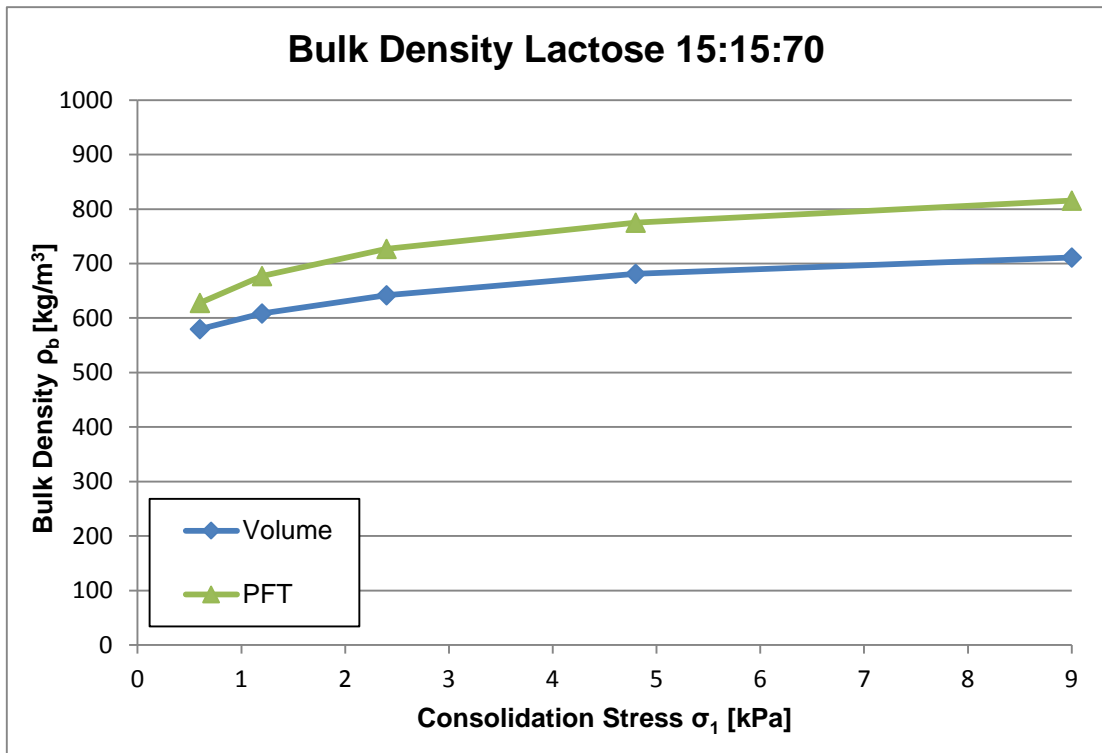


Figure A13

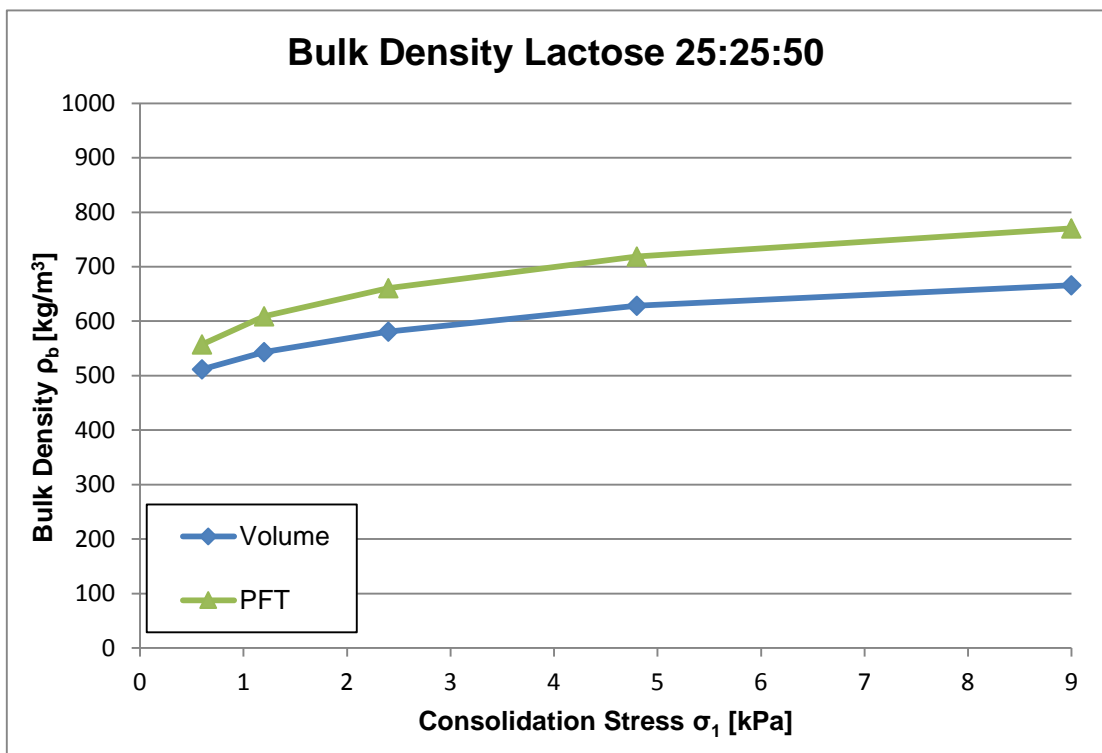


Figure A14

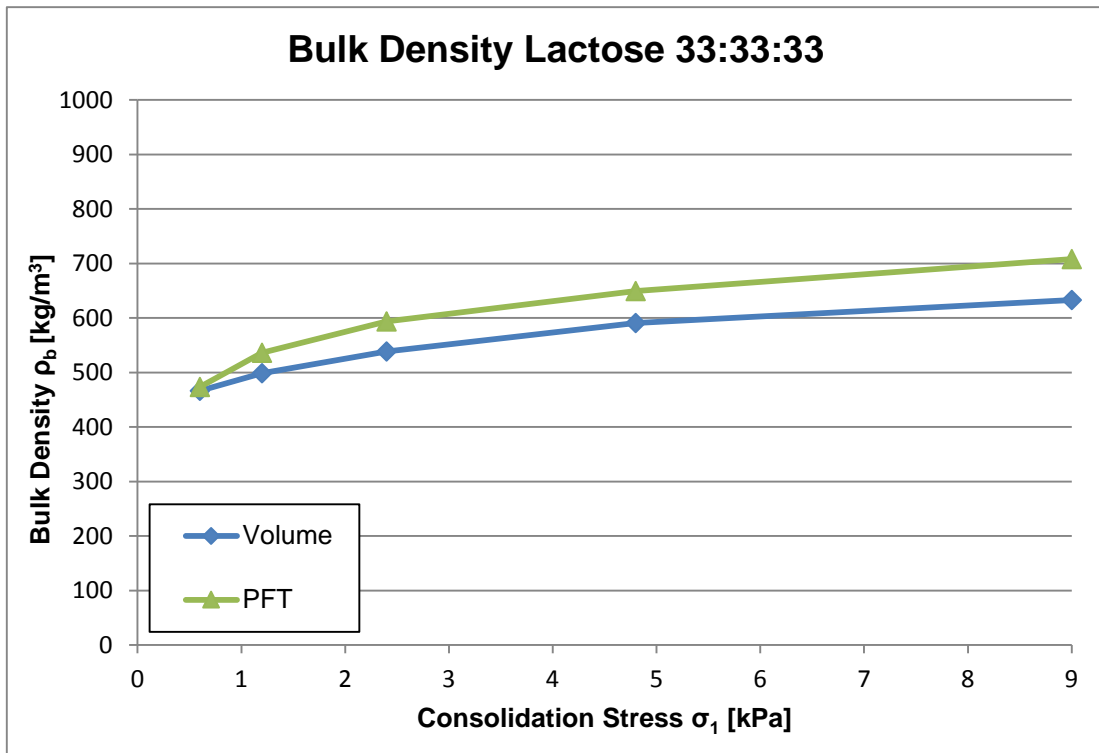


Figure A15

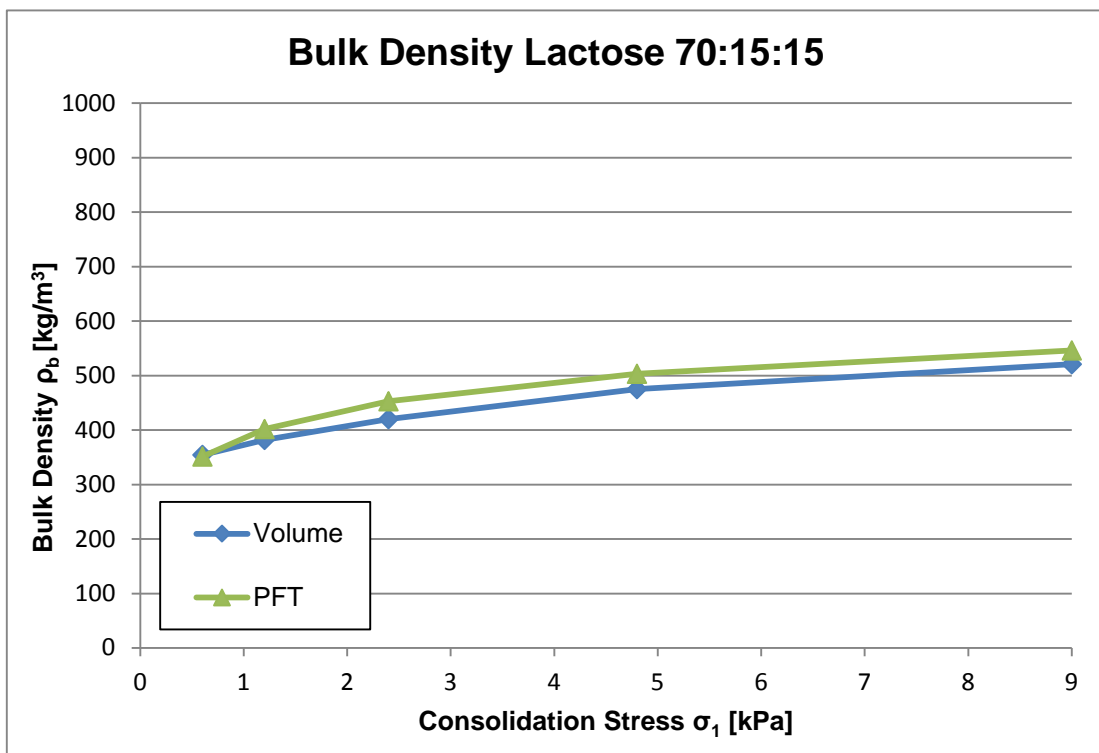


Figure A16

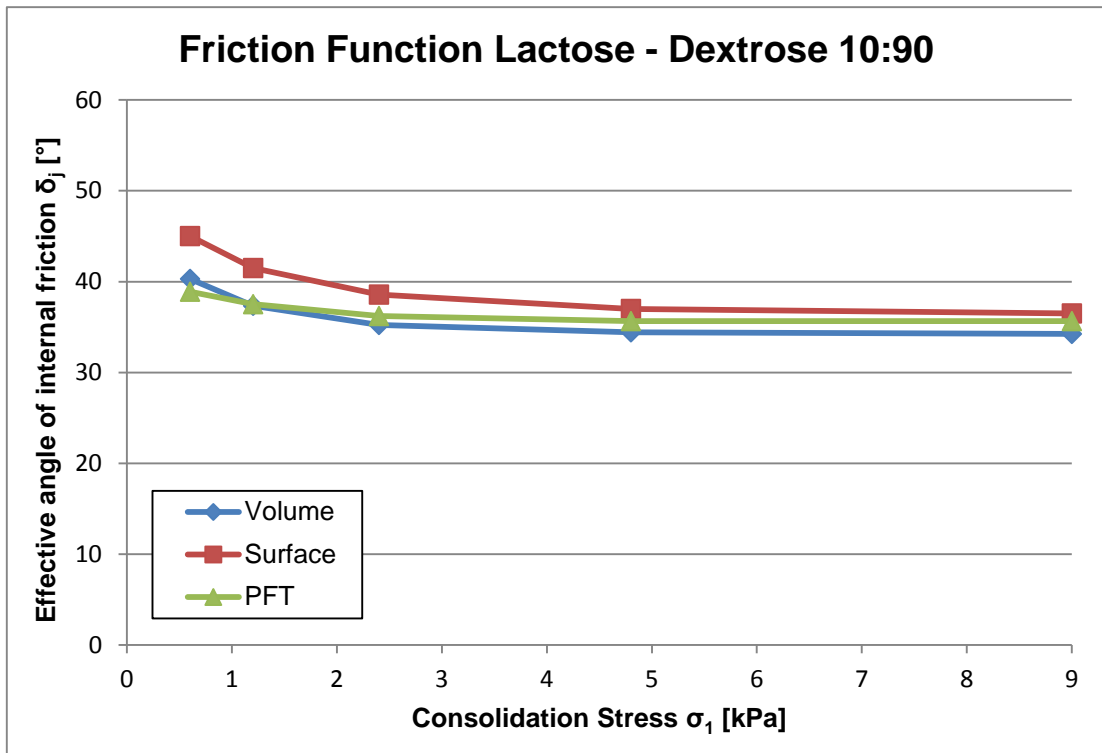


Figure A17

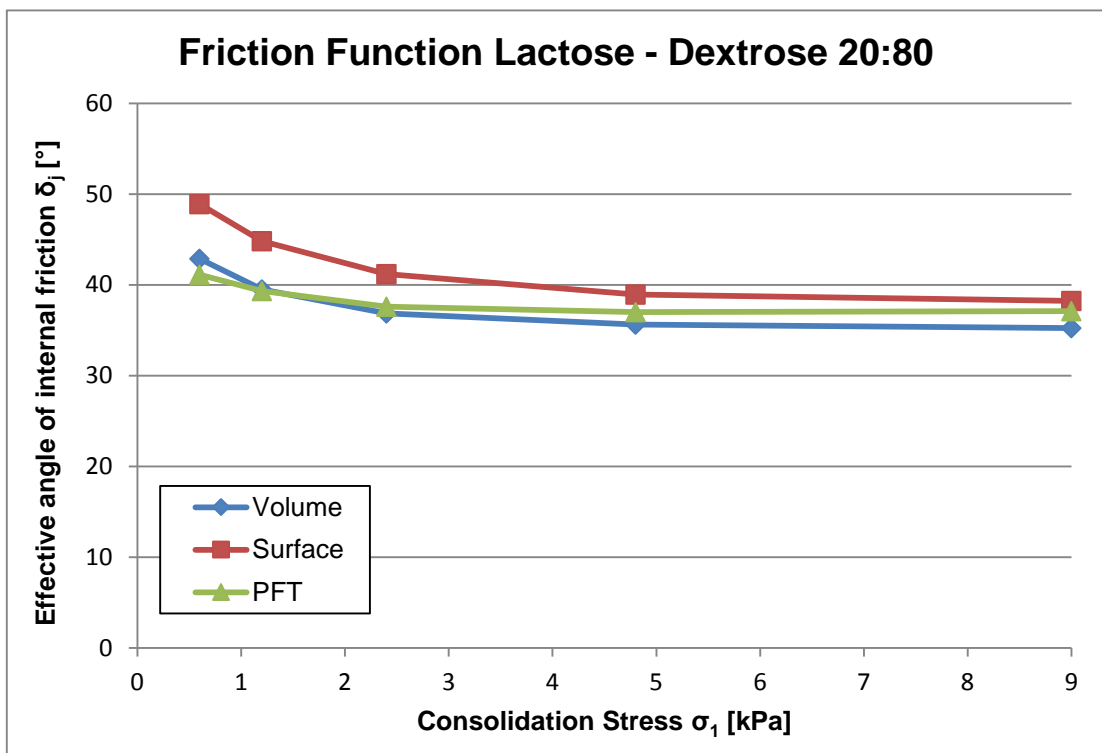


Figure A18

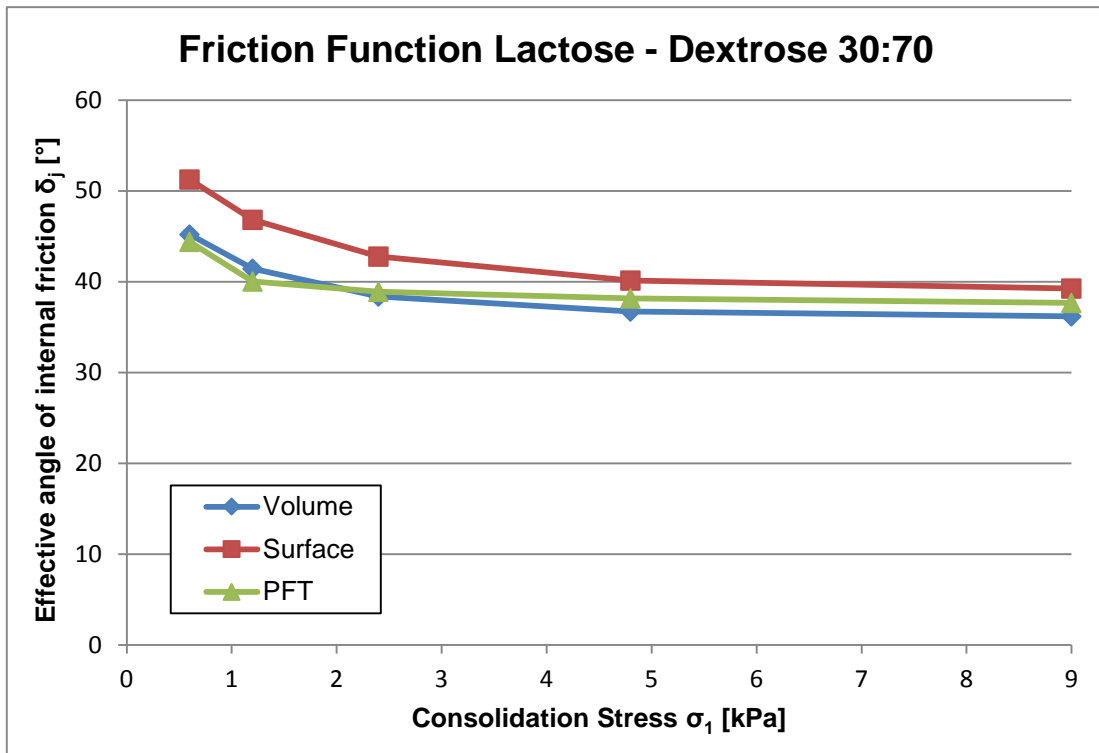


Figure A19

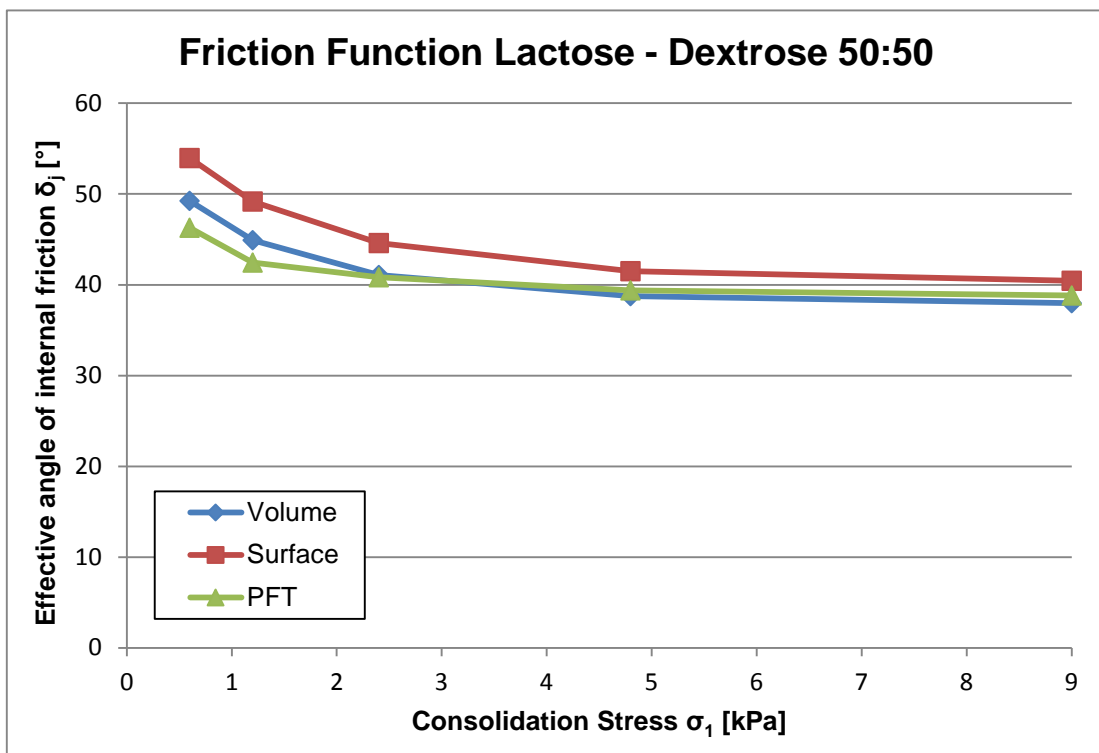


Figure A20

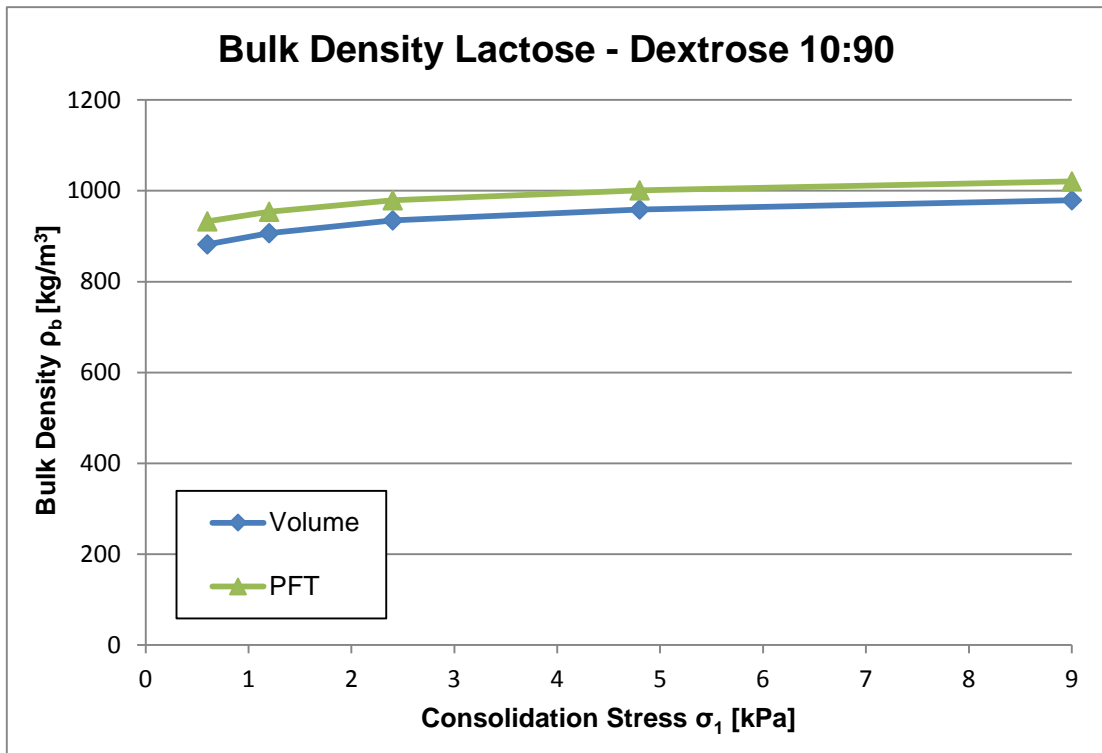


Figure A21

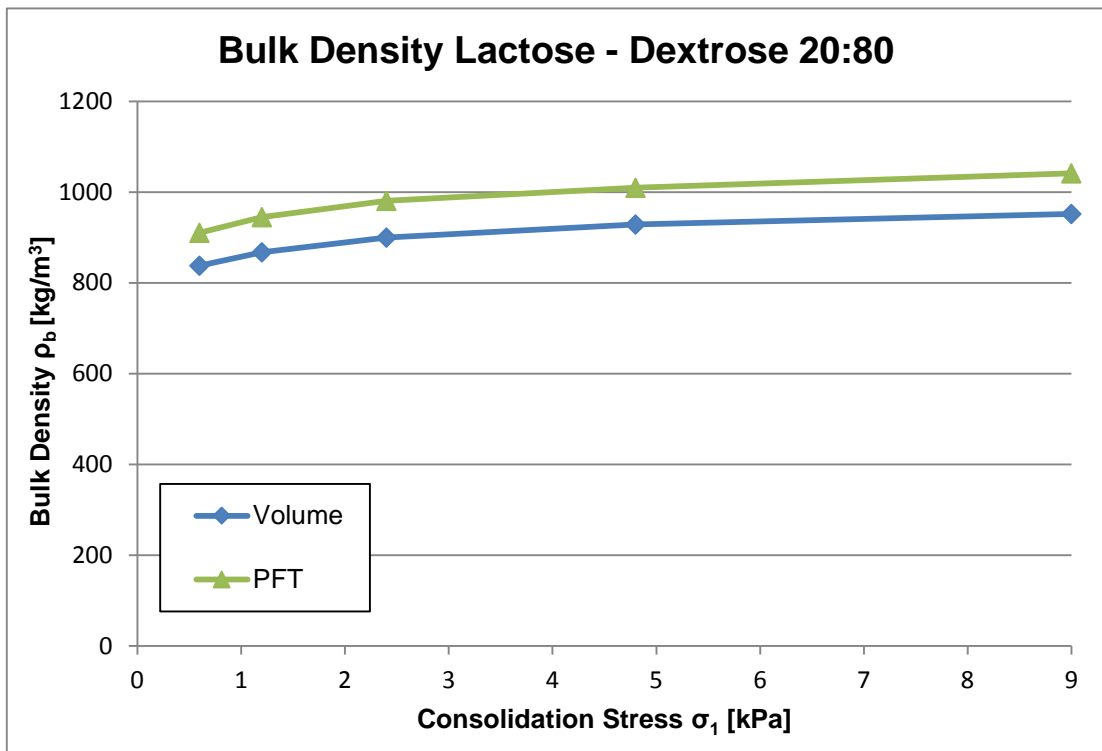


Figure A22

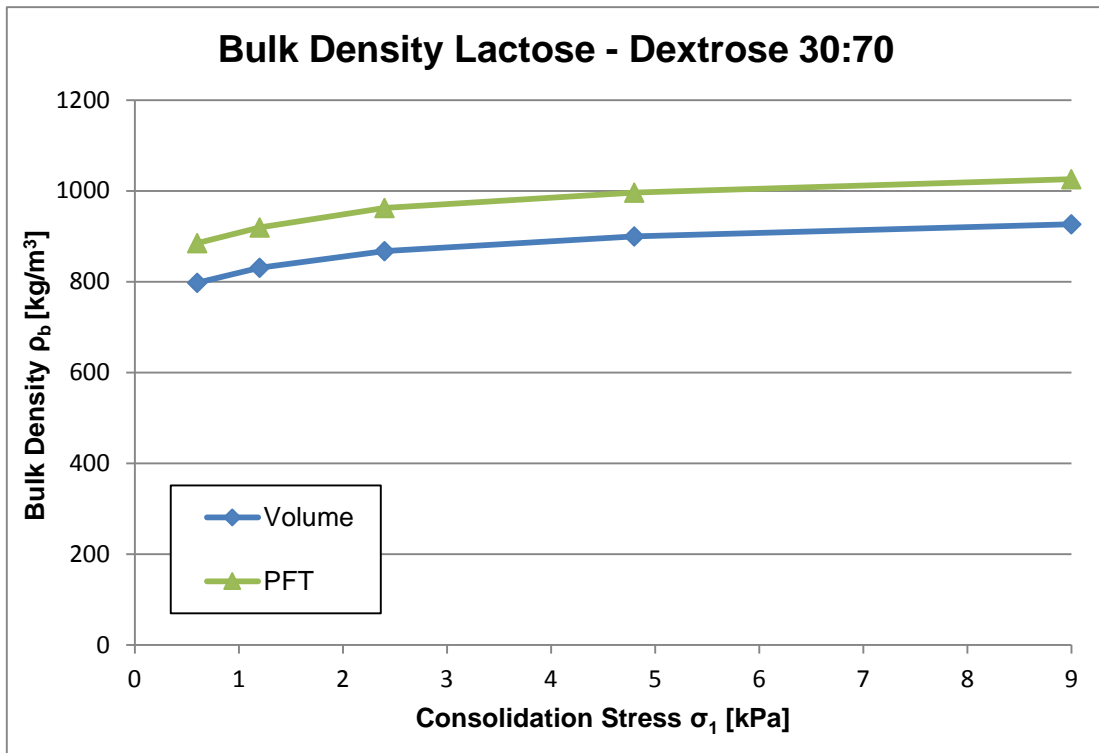


Figure A23

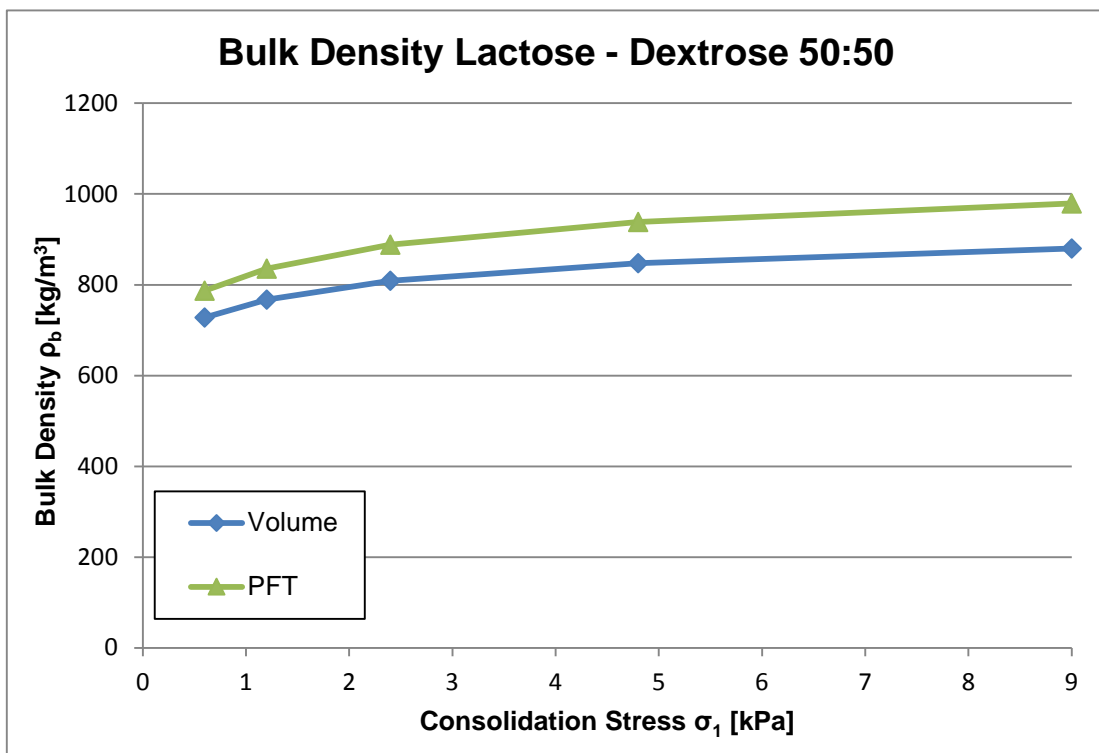


Figure A24

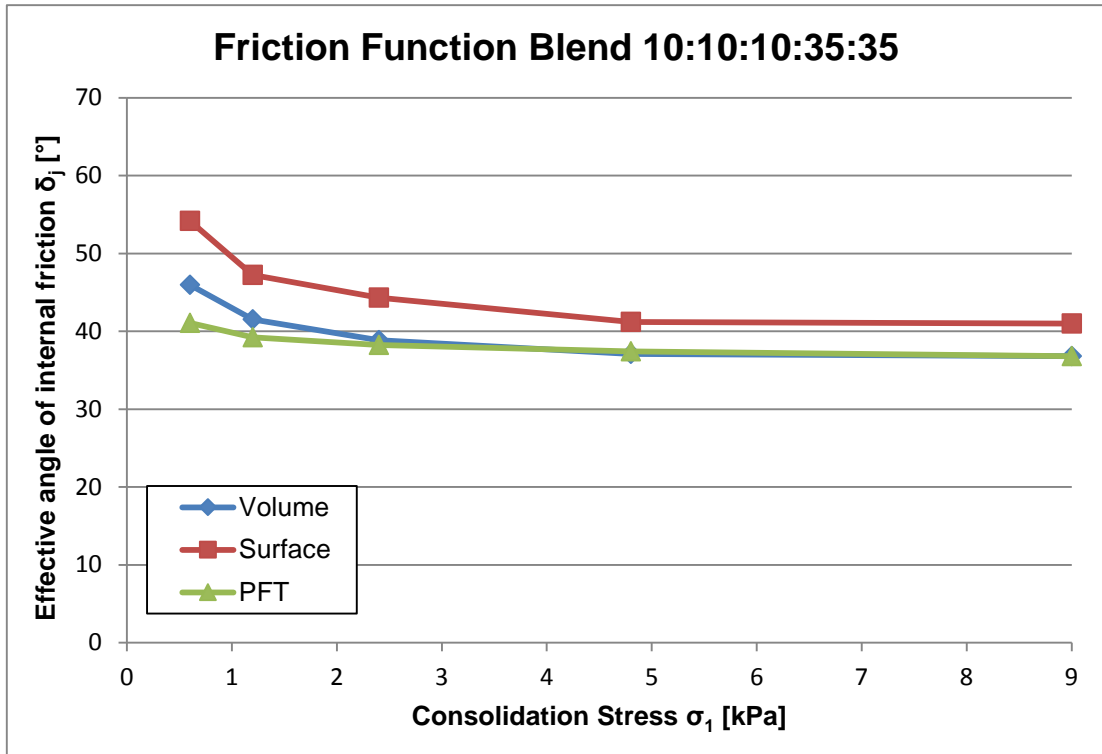


Figure A25

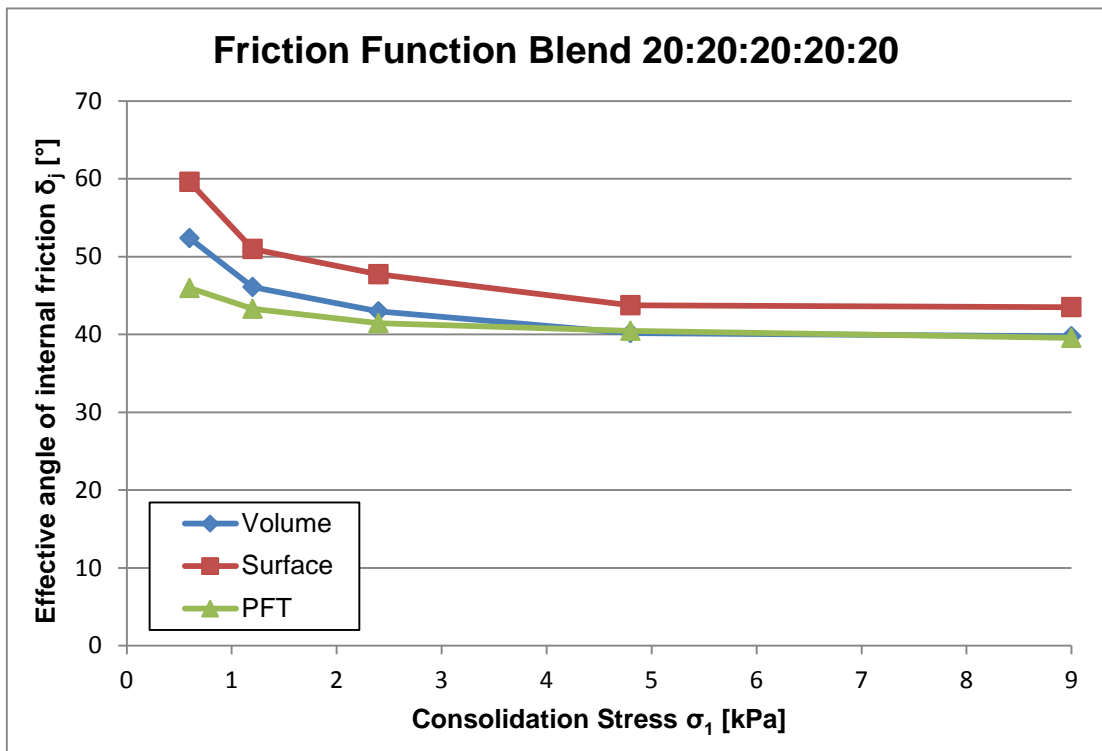


Figure A26

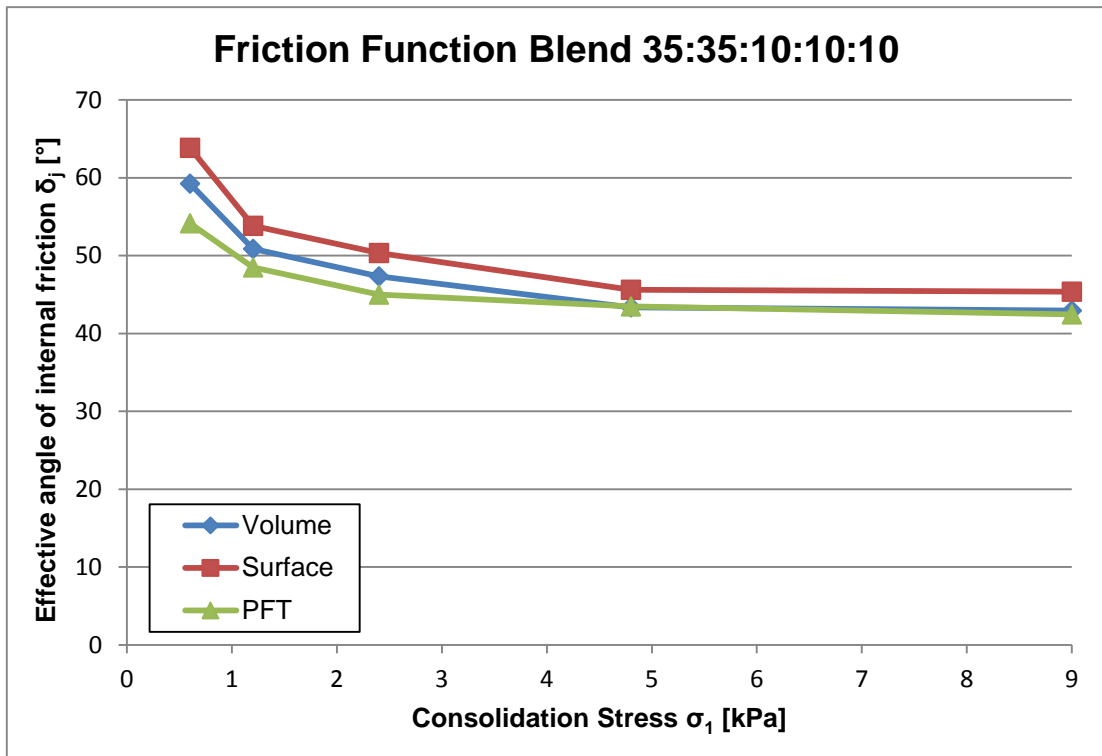


Figure A27

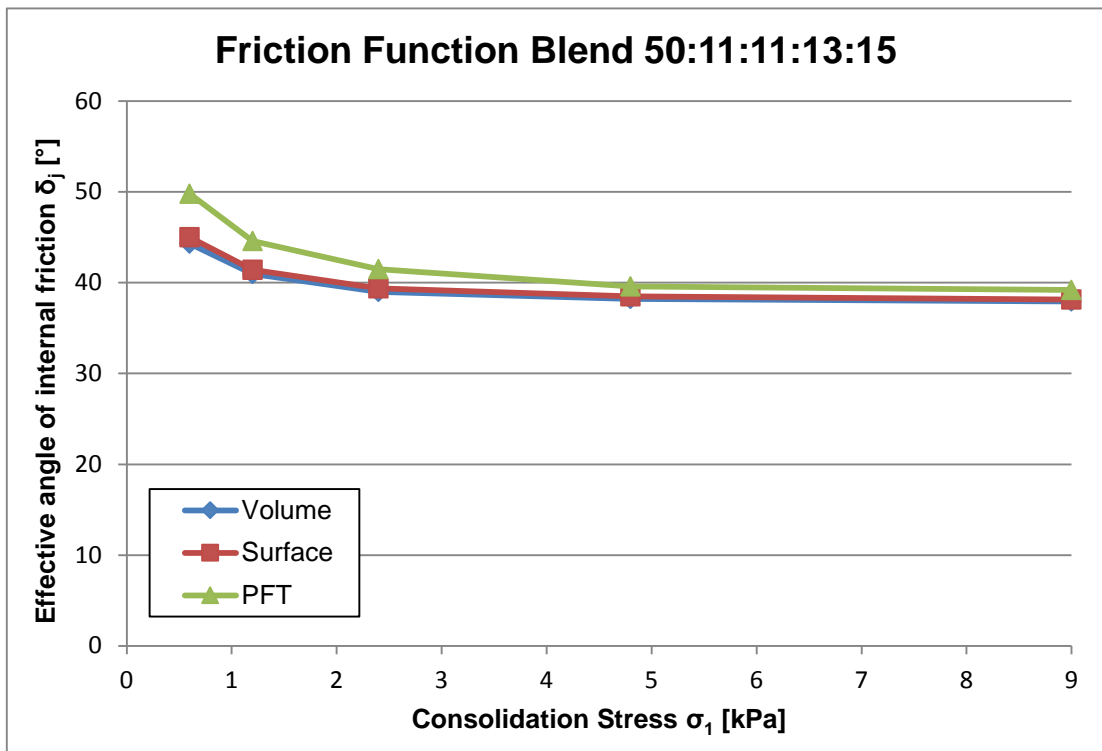


Figure A28

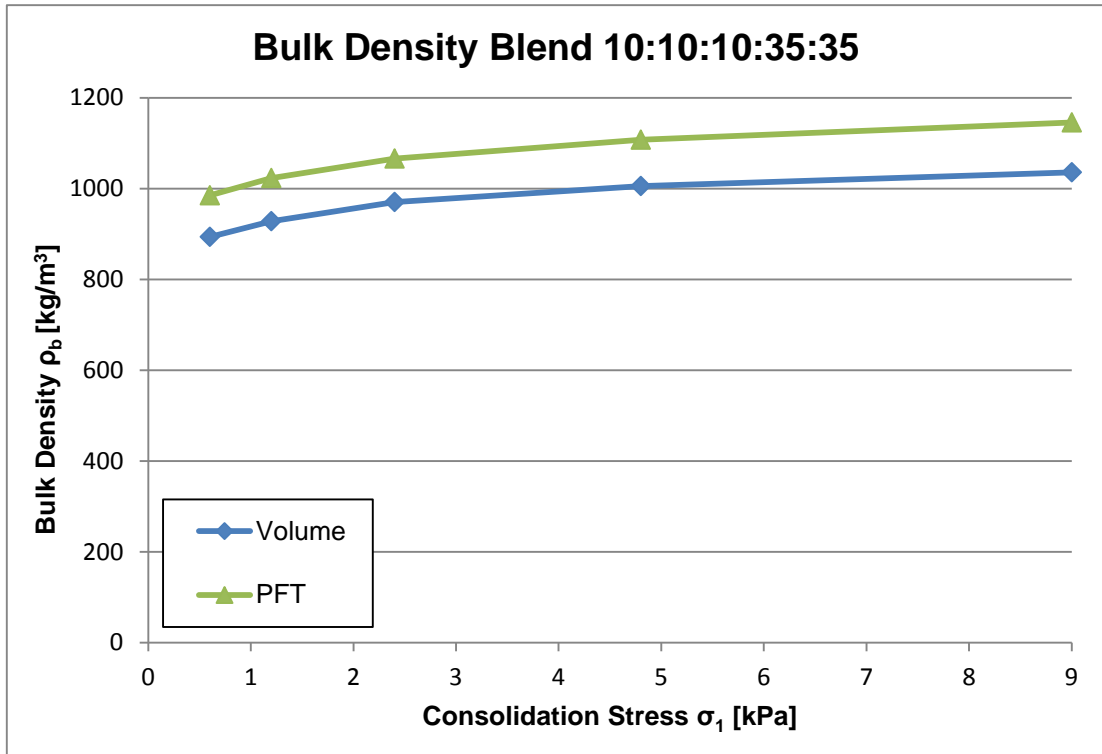


Figure A29

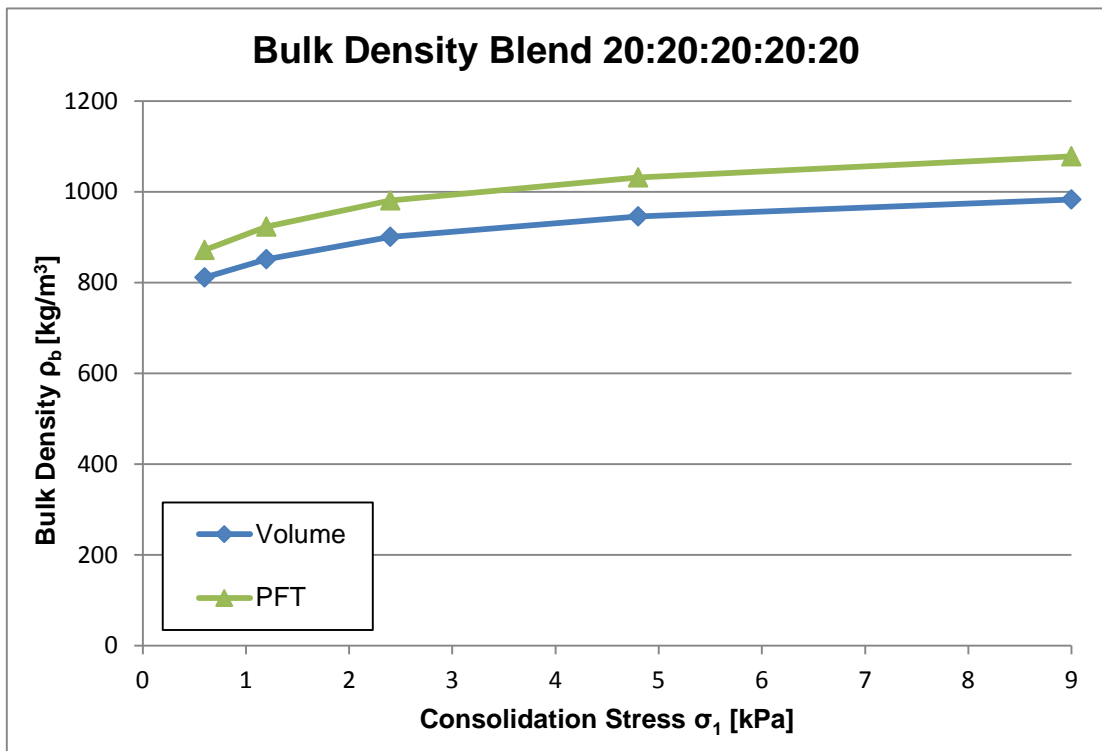


Figure A30

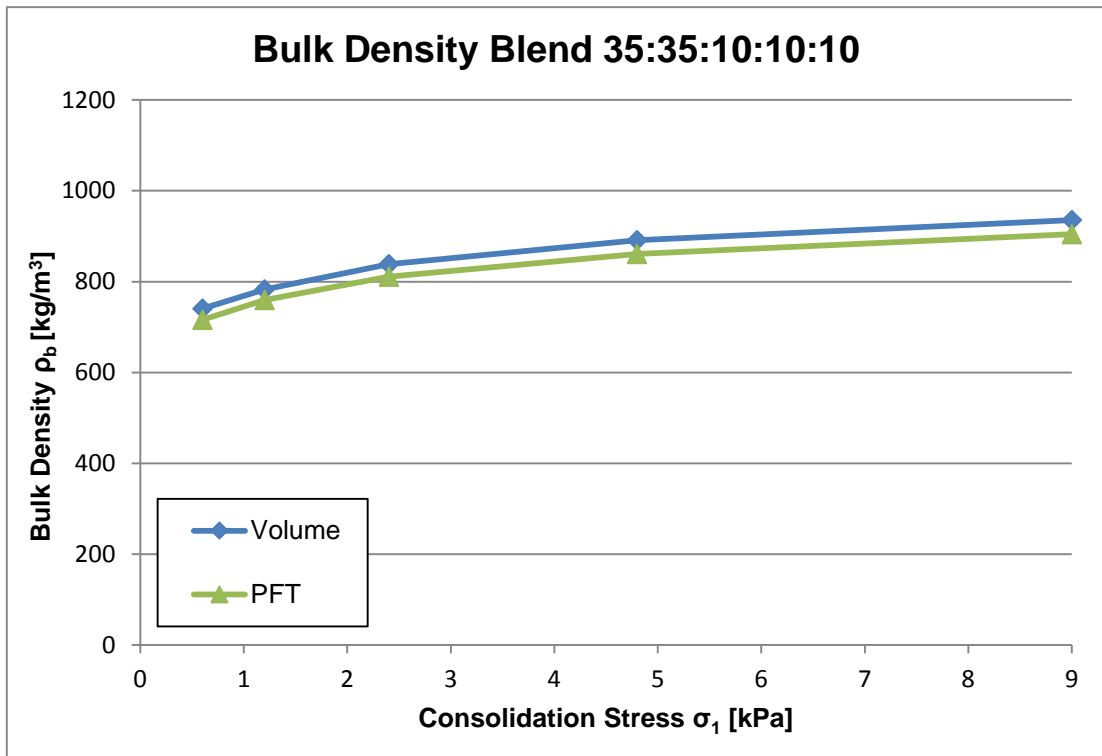


Figure A31

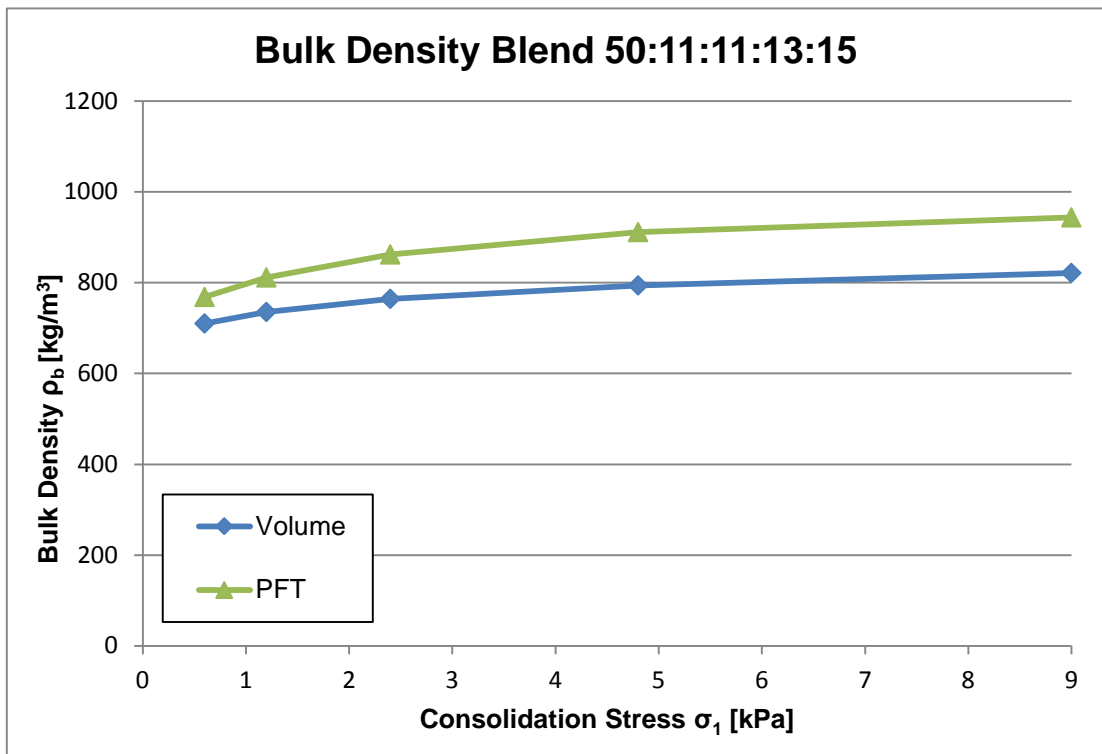


Figure A32

A4 Predictions of the flow functions for single powders

This section contains results of the validation of the logarithmic model developed to study the particle size scaling effect on dry powders. These are presented in the same two type of graphs explained in chapter 8 for maltodextrin, dextrose, sodium chloride and glass beads:

- 3) Plotting particle size against the values of Z for each powder at 0.6, 1.2, 2.4, 4.8, 9 and 10 kPa to study the effect of the consolidation stress selected on the accuracy of the predictions made by the model.
- 4) Plotting the measured and predicted flow functions for each size fraction or grade of the powders to study the influence of the particle size selected as a reference to make the predictions on the accuracy of the model.

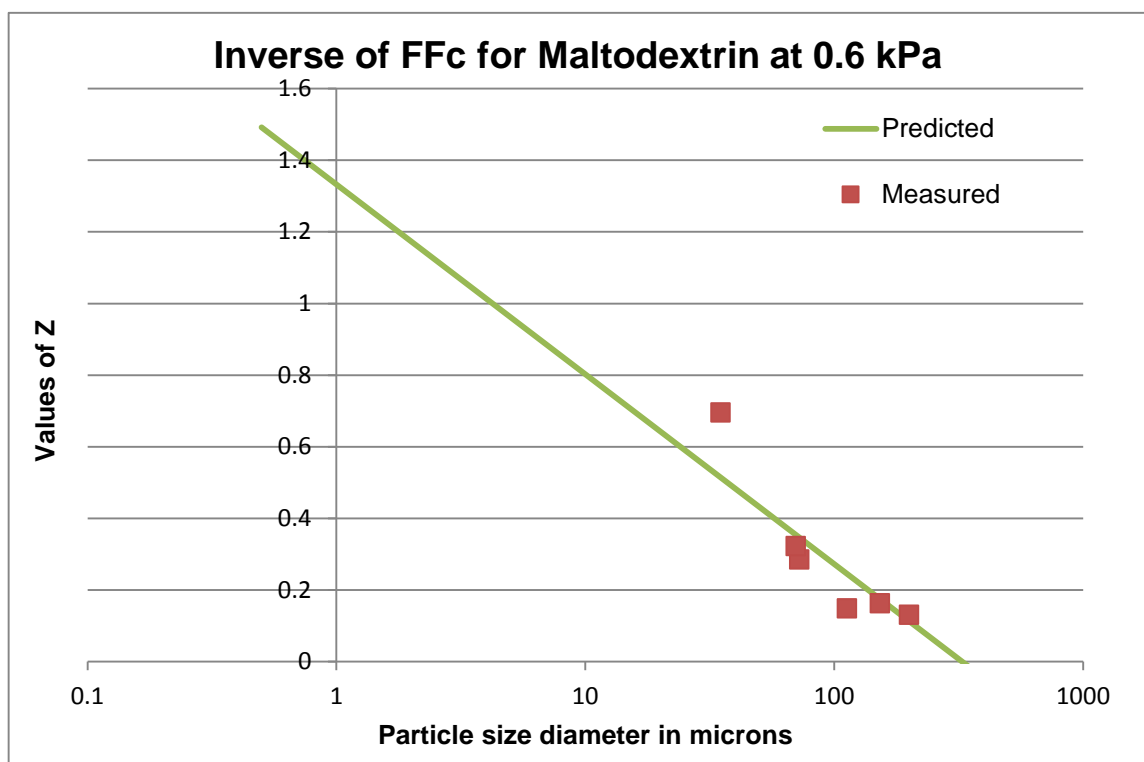


Figure A33

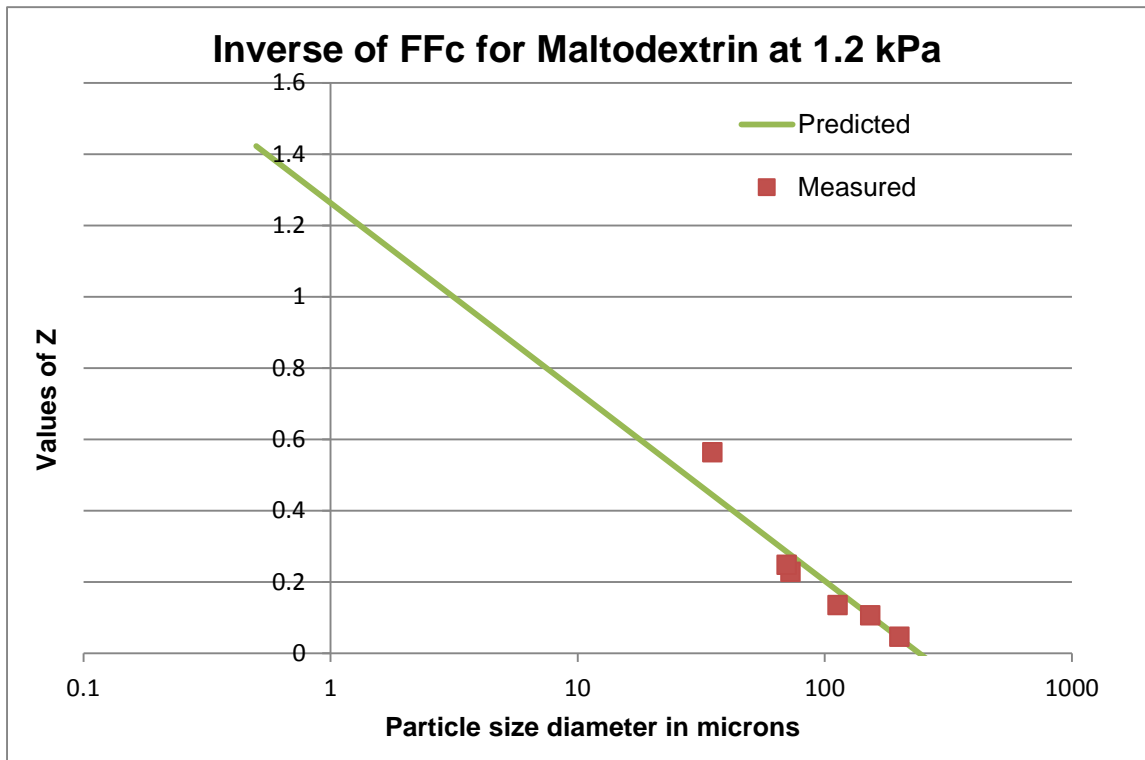


Figure A34

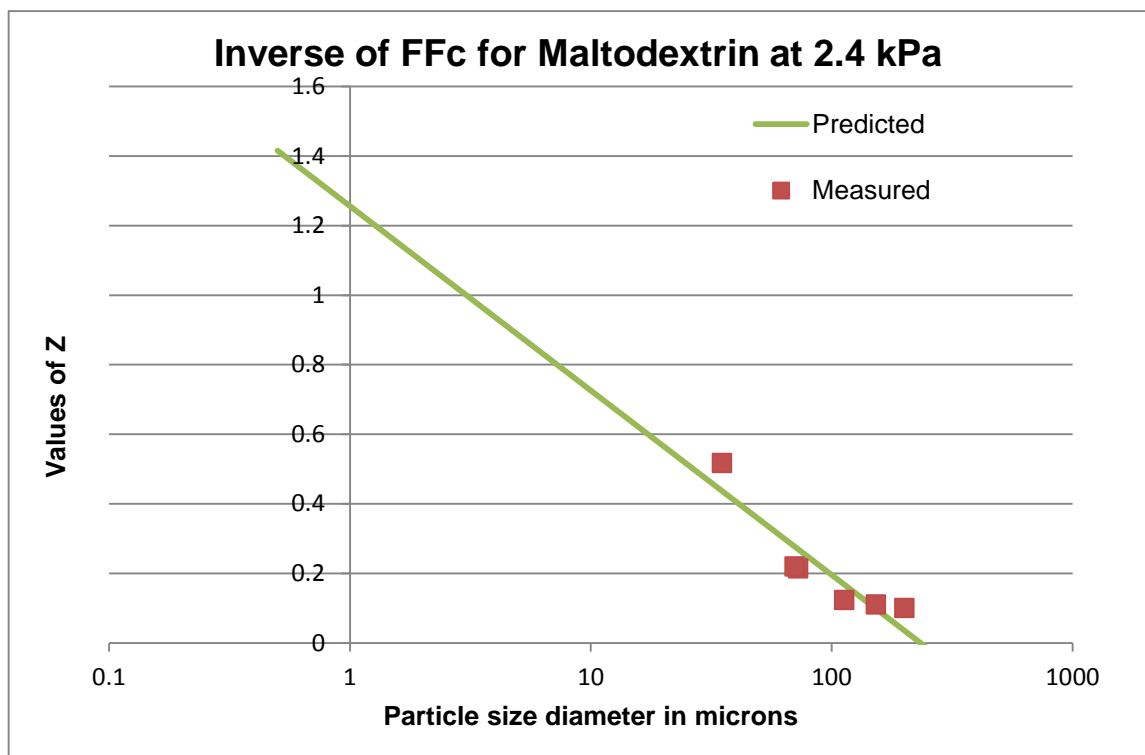


Figure A35

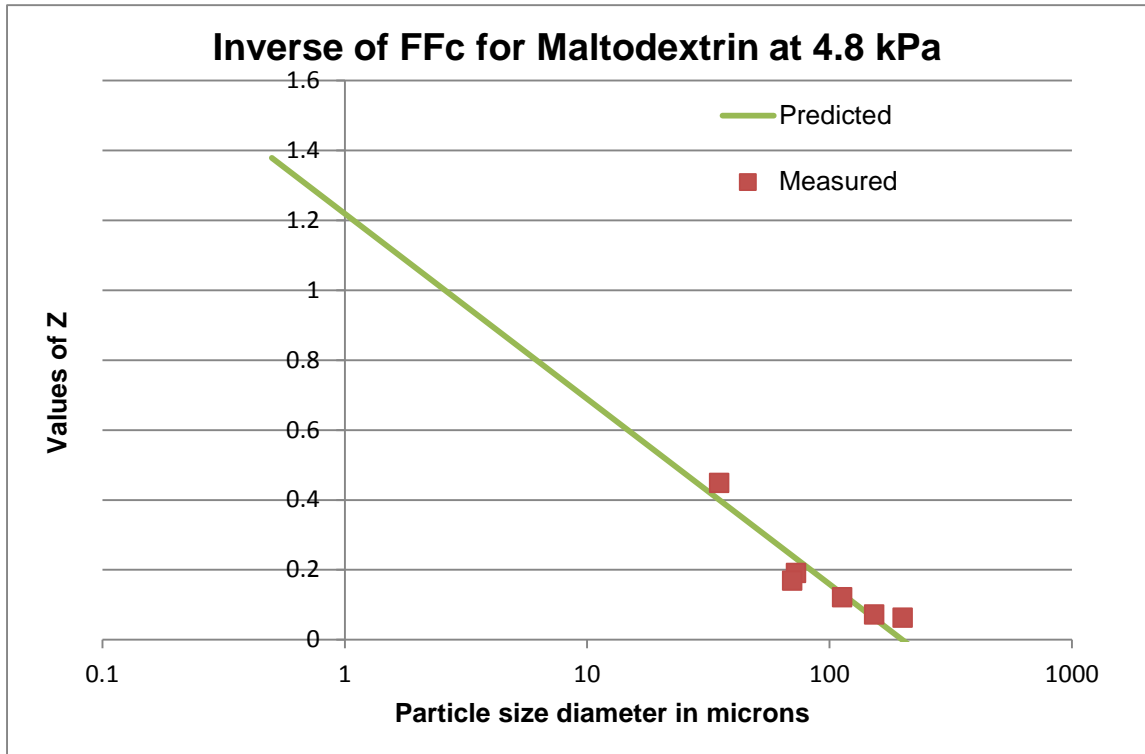


Figure A36

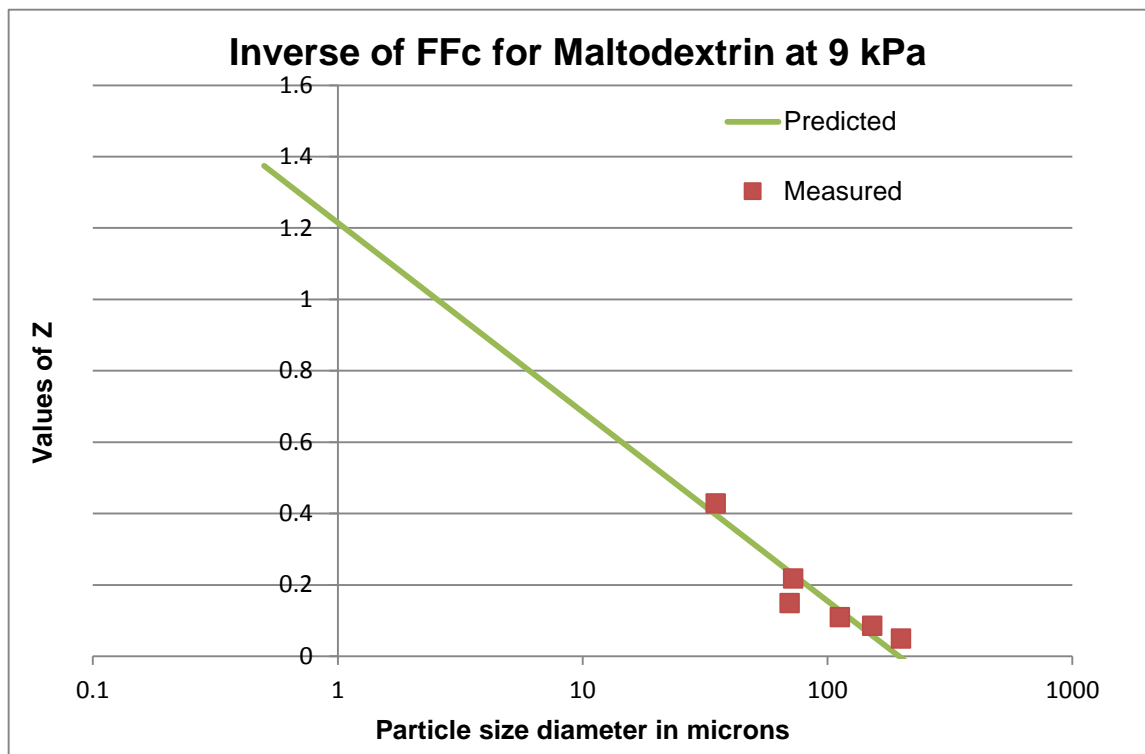


Figure A37

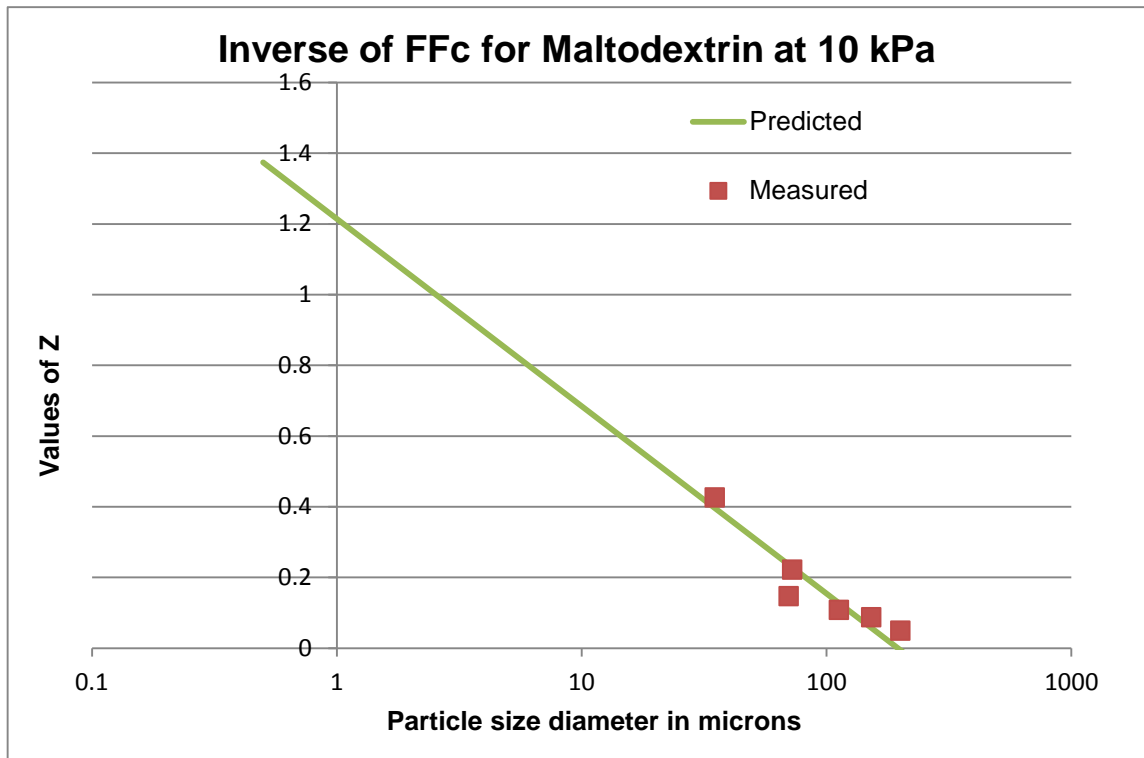


Figure A38

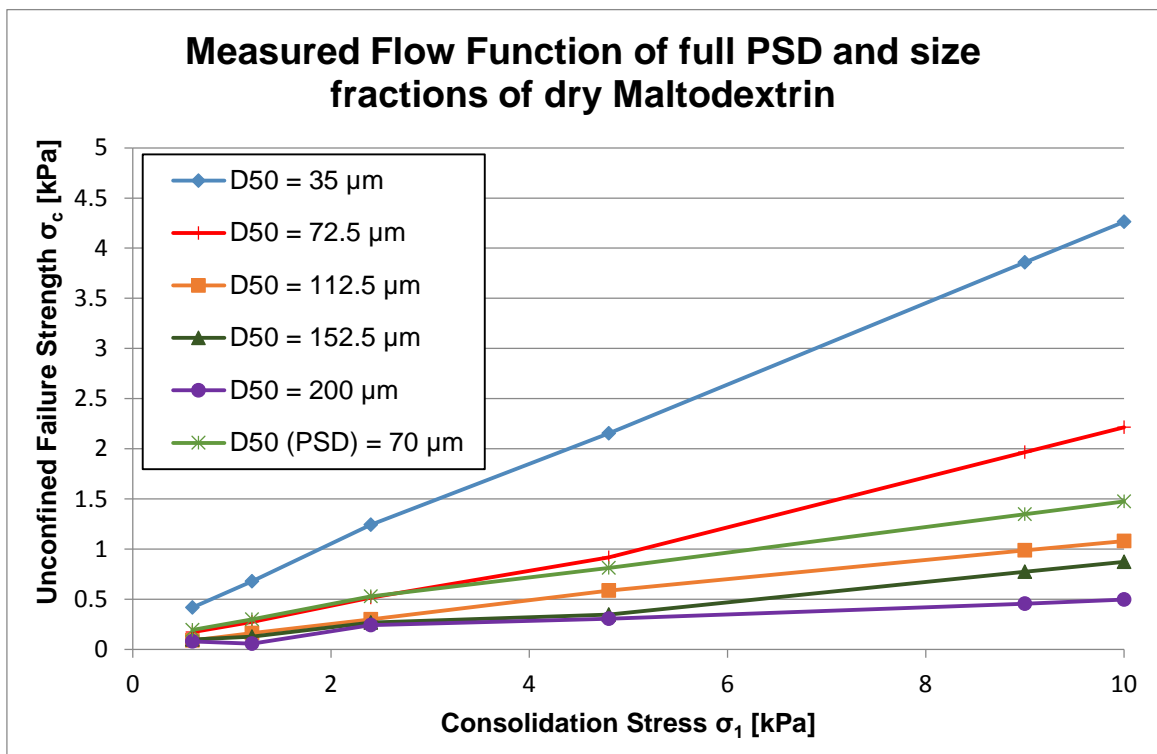


Figure A39

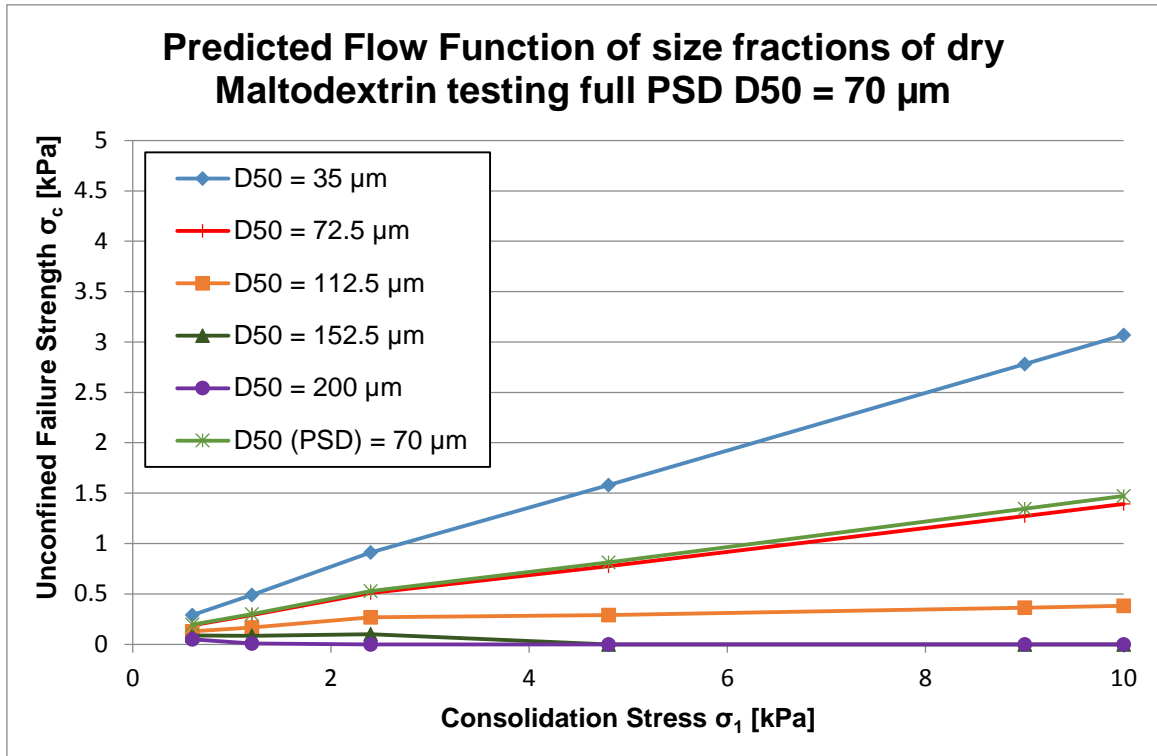


Figure A40

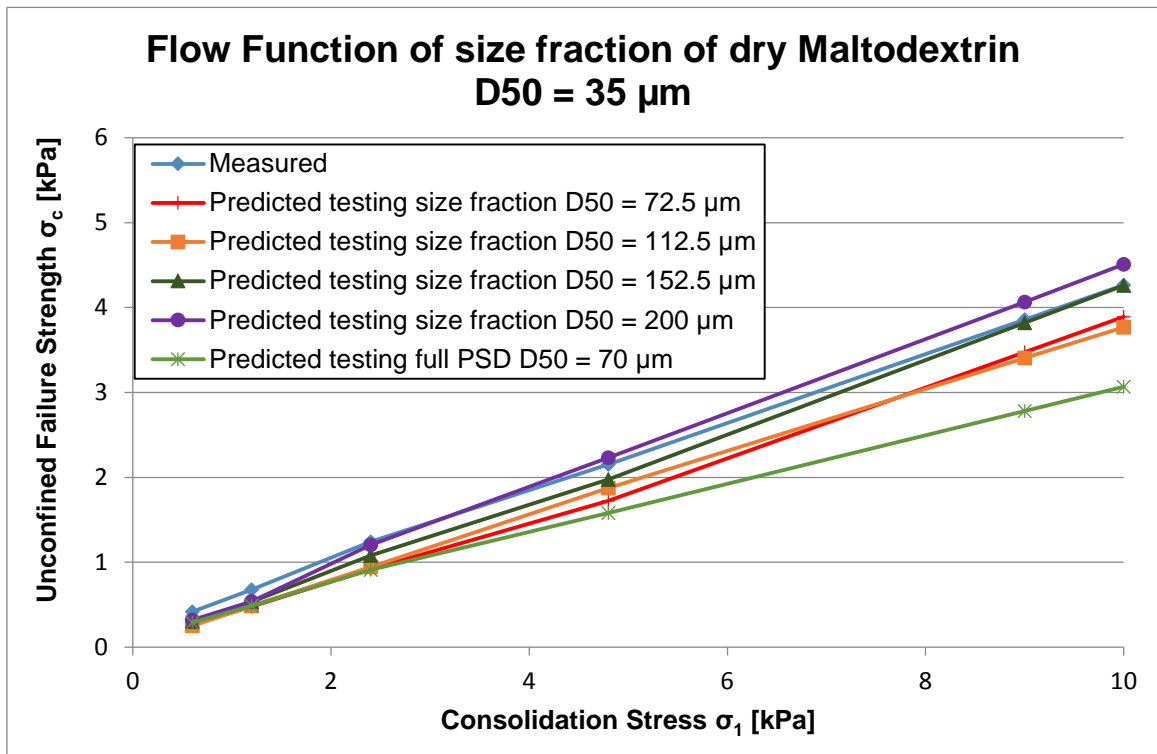


Figure A41

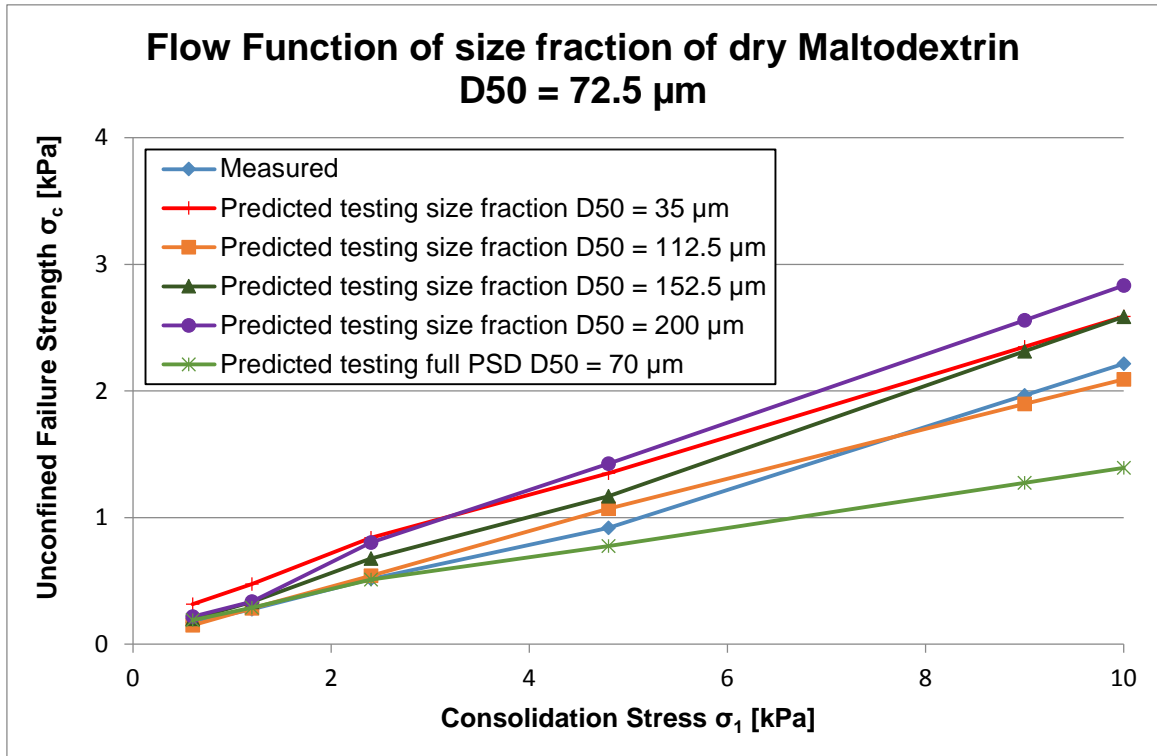


Figure A42

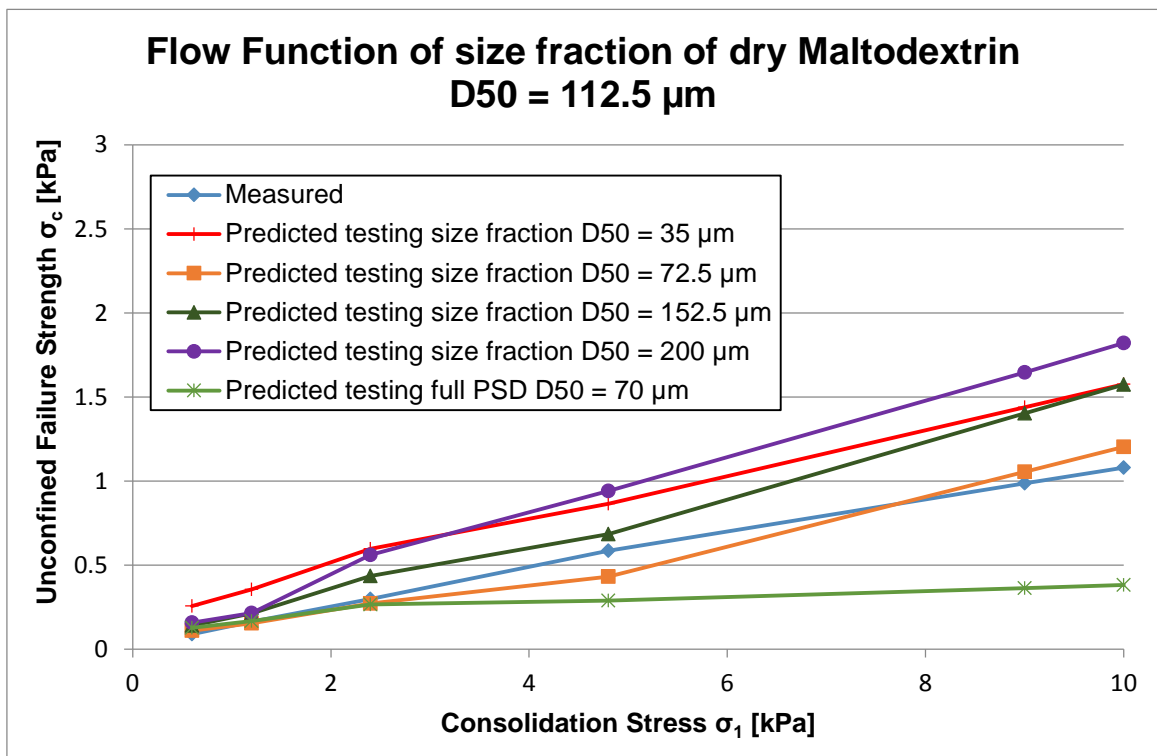


Figure A43

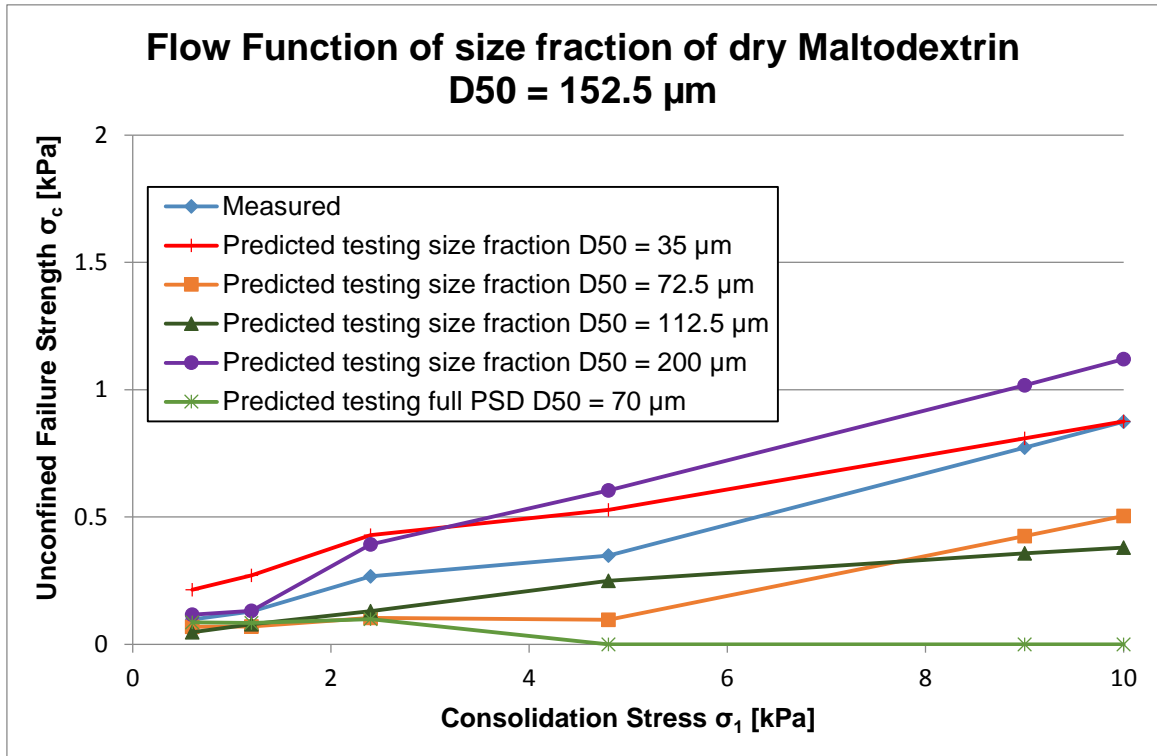


Figure A44

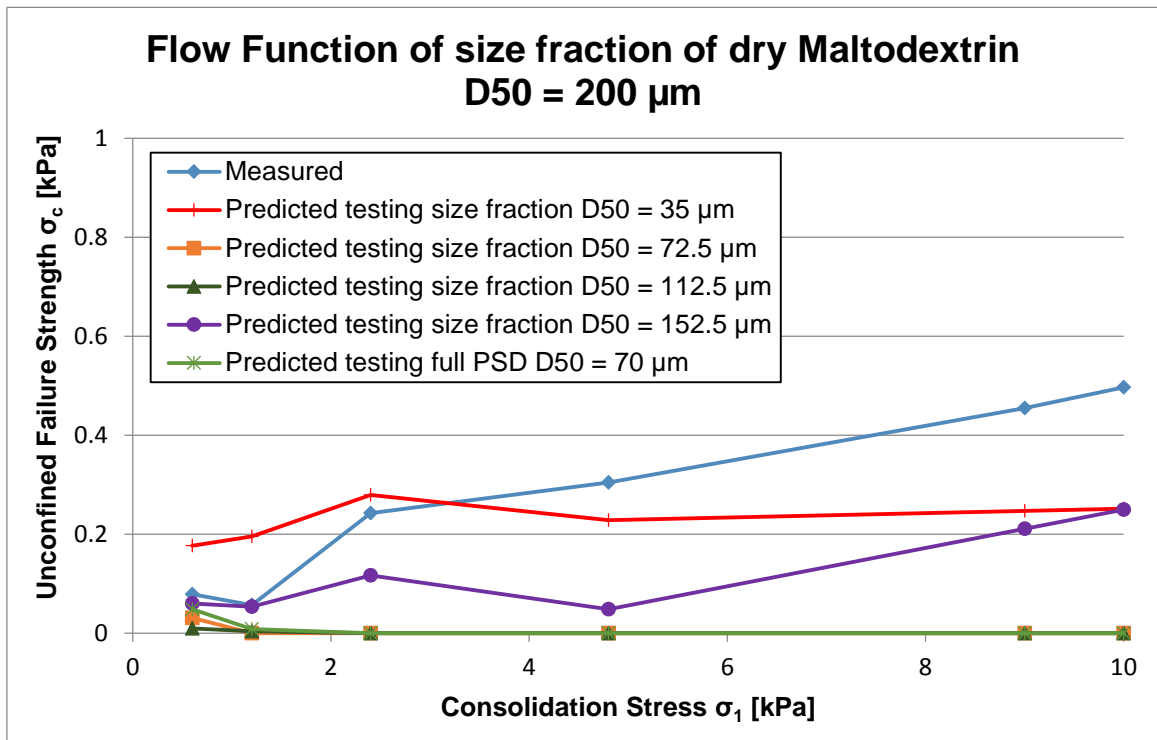


Figure A45

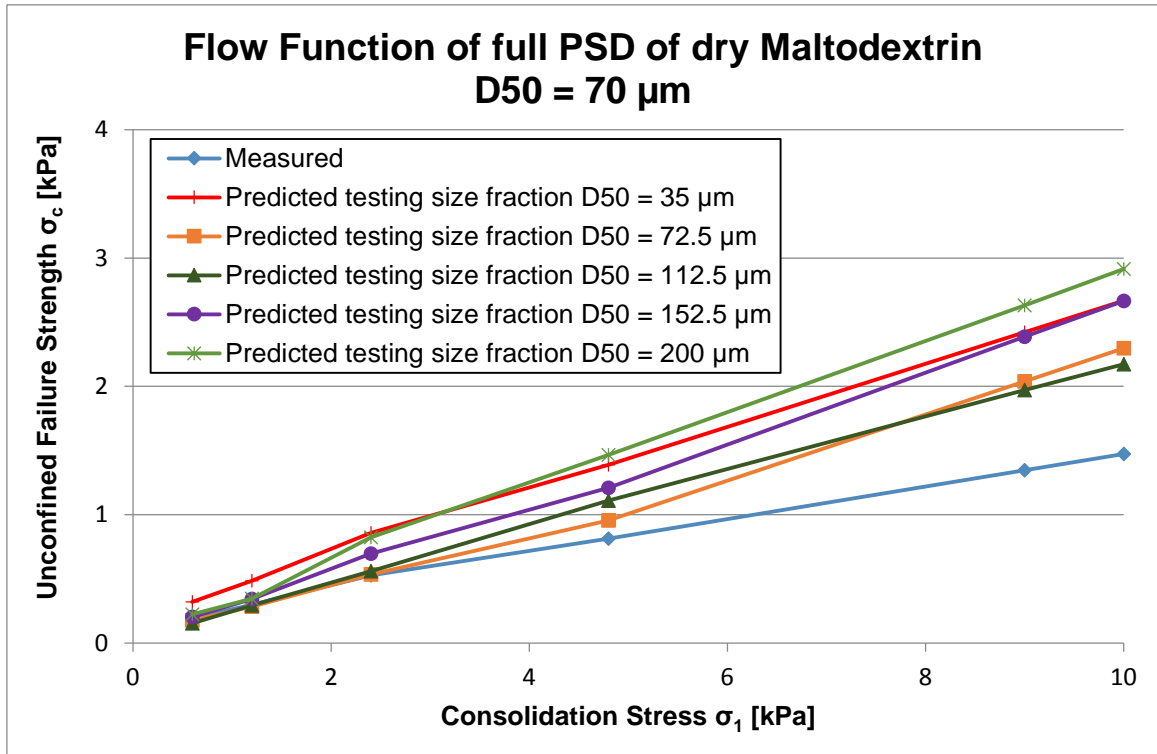


Figure A46

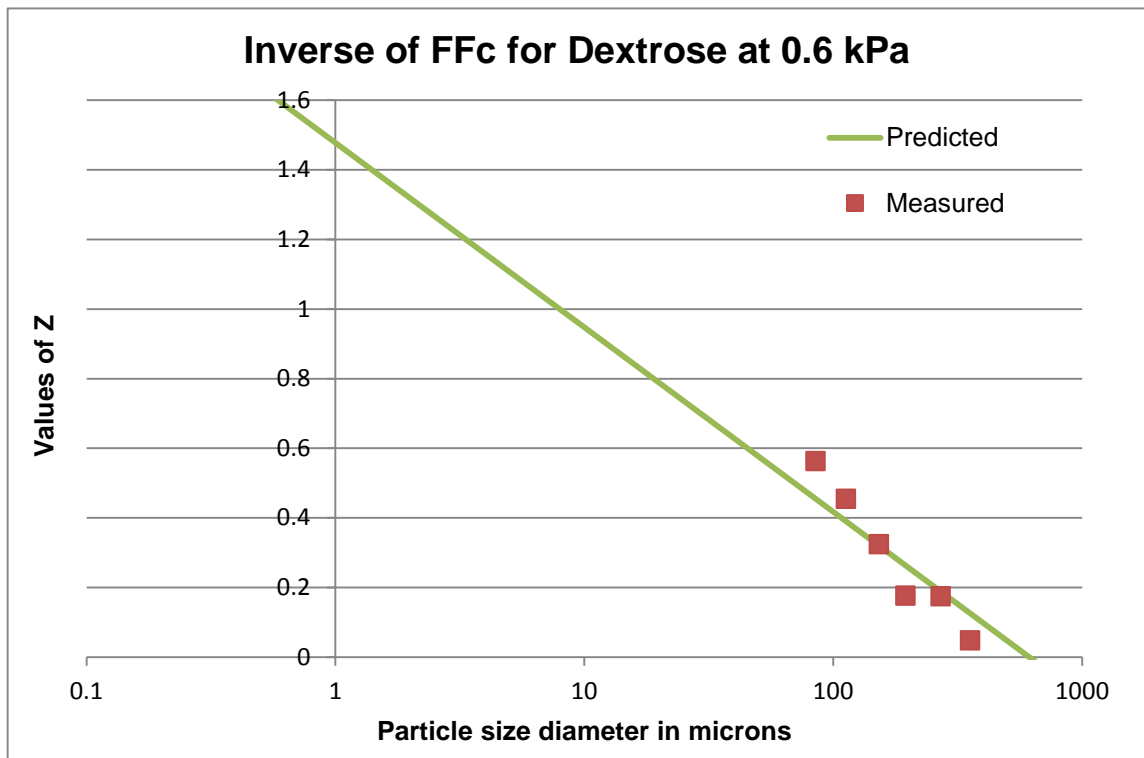


Figure A47

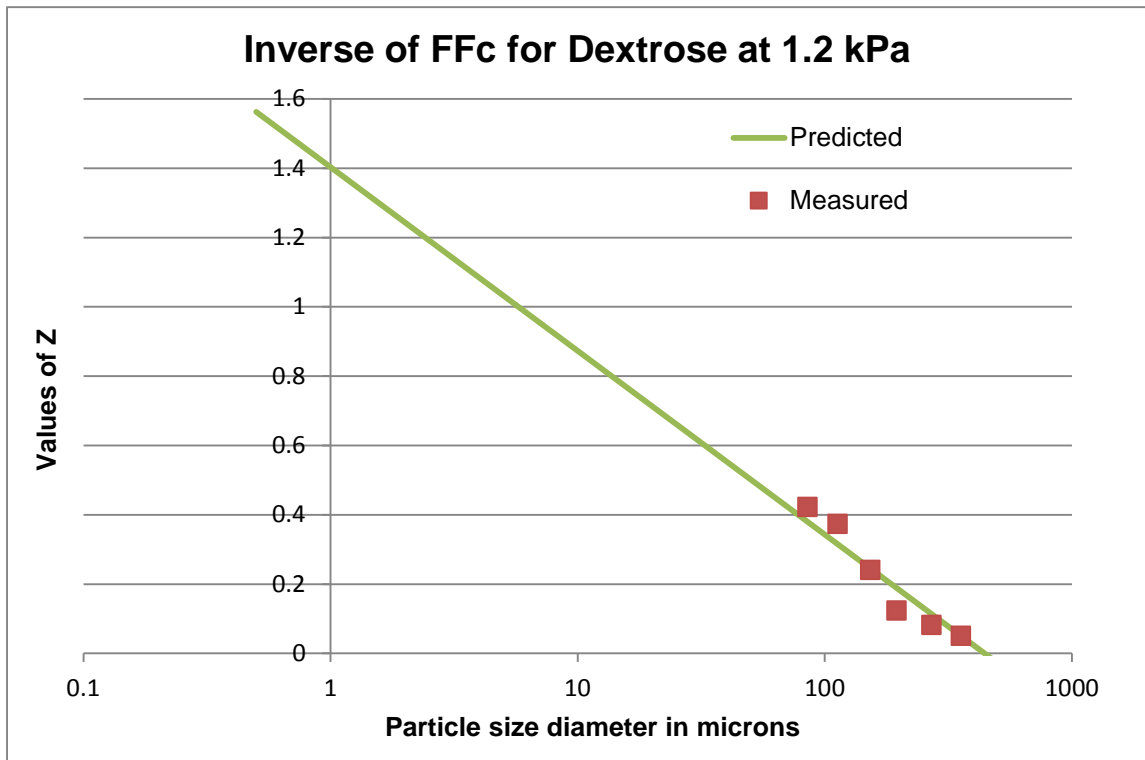


Figure A48

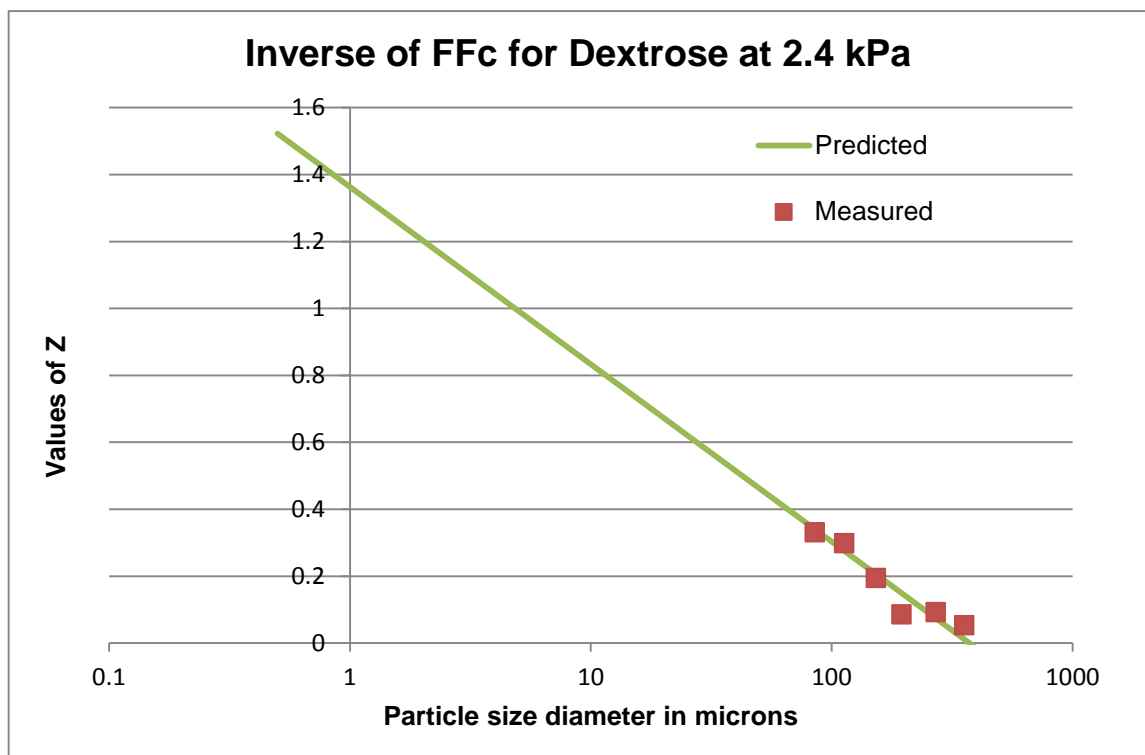


Figure A49

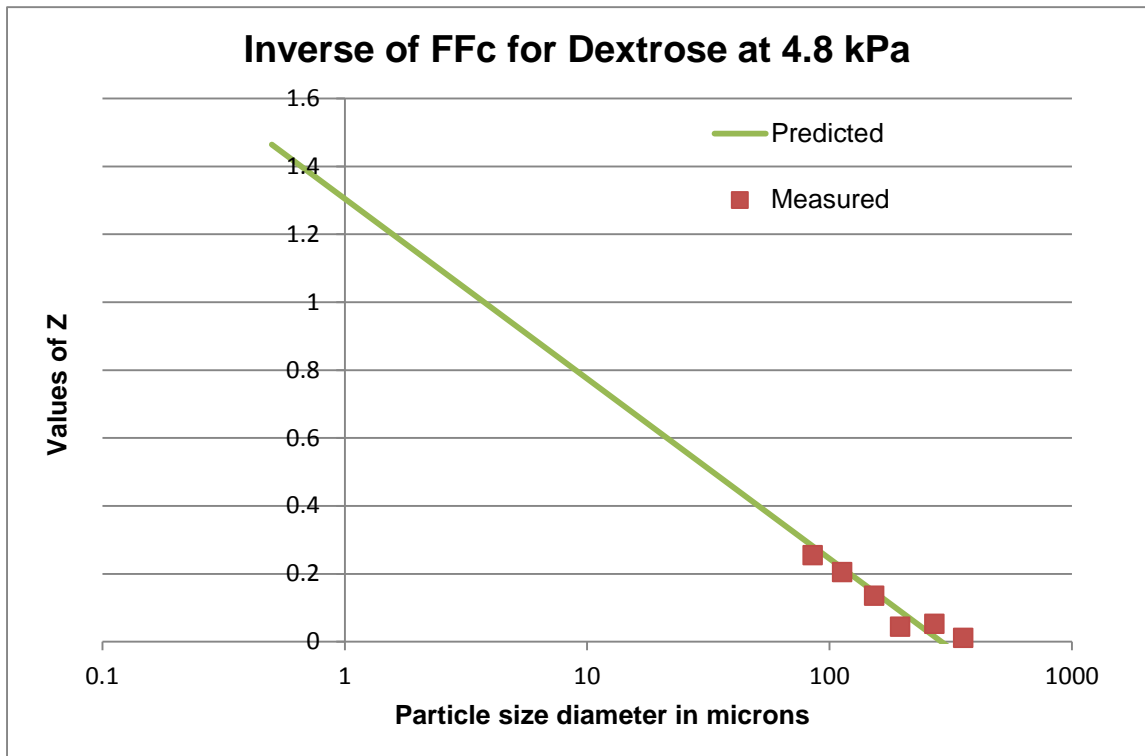


Figure A50

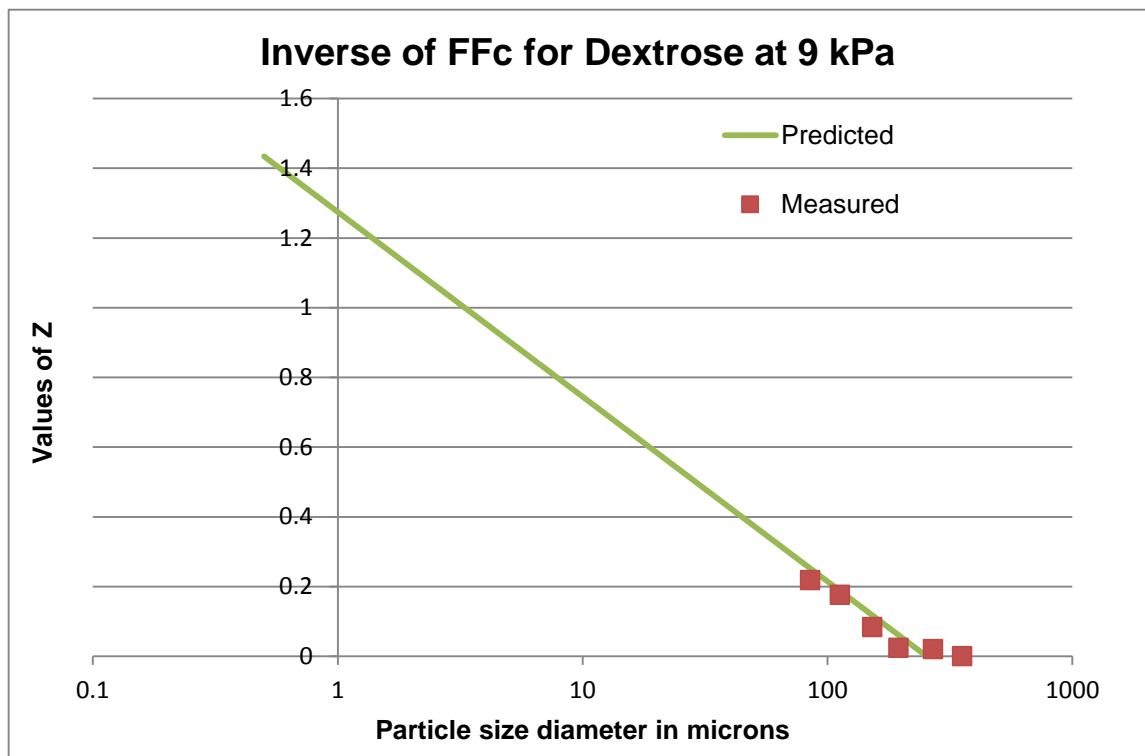


Figure A51

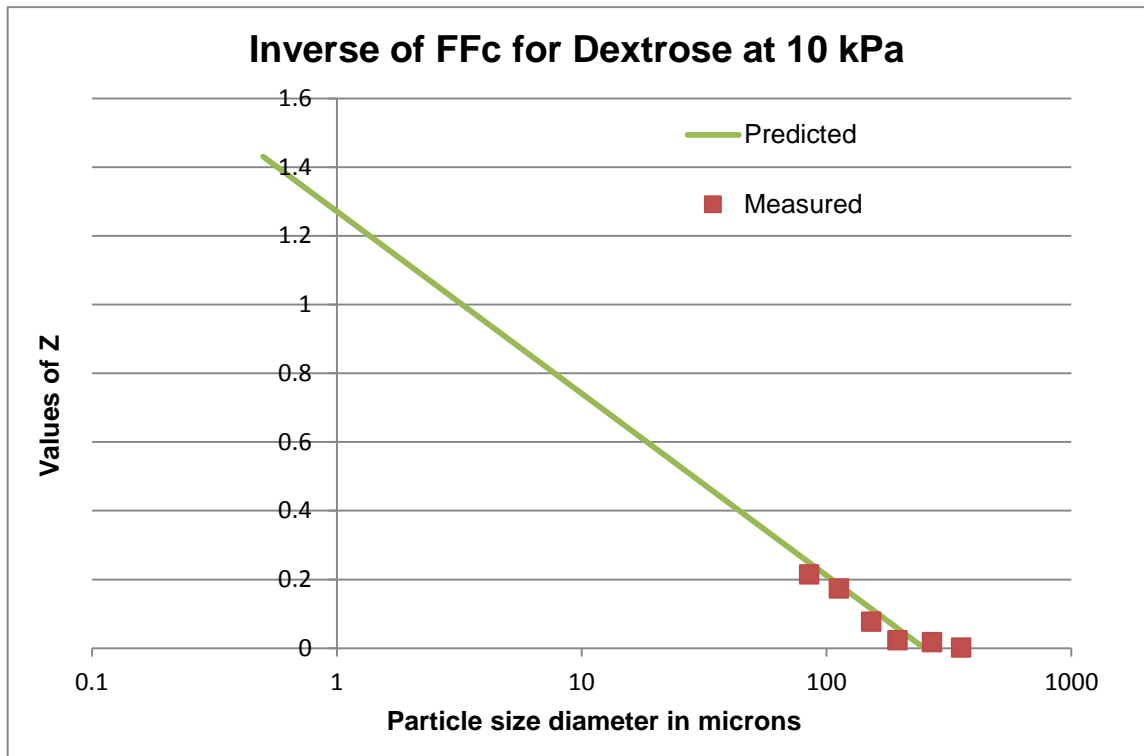


Figure A52

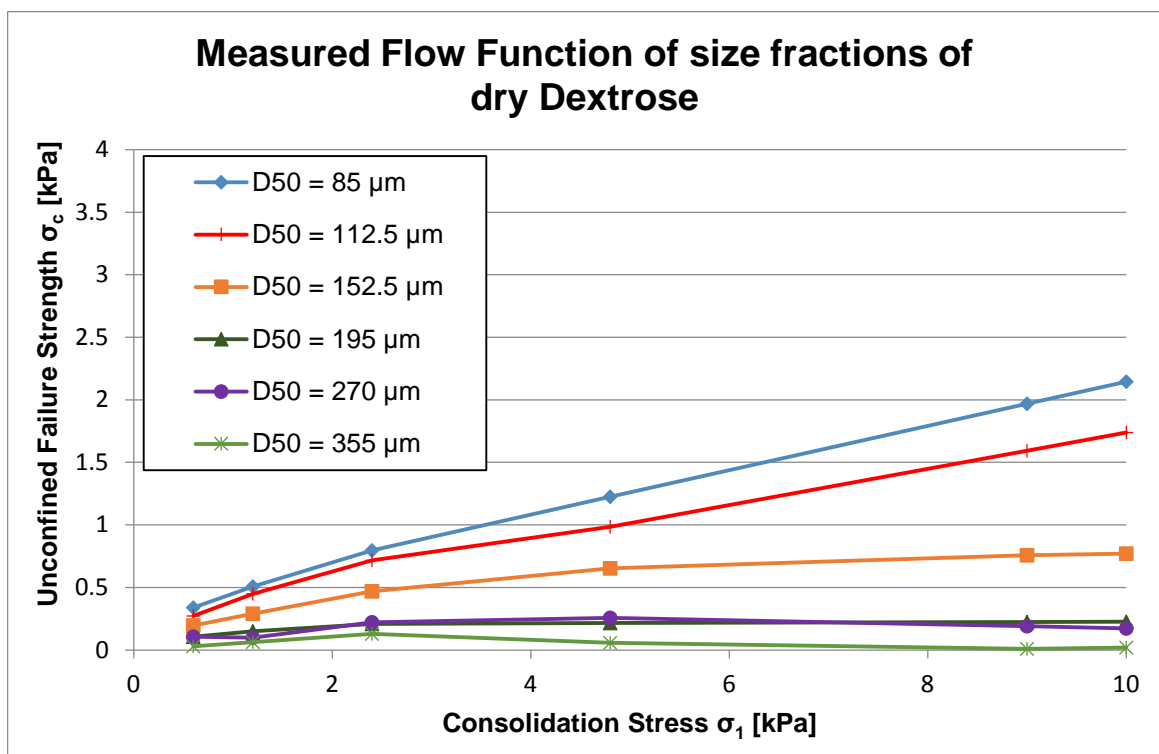


Figure A53

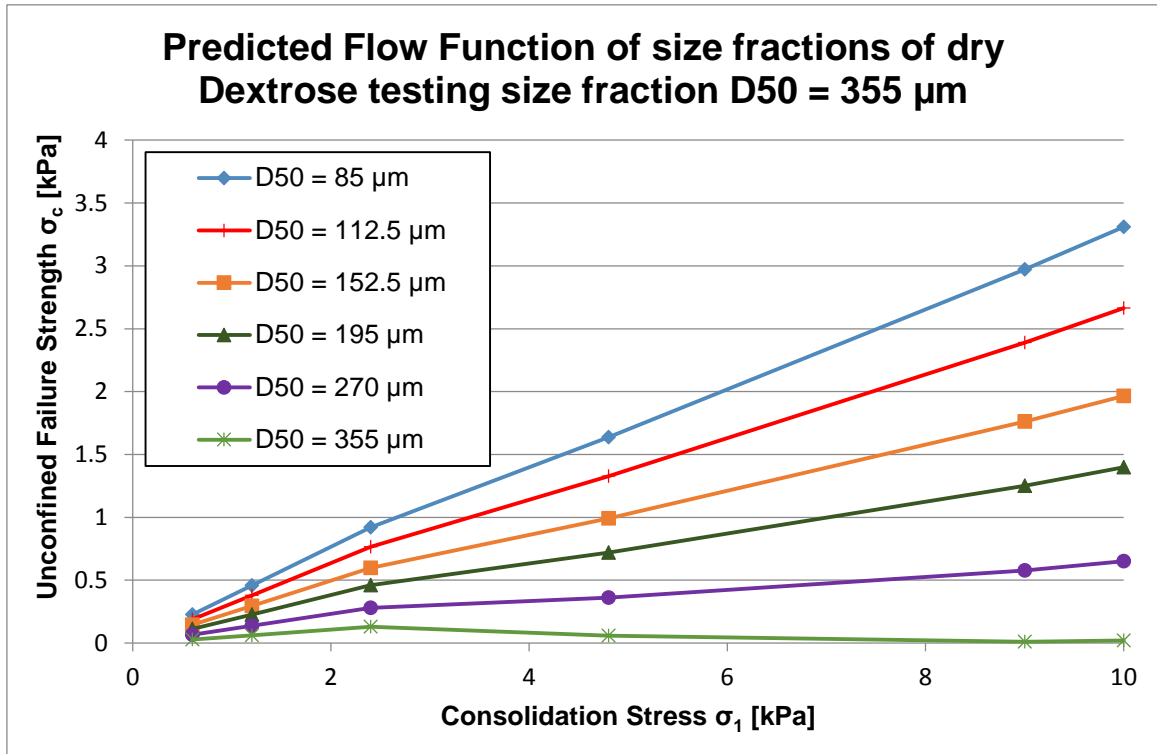


Figure A54

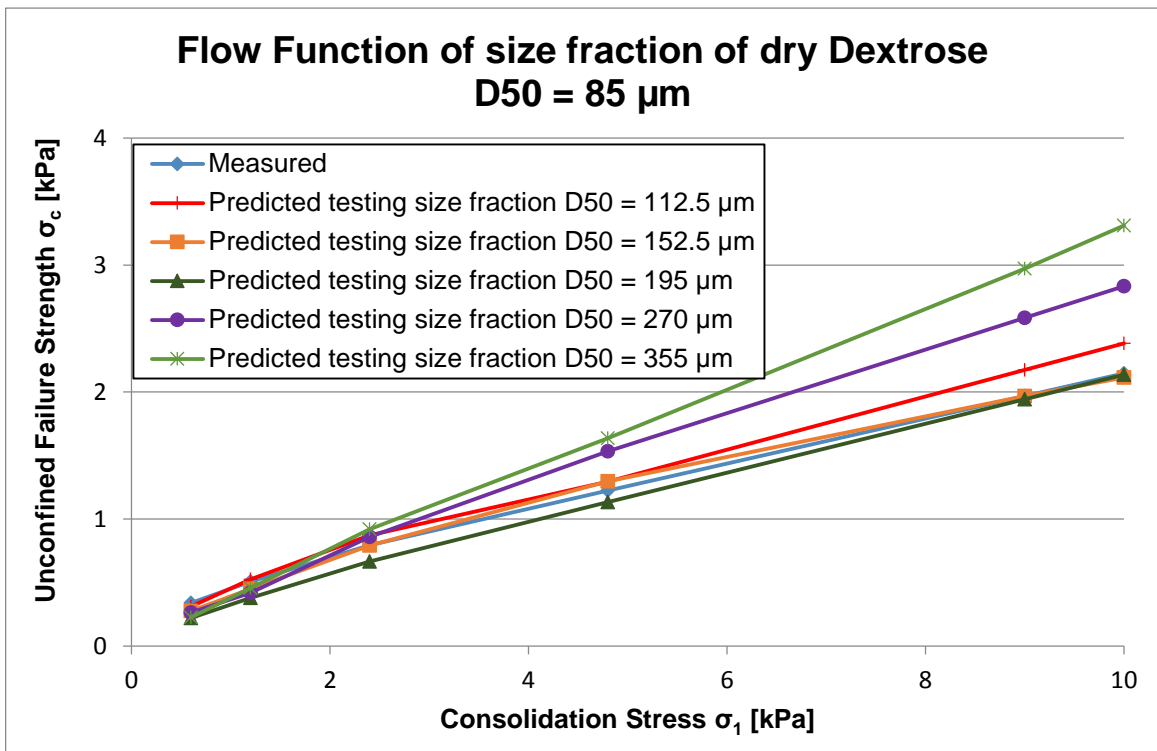


Figure A55

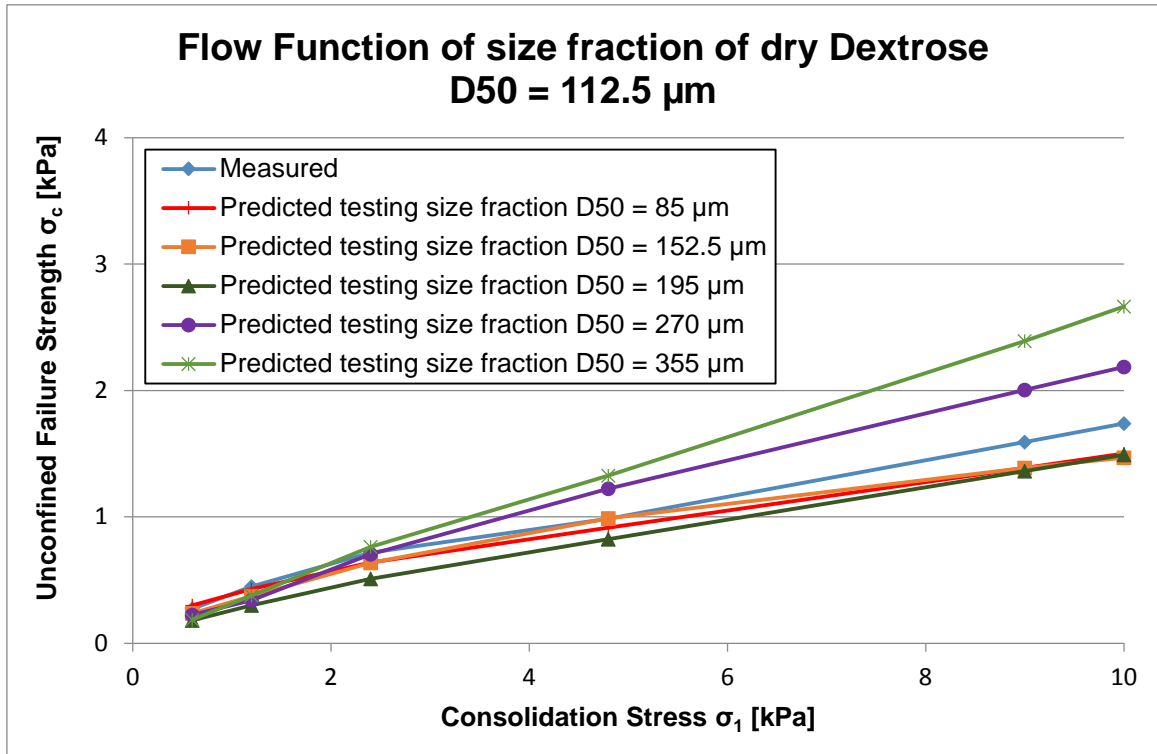


Figure A56

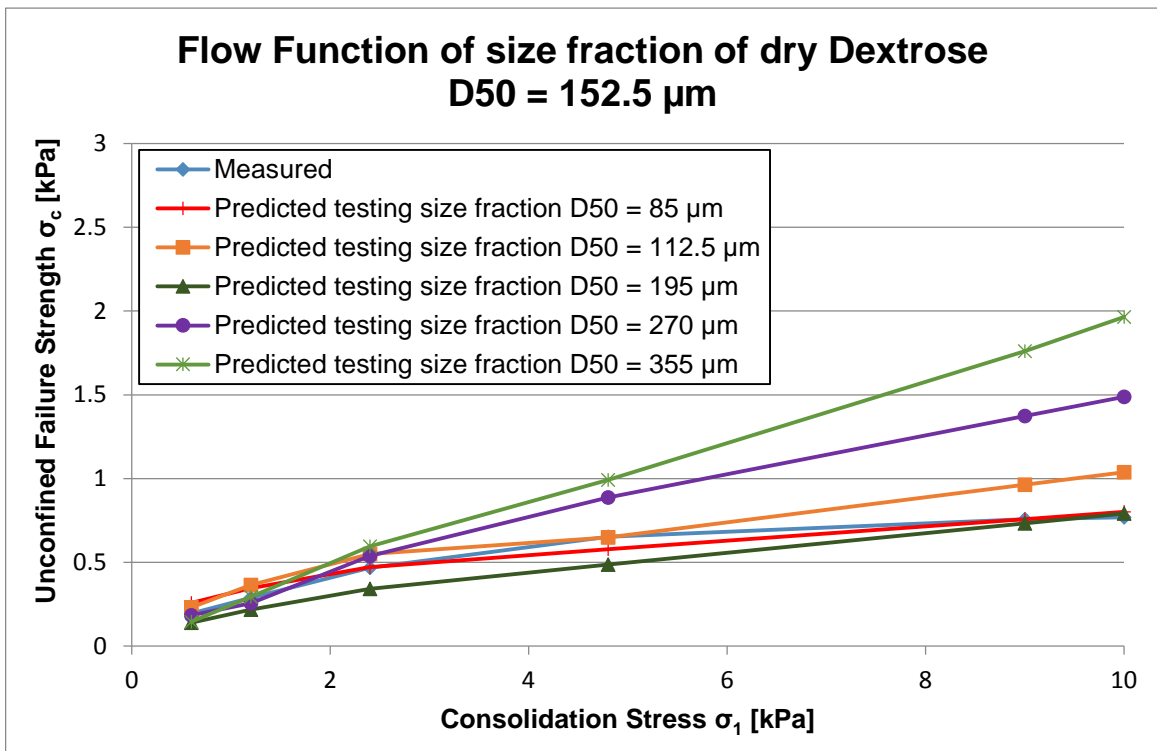


Figure A57

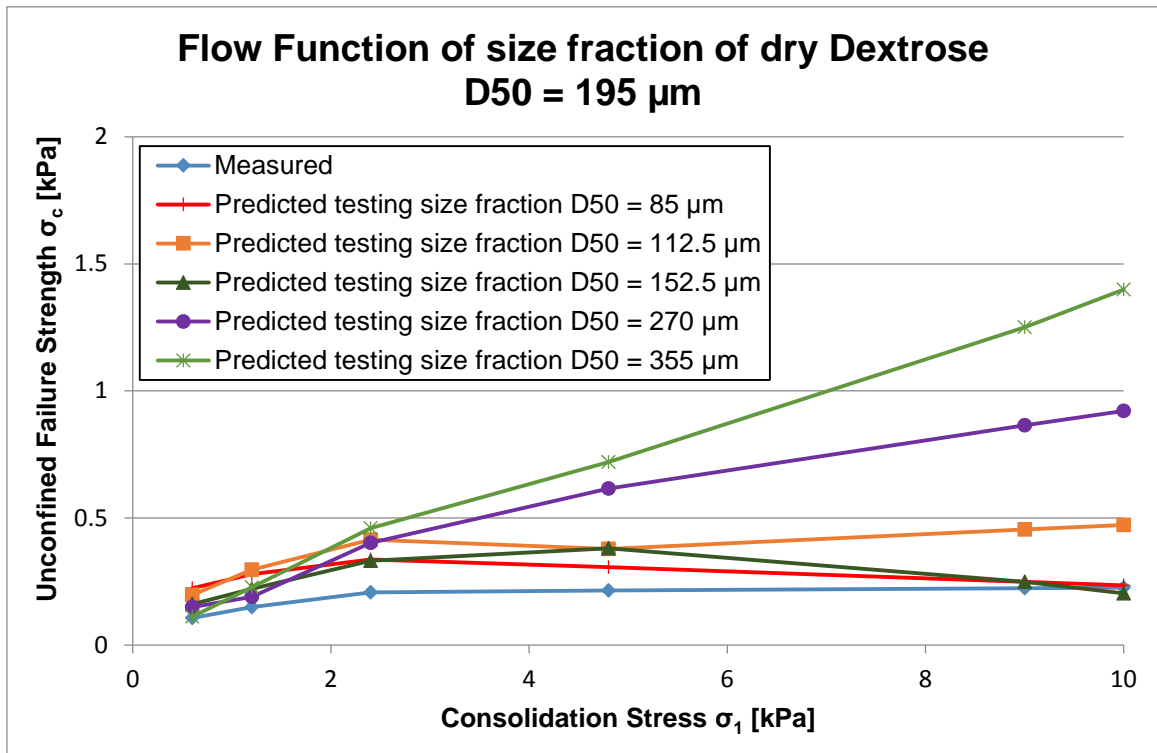


Figure A58

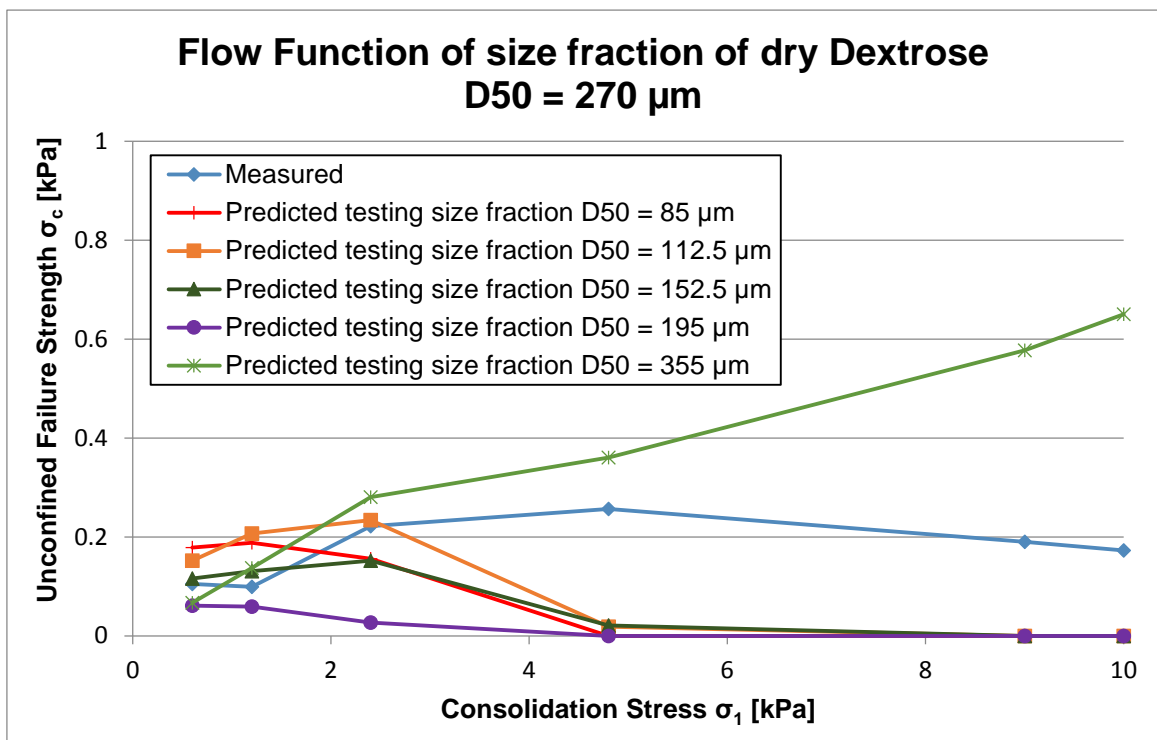


Figure A59

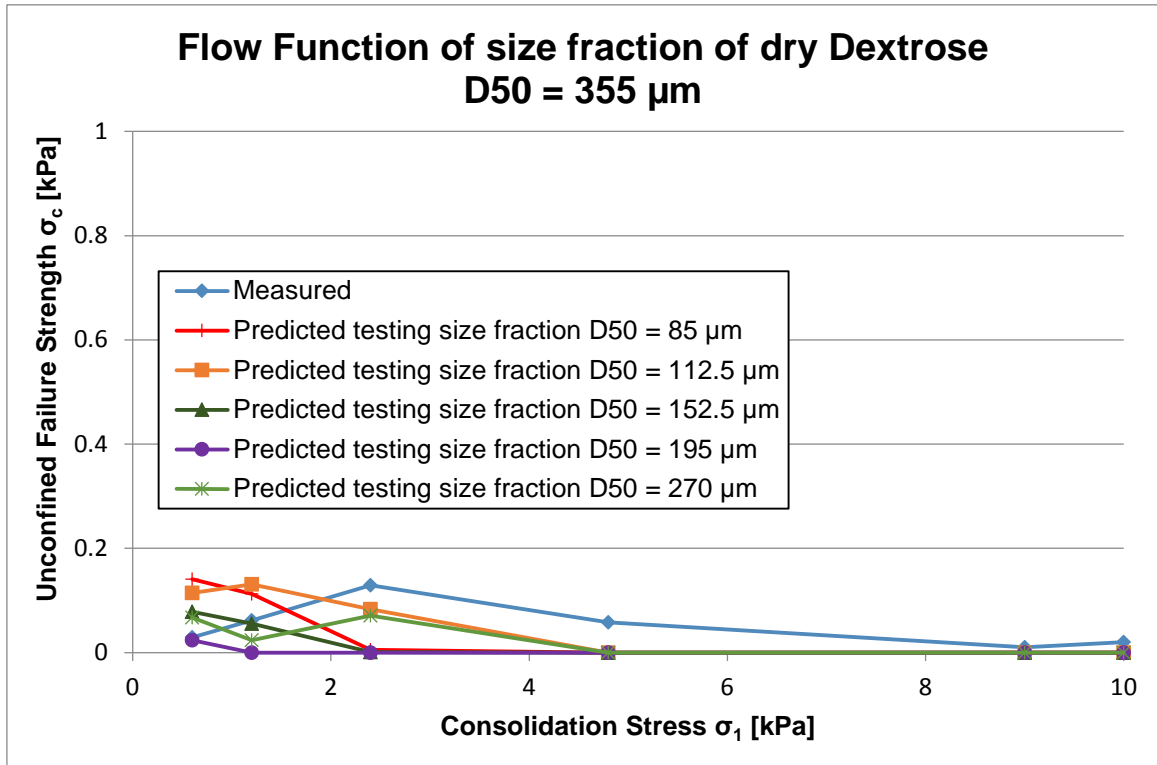


Figure A60

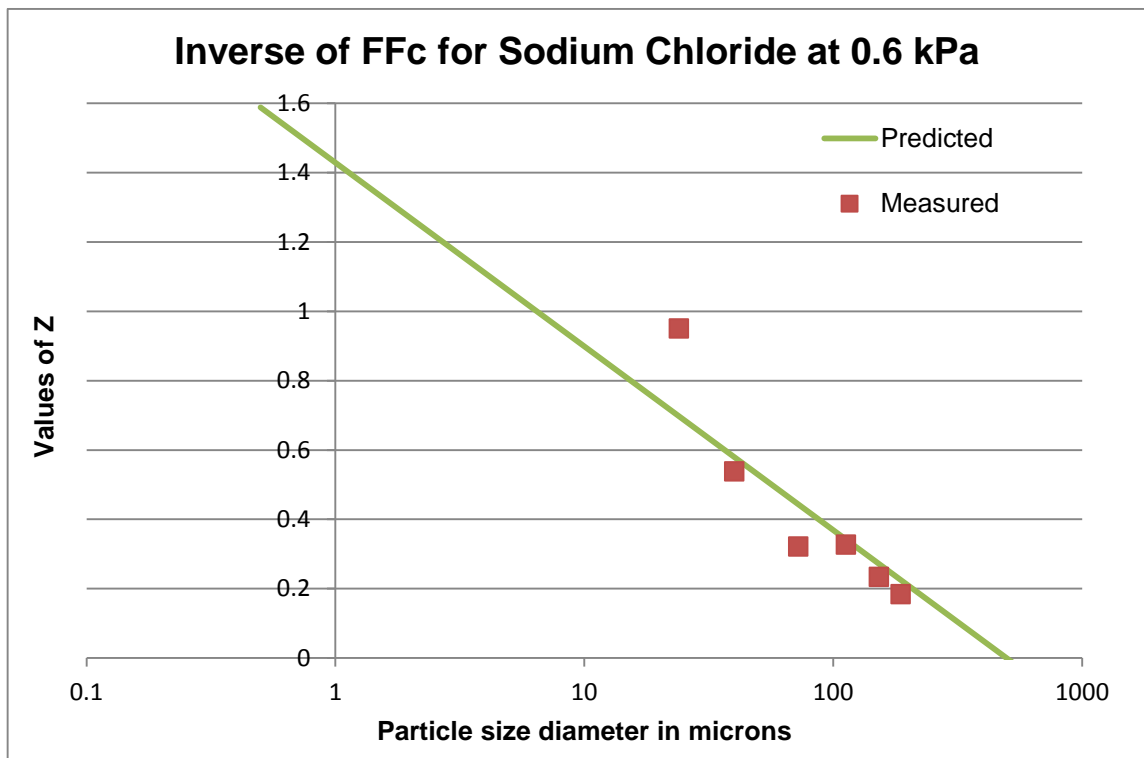


Figure A61

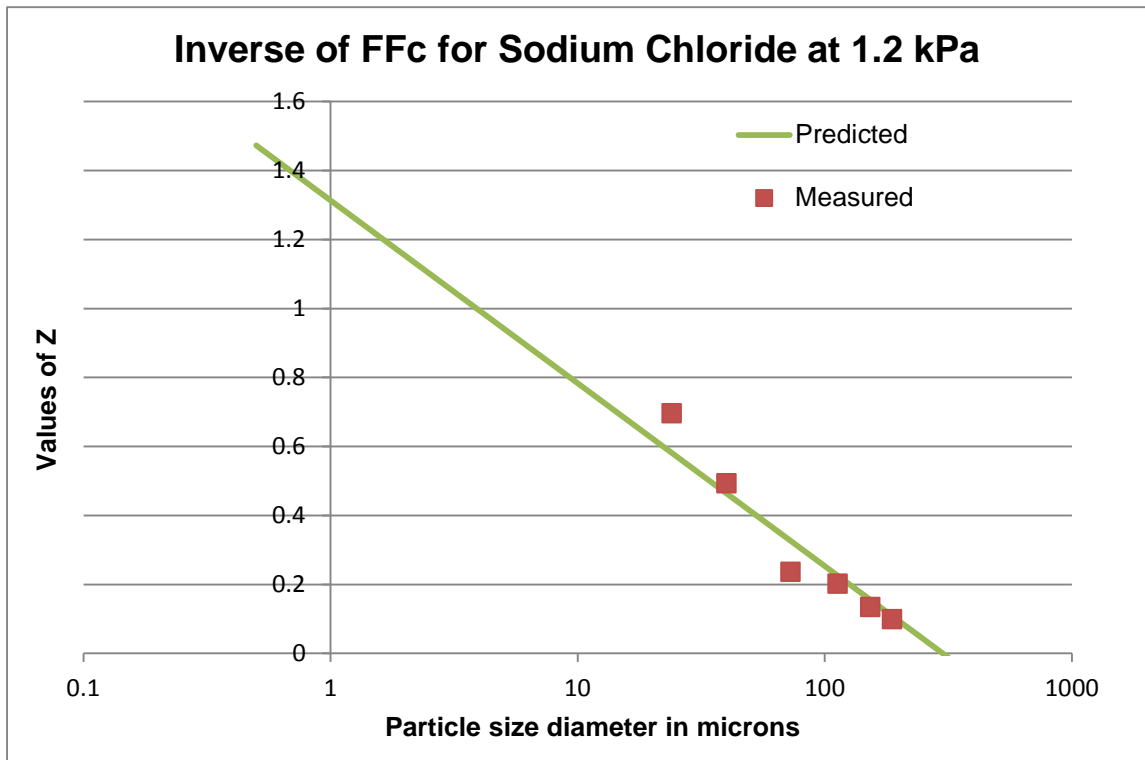


Figure A62

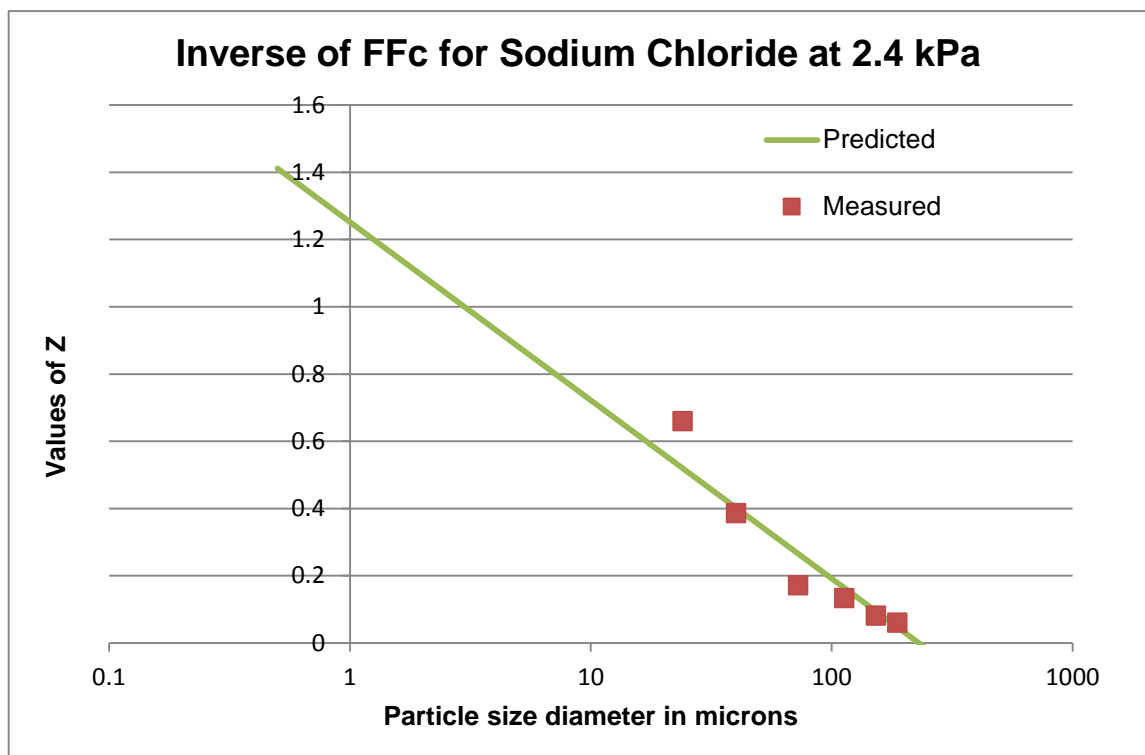


Figure A63

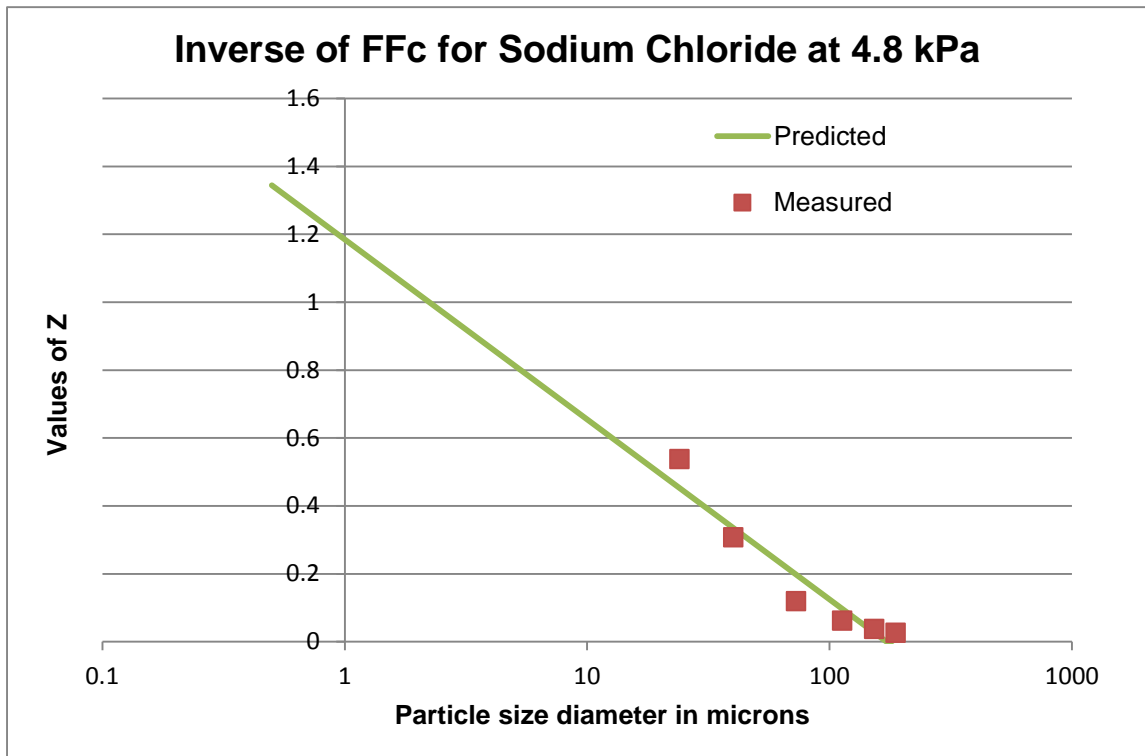


Figure A64

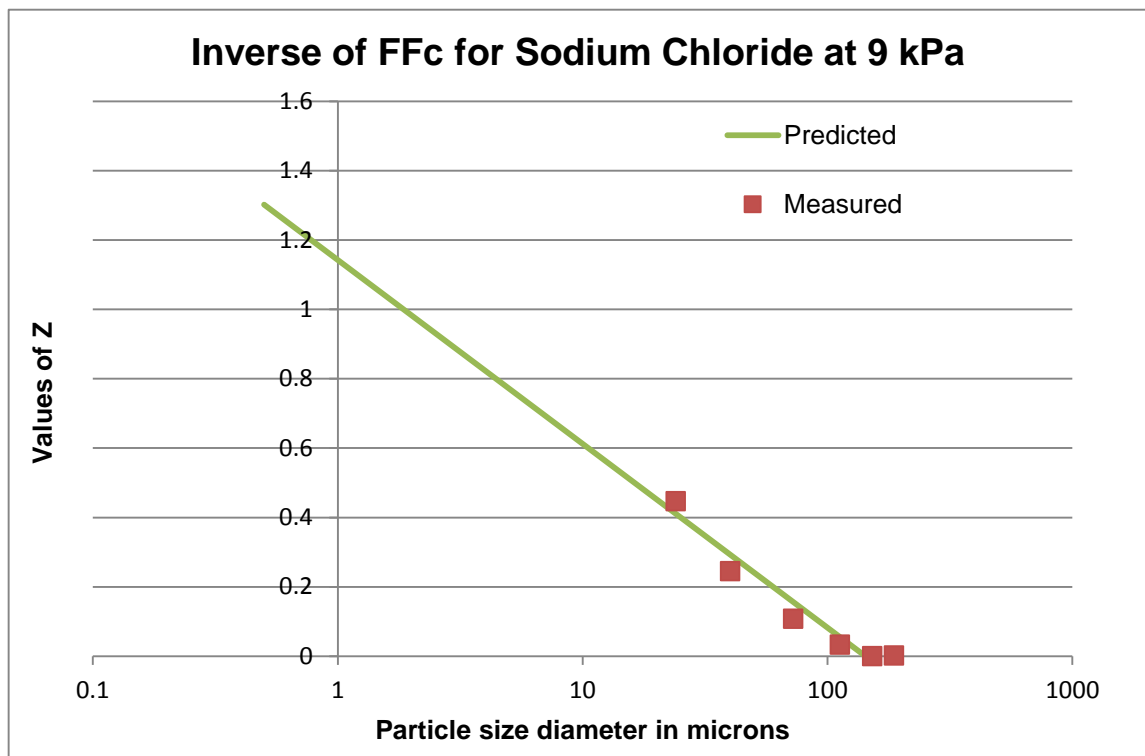


Figure A65

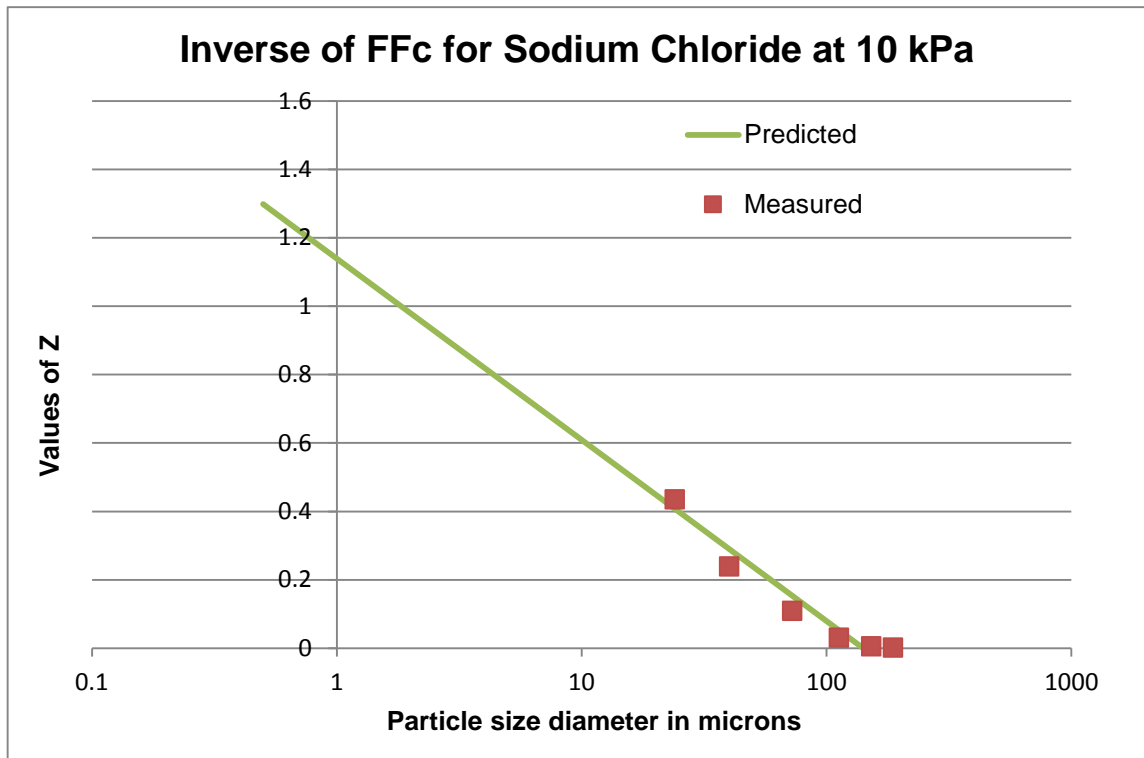


Figure A66

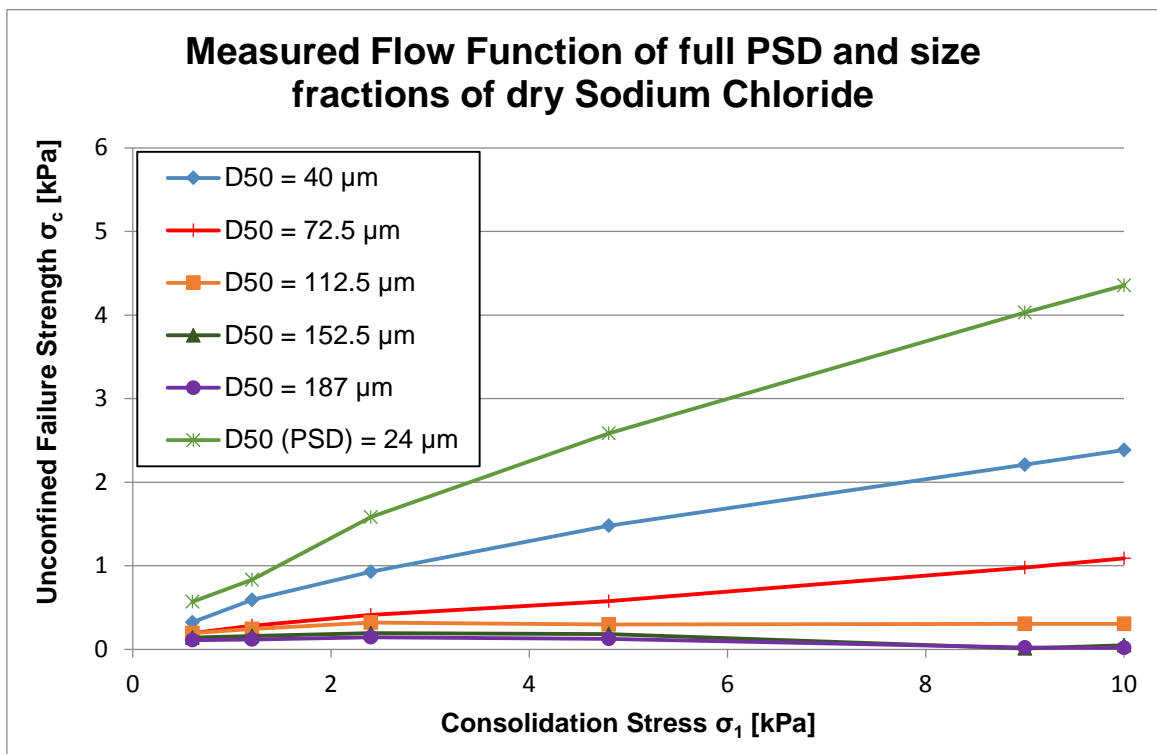


Figure A67

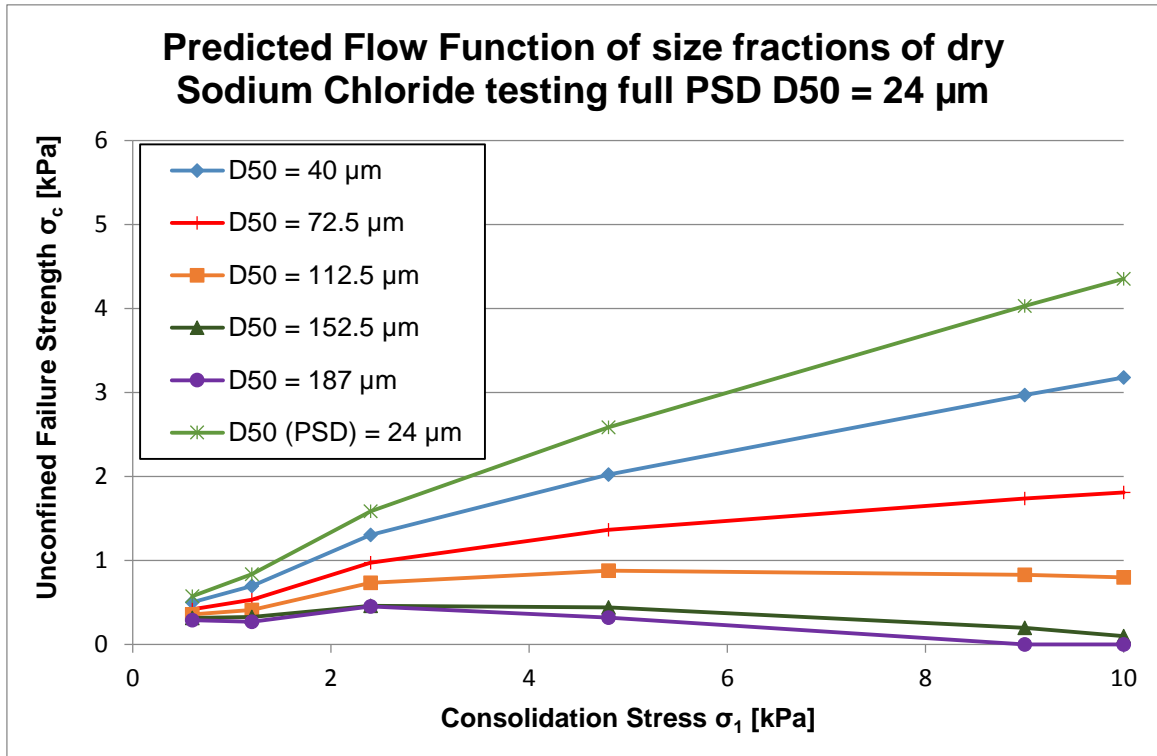


Figure A68

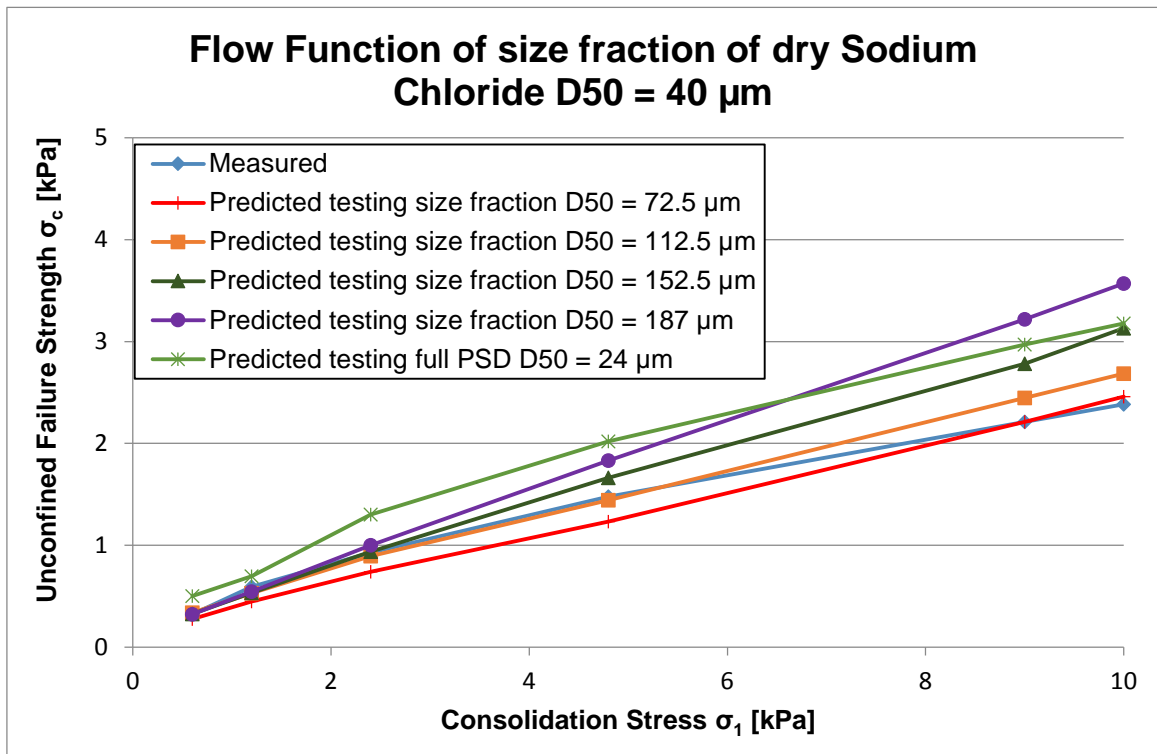


Figure A69

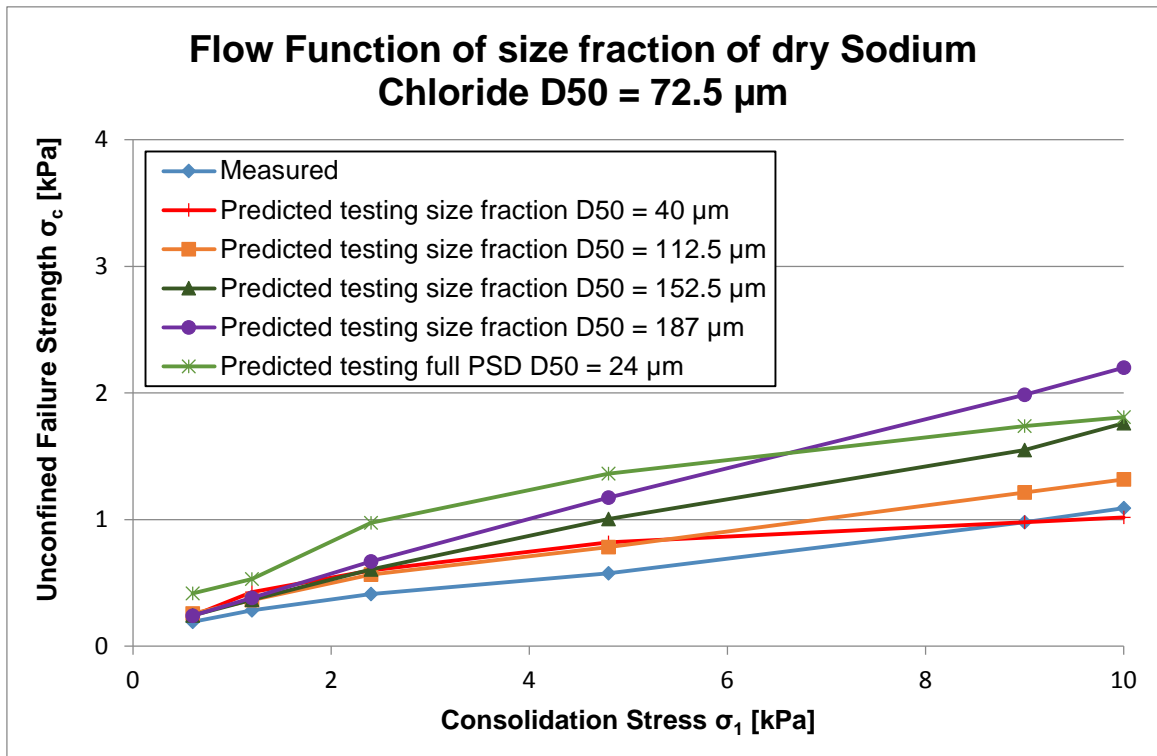


Figure A70

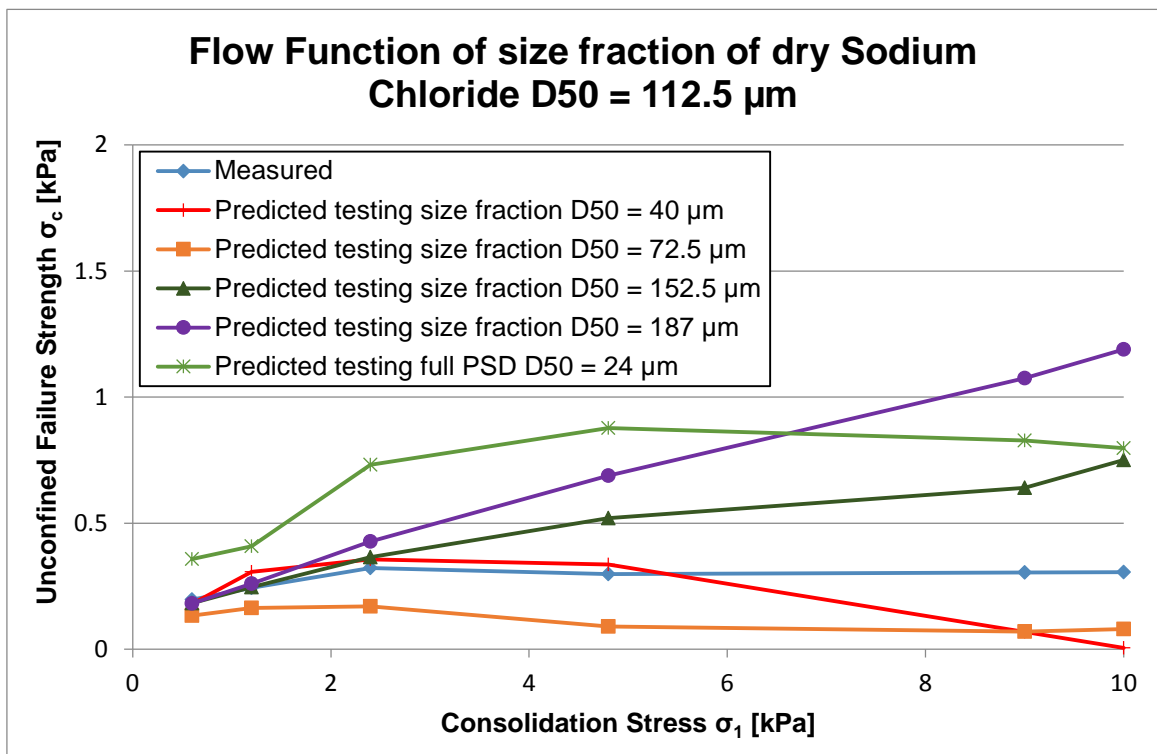


Figure A71

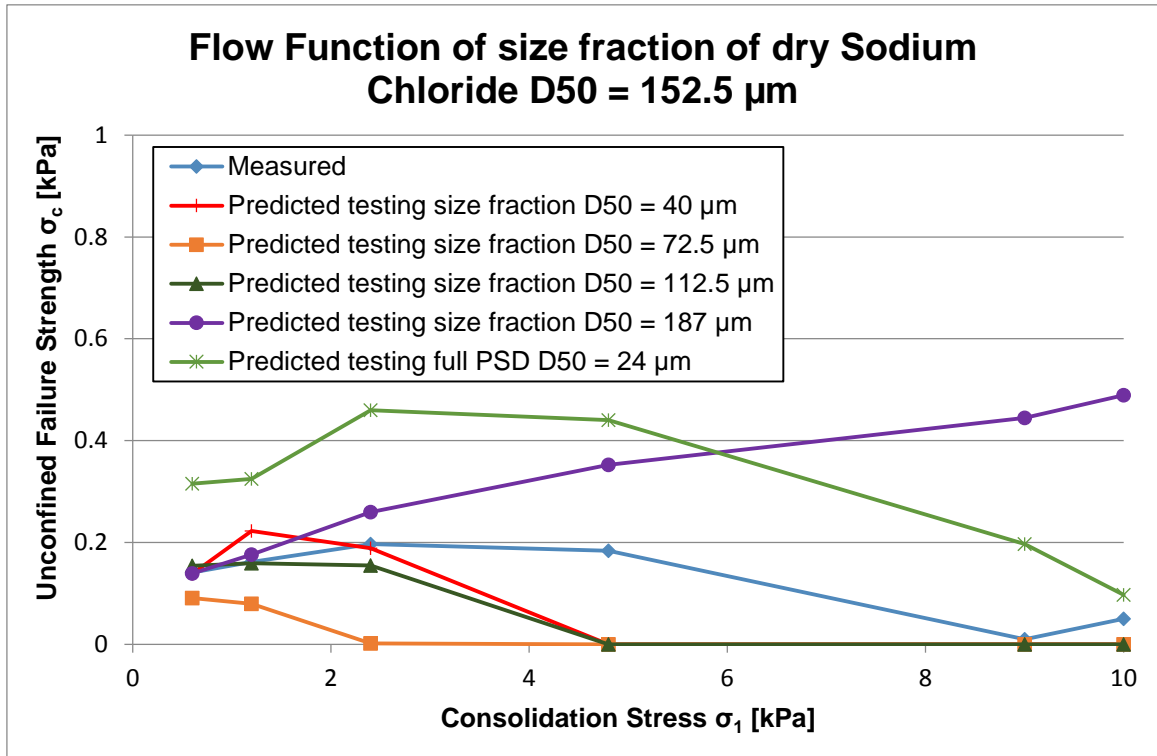


Figure A72

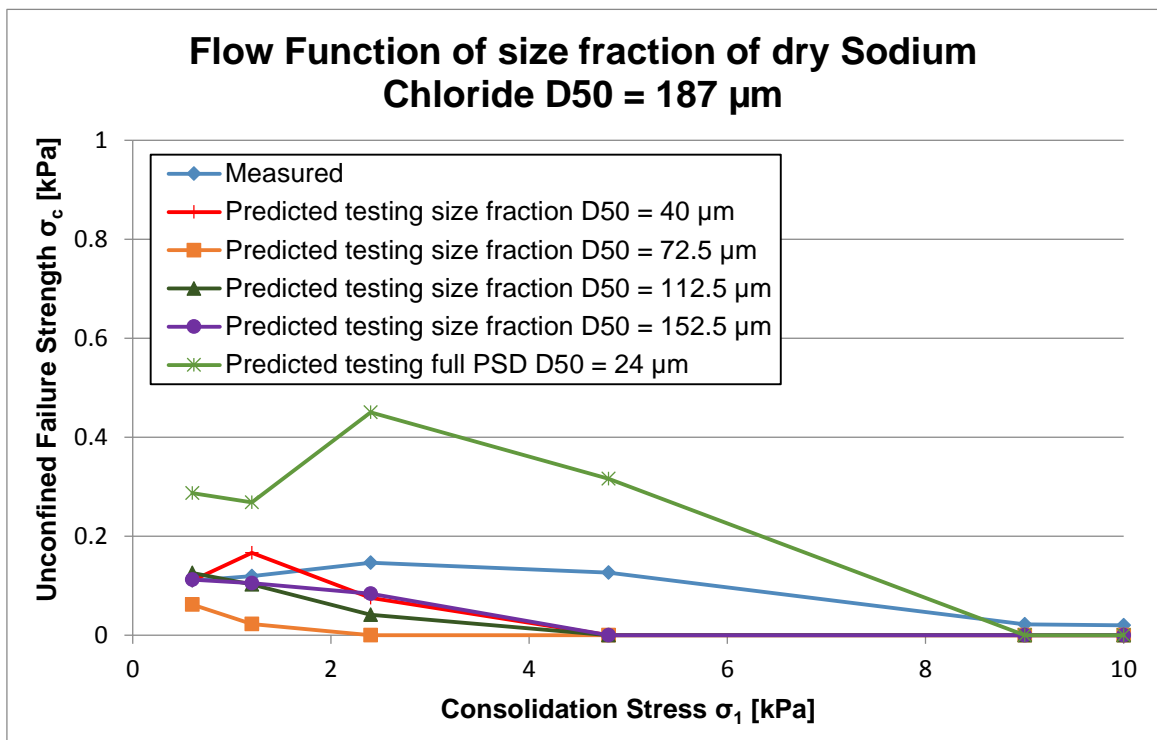


Figure A73

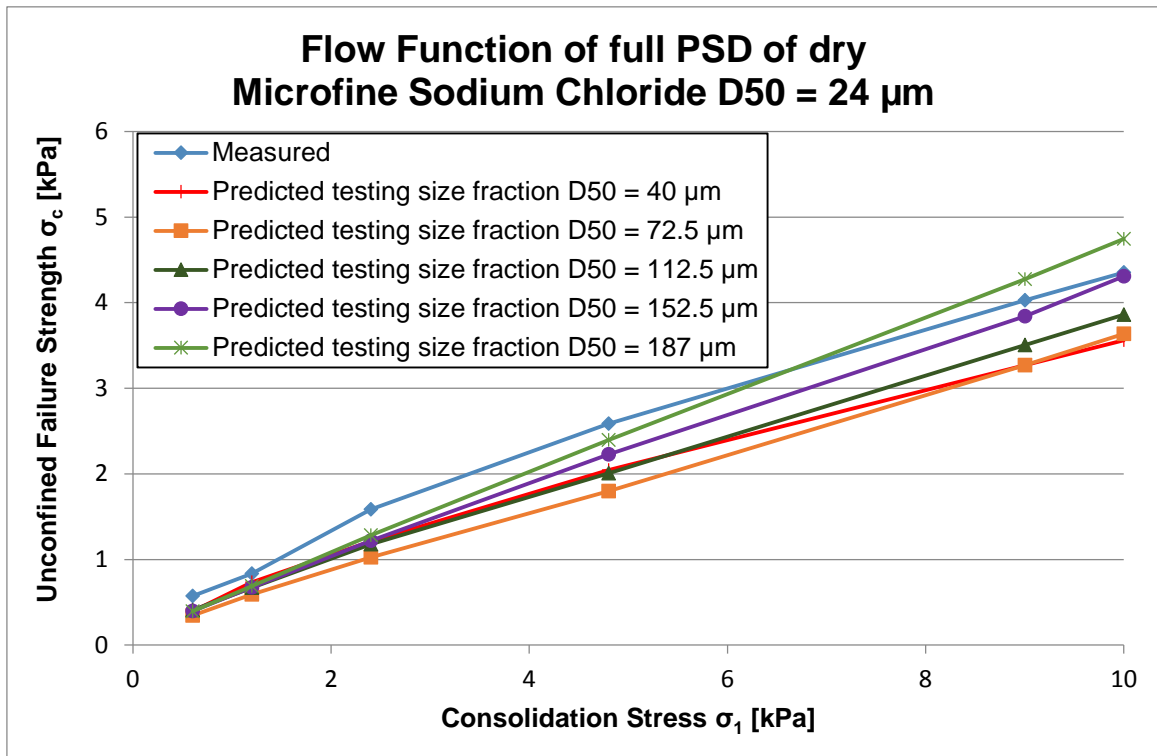


Figure A74

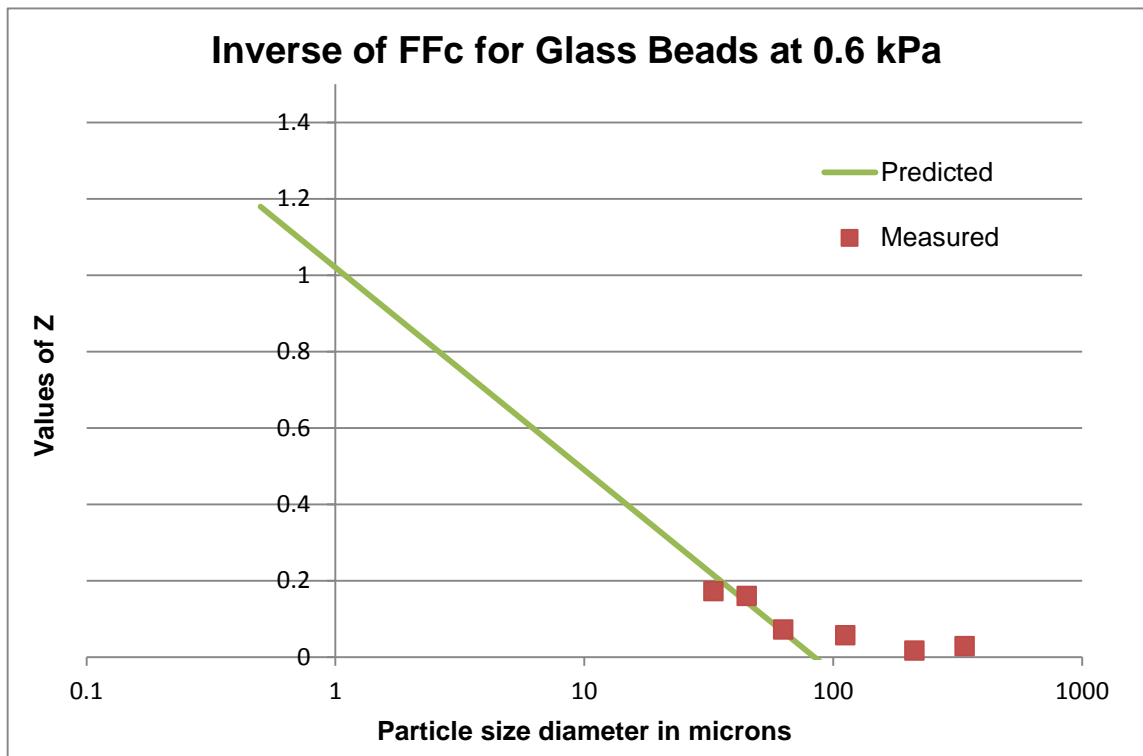


Figure A75

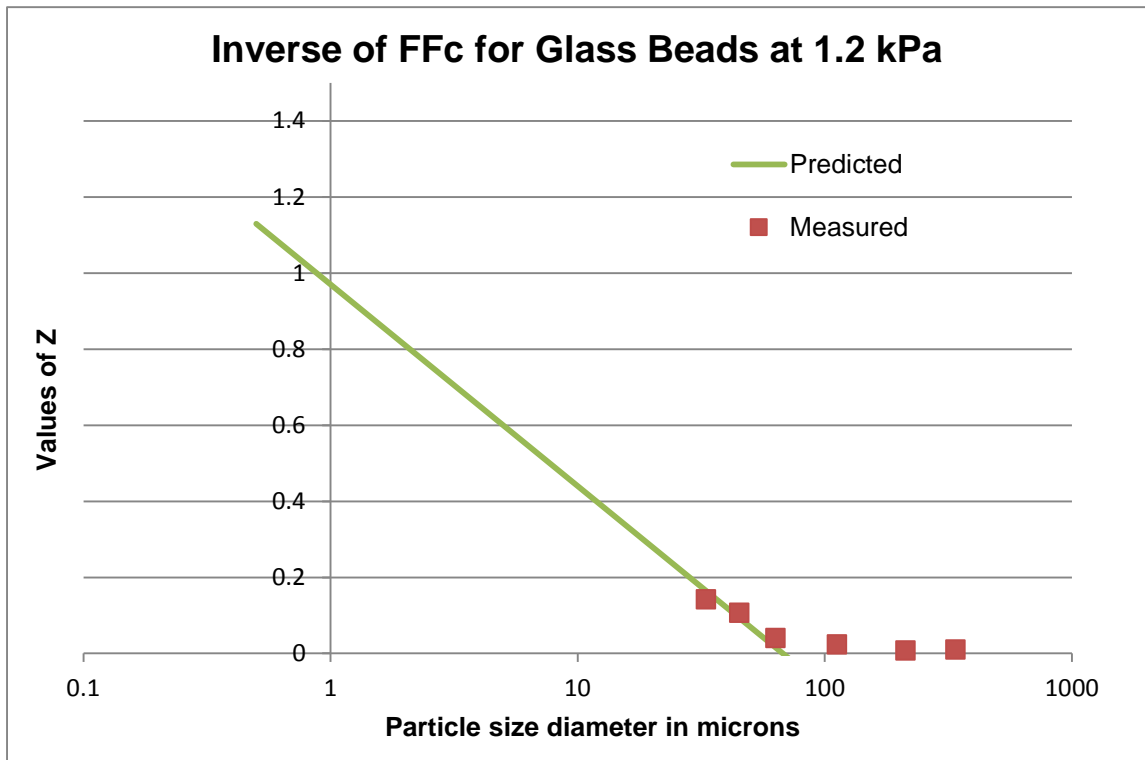


Figure A76

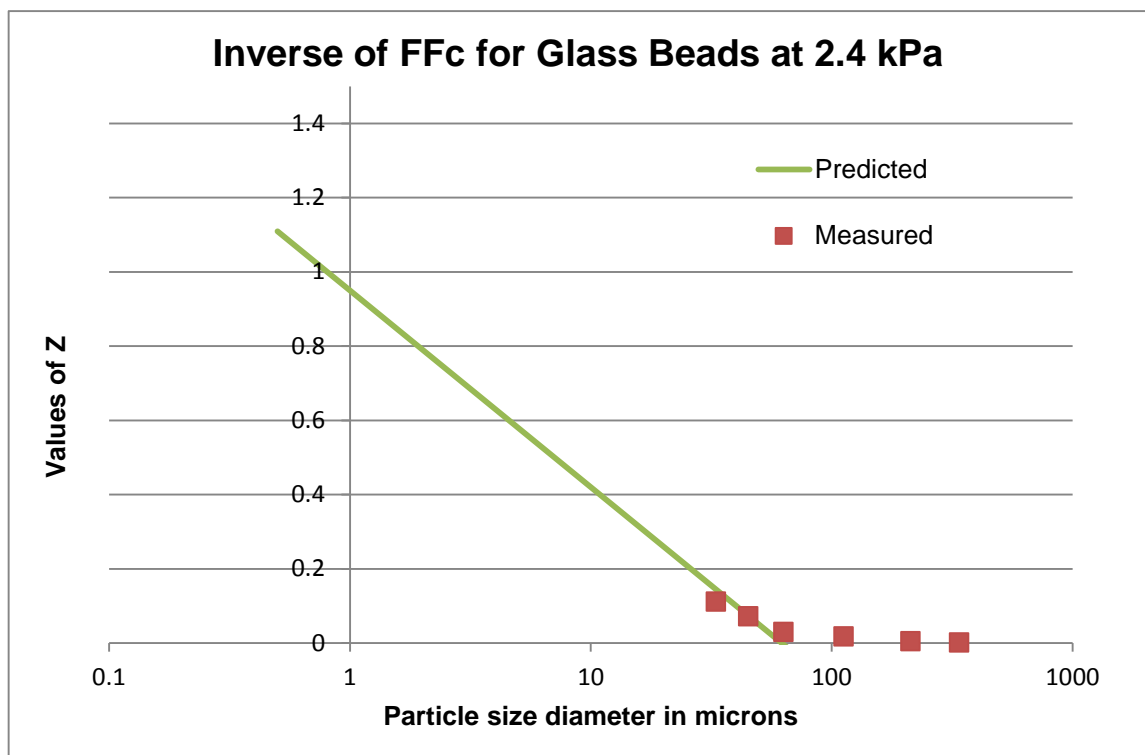


Figure A77

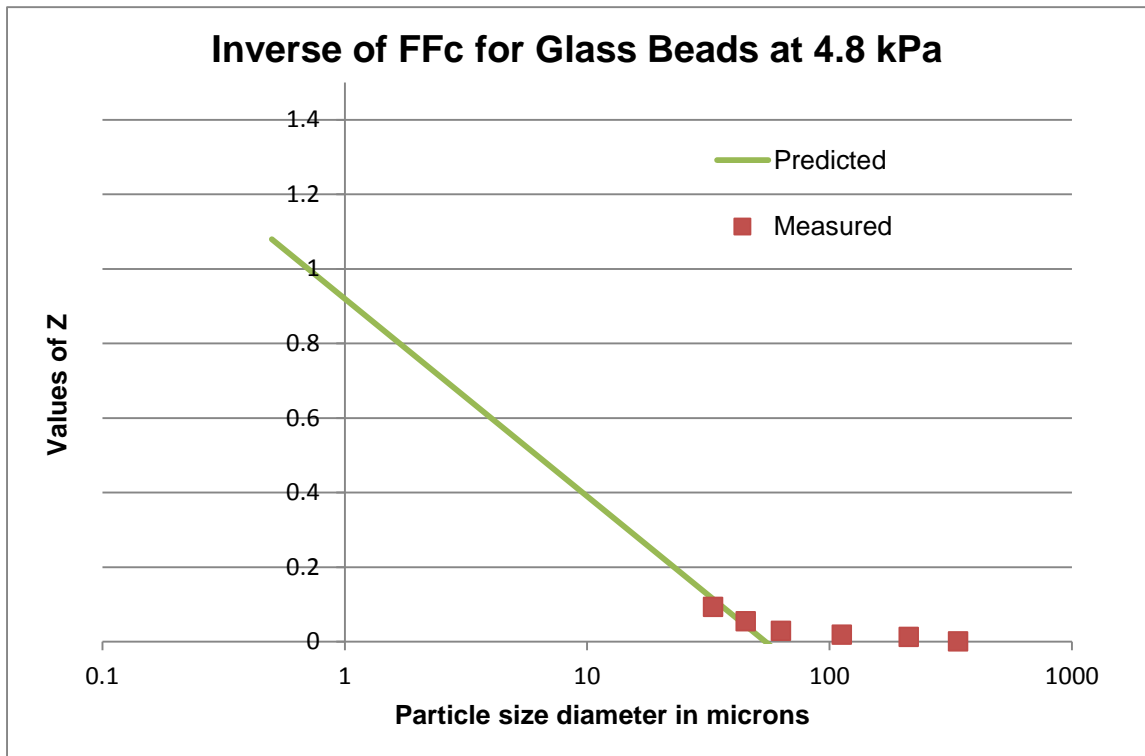


Figure A78

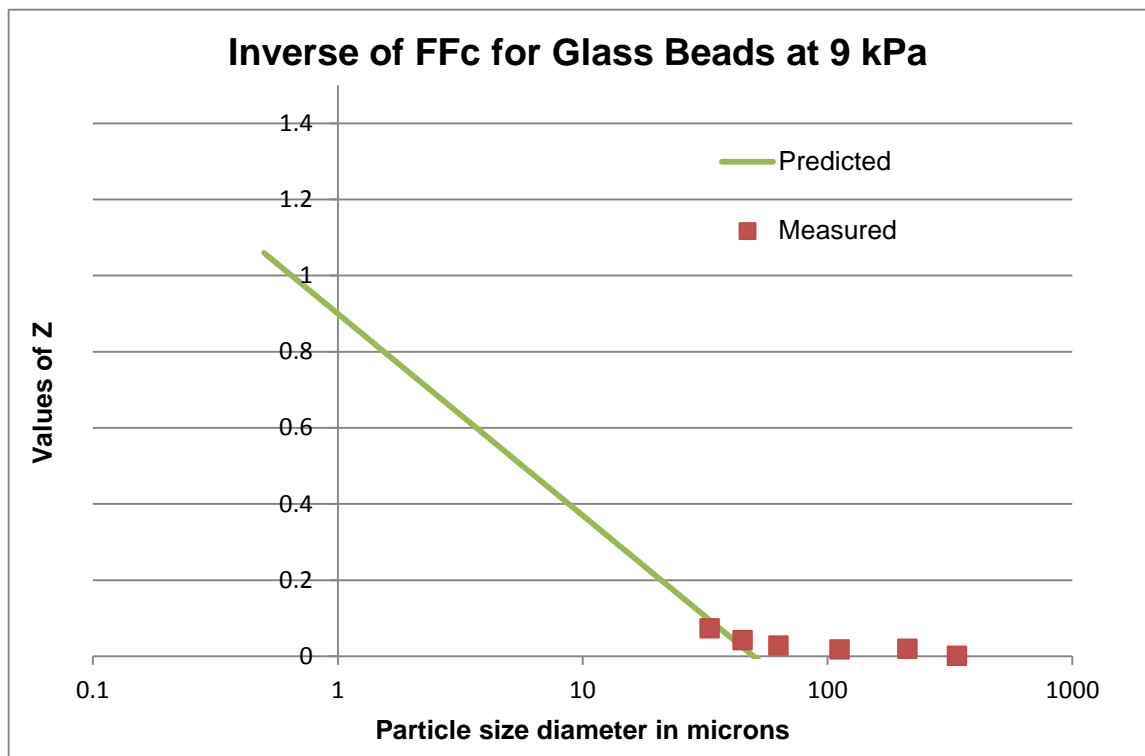


Figure A79

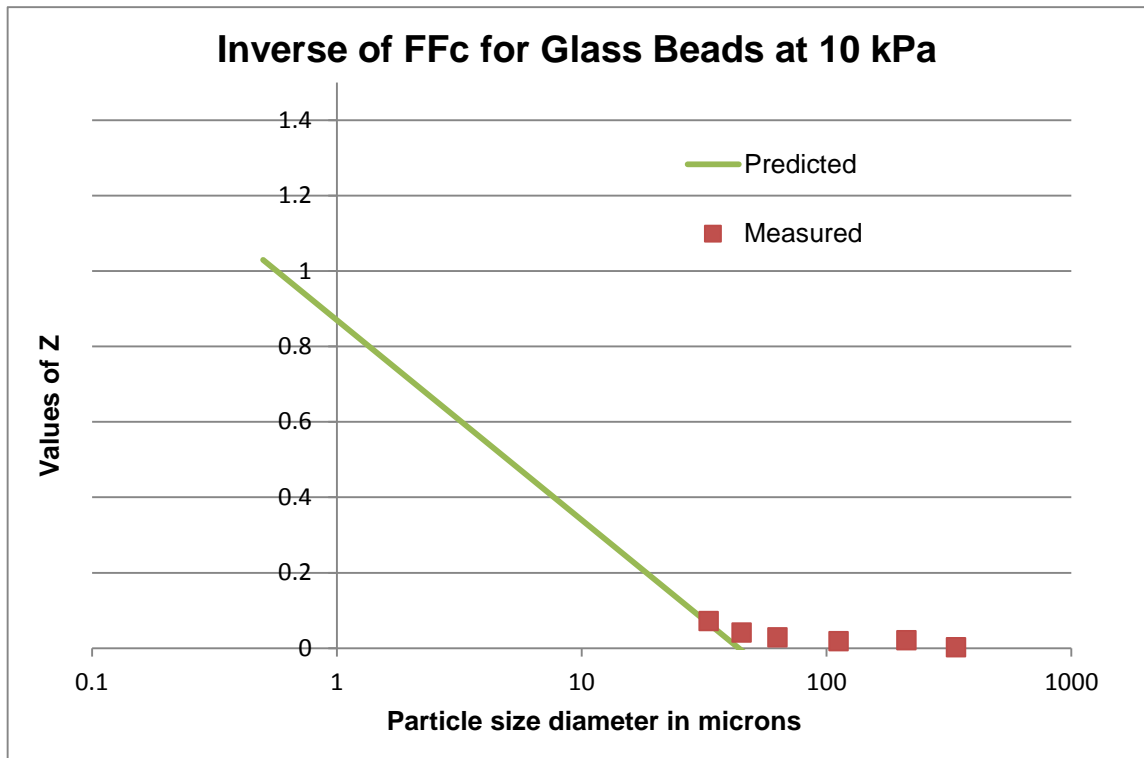


Figure A80

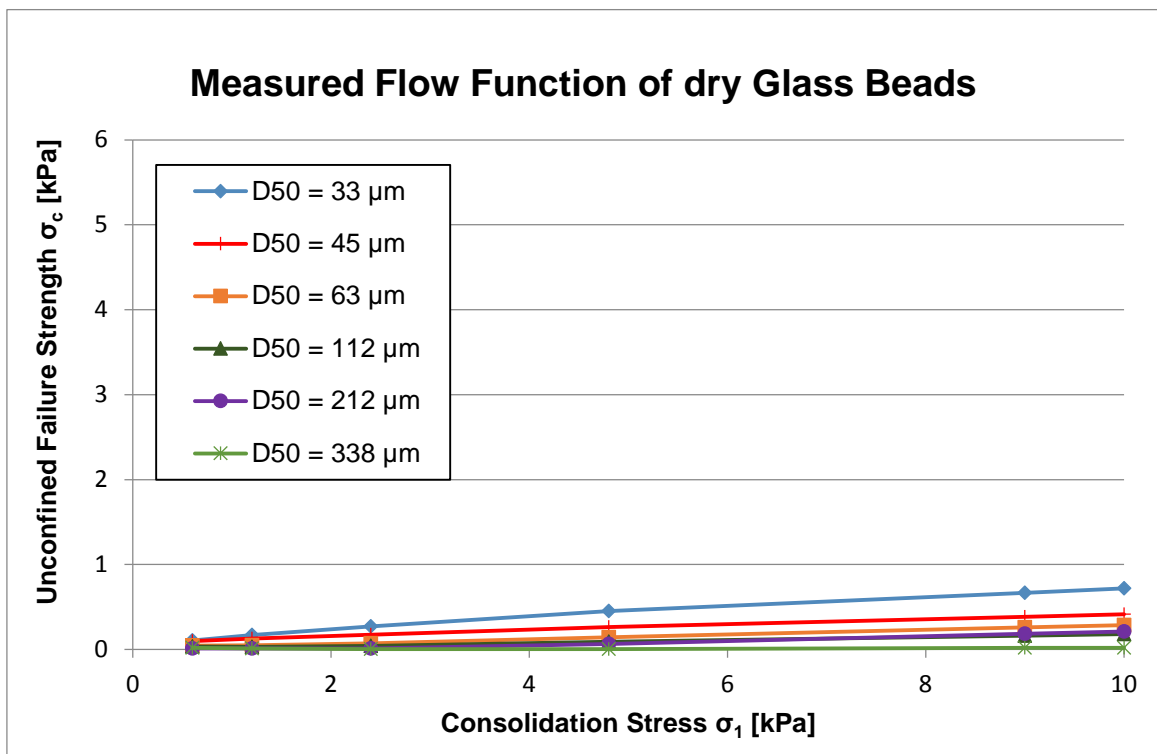


Figure A81

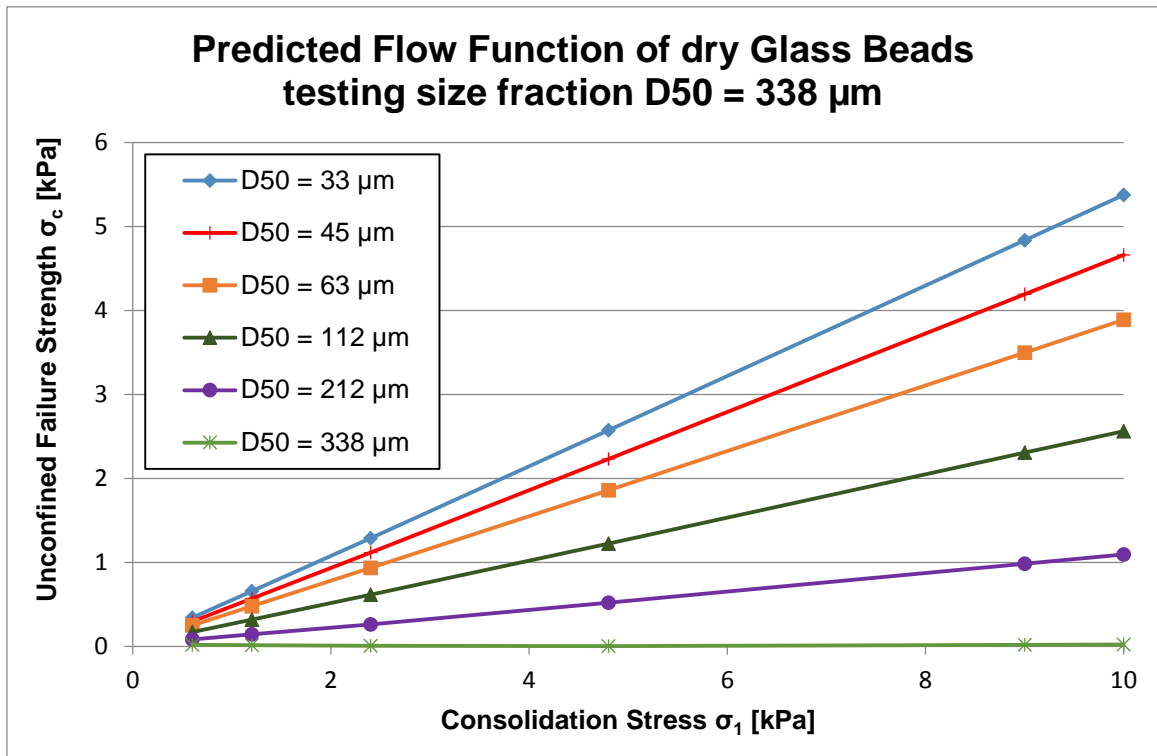


Figure A82

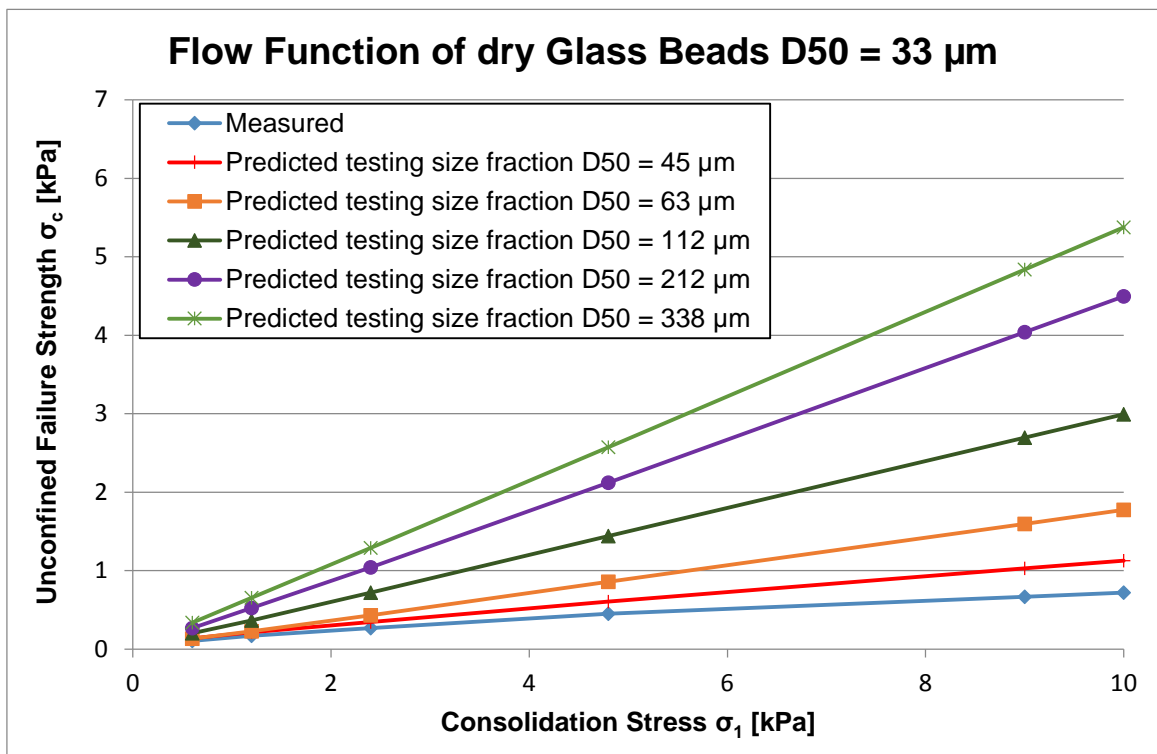


Figure A83

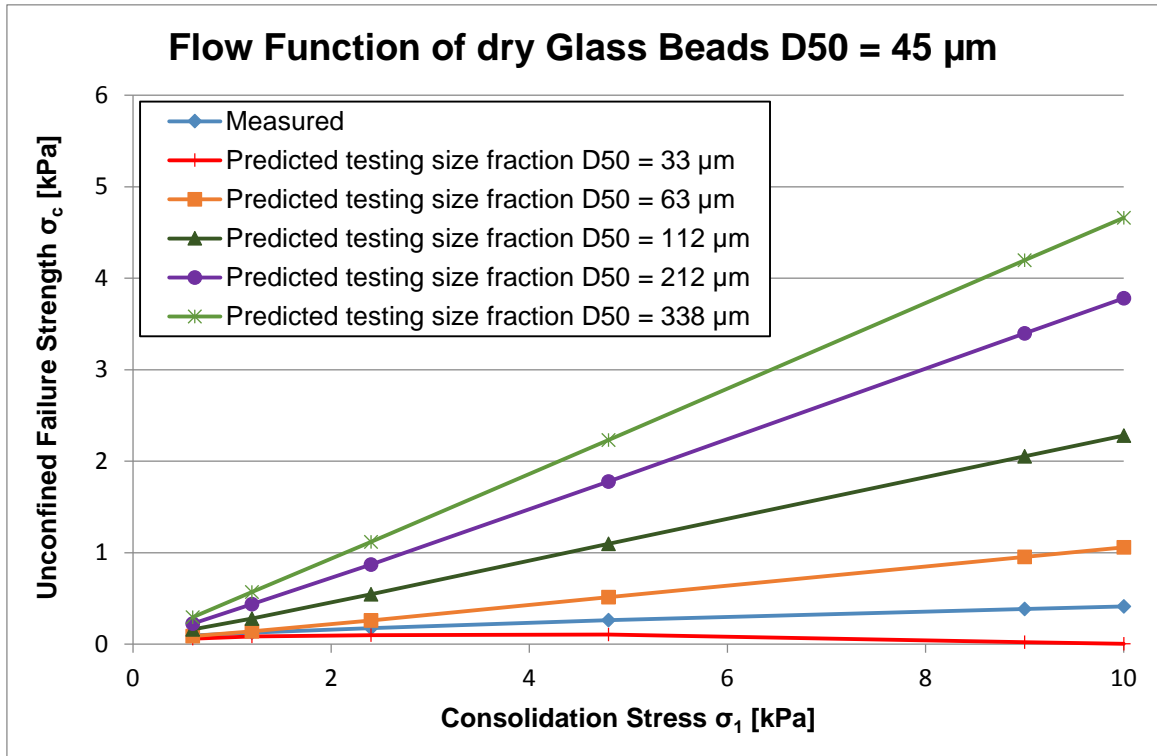


Figure A84

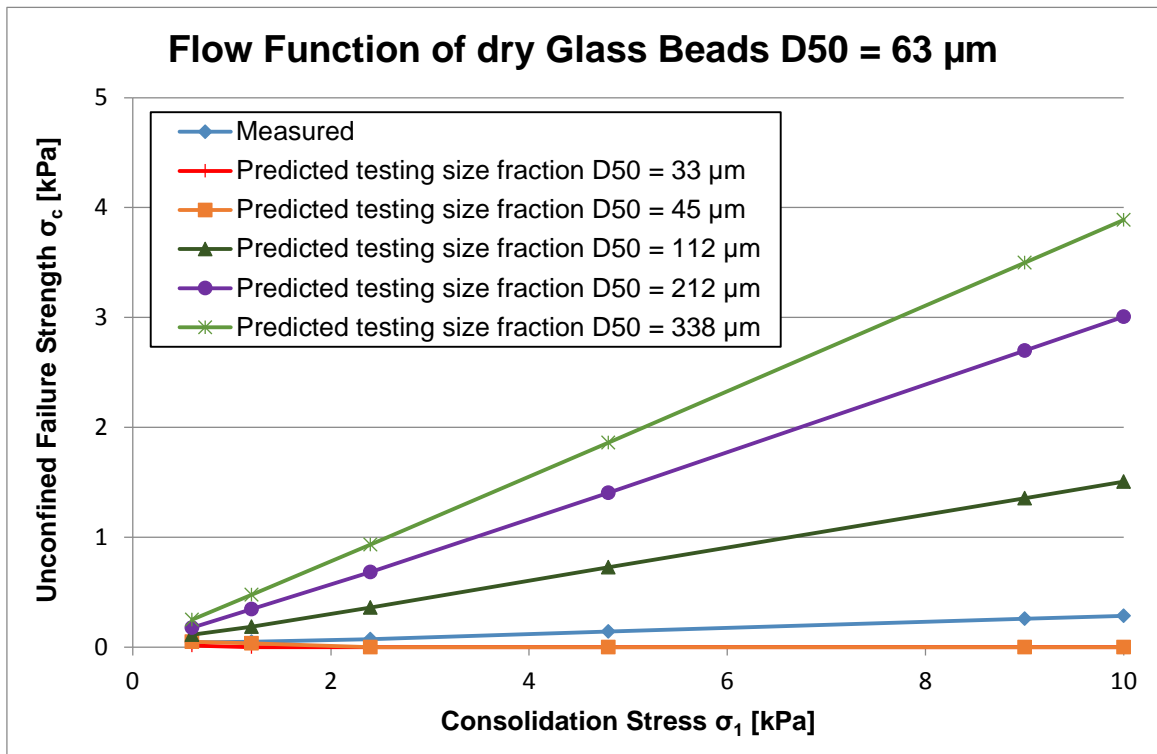


Figure A85

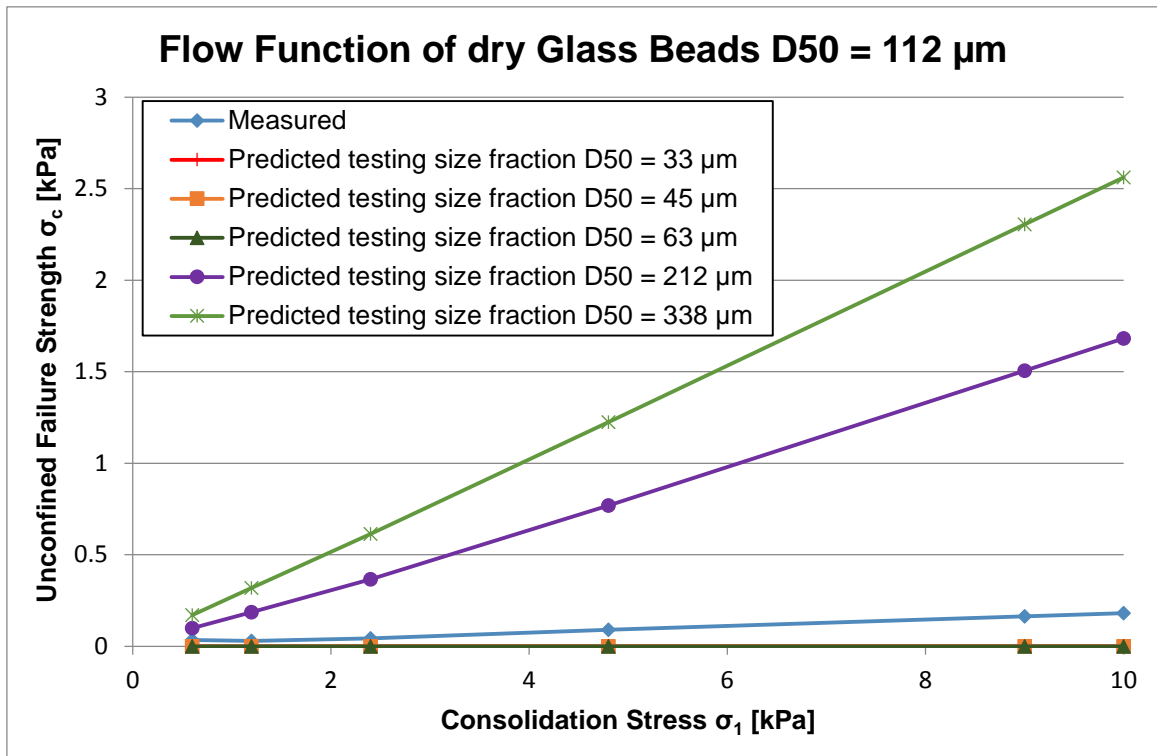


Figure A86

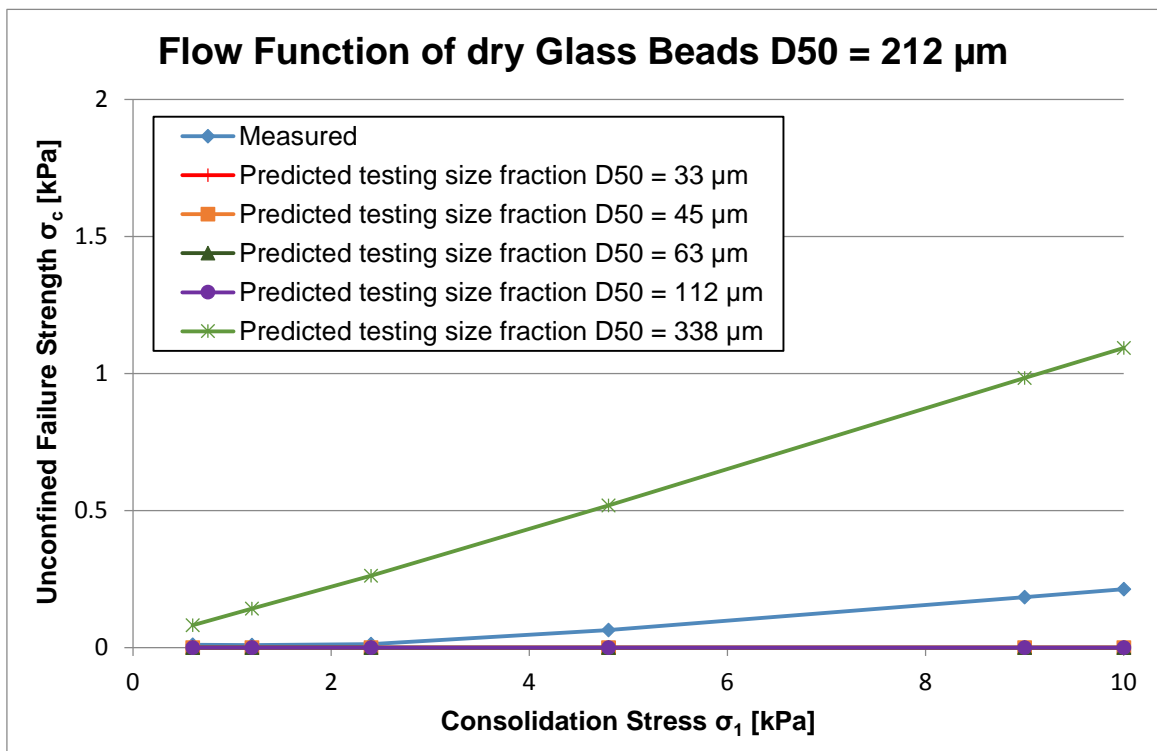


Figure A87

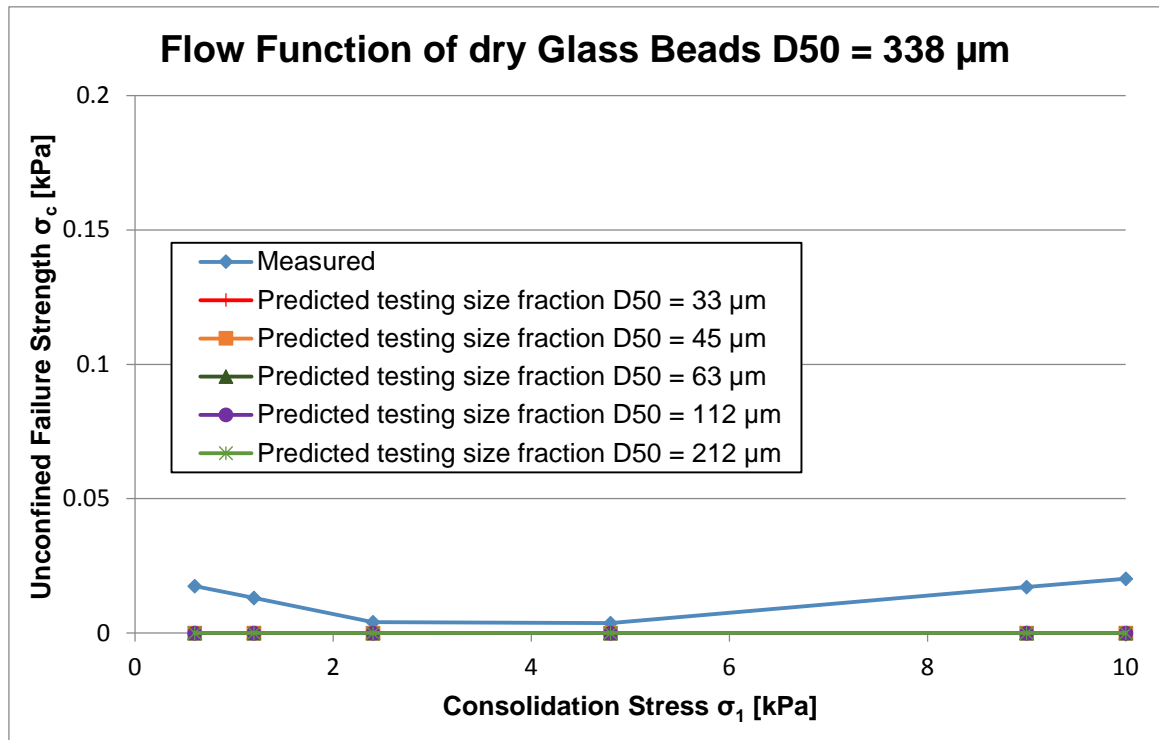


Figure A88

A5 *Effect of free flow additives on wet single powders*

This section shows more results of the effect of tricalcium phosphate on the bulk flow properties of wet single particulate materials as described in chapter 8.

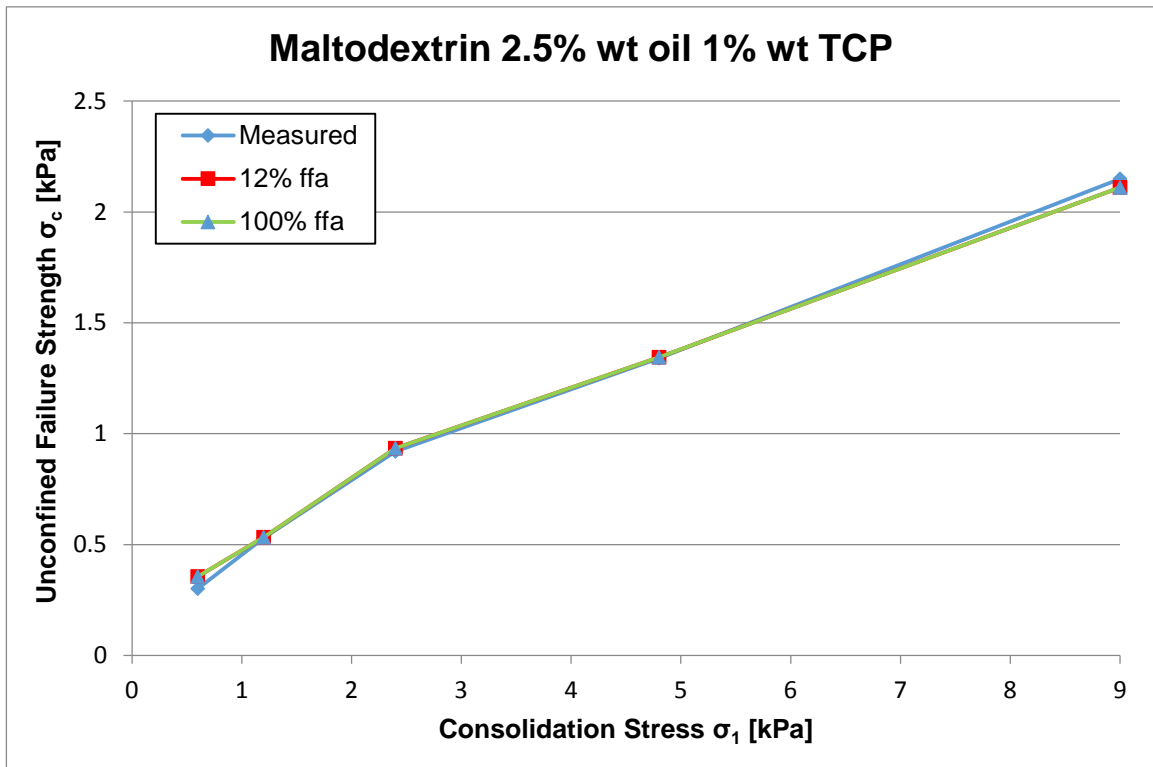


Figure A89

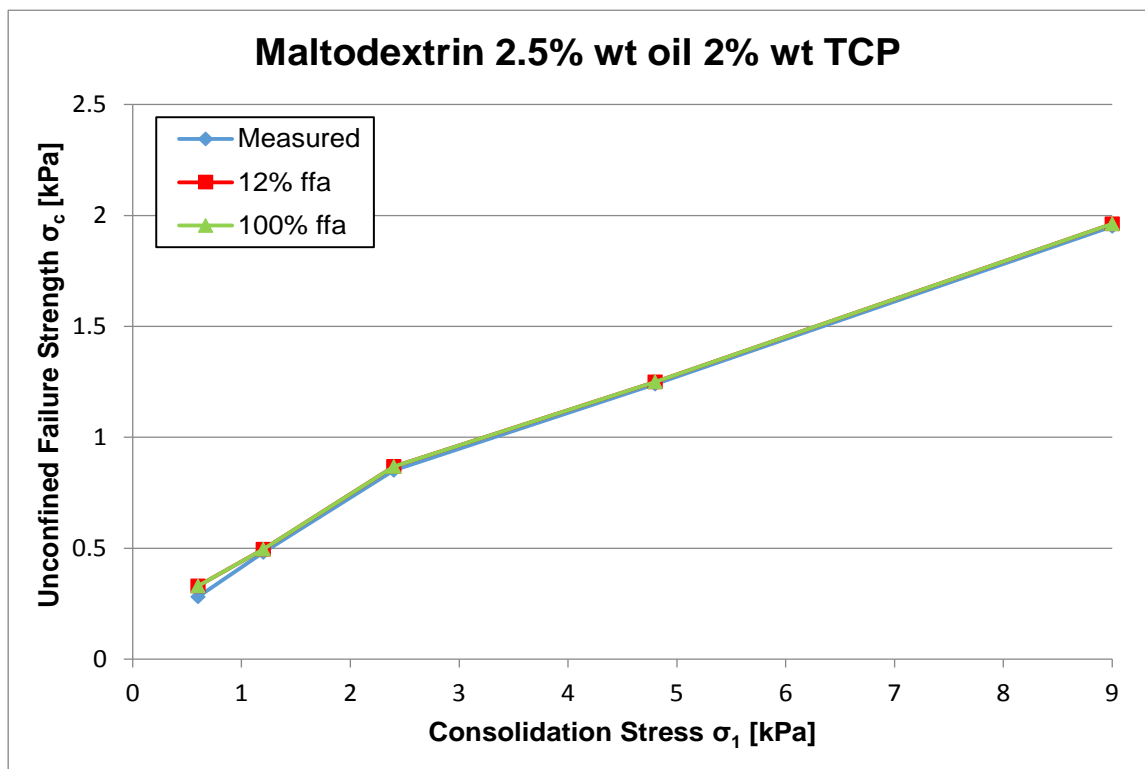


Figure A90

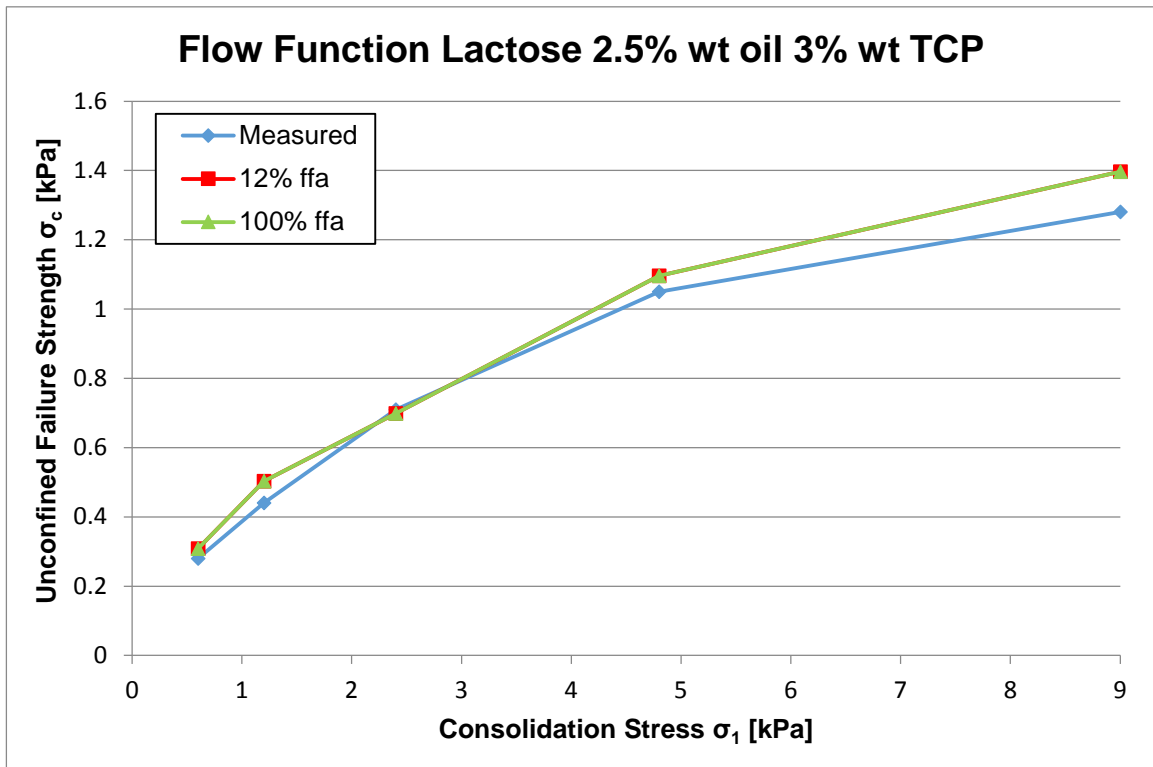


Figure A91

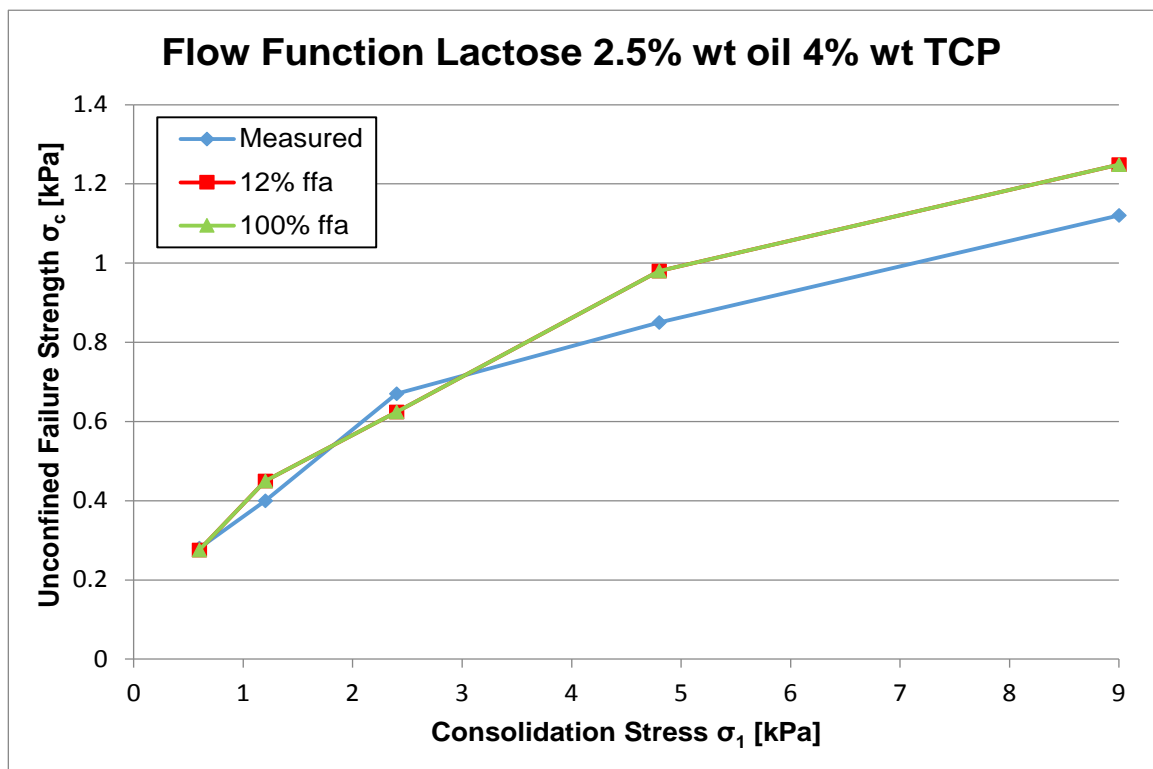


Figure A92

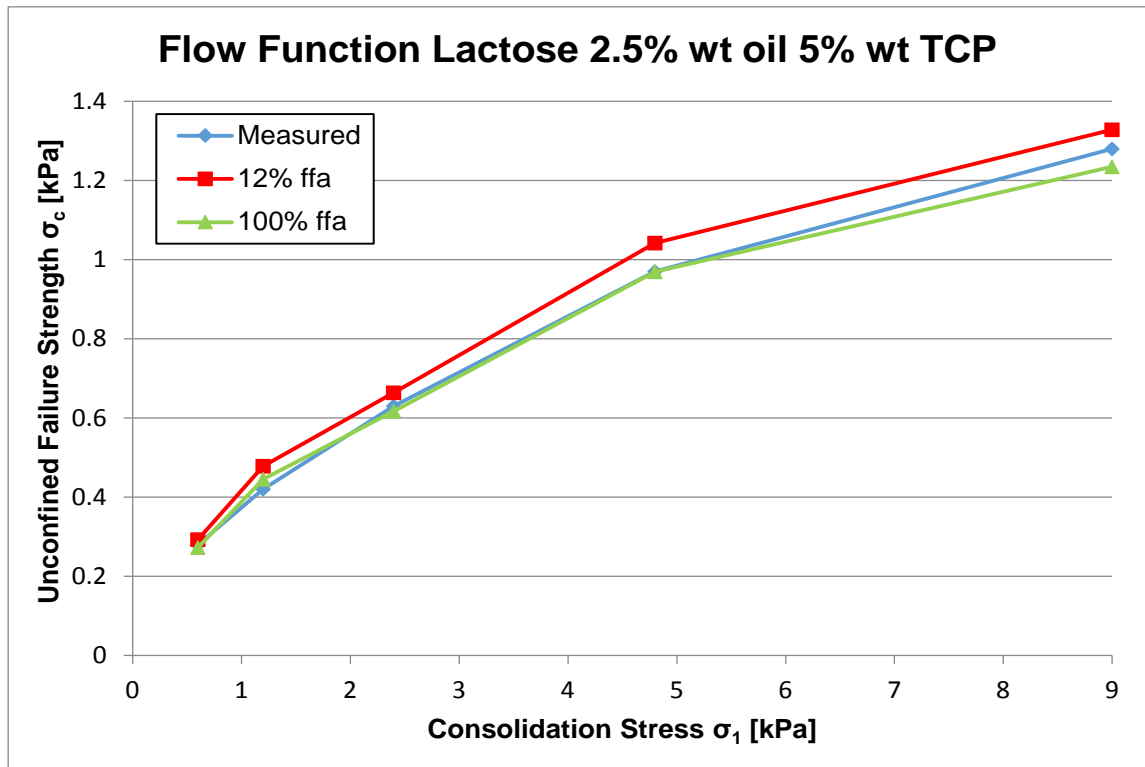


Figure A93

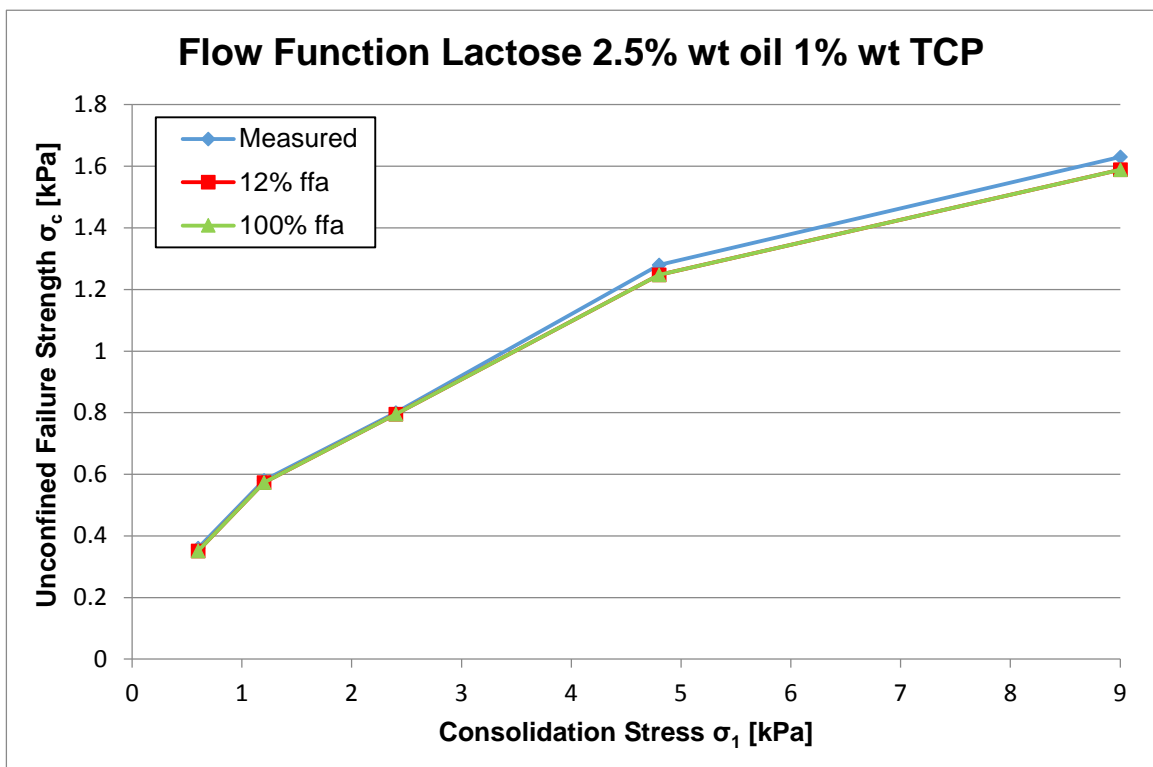


Figure A94

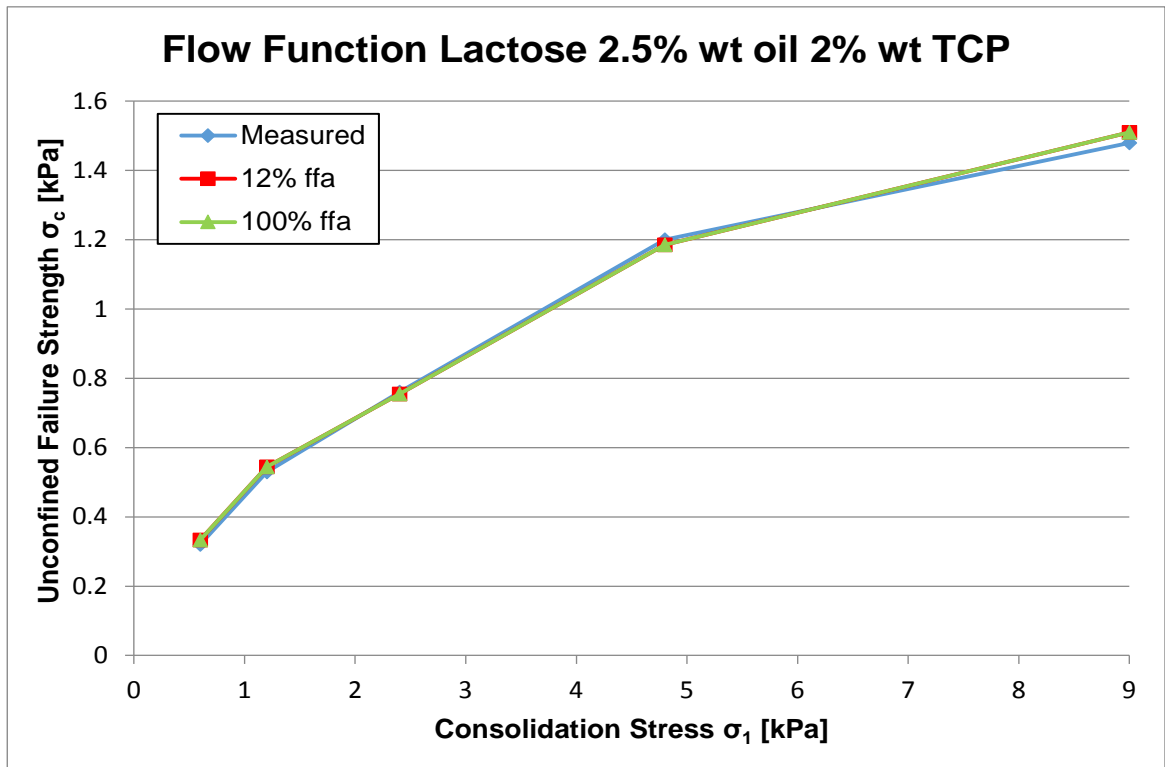


Figure A95

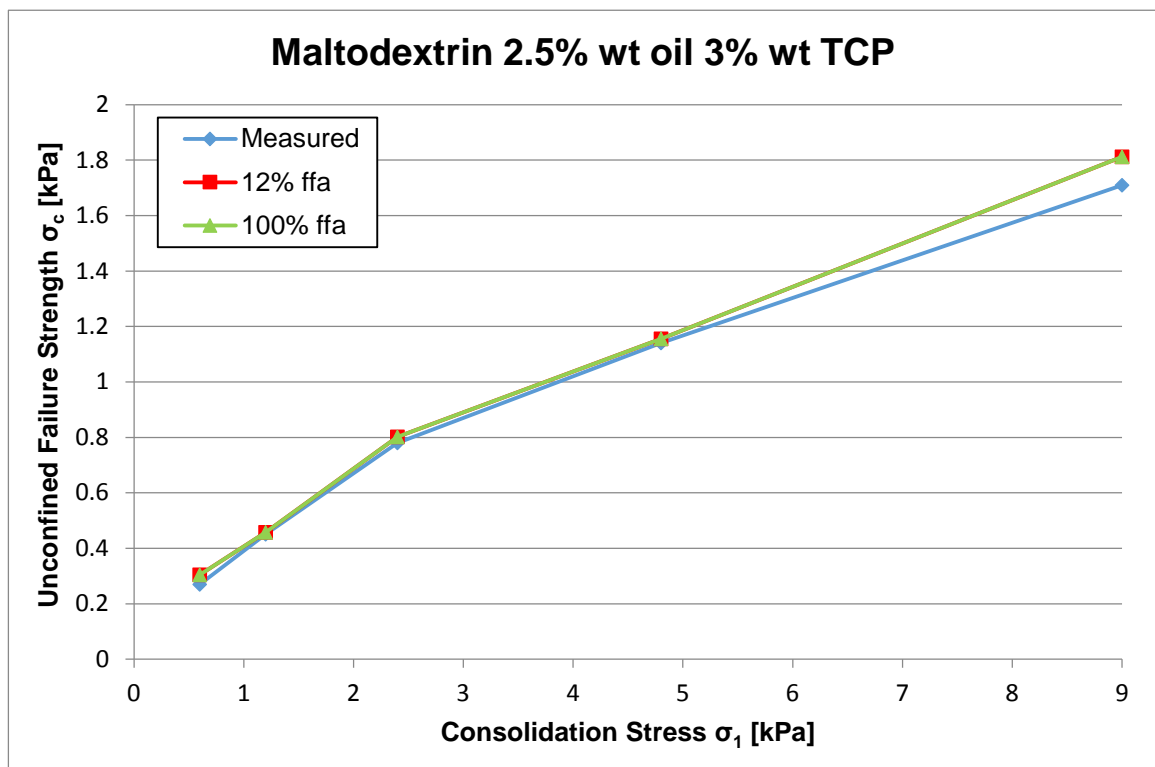


Figure A96

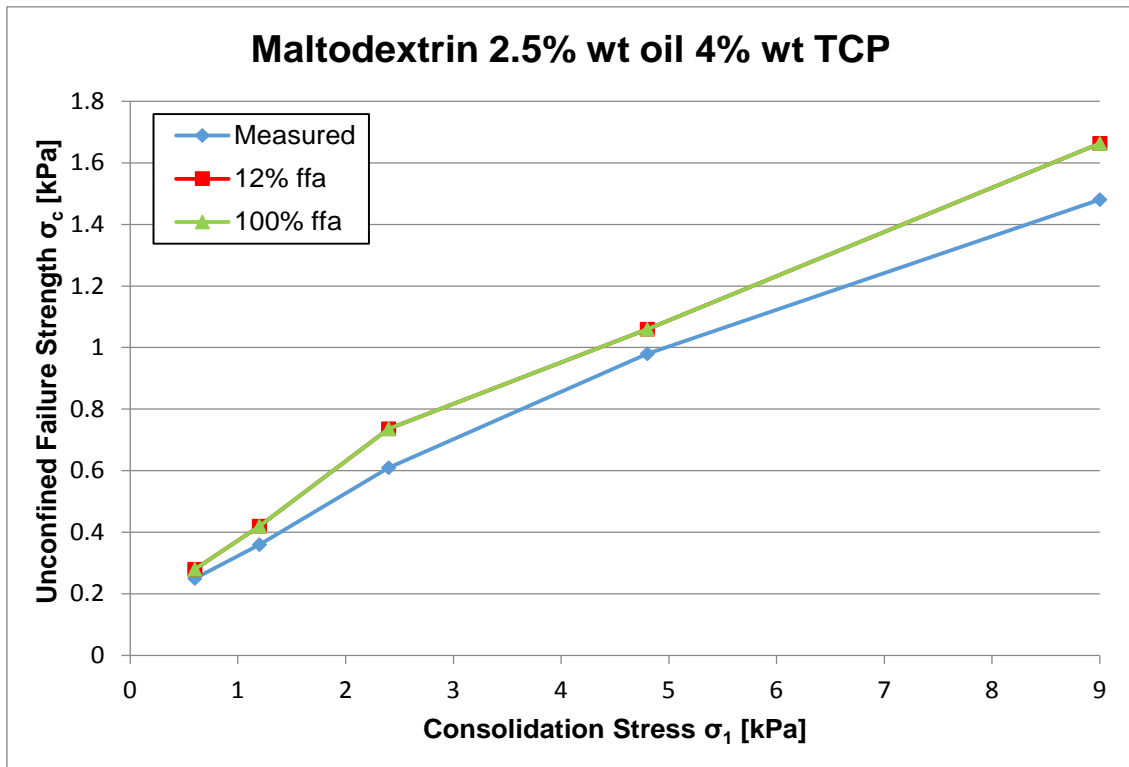


Figure A97

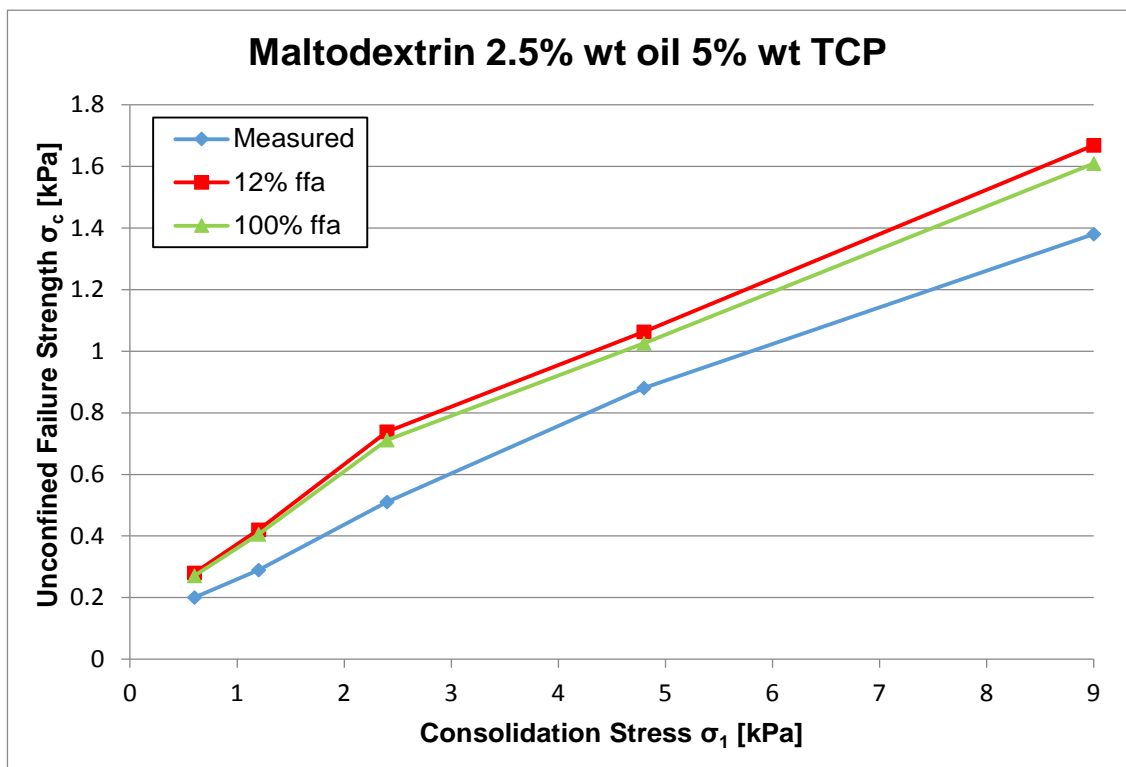


Figure A98

Appendix B: Experimental Work

B1 Introduction

The experimental work undertaken in this research generated a large amount of data and it was not possible to show all the data in chapter 6; this appendix contains the data not presented in the chapter.

B2 Effect of deconstructed particle size distribution

The aim of these test programmes is to study the influence of the particle size and distribution on four common filler materials named lactose, dextrose, sodium chloride and maltodextrin.

Test Parameters:

- Particle properties: size and breadths of the particle size distribution
- Type of powders: single food fillers
- Condition of the powders: dry
- Additives added: none

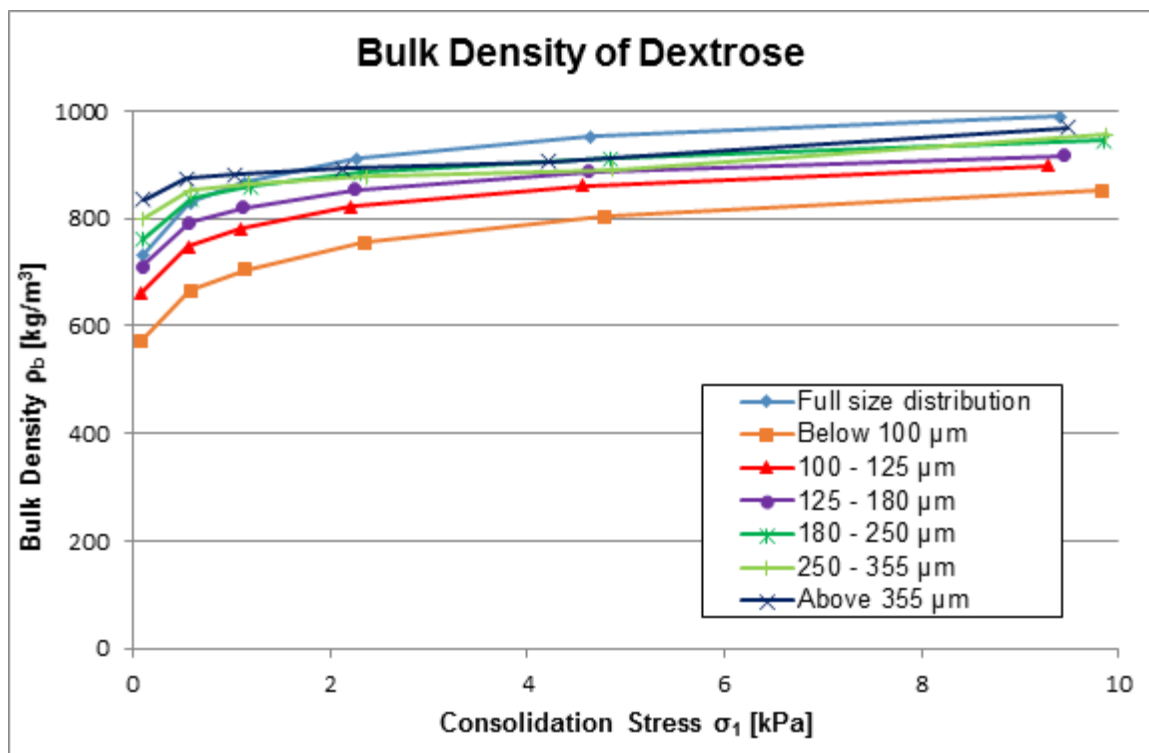


Figure B1

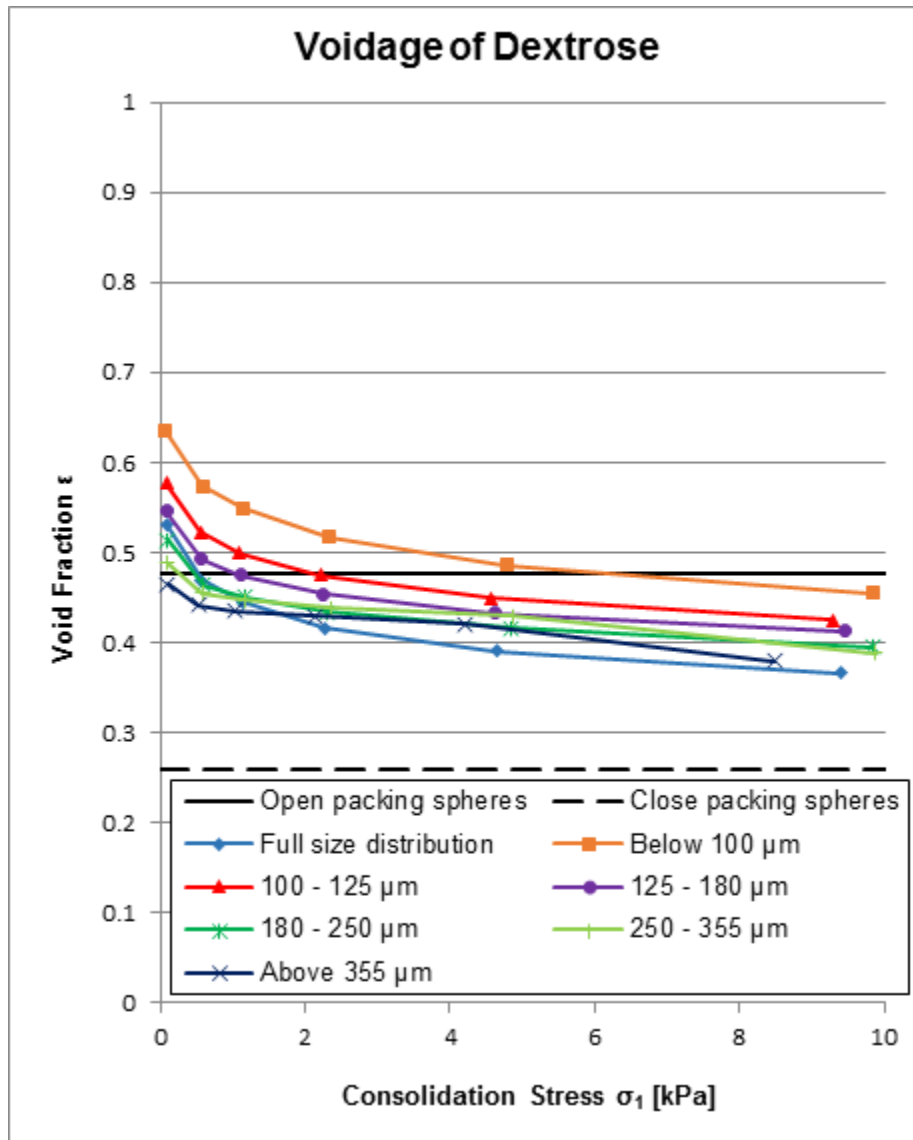


Figure B2

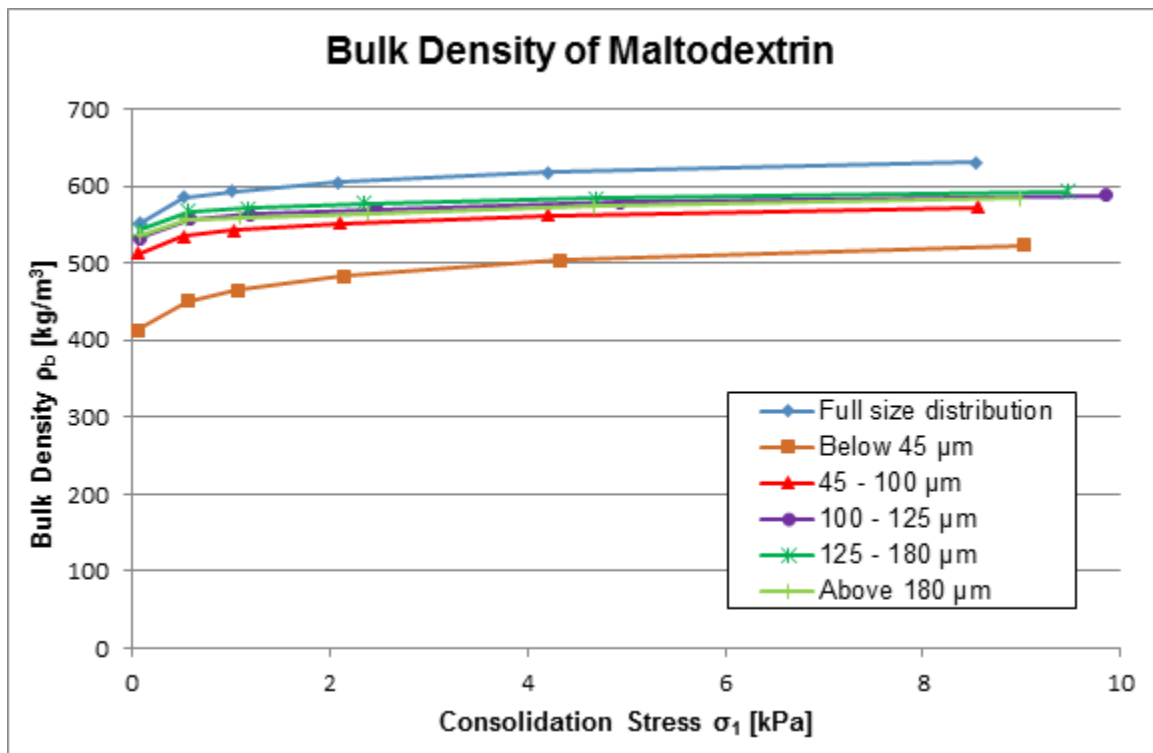


Figure B3

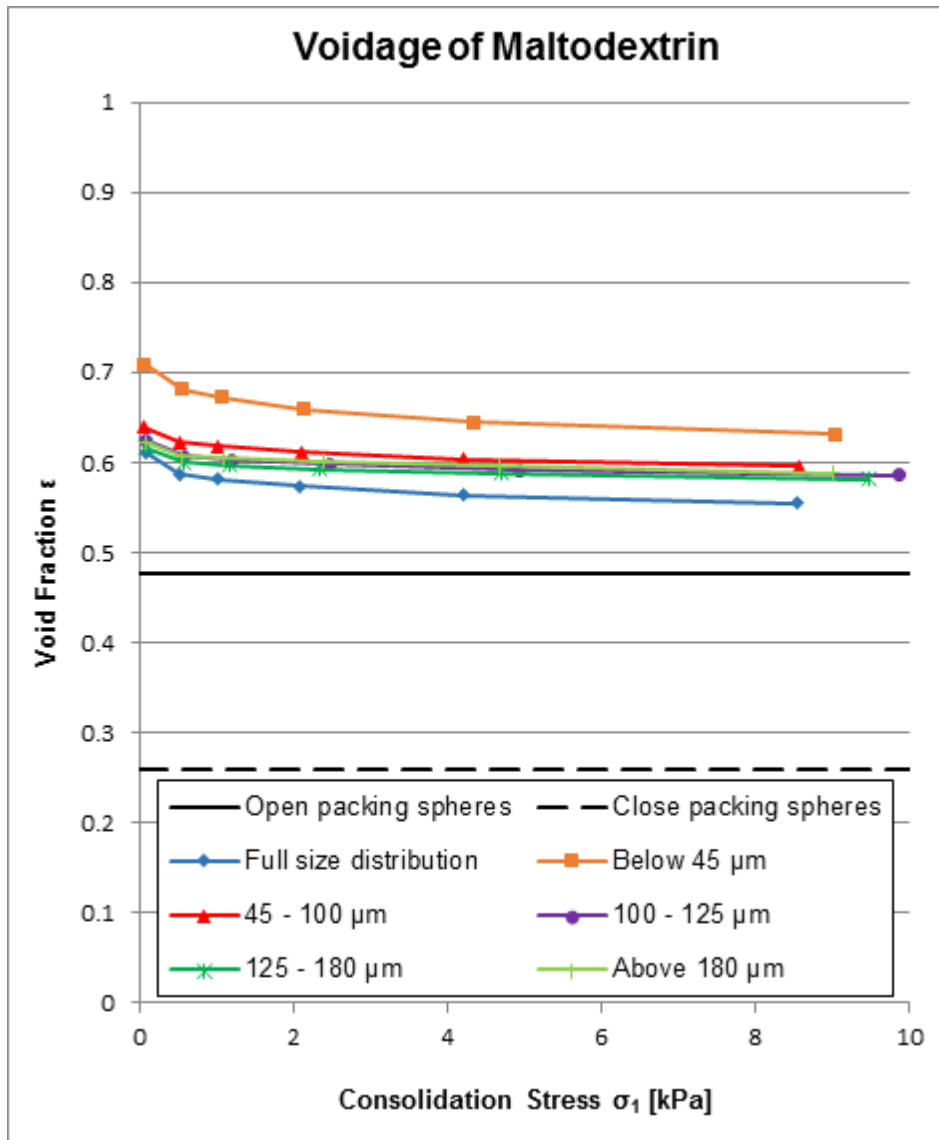


Figure B4

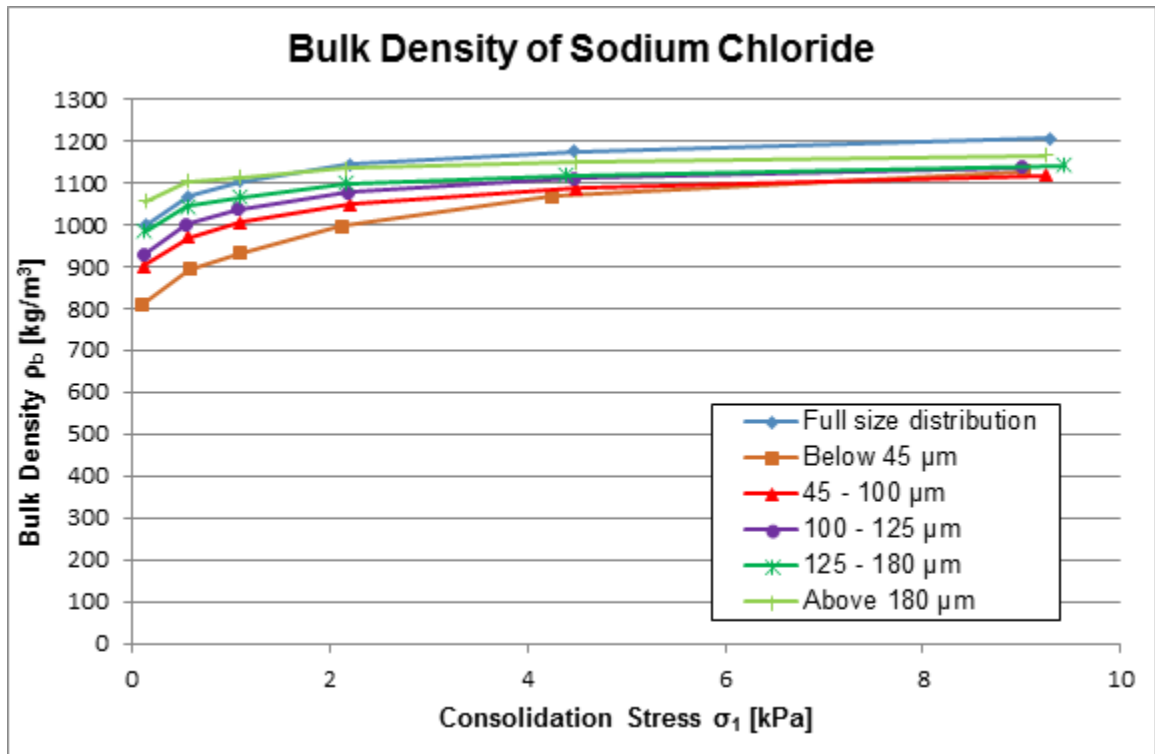


Figure B5

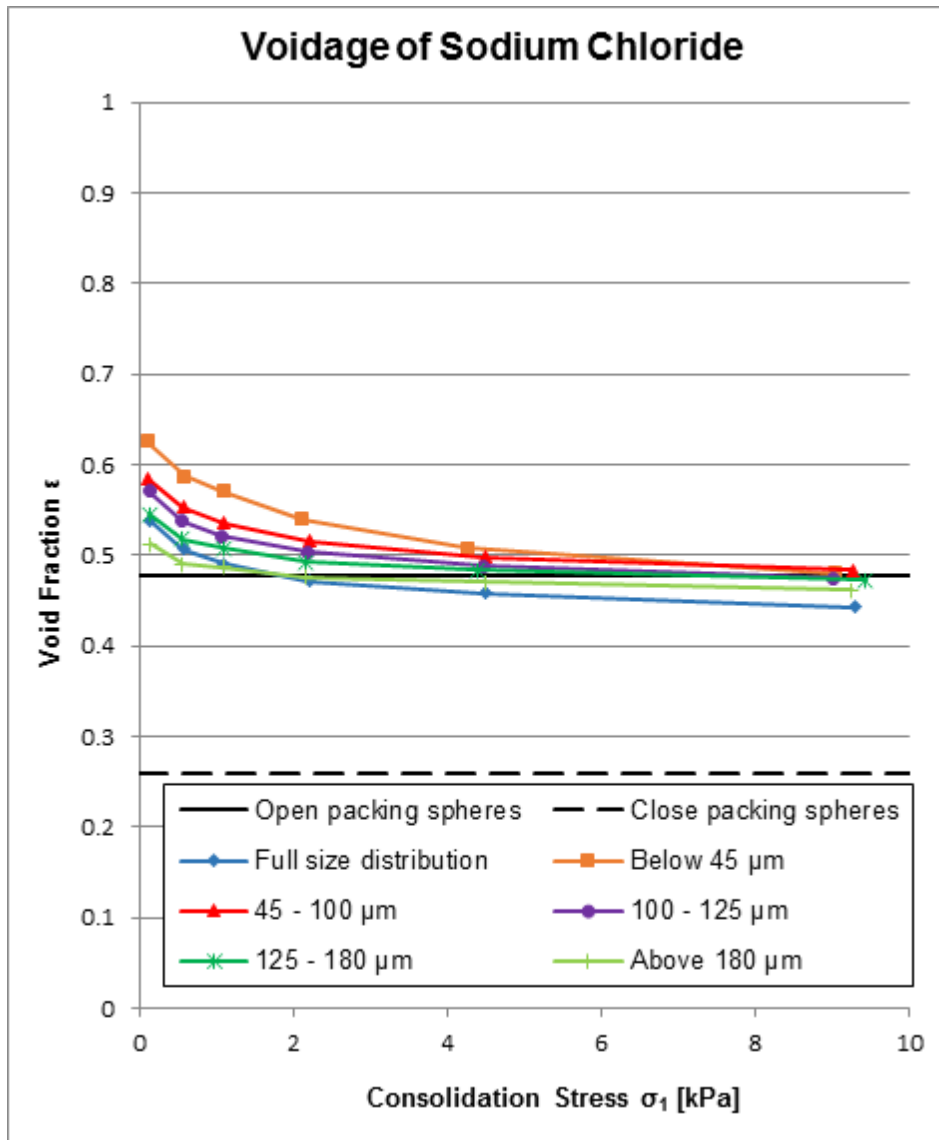


Figure B6

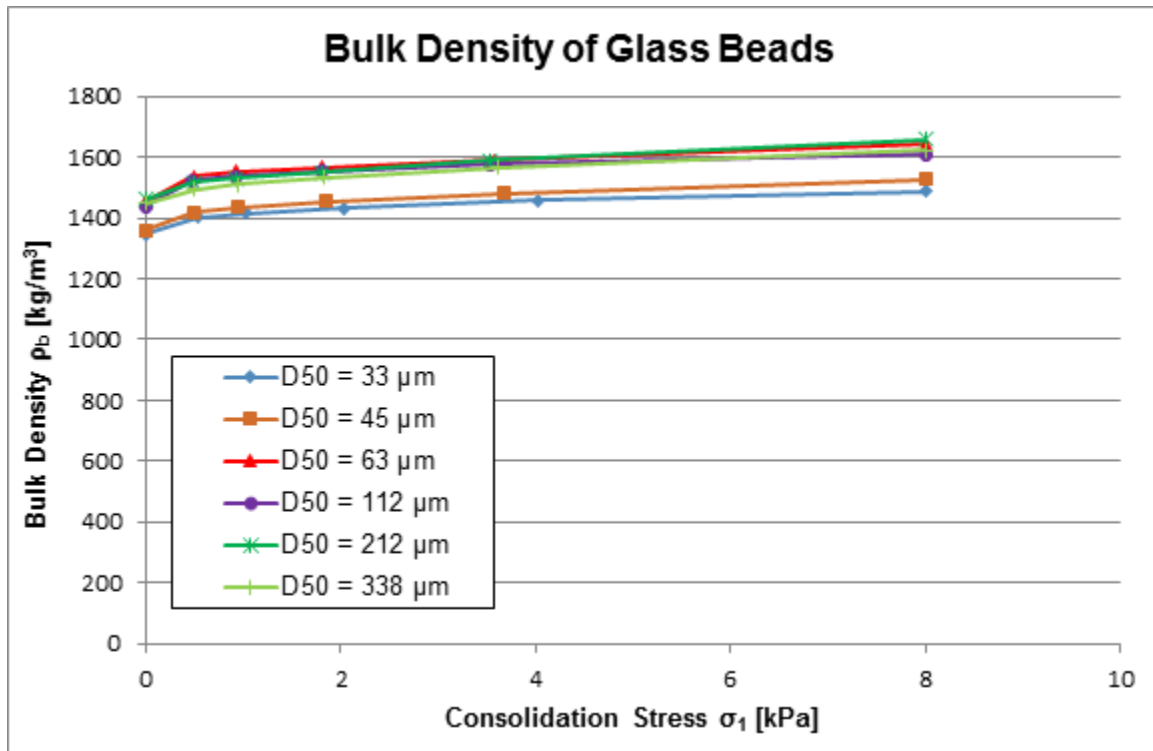


Figure B7

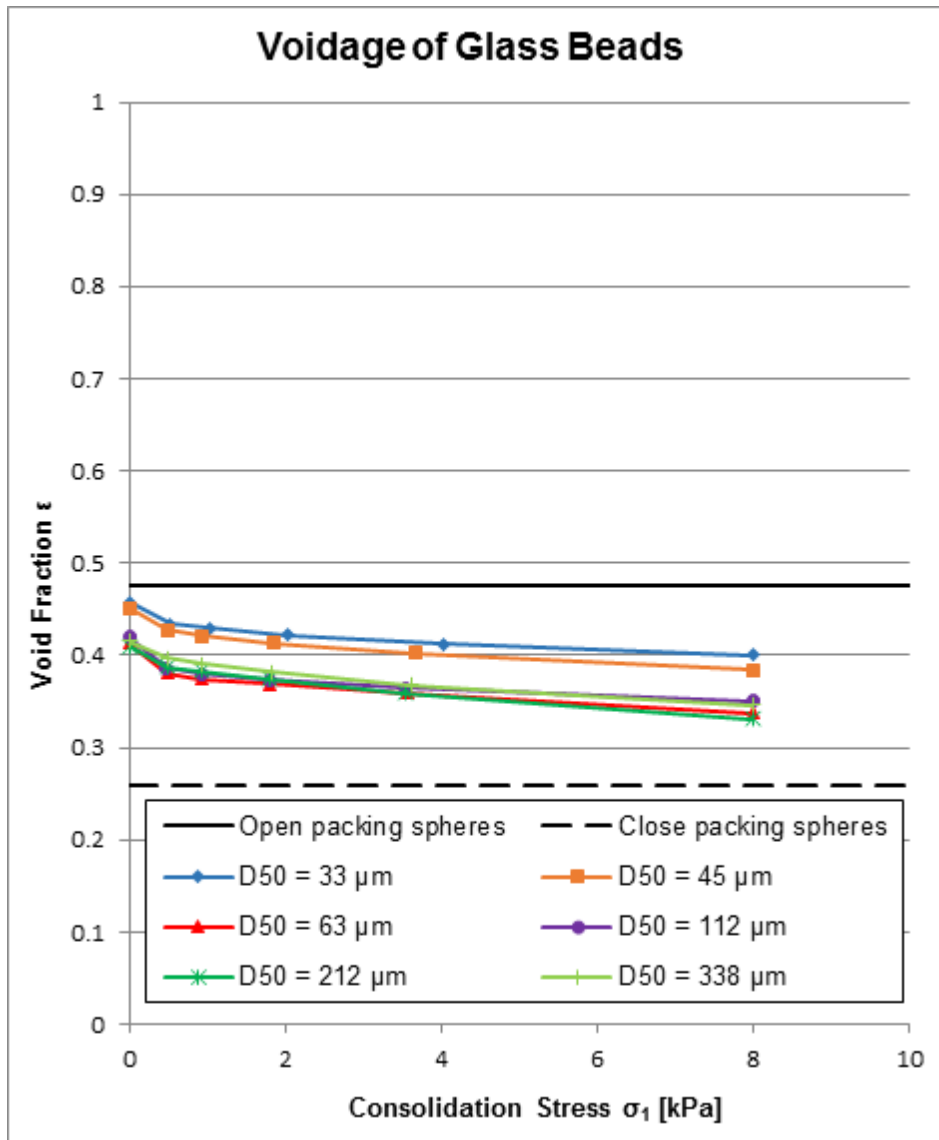


Figure B8

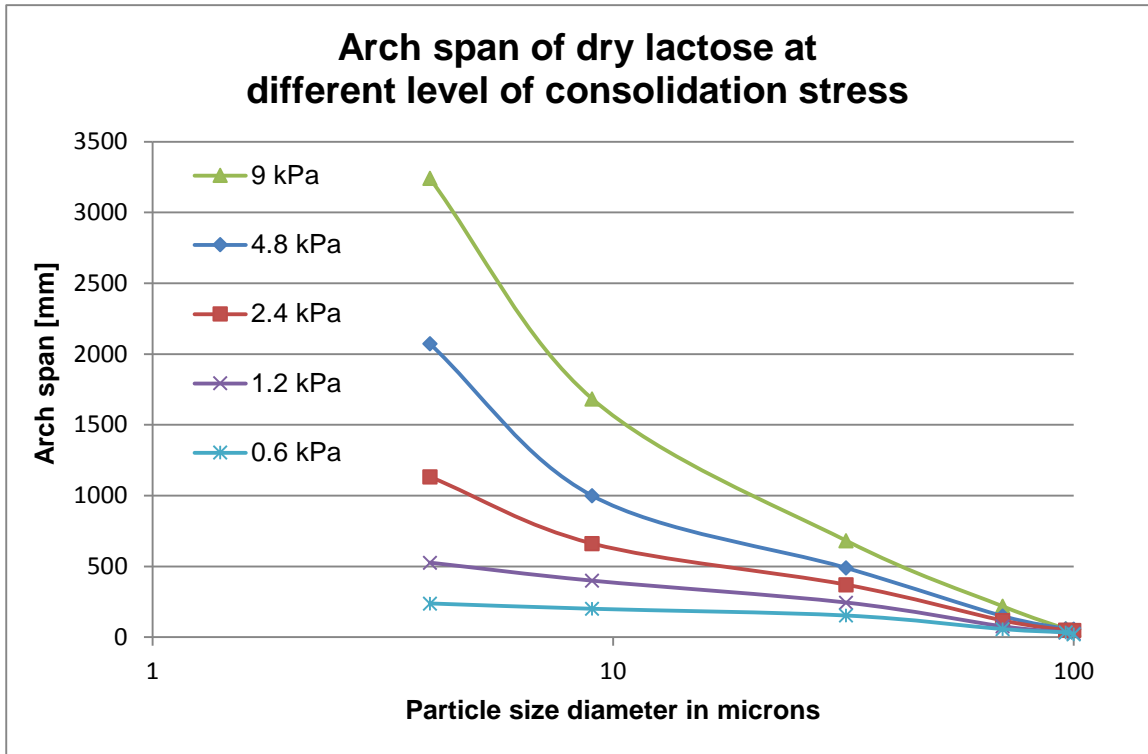


Figure B9

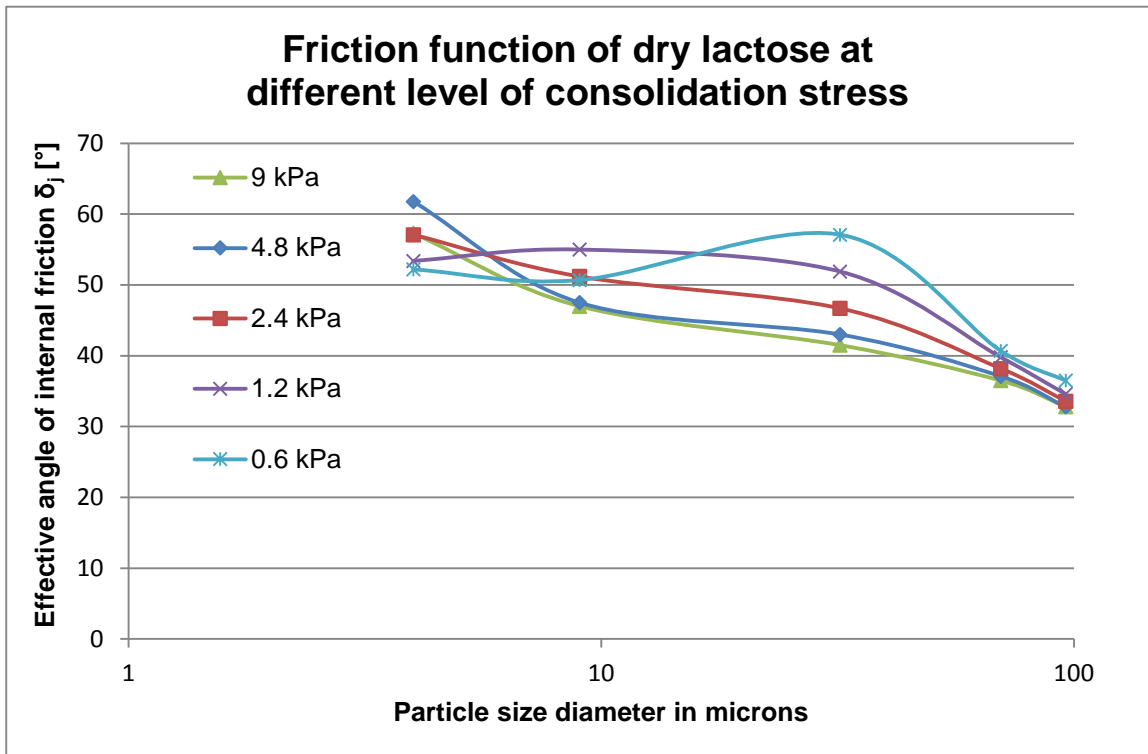


Figure B10

B3 Effect of particle shape, size and liquid content on powders

The aim of these test programmes is to study the influence of the particle shape, surface liquid content, liquid type and particle size on four idealised materials named glass beads, crushed glass and sodium chloride.

Test Parameters:

- Particle properties: size and shape
- Type of powders: single idealised particulate materials
- Condition of the powders: dry and wet
- Additives added: liquids

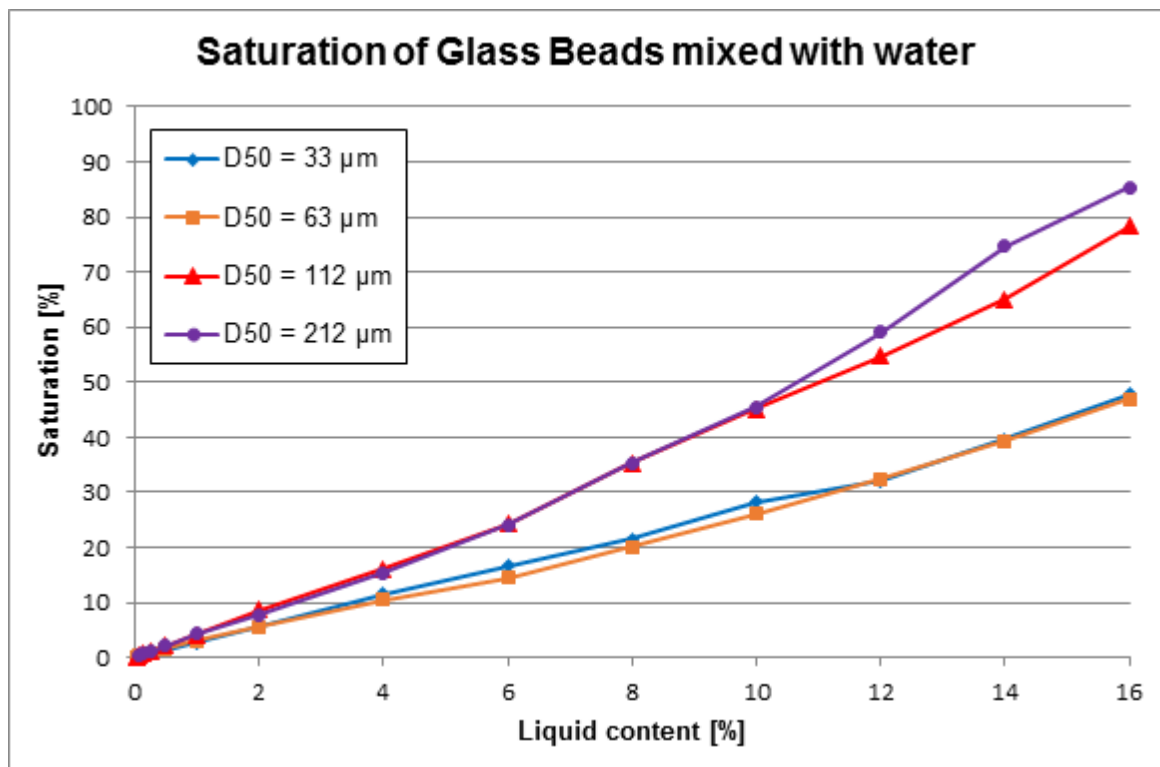


Figure B11

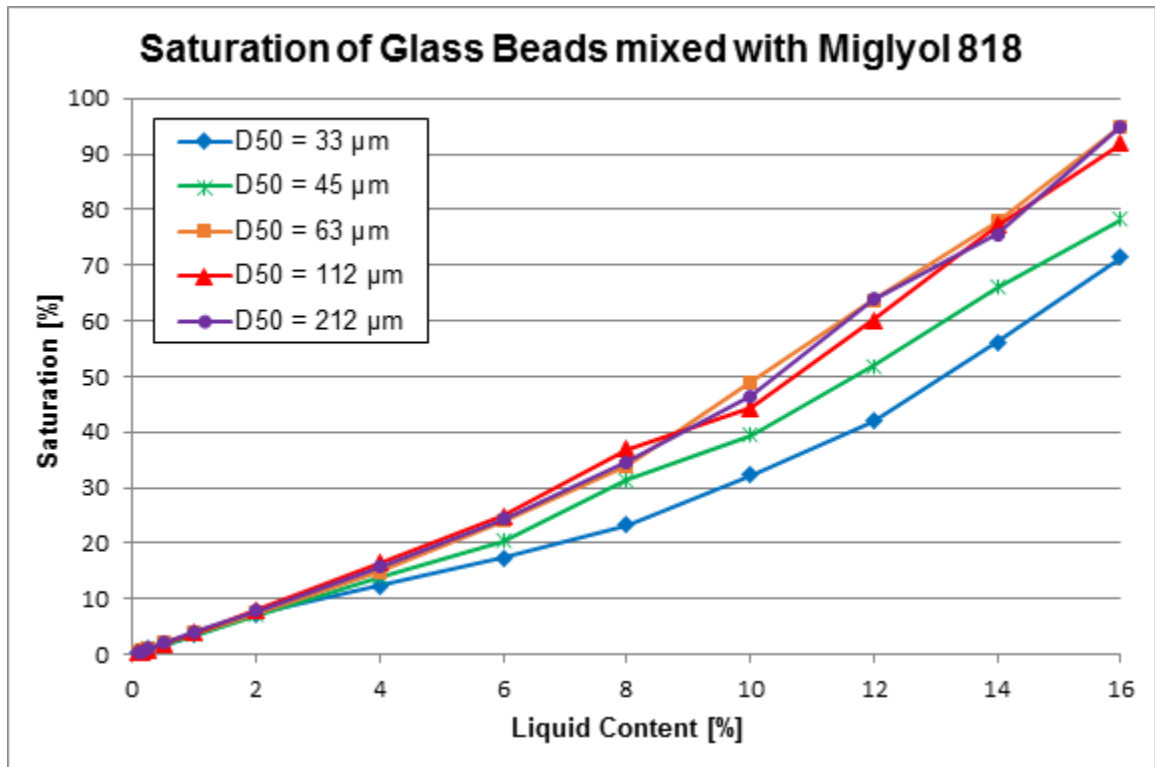


Figure B12

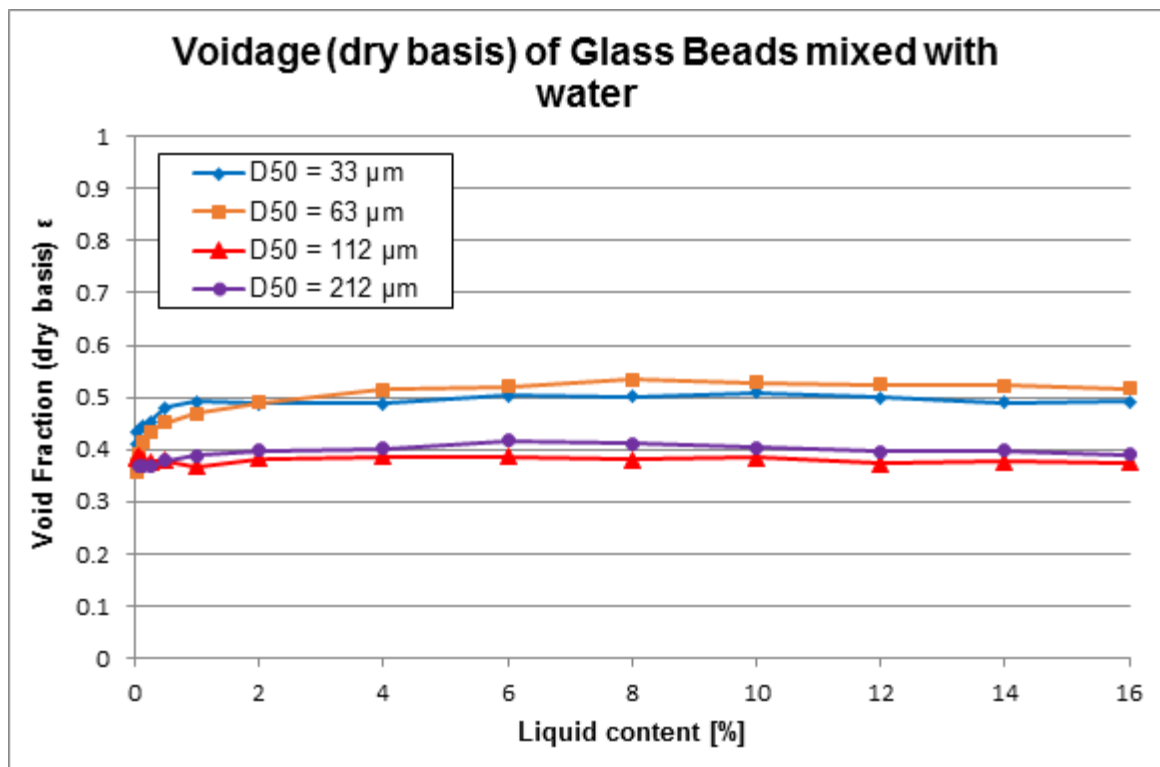


Figure B13

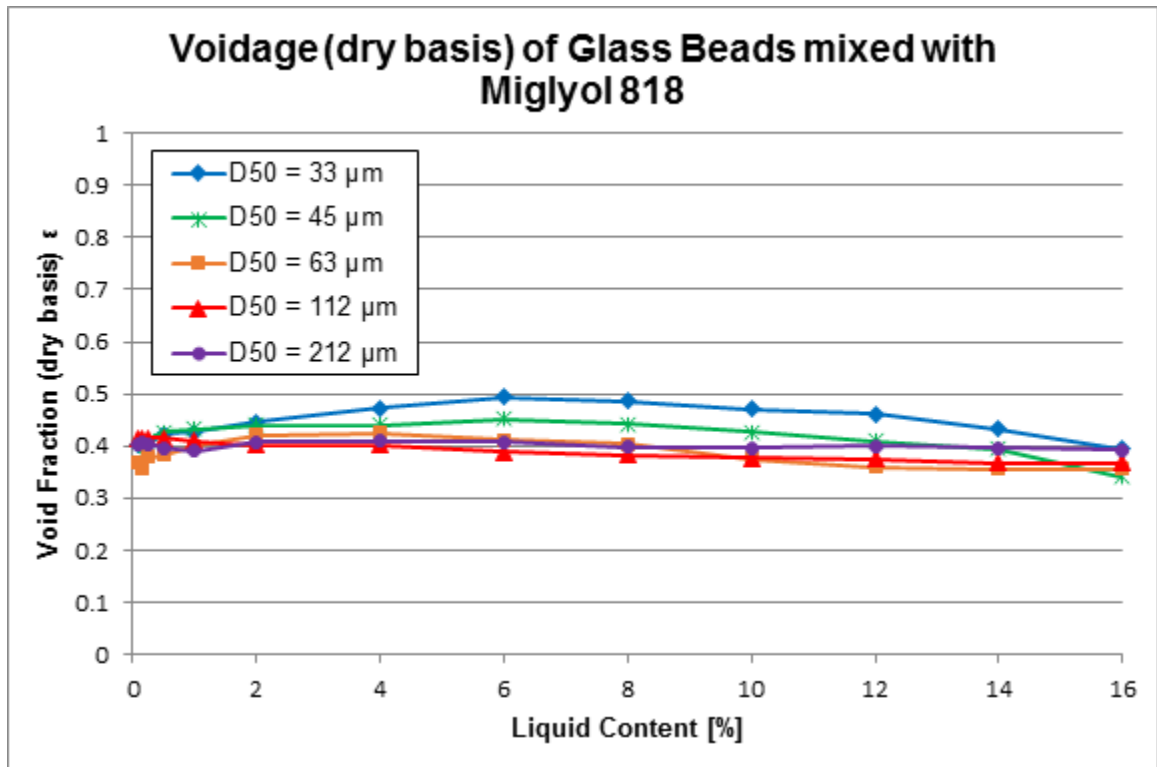


Figure B14

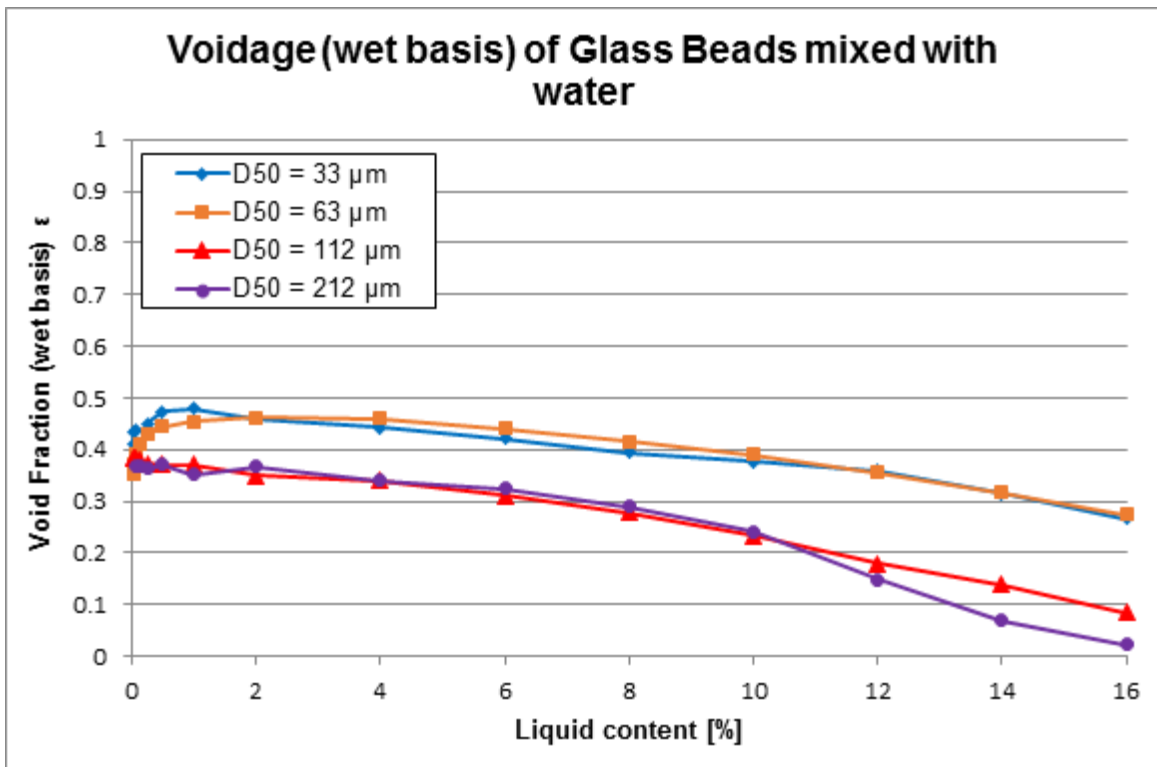


Figure B15

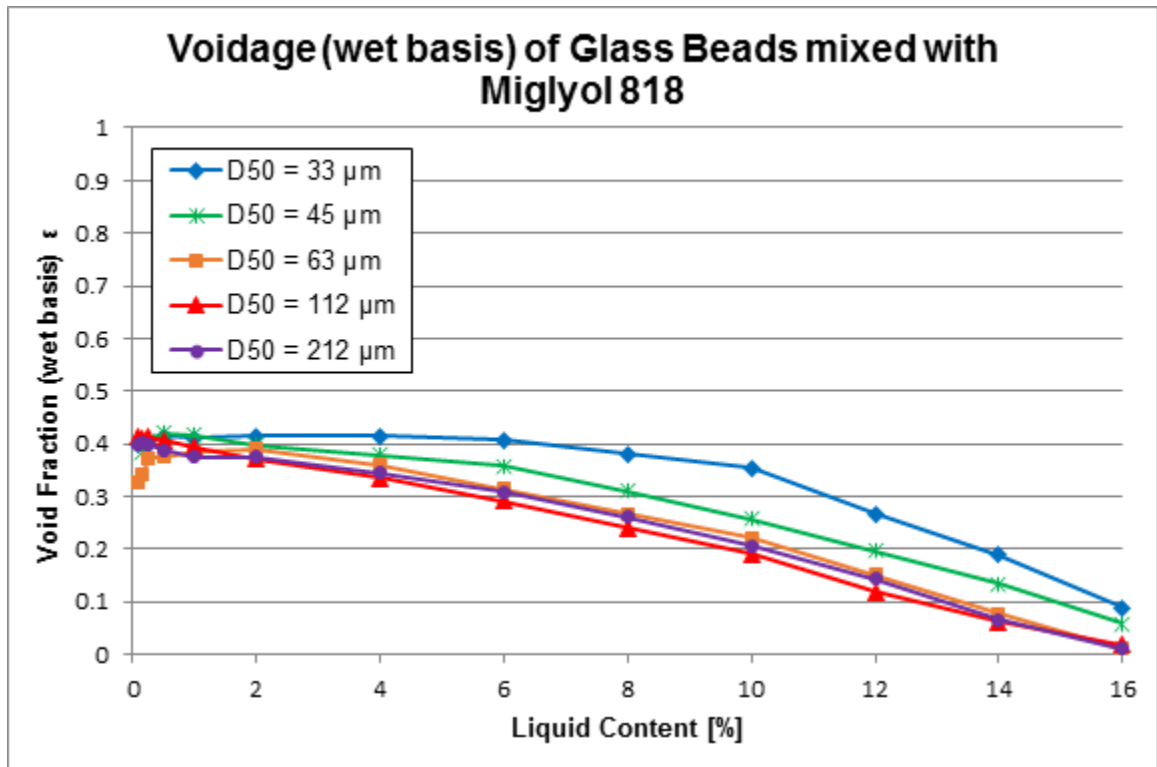


Figure B16

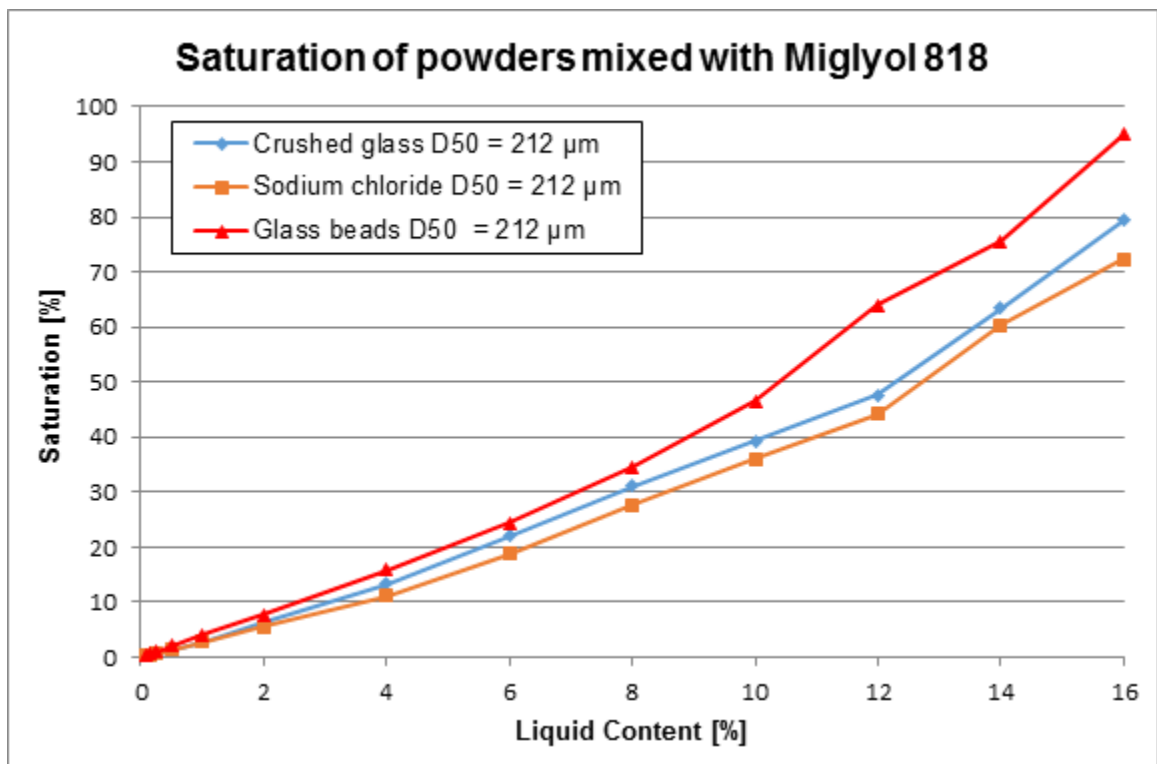


Figure B17

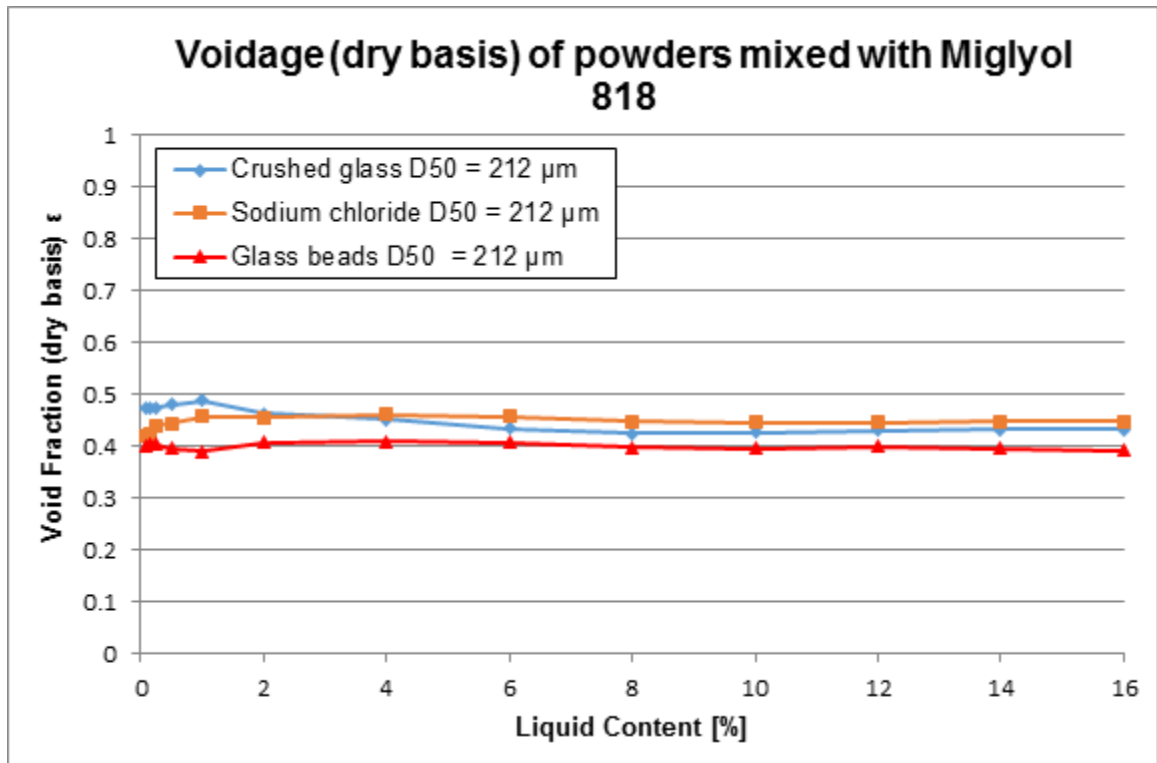


Figure B18

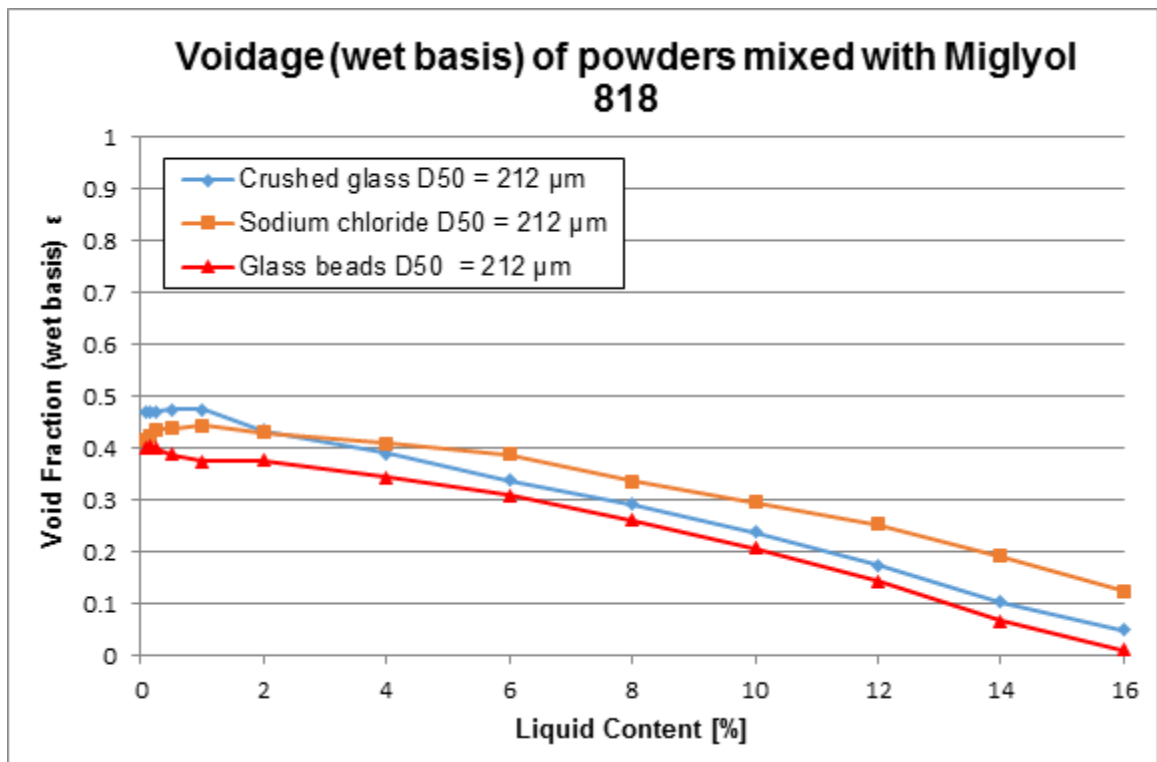


Figure B19

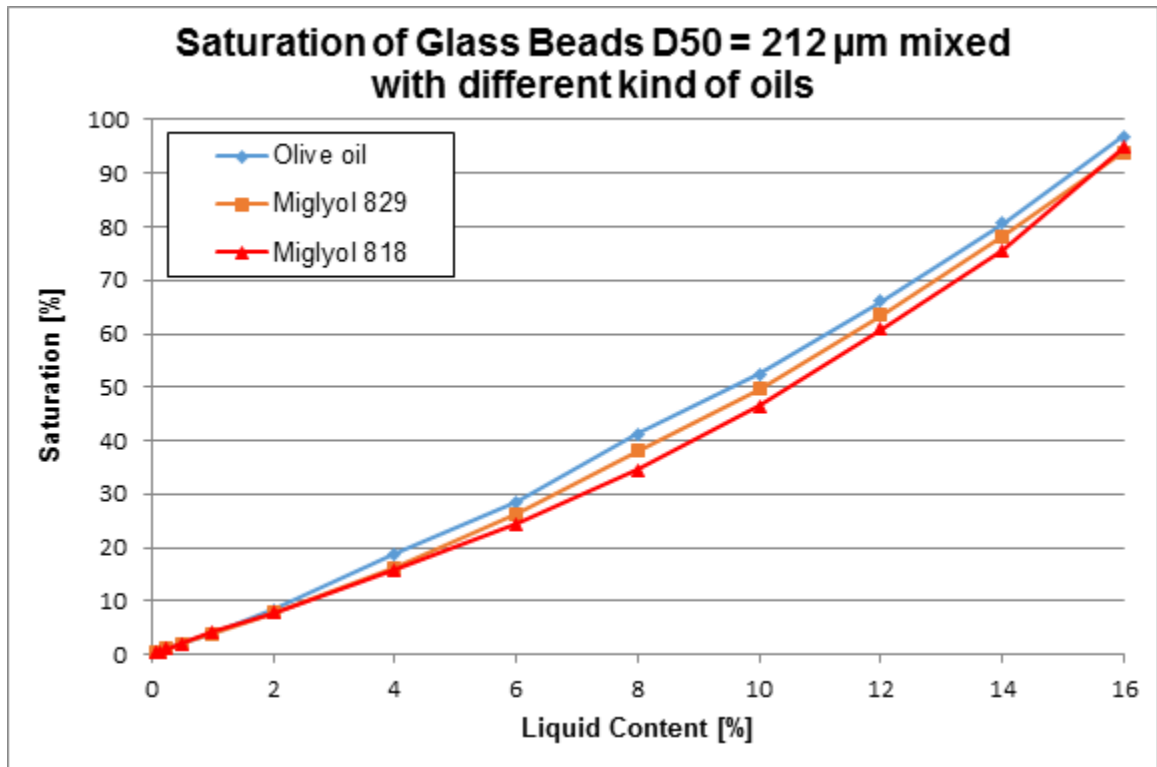


Figure B20

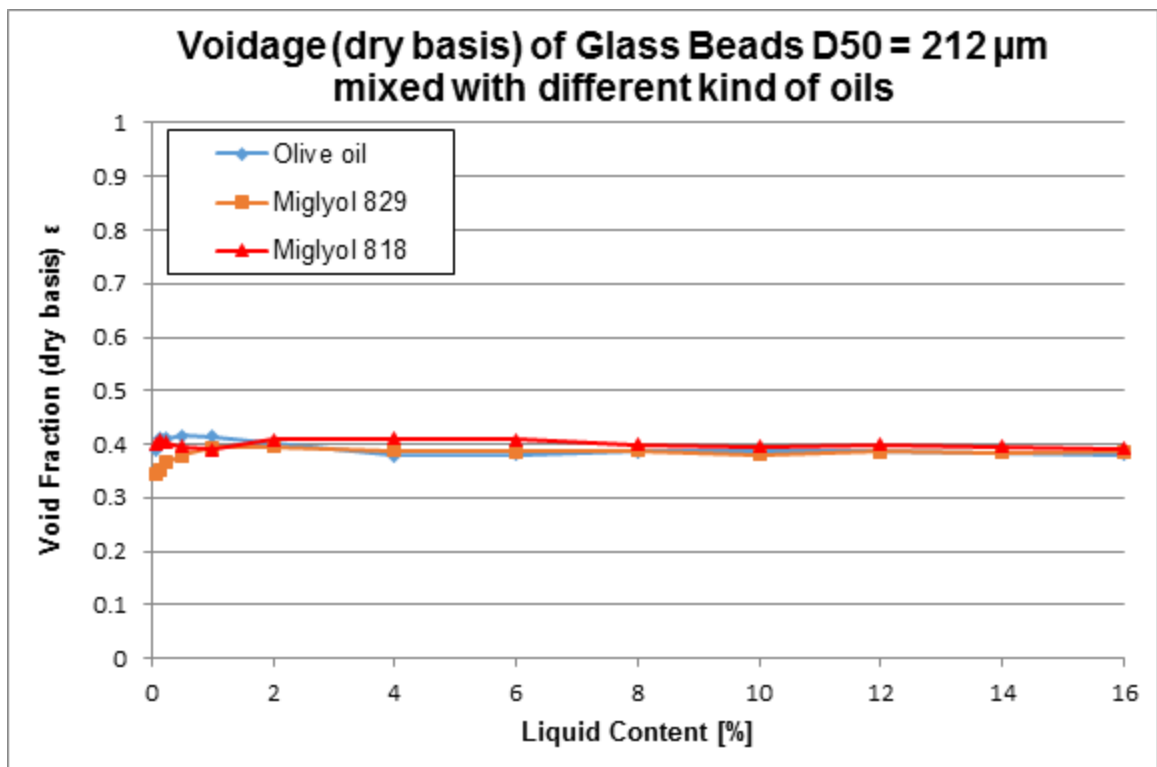


Figure B21

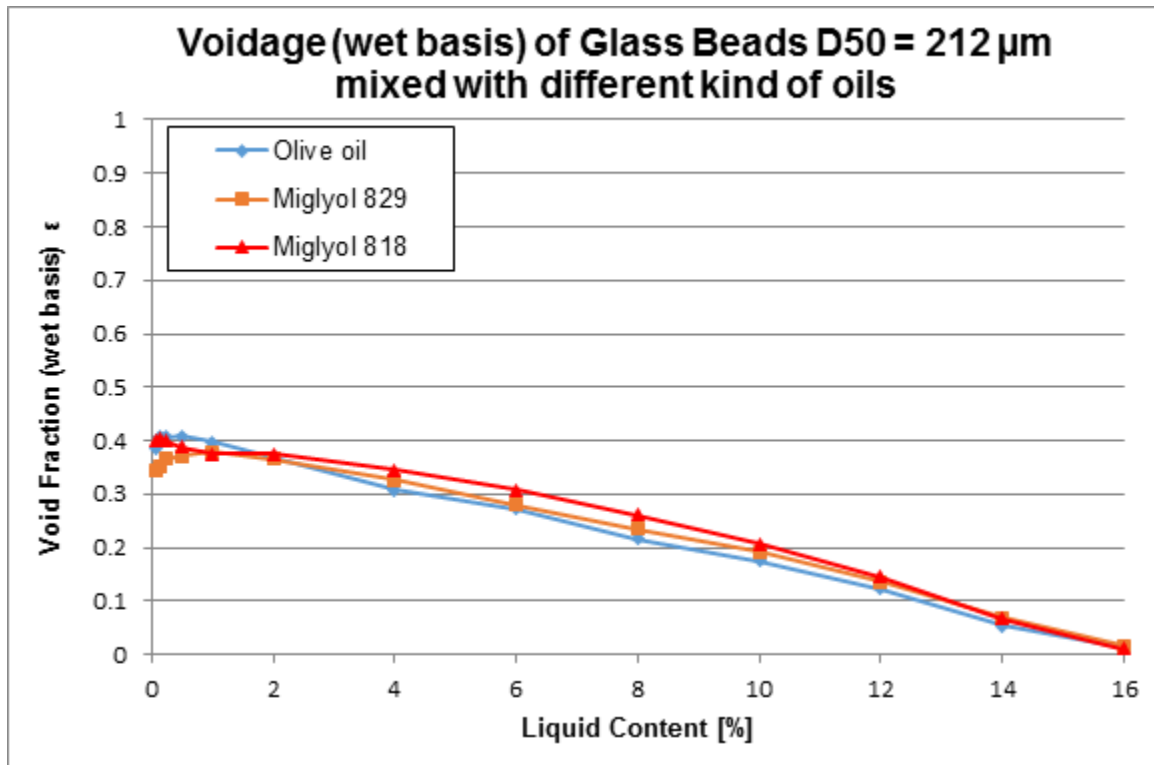


Figure B22

B4 Effect of particle size on dry blends

The aim of this test programme is to study the influence of the particle size of the constituent ingredients on dry blends of powders and idealised materials named dextrose, dextrose ex-wheat, lactose, sodium chloride and glass beads.

Test Parameters:

- Particle properties: size
- Type of powders: multicomponent simplified blends of food powders and idealised materials
- Condition of the powders: dry
- Additives added: none

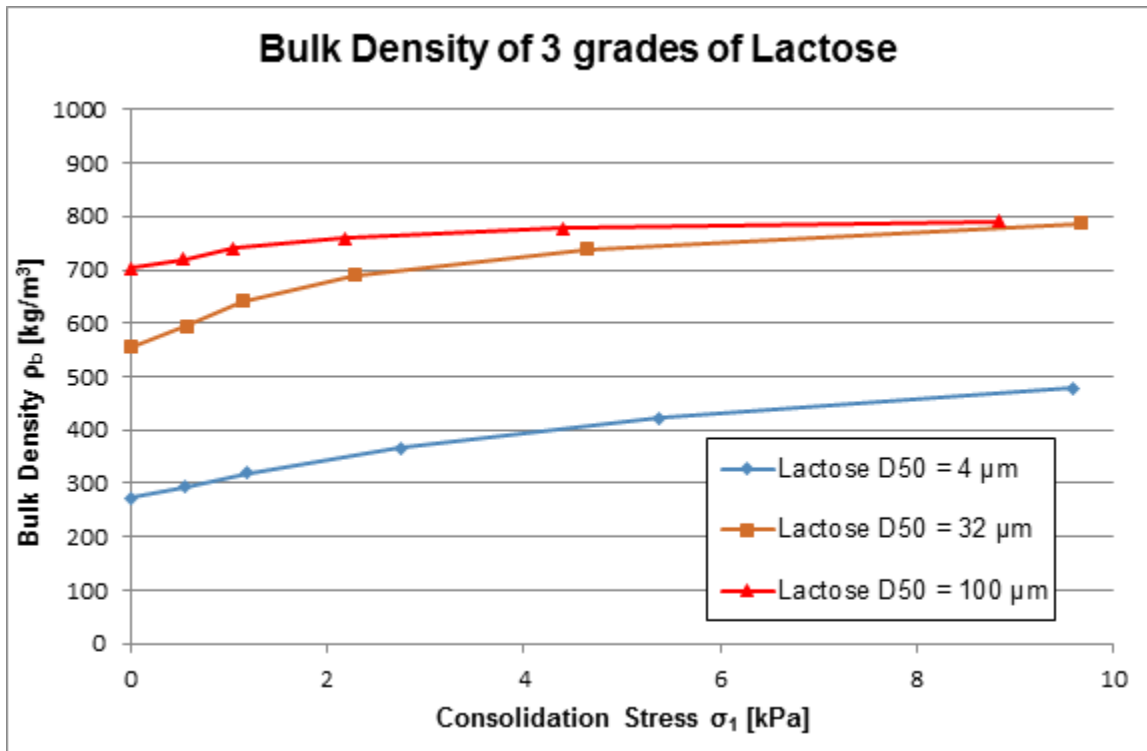


Figure B23

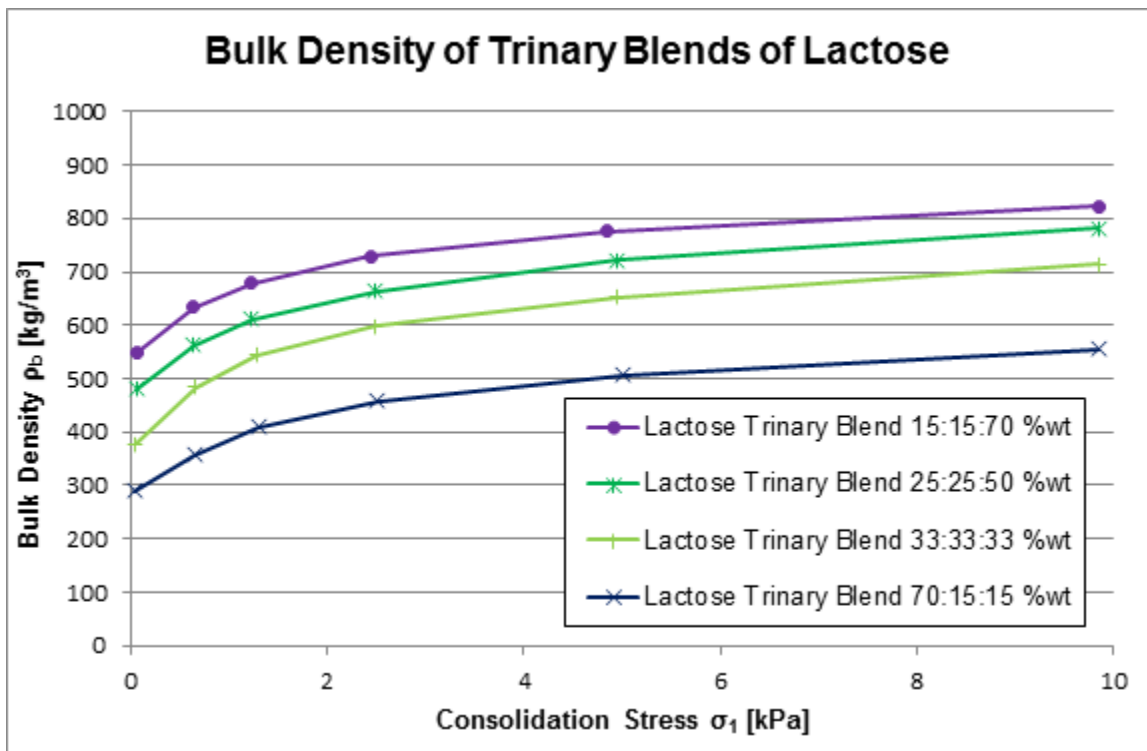


Figure B24

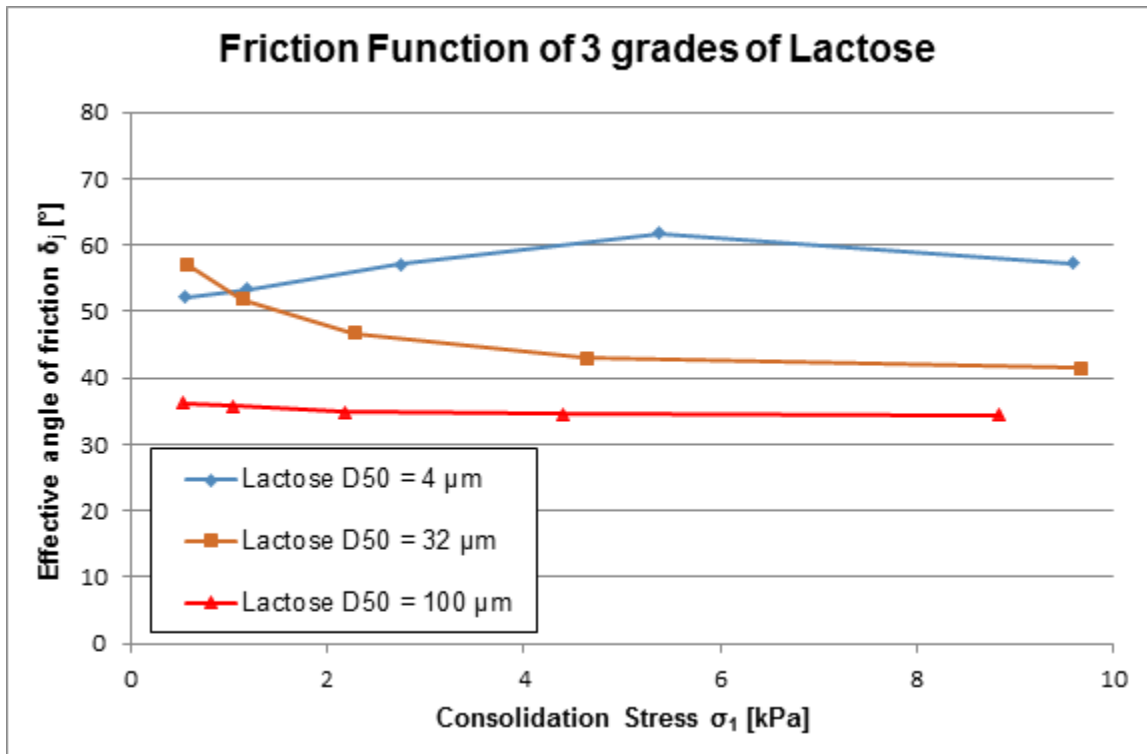


Figure B25

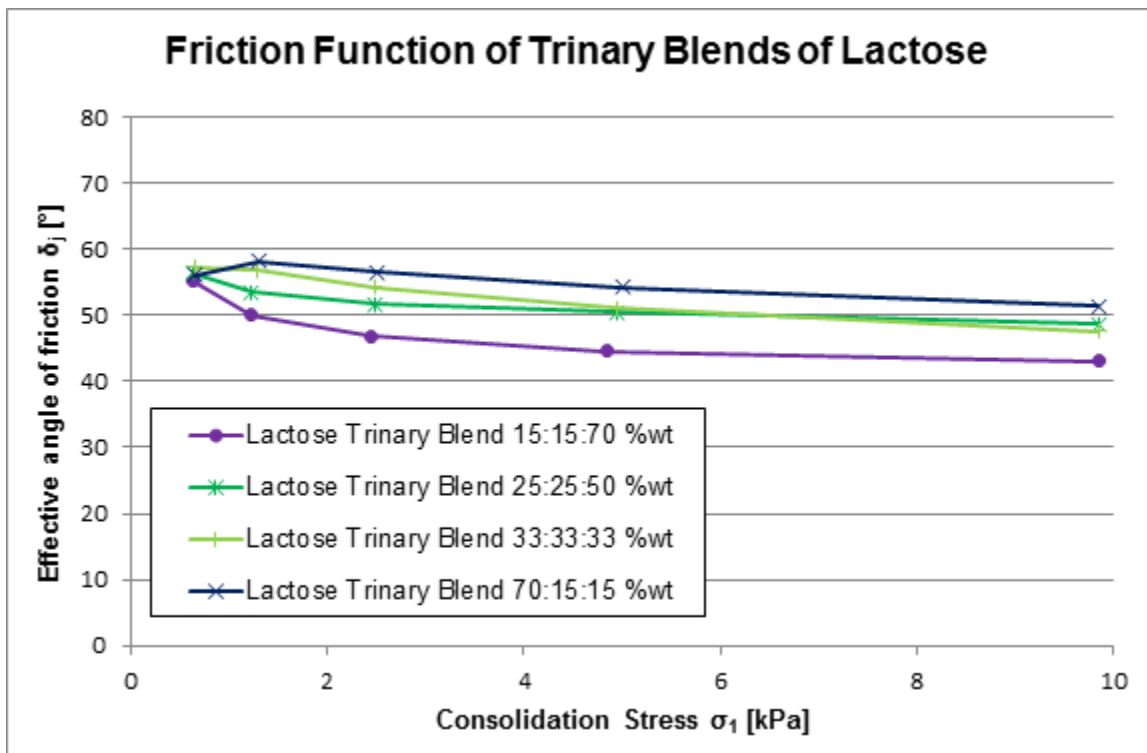


Figure B26

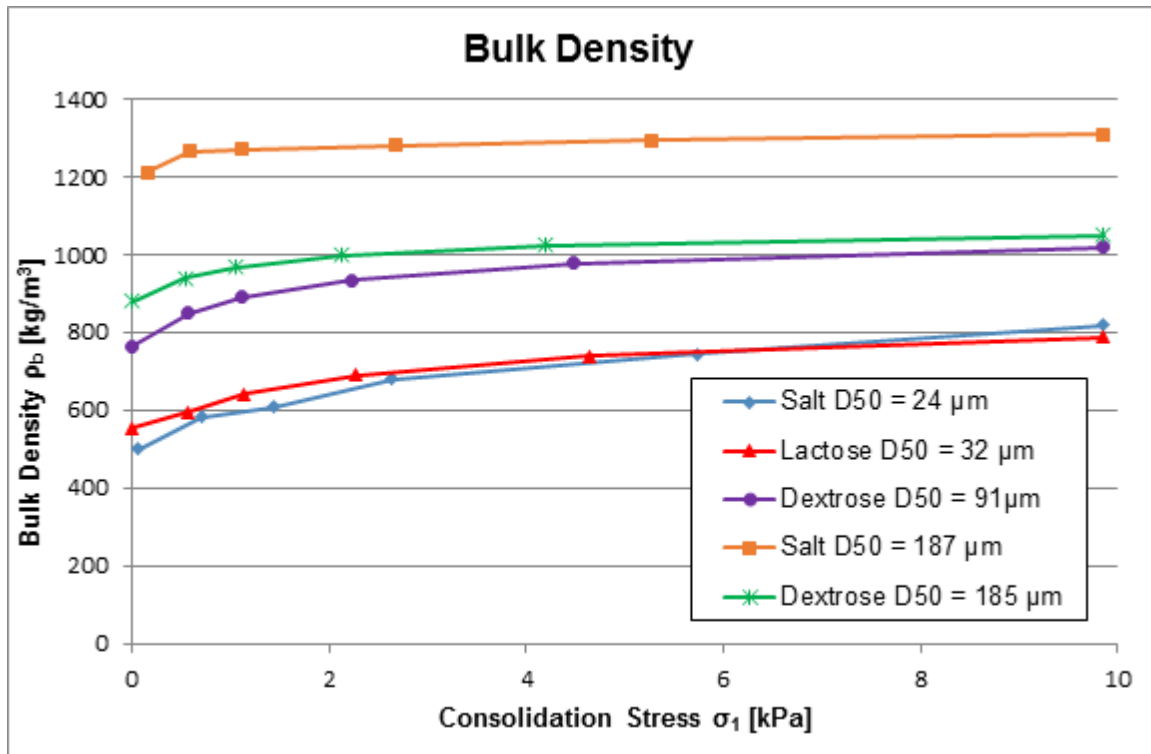


Figure B27

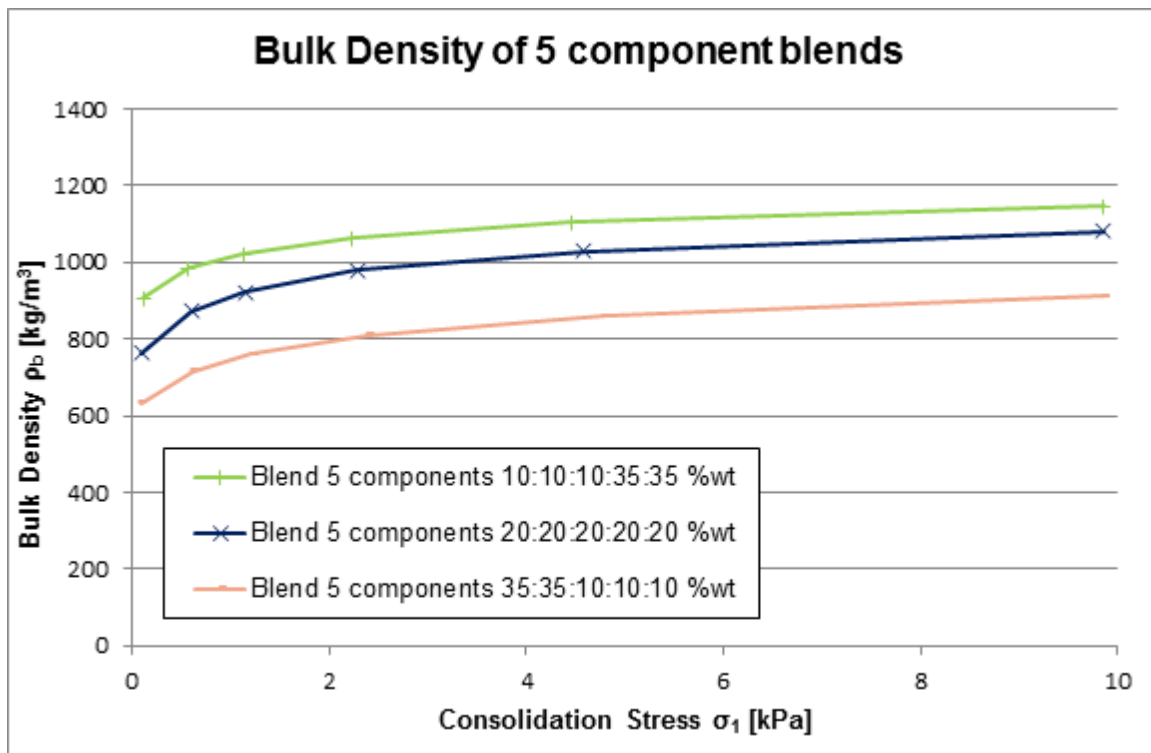


Figure B28

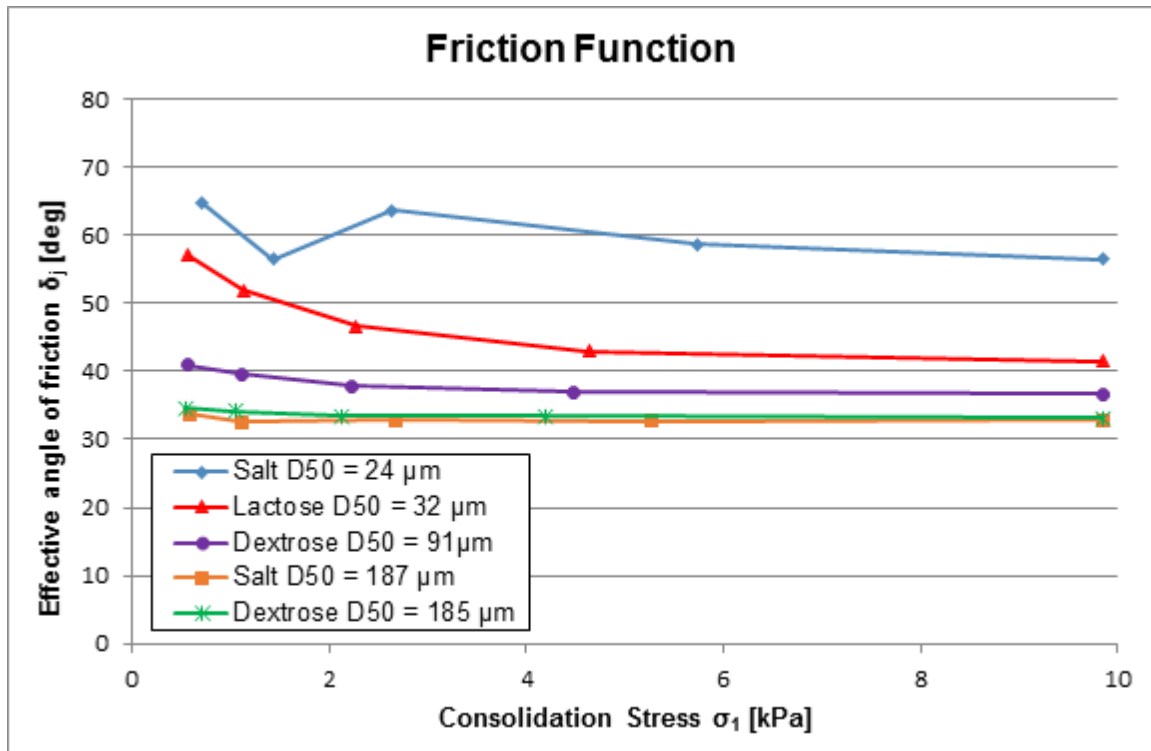


Figure B29

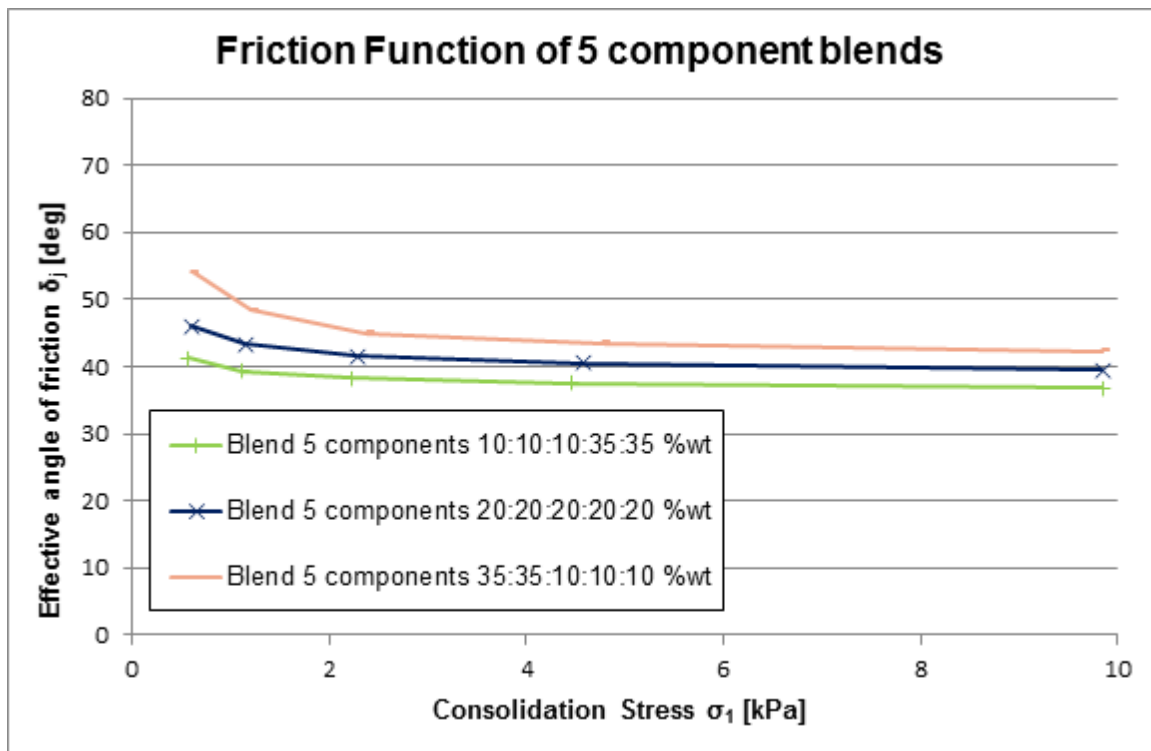


Figure B30

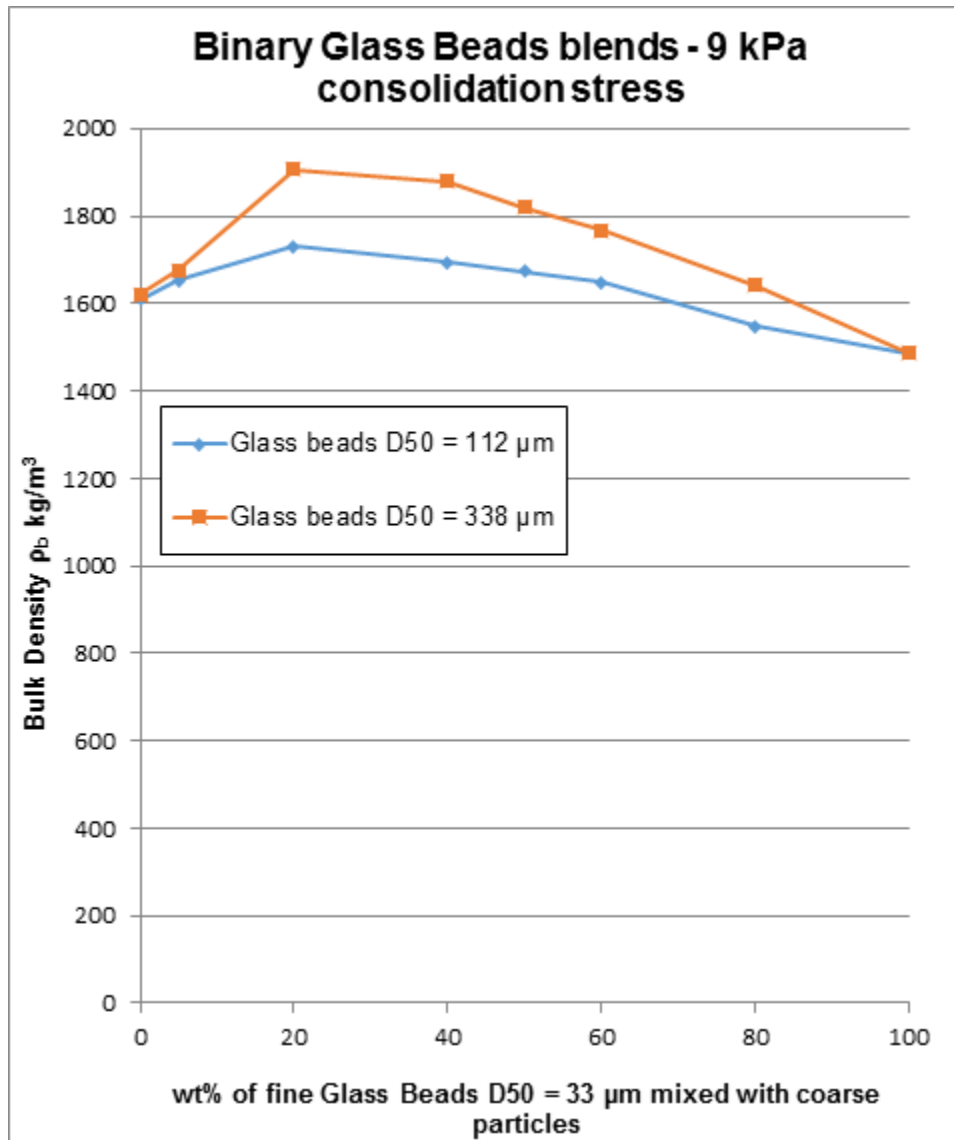


Figure B31

B5 *Interaction between oil and free flow additives*

The aim of these test programmes is to study the interaction between three common free flow additives named silicon dioxide, tricalcium phosphate and magnesium carbonate and oil at different liquid levels.

Test Parameters:

- Particle properties: none
- Type of powders: single flow property modifying ingredients
- Condition of the powders: wet
- Additives added: liquid and free flow additives

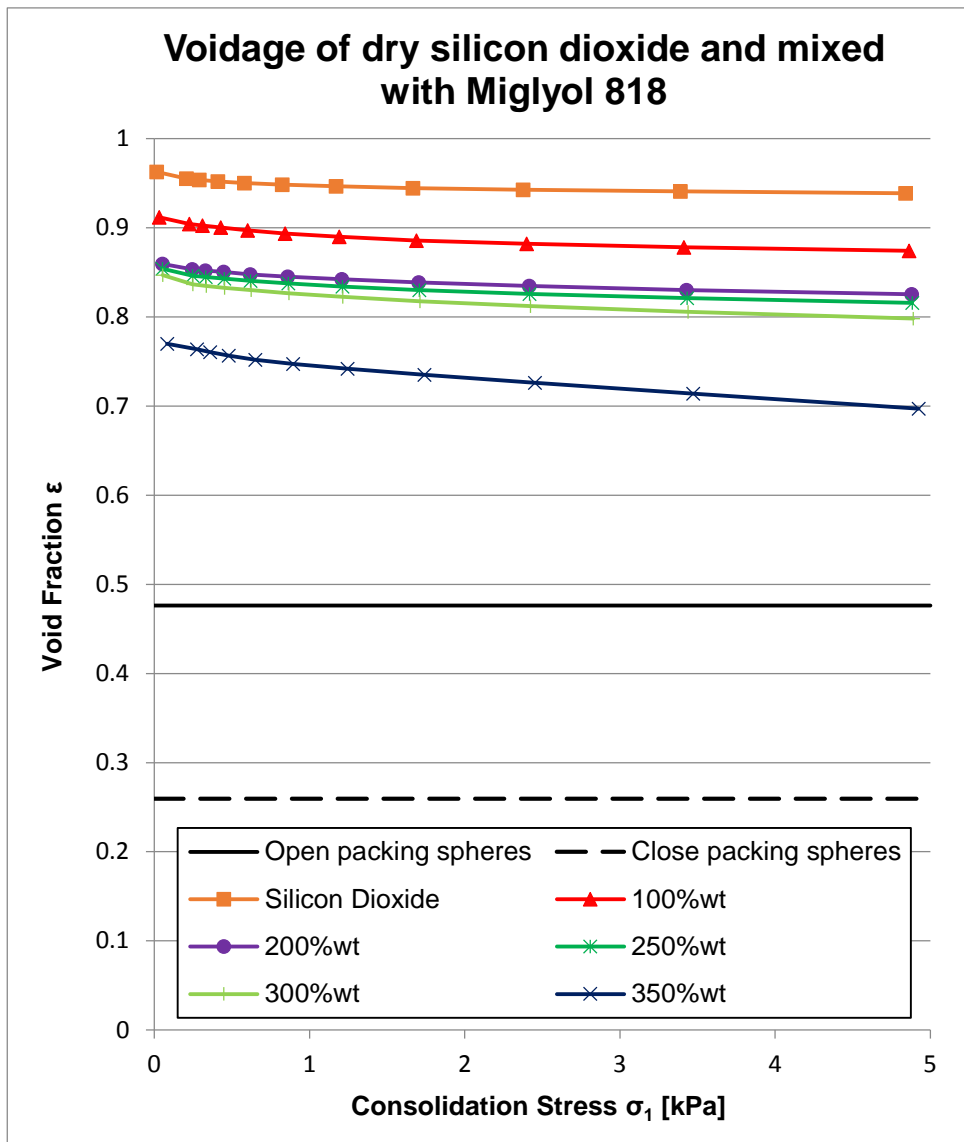


Figure B32

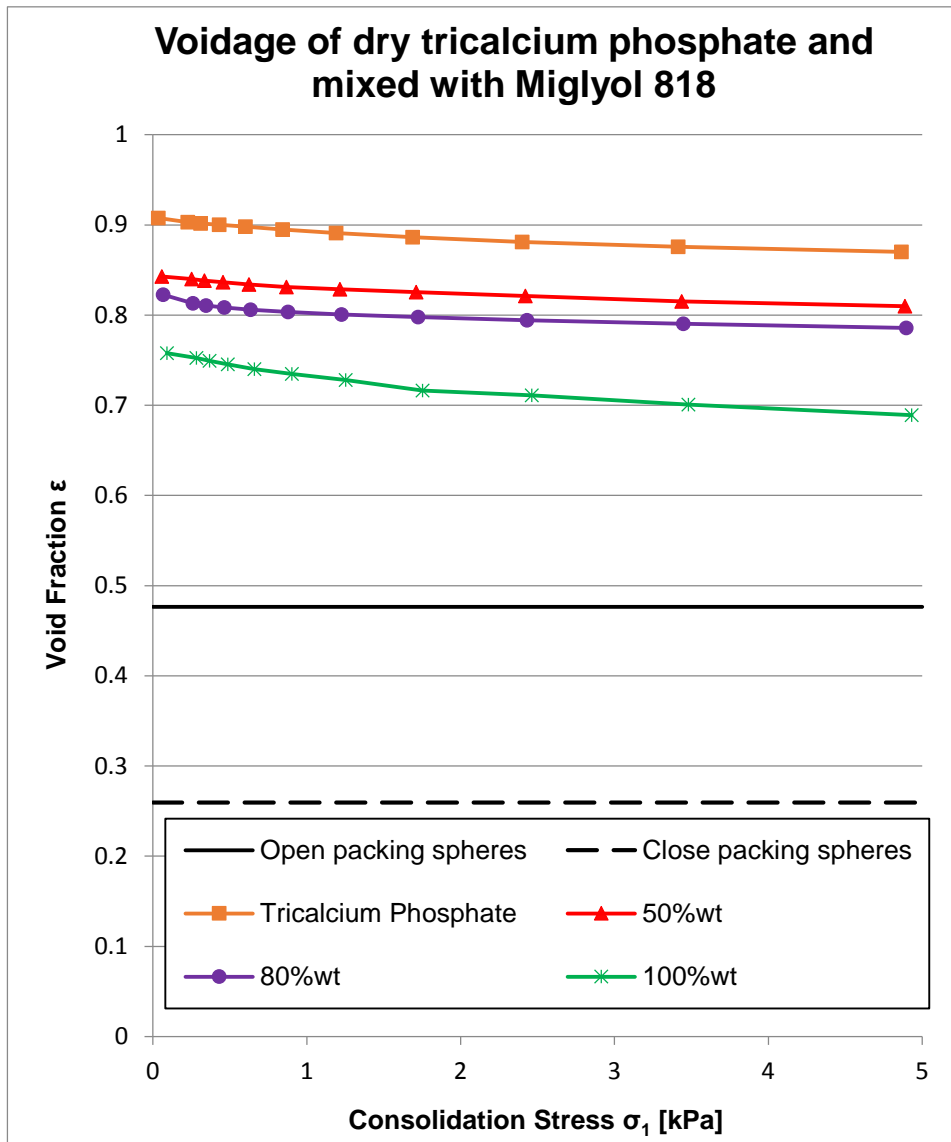


Figure B33

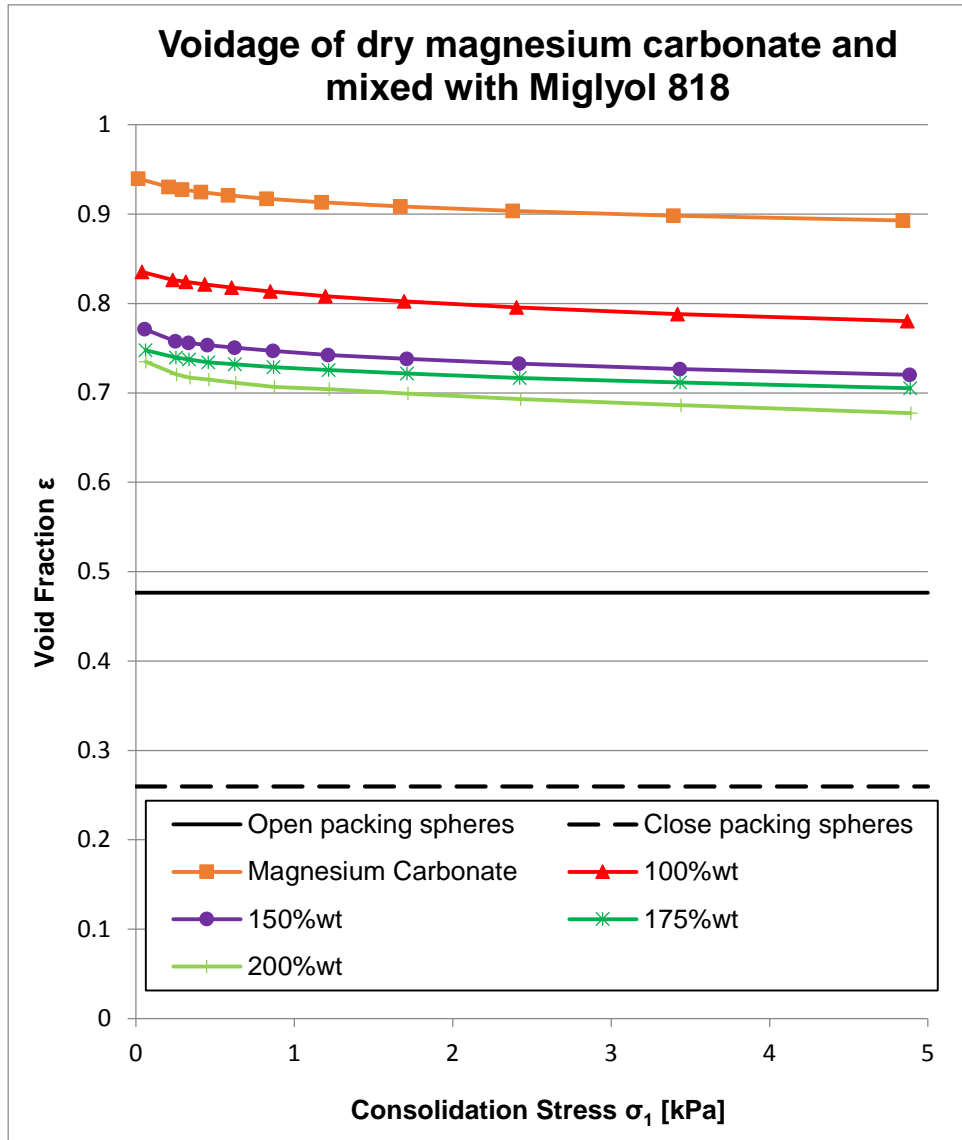


Figure B34

B5 Effect of free flow additives

The aim of these test programmes is to study the influence of the level and type of free flow additive on common filler powders (lactose and maltodextrin), idealised particulate materials (glass beads) and a blended snack flavour at different levels of oil.

Test Parameters:

- Particle properties: none
- Type of powders: blended snack flavour and single fillers & idealised materials
- Condition of the powders: dry and wet

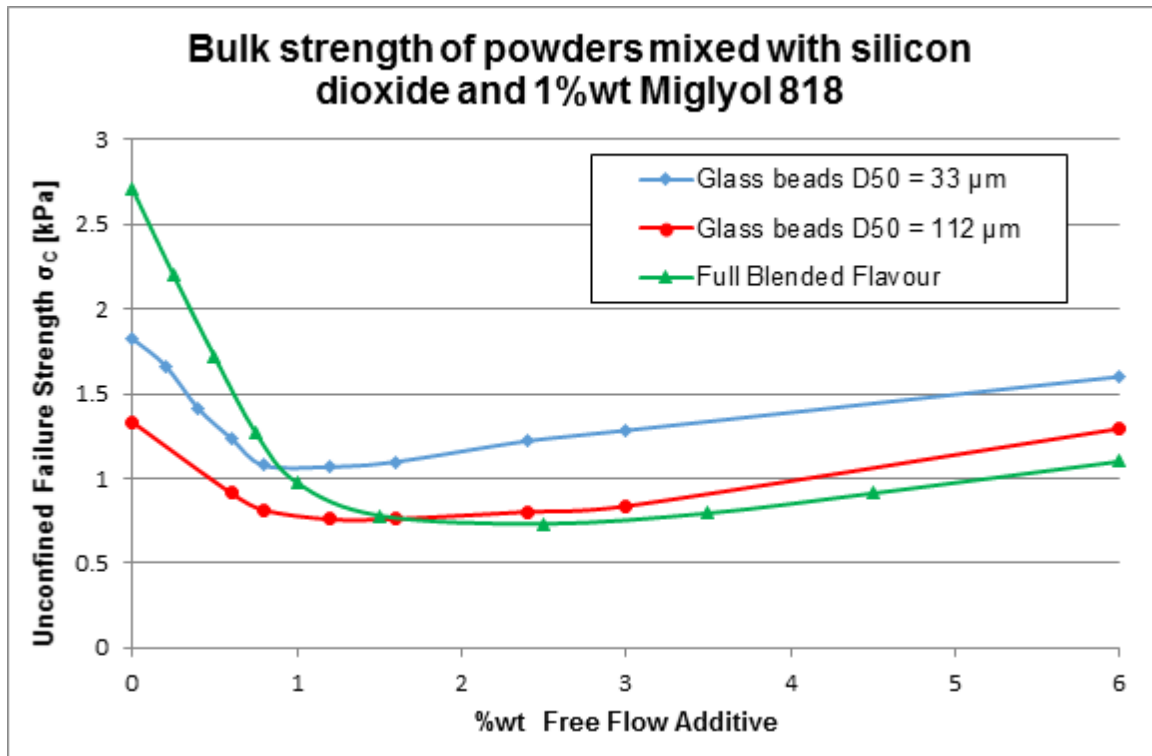


Figure B35

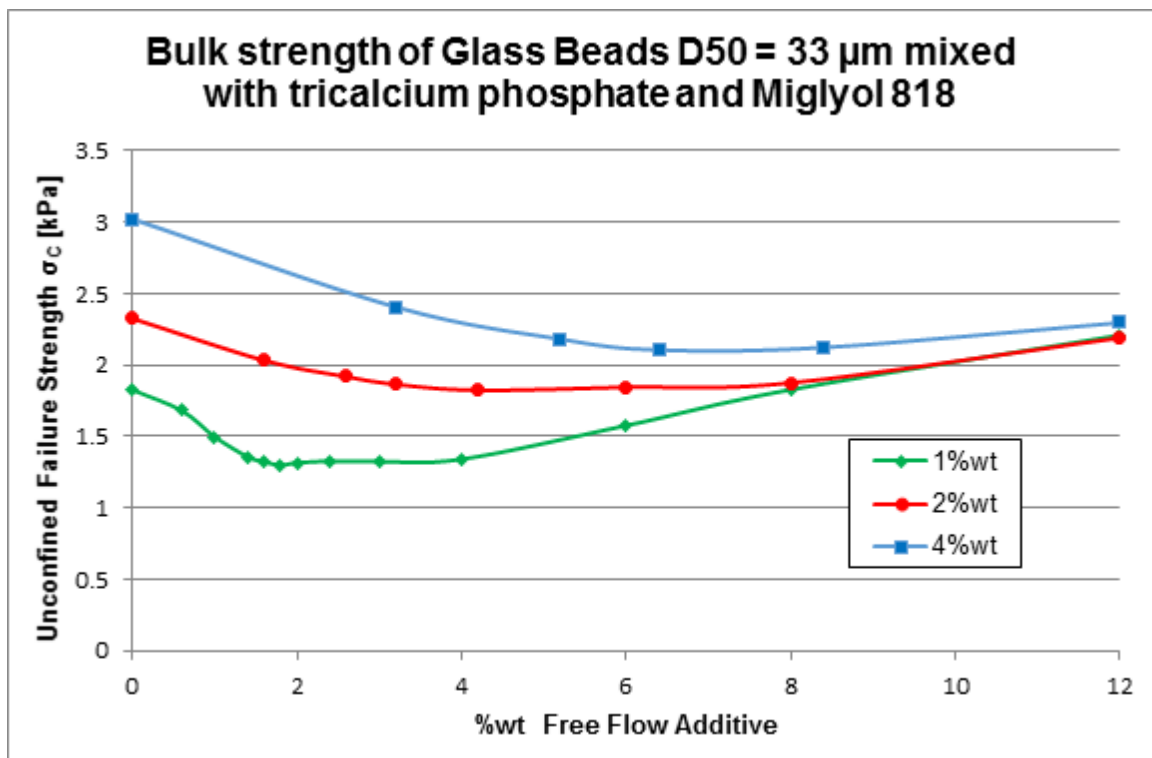


Figure B36

Appendix C: Industrial Case Study

C1 Introduction

The industrial case study undertaken in this research generated a large amount of data and it was not possible to show all the data in chapter 6; this appendix contains the data not presented in the chapter.

C2 Preliminary studies

Preliminary studies were undertaken to characterise the flow behaviour of blended powders with good and poor flow in the industrial process lines. This helped to define the window of the reformulated blended snack flavour without MSG. Standard Flame Grilled Steak snack flavour shows acceptable flowing in the process line.

The effect of the addition of the liquid and the flow agent on the flow behaviour of the standard formulation of the snack flavour was also studied. Meanwhile, bulk flow properties of the flavour were initially measured repeating the standard flow function test using the PFT 6 times to study the repeatability of the results from the shear tester in the case study.

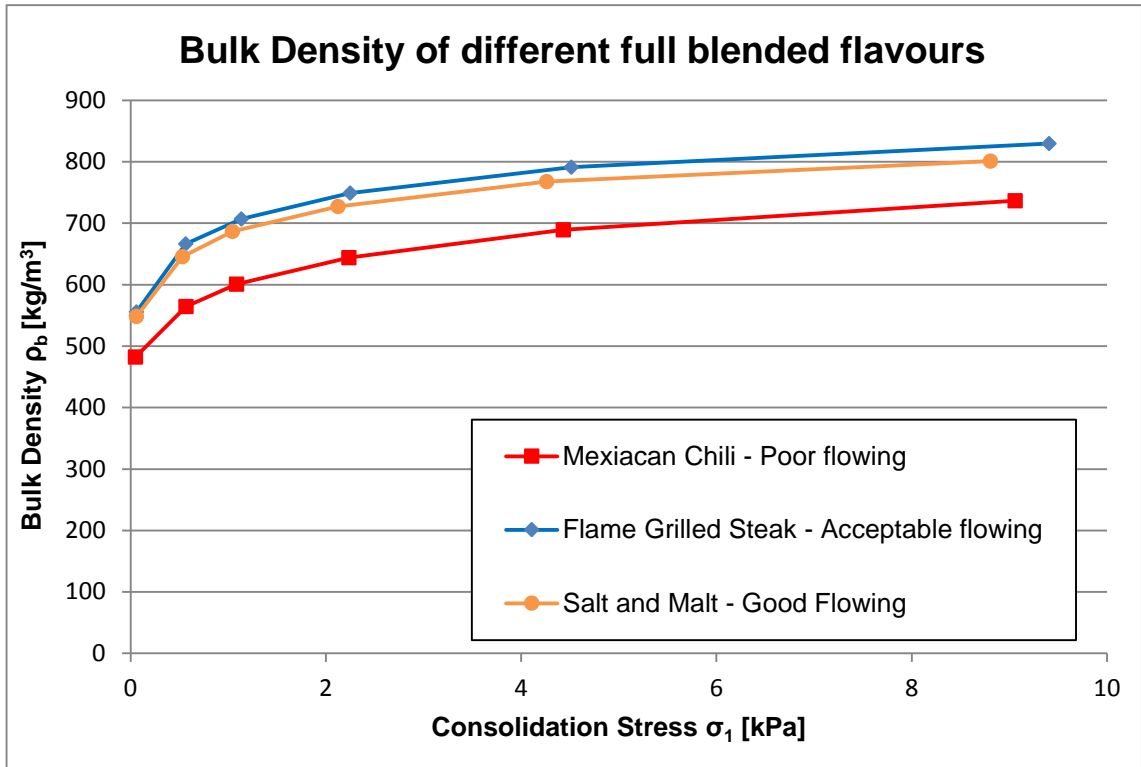


Figure C1

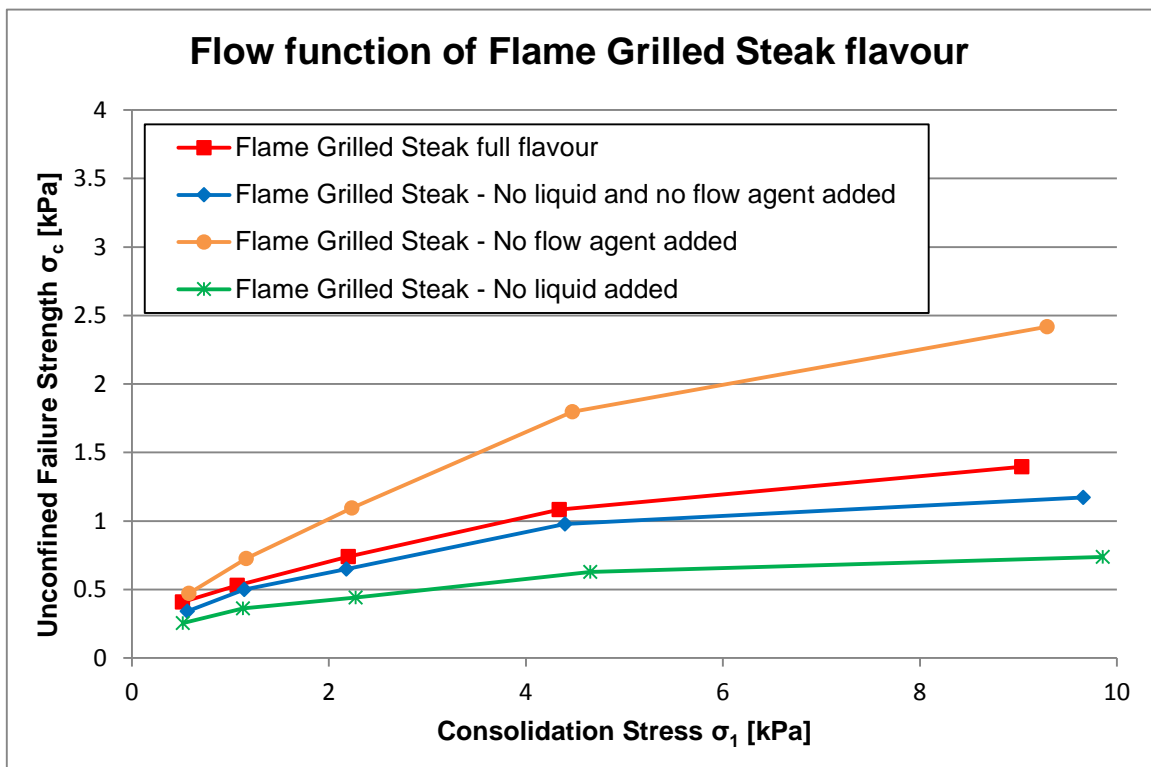


Figure C2

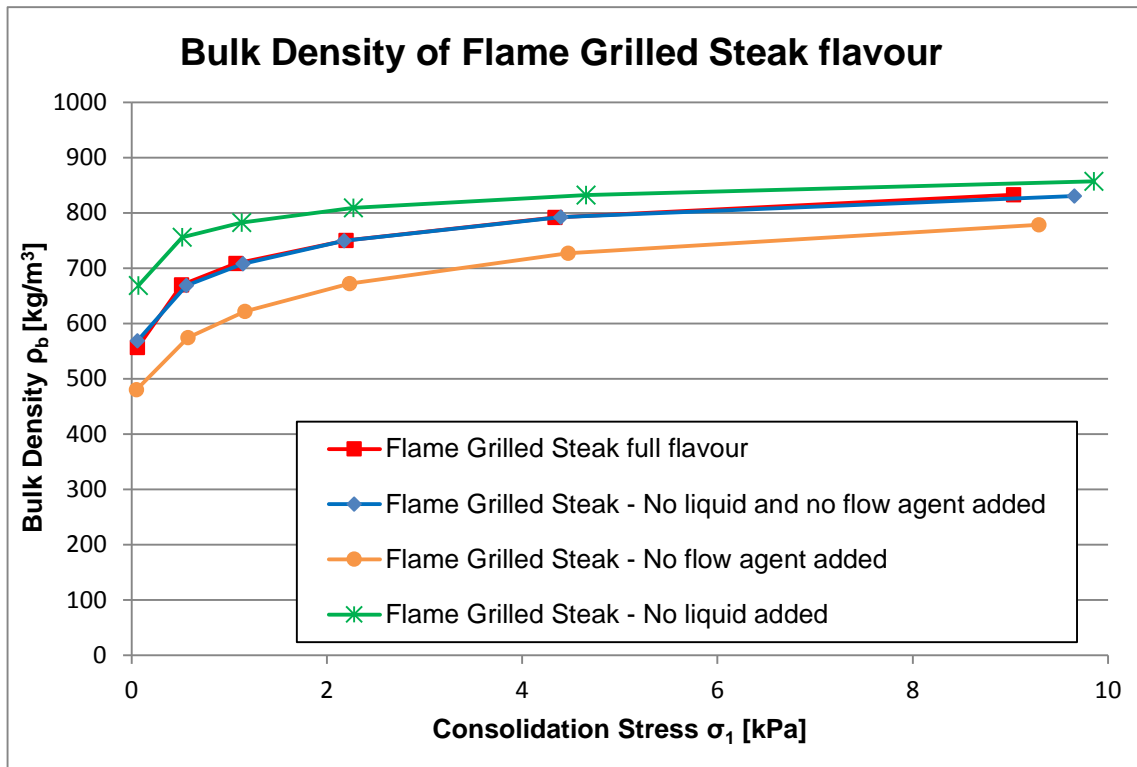


Figure C3



Figure C4

C3 Bulk flow properties results

This section shows more results of the measured bulk flow properties not presented in the chapter.

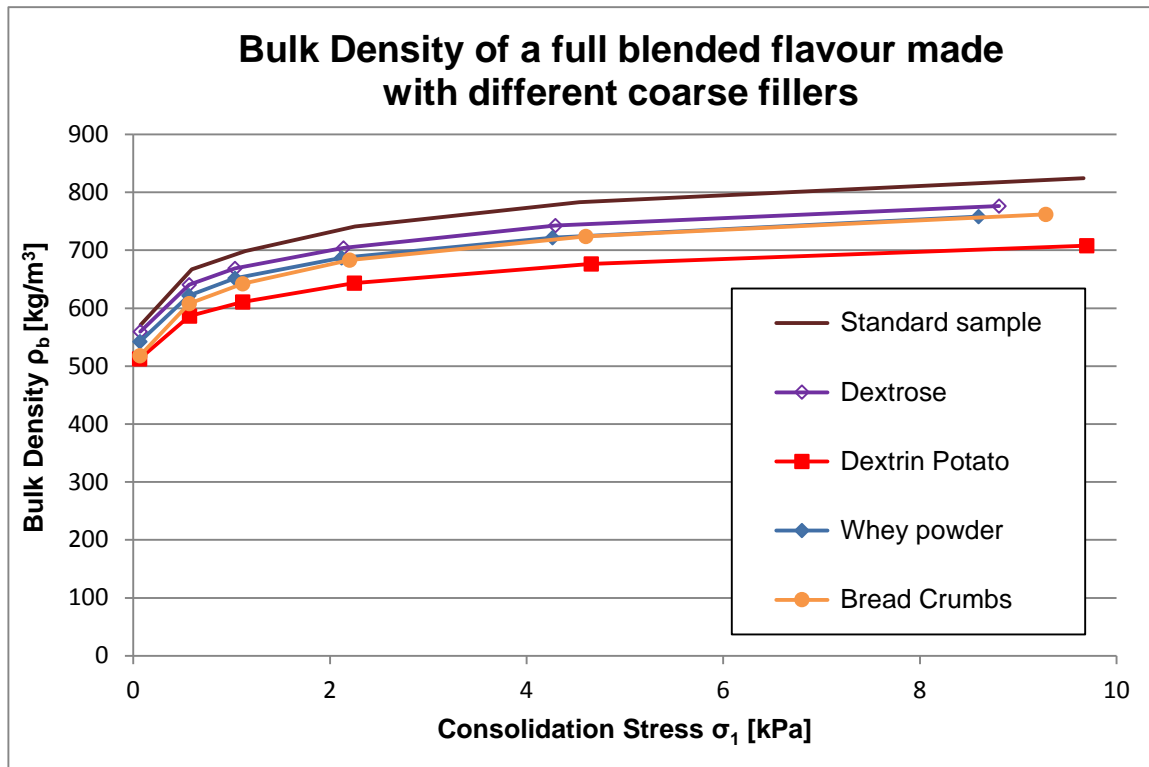


Figure C5

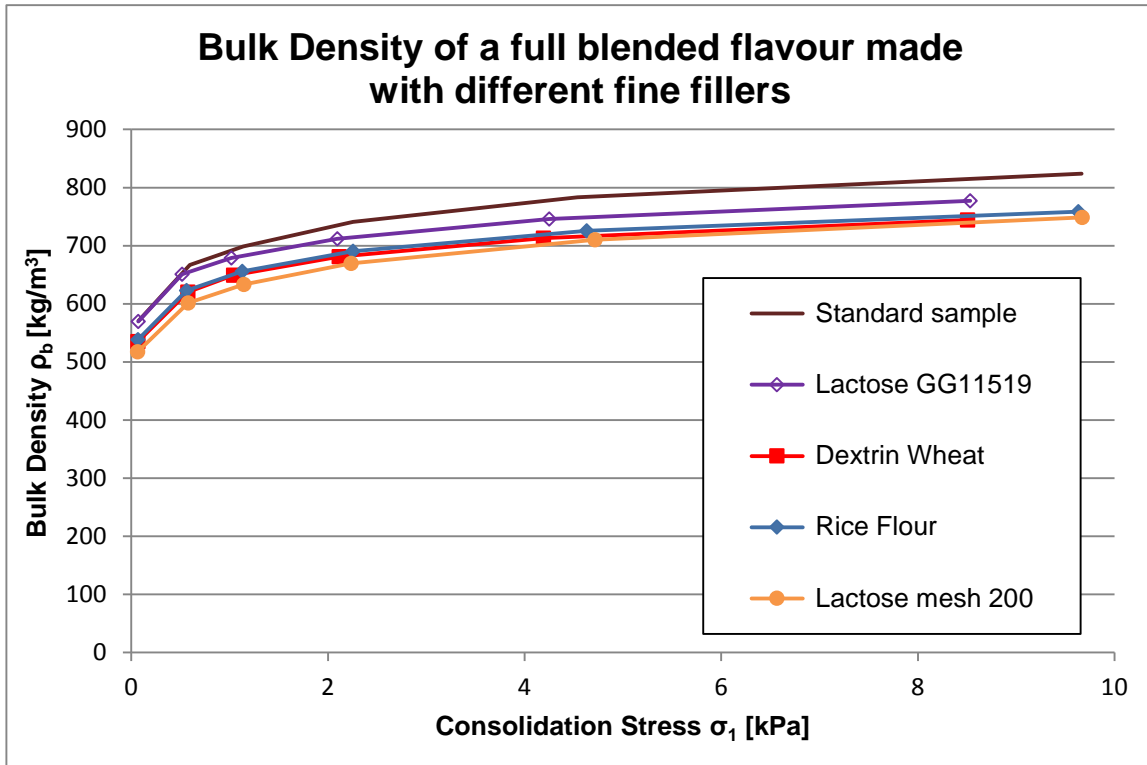


Figure C6

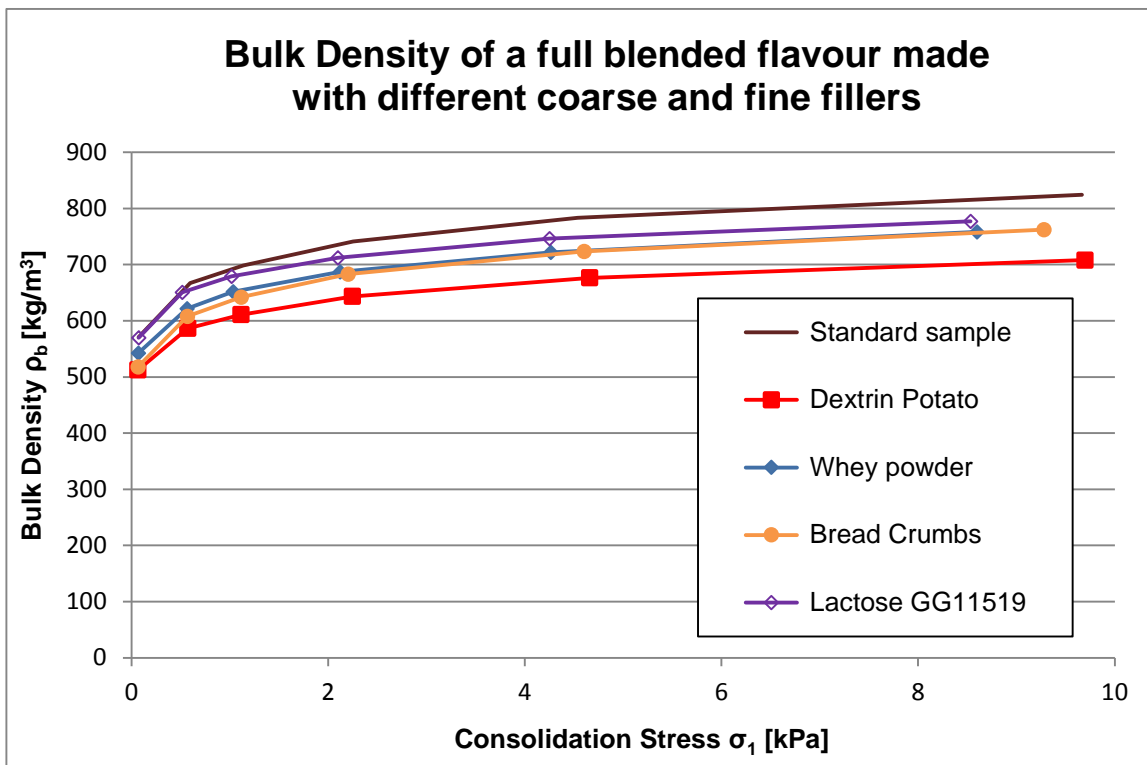


Figure C7

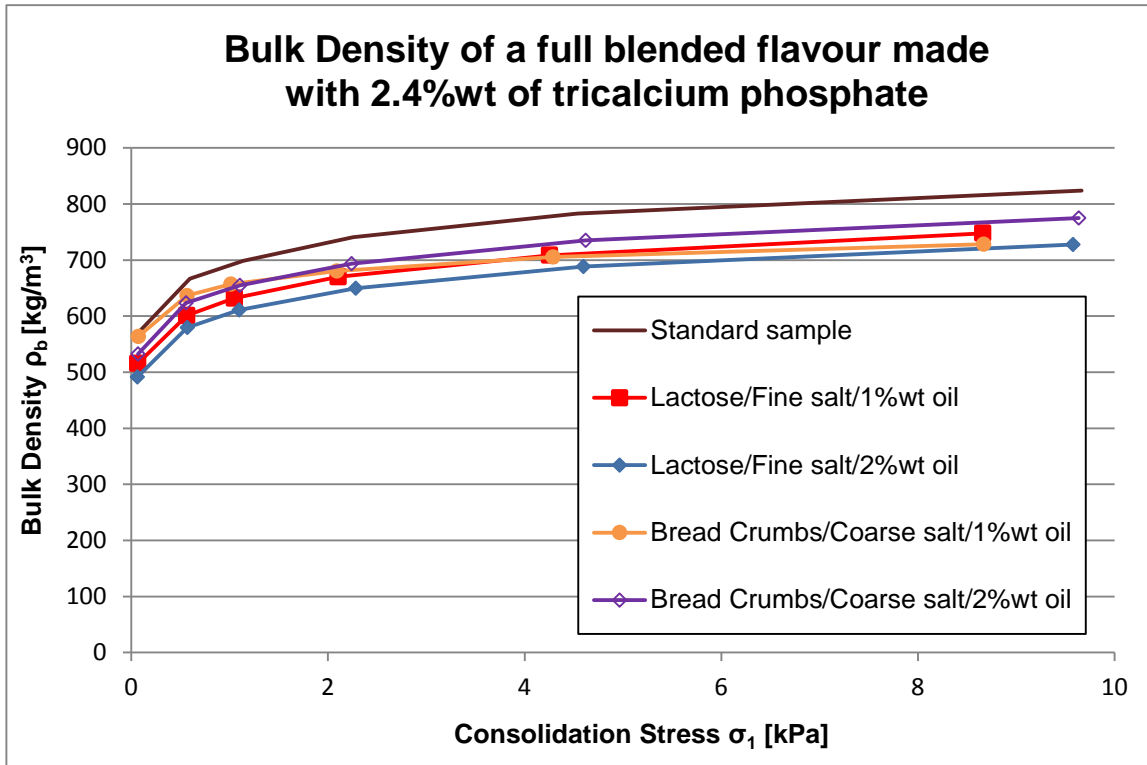


Figure C8

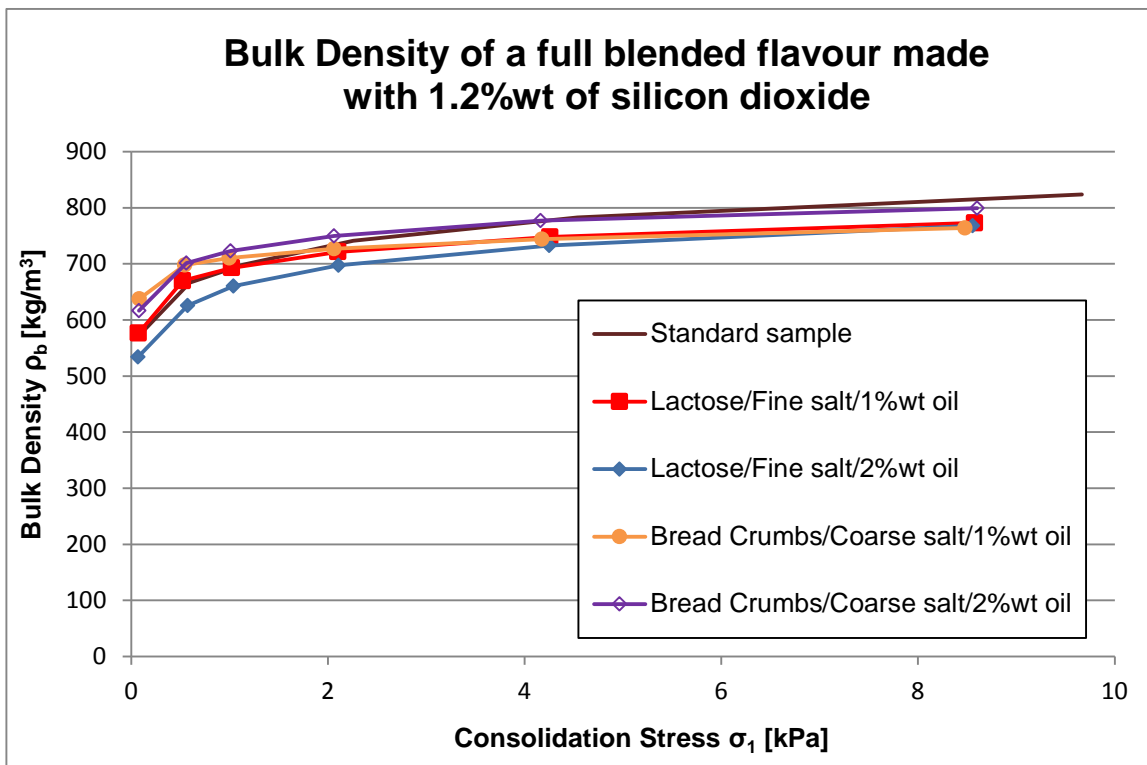


Figure C9

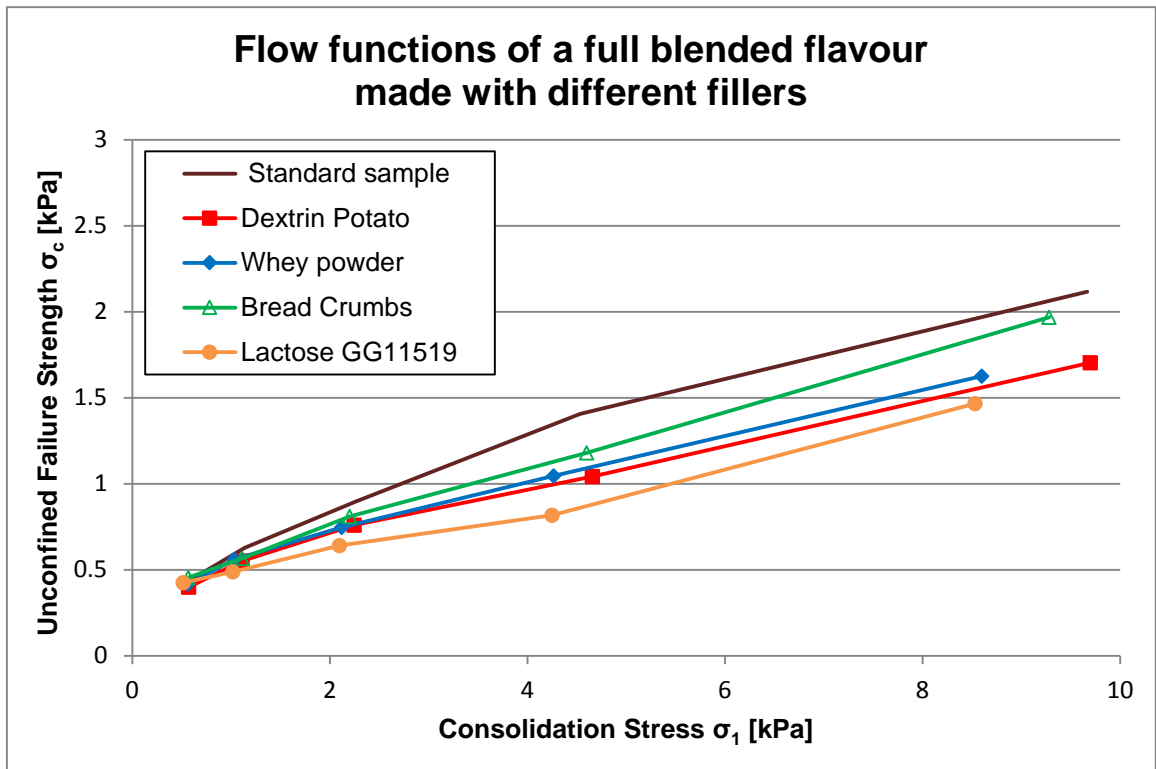


Figure C10

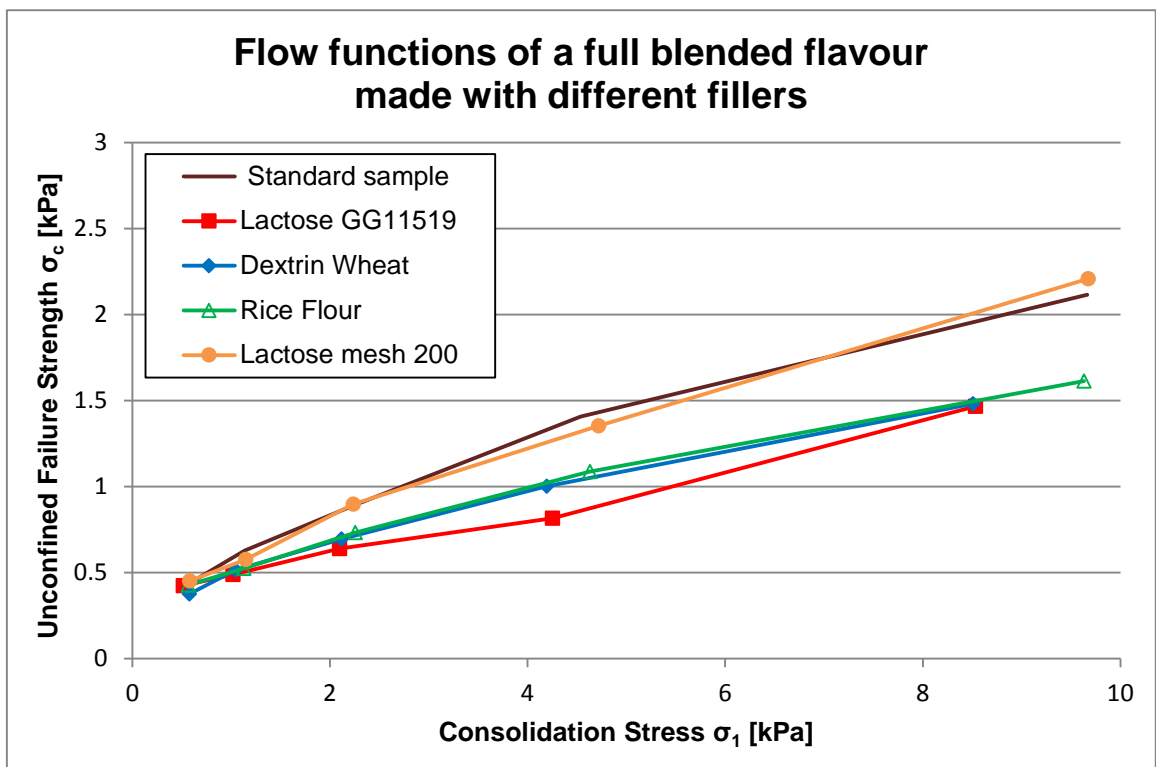


Figure C11

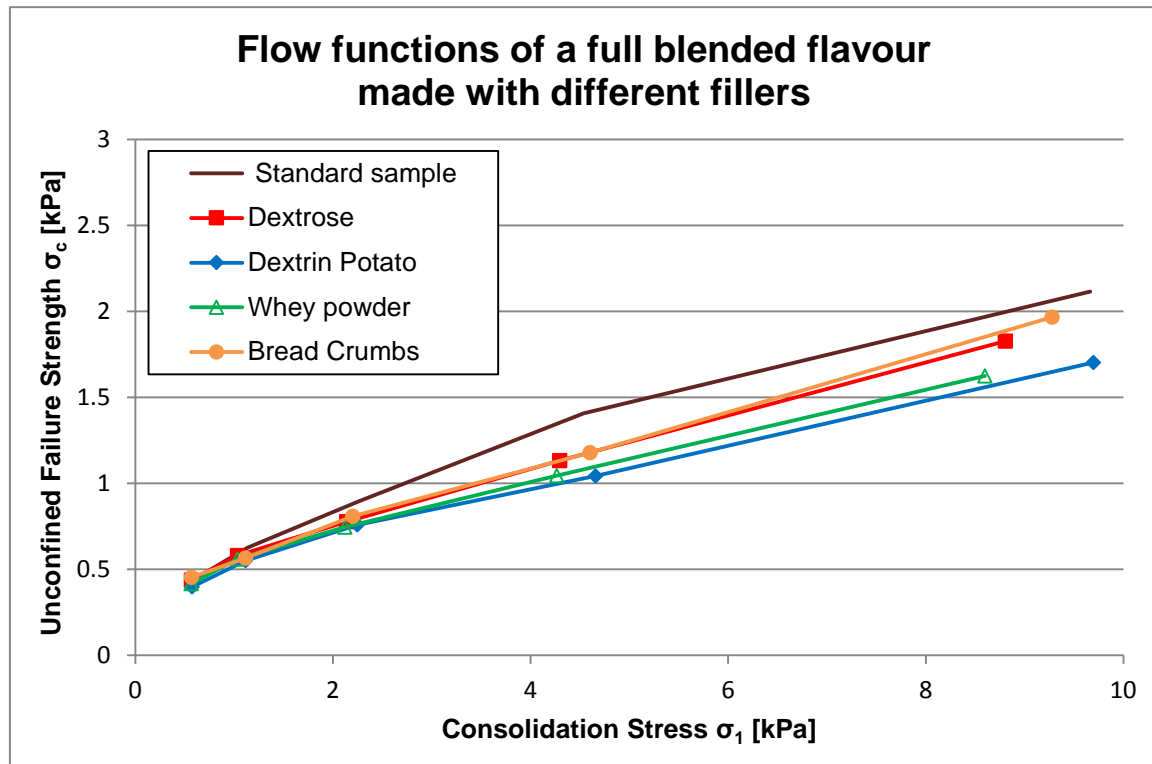


Figure C12

C4 Discharge of the powders in the Rospen unit

As explained in chapter 4, the reformulated blends were tested using the Rospen loss in weight feed hopper under adverse environmental conditions. Different flavours with poor flow behaviour in the handling process at the factory were also tested and compared with the reformulated trial blended powders. Conditions of the discharge were as follows:

- Temperature 35°C
- Relative humidity 40%
- Lid open all the time
- Single fill and non-stop discharge
- PFT samples taken over time
- Run at constant speed

Tests undertaken showed that the discharge consistency decreased with time, the worst flowing materials had more erratic discharge rates from the loss in weight feeder hopper when run at a constant speed; this demonstrates that there is a link between the flow properties of the snack flavours and the discharge behaviour.

Samples of the tested powders were taken every half an hour during the discharge from the Rospen loss in weight feeder hopper and subjected to measurements of their flow properties using PFT at the same environmental conditions.

This section presents the results of the tests for the trials of the reformulated blended powder, the standard Flame Grilled Steak snack flavour and snack flavours with poor flow behaviour at the factory such as Sizzling King Prawn flavour.

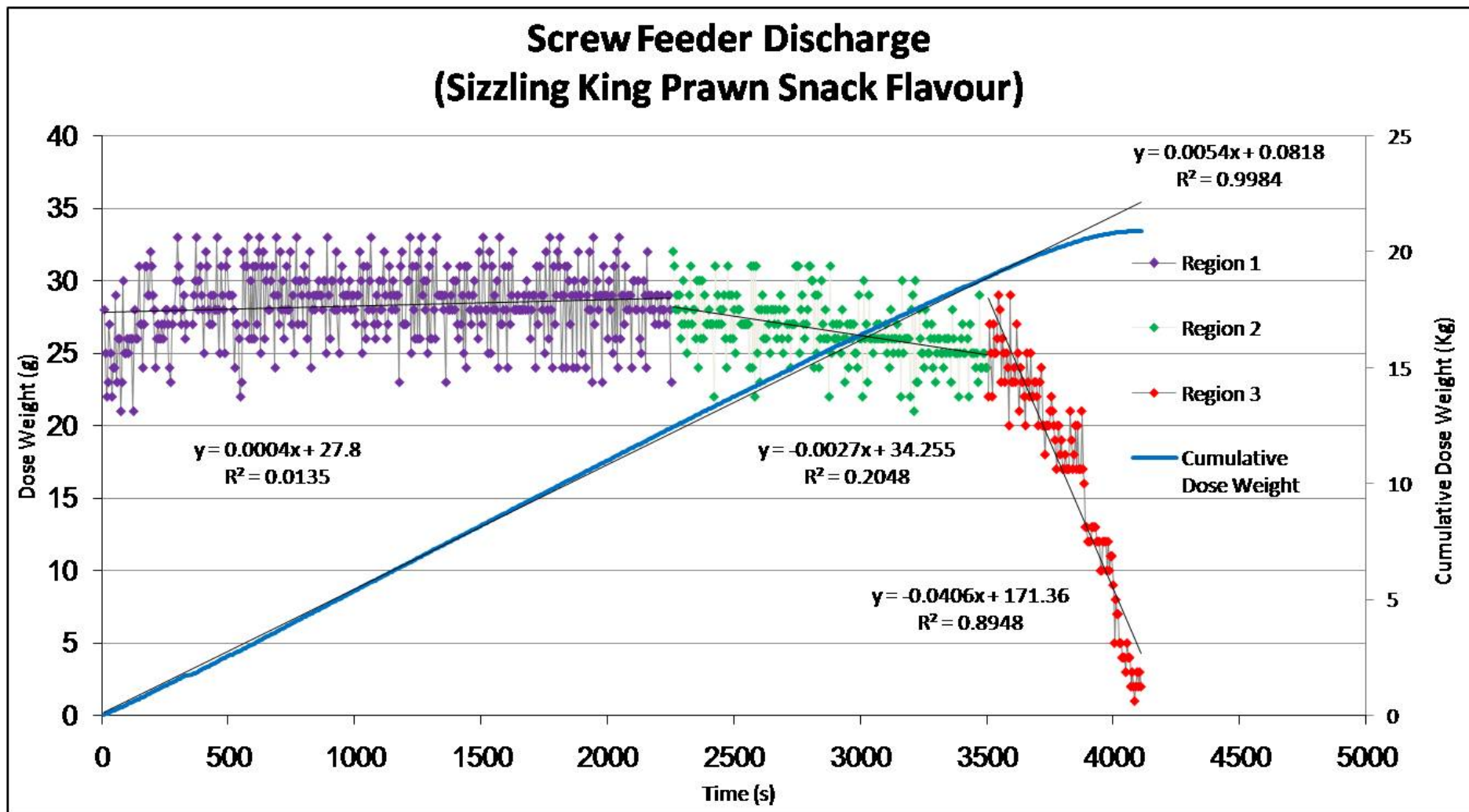


Figure C13

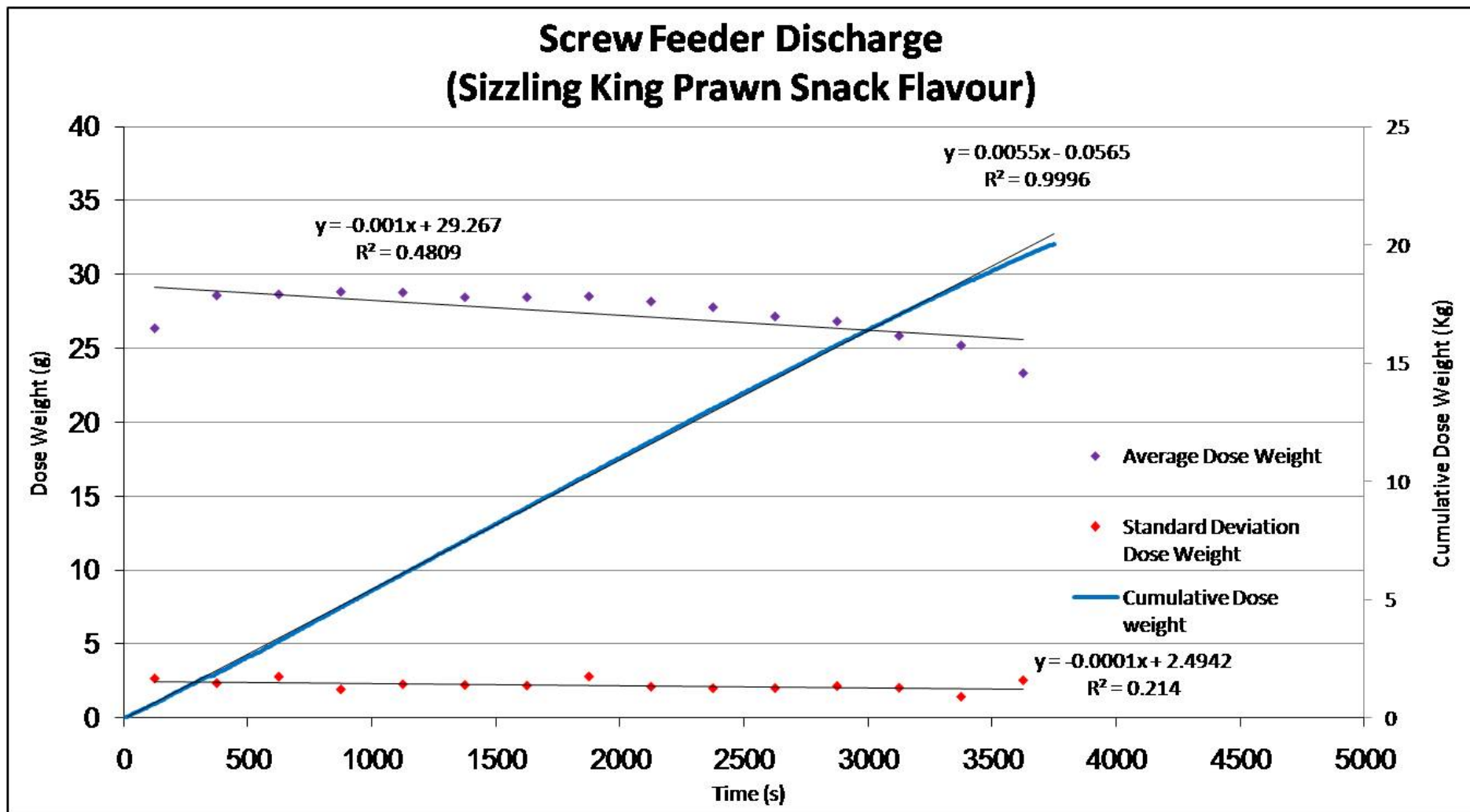


Figure C14

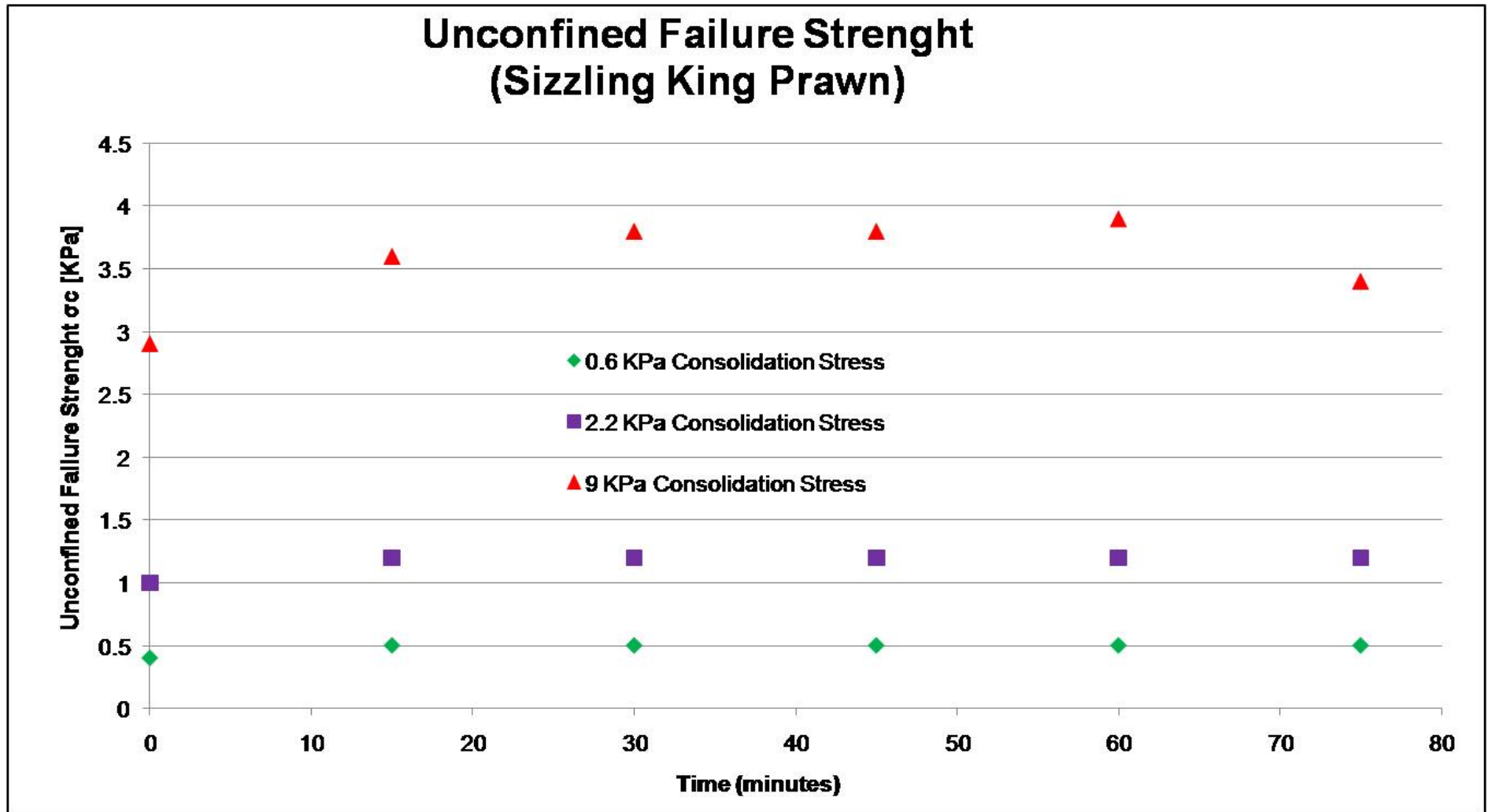


Figure C15

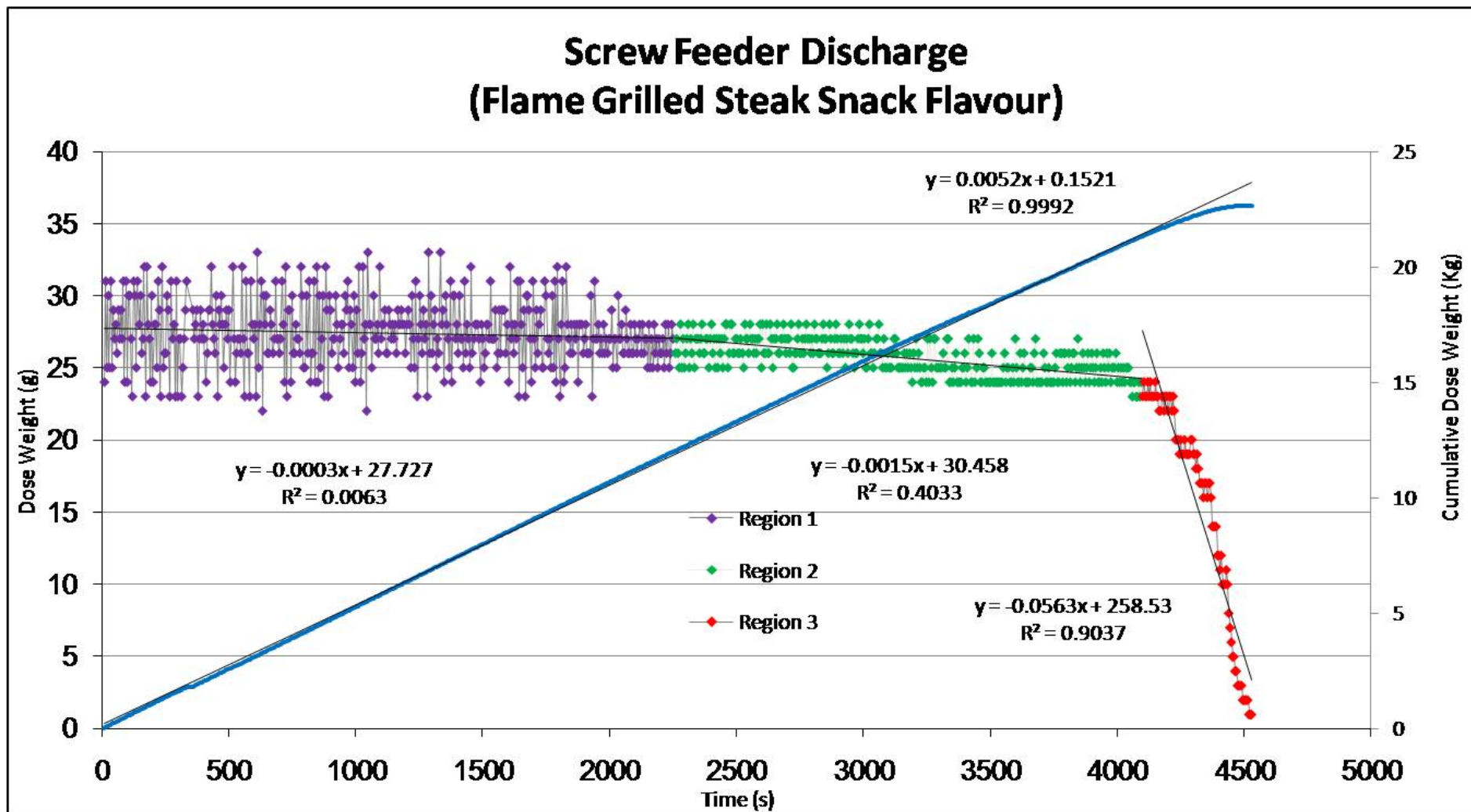


Figure C16

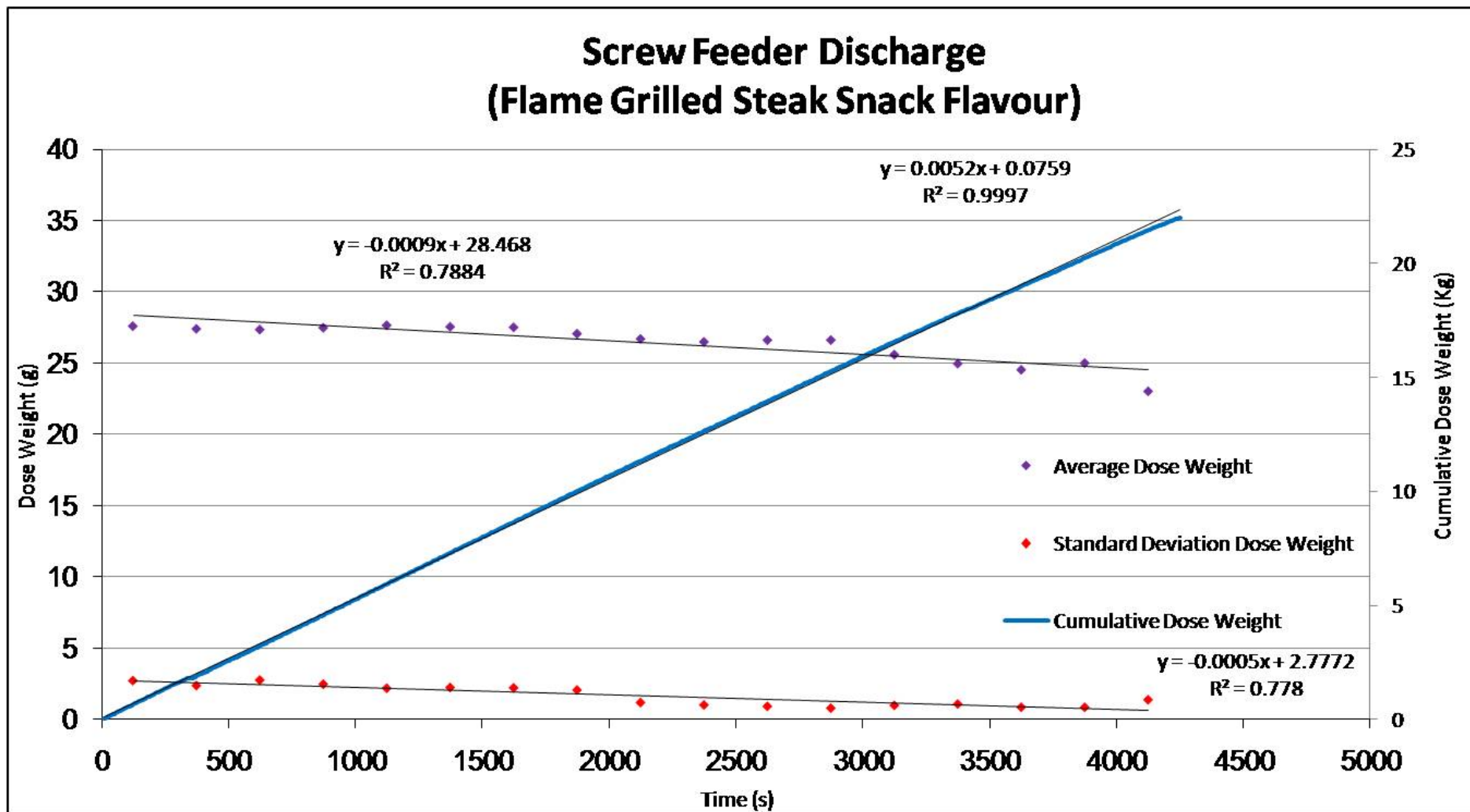


Figure C17

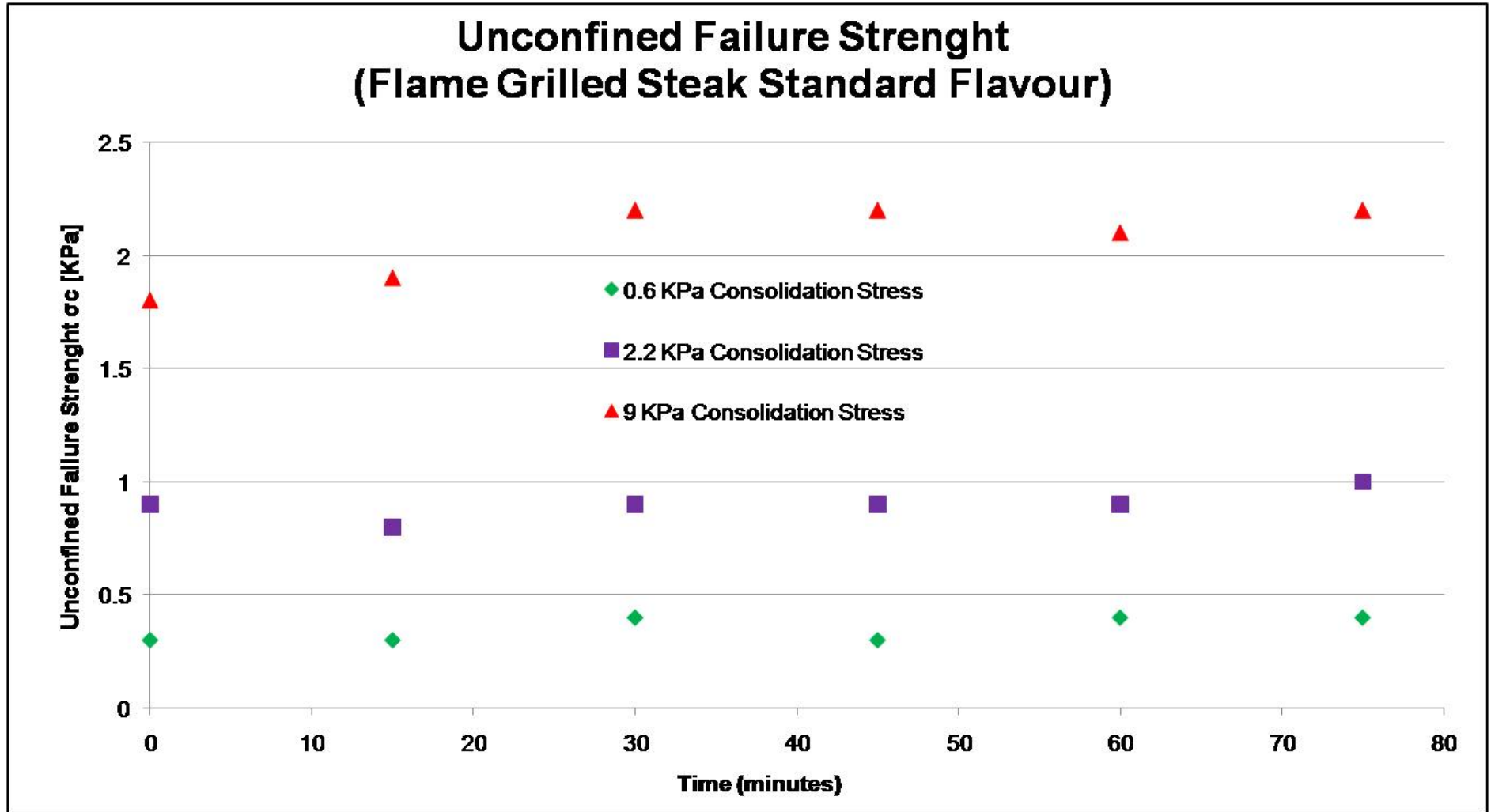


Figure C18

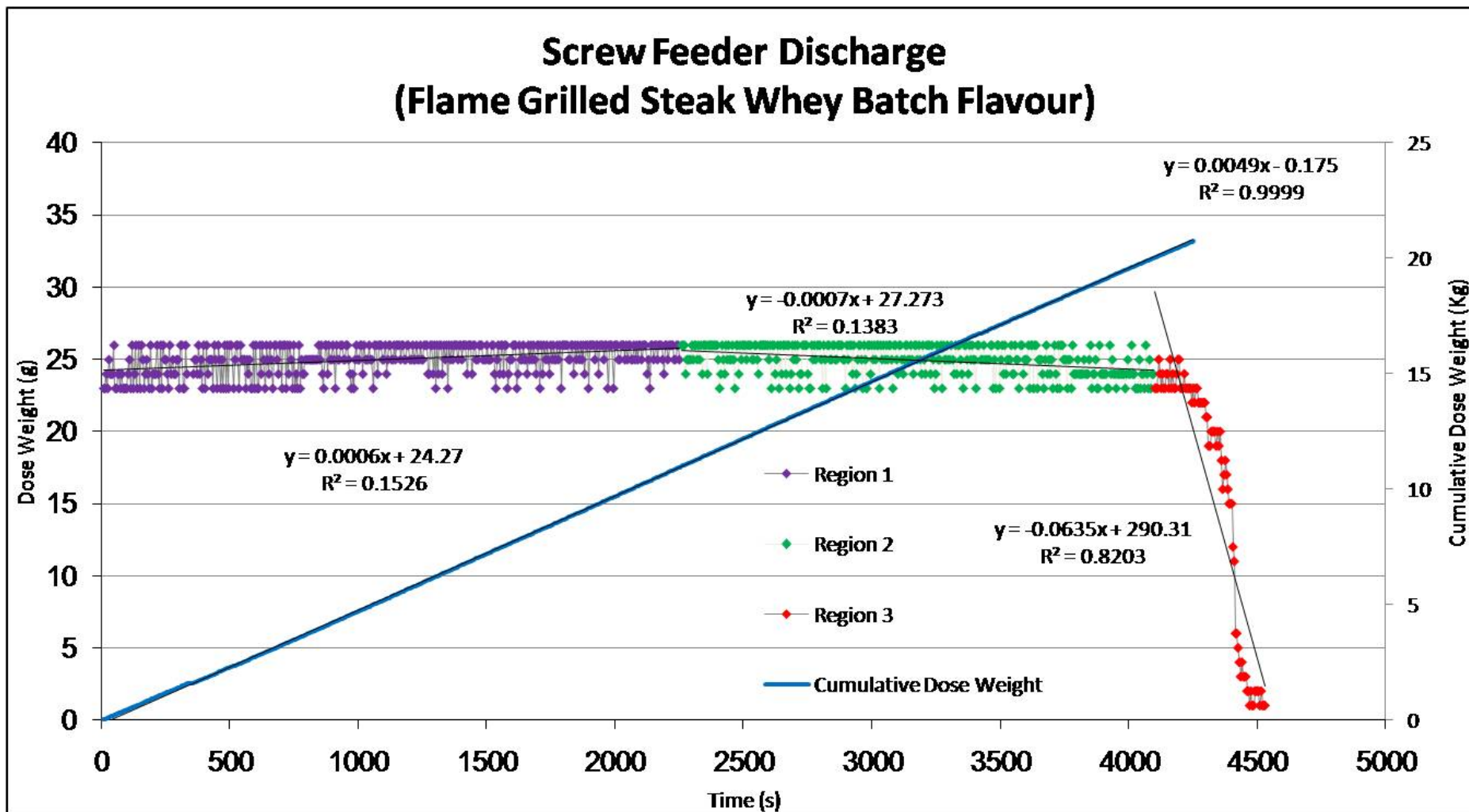


Figure C19

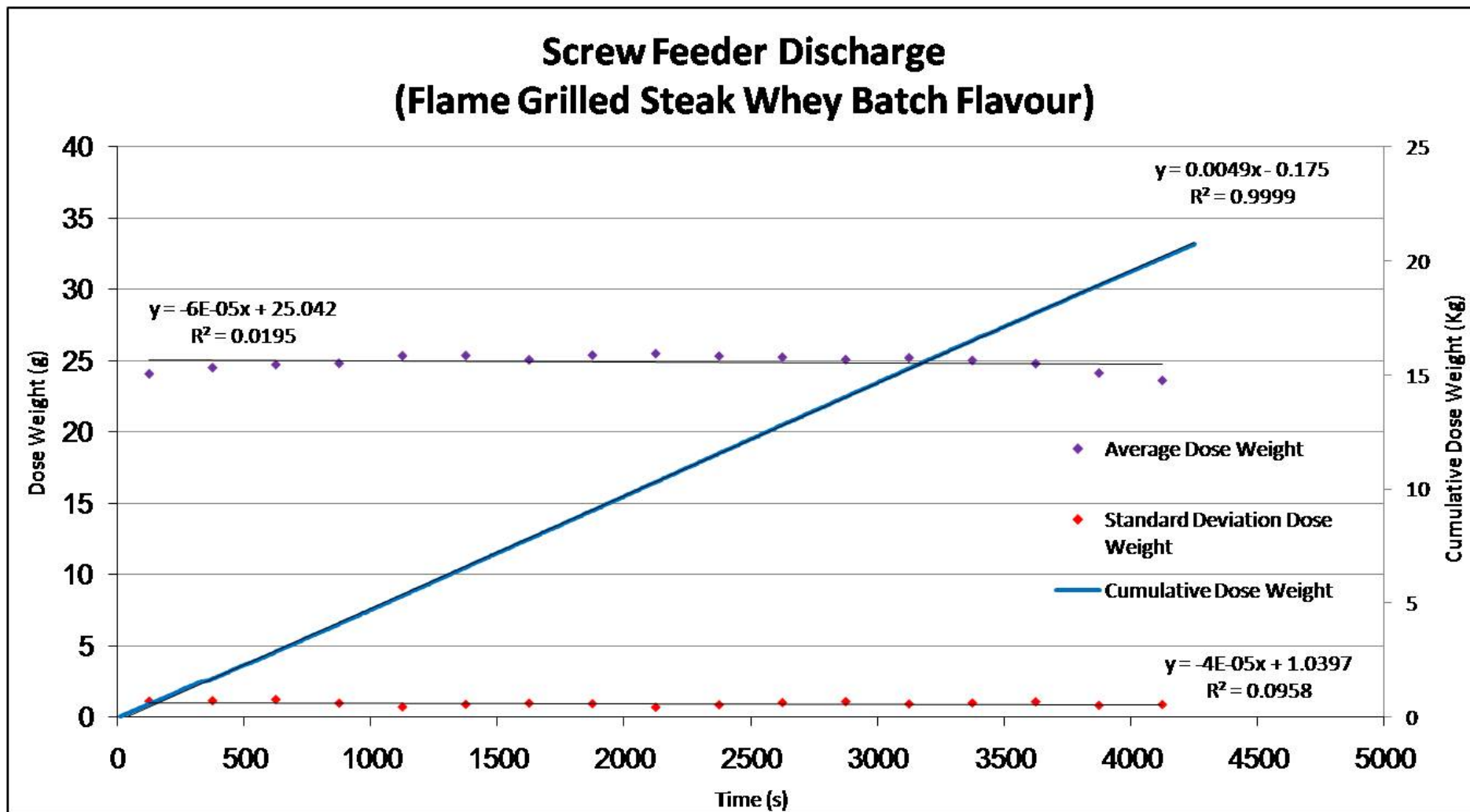
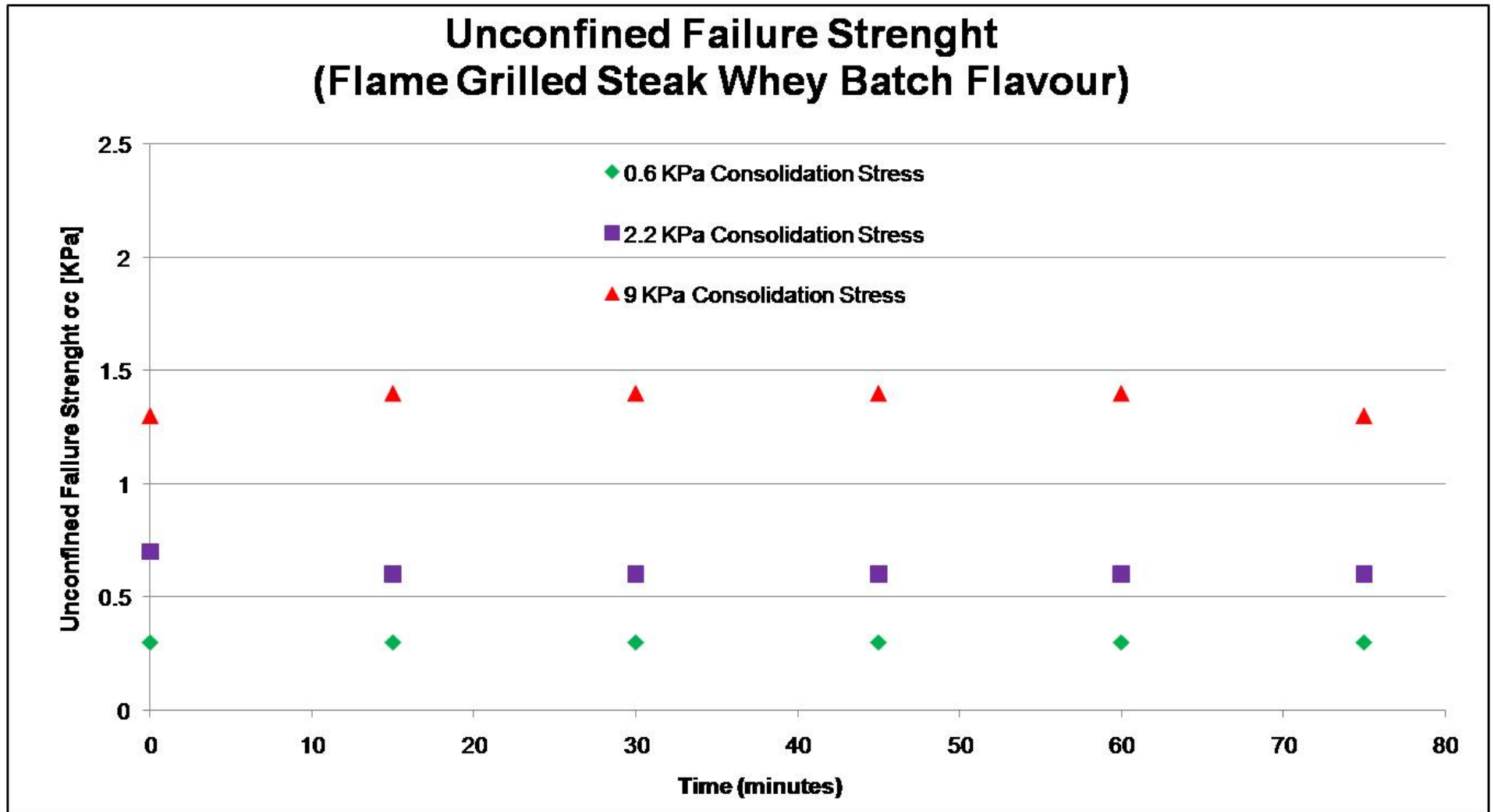


Figure C20

*Figure C21*

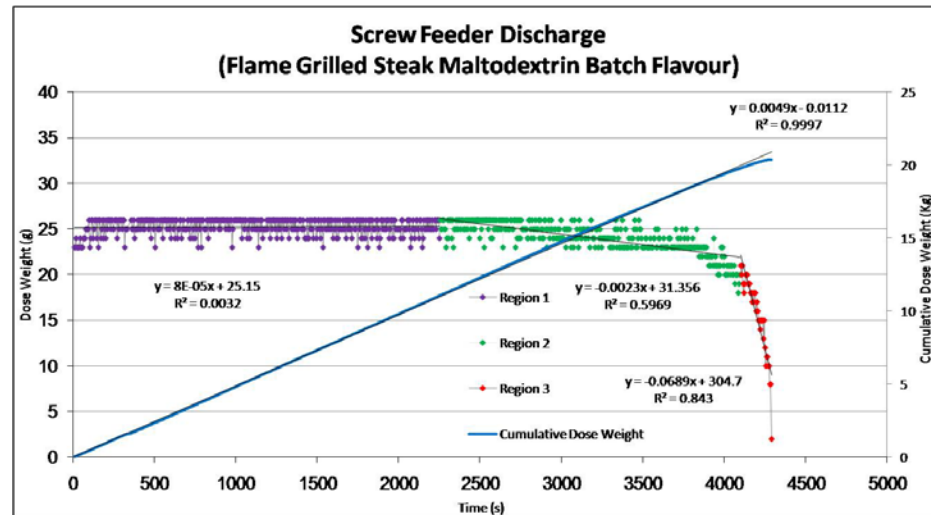
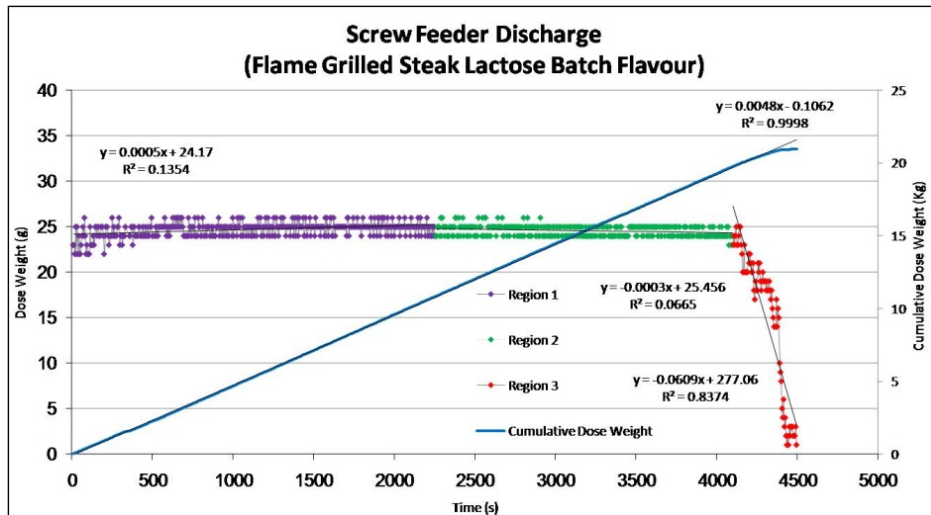
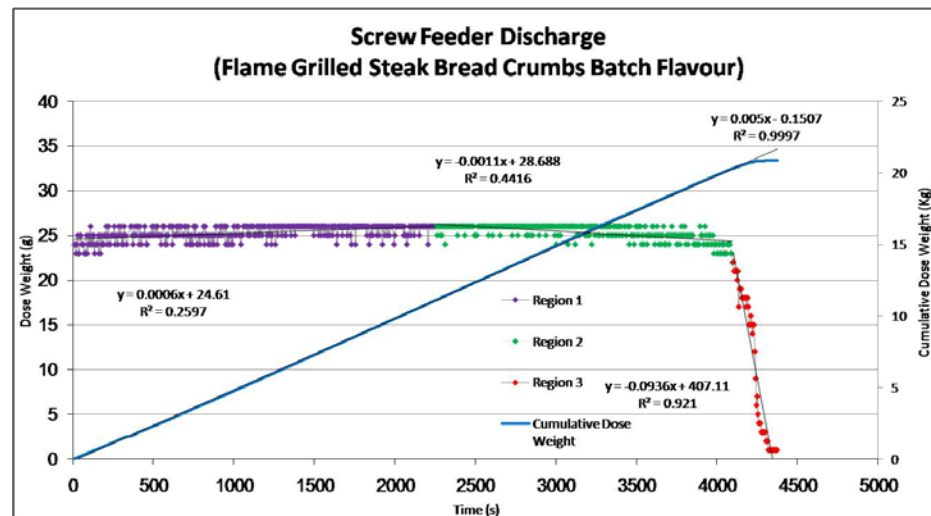
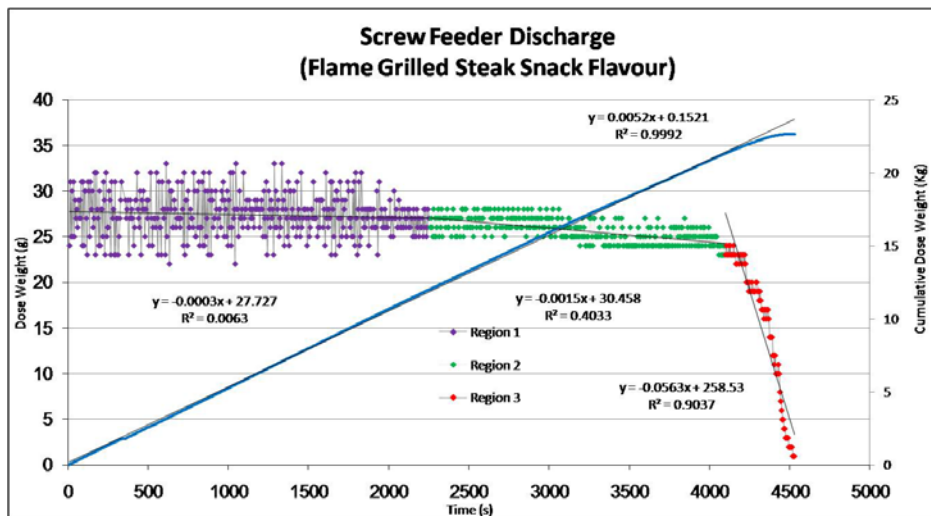


Figure C22

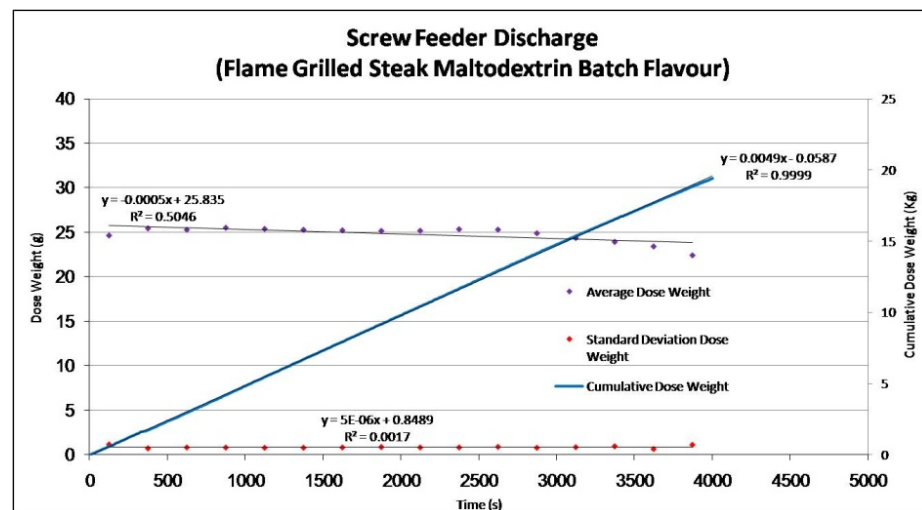
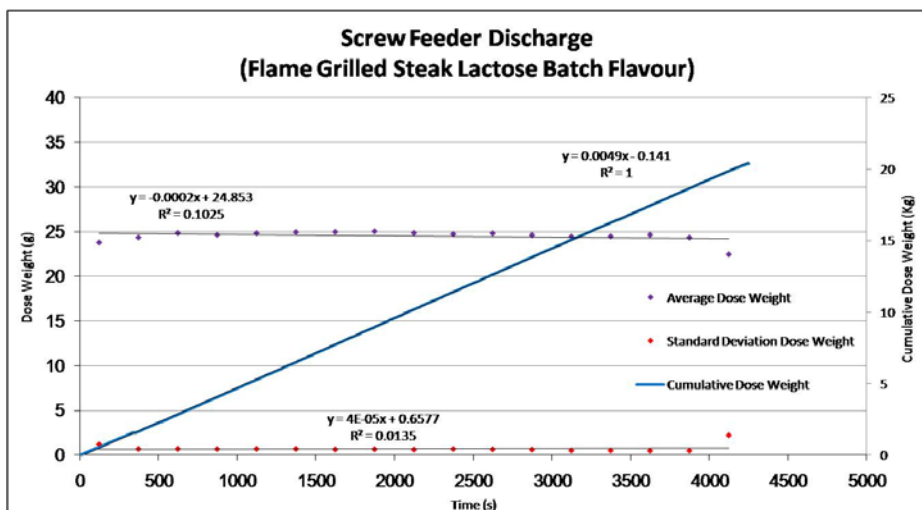
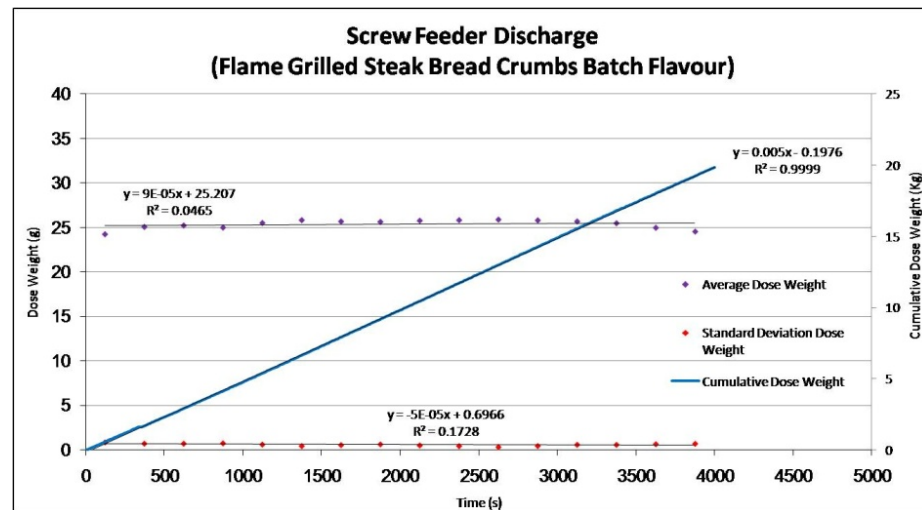
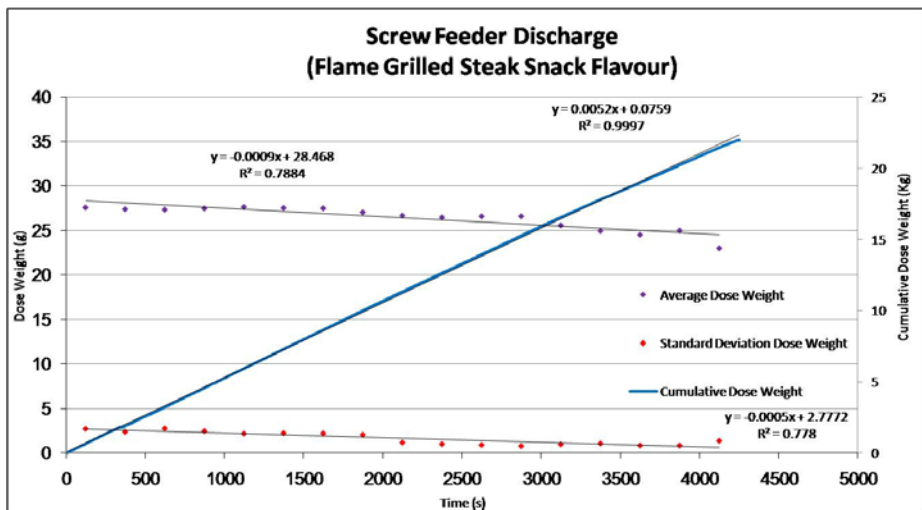


Figure C23

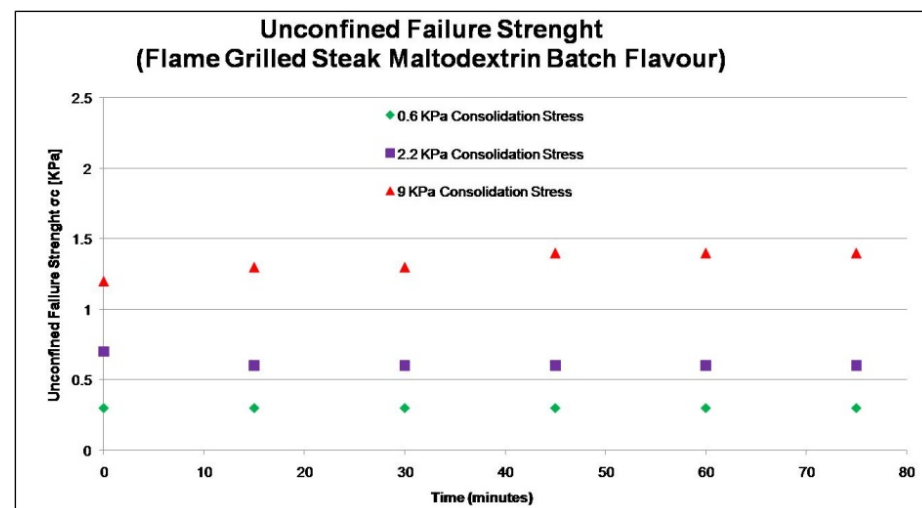
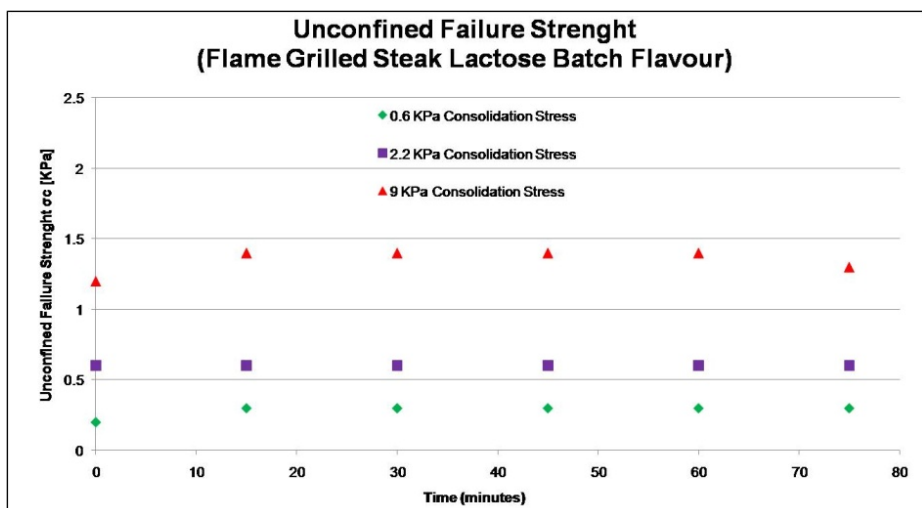
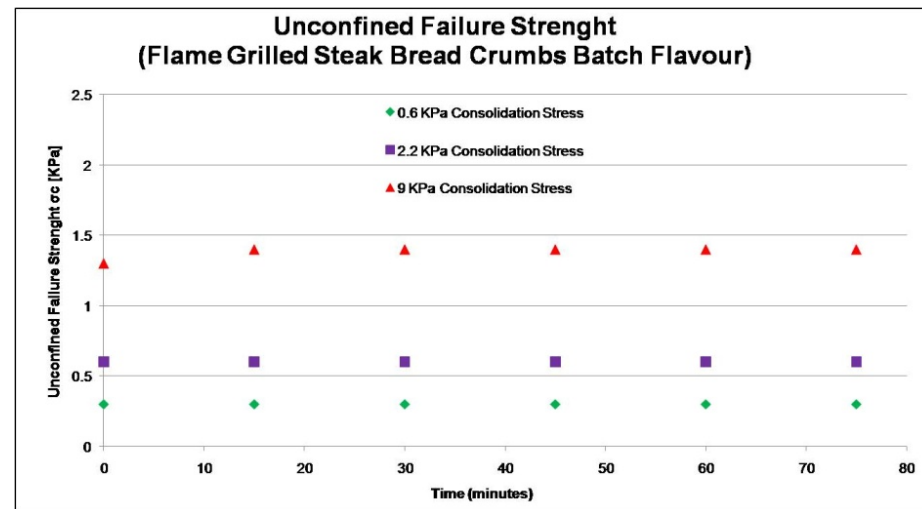
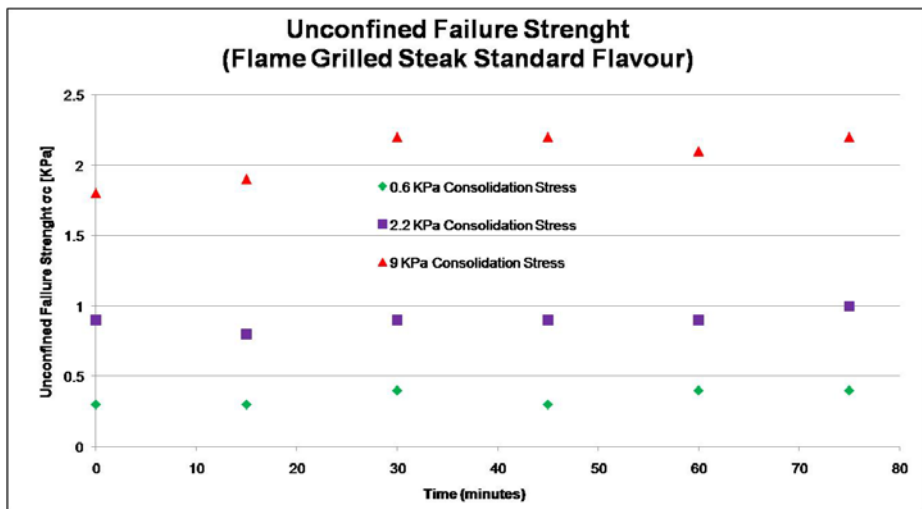


Figure C24